Proceedings of the Tenth American Peptide Symposium

Peptides

Garland R. Marshall

Chemistry and Biology

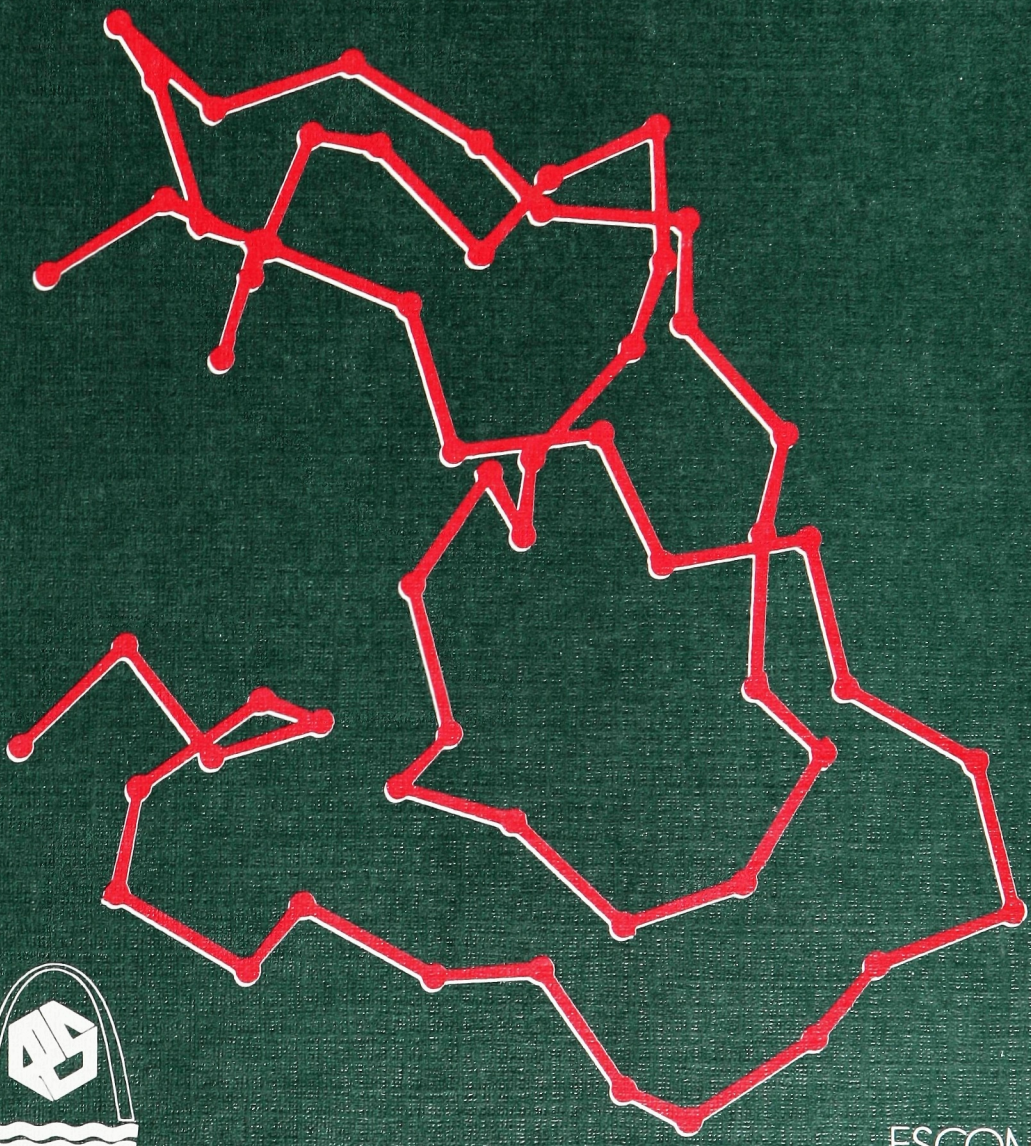

ESCOM

Peptides

Chemistry and Biology

Peptides

Chemistry and Biology

Proceedings of the Tenth American Peptide Symposium
May 23-28, 1987, St. Louis, Missouri, U.S.A.

Edited by

Garland R. Marshall
Department of Pharmacology
Washington University School of Medicine
St. Louis, Missouri 63110, U.S.A.

ESCOM ▪ Leiden ▪ 1988

CIP-Data Koninklijke Bibliotheek, Den Haag

Peptides

Peptides: Chemistry and Biology : Proceedings of the Tenth American Peptide Symposium / [Ed. by Garland R. Marshall]. - Leiden : ESCOM - Ill.
Includes bibliographies and indexes.
SISO 546 UDC 547.96(063)
Subject headings: Peptides; Chemistry; Congresses/Peptides; Biology; Congresses.

ISBN 90-72199-01-4 (hardbound)

Published by:

ESCOM Science Publishers B.V.
P.O. Box 214
2300 AE Leiden
The Netherlands

Printed in The Netherlands

Preface

The Tenth American Peptide Symposium was held on the campus of Washington University in St. Louis, Missouri, on May 23-28, 1987. More than 750 participants from around the world met to renew acquaintances, make new friends, and feast at the scientific explosion occurring in the field of peptide research. From over 85 oral presentations and 295 poster presentations, the manuscripts which make up this proceedings have been selected in order to present a synopsis of current research.

In many ways, this meeting represented a culmination of forces clearly perceptible in the proceedings of previous meetings in which synthetic chemistry, spectroscopy, molecular biology, molecular modeling, and protein chemistry all are blended as needed to focus on interesting scientific problems. As peptides assume an ever increasingly important role in biological phenomena, our domain as peptide chemists has obviously expanded, and we are the richer for it. The session on conformation was highlighted by both predictions of three-dimensional structures of proteins (i.e., interleukin and human growth hormone) as well as determination of solution structures by 2D NMR. A growing interest in peptide mimetics stimulated much interest in reverse turn mimics, nonpeptide antagonists of peptide hormones, and amide bond isosteres. Increased use of unusual amino acids created strong interest in approaches to asymmetric syntheses of amino acids and methodological improvements in peptide synthesis as well as recent advances in purification and characterization methods. A session on mechanism of action featured reviews of the second messenger role of inositol phosphate and genetic engineering of the insulin receptor as well as signal sequences which target both the export and specific transport of peptides to the nuclear compartment. Protein engineering both highlighted efforts to generate de novo structures as well as modification of known structures. The exciting developments in the specific interactions of peptides with nucleic acids in regulation of expression was the focus of another session. Structure-activity studies have long been a dominant interest of this community and presentations on the details of inhibition of thermolysin as well as new inhibitors of various peptides and proteins of biological interest such as vasopressin, bradykinin, parathyroid hormone, thrombin, and renin only served to emphasize the rapid progress being made. Four sessions were reserved to emphasize biological areas of enhanced activity. Antigen presentation, epitope definition and synthetic vaccines were well represented by

the immunology program. The growth factor/oncogene area was discussed with emphasis on TGF, *ras* oncogene proteins, EGF, and IGF. Neurochemistry focused on blood-brain barrier penetration by peptides, modulation by neuropeptides, new psychotomimetic peptides, satiety and precursor processing in the CNS. A final session emphasized cell-type specific adhesion, new developments in a potent immunosuppressive peptide, peptide inhibitors of viral enzymes and proteoglycan structure.

It is indeed appropriate that this year's Pierce Award was bestowed on a scientist whose career has exemplified the synergy resulting from the combination of a clear understanding of an important biological problem with the chemical expertise to characterize the structure of the relevant biologically active peptides. Professor Choh Hao Li characteristically chose to present yet another chapter in his lifetime treatise on molecular endocrinology by describing the characterization of novel gonadal peptides involved in endocrine regulation. A pioneer at the interface between peptide chemistry and relevant biology, Professor Li has served as both mentor and inspiration to the current generation of peptide scientists.

As the Chairman, it is my pleasure to acknowledge the contributions of those groups and individuals who contributed both physically as well as financially to the successful meeting we all enjoyed. Both the Planning Committee and the Program Committee were instrumental in suggestions and recruitment for the program. The Department of Pharmacology at Washington University School of Medicine, headed by Professor Philip Needleman, with Ms. Valorie Hambley as departmental administrator, were supportive in many substantive ways. The professional assistance of the St. Louis Scene was crucial in the organizational details of the meeting and our thanks to Ms. Peggy Schweig, Ms. Nell Lockhart, Ms. Pat Wyman, Ms. Lucy Tucker, and Ms. Margaret Craig for their professionalism and dedication to quality. Ms. Anne Dillon contributed her creative talents to the design of the logo and other graphics. Ms. Tootie Williams is the director of conference planning at Washington University and assisted at many stages of the meeting.

There is always another unsung group who sacrifices to make a meeting like this a success. Those are the members of the Chairman's research group who are alternatively ignored and then pressed into service with projectors, video equipment, and door monitoring. To the following individuals go my heartfelt thanks for their efforts: Drs. James Dunbar, Hiroshi Iijima, Tom Leplawy, Dorica Mayer, Chris Naylor, and Anne Richards. In addition, our publisher, Dr. Elizabeth Schram, has also contributed by her efforts to bring this book to press in a timely fashion and with the high publishing standards it exhibits.

Finally, there is the one individual that has truly been responsible for this meeting and the resulting proceedings. Ms. Melissa Taylor, the special project assistant for this meeting, has earned the gratitude and respect of all those with

whom she has dealt for her dedication to the success of this meeting and the quality of the publication. Hopefully, the quality of these proceedings reflects the outstanding quality of the science presented in St. Louis, which I believe was the dominant feature of the Tenth American Peptide Symposium.

Garland R. Marshall, Chairman
Tenth American Peptide Symposium

Tenth American Peptide Symposium

Washington University in St. Louis
May 23–28, 1987

Chairman

Garland R. Marshall, *Washington University School of Medicine*

Planning Committee

Irwin M. Chaiken, *National Institutes of Health*
Charles M. Deber, *Research Institute, Hospital for Sick Children, Toronto*
Lila M. Gierasch, *University of Delaware*
Ralph F. Hirschmann, *Merck Sharp and Dohme Research Laboratories*
Victor J. Hruby, *University of Arizona*
Kenneth D. Kopple, *Smith Kline and French Laboratories*
Maurice Manning, *Medical College of Ohio*
Garland R. Marshall, *Washington University School of Medicine*
Jean E. Rivier, *The Salk Institute*
Michael Rosenblatt, *Merck Sharp and Dohme Research Laboratories*
Peter W. Schiller, *Clinical Research Institute of Montreal*
Clark Smith, *The Upjohn Company*
Arno F. Spatola, *University of Louisville*
John M. Stewart, *University of Colorado Health Sciences Center*

Program Committee

Irwin M. Chaiken, *National Institutes of Health*
Roger M. Freidinger, *Merck Sharp and Dohme Research Laboratories*
Lila M. Gierasch, *University of Delaware*
William F. Huffman, *Smith Kline and French Laboratories*
Stephen B.H. Kent, *California Institute of Technology*
Garland R. Marshall, *Washington University School of Medicine*
James T. Sparrow, *Baylor College of Medicine*
John M. Stewart, *University of Colorado Health Sciences Center*
James P. Tam, *The Rockefeller University*

The Tenth American Peptide Symposium greatly appreciates the support and generous financial assistance of the following organizations:

Sponsors

BACHEM Feinchemikalien AG
BACHEM Inc.
Pierce Chemical Company
Sigma Chemical Company

Donors

Abbott Laboratories
CIBA-GEIGY Corporation
G.D. Searle Company
Hoechst-Roussel Pharmaceuticals Inc.
Hoffmann-La Roche Inc.
Johnson and Johnson Biotechnology Center Inc.
Kokusan Chemical Works Ltd.
Lilly Research Laboratories
Merck Sharp and Dohme Research Laboratories
Monsanto Company
Organon International B.V.
ORPEGEN GmbH
Peninsula Laboratories Inc.
Peptides International Inc.
Rorer Central Research
Smith Kline and French Laboratories
The Squibb Institute for Medical Research
Syntex Research
The Upjohn Company
Vega Biotechnologies Inc.

Contributors

Chemical Dynamics Corporation
Imperial Chemical Industries PLC
Ortho Pharmaceutical Corporation
Pfizer Inc.
Pharmacia Inc.
Sandoz Research Institute
Schering Corporation
Sterling-Winthrop Research Institute
UCB-Bioproducts S.A.
Warner-Lambert/Parke-Davis
Wyeth Laboratories

Abbreviations

Abbreviations used in the proceedings volume are defined below:

AII	angiotensin II
AAA	α-alkyl-α-amino acids; amino acid analysis
ABTS	2,2′-azinobis(3-ethylbenzthiazoline sulfonic acid)
ACE	angiotensin-converting enzyme
Acm	acetamidomethyl
ACP	acyl carrier protein
ACTH	corticotropin
AEC	3-amino-9-ethylcarbazol
AFP	antifreeze polypeptides
Aib	aminoisobutyric acid
AMD	actinomycin D
AMP	aminomethylpiperidine
ANF	atrial natriuretic factor
ANG II	angiotensin II
ANP	atrial natriuretic polypeptide; atrial natriuretic peptide
AP	aminopeptidase
APC	antigen presenting cell
APM	aminopeptidase M
APY	anglerfish peptide YG
ASW	artificial sea water
AVP	arginine vasopressin; arginine vasotocin
Bab	3,5-bis(2-aminoethyl)benzoic acid
Bal	β-alanine
BGH	bovine growth hormone
BHAR	benzhydrylamine resin
BHK	baby hamster kidney
BK	bradykinin
BnPeOH	2,2-[bis(4-nitrophenyl)]-ethanol
Boc	butyloxycarbonyl
BOP	benzotriazolyl-oxy-tris-(dimethylamino)-phosphonium hexafluorophosphate
BPA	benzylphenoxyacetamidomethyl
Bpoc	biphenylylpropyloxycarbonyl
BSA	bovine serum albumin
BTD	bicyclic β-turn dipeptide
Bzl	benzyl
Cbz	carbobenzoxy; benzyloxycarbonyl
CCD	countercurrent distribution
CCK	cholecystokinin
CD	circular dichroism
CPG	controlled pore glass
CPMAS	cross-polarization/magic angle spinning
CRF	corticotropin releasing factor
CTMS	chlorotrimethylsilane
DBU	1,8-diazobicyclo[5,4,0]-undec-7-ene
DCC	dicyclohexylcarbodiimide
DCCI	dicyclohexylcarbodiimide
DCM	dichloromethane
DDQ	dichlorodicyanoquinone
Deg	diethylglycine
DEPE	dielaidoylphosphatidylethanolamine
DHP	dihydroxypropyl
DIBAL	diisobutyl aluminum hydride
DIC	diisopropylcarbodiimide
DIEA	diisopropylethylamine
DKP	diketopiperazine
DLPS	dilauroylphosphatidylserine
DMAP	dimethylaminopyridine
DMBHA	dimethoxybenzhydryl amine
DMF	dimethylformamide
Dmp	dimethylphosphinyl
DMPC	dimyristoylphosphatidylcholine
DMS	dimethyl sulfide

DMSO	dimethyl sulfoxide
DNP	dinitrophenyl
DOPC	dioleoyl-*sn*-glycero-phosphocholine
DOPE	dioleoylphosphatidylethanol-amine
DPCDI	diisopropylcarbodiimide
DPPA	diphenylphosphorylazide
DPPC	dipalmitoylphosphatidyl-choline
Dtc	5,5-dimethylthiazolidine-4-carboxylic acid
Dts	dithiasuccinoyl
DTT	dithiothreitol
EA	ergotamine
EDAC	1-(3-dimethylaminopropyl)-3-ethylcarbodiimide hydro-chloride
EDTA	ethylenediaminetetraacetic acid
EGF	epidermal growth factor
ELISA	enzyme-linked immuno-sorbent assay
EP	endorphin
ER	endoplasmic reticulum
ESR	electron spin resonance
FABMS	fast atom bombardment mass spectrometry
FID	flame ionization detector
Fmoc	fluorenylmethoxycarbonyl
FSH	follicle stimulating hormone; follitropin
FTIR	Fourier transform infrared
GC	gas chromatography
GDA	glutaraldehyde
GEMSA	guanidino-ethylmercapto-succinic acid
GH	growth hormone
GLP	glucagonlike peptide
GnRH	gonadotropin releasing hormone
GPI	guinea pig ileum
GRF	growth hormone releasing factor
GRP	gonadotropin releasing-peptide
hBP	human serum binding protein
hCG	human chorionic gonado-tropin
hCGRP	human calcitonin gene-related peptide
HDL	high density lipoprotein
HF	hydrogen fluoride
HFBA	heptafluorobutyric acid
hF-GRP	human follicular gonado-tropin releasing peptide
HGH	human growth hormone
Hip	hydroxyisovalerylpropionic acid
HMP	hydroxymethylphenoxyacetic acid
HNP	human neutrophil peptide
HOBT	hydroxybenzotriazole
HODhbt	hydroxyoxodihydrobenzo-triazine
HOObt	hydroxyoxodihydrobenzo-triazine
HOSu	N-hydroxysuccinimide
HPLC	high pressure liquid chromatography
Hpp	3-(4-hydroxyphenyl)-propionyl
HSV	herpes simplex
HTH	hypertrehalosemic hormone
Ia	class II major histo-compatibility complex
IB	inhibin
IEC	ion-exchange chromato-graphy
IGF	insulinlike growth factor
IgG	immunoglobulin
IL	interleukin
IR	infrared; insulin receptor
KLH	keyhole limpet hemocyanin
LCAT	lecithin cholesterol acyl transferase
LEC	ligand-exchange chromato-graphy
LH	luteinizing hormone; lutropin
LHRH	luteinizing hormone releasing hormone
LPH	lipotropin
LVP	lysine-8-vasopressin

MAb	monoclonal antibody
MAP	membrane anchored protein; mean arterial pressure
Mbh	methoxybenzhydryl
MBHA	methylbenzhydrylamine
MBP	myelin basic protein
MBS	*m*-maleimidobenzoyl-*N*-hydroxysuccinimide ester
MCH	melanin concentrating hormone
MCPBA	*m*-chloroperbenzoic acid
MD	molecular dynamics
MHC	major histocompatibility complex
MNE	magnetic nonequivalence
MS	mass spectrometry
MSH	melanocyte stimulating hormone; melanotropin
Msob	methylsulfinylbenzyl
Mtr	methoxytrimethylphenyl-sulphonyl
MuLV	murine leukemia virus
MVD	mouse vas deferens
NBS	*N*-bromosuccinimide
NK	neurokinin
NMM	*N*-methylmorpholine
NMP	*N*-methylpyrrolidinone
NMT	*N*-myristoyl transferase
NOE	nuclear Overhauser effect
NP	neutrophil peptide; neurophysin
NPY	neuropeptide Y
OPA	*o*-phthaldialdehyde
OPA-ME	*o*-phthaldialdehyde-2-mercapto ethanol
OT	oxytocin
PAF	*p*-aminophenylalanine
PAGE	polyacrylamide gel electrophoresis
PAM	phenylacetamidomethyl
Pas	6,6-pentamethylene-2-aminosuberic acid
PBS	phosphate buffered saline
PCP	phencyclidine
PFP	pentafluoropropionyl
PG	proteoglycan
PGF	proteoglycan growth factor
PGPR	plant growth-promoting rhizobacteria
PhA	phenoxyacetal
PHA	phytohemagglutinin
PHBT	polymeric hydroxybenzotriazole
Phi	4-iodophenylalanine
PLP	poly-L-proline
Pmp	3,3-pentamethylene-3-mercaptopropionic acid
PP	pancreatic polypeptide
PPA	*n*-propylphosphoric anhydride
PPE	porcine pancreatic elastase
PSA	preformed symmetrical anhydride
PTH	phenylthiohydantoin; parathyroid hormone
PTK	protein tyrosine kinase
PVDF	polyvinylidene fluoride
PYY	peptide YY
RIA	radioimmunoassay
RNase	ribonuclease
ROE	rotating frame nuclear Overhauser effect
RPHPLC	reversed-phase high pressure liquid chromatography
RSV	respiratory syncytial virus
SA	symmetrical anhydrides
SAR	structure-activity relations
Sar	sarcosyl; sarcosine
SCP	small cardioactive peptide
SDC	sample displacement chromatography
SDS	sodium dodecyl sulfate
SFGF	Shope fibroma growth factor
SGPA	*Streptomyces griseus* protease A
SH	sulfhydryl
SMPS	simultaneous multiple peptide synthesis
SP	substance P
SPPS	solid phase peptide synthesis
SRP	signal recognition particle
SV	simian virus
TASP	template-assembled synthetic proteins

TBDMSCl	*tert*-butyldimethylsilyl chloride
TEA	triethylamine
TEAP	triethylamine phosphate
TFA	trifluoroacetic acid
TFE	trifluoroethanol
TFMSA	trifluoromethanesulfonic acid
TGF	transforming growth factor
THF	tetrahydrofuran
THTP	tetrahydrothiophene
TLC	thin layer chromatography
TM	transmembrane
TMSOTf	trimethylsilyl trifluoromethanesulfonate
TRNOE	transferred nuclear Overhauser effect
Tris	tris(hydroxymethyl)-aminomethane
UV	ultraviolet
VCD	vibrational circular dichroism
VP	vasopressin
WSCI	water soluble carbodiimide

Contents

Session II: Peptide mimetics

Session III: Analytic and synthetic methods

Session IV: Mechanism of action

Session V: Protein design/engineering

Session VI: Nucleic acid/peptide interactions

Session VII: Structure-activity relations

Session VIII: Immunology

Session IX: Growth factors/oncogenes

Session X: Neurochemistry

Session XI: New biological areas

Sixth Alan E. Pierce Award Lecture

Professor Choh Hao Li

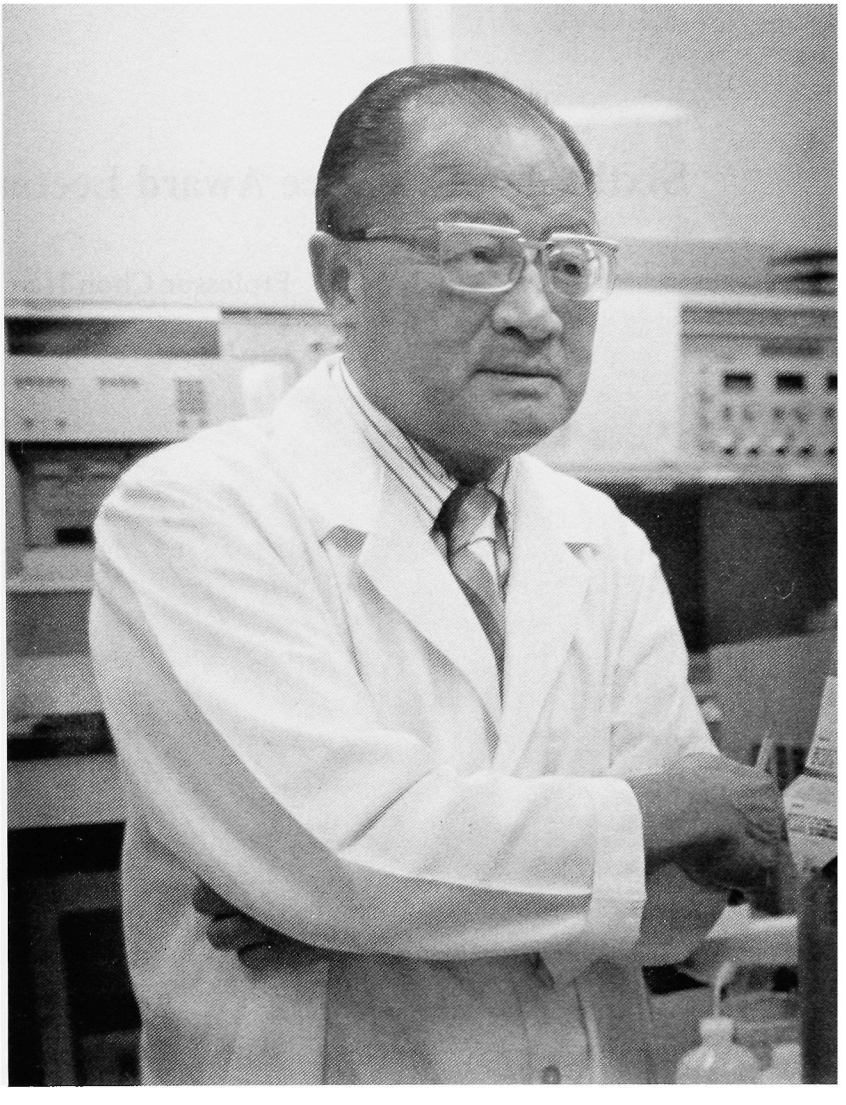

Professor Choh Hao Li

Recipient of the Sixth Alan E. Pierce Award

Naturally occurring active peptides from anterior pituitary and gonads

Choh Hao Li*
Laboratory of Molecular Endocrinology, University of California, San Francisco, CA 94143-0642, U.S.A.

Let us define that a molecule consisting of 90 amino acids is a peptide. Bovine ribonuclease A is not a peptide, as it has 124 amino acids, but it may be called a small protein or polypeptide. Ovine β-lipotropin consists of 91 amino acids and is a peptide. For our discussion, molecules are classified as peptides with 90 amino acids, polypeptides or small proteins with 90–200 amino acids, and proteins with over 200 amino acids. Hormones of the anterior pituitary are peptides [corticotropin (ACTH), α-melanotropin (α-MSH), β-MSH, β-lipotropin (β-LPH), γ-LPH, β-endorphin (β-EP)]; small proteins (growth hormone, prolactin); and glycoproteins [lutropin (LH), follitropin (FSH)].

Corticotropin

ACTH has been isolated and sequenced from porcine, ovine, bovine, human, whale, turkey, ostrich, and dogfish pituitary glands; however, the primary structure of ACTH from rat, mouse, and amphibian *Xenopus laevis* was deduced from the nucleotide sequence of cloned DNA complementary to mRNA. Fig. 1 presents the amino acid sequence of ACTH from various species. They all consist of 39 amino acids with an identical NH_2-terminal dodecapeptide, except that the amphibian has Ala as the NH_2-terminal residue.

A segment of human ACTH (α_h-ACTH) has been isolated, characterized, and synthesized [1]. This segment was identified as α_h-ACTH-(7–38). It has no intrinsic steroidogenic activity, but is capable of inhibiting the ACTH action on cAMP synthesis and corticosterone production in vitro and in vivo [2]. In rat adrenal capsular cells, α_h-ACTH-(7–38) antagonized ACTH-induced aldo-

* It is indeed an honor to be the recipient of the Sixth Alan E. Pierce Award. I would like to express my appreciation to the Planning Committee of the American Peptide Symposium and to thank our Chairman, Professor Garland R. Marshall, for the invitation to deliver the Pierce Award Lecture. For nearly 40 years, it has been my good fortune to be associated with a group of talented and able investigators in peptide chemistry. Without their contributions, this honor would never have been given to me.

	5								10
Human, Whale:	H-Ser-	Tyr-	Ser-	Met-	Glu-	His-	Phe-	Arg-	Trp-	Gly-
Turkey:										
Ostrich:										
Dogfish:										
Porcine:										
Ovine:										
Bovine:										
Amphibian:	H-Ala									
Mouse, Rat:										

	15								20
Human, Whale:	Lys-	Pro-	Val-	Gly-	Lys-	Lys-	Arg-	Arg-	Pro-	Val-
Turkey:					Arg-	Arg-	Lys			Ile
Ostrich:					Arg					
Dogfish:				Met	Arg					
Porcine:										
Ovine:										
Bovine:										
Amphibian:					Arg					Ile
Mouse, Rat:										

	25								30
Human, Whale:	Lys-	Val-	Tyr-	Pro-	Asn-	Gly-	Ala-	Glu-	Asp-	Glu-
Turkey:						Ser-	Val			
Ostrich:						Val-	Gln-	Glu		
Dogfish:					Ser-	Phe				
Porcine:										
Ovine:					Asp					
Bovine:										
Amphibian:							Val		Glu	
Mouse, Rat:						Val			Asn	

	35								39
Human, Whale:	Ser-	Ala-	Glu-	Ala-	Phe-	Pro-	Leu-	Glu-	Phe-	OH
Turkey:	Glu-	Gln-	Ala-	Ser-	Tyr		Val			
Ostrich:	Thr-	Ser								
Dogfish:				Asn-	Met-	Gly			Leu	
Porcine:	Leu									
Ovine:		Gln								
Bovine:		Gln								
Amphibian:				Ser-	Tyr		Met		Leu	
Mouse, Rat:										

Fig. 1. Primary structures of ACTH from various species.

sterone production [3]. Lypolysis induced by ACTH in isolated rabbit fat cells is also inhibited by the segment [4]. Thus, α_h-ACTH-(7–38) was designated corticotropin-inhibiting peptide (CIP).

β-Endorphin

β-EP has been isolated and sequenced from pituitary glands of various species including human, camel, bovine, ovine, porcine, equine, turkey, and ostrich. They all consist of 31 amino acids, and their primary structures (see Fig. 2) are highly conserved in evolution [5]. Met-enkephalin (Met-EK) is the NH-terminal segment of β-EP. The COOH-terminal residue is glutamine except in human β-EP.

A segment of β-EP was isolated and identified from pig [6], rat [7], and equine [8] pituitary glands and shown to be β-EP-(1–27). It was also found in rat [7] and bovine [9] brains and ectopic lung cancers [10]. In the mouse tail-flick assay, synthetic β_h-EP-(1–27) [11] inhibits competitively β_h-EP-induced analgesia [12, 13]. When compared with naloxone, the segment is at least 4 times more potent in antagonizing analgesia.

Intracerebroventricular (ICV) injection of β_h-EP-(1–27) in rats, while without cardiovascular effects of its own, significantly antagonized the bradycardic effects of the parent β-EP peptide [14]. Fifteen min following β-EP plus β-EP-(1–27), the heart rate was 380 ± 50 beats/min, whereas rats treated with β-EP alone were significantly bradycardic (270 ± 20 beats/min).

ICV injection of β-EP-(1–27) at a dose of 60μg caused little release of Met-EK from the spinal cord. This pretreatment of β-EP-(1–27) significantly inhibited

	5									10										
Human:	H-Tyr-	Gly-	Gly-	Phe-	Met-	Thr-	Ser-	Glu-	Lys-	Ser-										
Horse:							Ser													
Ostrich:							Ser				Arg-	Gly-								
Turkey:											His									

	15									20										
Human:	Gln-	Thr-	Pro-	Leu-	Val-	Thr-	Leu-	Phe-	Lys-	Asn-										
Horse:																				
Ostrich:	Arg-	Ala																		
Turkey:	Met			Leu																

	25									30										
Human:	Ala-	Ile-	Ile-	Lys-	Asn-	Ala-	Tyr-	Lys-	Lys-	Gly-	Glu-	OH								
Horse:								His			Gln									
Ostrich:		Val		Ser							Gln									
Turkey:		Val		Ser							Gln									
Porcine:		Val						His			Gln									
Camel, Bovine, Ovine, Whale:		Ile						His			Gln									
Rat:								Val-His			Gln									
Mouse:								His			Gln									

Fig. 2. Primary structures of β-EP from various species.

the release of Met-EK induced by subsequent ICV injection of 15 μg β-EP [15].

β-EP has been shown to have an effect on body temperature. In rats and mice, high doses of β-EP cause hypothermia and low doses produce hyperthermia. ICV injection of β-EP (0.25–4 μg) and β-EP-(1–27) (0.61 to 10 μg) in mice maintained at 10°C caused a dose-related hypothermia. The duration of hypothermia induced by β-EP-(1–27) was shorter than that induced by β-EP. The hypothermia induced by 2 μg of β-EP was antagonized by 5μg of β-EP-(1–27) [16].

β-EP-(1–27) has been shown to inhibit β-EP-induced growth hormone release but it does not affect β-EP-induced prolactin release in rats [17].

The remaining portion of the lecture will be devoted to recent studies on biologically active peptides from human gonads.

Gonadotropin-Releasing Peptide from Human Follicular Fluid

There are some indications for the occurrence of biologically active peptides in the follicular fluid and seminal plasma (for a review, see Ref. 18): FSH receptor binding inhibitor (seminal plasma), oocyte maturation inhibitor (follicular fluid), and LHRH-like factor (testes). None of these peptides have been purified and characterized.

A gonadotropin-releasing peptide has recently been isolated from human follicular fluid [19]. Its amino acid composition and sequence are completely different from the hypothalamic lutropin-releasing hormone. It is designated human follicular gonadotropin-releasing peptide and abbreviated as hF-GRP. The primary structure of this peptide (H-Thr-Asp-Thr-Ser-His-His-Asp-Gln-Asp-His-Pro-Thr-Phe-Asn-OH) has been confirmed by chemical synthesis. In the mouse pituitary incubation assay, the ED_{50} value for follitropin or lutropin release is estimated to be 1.2–1.6 nM per tube per ml. K. Ramasharma in his latest experiments showed that hF-GRP is active in releasing both FSH and LH in cultured rat pituitary cells (see Fig. 3). In comparison with the hypothalamic LHRH, hF-GRP is considerably less active in releasing gonadotropins in both the mouse pituitary incubation assay and cultured rat pituitary cell assay.

In computer homology search of protein sequences, hF-GRP is found in residues 11–24 of the primary structure of human α_1-antitrypsin [20, 21] as shown in Fig. 4. hF-GRP-(10–14) was also found in the amino acid sequence of bovine papilloma virus [22]. In addition, hF-GRP-(1–3),-(6–8) and -(10–12) are tripeptide sequences in the baboon α_1-antitrypsin structure [23]. Since there is only a single lysine in residue positions 10 and 25 of both human [20, 21] and baboon α_1-antitrypsin [23] sequences, it is possible that they are precursors for hF-GRP; however, it is generally accepted that cryptic domains of precursors for the formation of new peptide hormones are flanked by pairs of basic amino acids

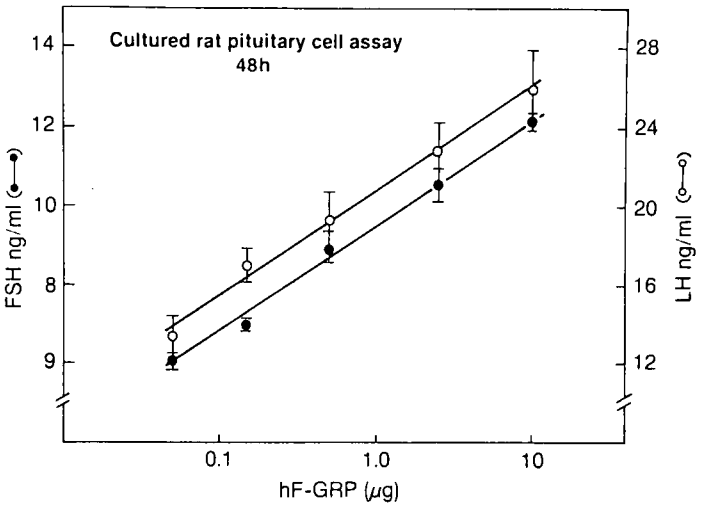

Fig. 3. FSH and LH release from cultured rat pituitary cells stimulated with hF-GRP.

[24–26]. It may be noted that α_1-antitrypsin does not exhibit gonadotropin-releasing activity [19].

α-Inhibin from Human Seminal Fluid

Inhibin (IB) is either a protein or peptide of gonadal origin that is involved in the regulation of pituitary FSH secretion in both sexes. Miyamoto et al. [27] were the first to isolate and characterize inhibin with a molecular weight of 32 kDa from porcine follicle fluid. Two groups of investigators [28, 29] subsequently confirmed the findings of Miyamoto et al. [27]. For a recent review on the chemistry and biology of inhibins from porcine, bovine, and human follicular fluids, see Ref. 30.

	6 10 15 20 25
α_1-Antitrypsin: (human)	-Asp-Ala-Ala-Gln-Lys-Thr-Asp-Thr-Ser-His-His-Asp-Gln-Asp-His-Pro-Thr-Phe-Asn-Lys-Ile-
α_1-Antitrypsin: (baboon)	-Asp-Ala-Ala-Gln-Lys-Thr-Asp-Thr-Pro-Pro-His-Asp-Gln-Asn-His-Pro-Thr-Leu-Asp-Lys-Ile-
Papilloma virus: (bovine)	-Glu-Val-Ser-Arg-Gly-Gln-Pro-Leu-Gly-Gly-Thr-Val-Thr-Gly-His-Pro-Thr-Phe-Asn-Ala-Leu-
	5 10
hF-GRP:	H-Thr-Asp-Thr-Ser-His-His-Asp-Gln-Asp-His-Pro-Thr-Phe-Asn-OH

Fig. 4. Comparison of hF-GRP primary structure with α-antitrypsin (human and baboon) and bovine papilloma virus amino acid sequences.

Ramasharma et al. [31] reported the isolation and structure of a peptide with IB-like activity from human seminal plasma. It was named IB-like peptide (ILP), and its structure is shown in Fig. 5. Antisera raised in rabbits to synthetic ILP [32] afford a highly synthetic [Tyr^4]-ILP analog as primary radioiodinated ligand [33].

Using the radioimmunoassay (RIA) for ILP, two new peptides structurally related to ILP have been isolated and characterized from human seminal plasma [34]. One consists of 52 amino acids and the other 92 amino acids. They are designated as α-IB-52 and α-IB-92. Sequence analyses show that the NH_2-terminal 31 amino acids of α-IB-52 are identical to the structure of ILP and the COOH-terminal 52 amino acids of α-IB-92 are identical to the structure of α-IB-52 (see Fig. 6). Bioassay data in mouse pituitaries in vitro show that α-IB-52 is 3.4 times and α-IB-92 over 40 times more active than ILP peptide in suppressing follitropin release.

Blake et al. [35] described the synthesis of α-IB-92 using the thiocarboxyl segment strategy. A new synthesis of α-IB-92 has now been devised by Donald Yamashiro with improved yield using 2,2′-dipyridyl disulfide as activator. Thiocarboxyl peptides were synthesized by the solid phase method on 4-[α-(Boc-Gly-*S*)benzyl]phenoxyacetamidomethyl-resin. The segments α-IB-92-(1–34) SH (I), Msc-α-IB-92-(35–65) SH (II), and Msc-α-IB-92-(66–92) OH (III) were prepared in good yields with use of crystalline symmetrical anhydrides in double coupling protocols. Segments I, II, and III were used in a 3-segment synthesis of α-IB-92. For comparison, all stepwise synthesis of α-IB-92 was also carried out using triple coupling protocol. The overall yield of α-IB-92 in the new 3-segment synthesis based on starting Boc-Gly-*S*-(BPA)-resin used for segment II was about 8%. It gave better yield than stepwise synthesis (4%) and the previous synthesis (0.8%). RIA and receptor-binding assay, which were performed by Ramasharma, showed that chemically synthesized products are equivalent to the natural α-IB-92.

RIA for α-IB-92 has been developed and used to estimate the amounts of immunoreactive material in human pituitary, hypothalamus and serum (36):

```
                    5                   10
H-His-Asn-Lys-Gln-Glu-Gly-Arg-Asp-His-Asp-

                15                  20
Lys-Ser-Lys-Gly-His-Phe-His-Arg-Val-Val-

                25                  31
Ile-His-His-Lys-Gly-Gly-Lys-Ala-His-Arg-Gly-OH
```

Fig. 5. Amino acid sequence of ILP.

```
                    5                   10                  15
H-Thr-Tyr-His-Val-Asp-Ala-Asn-Asp-His-Asp-Gln-Ser-Arg-Lys-Ser-

                   20                  25                  30
Gln-Gln-Tyr-Asp-Leu-Asn-Ala-Leu-His-Lys-Thr-Thr-Lys-Ser-Gln-

                   35                  40                  45
Arg-His-Leu-Gly-Gly-Ser-Gln-Gln-Leu-Leu-His-Asn-Lys-Gln-Glu-

                   50                  55                  60
Gly-Arg-Asp-His-Asp-Lys-Ser-Lys-Gly-His-Phe-His-Arg-Val-Val-

                   65                  70                  75
Ile-His-His-Lys-Gly-Gly-Lys-Ala-His-Arg-Gly-Thr-Gln-Asn-Pro-

                   80                  85                  90      92
Ser-Gln-Asp-Gln-Gly-Asn-Ser-Pro-Ser-Gly-Lys-Gly-Ile-Ser-Ser-Gln-Tyr-OH
```

Fig. 6. Amino acid sequence of α-IB-92. Residues 41–92 constitute α-IB-52 and residues 41–71 constitute ILP.

pituitary, 70 ng/g; hypothalamus, 13 ng/g; and serum, 7 ng/ml. In addition, concentrations of α-IB-92 in gonadal fluids or extracts from various species have also been estimated (K. Ramasharma, unpublished data). α-Inhibins are shown to be located in the Leydig cells of rodent testis [37].

Concluding Remarks

Feedback effects of gonadal steroids as well as hypothalamic LHRH on secretion of gonadotropins from the pituitary gland have been firmly established. After the observations for the existence of inhibin many years ago [38–40], inhibins have been isolated and characterized from human seminal plasma and porcine or bovine follicular fluid [30]. In addition, a simple peptide with 14 amino acids has now been discovered [19] in human follicle fluid with gonadotropin-releasing activity and named gonadotropin-releasing peptide (GRP). Fig. 7 presents the current knowledge on the control of FSH/LH release from the pituitary.

Naturally occurring segments of ACTH and β-EP are shown to inhibit the action of the parent hormone. This is also true for HCG [41] and ovine LH [42]. Thus, a new concept in endocrinology is emerging: A segment in the amino acid sequence of a peptide or protein hormone is an inhibitor of the hormone. When designing the hormone, Nature generally built in a system of checks and balances that allows hormonal activities to be closely regulated by opposing stimulatory and inhibitory influence. This may be referred to as the 'Ying-Yang concept of the peptide and protein hormones.'

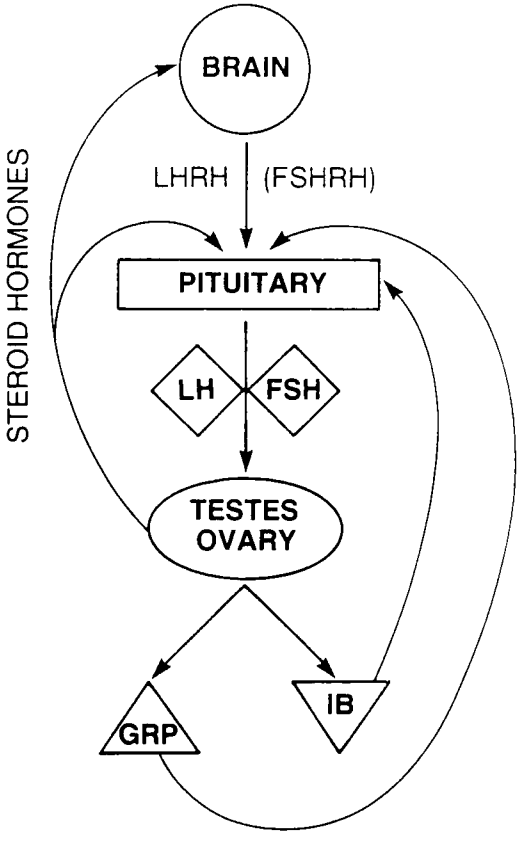

Fig. 7. Diagram for the control of FSH/LH secretion from the pituitary.

Acknowledgements

I thank Drs. D. Yamashiro and K. Ramasharma for their unpublished data. The work of the author and his collaborators was supported in part by grants from the U.S. Public Health Service (GM-2907, AM-6097, DA-03434, DA-04161) and the Hormone Research Foundation.

References

1. Li, C.H., Chung, D., Yamashiro, D. and Lee, C.Y., Proc. Natl. Acad. Sci. U.S.A., 75 (1978) 4306.
2. Lee, C.Y., McPherson, M., Licko, V. and Ramachandran, J., Arch. Biochem. Biophys., 201 (1980) 411.

3. Li, C.H., Ng, T.B. and Cheng, C.H.K., Int. J. Pept. Protein Res., 19(1982)361.
4. Ng, T.B. and Li, C.H., Int. J. Pept. Protein Res., 19(1982)562.
5. Li, C.H., Cell, 31(1982)504.
6. Smyth, D.G., Snell, C.R. and Massey, D.E., Biochem. J., 175(1978)261.
7. Zakarian, S. and Smyth, D.G., Proc. Natl. Acad. Sci. U.S.A., 76(1979)5972.
8. Ng, T.B., Chung, D. and Li, C.H., Int. J. Pept. Protein Res., 18(1981)443.
9. Ng, T.B., Chung, D. and Li, C.H., Int. J. Pept. Protein Res., 19(1982)343.
10. Suda, T., Tozawa, F., Yamaguchi, H., Shibasaki, T., Demura, H. and Shizume, K., J. Clin. Endocr. Metab., 54(1982)167.
11. Zaoral, M., Yamashiro, D., Hammonds, R.G., Jr. and Li, C.H., Int. J. Pept. Protein Res., 17(1981)292.
12. Hammonds, R.G., Jr., Nicolas, P. and Li, C.H., Proc. Natl. Acad. Sci. U.S.A., 81(1984)1398.
13. Nicolas, P. and Li, C.H., Biochem. Biophys. Res. Commun., 127(1985)649.
14. Kenner, J.R., Glatt, C.E., Li, C.H. and Holaday, J.W., Abstract No. 205, 5th Intl. Washington Spring Symposium, May 23–31, 1985.
15. Tseng, L-F. and Li, C.H., Int. J. Pept. Protein Res., 17(1986)394.
16. Suh, H.H., Tseng, L-F. and Li, C.H., Peptides, 8(1987)123.
17. Collado-Escobar, D., Rovati, L.C., Ganzetti, I., Cocchi, D., Panerai, A.E. and Li, C.H., Eur. J. Pharmacol., 129(1986)385.
18. Sairam, M.R. and Atkinson, L.E., In Sairam, M.R. and Atkinson, L.E. (Eds.) Gonadal Protein and Peptides and Their Biological Significance, World Sci. Publ. Co., Singapore, 1984, p. 3.
19. Li, C.H., Ramasharma, K., Yamashiro, D. and Chung, D., Proc. Natl. Acad. Sci. U.S.A., 84(1987)959.
20. Carrell, R.W., Jeppsson, J.-O., Laurell, C.-B., Brennan, S.O., Owen, M.C., Vaughan, L. and Boswell, D.R., Nature, 298(1982)329.
21. Bollen, A., Herzog, A., Cravador, A., Herion, P., Chuchana, P., Vander Straten, A., Loriau, R., Jacobs, P. and Van Elsen, A., DNA, 2(1983)255.
22. Chen, E.Y., Howley, P.M., Levinson, A.D. and Seeburg, P.M., Nature, 298(1982)529.
23. Kurachi, K., Chandra, T., Degen, S.J.F., White, T.T., Marchioro, T.L., Woo, S.L.C. and Davie, E.W., Proc. Natl. Acad. Sci. U.S.A., 78(1981)6826.
24. Steiner, D.F., Quin, P.S., Chan, S.J., March, J. and Stager, H., Ann. N.Y. Acad. Sci., 343(1980)1.
25. Chrétien, M. and Seidah, N.G., Int. J. Pept. Protein Res., 23(1984)335.
26. Douglas, J., Civelli, O. and Herbert, E., Ann. Rev. Biochem., 53(1984)665.
27. Miyamoto, K., Hasegawa, Y., Fukuda, M., Nomura, M., Igarashi, M., Kangawa, K. and Matsuo, H., Biochem. Biophys. Res. Commun., 239(1985)396.
28. Ling, N., Ying, S.Y., Ueno, N., Esch, F., Denoroy, L. and Guillemin, R., Proc. Natl. Acad. Sci. U.S.A., 82(1985)7217.
29. Rivier, J., Spiess, J., McClintook, R., Vaughan, J. and Vale, W., Biochem. Biophys. Res. Commun., 133(1985)120.
30. Li, C.H. and Ramasharma, K., Ann. Rev. Pharmacol. Toxicol., 27(1987)1.
31. Ramasharma, K., Sairam, M.R., Seidah, N.G., Chrétien, M., Manjunath, P., Schiller, P.W., Yamashiro, D. and Li, C.H., Science, 223(1984)1199.
32. Yamashiro, D., Li, C.H., Ramasharma, K. and Sairam, M.R., Proc. Natl. Acad. Sci. U.S.A., 81(1984)5399.
33. Hammonds, R.G., Jr., Li, C.H., Yamashiro, D., Cabrera, C.M. and Westphal, M., J. Immunoassay, 6(1985)363.
34. Li, C.H., Hammonds, R.G., Jr., Ramasharma, K. and Chung, D., Proc. Natl. Acad. Sci. U.S.A., 82(1985)4041.

35. Blake, J., Yamashiro, D., Ramasharma, K. and Li, C.H., Int. J. Pept. Protein Res., 28 (1986) 468.
36. Ramasharma, K. and Li, C.H., Proc. Natl. Acad. Sci. U.S.A., 83 (1986) 3484.
37. Lau, Y-F. and Li, C.H., Biochem. Biophys. Res. Commun., (1987) in press.
38. Mottram, J.C. and Cramer, W., J. Exp. Physiol., 13 (1923) 209.
39. Martins, T. and Rocha, A., Endocrinology, 15 (1931) 421.
40. McCullagh, D.R., Science, 76 (1932) 19.
41. Moudgal, N.R. and Li, C.H., Proc. Natl. Acad. Sci. U.S.A., 79 (1982) 2500.
42. Sairam, M.R., In Li, C.H. (Ed.) Hormonal Proteins and Peptides, Vol. II, Academic Press, New York, 1983, p. 1.

Session I
Conformation of peptides

Chair: Lila Gierasch
University of Delaware
Newark, Delaware, U.S.A.

Circular dichroism measurement of peptide helix unfolding

Kevin R. Shoemaker[a], Robert Fairman[a], Eunice J. York[b], John M. Stewart[b] and Robert L. Baldwin[a]

[a]*Department of Biochemistry, Stanford University School of Medicine, Stanford, CA 94305, U.S.A.*

[b]*Department of Biochemistry, University of Colorado School of Medicine, Denver, CO 80262, U.S.A.*

Introduction

α-Helix formation in a monomolecular reaction in aqueous solution is now well demonstrated for a few short peptides: the C-peptide (residues 1–13) [1, 2] and the S-peptide (residues 1–20) [3–5] of RNase A (bovine pancreatic ribonuclease A), both of which contain residues 3–13 that form a helix in RNase A, as well as chemically modified derivatives [6, 7] and chemically synthesized analogs [8] of these peptides. Some short alanine-based peptides of de novo design that contain pairs of (Glu, Lys) residues in simple, repetitive sequences also form an α-helix in aqueous solution (Marqusee and Baldwin, in preparation).

Those results focus interest on the quantitative determination of helix content and the unfolding transitions of these peptides. Circular dichroism (CD) is particularly wellsuited to the measurements of overall helix content for several reasons:

(i) It can be measured at low peptide concentration (our measurements are typically made at 0–40 μM) which is important for avoiding aggregation of helical molecules. Sedimentation equilibrium measurements [1], lack of concentration dependence for CD signal [2], and gel filtration experiments [9] all indicate that helix formation by C-peptide and its analogs is monomolecular.

(ii) The $n \rightarrow \pi^*$ band centered at 222 nm is a reliable indicator of the α-helix [11], provided that the spectrum shows a genuine minimum at 222 nm.*

(iii) The change in ellipticity for $0 \rightarrow 100\%$ helix is nearly the same for different residues and to a first approximation depends only on helix length [14]. Moreover, the relation between the CD spectrum and peptide conformation is reasonably well understood theoretically [15].

---

* CD spectra resembling that of α-helical polypeptides have been observed for small cyclic peptides possessing type I β-bends [12, 13].

We consider here the problem of obtaining a reliable CD baseline for 0% helix when guanidinium chloride (GuHCl) and/or temperature is used for unfolding. This problem has been discussed previously in the context of C-peptide and S-peptide by Brown and Klee [1] and by Filippi et al. [16, 17], respectively. Recently, helix-enhancing and -destabilizing replacements have been found for C-peptide [8, 9] and we use them here to study the unfolding behavior of strong, moderate and weak helix-formers. Data are also given for a shorter peptide (P-peptide, residues 1–8 of RNase A) that shows no observable helix formation and provides a control for the effects of GuHCl on the CD spectrum of a random-coil peptide.

The problem of how to obtain 100% helix is not discussed here, but complete helix formation by residues 3–13 can be obtained by adding S-peptide [16, 18] or analogs of S-peptide 1–15 [10] to folded S-protein, and the change in ellipticity for 0 → 100% helix for residues 3–13 has been derived from these data, subject to certain assumptions. The approach of adding trifluoroethanol (TFE) to induce complete helix formation has to be treated with caution in the C-peptide system, both because the TFE transitions are broad (almost noncooperative) and large amounts of TFE must be added [16, 17, 19], and because the C-peptide helix is stabilized by specific side-chain interactions [2, 6–9, 20] that are likely to be affected by TFE.

Results and Discussion

(a) *P-peptide as a model for a random-coil peptide*

Fig. 1A shows CD spectra from 260 to ~206 nm for P-peptide om 0.1 M NaCl at temperatures from 3.0°C to 58.9°C. A minor positive band, centered at ~215 nm, is present at low temperatures; its rotational strength decreases with increasing temperature. This band has been seen in earlier studies of random-coil model compounds [21–23], as well as C-peptide [1], S-peptide [24], and S-peptide derivatives [16, 17]. It is primarily responsible for the temperature dependence of the mean residue ellipticity at 222 nm ($[\theta]_{222}$), the wavelength used for measurement of α-helix content. The decrease in intensity of this band with temperature is also unaffected by GuHCl, as shown in Fig. 1B, which compares the plots of $[\theta]_{222}$ versus temperature in 0 M and 3 M GuHCl. Fig. 1C shows that there is little change in $[\theta]_{222}$ with GuHCl concentration at 3°C. The value in 8 M GuHCl (~+3,000 deg cm^2 dmol^{-1} at 3°C) is close to the value (+3600) reported by Filippi et al. [16] for [Pro^6, Orn^{10}]-S-peptide analog in 8 M GuHCl at 1°C. Neglecting sequence-specific effects, we conclude that P-peptide provides a good model for a random-coil peptide in 0.1 M NaCl and that the CD spectrum of P-peptide is nearly unaffected by GuHCl.

(b) *GuHCl-induced unfolding of strong, moderate and weak helix-formers*

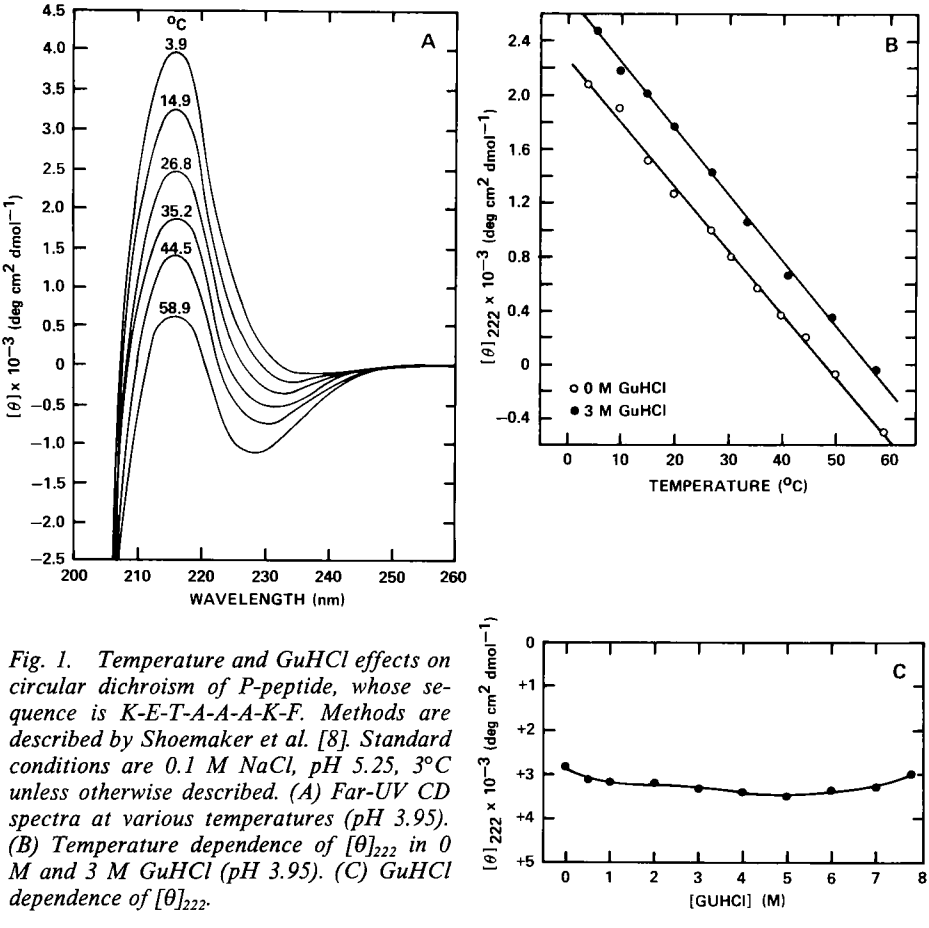

Fig. 1. Temperature and GuHCl effects on circular dichroism of P-peptide, whose sequence is K-E-T-A-A-A-K-F. Methods are described by Shoemaker et al. [8]. Standard conditions are 0.1 M NaCl, pH 5.25, 3°C unless otherwise described. (A) Far-UV CD spectra at various temperatures (pH 3.95). (B) Temperature dependence of $[\theta]_{222}$ in 0 M and 3 M GuHCl (pH 3.95). (C) GuHCl dependence of $[\theta]_{222}$.

Three analogs of C-peptide were chosen as representatives of strong (RN 44), moderate (RN 54), and weak (RN 56) helix-formers. Their sequences are given in the legend to Fig. 2. All three peptides show broad helix-coil transitions induced by GuHCl. At 3°C, complete unfolding is approached in 8 M GuHCl by all three peptides, as judged by the P-peptide control (Fig. 2A). At 70°C, the helix contents at 0 M GuHCl are considerably reduced compared to 3°C, but again the unfolding transitions are broad and complete unfolding is barely reached at 8 M GuHCl (Fig. 2B).

Fig. 3 compares spectra taken at 3°C in 0 and 8 M GuHCl for the strong helix-former RN44 (Fig. 3A) and for the weak helix-former RN56 (Fig. 3B). The spectra taken in 8 M GuHCl are similar and resemble that of P-peptide (Fig. 1), although the spectra in 0 M GuHCl are quite different.

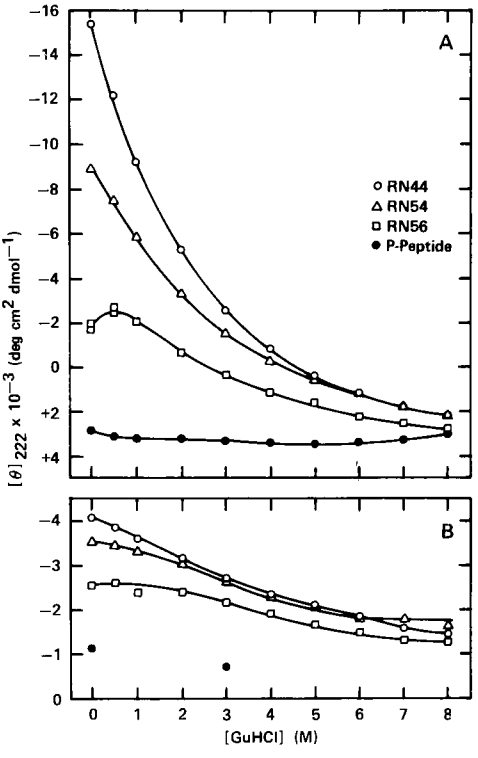

Fig. 2. Comparison of GuHCl-induced unfolding for strong (RN44), moderate (RN54), and weak (RN56) helix-formers. $[\theta]_{222}$ is measured at (A) 3°C and (B) 70°C in 0.1 M NaCl, pH 5.25. P-peptide (Fig. 1C) is used as reference in (A). In (B), the values of $[\theta]_{222}$ for complete unfolding, extrapolated from the P-peptide results (Fig. 1B), are also shown. Sequences: RN44: Succinyl-A-A-T-A-A-A-K-F-L-A-A-H-A-CONH$_2$; RN 54: RN 44 (Suc-Ala → acetyl-Ala); RN 56: RN 44 (Suc-Ala → Lys).

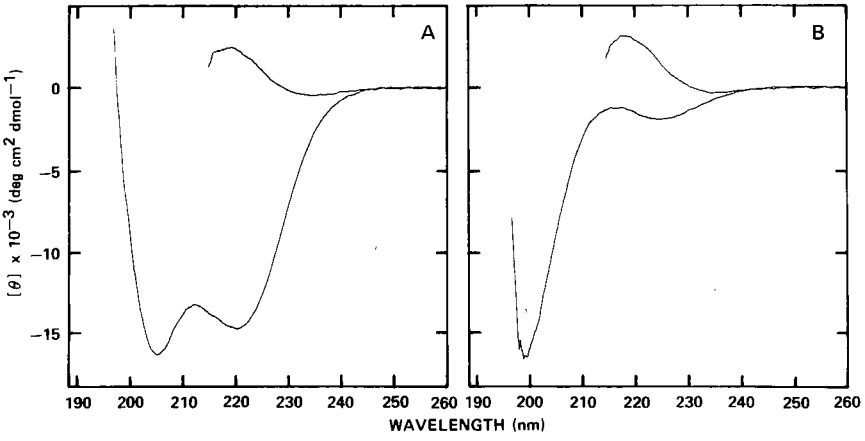

Fig. 3. Comparison of far-UV CD spectra for (A) RN 44 and (B) RN 56 in 0 M and 8 M GuHCl. Standard conditions are 0.1 M NaCl, pH 5.25, 3°C.

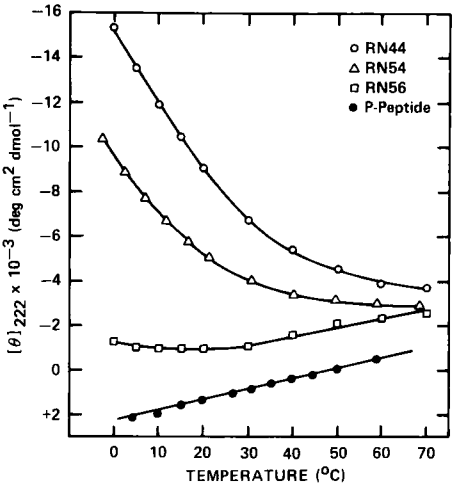

Fig. 4. Comparison of thermal unfolding for RN 44, RN 54, and RN 56, monitored by $[\theta]_{222}$. P-peptide is used as reference. Standard conditions are 0.1 M NaCl, pH 5.25, 3°C.

(c) *Thermal unfolding of strong, moderate, and weak helix-formers*

The thermal unfolding transitions of these three peptides in 0.1 M NaCl are broad (Fig. 4), although complete unfolding for all of them is approached by 70°C. It is not surprising that such short helices should show broad thermal transitions (compare the thermal unfolding curve of a 26-residue helix [25]), but we are not yet able to compare these experimental curves with theoretical ones, for two reasons. First, the enthalpy change of unfolding has not yet been measured for helix-forming peptides such as these. The transition curves from calorimetry are too broad to permit a reliable determination of ΔH (J.M. Sturtevant, personal communication). Second, these peptide helices are considerably more stable [8] than predicted using the Zimm-Bragg equation [26] with host-guest data [27], because specific intrahelical side-chain interactions help to stabilize the helix. Although the Zimm-Bragg theory has been generalized to take these side-chain interactions into account [28, 29], the extended theory has not yet been applied to the problem of predicting thermal unfolding curves.

Acknowledgements

We gratefully acknowledge the helpful discussion of Dr. Peter Kim and support from NIH Research Grant GM 31475.

References

1. Brown, J.E. and Klee, W.A., Biochemistry, 10 (1971) 470.
2. Bierzynski, A., Kim, P.S. and Baldwin, R.L., Proc. Natl. Acad. Sci. U.S.A., 79 (1982) 2470.
3. Kim, P.S., Bierzynski, A. and Baldwin, R.L., J. Mol. Biol., 162 (1982) 187.
4. Rico, M., Nieto, J.L., Santoro, J., Bermejo, F.J., Herranz, J. and Gallego, E., FEBS Lett., 162 (1983) 314.
5. Kim, P.S. and Baldwin, R.L., Nature, 307 (1984) 329.
6. Rico, M., Gallego, E., Santoro, J., Bermejo, F.J., Nieto, J.L. and Herranz, J., Biochem. Biophys. Res. Comm., 123 (1984) 757.
7. Rico, M., Santoro, J., Bermejo, F.J., Herranz, J., Nieto, J.L., Gallego, E. and Jiménez, M.A., Biopolymers, 25 (1986) 1031.
8. Shoemaker, K.R., Kim, P.S., Brems, D.N., Marqusee, S., York, E.J., Chaiken, I.M., Stewart, J.M. and Baldwin, R.L., Proc. Natl. Acad. Sci. U.S.A., 82 (1985) 2349.
9. Shoemaker, K.R., Kim, P.S., York, E.J., Stewart, J.M. and Baldwin, R.L., Nature, 326 (1987) 563.
10. Mitchinson, C. and Baldwin, R.L., Proteins, 1(1986) 23.
11. Holzwarth, G. and Doty, P., J. Am. Chem. Soc., 87 (1965) 218.
12. Bandekar, J., Evans, D.J., Krimm, S., Leach, S.J., Lee, S., McQuie, J.R., Minasian, E., Nemethy, G., Pottle, M.S., Scheraga, H.A., Stimson, E.R. and Woody, R.W., Int. J. Pep. Prot. Res., 19 (1982) 187.
13. Gierasch, L.M., Deber, C.M., Madison, V., Niu, C.-H. and Blout, E.R., Biochemistry, 20 (1981) 4730.
14. Chen, Y.-H., Yang, J.T. and Chau, K.H., Biochemistry, 13 (1974) 3350.
15. Schellman, J.A. and Becktel, W.J., Biopolymers, 22 (1983) 171.
16. Filippi, B., Borin, G., Anselmi, U. and Marchiori, F., Biopolymers, 17 (1978) 2525.
17. Filippi, B., Borin, G., Moretto, V. and Marchiori, F., Biopolymers, 17 (1978) 2545.
18. Labhardt, A.M., Biopolymers, 20 (1981) 1459.
19. Nelson, J.W. and Kallenbach, N.R., Proteins, 1 (1986) 211.
20. Shoemaker, K.R., Fairman, R., Kim, P.S., York, E.J., Stewart, J.M. and Baldwin, R.L., Cold Spring Harbor Symp. Quant. Biol., 52 (1987) in press.
21. Greenfield, N. and Fasman, G.D., Biochemistry, 8 (1969) 4108.
22. Mattice, W.L., Lo, J.-T. and Mandelkern, L., Macromolecules, 5 (1972) 729.
23. Mattice, W.L., Biopolymers, 13 (1974) 169.
24. Klee, W.A., Biochemistry, 7 (1968) 2731.
25. Zimm, B.H., Doty, P. and Iso, K., Proc. Natl. Acad. Sci. U.S.A., 45 (1959) 1601.
26. Zimm, B.H. and Bragg, J.K., J. Chem. Phys., 31 (1959) 526.
27. Sueki, M., Lee, S., Powers, S.P., Denton, J.B., Konishi, Y. and Scheraga, H.A., Macromolecules, 17 (1984) 148.
28. Vasquez, M., Pincus, M.R. and Scheraga, H.A., Biopolymers, 26 (1987) 351.
29. Vasquez, M. and Scheraga, H.A., Biopolymers (1987) in press.

Theoretical studies of protein structure

Fred E. Cohen and I.D. Kuntz
Department of Pharmaceutical Chemistry, UCSF, San Francisco, CA 94143, U.S.A.

Early experiments by Anfinsen [1] proved that an amino acid sequence contains sufficient information to determine the precise three-dimensional structure of a native globular protein. Since that time, theoreticians [2–6] and experimentalists [7, 8] have searched for constructive solutions to the chain-folding problem. In spite of the large number of protein structures known to atomic resolution and the much larger data base of protein sequences, solutions to the folding problem remain elusive.

Theoretical efforts have focused along three lines: energetic, heuristic, and statistical. Following the physically reasonable assumption that a protein folds so as to minimize the free energy of the system, many investigators [2, 3, 9, 10] have developed potential functions to describe the energy surface of a polypeptide chain. Minimum energy conformations are sought computationally. Alternatively, conformational space is probed from a starting point by integrating the equations of motion over time. Energy minimization schemes have failed to predict chain folding accurately [11, 12]. Presumably, this stems from difficulties in modeling protein-solvent interactions, the use of analytic functions to approximate the chemical potential and the compounding of these errors in the computed gradient, and because the energy surface has multiple minima which makes it nearly impossible to locate the global minimum. Efforts to overcome these problems are underway. Molecular dynamics offers many attractive features, but remains computationally limited as a technique for studying chain folding [9]. Presumably, chain folding will take place on the millisecond time scale [13]. Extreme computing resources must be expended to sample 100 nanoseconds in the life of a small protein [14].

The success of statistical or data base methods relies heavily on the ability to recognize a known structural theme in a new protein sequence. While highly homologous sequences can be recognized through a variety of methods [15–18], the significance of limited homology is much harder to evaluate. Certainly, some structures which have been proved similar by X-ray crystallography bear little or no sequence homology [5]. In principle, local homology could be used to identify structural features in a piecemeal fashion; however, several investigators have observed a five- or six-amino acid sequence adopting α-helical structure in one protein and β-structure in another [19]. Clearly, this poses great

difficulty for data base methods. In spite of these caveats, it is likely that these methods will offer significant structural information for a limited set of proteins [20]. To the extent that there is a very finite set of possible protein folds that can be easily catalogued, this approach would be increasingly useful.

Heuristic methods attempt to exploit structural inferences gained from the study of known protein structures. A large number of analyses of the topological, sequential, packing, and surface characteristics of proteins have been done [21–27]. These conclusions have been incorporated into a hierarchical condensation model. Protein class (α/α, β/β, α/β, misc) is determined [27], and secondary structure is located along the chain through statistical [25, 26, 28] or class-dependent, pattern-based [29–31] algorithms. Attention is paid to the super-secondary and tertiary restraints on a chain which follows a particular folding motif. Turn prediction accuracy is enhanced by searching for segments of chain well suited for a protein surface location which are spaced through the chain at intervals compatible with secondary structure pitch and domain diameter. α-Helices and β-strands can be more easily identified between these turns because of the restrictions imposed by protein class. Once identified, all possible juxtapositions of these secondary structures are generated using combinatorial algorithms [32–36]. Proposed structures which are inconsistent with the known chain connectivity and steric properties of the secondary structure segments are rejected. Additional structures which violate topological properties, surface-volume relationships, or experimental data are discarded.

When applied to myoglobin, 13 docking sites were identified on six of the eight helices, and 3.4×10^8 possible tertiary structures were generated which matched helix docking sites in geometries consistent with known packing constraints [33]. Of these structures, only 20 were connected and sterically reasonable [33], and two could bind a heme group between the proximal and distal histidine [34]. These two latter structures were very similar (r.m.s. deviation 0.3Å) and resembled the myoglobin X-ray structure (r.m.s. deviation 3.6Å). Subsequent studies on a number of proteins with known structures suggested that similar results could be obtained in approximating the X-ray structure; however, frequently many alternative conformations were produced which could not be distinguished from the nativelike structure on theoretical grounds.

Recently, this approach has been applied to two proteins of known sequence but unknown structure: interleukin-2 (Il-2) [37] and human growth hormone (HGH) [38]. Since the completion of these calculations, preliminary X-ray crystallographic information has become available. This provides a unique opportunity to document the successes and failures of the heuristic approach and points to key problems for future study.

Il-2 is a lymphokine which promotes T-cell growth [39, 40]. Analysis of the amino acid sequence suggested a predominance of α-helical structure, which was confirmed by circular dichroism [37]. Four helices were identified in the

human sequence A(17–31), B(64–73), C(83–97), and D(116–132) by identifying turns [31] and subsequently locating helical patterns between the turns. Ten helix docking sites were located using the method of Richmond and Richards [32] and 3.9×10^4 structures were generated. Of these structures, 27 satisfy steric constraints while simultaneously maintaining the connectivity of the chain and permitting a disulfide bridge between residues Cys-58 and Cys-105. The five topological families of four-helix bundles which remained are shown in Fig. 1a. The right-handed cylinder was reminiscent of other four-helix bundle structures [41] and was selected as the most likely structure (see Fig. 1b). Preliminary crystallographic data at 5Å resolution suggest that Il-2 is probably a four-helix bundle (McKay, personal communication); however, details of the helix boundaries and chain connectivity are not yet available and will be needed before the success of this model can be judged. In the interim, this model has served as a guide to site-directed and semisynthetic mutagenesis to deduce structure-activity relationships in Il-2 [42].

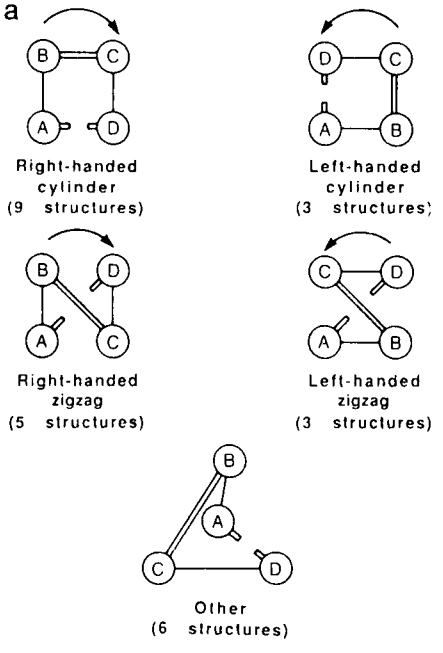

Fig. 1a. Schematic representation of four-helix bundle topologies generated by a combinatorial search of possible structures for interleukin-2. Single lines show connections behind the page, and double lines represent loops in front of the page.

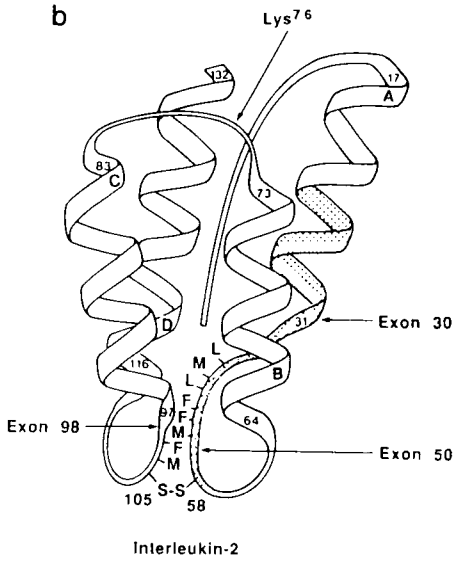

Fig. 1b. Ribbon diagram of the most likely model for Il-2. The disulfide bridge and exon boundaries are shown. A hydrophobic region in the AB and CD loops is a potential candidate for the ligand receptor binding site.

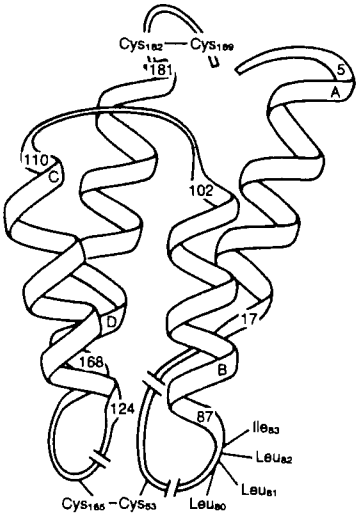

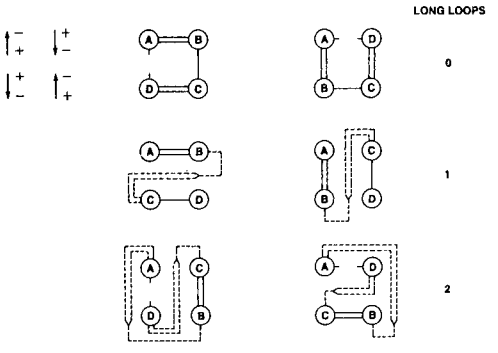

Fig. 2a. A schematic diagram of the right-handed fourfold α-helical structure predicted for human growth hormone. Helices are labeled sequentially A through D, and the residue numbers of the N-terminii and C-terminii are marked. Loops are added for clarity, and breaks are placed in the longer loops. Disulfide bridges are shown between Cys_{53} and Cys_{165} and between Cys_{182} and Cys_{189}. Four hydrophobic residues predicted to be important to receptor binding, Leu_{80}, Leu_{81}, Leu_{82}, and Ile_{83}, are marked.

Fig. 2b. A schematic representation of four α-helix bundle topologies which are favored by helix dipole interactions. Helices are labeled sequentially A through D with double lines showing connections in front of the page, single lines showing connections behind the page, and long loops which traverse the diameter of the molecule shown as transitions from single to double lines. For clarity, the relative directions of the chain for each helix are highlighted in the upper left-hand corner of the figure.

HGH was studied in a similar fashion. Four helices were identified along the sequence, and a most likely structure was selected from a list of 186 possibilities (see Fig. 2a). Abdel-Meguid et al. (personal communication) have determined the crystal structure. Both are four-helix bundles with a right-handed sense. Helices are consistently shorter in the predicted structure regardless of where the major packing interfaces are located. Unfortunately, the topological arguments used to process the list of 186 structures proved too limiting [38]. The crystal structure connectivity can be obtained from the model structure (Fig. 2a) by interchanging the position and direction of the B and C helices. The crystal structure requires long loop connections between helices A and B and between helices C and D. This connectivity was generated by the combinatorial

algorithm; however, in an attempt to find the most likely predicted structure, it was rejected on statistical grounds. As suggested by the breaks in the chain in Fig. 2a, such long connections are sterically possible but had been thought to be kinetically unreasonable. Clearly, a reevaluation of this presumption is indicated.

Baldwin and co-workers [7] have shown that the helix dipole is important to the stability of isolated α-helices. If this effect is important for stabilizing helix pairs that adopt the relatively parallel orientation observed in four-α-helical bundles, then six connectivities should be observed. These are shown schematically in Fig. 2b. Obviously, those which require long loop connections would be possible only when sufficient chain is present between the helices. It is tempting to speculate that long loop connections have not been observed in the previously studied four-α-helix bundles [41] because they are consistently smaller than HGH.

Current heuristic methods are capable of generating plausible structural models which can be subjected to experimental testing. These methods fail to produce a unique answer. The HGH example clearly shows an inability of the method to distinguish the native structure from a reasonable, but incorrect, alternative. Significant progress in understanding protein stability is necessary before it will be possible to sort between alternative structures. Mutagenesis experiments may provide this insight. In the interim, a close collaboration between experimentalist and theoretician is vital if these modeling efforts are to have any utility.

Acknowledgements

This work was supported by the Defense Advanced Research Projects Agency under contract N00014-86-K-0757 administered by the Office of Naval Research. The authors thank Dr. Langridge for his ongoing help and encouragement.

References

1. Anfinsen, C.B., Haber, E., Sela, M. and White, F.H., Proc. Natl. Acad. Sci. U.S.A., 47 (1961) 1309.
2. Levitt, M. and Warshel, A., Nature, 253 (1975) 694.
3. Nemethy, G. and Scheraga, H.A., Quart. Rev. Biophys., 10 (1977) 239.
4. Karplus, M. and Weaver, D.L., Biopolymers, 18 (1979) 1421.
5. Schulz, G.E. and Schirmer, R.H., Principles of Protein Structure, Springer-Verlag, New York, 1979.
6. Sternberg, M.J.E., In Geisow, M. and Barrett, A. (Eds.) Computing in Biological Science, Elsevier, Amsterdam, 1983, p. 143.
7. Shoemaker, K.R., Kim, P.S., York, E.J., Stewart, J.M. and Baldwin, R.L., Nature, 326 (1987) 563.
8. Creighton, T.E., Prog. Biophys. Mol. Biol., 33 (1978) 231.
9. McCammon, J.A., Gelin, B.R. and Karplus, M., Nature, 267 (1977) 585.

10. Weiner, S.J., Kollman, P.A., Case, D.A., Singh, U.C., Ghio, C., Alagona, G., Profeta, S. and Weiner, P., J. Am. Chem. Soc., 106 (1984) 765.
11. Hagler, A.T. and Honig, B., Proc. Natl. Acad. Sci. U.S.A., 75 (1978) 554.
12. Cohen, F.E. and Sternberg, M.J.E., J. Mol. Biol., 138 (1980) 321.
13. Baldwin, R.L., In Jaenicke, R. (Ed.) Protein Folding, Elsevier, Amsterdam, 1980, p. 369.
14. Post, C.B., Brooks, B.R., Karplus, M., Dobson, C.M., Artymiuk, P.J., Cheetham, J.C. and Phillips, D.C., J. Mol. Biol., 190 (1986) 455.
15. Needleman, S. and Wunsch, C., J. Mol. Biol. 48 (1970) 443.
16. Dayhoff, M., Atlas of Protein Sequence and Structure, National Biomedical Research Foundation, Silver Spring, Maryland, 1978.
17. Doolittle, R.F., Feng, D.F. and Johnson, M.S., Nature, 307 (1984) 558.
18. Martinez, H.M., Katzung, B. and Farrah, T., Sequence Analysis Program Manual, Biomathematical Computation Laboratory, University of California, San Francisco, 1983.
19. Kabsch, W. and Sander, C., Proc. Natl. Acad. Sci. U.S.A., 81 (1984) 1075.
20. Blundell, T.L., Sibanda, B.L., Sternberg, M.J.E. and Thornton, J.M., Nature, 326 (1987) 347.
21. Richardson, J.S., Adv. Protein Chem., 34 (1981) 167.
22. Sternberg, M.J.E. and Thornton, J.M., Nature, 271 (1978) 15.
23. Richards, F.M., Ann. Rev. Biophys. Bioeng., 6 (1977) 151.
24. Lee, B.K. and Richards, F.M., J. Mol. Biol., 55 (1971) 379.
25. Chou, P.Y. and Fasman, G.D., Biochemistry, 13 (1974) 211.
26. Chou, P.Y. and Fasman, G.D., J. Mol. Biol., 115 (1977) 135.
27. Sheriden, R.P., Dixon, J.S., Venkataraghavan, R., Kuntz, I.D. and Scott, K.P., Biopolymers, 24 (1985) 1995.
28. Taylor, W.R. and Thornton, J.M., J. Mol. Biol., 173 (1984) 487.
29. Lim, V.I., J. Mol. Biol., 88 (1974) 857.
30. Cohen, F.E., Abarbanel, R.A., Kuntz, I.D. and Fletterick, R.J., Biochemistry, 22 (1983) 4894.
31. Cohen, F.E., Abarbanel, R.A., Kuntz, I.D. and Fletterick, R.J., Biochemistry, 25 (1986) 266.
32. Richmond, T.J. and Richards, F.M., J. Mol. Biol., 119 (1978) 537.
33. Cohen, F.E., Richmond, T.J. and Richards, F.M., J. Mol. Biol., 132 (1979) 275.
34. Cohen, F.E. and Sternberg, M.J.E., J. Mol. Biol., 137 (1980) 9.
35. Cohen, F.E., Sternberg, M.J.E. and Taylor, W.R., Nature, 285 (1980) 378.
36. Cohen, F.E., Sternberg, M.J.E. and Taylor, W.R., J. Mol. Biol., 156 (1982) 821.
37. Cohen, F.E., Kosen, P.A., Kuntz, I.D., Epstein, L.B., Ciardelli, T.L. and Smith, K.H., Science, 234 (1986) 349.
38. Cohen, F.E. and Kuntz, I.D., Proteins: Structure, Function and Genetics (1987) in press.
39. Morgan, D.A., Ruscetti, F.W. and Gallo, R., Science, 193 (1976) 1007.
40. Gillis, S. and Smith, K.A., Nature, 268 (1977) 154.
41. Weber, P.C. and Salemme, F.R., Nature, 287 (1980) 82.
42. Ciardelli, T.L., Cohen, F.E., Gadski, R., Butler, L., Landgraf, B. and Smith, K.A., In Marshall, G.R. (Ed.) Peptides: Chemistry and Biology, Proceedings of the Tenth American Peptide Symposium, ESCOM, Leiden, 1988, p. 364.

Solution structures of defensins: Naturally occurring peptide antibiotics

Alvin C. Bach II[a], Xiao-Lu Zhang[a], Dennis R. Hare[b] and Arthur Pardi[a,*]

[a]*Department of Chemistry, Rutgers, The State University of New Jersey, New Brunswick, NJ 08903, U.S.A.*

[b]*Hare Research, Inc., Woodinville, WA 98072, U.S.A.*

Introduction

Defensins form part of the oxygen-independent mammalian defense system against microbial infection. They possess various degrees of in vitro microbicidal activity against a wide range of pathogens including gram-positive and gram-negative bacteria, fungi, and enveloped viruses [1–3]. Selsted, Lehrer, and co-workers have purified and characterized ten defensins from mammalian phagocytic leukocytes: one guinea pig, three human, and six rabbit peptides [2–4]. These homologous peptides are all cysteine- and arginine-rich, 29–34 residues in length, highly charged, and have eight conserved residues in the whole family. The conserved residues are the six cysteines arranged in three disulfide bonds, one glycine, and one arginine.

The three-dimensional structures of two members of the defensin family of antimicrobial peptides have been determined by two-dimensional (2D) nuclear magnetic resonance (NMR) and distance geometry techniques. A variety of 2D NMR experiments, including multiple quantum spectroscopy, total correlation spectroscopy, as well as standard correlation and nuclear Overhauser effect (NOE) spectroscopy, were used to make resonance assignments for all backbone and most side-chain protons in rabbit neutrophil peptide 5 (NP-5) and human neutrophil peptide 1 (HNP-1) [5]. Structural information was then obtained from 2D NOE experiments. The measured NOEs were used to calculate proton-proton internuclear distances less than 4.5Å. Short distances between protons on residues far apart in the sequence give information on the folding of the peptide backbone [6]. These short distance constraints were used as input for a distance geometry program to generate three-dimensional structures for these peptides. These NMR data show that the predominant structural feature of the homologous peptides is an antiparallel β-sheet in a hairpin conformation, extending from residues

*To whom correspondence should be addressed.

19 to 29 in NP-5. No regions of extended helical structure were found in these peptides.

Results and Discussion

Rabbit NP-5 and human HNP-1 were isolated and purified as previously described [1, 2]. The amino acid sequences for these two peptides are shown in Table 1. The first step in any structure determination process by NMR spectroscopy involves resonance assignment of the molecule. Nearly complete proton resonance assignments have been made on NP-5 and are described elsewhere [5]. A similar set of assignments has been made on HNP-1 (X.L. Zhang and A. Pardi, manuscript in preparation). Once resonance assignments have been made in a molecule, it is possible to use distance information derived from 2D NOE experiments to generate structures. The magnitude of the NOE is proportional to r_{ij}^{-6}, where r_{ij} is the internuclear distance between protons i and j. Most of the observed NOEs in peptides arise from intraresidue, or nearest neighbor residue, interactions [6, 7]. Statistical studies of X-ray crystal structures have shown that there are correlations between the short distances between protons on neighboring amino acid residues and regular secondary structure in proteins [8]. These sequential NOE connectivities for NP-5 and HNP-1 have been measured, and the absence of long stretches (>3 residues) of short NH-NH distances indicates that these defensins have little or no helical secondary structures [5, 6, 8].

In addition to the sequential NOE connectivities, a large number of NOEs were observed between protons on nonneighboring residues in NP-5 and HNP-1. NOEs for NP-5 and HNP-1 are illustrated in the diagonal plots in Figs.

Table 1 *Amino acid sequence of HNP-1 and NP-5*

	1									10
HNP-1:		Ala	Cys	Tyr	Cys	Arg	Ile	Pro	Ala	Cys
NP-5:	Val	Phe	Cys	Thr	Cys	Arg	Gly	Phe	Leu	Cys
	11									20
HNP-1:	Ile	Ala	Gly	Glu	Arg	Arg	Tyr	Gly	Thr	Cys
NP-5:	Gly	Ser	Gly	Glu	Arg	Ala	Ser	Gly	Ser	Cys
	21									30
HNP-1:	Ile	Tyr	Gln	Gly	Arg	Ler	Trp	Ala	Phe	Cys
NP-5:	Thr	Ile	Asn	Gly	Val	Arg	His	Thr	Leu	Cys
	31									
HNP-1:	Cys									
NP-5:	Cys	Arg	Arg							

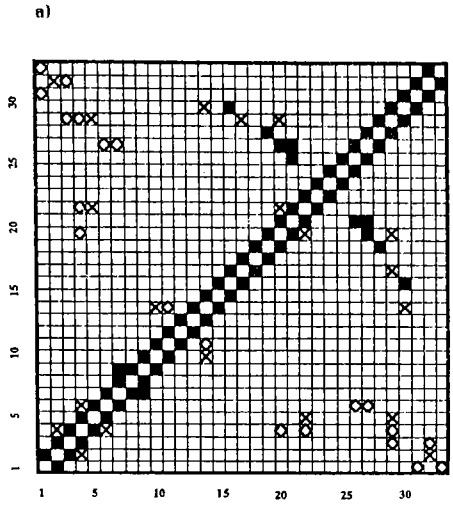

Fig. 1a. Diagonal plot of the observed NOEs in NP-5. Both axes are calibrated with numbers corresponding to the amino acid sequence in the peptide. The solid black squares indicate NOEs between backbone protons, the diamond shapes indicate NOEs between backbone and side-chain protons, and the crosses indicate NOEs between side-chain protons. Where a black square and diamond occupy the same location, only the square is shown.

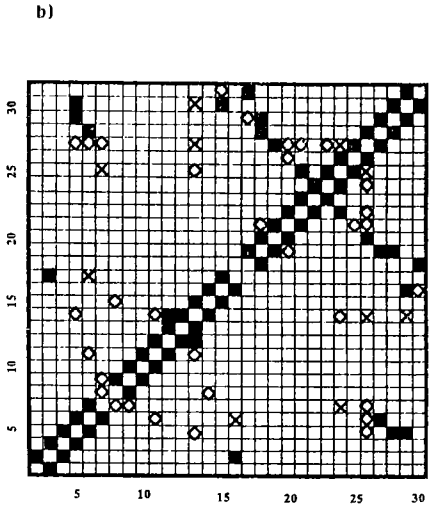

Fig. 1b. Diagonal plot for the observed NOEs in HNP-1.

1a and 1b, respectively. Diagonal plots provide an easily visualized format for presenting characteristic patterns of NOEs that can be used to identify regular secondary structure in proteins. For example, an antiparallel β-sheet is characterized by a line running perpendicular to the diagonal. Such patterns are seen in Figs. 1a and 1b, which indicate the presence of an antiparallel β-sheet involving residues 19–29 in NP-5 and HNP-1. These β-sheets were the only secondary structure that could be confidently obtained from qualitative analysis of the measured NOEs. As seen in the diagonal plots in Fig. 1, there are a large number of NOE connectivities that arise from close contacts between residues far apart in the sequence. These NOEs are useful for defining the tertiary structure of the peptide and were used as input for a distance geometry algorithm to generate the three-dimensional structures of the NP-5 and HNP-1.

The distance geometry program DSPACE (Hare Research, Inc.) was used to calculate structures of NP-5 using distances estimated from NMR data. This program uses a metric-matrix embedding technique [9, 10] to generate trial structures that are subsequently refined using nonlinear optimization techniques

to minimize the disagreement between the structure and the input distances. Since it is not possible to extract exact distances from NMR data, there is no single structure that is consistent with these input distances. Therefore, an important question is how well these NMR distances restrict possible structures to limited regions of conformation space. To address this question, eight distance geometry calculations were run on NP-5, where the input consisted of distance constraints estimated from 46 sequential NOEs involving protons on neighboring amino acid residues and 63 NOEs between protons on nonneighboring residues. Besides the NOE distance constraints and the covalent structure of NP-5, the only additional information used in the distance geometry calculations was the assumption of L-amino acids, *trans* peptide bonds, and knowledge of the disulfide linkages between residues C5-C20, C10-C30 and C3-C31 (M.E. Selsted and A. Pardi, unpublished results).

Fig. 2 shows a superposition of the backbone structures of NP-5 produced by four separate runs of the distance geometry program. These structures are all equally consistent with the input distance data, with no violations of any of the input distance constraints greater than 0.15Å. The chain proceeds from residue 1 over and across the antiparallel β-sheet and then curves around the sheet with a tight turn involving residues G11-S12-G13-E14. The chain then proceeds to the beginning of the antiparallel β-sheet at residue 19 and forms a hairpin turn for residues 21–24. The chain runs from the end of the β-sheet to the C-terminus which is in close contact with the N-terminus. Fig. 2 illustrates that the peptide backbone of NP-5 is quite well defined by these NMR data. Distance geometry calculations on HNP-1 show that it has a very similar backbone structure to that seen for NP-5 in Fig. 2 (data not shown). Detailed analysis of both of these structures will be presented elsewhere, but the preliminary results

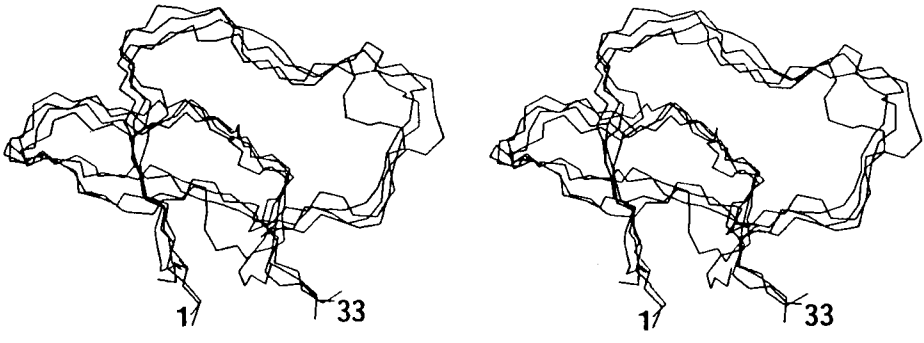

Fig. 2. Stereo pair of a superposition of four structures of NP-5 calculated by distance geometry methods. The C- and N-terminal residues are labeled in the figure.

shown here indicate that it is possible to use 2D NMR data to determine the three-dimensional structure of these antimicrobial peptides in solution.

Acknowledgements

We wish to thank Drs. R.I. Lehrer and M.E. Selsted (Departments of Medicine and Pathology, UCLA) for helpful discussions and providing us with purified peptides. This work was supported in part by grants from the Searle Scholars Program of the Chicago Community Trust (85-C110), NIH GM3501, a Henry Rutgers Research Fellowship, and a Biomedical Research Support Grant PHS RR 07058-21 to A.P. The 400 MHz NMR spectrometer was purchased with partial support from NSF grant CHEM-8300444.

References

1. Ganz, T., Selsted, M.E., Szklarek, D., Harwig, S.S.L., Daher, K. and Lehrer, R.I., J. Clin. Invest., 76 (1985) 1427.
2. Selsted, M.E., Szklarek, D. and Lehrer, R.I., Infect. Immun., 45 (1984) 150.
3. Selsted, M.E., Brown, D.M., DeLange, R.J. and Lehrer, R.I., J. Biol. Chem., 258 (1983) 14485.
4. Selsted, M.E., Harwig, S.S.L., Ganz, T., Schilling, J.W. and Lehrer, R.I., J. Clin. Invest., 76 (1985) 1436.
5. Bach II, A.C., Selsted, M.E. and Pardi, A., Biochemistry, 26 (1987) 4389.
6. Wuethrich, K., In NMR of Proteins and Nucleic Acids, John Wiley and Sons, New York, 1986, 117 pp (and references therein).
7. Billeter, M., Braun, W. and Wuethrich, K., J. Mol. Biol., 155 (1982) 321.
8. Wuethrich, K., Billeter, M. and Braun, W., J. Mol. Biol., 180 (1984) 715.
9. Crippen, G.M., J. Comp. Phys., 24 (1977) 96.
10. Kuntz, I.D., Crippen, G.M., Kollman, P.A. and Kimmelman, D., J. Mol. Biol., 106 (1976) 983.

Action of alanine-rich antifreeze polypeptides: Dipole moment of α-helix for ice recognition

Avijit Chakrabartty[a], Choy L. Hew[a,*], Daniel Yang[b] and Martin Sax[b]
[a]Research Institute, Hospital for Sick Children, Toronto, Ontario, Canada M5G 1X8
[b]Department of Crystallography, VAMC, Pittsburgh, PA, U.S.A.

Introduction

Isolation and characterization of the antifreeze polypeptides (AFP) from the right-eye flounder and cottid families have established the homologies of their chemical structures. These alanine-rich AFP are α-helical and contain an 11-amino acid repeating structure consisting of Thr-X_2-polar amino acid-X_7, where X is mainly alanine [1]. The two major AFP from winter flounder contain three of these repeats [1], whereas four similar repeats are found in the yellowtail flounder (P.L. Davies, personal communication).

Results and Discussion

The following experiments have been done to investigate the structure and function of these AFP.

1. *Chemical modification and peptide synthesis studies*

Complete modification of carboxyl and amino groups eliminated all antifreeze activity of the AFP from both families of fish. Partial modification of one or two of the four free amino groups of a shorthorn sculpin AFP (SS-8) reduced AFP activity at low concentrations but not at high concentrations. Acetylation of the α-amino group of Asp-1 and ε-amino group of Lys-18 in the winter flounder AFP (HPLC-6) did not affect activity at high concentrations, whereas citraconylation of the same groups eliminated activity.

Synthetic peptides corresponding to residues 1–37, 11–37, and 22–37 of flounder HPLC-6 were synthesized. The two shorter peptides did not exhibit antifreeze activity but the 37-mer was active, thus confirming the minimum requirement of at least three repeats for antifreeze activity.

*To whom correspondence should be addressed.

2. *Conformation*

The X-ray crystallographic structure of winter flounder AFP (HPLC-6) at 2.5Å was determined by direct analysis of the Patterson function. This polypeptide is a single 100% α-helix, 54Å in length, and completely amphiphilic. Examination of the electron density map and Nicholson models revealed various structural features which may stabilize the helix. First, a charge-charge interaction between Lys-18 and Glu-22 was observed. Second, interactions between the dipole of the α-helix [2] and charged side chains of the terminal amino acid residues were possible. The charged γ-carboxyl of Asp-1 may interact with the positive pole of the α-helix macrodipole, which is located at the N-terminal of the molecule. The C-terminal of the AFP contains an arginine-amide [3], thus allowing a second charge-dipole interaction between the guanidino group and the negative pole of the α-helix macrodipole. These charge-dipole interactions have been shown to play a critical role in the stabilization of the isolated C-peptide α-helix (a CNBr fragment of RNAse A) [4].

3. *Mechanism of action*

The two major aspects of AFP action are the preferential binding of the AFP to the ice nuclei and the subsequent inhibition of ice crystal growth [5]. The side chains of the polar amino acids of the AFP helix hydrogen bond to the oxygen atoms of ice, whereas the hydrophobic amino acids prevent further ice-water interactions. The AFP molecules preferentially adsorb to the prism faces (the planes of the ice crystal that are parallel to the c-axis), which are the fastest growing faces of the ice crystal [6].

The interaction of the dipole of the AFP helix with those of the water molecules in the bound ice nucleus may provide an explanation for the preferential binding of the AFP to the prism faces of ice. The dipoles of the water molecules in the ice nucleus adjacent to the AFP helix would align themselves in a direction antiparallel to the helix-dipole. The interaction of the resultant of the local dipoles on the ice surface with the macrodipole of the AFP helix would explain the preferential binding of the AFP to the prism faces of ice.

Acknowledgements

This work was supported by MRC, Canada.

References

1. Hew, C.L. and Fletcher, G.L., In Gilles, R. (Ed.) Circulation, Respiration, and Metabolism, Springer-Verlag, 1985, p. 553.
2. Hol, W.G.J., van Duijnen, P.T. and Berendsen, H.J.C., Nature, 273 (1978) 443.

3. Hew, C.L., Wang, N.C., Yan, S., Cai, H., Sclater, A. and Fletcher, G.L., Eur. J. Biochem., 160 (1986) 267.
4. Shoemaker, K.R., Kim, P.S., York, E.J., Stewart, J.M. and Baldwin, R.L., Nature, 326 (1987) 563.
5. Raymond, J.A. and DeVries, A.L., Proc. Natl. Acad. Sci. U.S.A., 74 (1977) 2589.
6. DeVries, A.L., Phil. Trans. R. Soc. Lond., B304 (1984) 575.

Conformational analysis of a cyclic hexapeptide by rotating frame NOE (ROE) evaluation and molecular dynamics (MD) calculations

Horst Kessler, Klaus Wagner and Martin Will

Institut für Organische Chemie, J.W. Goethe-Universität, Niederurseler Hang, D-6000 Frankfurt 50, F.R.G.

We report here the conformational analysis of cyclo[-D-Pro^1-Phe^2-Val^3-Lys(Z)^4-Trp^5-Phe^6-] **1** which is an analog of the potent cytoprotective hexapeptide cyclo(-D-Pro^1-Phe^2-Thr^3-Lys^4-Trp^5-Phe^6-) **2**. In **2**, intramolecular H-bridges of the Thr hydroxyl group are found; it acts as an H-donor to the carbonyl group of Phe^6 and accepts H-bridges from the NH-protons of Trp^5 and Phe^6. This stabilizes the region about the originally assumed βI-turn (Thr^3-Lys^4-Trp^5-Phe^6); however, the βI-turn is not strongly populated in the mean of the MD trajectory over 100 ps (Kessler et al., manuscript submitted for publication). In **1**, which exhibits an even higher biological activity than **2** [1], the Thr hydroxyl group is omitted and the conformation of **1** is therefore of special interest.

Only a few tiny cross peaks in the NOESY spectrum are observed; therefore, we performed a ROESY experiment [2, 3]. It is essential for a quantitative ROE evaluation to use *small flip angles* ($\beta = 20°$) and a *weak lockfield* ($B_1 = 2$ kHz). The mixing time was 200 ms. Frequency offset effects of the cross peak intensities were corrected [4]. For the transformation of these values into distances, the NH-C^{7}H cross peak of the indole ring (282 pm) was used for calibration. Independent confirmation was obtained by the distance of the diastereotopic β-protons of Phe^2 (180 pm). Seventeen experimentally determined distances were used as constraints in the MD calculations using the GROMOS package [5]. The mean conformation of a 31 ps run is shown in Fig. 1 and compared to that of **2**.

The results show an identical βII'-region, but distinct differences in the Lys^4-Trp^5 region. Here, a βII-turn is formed which is populated in most of the MD time steps (98.5%, distance NH-O 204 pm, angle 153°), although it is unusual in β-bends containing two L-amino acids in the i + 1 and i + 2 position [6]. The difference between the solution structures of **1** and **2** is obviously caused by the lack of the Thr hydroxyl group in compound **1**. Therefore, the upright fixation of the NH of Trp^5 in **1** is lost and the molecule adopts a more relaxed β-type conformation.

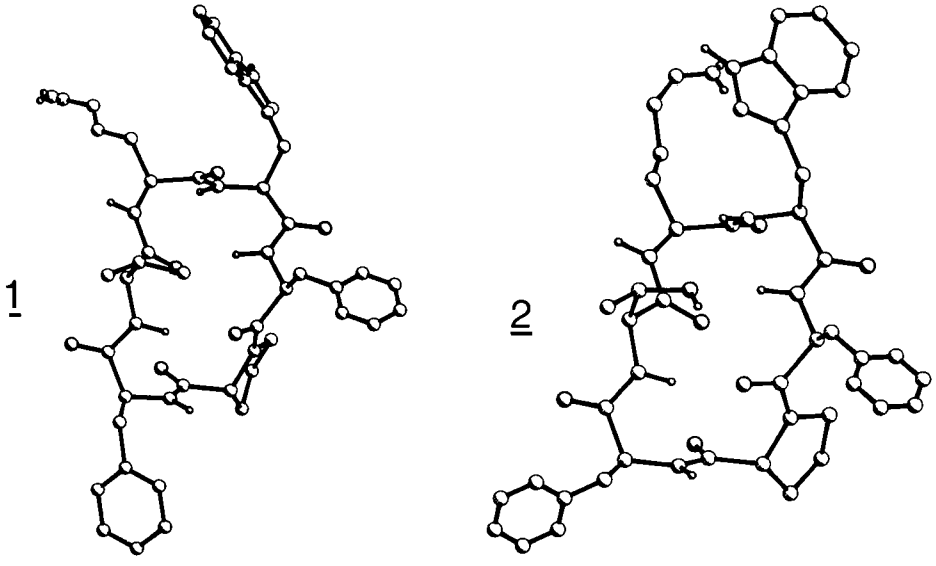

Fig. 1. Solution conformation of **1** *and* **2**. *For* **2**, *no side-chain restrictions are used in the calculations; for* **1**, *the preferred side chains are shown.*

References

1. Ziegler, K., Frimmer, M., Kessler, H., Damm, I., Eiermann, V., Koll, S. and Zarbock, J., Biochim. Biophys. Acta, 845 (1985) 86.
2. Bothner-By, A.A., Stephans, R.L., Warren, C.D. and Jeanloz, R.W., J. Am. Chem. Soc., 106 (1986) 811.
3. Kessler, H., Griesinger, C., Kerssebaum, R., Wagner, K. and Ernst, R.R., J. Am. Chem. Soc., 109 (1987) 607.
4. Bax, A. and Davis, D.G., J. Magn. Reson., 63 (1985) 207.
5. van Gunsteren, W.F., Boelens, R., Kaptein, R., Scheek, R.M. and Zuiderweg, E.R.P., In Hermans, J. (Ed.) Molecular Dynamics and Protein Structure, Polycrystal Book Service, Western Springs, Illinois, 1985, p. 92.
6. Smith, J.A. and Pease, L.G., CRC Crit. Rev. Biochem., 8 (1980) 3.

^{13}C NMR T_1 studies and enantiotopomerisations of 3_{10}-helical polypeptides

Günther Jung[a,*], Rolf-Peter Hummel[a], Klaus-Peter Voges[a], Klaus Albert[a] and Claudio Toniolo[b]

[a]Institut für Organische Chemie, Universität Tübingen, D-7400 Tübingen, F.R.G.
[b]Instituto di Chimica Organica, Università di Padova, I-35131 Padova, Italy

α-Aminoisobutyryl (Aib) residues induce preferentially right-handed 3_{10}-helices in tri- to octapeptide peptaibol segments containing L-amino acids. In exceptional cases, the left-handed 3_{10}-helix can be found even in peptides with L-residues [1]. The homopeptides $(Aib)_n$ (n = 5,8) [2] and poly(Aib) [3] were shown to crystallize in the form of enantiomeric 3_{10}-helices. Compared with this large data set available from 3_{10}-helical oligopeptides, there also exists a representative series of crystal structures of α-helical Aib-containing polypeptides [1, 4], including the 20-peptide antibiotic alamethicin, its synthetic C-terminal nonapeptide segment and N-terminal decapeptide model, and recently the N-terminal zervamicin decapeptide [5].

Using independent methods, it has been demonstrated that most of these 3_{10}-helices and the α-helices as well maintain their conformation in solution. Furthermore, it has been concluded that the α-helix content increases with increasing Aib content (30–50%) in polypeptides of similar length. And it was shown that alamethicin adopts a particularly rigid and heat-stable, α-helical, rodlike structure in a lipophilic environment, contributing the high dipole moment required for voltage-dependent channel formation [6].

Here, we wish to stress the first finding of an enantiotopomerisation between left- and right-handed 3_{10}-helices. During ^{13}C NMR T_1 measurements of the peptide series Z-$(Aib)_n$-OtBu [2], only one sharp single signal was recorded for the 20 methyl groups of Z-$(Aib)_{10}$-OtBu, whereas a conformationally stable enantiomeric homopeptide 3_{10}-helix was expected to show diastereotopic splitting of the geminal α,α-methyl signals of each Aib residue as observed in the α-helical alamethicin [7, 8]. Such a magnetic nonequivalence (MNE) of pro-*R* and pro-*S*-C_β atoms should also be observable in a racemate of 3_{10}-helices. Indeed, upon cooling down to 203K, Z-$(Aib)_{10}$-OtBu exhibits two distinct signal groups at 26.7 and 21.4 ppm (MNE = 5.3 ppm). Similar values are found for all Aib-containing right-handed α-helical peptaibols and for sequential polypeptides Boc-

*To whom correspondence should be addressed.

(L-Ala-Aib-L-Ala-Aib-L-Ala)$_n$-OMe (n = 2–4) [6] with increasing chain length at room temperature. Upon raising the temperature to 265K coalescence of the C_β signals of Z-(Aib)$_{10}$-OtBu was observed corresponding to the free energy of activation $\Delta G^{\ddagger} = 46$ KJ/mole (4.6 KJ/mole Aib residue), a much lower value than that found for α-helices. The high MNE obtained also by solid-state ^{13}C NMR (CPMAS), T_1 relaxation time measurements (see below), and vibrational spectroscopy support our interpretation of the effects observed during freezing the $3^r_{10} \rightleftharpoons 3^l_{10}$ helix interconversion of Z-(Aib)$_{10}$-OtBu. This interconversion occurs very rapidly at room temperature (1200 Hz) in dichloromethane or chloroform solution, and it can be described as a monomolecular all-or-nothing process between the enantiomeric helices.

Our finding may be of relevance with respect to the peculiar burst-like pore formation in lipid bilayer experiments of some Aib-rich alamethicin analogs such as trichotoxin. At room temperature, conformationally labile 3_{10}-helical segments could be inter alia the reason for nonresolvable pore states, whereas the particularly rigid α-helix of alamethicin contributes all steric requirements for defined ion-conducting helix aggregates.

At room temperature (298K), the 3_{10}-helices of different lengths of Z-(Aib)$_n$-OtBu (n = 5, 6, 10, 11) show almost no differences in their ^{13}C T_1 relaxation times for their Aib-C_β carbon atoms because of rapid interconversion. Slightly increasing differences were observed with decreasing temperature for Z-(Aib)$_{10}$-OtBu at 250K ($\Delta T_1 = 35$ ms) and at 240K ($\Delta T_1 = 51$ ms). In analogy to the α-helical pro-*R*-C_β in alamethicin [7, 8], the downfield shifted group of methyl carbons relaxes faster than the group at higher field. In contrast to these ΔT_1 values found for the 3_{10}-helical homopeptides Z-(Aib)$_n$-OtBu (n = 10, 11), all α-helical Aib peptides including alamethicin [7, 8] and Boc-(L-Ala-Aib-L-Ala-Aib-L-Ala)$_n$-OMe (n = 2–4) [6] show very large differences in Aib-C_β T_1 values: $\Delta T_1 = 250$–290 ms already at room temperature.

References

1. Bosch, R., Jung, G., Schmitt, H., Sheldrick, G.M. and Winter, W., Angew. Chem. Int. Ed., 23 (1984) 450 (and refs. cited therein).
2. Bavoso, A., Benedetti, E., Di Blasio, B., Pavone, V., Pedone, C., Toniolo, C. and Bonora, G., Proc. Natl. Acad. Sci. U.S.A., 83 (1986) 1988.
3. Malcolm, B.R. and Walkinshaw, M.D., Biopolymers, 25 (1986) 607.
4. Bosch, R., Jung, G., Schmitt, H. and Winter, W., Biopolymers, 24 (1985) 961 and 979.
5. Karle, I.L., Sukumur, M. and Balaram, B., Proc. Natl. Acad. Sci. U.S.A., 83 (1986) 9284.
6. Menestrina, G., Voges, K.-P., Jung, G. and Boheim, G., J. Membr. Biol., 93 (1986) 111.
7. Schmitt, H. and Jung, G., Liebigs Ann. Chem. (1985) 321 and 345.
8. Jung, G. and Schmitt, H., In Ragnarsson, U. (Ed.) Peptides 1984, Almquist and Wiksell, Uppsala, 1984, p. 569.

The conformation of oxytocin bound to neurophysin I

Klaas Hallenga[a], N.R. Nirmala[a], D. David Smith[b] and Victor J. Hruby[b]
[a]*Department of Chemistry, Michigan State University, East Lansing, MI 48824, U.S.A.*
[b]*Department of Chemistry, University of Arizona, Tucson, AZ 85721, U.S.A.*

Introduction

Knowledge of the conformation of a peptide when it is bound is crucial for the understanding of hormone receptor interactions as well as for the design of biologically more active or more selective analogs. We have studied the oxytocin/bovine-neurophysin I complex by two-dimensional (2D) NMR as a model for peptide-hormone receptor interaction.

Results and Discussion

A single conformation has been found for oxytocin in the bound form, which was determined in considerable detail from a series of proton 2D NMR studies at 360 MHz and 500 MHz. Sizeable and unambiguous transfer nuclear Overhauser effects (NOE) were established in both D_2O and H_2O.

The cross peaks seen in the 2D NOE spectra can be broadly classified into four categories:

(1) Intraresidue cross peaks;
(2) Interresidue cross peaks;
(3) Protein-peptide cross peaks; and
(4) Cross peaks between protons on the protein.

Of these, type 1 cross peaks serve to supplement information in the COSY spectrum and, to a limited extent, give us information about the orientation of the side chain in the amino acid residues. Type 2 cross peaks are crucial for obtaining the conformation of the bound peptide. Cross peaks of type 3 indicate which peptide residues are very close to the protein. Cross peaks of type 4 are relevant for studying the structure of the protein and will not be considered here. Most of the interresidue cross peaks present are from the i^{th} residue to the $(i+1)^{th}$ residue (i.e., they are short-range cross peaks). The only type of long-range interresidue cross peaks is from the ^{2}Tyr residue to the ^{5}Asn residue. Since this is a peak that occurs across the ring, it is crucial in determining the conformation of the bound oxytocin.

A model of the oxytocin molecule was constructed based on the X-ray structure [1]. Examination of this model reveals that the strongest cross peak in the 2D

NOE spectrum should be that between the ^{2}Tyr-NH proton and the ^{6}Cys-α proton since the interproton distance in the X-ray structure is only 1.1 Å; however, such a cross peak does not exist.

Similarly, the model based on the X-ray structure indicates that the ^{5}Asn-β is $\approx$4.8 Å away from the ^{2}Tyr-NH. This means that one should not be able to observe the corresponding cross peak in the spectrum. However, a cross peak is indeed observed between ^{5}Asn-β and ^{2}Tyr-NH, where the cross peak is about 1.4% of the intensity of the diagonal peak.

A model could be constructed based upon the 2D NOE data such that all NOE constraints are satisfied. Furthermore, in this model the ^{6}Cys-α-^{2}Tyr-NH are about 5 Å apart while the ^{5}Asn-β moves closer to the ^{2}Tyr protons, explaining the absence of cross peaks in the former case and their presence in the latter. This model is also consistent with the fact that all the cross peaks seen but not compatible with the X-ray structure can be expected based on the interproton distances. The dihedral angles of the ^{1}Cys, ^{2}Tyr, ^{3}Ile, and ^{6}Cys residues are drastically different from those in the X-ray structure. In addition, the tail, consisting of ^{7}Pro, ^{8}Leu, and ^{9}Gly, also undergoes some change that gives rise to a strong ^{7}Pro-α-^{8}Leu-NH cross peak.

The information obtained in the D_2O experiments serves to substantiate information from the NOESY experiments in H_2O. Since the molecule is a relatively small peptide, the NH-α, NH-β and NH-NH cross peaks offer the maximum information on interresidue spatial relationships. The presence of a very strong cross peak between the ^{6}Cys-α and the ^{7}Pro-δ, however, is to be noted in the D_2O spectra. This strong cross peak is possible only if the configuration of the ^{7}Pro residue is *trans*. This is also borne out by the X-ray structure and by previous structural studies on oxytocin. In addition, since it is possible to look at really low contours in the D_2O spectra (unlike the spectra of oxytocin-neurophysin complex in H_2O where the solvent peak is so intense that peaks of lower intensity can just not be seen very easily without interference from the solvent ridges), one can see cross peaks between the following peptide residues and the protein: ^{2}Tyr, ^{3}Ile, ^{4}Gln, and ^{5}Asn.

This information, in addition to the suggested conformation for the bound oxytocin, shows that the peptide-protein NOEs are all on one side of the oxytocin molecule. It may be speculated that the mode of approach of the peptide towards the protein is from the side containing the above-mentioned residues.

Acknowledgements

This work is supported in part by NIH grant No. AM17420.

References

1. Wood, S.P., Tickle, I.J., Treharne, A.M., Pitts, J.E., Mascarenhas, Y., Li, J.Y., Husain, J., Cooper, S., Blundell, T.L., Hruby, V.J., Buku, A., Fischman, A.J. and Wyssbrod, H.R., Science, 232 (1986) 633.

Conformational analysis of human atrial natriuretic polypeptide by NMR and distance geometry algorithm

Y. Kobayashi[a], T. Ohkubo[a], Y. Kyogoku[a], S. Koyama[b], M. Kobayashi[b] and N. Gō[c]

[a]Institute for Protein Research, Osaka University, Suita, Osaka 565, Japan
[b]Research Laboratory, Fujisawa Pharmaceutical Co. Ltd., Kashima, Yodogawa, Osaka 532, Japan
[c]Faculty of Science, Kyoto University, Kyoto 606, Japan

Introduction

Atrial natriuretic polypeptides (ANP) which possess potent diuretic and vasodilating activities have been isolated from human and rat atrial tissues, and their amino acid sequences have been determined. Various analogs have been synthesized and much work has been done to elucidate the structure-activity relationships. Conformational analysis is required to gain a better understanding of the unique activities of ANP. In the present study, we describe the solution conformation of a human atrial natriuretic polypeptide, α-hANP. The primary structure of α-hANP was determined by Kangawa and Matsuo [1] to be H-Ser-Leu-Arg-Arg-Ser-Ser-Cys-Phe-Gly-Gly-Arg-Met-Asp-Arg-Ile-Gly-Ala-Gln-Ser-Gly-Leu-Gly-Cys-Asn-Ser-Phe-Arg-Tyr-OH.

Results and Discussion

Three-dimensional structural analysis was carried out using NMR and a distance geometry algorithm as follows: Two-dimensional COSY, NOESY, and relayed-COSY experiments were performed in DMSO-d_6 with α-hANP, which was produced in *E. coli* by recombinant DNA techniques. The peak assignments of these spectra were determined in a sequential manner, and the peak intensities of the NOESY spectra were subsequently interpreted as constraints on the proton-proton distances. Using our recently developed algorithm [2], distance geometry calculations were carried out with these constraints. The algorithm consists of construction of an initial conformation with random dihedral angles and minimization of the sum of the squared differences between mutual atomic distances d_{ij} in the calculated conformation and experimental values of the corresponding distances.

Results obtained from different initial conformations were compared. One of the conformations which has the lowest conformational energy is shown in Figs. 1 and 2.

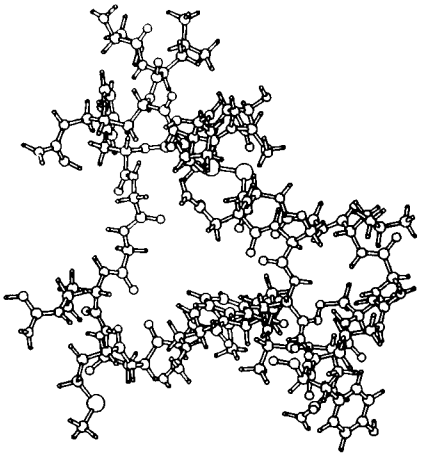

Fig. 1. Molecular conformation of α-hANP.

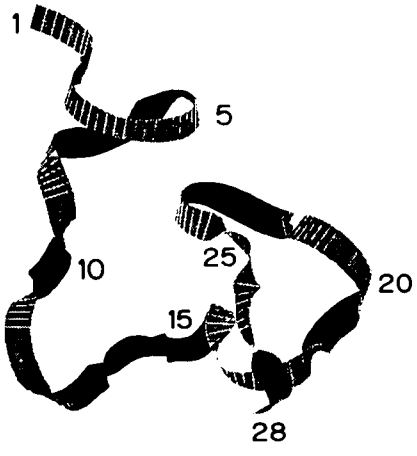

Fig. 2. Ribbon drawing of backbone structure of α-hANP.

Fesik et al. [3] carried out NMR analysis on the conformation of rat ANP, which has a primary structure identical to that of α-hANP (5–27) with a single amino acid replacement at position 12 of Ile for Met, and reported that it has a β-type structure or an averaged conformation (random coil). Our present results, however, show that the cyclic moiety (7–23) has an ordered structure, and the C-terminal part (24–28) is folded back toward the ring moiety. The N-terminal region might be spread in space because of the lack of long-range NOE peaks.

References

1. Kangawa, K. and Matsuo, H., Biochem. Biophys. Res. Commun., 118(1984)131.
2. Ohkubo, T., Kobayashi, Y., Shimonishi, Y., Kyogoku, Y., Braun, W. and Go, N., Biopolymers, 25(1986)S123.
3. Fesik, S.W., Holleman, W.H. and Perun, T.J., Biochem. Biophys. Res. Commun., 131(1985)517.

The structure of a new hexameric form of human insulin

G.D. Smith[a], D.C. Swenson[a], Z. Derewenda[b], E.J. Dodson[b], G.G. Dodson[b], C.D. Reynolds[c] and K. Sparks[c]

[a]*Medical Foundation of Buffalo, Inc., 73 High Street, Buffalo, NY 14203, U.S.A.*
[b]*University of York, Heslington York, U.K.*
[c]*Liverpool Polytechnic, Liverpool, U.K.*

Introduction

Crystallographic studies of different crystalline forms of insulin have shown that certain portions of the insulin molecule are flexible and can exist in different conformational states. Changes in the conformation of the insulin molecule displace specific amino acid residues which help hold the dimer and the hexamer together through hydrophilic and hydrophobic interactions. The aggregation properties of insulin which are exploited in the management of diabetes are very much dependent upon the identity and the nature of these dimer- and hexamer-forming interactions.

Results

Addition of phenol to the crystallizing media produces a crystalline modification called monoclinic insulin. We have solved this form of human insulin and have refined the structure using 2.25 Å resolution data to a residual of 0.22. Unlike the 2-zinc structure [1], which has the N-terminus of all six B-chains in an extended conformation, or the 4-zinc structure [2], for which three B-chains are extended and three are α-helical, all six B-chains in the monoclinic form are α-helical. Fig. 1a shows a comparison of one monoclinic B-chain to a 4-zinc B-chain; while the α-helical regions are very similar, the last five residues have undergone a shift. The conformation of these five residues, however, is nearly identical to that of 2-zinc, shown in Fig. 1b. Thus, each of the six molecules of the monoclinic form have structural features in common with the 2-zinc and the 4-zinc structures.

The change in conformation of the B-chains from extended to α-helical has a profound influence on the dimer- and hexamer-stabilizing surfaces. Four antiparallel hydrogen bonds between B24 and B26 of molecule 1 and their counterparts in molecule 2 produce a pleated sheet structure and are important for stabilizing the 2-zinc, 4-zinc, and monoclinic dimers. Additional stabilization of the dimer is produced in 4-zinc insulin, since three of the B-chains have

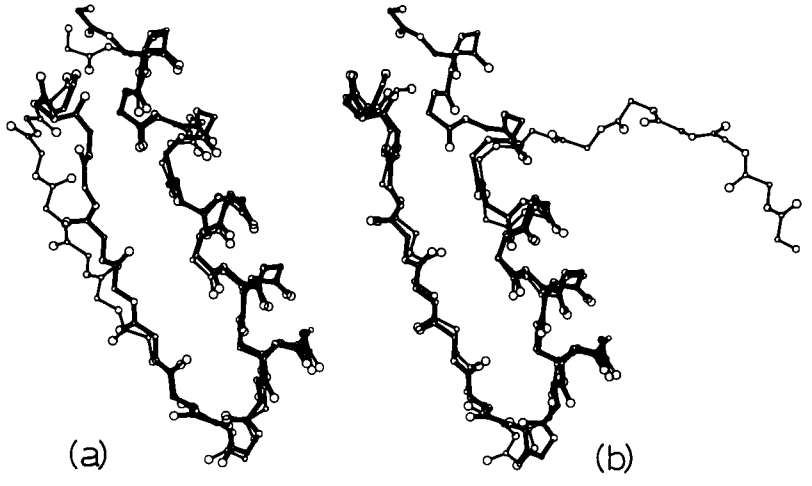

Fig. 1. A comparison of one of the B-chains in monoclinic insulin (thick bonds) with the B-chain of (a) molecule 1 of 4-zinc insulin and (b) molecule 2 of 2-zinc insulin. The carboxyl terminus is at the left of both figures.

moved from the hexamer-forming surface to the dimer-forming surface where they participate in six hydrogen bonded interactions. In the monoclinic form, all six of the B-chains have migrated to the dimer-forming surface. This results in a total of 18 hydrogen bonds and provides additional stability for the formation of the dimer.

In 2-zinc insulin, interactions which stabilize the formation of the hexamer occur exclusively between a single pair of molecules. The B1 Phe residue plays an important role in hexamer stabilization since its amino group forms a salt bridge to the A17 carboxyl group and its side chain makes hydrophobic interactions with the side chains of A13 Leu and A14 Tyr on the adjacent monomer surface. The movement of the N-terminus of the B-chain alters the nature of the hexamer-stabilizing interactions in the 4-zinc and monoclinic forms. The loss of one of the B-chains from the hexamer-forming surface in the 4-zinc structure allows the second B-chain to undergo a shift of approximately 4 Å where it can form hydrogen bonds to the B16 Tyr and B17 Leu residues in the adjacent monomer. In the monoclinic form, a deep cleft is produced on the surface of the hexamer by the absence of both B-chain N-termini. The strong hexamer-forming contacts observed in the 2-zinc and 4-zinc structures are replaced by several weak interactions involving A13, B14, B17, and B18 of both monomers. The new position of the B1 Phe residue permits it to make weak contacts with A-chain residues of a neighboring monomer.

Acknowledgements

The authors are grateful to Professor Dorothy Hodgkin for helpful discussions. Research supported by the James H. Cummings Foundation, the Juvenile Diabetes Foundation, and the Diabetes Research and Education Foundation.

References

1. Dodson, E.J., Dodson, G.G., Hodgkin, D.C. and Reynolds, C.D., Can. J. Biochem., 57 (1979) 469.
2. Smith, G.D., Swenson, D.C., Dodson, E.J., Dodson, G.G. and Reynolds, C.D., Proc. Natl. Acad. Sci. U.S.A., 81 (1984) 7093.

Comparative 2D NMR studies of the Phe B24 → Leu mutant human insulin

Michael A. Weiss[a,b], Erin O'Shea[a], Ken Inouye[c], Bruce H. Frank[d], Igor Khait[a], Dzung Nguyen[e], Leo J. Neuringer[a] and Steven E. Shoelson[b,f]

[a]*Francis Bitter National Magnet Laboratory, Massachusetts Institute of Technology, Cambridge, MA 02139, U.S.A.*
[b]*Brigham and Women's Hospital, Boston, MA 02115, U.S.A.*
[c]*Shionogi Research Laboratory, Osaka 553, Japan*
[d]*Lilly Research Laboratories, Indianapolis, IN 46285, U.S.A.*
[e]*Chemistry Department, Harvard University, Cambridge, MA 02138, U.S.A.*
[f]*Joslin Diabetes Center, Boston, MA 02215, U.S.A.*

Introduction

Insulin provides a paradigm for the cellular control of metabolism by peptide hormones. Recent advances in the cloning of the insulin receptor have led to renewed interest in structure-function relationships [1]. We demonstrate that high-resolution ^{1}H NMR spectra of human insulin may be obtained. Comparative studies of mutant insulins [2], identified from patients with Type II diabetes mellitus, enable key resonances to be assigned and structural perturbations to be characterized. We describe here the NMR features of one such mutant, Phe B24 → Leu. This substitution selectively perturbs dimer packing.

In the wild-type hormone, Phe B24 lies in the extended C-terminal region of the B-chain (Fig. 1). This region is thought to be part of the receptor-binding surface [3]. In addition, it forms part of the insulin dimer contact in the crystal [4]. The physiologic importance of this residue is underscored by the discovery of mutations at this position in certain diabetic patients. Among mammalian insulins, phenylalanine is the conserved amino acid [5].

Results and Discussion

Human insulin was obtained from Lilly Research Laboratories; zinc was removed by gel filtration in 1% acetic acid. Mutant insulins were prepared by semisynthesis at Shionogi Research Laboratory as described [6]. Two-dimensional ^{1}H NMR spectra were obtained at 500 MHz by the pure-phase method of States et al. [7], and processed as described [8].

The aromatic resonances in the two-dimensional ^{1}H NMR spectrum of human insulin are shown in Fig. 2. Assignments shown are based on a variety of two-

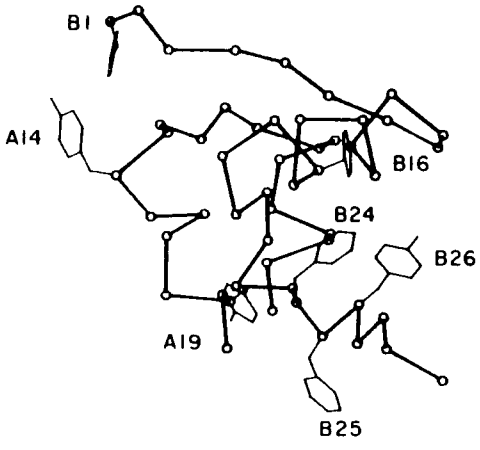

Fig. 1. α-Carbon representation of the A-B monomer in 2-Zn insulin.

dimensional ^{1}H NMR experiments of native and modified insulins, as will be described elsewhere. At the concentration and conditions used (37°C, 200 μM protein concentration, 20% acetic acid, pD 3.0), insulin is predominantly monomeric. At lower temperatures, higher pH or protein concentration, intermediate exchange is observed between monomer, dimer, and higher-order oligomers (data not shown). The ^{1}H NMR resonances of residues involved in dimerization selectively broaden; those whose environments are not perturbed by dimerization remain sharp. These ^{1}H NMR features may be used to monitor the extent of dimerization under defined conditions.

The pure-phase COSY spectrum of the mutant insulin Phe B24 → Leu is shown in Fig. 3. One phenylalanine spin system is absent (arrow), identifying the resonances of Phe B24 in the native spectrum (Fig. 2). These resonances are unusual in that they are shifted to higher field and are broader than the resonances of the Phe B1 and Phe B25. These properties reflect the distinctive structural environment of Phe B24 in the native structure. The B24 Phe → Leu substitution does not significantly perturb the remaining aromatic resonances, indicating that it is structurally conservative in the monomer; however, no monomer-dimer transition is observed at lower temperatures or higher protein concentrations, indicating that Leu B24 disrupts dimer packing. We suggest that receptor-binding may be similarly destabilized.

These studies are part of a broader structural investigation of insulin and its genetic variants in solution. Studies of additional diabetes-related mutations at the A3, B24, and B25 positions will be described elsewhere.

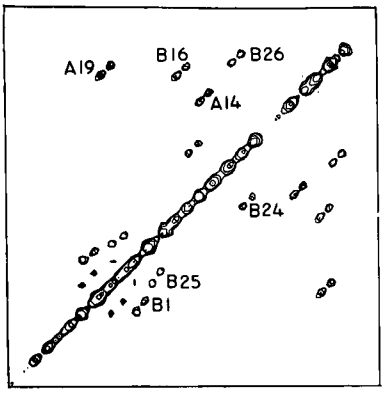

Fig. 2. Two-dimensional ^1H NMR COSY spectrum at 500 MHz of human insulin showing the phenylalanine (B1, B24, B25) and tyrosine (A14, A19, B16, B26) resonances.

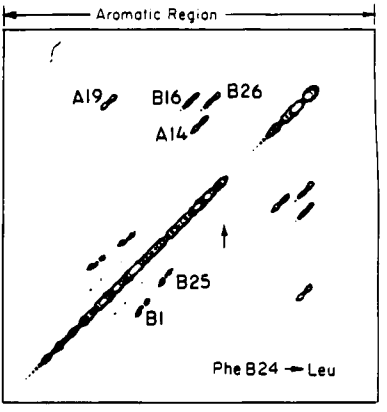

Fig. 3. Pure-phase two-dimensional ^1H NMR COSY spectrum at 500 MHz of the mutant insulin Phe B24 → Leu. The Phe B24 resonance (arrow) is missing.

Acknowledgements

We acknowledge the High Field NMR Resource of the Francis Bitter National Magnet Laboratory (supported by NIH Grant No. RR-00995); we also thank Professor Martin Karplus (Harvard Chemistry Department) for use of computer graphics facilities and Professor Robert Sauer (M.I.T. Biology Department) for making available laboratory facilities.

References

1. Ellis, L.E., Clauser, E., Morgan, D.O., Edery, M., Roth, R.A. and Rutter, W.J., Cell, 45 (1986) 721.
2. Haneda, M., Polonsky, K.S., Bergenstal, R.M., Jaspan, J.B., Shoelson, S.E., Blix, P.M., Chan, S.J., Kwok, S.C.M., Wishner, W.B., Zeidler, A., Olefsky, J.M., Freidenberg, G., Tager, H.S., Steiner, D.F. and Rubenstein, A.H., N. Engl. J. Med., 310 (1984) 1288.
3. Pullen, R.A., Lindsay, D.G., Wood, S.P., Tickle, I.J., Blundell, T.L., Wollmer, A., Krail, G., Brandenburg, D., Zahn, H., Gliemann, J. and Gammeltoft, S., Nature, 259 (1976) 369.
4. Blundell, T.L., Cutfield, J.F., Cutfield, S.M., Dodson, E.J., Dodson, G.G., Hodgkin, D.S., Mercola, D.A. and Vijayan, M., Nature, 231 (1971) 506.
5. Cutfield, J.F., Cutfield, S.M., Dodson, E.J., Dodson, G.G., Emdin, S.F. and Reynolds, C.D., J. Mol. Biol., 132 (1979) 85.

6. Inouye, K., Watanabe, K., Tochino, Y., Kanaya, T., Kobayashi, M. and Shigeta, Y., Experientia, 37(1981)811.
7. States, D.J., Haberkorn, R.A. and Ruben, D.J., J. Magn. Reson., 48(1982)286.
8. Weiss, M.A., Karplus, M. and Sauer, R.T., Biochemistry, 26(1987)890.

Hexapeptide metal binding domains in proteins

H.A. Anderson[a], M.A. Eastman[b], L.G. Pedersen[c], R.G. Hiskey[c] and A.T. Hagler[a]

[a]*The Agouron Institute, 505 Coast Blvd So., La Jolla, CA 92038, U.S.A.*
[b]*Cornell University, Baker Laboratory of Chemistry, Ithaca, NY 14853, U.S.A.*
[c]*University of North Carolina at Chapel Hill, Venable and Kenan Laboratories 045A, Chapel Hill, NC 27514, U.S.A.*

Introduction

Calcium metal binding plays important roles in the regulation and function of proteins. Among these roles include both catalytic regulation and structural integrity in protein function and conformation. The conformation of a proposed Ca^{2+} binding site for bovine prothrombin fragment 1, 18–23 region, was minimized using ECEPP [1] and VFF [2, 3] energy calculations. Further analyses of the resulting minimum energy conformation, using *template forcing* techniques, found the same conformation compatible for five homologous blood protein sequences (Eastman et al., manuscript in preparation). Comparison of the prothrombin metal binding conformation to Brookhaven crystal structures has led to a hypothesis for calcium metal binding requirements.

Hypothesis

Here we report on the characteristics, both the nature of the primary sequence and conformational properties of a proposed calcium binding fragment. In attempting to define a generalized domain and compare metal binding sites, we consider three properties of the proposed region: (1) The *loop* nature of the binding region (i.e., a measure of the C_1^α–C_6^α distances); (2) the conformational similarity between structures as measured by the root mean square (RMS) deviation of the backbone; and (3) the sequence homology of residues involved in the binding loop. We have examined and compared known calcium binding domains in the Brookhaven data base, using interactive graphics [4] on an Evans and Sutherland PS 300 graphics terminal. The results are given in Table 1.

Results and Discussion

We compared the calculated minimum energy calcium binding conformation for the family of blood proteins to those calcium binding proteins whose structures

Table 1 *Physical data comparisons of Brookhaven calcium binding domains*

Protein	Sequence	RMS (Å)[a]	C_1^{α}–C_6^{α} distance (Å)	Metal–metal distance (Å)[b]
Prothrombin 18–23 model	C-L-E[c]-E[c]-P-C	0.00	6.33	4.83
Actinoxanthin 83–88	C-A-T-D-A-C	0.81	5.21	0.00
Staphylococcus nuclease 18–23	I-D-G-D-T-V	2.02	5.38	0.94
Southern bean mosaic virus c136–c141	Q-Y-D-M-A-D	2.23	7.49	3.72
Porcine phospholipase 89–94	N-A-C-E-A-F	2.53	8.69	0.94
Erabutoxin *b* 55–60	C-E-S-E-V-C	1.86	6.11	–
α-Bungarotoxin 60–65	C-S-T-D-K-C	1.88	6.28	–
Parvalbumin b 51–56	D-Q-D-K-S-G	1.63	6.46	5.92
Parvalbumin b 90–95	D-S-D-G-D-G	1.60	6.52	5.52
Tobacco mosaic virus 53–58	Q-G-D-D-I-N	1.64	9.13	9.35
Tobacco mosaic virus 136–141	S-L-T-G-E-S	1.75	4.66	6.80
Thermolysin 56–61	A-D-A-D-N-Q	2.25	10.77	6.66
Thermolysin 194–199	T-P-G-I-S-G	2.17	9.61	9.17
Intestinal calcium-binding protein 14–19	N-A-K-E-G-D	1.75	7.10	7.27
Intestinal calcium-binding protein 54–59	N-G-N-G-D-G	1.71	6.64	5.83

[a] Comparison to prothrombin 18–23 model conformation.
[b] Distances from heavy metal ion, UO_2^{2+}, after superimposed to actinoxanthin 83–88 structure.
[c] These residues are γ-carboxyglutamic acids.

have been solved by X-ray (Brookhaven crystallographic data base) in search of similar structures. Confining our original search to Cys^1–Cys^6 cyclic sequences, we found 14 such regions in 11 proteins of known crystal structure. A very close comparison was found in actinoxanthin, an antitumor, antibiotic class of protein (Eastman et al., manuscript in preparation). It was also found that this six-residue disulfide-bridged loop was responsible for binding heavy metal ions, UO_2^{2+} and Pb^{2+}, used for phase determination of the crystal coordinates. This discovery prompted us to expand our search to include all known linear sequences involving calcium ion binding regions. This expanded investigation resulted in the working hypothesis that calcium binding sites may be defined by a six-residue backbone sequence possessing hydrophilic side-chain carboxyl or hydroxyl groups within a *loop* region. The constraint inherent in Cys^1–Cys^6 rings, along with the aspartic, glutamic, threonine, or serine residues within the disulfide-bridged segment results in a loop capable of functioning as metal (Ca^{2+}) binding regions in proteins. In addition, linear six-residue calcium binding loop regions found in Brookhaven have remarkable conformational and sequential similarities to the original, constrained disulfide-bridged structures. Within this basic motif several variations of metal liganding are found as seen by some of the large distances reported for metal–metal comparisons. The model structure has the metal bound *away* from the loop, while several structures induce the metal into a region closer to the *center* of the loop. Finally, the metal can bind on either side of the loop.

We have, in addition, searched the National Biomedical Research Foundation data base (NBRF) for evidence of other possible cyclic 1,6-disulfide-bridged calcium binding loops. Metal binding properties for the majority of these identified Cys^1–Cys^6 loops remain to be determined; however, the conserved nature of these disulfide bridges among species, along with their hydrophilic side-chain homology strengthens the hypothesis that such structures are capable of functioning as a metal binding domain.

References

1. Eastman, M.A., Pedersen, L.G., Hiskey, R.G., Pique, M., Koehler, K.A., Gottschalk, K.E., Némethy, G. and Scheraga, H.A., Int. J. Pept. Prot. Res., 27 (1986) 530.
2. Struthers, R.S., Rivier, J. and Hagler, A.T., In Vida, J.A. and Gordon, M. (Eds.) ACS Symposium Series, Conformationally Directed Drug Design: Peptides and Nucleic Acids as Templates or Targets, American Chemical Society, Washington, DC, 1984, pp. 239–261.
3. Hagler, A.T., In Hruby, V.J. (Ed.) The Peptides: Analysis, Synthesis, Biology, Vol. 7, Academic Press, New York, NY, 1985, pp. 213–299.
4. The graphics software package is INSIGHT provided by BIOSYM Technologies, Inc., 10065 Barnes Canyon Road, Suite A, San Diego, CA 92121, U.S.A.

Conformation of the flap of human renin

J.A. Fehrentz[a], A. Heitz[a], F. Heitz[b], C. Carelli[c], F.X. Galen[c], P. Corvol[c] and B. Castro[a]

[a]CCIPE, rue de la Cardonille, F-34094 Montpellier Cedex, France
[b]Laboratoire de Physico-Chimie des Systèmes Polyphasés, F-34033 Montpellier, France
[c]INSERM U36, 17 rue du Fer à Moulin, F-75005 Paris, France

Introduction

Renin is a key hormone in the regulation of blood pressure; as other aspartyl proteases, it contains a flexible region named flap, which is thought to play a major role in the enzymatic activity [1]. A β-hairpin structure has been proposed [2] for the flap on the basis of crystallographic data obtained on other aspartyl proteases. In order to check this possible conformation, four peptides containing the flap sequence of human renin were synthesized. Two of them are linear while the other two are ring-closed through appropriately designed disulfide bridges.

L R Y S T G T V S G: Peptide I, [81–90]-human renin
T E L T L R Y S T G T V S G F L S: Peptide II, [77–93]-human renin
C L R Y S T G T V C: Peptide III, (Cys-80, Cys-89) [80–89]-human renin
C L T L R Y S T G T V S G C: Peptide IV, (Cys-78, Cys-91) [78–91]-human renin

Results and Discussion

Conformational investigations based mainly on ^{1}H NMR and IR techniques show that all peptides adopt a secondary structure in DMSO. All the NMR observations confirm the presence of the reversal in the four peptides. In peptides III and IV, the temperature coefficients and the observed NOEs [3] reveal typical features as expected for two strands with an antiparallel disposition. Fig. 1 represents a conformation identified for peptide IV consistent with the observed NOEs.

The fact that the two cyclic peptides are both recognized by polyclonal and monoclonal antibodies [4] raised against human renin while the two linear peptides do not bind them suggest that (a) the cyclic peptides present a conformation very close to that expected for the human renin flap, (b) the flap is an immunopotent region of human renin which can belong to a discontinuous

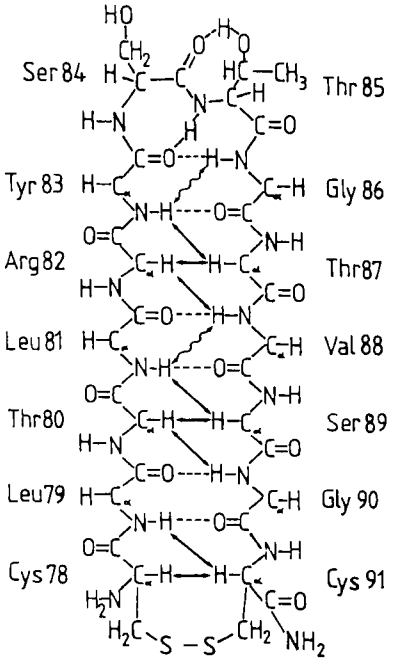

Fig. 1. Schematic drawing of the proposed conformation of the flap based on NMR observations. Observed NOEs only on peptide III (⟿), and on peptides III and IV (⟷).

epitope, and (c) the presence of the two antiparallel strands seems to be necessary for recognition by the antibodies (since the two linear peptides contain the turn region but not the complete antiparallel strands).

Conclusion

From these observations, it can be concluded that all four peptides adopt a secondary structure in DMSO close to that expected for human renin; however, a higher flexibility exists for peptide I, which is probably due to the shortness of the peptide chain. The β-hairpin loop structure is strongly stabilized by the presence of a disulfide bridge and acts in a manner similar to the remainder of the protein, as revealed by the cyclic peptides' ability to bind antirenin antibodies.

References

1. James, M.N.G. and Sielecki, A.R., Biochemistry, 24 (1985) 3701.
2. James, M.N.G. and Sielecki, A.R., J. Mol. Biol., 163 (1983) 299.
3. Kuo, M.C. and Gibbons, W.A., Biophys. J., 32 (1980) 807.
4. Galen, F.X., Devaux, C., Atlas, S., Guyenne, T., Ménard, J., Corvol, P., Simon, D., Cazaubon, C., Richer, P., Badouaille, G., Richaud, J.P., Gros, P. and Pau, B., J. Clin. Invest., 74 (1984) 723.

Isotope-filtered proton NMR experiments for the conformational determination of peptides in solution and bound to biomacromolecules

Stephen W. Fesik, Robert T. Gampe, Jr., Edward T. Olejniczak, Jay R. Luly, Herman H. Stein and Todd W. Rockway

Pharmaceutical Discovery Division, Abbott Laboratories, Abbott Park, IL 60064, U.S.A.

Introduction

Extracting structural information from proton NMR spectra of large peptides in solution or of small peptides bound to biomacromolecules can be extremely difficult due to the severe overlap of many signals. Recently, however, experimental approaches have been introduced to overcome some of these limitations by selectively detecting protons attached to an isotopically labeled nucleus [1, 2] and their scalar [2, 3] or dipolar coupled [3–6] partners. Here, we report on the application of isotope-filtered NMR experiments in the conformational analysis of atrial natriuretic factor [7–23] in sodium dodecyl sulfate (SDS-d25) micelles and in a structural study of a pepsin/inhibitor complex using experimental schemes containing an echo difference pulse sequence.

Results and Discussion

As will be described in detail elsewhere (manuscript submitted for publication), isotope-filtered 2D NOE spectra were acquired of a trilabeled analog of atrial natriuretic factor, [^{15}N-G10, A17, G20] ANF(7–23), in SDS. From the spectral simplification achieved in the experiment, cross peaks were resolved which could not be analyzed in conventional 2D NOE spectra. Proton-proton distances derived from this data as well as those calculated from a quantitative analysis [7] of several conventional 2D NOE data sets were used to generate three-dimensional structures of ANF(7–23) using distance geometry and restrained energy minimizations. Unlike the conformational averaging observed in NMR studies of ANF analogs in bulk solvents (H_2O, DMSO) [8], the NMR data of ANF(7–23) in SDS micelles was indicative of a more ordered three-dimensional structure composed of defined loops.

Isotope-filtered proton NMR experiments were also applied in a structural study of a porcine pepsin/inhibitor (**1**) complex. Fig. 1A depicts an ^{15}N-decoupled

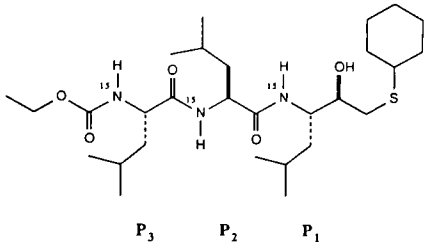

1

isotope-filtered proton NMR spectrum of the complex in H_2O/D_2O (9/1). Only those NMR signals corresponding to protons of **1** that are attached to ^{15}N are observed. Excellent suppression of the remaining proton NMR resonances of the inhibitor and pepsin was achieved in these experiments, as illustrated by a comparison with the conventional proton NMR experiment (Fig. 1B).

In order to measure the NH exchange rates of the bound ligand, a series of isotope-filtered proton NMR spectra was acquired after the addition of D_2O. Under the experimental conditions employed, the P_1 NH exchanged more slowly than the P_2 NH and P_3 NH. These results were used to define the relative solvent

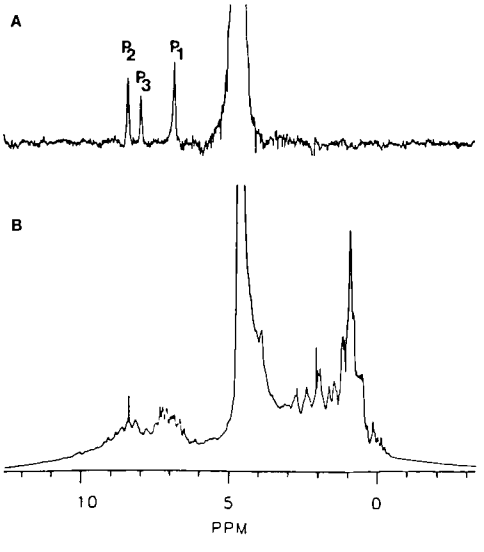

*Fig. 1. Proton NMR experiments of a pepsin/inhibitor (**1**) complex: (A) isotope-filtered; (B) conventional. Assignments were made by studying singly labeled inhibitors.*

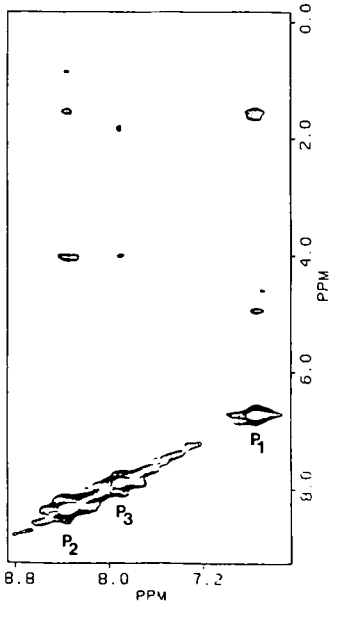

*Fig. 2. Contour plot of an isotope-filtered 2D NOE experiment of a 1 mM pepsin/inhibitor (**1**) complex.*

accessibility for the different parts of the bound inhibitor and/or the NH protons involved in hydrogen bonds.

Fig. 2 depicts part of a contour map from an isotope-filtered 2D NOE experiment ($\tau m = 30$ ms) of the pepsin/inhibitor (**1**) complex. NOEs were observed along ω_1 between the protons attached to the ^{15}N labeled nuclei of the ligand and the protons in close proximity to these nuclei within the inhibitor and pepsin. NOE cross peaks were assigned from additional experiments using inhibitors with perdeuterated residues. From an analysis of the NOE data, the conformation of the bound ligand was deduced.

References

1. Griffey, R.H., Redfield, A.G., Loomis, R.E. and Dahlquist, F.W., Biochemistry, 24 (1985) 817.
2. Wilde, J.A., Bolton, P.H., Stolowich, N.J. and Gerlt, J.A., J. Magn. Reson., 68 (1986) 168.
3. Otting, G., Senn, H., Wagner, G. and Wüthrich, K., J. Magn. Reson., 70 (1986) 500.
4. Bax, A. and Weiss, M.A., J. Magn. Reson., 71 (1987) 571.
5. Rance, M., Wright, P.E., Messerle, B.A. and Field, L.D., J. Am. Chem. Soc., 109 (1987) 1591.
6. Griffey, R.H., Jarema, M.A., Kunz, S., Rosevear, P.R. and Redfield, A.G., J. Am. Chem. Soc., 107 (1985) 711.
7. Olejniczak, E.T., Gampe, R.T., Jr. and Fesik, S.W., J. Magn. Reson., 67 (1986) 28.
8. Fesik, S.W., Holleman, W.H. and Perun, T.J., Biochem. Biophys. Res. Commun., 131 (1985) 517.

Modulation of membrane morphology by basic proteins and polypeptides

Paul E. Fraser and Charles M. Deber

Research Institute, Hospital for Sick Children, Toronto M5G 1X8 and Department of Biochemistry, University of Toronto, Toronto M5S 1A8, Ontario, Canada

Introduction

Central nervous system myelin exhibits instability and eventual breakdown under certain pathological conditions [1]. Myelin contains an extrinsic membrane protein – myelin basic protein (MBP) – which may assist in the maintenance of the myelin bilayers [2]. In view of recent investigations demonstrating the potential of nonbilayer lipid structures to destabilize membranes [3, 4], we have been examining – principally by X-ray diffraction and ^{31}P NMR – the ability of basic proteins and polypeptides to preferentially stabilize the bilayer arrangement from a preexisting hexagonal phase (H_{II}). The H_{II}-forming dioleoylphosphatidylethanolamine (DOPE) has been used as a representative model of such membrane-destabilizing lipids.

Results and Discussion

At pH 9, DOPE is negatively charged due to deprotonation of its head group amine. The presence of this charge allows for electrostatic binding of the basic proteins and, as shown by the X-ray diffraction data in Table 1, the conversion of DOPE from a hexagonal to lamellar phase was induced by MBP, histone IV (H4), and poly-lysine (PL). Lysozyme, however, appeared to maintain the DOPE hexagonal phase (confirmed by ^{31}P NMR; spectra not shown), while the bee venom peptide melittin produced disordering of the lipid packing (i.e., membrane disruption) as indicated by the lack of coherent X-ray reflections. Titration to pH 7 (where DOPE becomes a neutral lipid) resulted in the dissociation of all proteins, except melittin, from the lipid. This latter result demonstrates the importance of the initial electrostatic interaction between protein and lipid (i.e., the loss of this interaction creates a situation where only the hydrophobic component can provide the attractive force). With the exception of melittin, which is known to contain a significant membrane-penetrating hydrophobic segment, the other proteins, however, did not appear to display sufficient non-electrostatic binding sites.

Table 1 *X-ray diffraction data on morphological states of model lipid systems*

Sample	DOPE[a] pH 9	DOPE[a] pH 7	DOPE : PS[a] (95 : 5 w/w)
Lipids only	HEX (67.1 Å)[b]	HEX (64.3 Å)[b]	HEX (66.0 Å)[b]
+ MBP (40% w/w)	LAM (74.0 Å)[b]	HEX (66.6 Å)[b]	LAM/HEX (78.0/66.0 Å)[b]
+ Histone IV (40%)	LAM (66.4 Å)[b]	HEX (65.4 Å)[b]	HEX (66.0 Å)[b]
+ Poly-lysine (20%)	LAM (58.6 Å)[b]	HEX (64.7 Å)[b]	HEX (66.6 Å)[b]
+ Lysozyme (40%)	HEX (71.0 Å)[b]	HEX (65.2 Å)[b]	–
+ Melittin (40%)	Central scatter	Central scatter	–

[a]DOPE = dioleoylphosphatidylethanolamine; PS = phosphatidylserine.
[b]Lipid phases: HEX = hexagonal; LAM = lamellar. Repeat dimensions given in angstroms (Å).

To examine the contributions of both electrostatic and hydrophobic protein/lipid interactions, DOPE was combined with a small quantity of the anionic lipid phosphatidylserine (PS). As seen in Table 1, among previously lamellar-promoting proteins (MBP, H4, and PL), only MBP was capable of incorporating a significant proportion of the uncharged DOPE into an overall lamellar lipid structure.

These results indicate that bilayer stabilization may be dependent on a number of physical-chemical protein properties, which include: (i) sufficient complementation of protein-lipid electrostatic interactions; (ii) the inclusion of a sufficient hydrophobic component; (iii) balanced distribution of protein charged and uncharged residues (viz. the case of melittin); and (iv) an extended chain conformation (as demonstrated by the lysozyme case). The property of MBP to stabilize the bilayer under a variety of conditions may provide an important myelin stabilization factor.

References

1. Wood, D.D. and Moscarello, M.A., J. Membr. Biol., 79 (1984) 195.
2. Fraser, P.E., Moscarello, M.A., Rand, R.P. and Deber, C.M., Biochim. Biophys. Acta, 863 (1986) 282.
3. Cullis, P.R., Hope, M.J., de Kruijff, B., Verkleij, A.J. and Tilcock, C.P.S., In Kuo, J.F. (Ed.) Phospholipids and Cellular Regulation, CRC Press, Boca Raton, Florida, 1985, p. 1.
4. Siegel, D.P., Biophys. J., 49 (1986) 1155.

An application of distance geometry in the modeling of peptides: A molecular complex of the aglycon of aridicin A

Judith C. Hempel, Luciano Mueller, Sarah L. Heald and Peter W. Jeffs
Smith Kline and French Laboratories, 709 Swedeland Road, Swedeland, PA 19479, U.S.A.

Introduction

The glycopeptide antibiotic aridicin A is thought to exert its effect by binding to the C-terminal D-alanyl-D-alanine residues of bacterial cell wall components [1]. Distance geometry [2] has been used to generate models for a molecular complex of the aglycon of aridicin A bound to Ac-Lys(Ac)-D-Ala-D-Ala which are consistent with over 100 NOEs derived from 2D NMR studies. Questions which arise in distance geometry studies include: which features of the conformations generated characterize all possible conformers and has the algorithm sampled the full range of possible conformations. In this study, an identification of NOE-defined structural templates allows us to identify conformationally stable regions of the molecular complex and predict regions of conformational variability in the models.

Results

There are 55 structural templates in our data set in addition to those derived from chemical bonding. These are sets of atoms for which all interatomic distances are specified by chemical bonding and/or NOE information. Fig. 1 is a graphical analysis of the NOE structural templates. Heights of the diagonal peaks are proportional to the number of atoms in each template. Off-diagonal entries indicate that atoms are shared between templates. NOE structural templates for the molecular complex are ordered by chemical structure in Fig. 1, proceeding logically from the N- to C-terminus of the aglycon heptapeptide, as indicated by the residue labels of the aglycon, and from the C- to N-terminus of the bound tripeptide.

As implied by an inspection of Fig. 1, models generated by distance geometry vary primarily in the relative orientation of the GCFB and BEAD regions of the aglycon. Conformational variation is minor. The peptide backbones of aglycon and tripeptide are antiparallel, and the C-terminus region of the tripeptide fits snugly into the binding conformation of the aglycon. An example is given in Fig. 2. Fig. 2, derived solely from chemical structure and NOE distance

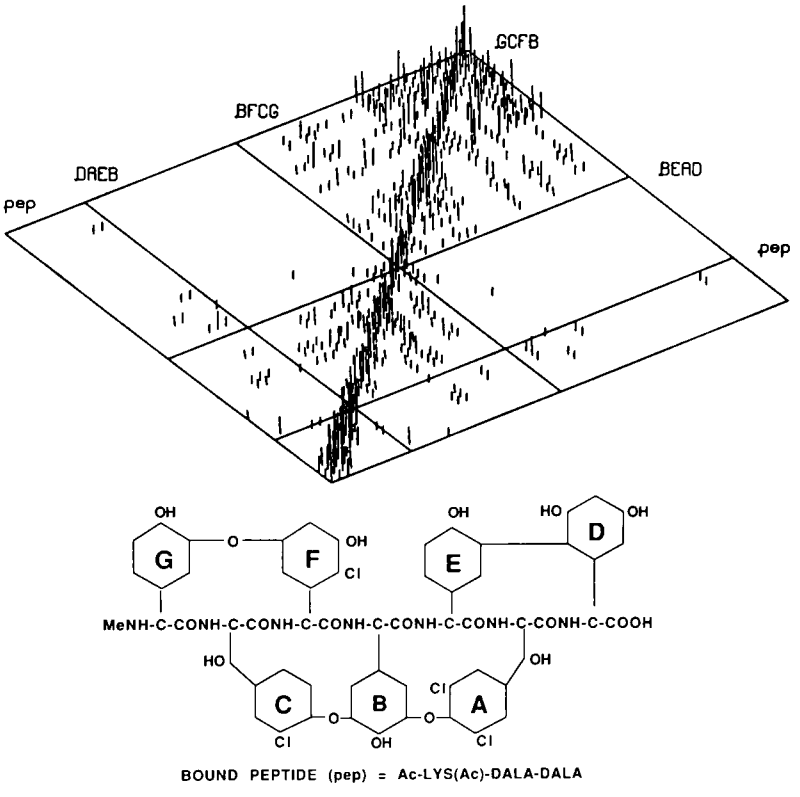

Fig. 1. NOE template analysis molecular complex.

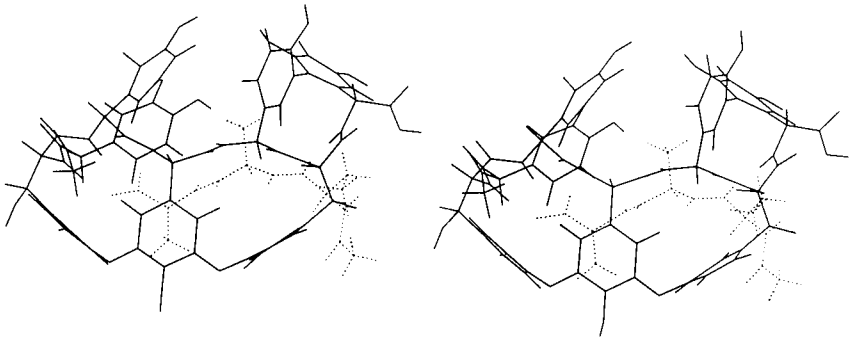

Fig. 2. Solution conformation model.

constraints, is similar to a previously proposed model for aridicin A (unbound) [3] and for ristocetin bound to the tripeptide Ac-Lys(Ac)-D-Ala-D-Ala [4].

References

1. Williams, D.H., Rajananda, V., Williamson, M.P. and Bojesen, G., Top. Antiobiotic Chem., 5 (1980) 119.
2. Havel, T.F., Kuntz, I.D. and Crippen, G.M., Bull. Math. Biol., 45 (1983) 665.
3. Jeffs, P.W., Mueller, L., DeBrosse, C., Heald, S.L. and Fisher, R., J. Am. Chem. Soc., 108 (1986) 3063.
4. Fesik, S.W., O'Donnell, T.J., Gampe, Jr., R.T. and Olejniczek, E.T., J. Am. Chem. Soc., 108 (1986) 3165.

Vibrational circular dichroism of polyproline

Rina Kobrinskaya, Sritana C. Yasui and Timothy A. Keiderling
Department of Chemistry, University of Illinois at Chicago, Box 4348, Chicago, IL 60680, U.S.A.

Introduction

Poly-L-proline (PLP) exists in two forms, designated as I and II. In the solid state, form I is a right-handed 3_1-helix of *cis* amides and form II is a left-handed 10_3-helix of *trans* amides. Considerable work has been reported on the conformation of PLP in solution, particularly as determined with electronic circular dichroism (CD). Controversy has arisen over the relationship of these spectra to that obtained from a random coil of polypeptides [1, 2]. In this paper, we present our initial vibrational circular dichroism (VCD) studies for PLP in helical and random-coil conformations. These are designed both to shed light on the random-coil problem and to determine if the PLP I and II conformers give unique VCD differentiable from that of the other helix forms we have studied.

Results and Discussion

Experimental techniques for obtaining VCD of polypeptides in solution have been described previously [3, 4]. Two PLP samples (MW = 5,500 and 19,000) and collagen from human placenta were obtained from Sigma. PLP I was obtained from PLP II by the method of Steinberg et al. [5]. The VCD and IR spectra in Fig. 1 are normalized to $A_{max} = 1.0$ for sake of comparison.

In trifluoroethanol (TFE), both forms have a negative VCD couplet with PLP II (solid line) being about twice the magnitude of PLP I (dotted line) and shifted ~ 10 cm^{-1} to higher energy. Similar results in terms of magnitude and frequency are obtained for PLP II in D_2O, but mutarotation from I to II occurred during measurement, even at 3°C. While $\Delta A/A$ values for PLP II in TFE and D_2O are approximately the same, in D_2O the zero-crossing frequency is ~ 20 cm^{-1} lower.

In Fig. 1b, VCD and absorption spectra of PLP II in 6 M $CaCl_2$ are compared to the D_2O result. While the absorbance broadens, the $\Delta A/A$ values are similar, with the negative lobe being broader and weaker. In 6 M $CaCl_2$, PLP has been reported to be unordered as measured by electronic CD [1, 2]; however, we find that PLP-II-like VCD remains. In 6 M LiBr, we observe broadening of

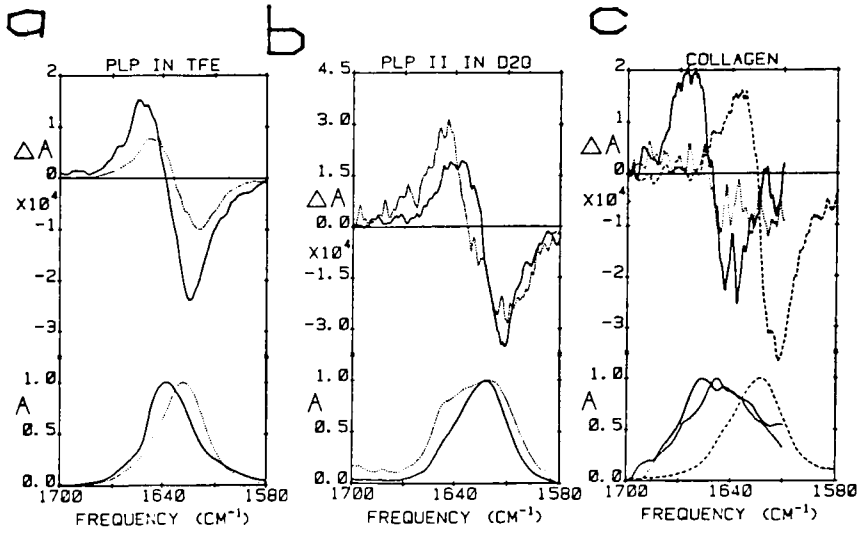

Fig. 1. VCD and absorption of (a) PLP I (·····) and PLP II (——) in TFE, (b) PLP II in D_2O (——) and 6 M $CaCl_2$ (·····) and (c) collagen at 25°C (——) and *45°C (·····) compared to PLP II in D_2O at 25°C (-----).*

the positive peak; and, with heating to ~65°C, the negative peak collapses to less than a third of its original intensity. Unordered structure formation is thus obtained only at high temperatures.

Collagen is expected to have a triple 10_3-helix and exhibits an electronic CD consistent with PLP II. The collagen VCD was obtained by dissolving 10 mg in 2 ml of $D_2O + 2$ μl of acetic acid (Fig. 1c). While the collagen couplet (solid line) resembles that of PLP II (dashed line), the frequency is shifted up almost 30 cm^{-1} and the absorption is broadened due to the presence of secondary and tertiary amides in collagen. When the sample temperature is raised to ~45°C, the VCD collapses (dotted line) appropriate to the unordered form [6]. PLP II is more stable, requiring both salt and high temperature to lose its characteristic VCD.

In summary, we have demonstrated that PLP structures give VCD differentiable from that of other helices and consistent with the spectra we have found for a series of random-coil conformations of charged and aromatic side-chain polypeptides[7, 8].

Acknowledgements

This work was supported by the National Institutes of Health (GM 30147), which we gratefully acknowledge.

References

1. Balasubramanian, D., Biopolymers, 13 (1974) 407.
2. Tiffany, M.L. and Krimm, S., Biopolymers, 6 (1968) 1767.
3. Keiderling, T.A., Appl. Spectrosc. Rev., 17 (1981) 189.
4. Keiderling, T.A., Nature, 322 (1986) 851.
5. Steinberg, I.Z., Berger, A. and Katchalski, E., Biochim. Biophys. Acta, 28 (1958) 647.
6. Tiffany, M.L. and Krimm, S., Biopolymers, 8 (1969) 346.
7. Yasui, S.C. and Keiderling, T.A., J. Am. Chem. Soc., 108 (1986) 5576.
8. Yasui, S.C. and Keiderling, T.A., Biopolymers, 25 (1986) 5.

Conformational mobility in the vasopressin series

Charles W. DeBrosse, Judith C. Hempel and Kenneth D. Kopple*
L-940, Smith Kline and French Laboratories, Research and Development Division, P.O. Box 1539, King of Prussia, PA 19406-0939, U.S.A.

To assess conformational mobility in vasopressin analogs, the proton NMR spectrum of arginine vasopressin (AVP) and the analog [Pmp[1], D-Tyr(Et)[2], Val[4], desGly[9]]AVP (Pmp = 3,3-pentamethylene-3-mercaptopropionic acid) (I) have been investigated in methanol at low temperatures [1]. Differential line broadening below −20°, suggesting slow conformational exchange, is observed. This is illustrated in the spectra of I (Fig. 1). For example, the resonances of the backbone Val H^{α} (A, 4.07 ppm) and Pmp H_2 (B, 2.5 ppm) can be seen to be more broadened in the 246 K spectrum than the resonances of the side chain Tyr(Et) – OCH_2 – (C, 3.95 ppm) or the 'tail' Arg^8 H^{α} (4.35 ppm).

Differential broadening under similar conditions among the α-proton resonances of AVP is also obvious in the AVP spectrum (not shown). Such effects are the result of chemical exchange, not the consequence of an increase in overall

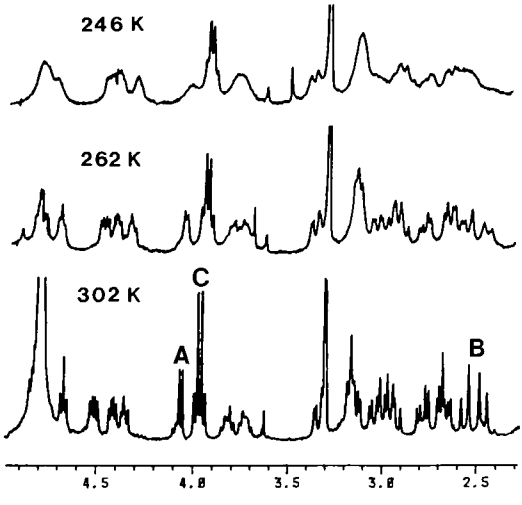

Fig. 1. NMR spectra of analog I.

*To whom correspondence should be addressed.

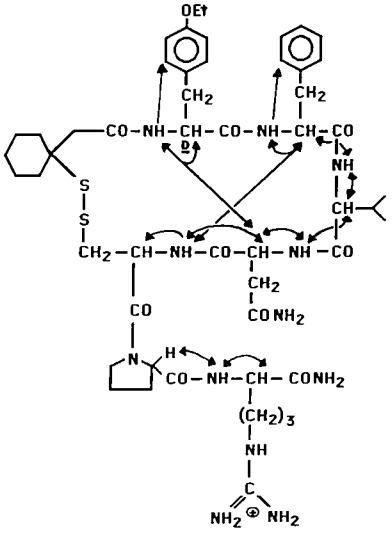

Fig. 2. Observed NOEs for analog I.

rotational correlation time. (The viscosity of methanol at 230 K is about 2 cP, comparable to dimethyl sulfoxide at room temperature.) Separate conformations of AVP or I have not gone into slow exchange at 200 K.

Observation of exchange broadening at low temperatures indicates that these vasopressin analogs must be rapidly exchanging mixtures of conformations at room temperature. This is consistent with the recently reported [2] disorder in the crystal structure of deamino oxytocin, and it explains inconsistencies we find in constructing models of I from coupling constant and nuclear Overhauser enhancement (NOE) data.

In DMSO at room temperature, the NOEs shown in Fig. 2 are observed for I. Of particular interest as indicators of ring conformation are the transannular interactions Tyr NH <-> Asn H^{α} and Cys NH <-> Phe H^{α}.

Taking the observed NOEs to indicate interproton distances of ≤ 3.5 Å, and using all combinations of ranges of ϕ suggested by the HNCH coupling constants (all ≥ 8 Hz except for $Asn^5 = 6$ Hz), we employed distance geometry [3] to construct several hundred models of the backbone of I.

When both transannular NOEs were incorporated as constraints in the distance geometry calculation, all of the resulting models that were physically realistic contained short interproton distances that should result in additional, but unobserved, NOEs. When the interproton distances not corresponding to observed NOEs were constrained to > 3.2 Å, physically unrealistic models were obtained. Only when the transannular NOE constraints were used singly were

models obtained that predict just the experimentally observed NOEs. Each of the two observed transannular effects thus most probably arises from a different ring conformation type (i.e., the observed effects are averages over rapidly exchanging conformations).

We suggest that studies at low temperature will show that many other cyclic peptides are mixtures of rapidly exchanging backbone conformations at room temperature. The need for caution in constructing models in such cases is obvious.

References

1. Huffman, W.F., Ali, F.E., Bryan, W.M., Callahan, J.F., Moore, M.L., Silvestri, J.S., Yim, N.C.F., Kinter, L.B., McDonald, J.E., Ashton-Shue, D., Stassen, F.L., Heckman, G.D., Schmidt, D.B. and Sulat, L., J. Med. Chem., 28 (1985) 1759.
2. Wood, S.P., Tickle, I.J., Treharne, A.M., Pitts, J.E., Mascarenhas, Y., Li, J.Y., Husain, J., Cooper, S., Blundell, T.L., Hruby, V.J., Buku, A., Fischman, A.J. and Wyssbrod, H.R., Science, 232 (1986) 633.
3. Havel, T.F., Kuntz, I.D. and Crippen, G.M., Bull. Math. Biol., 45 (1983) 665.

Conformation and motion of biologically active peptides as bound to phospholipid membrane

Alain Milon[a,b], Kaori Wakamatsu[a], Kazuki Saito[a], Akihiko Okada[a], Tatsuo Miyazawa[a] and Tsutomu Higashijima[a]

[a]*Department of Biophysics and Biochemistry, Faculty of Science, University of Tokyo, 7-3-1 Hongo, Bunkyo-ku, Tokyo 113, Japan*

[b]*Laboratoire de Chimie des Substances Naturelles, Associe au CNRS, Université Louis Pasteur, Centre de Neurochimie, 5 rue Blaise Pascal, 67084 Strasbourg, France*

Introduction

For many physiologically active peptides, the first step involved in the activity is the binding to a receptor embedded in a membrane. In this recognition process, the membrane itself plays an important role [1]. Therefore, in order to understand conformation-activity relationships, it is interesting to analyze the conformation and mobility of peptides as bound to phospholipid membranes. Liposomes made of mixtures of natural phospholipids organized in bilayers are convenient models of natural membranes, preferable for instance to micelles.

For peptides bound to liposomes, however, ^{1}H NMR signals are too broad to be observed and they overlap with those of the phospholipids. To overcome this difficulty, perdeuterated phospholipids (DPPC and DLPS) have been synthesized [2]. By carefully adjusting the experimental conditions (temperature, pH, ionic strength, peptide-to-phospholipid ratio), it is possible, for many small amphiphilic peptides, to establish an equilibrium between a free state and a membrane-bound state and to observe transferred nuclear Overhauser effect (TRNOE). We have thus determined the conformation in the membrane-bound state of several active peptides, including α-mating factor from *S. cerevisiae*, enkephalin, melittin, mastoparan, LHRH, and their analog peptides [2–5].

Results and Discussion

α-Mating factor is a pheromone secreted by the α type cell of *S. cerevisiae*. Its primary structure is: Trp-His-Trp-Leu-Gln-Leu-Lys-Pro-Gly-Gln-Pro-Met-Tyr. The minimal structure required for activity is His^2-Gln^{10}. By the ^{1}H TRNOE method in the presence of perdeuterated DPPC, we have found intramolecular proximities. These data, together with circular dichroism analyses, are consistent with the existence of a compact 3_{10}-helix for the Trp^1-Gln^5 residues (many i,

i+3 interresidue TRNOEs were observed for the first five residues) and an extended structure for the Leu^6-Gln^9 residues. The last four C-terminal residues give very weak intraresidue TRNOEs which indicates that those residues are not tightly bound to the bilayer. Interestingly, a similar TRNOE pattern was observed for an active decapeptide analog Trp^1-Gln^{10}, thus indicating a similar conformation (collaboration with Y. Masui and S. Sakakibara).

We have analyzed the conformation of several analogs of Leu-enkephalin (Tyr-Gly-Gly-Phe-Leu) bound to liposomes (DPPC-d + DLPS-d; the presence of DLPS in the bilayer increases the binding of these peptides). Gly^2 has been substituted by D-Ala (10-times increase in the activity) and by L-Ala (complete loss of the activity). The TRNOE patterns of these two analogs in H_2O are clearly different from each other. For the D-Ala^2 derivative, all the proximities among NH, α, and β protons have been determined and are consistent with a type II' β-turn involving the C-terminal four residues. The Tyr residue shows very weak intra- and interresidue TRNOEs and is believed to protrude outside the bilayer in the aqueous phase. In the case of the L-Ala^2 derivative, the data indicate a hydrogen bond between the carboxylate and the NH of Gly^3. The Tyr residue is folded below this turn, inside the bilayer (we observed strong TRNOEs with Tyr in this case). We suggest that the location of Tyr with respect to the bilayer may be of critical importance for the activity.

Finally, the dynamics of mastoparan (Ile-Asn-Leu-Lys-Ala-Leu-Ala-Ala-Leu-Ala-Lys-Lys-Ile-Leu-NH_2) was studied by ^{2}H NMR [6]. Five analogs, in which one residue was perdeuterated, were synthesized by solution method: [Ala-d^5], [Ala-d^8], [Ala-d^{10}], [Val-d^1, Val^{13}], and [Val^1, Val-d^{13}]. The quadrapole splitting of each compound has been determined at different temperatures and different peptide-to-lipid ratio. Mastoparan is tightly bound to the bilayer, even below the phase transition. The membrane-bound mastoparan was found to be composed of a rigid α-helix core in the C-terminal part and a dangling N-terminal.

These results show that ^{2}H NMR and ^{1}H TRNOE using perdeuterated phospholipids are efficient methods for the analysis of membrane-bound peptides. As further experiments are performed in this direction, the correlation between activity and conformation of membrane-bound peptides is clearly exemplified.

References

1. Schwyzer, R., In Imura, H., Goto, T., Nakajima, T. and Murachi, T. (Eds.) Natural Products and Biological Activities, University of Tokyo Press, Tokyo, 1986, p. 197.
2. Wakamatsu, K., Okada, A., Suzuki, M., Higashijima, T., Masui, Y., Sakakibara, S. and Miyazawa, T., Eur. J. Biochem., 154 (1986) 607.
3. Wakamatsu, K., Okada, A., Higashijima, T. and Miyazawa, T., Biopolymers, 25 (1986) S193.

4. Wakamatsu, K., Higashijima, T., Fujino, M., Nakajima, T. and Miyazawa, T., FEBS Lett., 162 (1983) 123.
5. Wakamatsu, K., Okada, A., Miyazawa, T., Masui, Y., Sakakibara, S. and Higashijima, T., Eur. J. Biochem., 163 (1987) 331.
6. Saito, K., Wakamatsu, K., Higashijima, T., Fujino, M., Nakajima, T. and Miyazawa, T., J. Pharmacobiodyn., 8 (1985) S85.

Two-dimensional NMR and computer modeling studies of two conformers of an actinomycin-related peptide lactone

Anthony B. Mauger[a], James A. Ferretti[b], Kathleen S. Gallagher[b] and James V. Silverton[a]

[a]*Research Foundation of the Washington Healthcare Corp., 108 Irving St., N.W., Washington, D.C. 20010, U.S.A.*

[b]*NHLBI, NIH, Bethesda, MD 20892, U.S.A.*

Introduction

An NMR study by Lackner [1] revealed that I ($R = CH_3$ or $C_6H_5CH_2$) in CD_3COCD_3 adopted a conformation, designated 'A', resembling that of the peptide units of actinomycin D [2]. In $CDCl_3$, a different conformation, designated 'C', was observed and a molecular model proposed.

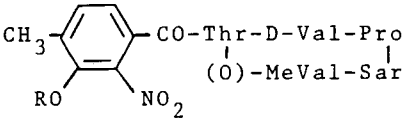

I: R = H
II: R = H and MeAla replaces MeVal

We have reported the assignments of the proton 2D NMR spectra of the A and C conformations of I and II [3]. This paper describes the determination of the solution conformations of A and C using 2D cross-relaxation data (NOESY) in combination with energy minimization computations.

Methods and Results

1. *NMR*

All experiments were performed at room temperature on a Varian XL-300. Resonance assignments for the A and C conformations were made from 2D COSY spectra obtained in CD_3COCD_3 and $CDCl_3$ respectively. Backbone interproton distance measurements were obtained from build-up rates of cross peaks in 2D NOESY spectra. The geminal sarcosine α-protons were used as a calibration distance (1.77 Å). The resulting data were used to construct models as starting points in the energy minimization computations. The primary difference between the two conformers is the presence of *cis* Val-Pro and Pro-Sar peptide bonds in the A conformer; all others are *trans*. This follows from

the contacts $\alpha H^i - \alpha H^{i+1}$ and $\alpha H^i - NH^{i+1}$ observed in *cis* and *trans* peptide bonds, respectively. An intense cross peak between the Pro αH and Sar NCH_3 in the C conformation is incompatible with the previously proposed model [1].

2. *IR*

In a spectrum of I in $CHCl_3$, the only absorption band in NH region was at 3420 cm^{-1}. This implies absence of any intramolecular hydrogen bond such as that postulated in the previously proposed model [1].

3. *Energy minimization*

The XICAMM program [4] was used on an IBMPC/AT/80287 computer. The starting points for refinement were: A conformer, the crystal structure [3]; C conformer, the NMR-derived model; the previously proposed model [1] was also refined without numerical restraints. The three models were refined to completion, and the final strain energies were 10.8, 11.2, and 16.8 kcal/mole, respectively. A and C are shown in Figs. 1 and 2. Interproton distances are in reasonable agreement with those from the NMR study for these structures but not for the earlier model [1], which also has a higher strain energy.

Conclusions

Two solvent-dependent conformations have been characterized for I using measurements obtained by NMR in combination with minimum energy calculations. The energy-minimized A conformer has two *cis* peptide bonds and closely

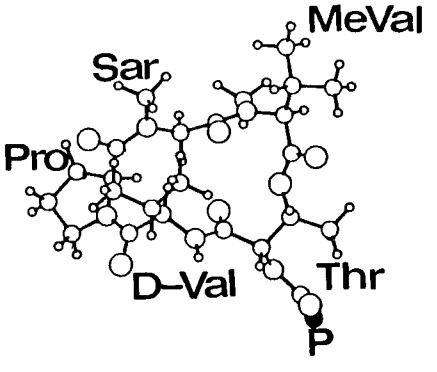

Fig. 1. A Conformation. P = protecting group (3-hydroxy-4-methyl-2-nitrobenzoyl).

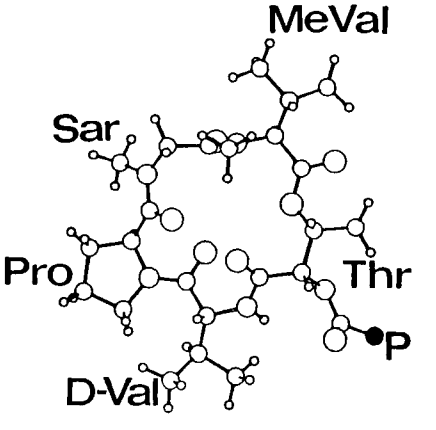

Fig. 2. C Conformation.

resembles the X-ray crystal structure of II [3]. This conformation is similar to that of the peptide units of actinomycin D in solution [1] in its crystalline deoxyguanosine complex [2]. For the C conformation, all peptide bonds were found to be *trans*. It is an open structure with no intraannular hydrogen bonds, in contrast to the previously proposed model. As yet, no suitable crystals of the C conformation have been obtained for X-ray analysis. The results described here demonstrate that the crystal and solution conformations of oligopeptides need not be the same.

Acknowledgements

This investigation was supported in part by PHS grant #CA-11627 awarded (to A.B.M.) by the National Cancer Institute, DHHS.

References

1. Lackner, H., Angew. Chem. Internat. Ed. Engl., 14 (1975) 375.
2. Jain, S.C. and Sobell, H.M., J. Mol. Biol., 68 (1972) 1.
3. Mauger, A.B., Stuart, O.A., Ferretti, J.A. and Silverton, J.V., J. Am. Chem. Soc., 107 (1985) 7154.
4. Brugger, W.E., XICAMM, Xiris Corp., New Monmouth, N.J. 07748 (1986).

2D NMR evaluation of 3D structure of scorpion *Buthus eupeus* neurotoxin M_9 in solution

Vladimir S. Pashkov, N. Anh Hoang, Vladimir N. Maiorov and Vladimir F. Bystrov

Shemyakin Institute of Bioorganic Chemistry, USSR Academy of Sciences, Ul. Miklukho-Maklaya, 16/10, Moscow, V-437 U.S.S.R.

Introduction

Most of the polypeptide toxins separated from scorpion venoms consist of 60–80 amino acid residues (act on mammals or insects), while some insectotoxins are composed of 35–36 residues [1]. Both groups contain four disulfide bonds. This paper deals with NMR investigation of neurotoxin M_9 *Buthus eupeus* (66 amino acid residues). As do other mammalian scorpion toxins, M_9 acts on the sodium channels of excitable membranes [1].

Results and Discussion

Two slowly exchangeable conformers of M_9 are manifested by splitting of the proton NMR signals at acidic pH. The conformational equilibrium apparently is due to the protonation of one or more carboxyl groups with $pK_a \sim 2$ [2]. To determine the spatial structure of the conformer, which predominates under physiologically relevant conditions, the 2D ^1H NMR (COSY and NOESY) spectra were recorded with a Bruker WM-500 spectrometer. Most proton signals of the conformer were assigned, and the data on interproton NOE contacts, coupling constants $^3J(H\text{-}NC^{\alpha}\text{-}H)$, and deuterium exchange rates for the peptide NHs were collected. The data were treated by distance geometry algorithm with amino acid residues represented by two pseudoatoms [2]. Ten conformations consistent with the NOE distance constraints (Fig. 1) were computed. Average root-mean-square deviation between these structures is ~ 0.2 nm. Further refinement of the experimental data in atomic representation with the molecular model showed that the conformer contains the right-handed α-helix (residues 22–31), three-stranded β-sheet (residues 1–5, 46–52, 35–40), and β-turn of type I (residues 54–57). All five X-Pro bonds are in the *trans* configuration. Similar secondary structure patterns (Fig. 2) were revealed for insectotoxin v-3 *Centruroides sculpturatus* (65 residues) [3] and insectotoxin I_5A *Buthus eupeus* (35 residues) [4]. The difference in biological specificity between M_9 and I_5A could be explained

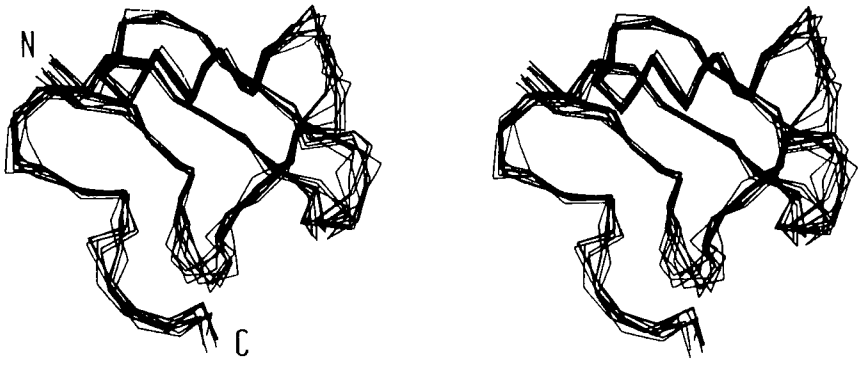

Fig. 1. Stereo drawing of backbone folding of ten calculated M_9 structures.

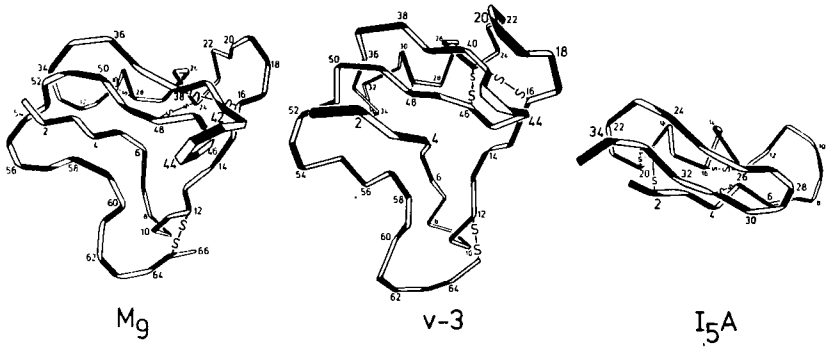

Fig. 2. Backbone folding of the M_9, v-3, and I_5A scorpion toxins.

by additional amino acid residues in M_9. In the case of M_9 and v-3, the difference might be related with the residue substitutions [2].

References

1. Ovchinnikov, Yu.A., Pure Appl. Chem., 56 (1984) 1049.
2. Pashkov, V.S., Hoang, N.A., Maiorov, V.N. and Bystrov, V.F., Bioorgan. Khim. (USSR), 12 (1986) 1306.
3. Zell, A., Ealick, S.E. and Bugg, C.E., In Bradshaw, R.A. and Tang, J. (Eds.) Molecular Architecture of Proteins and Enzymes, Academic Press, New York, 1985, p. 65.
4. Arseniev, A.S., Kondakov, V.I., Maiorov, V.N. and Bystrov V.F., FEBS Lett., 165 (1984) 57.

^{1}H NMR and CD studies of *des*-Trp^1, Nle^{12}-minigastrin in H_2O/TFE

Nancy J. Mammi, Stefano Mammi and Evaristo Peggion
Biopolymer Research Center, Department of Organic Chemistry, University of Padua, Via Marzolo 1, 35131 Padua, Italy

Introduction

Previous conformational and in vivo biological activity studies on gastrin-related peptides led to the hypothesis that the structure assumed by gastrin hormones in TFE is of biological importance. Based on circular dichroism (CD) results, we proposed a conformational model for the minigastrin analog comprising an α-helical segment at the N-terminus and a β-bend located in the central sequence Ala-Tyr-Gly-Trp. To test our hypothesis, we have carried out CD and 400 MHz proton NMR studies on *des*-Trp^1, Nle^{12}-minigastrin in H_2O/TFE mixtures.

Results and Discussion

The assignment of the NMR spectrum of *des*-Trp^1, Nle^{12}-minigastrin in 90% TFE proved to be extremely difficult by the usual methods because of the large OH peak and the methylene quartet of the solvent. We chose to assign the spectrum in water and then to follow the displacement of the resonance peaks from water to TFE. The NMR spectrum in water (not shown) was assigned using 2-D Hartmann-Hahn and one-dimensional NOE spectra. The assigned spectrum in 90% TFE is shown in Fig. 1. At this solvent composition, the CD spectrum indicates the same conformation as in 98% TFE. Temperature-dependence studies indicated that the following amide protons have low temperature coefficients (indicated in parentheses and expressed in -ppb/K): Glu(0.89); Glu(0.70); Trp(2.31); Nle (1.56); Asp(1.76); Phe(2.99). These results are consistent with the presence of an α-helical segment at the N-terminus, comprising the sequence -$(Glu)_5$-, (hydrogen bonding of Glu^5-NH and Glu^6-NH to Leu^1-CO and Glu^2-CO, respectively). Trp-NH also appears to be hydrogen bonded, consistent with the proposed β-turn, which implies a hydrogen bond between Trp-NH and Ala-CO. A new feature revealed by NMR studies is the presence of three additional hydrogen bonds at the C-terminus. A possible

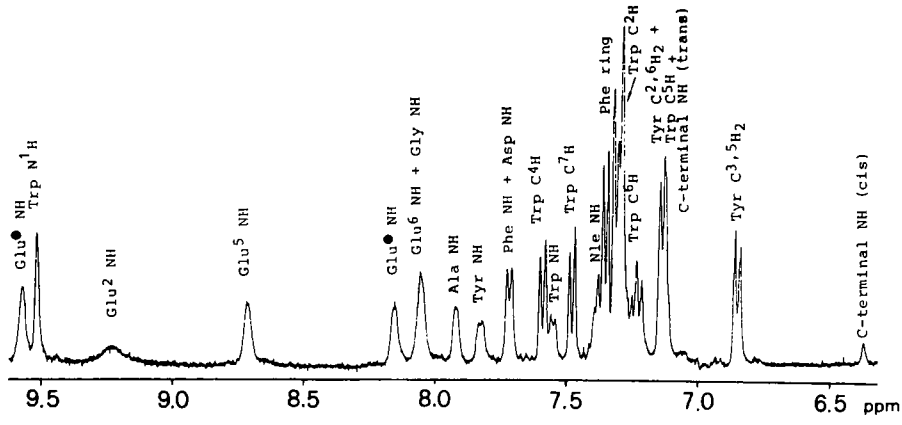

Fig. 1. Downfield region of the assigned 400 MHz spectrum of des-*Trp*[1]*, Nle*[12]*-minigastrin in 90% TFE/10% D_2O. (•) Glu*[3] *and Glu*[4] *cannot be distinguished.*

structure accounting for these results and also consistent with the CD properties is a series of concatenated type I or type III β-turns, with hydrogen bonds of Nle-NH to Tyr-CO, Asp-NH to Gly-CO, and Phe-NH to Nle-CO. This is equivalent to a segment of 3_{10}-helix starting with Ala-CO and including the six C-terminal residues. The data also suggest the presence of a flexible region in the center of the molecule, about the φ and ψ angles of Glu[6] and Ala. This flexibility might allow an interaction between the two proposed helical segments at the two ends of the molecule.

Acknowledgements

Thanks are due to Prof. E. Wünsch for the sample of the minigastrin analog. N.J.M. was supported by an NSF-NATO fellowship.

References

1. Peggion, E., Foffani, M.T., Wünsch, E., Moroder, L., Borin, G., Goodman, M. and Mammi, S., Biopolymers, 24 (1985) 647.
2. Bax, A. and Davis, D., J. Magn. Reson., 65 (1985) 355.

Conformational analysis of 5,5-dimethylthiazolidine-4-carboxylic acid (Dtc), a readily available proline analog

James Samanen[a], Theresa Cash[a], Drake S. Eggleston[a] and Martin Saunders[b]
[a]*Smith Kline and French Laboratories, P.O. Box 1539, King of Prussia, PA 19406-0939, U.S.A.*
[b]*Smith Kline and French Laboratories, The Frythe, Welwyn, Hertfordshire, AL6 9AR, U.K.*

Introduction

5,5-Dimethylthiazolidine-4-carboxylic acid (Dtc) (Samanen et al., manuscript in preparation) is a proline analog readily available from penicillamine. As had been observed [1] with *syn*-(βMe)Pro, the *syn* beta methyl in Dtc could sterically interact with the carboxyl group to destabilize the gamma turn conformation (C_7) preferred by proline. If steric effects of Dtc beta methyl groups on conformation could be defined, then substitution of Dtc for Pro in peptides could provide more information about bioactive conformation.

Results and Discussion

Systematic search via SYBYL (Tripos Associates, St. Louis, MO) of Dtc ring conformations produced seven ring conformations [2]: DENN, DEGN, SGE, SBE, SGN, SBN, and SAN. Boc-L-Dtc X-ray crystal structure unit cell (Samanen et al., manuscript in preparation) contains conformers SGE and SBE. Total conformational energy vs. psi angle (with complete minimization for each value of psi) was calculated via Spin 01 in COSMIC [3] for conformers of Ac-L-[Dtc,(*syn*-βMe)Pro, Tpr, and Pro]-NMe. All conformers are flexible, displaying <8 kcal/mole maximum rotational barriers for psi. Fig. 1 compares E_{TOT} minimum energy regions and coulombic energy (E_{COUL}) minima (*) of Ac-L-Pro-NMe with Ac-L-Dtc-NMe. Ac-L-Pro-NMe (and Ac-L-Tpr-NMe) E_{TOT} and E_{COUL} minima coincide at C_7 where hydrogen bonding occurs. Ac-L-Dtc-NMe [and Ac-L-(*syn*-βMe)Pro-NMe] E_{TOT} and E_{COUL} minima do not coincide at C_7 since *syn*-beta methyl/carboxyl group interactions contribute nonbonded (steric) and angle strain energies to E_{TOT} at C_7 where hydrogen bonding can occur. Six of seven Ac-L-Dtc-NMe conformers display E_{TOT} minima at psi 120–140° and 340°. The lowest energy conformation, SAN, in which nonbonded interactions are minimized, displays an E_{TOT} minimum (80°) much closer to E_{COUL} minimum (60°) than the other conformers. The contribution of SAN and other conformers to Dtc

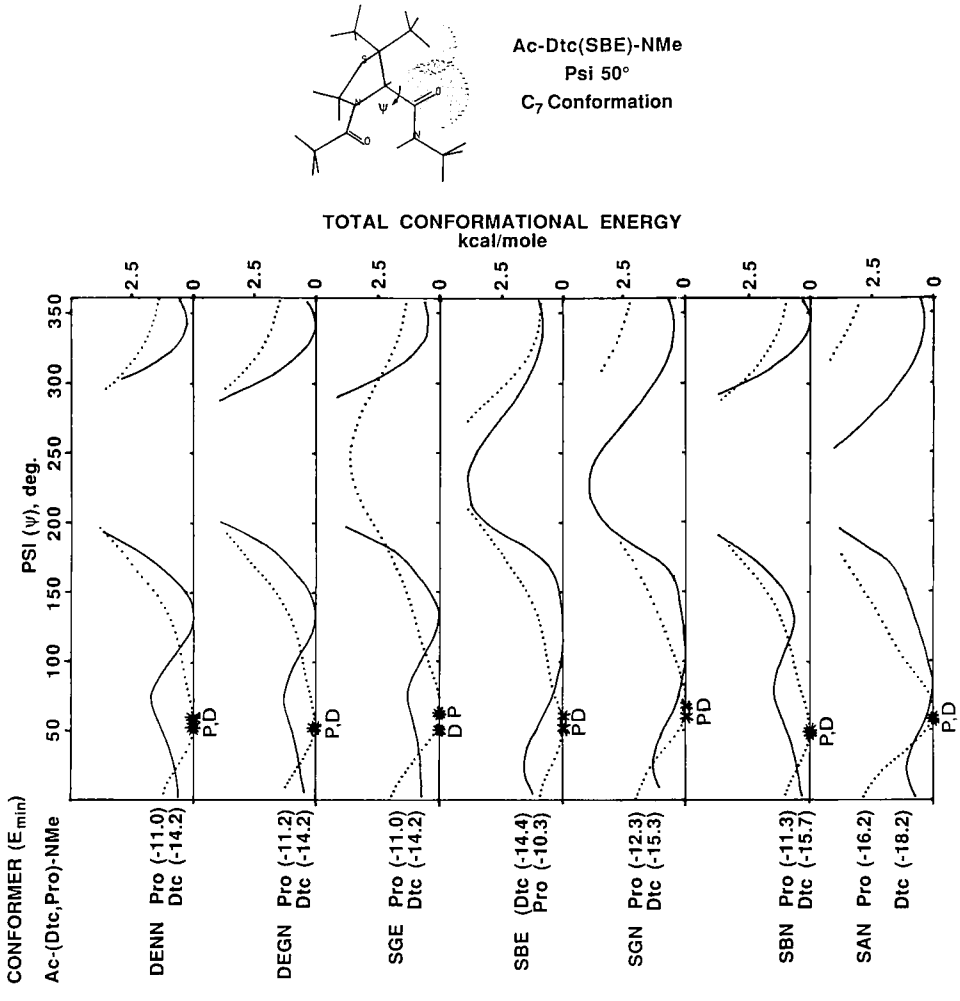

*Fig. 1. Relative total conformational energy vs. psi for conformers of Ac-Pro-NMe (···) and Ac-Dtc-NMe (—). (Left margin displays E_{TOT} minimum, kcal/mole, for each conformer; E_{COUL} minimum = * for Pro = P, Dtc = D.)*

conformer population will be envrionmentally determined (e.g., SAN is absent in the crystal of Boc-L-Dtc); C_7 is diminished in the IR spectrum (CCl_4) of Boc-Dtc-Ile-OMe (Samanen et al., manuscript in preparation). Thus, C_7 is allowed for Dtc-containing peptides, but it may no longer be the preferred conformation. In the absence of other structural influences, peptides that adopt a hydrogen bonded C_7 about a proline residue may adopt other conformations when Dtc is substituted for Pro.

References

1. Delaney, N. and Madison, V., J. Am. Chem. Soc., 104 (1982) 6635.
2. Via Madison, V., Biopolymers, 16 (1977) 2671. Conformers are symmetrical envelope with one atom exo or endo to carboxylate (e.g., SGE = symmetrical-gamma-exo) or half chair with one atom exo to carboxyl and one atom endo (e.g., DEGN = delta-exo-gamma-endo).
3. Vinter, J.G., Davis, A. and Saunders, M.R., J. Comput.-Aided Mol. Design, 1 (1987) 31.

Conformational analysis of model cyclic endothiopeptides by NMR and molecular modeling techniques

Douglas B. Sherman, Richard A. Porter and Arno F. Spatola
Department of Chemistry, University of Louisville, Louisville, KY 40292, U.S.A.

Introduction

Thioamide substitutions in the peptide backbone represent structurally subtle yet conceptually intriguing modifications. Over the past few years, conformational analysis of thionopeptides has been limited to di- and tripeptides [1, 2]. These studies have shown that the thioamide surrogate adopts a *trans* conformation, and there is a marked difference in the folding and hydrogen bonding properties of these pseudopeptides in polar and nonpolar solvents. A next step in conformational analysis would be to examine the compatibility of the thioamide moiety in structural features such as β- and γ-turns. To this end, we have synthesized two model cyclic pseudopentapeptides, cyclo(D-Phe-Proψ[CSNH] Gly-Pro-Gly) **I** and cyclo(D-Phe-Pro-Gly-Proψ[CSNH]Gly) **II** (Fig. 1). The all-amide parent molecule belongs to a class of cyclic pentapeptides known to contain both a β- and a γ-turn [3].

Results and Discussion

Compounds **I** and **II** were synthesized by solution phase methods and characterized by amino acid and FABMS analyses, HPLC, TLC, and spectral

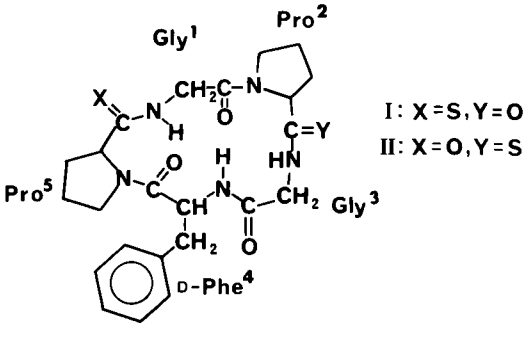

Fig. 1. Proposed structure of the cyclic pseudopentapeptides.

characteristics. Both **I** and **II** exhibit a single conformation in $CDCl_3$ consistent with that of the parent compound. The Pro^2 H^{α}s appear as triplets in the ^1H spectra, while the Pro^5 H^{α}s appear as doublets, the latter feature characteristic of Pro in a γ-turn with a low ψ angle. Supportive evidence can be seen in the ^{13}C spectrum of **II** (Fig. 2A), in which the Pro^5 C^{β} is shifted upfield from a normal 28 ppm to 25 ppm. In compound I (Fig. 2B), this diagnostic shift is effectively canceled by the deshielding effect of sulfur, so that the Pro^5 C^{β} now resonates at 28 ppm along with the unstrained Pro^2 C^{β}.

Temperature dependence in $CDCl_3$ of Gly^1 N-H in **I** ($\Delta\delta/\Delta T = 5.5$ ppb/deg) and **II** ($\Delta\delta/\Delta T = 7.6$ ppb/deg) indicates that the γ-turn hydrogen bonds are weaker than in the parent ($\Delta\delta/\Delta T = 1.8$ ppb/deg), while the D-Phe^4 N-H values for **I** ($\Delta\delta/\Delta T = 0$ ppb/deg) and **II** ($\Delta\delta/\Delta T = 3.2$ ppb/deg) suggest that the β-turn hydrogen bonds are stronger than in the parent ($\Delta\delta/\Delta T = 3.9$ ppb/deg). Nevertheless, there is remarkable consistency between the overall conformational preferences of these thionopeptides relative to the parent.

In DMSO, compound **II** again shows a single conformation, but compound I displays two interconverting conformers in a ratio of 2 : 1 based on integration in the ^1H spectrum (Fig. 3A). The Pro $C^{\beta,\gamma}$ region of the ^{13}C spectrum (Fig. 3B) and temperature dependence data suggest that the minor conformer may be a one-*cis* X-Pro conformer, in which rotation occurs about the Gly^1-Pro^2 bond. The major and minor amide peaks were correlated through magnetization transfer. Because of exchange, saturation of a major amide peak could be detected in the corresponding minor amide peak by a change in intensity of the signal. Quantitative analysis by this technique at various temperatures should make it possible to determine the energy barrier for exchange [4].

Application of energy minimization programs in the SYBYL (Tripos Associates, St. Louis, MO) software to these structures consistently revealed an increase in the ψ angle of the thionated Pro by 3–5°, a factor which may account for

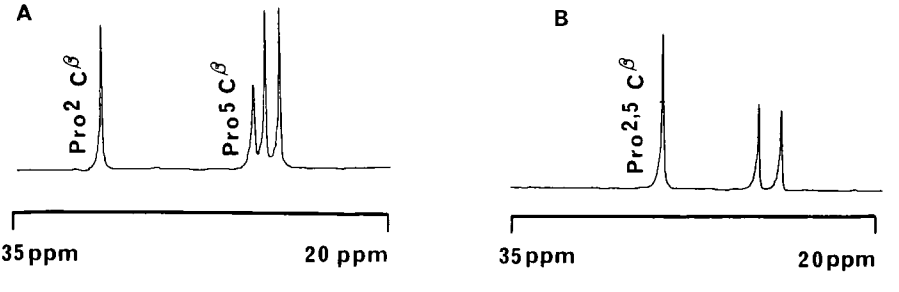

*Fig. 2. $Pro^{2,5}$ $C^{\beta,\gamma}$ region of (A) **II** and (B) **I** in $CDCl_3$.*

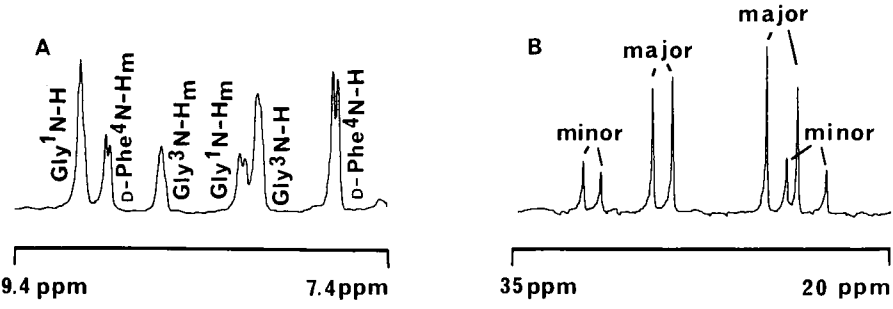

Fig. 3. (A) Amide region of I in DMSO; (B) Pro^{2,5} $C^{\beta,\gamma}$ region of I in DMSO.

the weaker γ-turn hydrogen bond in I due to steric interactions of the thiocarbonyl with the β-methylene.

Future studies will emphasize the biological consequences of thioamide replacements and comparisons with other types of backbone modifications.

Acknowledgements

This work is supported by NIH GM-33376.

References

1. Kajtar, M., Hollosi, M., Kajtar, J. and Majer, Zs., Tetrahedron, 42 (1986) 3931 (and references therein).
2. Jensen, O. and Senning, A., Tetrahedron, 42 (1986) 6555.
3. Spatola, A.F., Anwer, M.K., Rockwell, A.L. and Gierasch, L.M., J. Am. Chem. Soc., 108 (1986) 825.
4. Led, J.J. and Gesmar, H., J. Magn. Reson., 49 (1982) 444.

Peptide inhibitor binding to bacterial collagenase by proton NMR relaxation studies: A direct approach to structure–activity relationships

Flavio Toma[a], Vincent Dive[b] and Athanasios Yiotakis[b]

[a]*Service de Biochimie, Département de Biologie, CEN-Saclay, F-91191 Gif/Yvette, France*
[b]*Laboratory of Organic Chemistry, University of Athens, 10660 Athens, Greece*

We report a preliminary NMR study of peptide inhibitor–bacterial collagenase interactions using two inhibitors of the series recently developed in our laboratory [1–3].

The proton selective spin-lattice relaxation rate, $R^s = 1/T_1^s$, is a powerful NMR parameter for observing the binding of small ligands to macromolecules [4–7]. For a given proton pair i,j in the ligand molecule, R_i^s increases linearly with the motional correlation time τ_c (R_i^s is proportional to τ_c/r_{ij}^6, with r_{ij} = interproton distance) when the condition $(2\omega\cdot\tau_c)^2 >> 1$ is satisfied [4], i.e. for $\tau_c >> 2\times10^{-10}$ s at 500 MHz. The R_{obs}^s measured on the single proton signals of the ligand in the presence of the macromolecule increases with respect to the free ligand as a consequence of the binding (τ_c varies from 10^{-10} to 10^{-11} s in the free state to values $> 10^{-9}$ s in the complex) even for small amounts of bound form (< 3%) provided the ligand molecules undergo fast exchange in the NMR time scale between the free and the bound state [4, 5]. Under these conditions $R_{obs}^s = x_F R_F^s + x_B R_B^s$ (x = molar fractions; F = free state; B = bound state) from which R_B^s can be obtained. Nonselective relaxation rates in the bound form can be determined in the same way and therefore $(R^{ns}/R^s)_B$ can be deduced. The R^{ns}/R^s ratio is a function of only the $\omega\cdot\tau_c$ variable [4] – the $1/r_{ij}^6$ dependence is deleted – and equals 1.5 for $(\omega\cdot\tau_c)^2 << 1$, whereas it decreases rapidly for $(\omega\cdot\tau_c)^2 >> 1$, i.e. for $\tau_c >> 5\times10^{-10}$ s at 500 MHz. The observation of different $(R^{ns}/R^s)_B$ values for protons in different parts of the molecule may be assumed to qualitatively reflect differential residual mobilities of the bound ligand. Smaller $(R^{ns}/R^s)_B$ values (i.e., longer τ_c) are expected for proton pairs belonging to, or in proximity of, groups involved in stronger ligand–macromolecule interactions. The results reported in Tables 1 and 2 for two peptide inhibitors, Suc-Pro-Ala ($K_i \sim 4\times10^{-4}$ M) and Suc-Pro-Lys ($K_i \sim 2\times10^{-5}$ M), respectively, with and without *Achromobacter iophagus* collagenase show a large increase of R^s in the presence of approx. 3% collagenase–inhibitor complex both for single proton signals (e.g., H^{α}-Ala^3) and for chemically equivalent methylene protons ($H^{\gamma}H^{\gamma'}$-Lys^3 and $H^{\epsilon}H^{\epsilon'}$-Lys^3). In Suc-Pro-Ala, the smallest $(R^{ns}/R^s)_B$ value is observed

Table 1 *Proton relaxation parameters of (2,3-dideutero)Suc-Pro-Ala at 500 MHz (25°C)*

	Suc-Pro-Ala[a]		Suc-Pro-Ala[a] + collagenase[b]		
	R^s (s^{-1})	(R^{ns}/R^s)	R^s (s^{-1})	(R^{ns}/R^s)	$(R^{ns}/R^s)_B$
C_2HD-Suc[1]	0.37	0.82	1.17	0.68	0.4
C_3HD-Suc[1]	0.44	0.76	1.27	0.63	0.3
H^{α}-Pro[2]	0.45	0.95	1.04	0.77	0.6
H^{α}-Ala[3]	0.37	1.03	2.30	0.30	0.2

[a] 2.6 mM.
[b] From *A. iophagus*: 0.08 mM; $CaCl_2$ 1 mM; pH 6.8.

Table 2 *Proton relaxation parameters of Suc-Pro-Lys at 500 MHz (25°C)*

	Suc-Pro-Lys[a]		Suc-Pro-Lys[a] + collagenase[b]		
	R^s (s^{-1})	(R^{ns}/R^s)	R^s (s^{-1})	(R^{ns}/R^s)	$(R^{ns}/R^s)_B$
C_3H-Suc[1]	1.2	1.39	4.8	0.34	0.01
H^{α}-Pro[2]	0.5	1.20	1.2	0.75	0.48
H^{α}-Lys[3]	0.6	1.11	1.9	0.48	0.24
$H^{\gamma,\gamma'}$-Lys[3]	2.0	0.90	3.0	0.59	0.06
$H^{\epsilon,\epsilon'}$-Lys[3]	1.0	1.0	3.8	0.31	0.08

[a] 2.5 mM.
[b] From *A. iophagus*: 0.08 mM; $CaCl_2$ 1 mM; pH 6.8.

for H^{α}-Ala. This result, along with the 50-fold decrease of the activity of the methylester derivative, Suc-Pro-Ala-OMe, hints at the implication of the free carboxylate group of Ala[3] in a strong interaction with the enzyme [3]. The $(R^{ns}/R^s)_B$ values found for Suc[1] in the same inhibitor are consistent with the fact that the carboxylate group of Suc[1] binds to the Zn atom in the active site of the enzyme [1–3]. In Suc-Pro-Lys, the smallest $(R^{ns}/R^s)_B$ values are found for C_3H-Suc[1] and H^{γ}- and H^{ϵ}-Lys. This clearly indicates that the lysine side chain interacts with the S'_3 subsite of collagenase. This novel interaction favors, as compared to Suc-Pro-Ala, a stronger binding of the succinyl part to the S'_1 subsite of collagenase. Such a cooperative effect – which cannot be shown by the usual structure–activity approach – can explain the 20-fold higher activity of Suc-Pro-Lys with respect to Suc-Pro-Ala.

References

1. Dive, V., Yiotakis, A. and Toma, F., In Bertini, I., Luchinat, C., Maret, W. and Zeppezauer, M. (Eds.) Zinc Enzymes, Birkhäuser, Boston, MA, 1986, p. 289.

2. Yiotakis, A. and Dive, V., Eur. J. Biochem., 160 (1986) 413.
3. Dive, V., Thèse de Doctorat d'Etat, Université de Paris VI, 1986.
4. Valensin, G., Kushnir, T. and Navon, G., J. Magn. Reson., 46 (1982) 23.
5. Barni Comparini, I., Gaggelli, E., Marchettini, N. and Valensin, G., Biophys. J., 48 (1985) 247.
6. Valensin, G., Lepri, A. and Gaggelli, E., Biophys. Chem., 22 (1985) 83.
7. Gaggelli, E., Lepri, A. Marchettini, N. and Ulgiati, S., In Niccolai, N. and Valensin, G. (Eds.) Advanced Magnetic Resonance Techniques in Systems of High Molecular Complexity, Birkhäuser, Boston, MA, 1986, p. 109.

Vibrational circular dichroism of aromatic polypeptides

Sritana C. Yasui and Timothy A. Keiderling
Department of Chemistry, University of Illinois at Chicago, Box 4348, Chicago, IL 60680, U.S.A.

Introduction

It has been demonstrated that vibrational circular dichroism (VCD) is capable of distinguishing common polypeptide secondary structures even when restricted to study of the amide I band [1, 2]. Recently we have shown that the inherent resolution characteristics of the vibrational spectrum allow VCD to determine the secondary structure of aromatic polypeptides [e.g., poly-L-tyrosine and poly (L-Lys(Z)$_2$-(A)Ala), A = aromatic] in cases where electronic CD techniques are ambiguous at best [3, 4]. By using VCD band shape, frequency and $\Delta A/A$ values, α-helical structures are distinguishable from random and β-conformers in various solvent environments. In this report, we present the VCD of poly-L-tryptophan (PLT), poly-L-phenylalanine (PLPA), and poly-L-histidine·HCl (PLH), all of which contain aromatic side chains. These results are complex and, in some cases, give rise to new interpretations to polypeptide conformation and its characteristic VCD.

Results and Discussion

VCD spectra were measured on the UIC dispersive spectrometer using

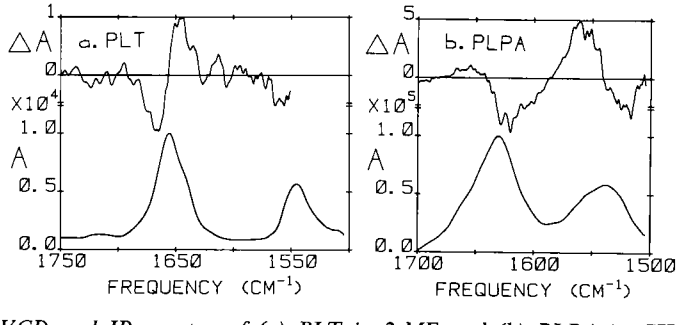

Fig. 1. VCD and IR spectra of (a) PLT in 2-ME and (b) PLPA in CH_2ClCH_2Cl + 1% TFA.

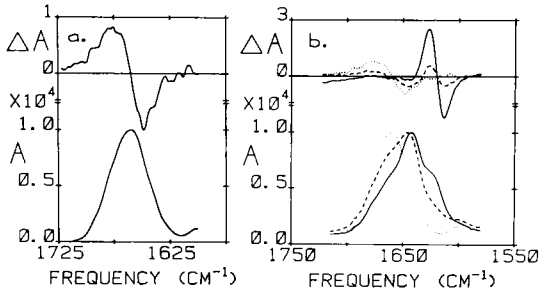

Fig. 2. VCD and IR spectra of (a) PLH in D_2O, pH 4.4, and (b) PLH with pH varying from 4.4 (.....) to 5.7 (-----) and overnight (——).

techniques and sampling methods described earlier. [1–4]. PLT (MW = 9,000 and 34,000), PLPA (MW = 16,000), and PLH (MW = 18,000) were obtained from Sigma. In Fig. 1 are the amide I VCD and absorption spectra of PLT (a) and PLPA (b).

The positive couplet result for PLT closely resembles the previously reported VCD for right-handed α-helical polypeptides and provides a simple confirmation of earlier proposals that PLT in 2-methoxyethanol (2-ME) was α-helical which were based on a complex CD and fluorescence-detected CD study [5]. Based on the two molecular weights studied, degree of polymerization had no effect on $\Delta A/A$ values obtained or band shape which is a conservative couplet as in poly-L-tyrosine [3, 4]. Solvent interference precluded measurement of the amide II VCD.

While solubility of PLPA in pure CH_2ClCH_2Cl is low, addition of 1% TFA gave a solution whose VCD spectrum was measurable. The amide I result is a strongly negatively biased couplet, shifted down in energy and opposite in sign from that of PLT. Aside from frequency, this result is consistent with spectra seen for random-coil structures [1–4]. Surprisingly, a relatively large VCD couplet is seen at $\sim$ 1540 cm^{-1} which must come from the phenyl ring deformation modes. Such strong coupling indicates significant residual local order in the side chains.

In Fig. 2 are VCD for PLH in the amide I at pH values from 4.4 to 5.7 (in D_2O, uncorrected). At lower pHs (1–4), there was no change in this random-coil VCD, consistent with earlier predictions [6]. As pH is increased, however, the spectrum changes to one which we have never seen in polypeptides. We cannot conclude what the structure is other than to eliminate the α-helix that has been proposed as an intermediate [6] and the (polylysinelike) antiparallel β-sheet [1, 2].

In conclusion, we have shown that VCD can give new insight into polypeptide conformation and a new interpretation to some long-standing questions in peptide chemistry.

Acknowledgements

This work was supported by the National Institutes of Health (GM-30147) which we gratefully acknowledge.

References

1. Yasui, S.C. and Keiderling, T.A., J. Am. Chem. Soc., 108 (1986) 5576.
2. Keiderling, T.A., Nature, 322 (1986) 851.
3. Yasui, S.C. and Keiderling, T.A., Biopolymers, 25 (1986) 5.
4. Yasui, S.C., Keiderling, T.A. and Sisido, M., Macromolecules, 20 (1987) 2403.
5. Muto, K., Mochizuki, H., Yoshida, R., Ishii, T. and Handa, T., J. Am. Chem. Soc., 108 (1986) 6416.
6. Woody, R.W., J. Polym. Sci., Macromol. Rev., 12 (1977) 181.

Crystal and molecular structure of *S*-deoxo [γ(*R*) hydroxy-Ile^3]-amaninamide: A synthetic analog of *Amanita* toxins

Giancarlo Zanotti[a], Theodor Wieland[b], Ettore Benedetti[c], Benedetto Di Blasio[c], Vincenzo Pavone[c] and Carlo Pedone[c]

[a]*Centro di Studio per la Chimica del Farmaco del CNR, Instituto di Chimica Farmaceutica, Università "La Sapienza", I-00185 Rome, Italy*

[b]*Max-Planck-Institut für medizinische Forschung, D-6900 Heidelberg, F.R.G.*

[c]*Dipartimento di Chimica, Università di Napoli, I-80134 Naples, Italy*

The amatoxins are the most toxic components of *Amanita* mushrooms (Fig. 1). They inhibit the eukaryotic RNA polymerase B with which they form a strong 1:1 complex [1]. The nature of the side chain of residue 3 is decisive for their toxicity. This position is held by a di- or monohydroxylated isoleucine as in compounds **1** and **2**, respectively. Of the two, only the γ-hydroxyl group

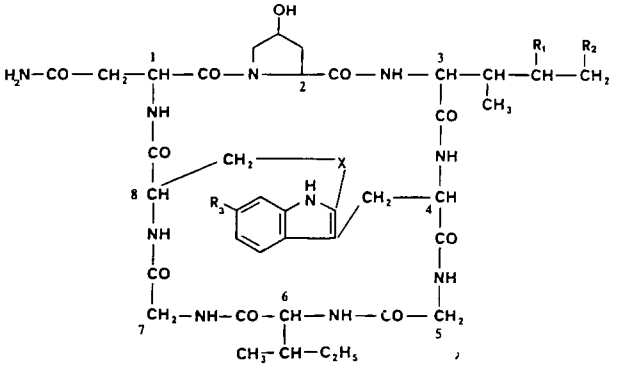

Amatoxins	R1	R2	R3	X	LD_{50}	$K_i \cdot 10^{-8}$
α-Amanitin (**1**)	OH	OH	OH	SO	0.3	0.23
γ-Amanitin (**2**)	OH(*S*)	H	OH	SO	0.2	0.5
Amaninamide (**3**)	OH	OH	H	SO	0.3	0.5
S-deoxo-Ile^3-amaninamide (**4**)	H	H	H	S	/	8.0
S-deoxo-[γ (*R*)OH-Ile^3]-amaninamide (**5**)	OH(*R*)	H	H	S	/	8.0

Fig. 1. Chemical structure, inhibition capacity and toxicity (LD_{50} in mg/kg white mouse) of some natural and synthetic amatoxins.

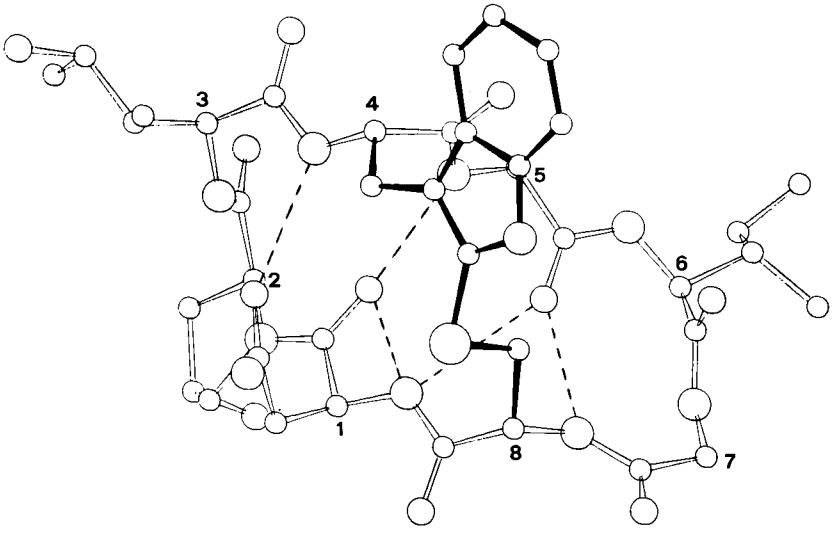

Fig. 2. Molecular model of toxin **5**. *Intramolecular H-bonds are indicated as dashed lines; the sulfur bridge is given as solid lines.*

is necessary. We report on the crystal and molecular structure of *S*-deoxo[γ (*R*)OH-Ile^3]-amaninamide (**5**), the first synthetic amatoxin analog containing the difficult γ-hydroxyisoleucine residue (HyIle). The absolute configuration of the γ-carbon of the HyIle side chain in **5** is opposite to that found in the natural toxins. Analog **5** is nontoxic and its inhibition capacity is reduced to about 5% of that of α-amanitin (**1**). As determined by X-ray analysis, analog **5** is nearly isomorphous to toxin **4** [2]. It crystallizes with 4 H_2O and 2 ethanol molecules in the $P2_1$ monoclinic space group with a = 12.251, b = 11.287, c = 19.053 Å, β = 95.46° and Z = 2. The structure of **5** is very close to that of **4**. The C^β and C^γ atoms of residue 3 (HyIle) both have the R configuration. The best fit between the structures of **4** and **5** shows an rms deviation of the atoms of 0.3 Å. The only gross 'mismatch' occurs for the side-chain atoms of residue 3. The intramolecular H-bonding scheme remains the same as described for **4**, while the intermolecular H-bonds involve the co-crystallized solvent molecules in different ways.

References

1. Wieland, T., In Rich, A. (Ed.) Peptides of Poisonous *Amanita* Mushrooms, Springer-Verlag, New York, NY, 1986, and references therein.
2. Shoham, G., Rees, D.C., Lipscomb, W.N., Zanotti, G. and Wieland, T., J. Am. Chem. Soc., 106(1984)4606.

Session II
Peptide mimetics

Chair: Ralph Hirschmann
Merck Sharp and Dohme Research Laboratories
Rahway, New Jersey, U.S.A.

Design and comparison of nonpeptide and peptide CCK antagonists

Roger M. Freidinger, Paul S. Anderson, Mark G. Bock, Raymond S.L. Chang, Robert M. DiPardo, Ben E. Evans, Victor M. Garsky, Victor J. Lotti, Kenneth E. Rittle, Daniel F. Veber and Willie L. Whitter

Merck Sharp & Dohme Research Laboratories, West Point, PA 19486, U.S.A.

Introduction

An increasingly attractive objective in research on biologically active peptides is the design of peptide mimetics. The goal is to obtain a more pharmacologically useful agent by eliminating undesirable properties (e.g., cleavage by proteases) while retaining affinity for the peptide's receptor. The most attractive outcome of such an exercise would be the development of an effective, totally nonpeptide ligand for the peptide receptor. This agent might be either an agonist or antagonist and would represent a unique tool for elucidating the role of the parent peptide in physiological processes and could also have value in therapy.

Two general approaches to such nonpeptide ligands can be envisaged. A stepwise, rational design process has received the greatest attention to date. Considerable progress has been made in developing partially peptidal and/or conformationally modified agents with improved properties. Extension of this process to an orally active, nonpeptide structure, however, has proven to be very difficult. An alternative is to search for nonpeptide receptor ligand leads using receptor-based technology for screening. Such a lead could serve as a starting point from which medicinal chemists could design an optimal structure. The application of both approaches to the design of antagonists of cholecystokinin (CCK) is described here.

Results and Discussion

CCK is a peptide hormone for which the minimum fully potent in vivo-occurring sequence is the C-terminal octapeptide H-Asp-Tyr(SO_3H)-Met-Gly-Trp-Met-Asp-Phe-NH_2 (CCK-8). Its involvement in such processes as satiety and pancreatic secretion has been widely studied, and more recent evidence has supported a role as a neurotransmitter. Until recently, the lack of potent antagonists has hindered progress of such studies. Two years ago, the discovery from fermentation broths of the novel CCK antagonist asperlicin utilizing a radioligand binding

assay was reported [1]. Asperlicin represented a key breakthrough to a nonpeptide, competitive, and selective antagonist ($K_i = 600$ nM) at the CCK receptor, and an effort was initiated to design more potent and orally effective agents from this lead.

One approach to this problem focused on structural features of asperlicin which might be key to its CCK receptor affinity and which could be incorporated into simpler molecules. Particularly attractive were the 1,4-benzodiazepine and indoline moieties. Recent studies in the antianxiety and opiate areas support the idea that benzodiazepines may be previously unrecognized nonpeptide ligands of receptors for which the endogenous ligand is a peptide [2, 3]. The existence of common features of structure and conformation among certain peptides suggested that this bicyclic system could have broader application in the design of other peptide receptor ligands. The indoline part structure was attractive because of its resemblance to the key tryptophan side chain of CCK. The basic design hypothesis then involved a fusion of the elements of the 5-phenyl-1,4-benzodiazepine with tryptophan. As is detailed in Fig. 1, to achieve maximum correspondence of the aromatic moieties of asperlicin and the proposed structure, D-tryptophan was employed.

The target 3R-3-indolylmethylbenzodiazepine **2** was synthesized and proved to have pancreas CCK receptor affinity comparable to asperlicin ($IC_{50} = 3.4\ \mu M$). In accord with the design hypothesis, the 3S enantiomer **1** was 10-fold less potent. A detailed structure-activity study based on this simplified antagonist was then performed to identify key features for optimal interaction with the CCK receptor.

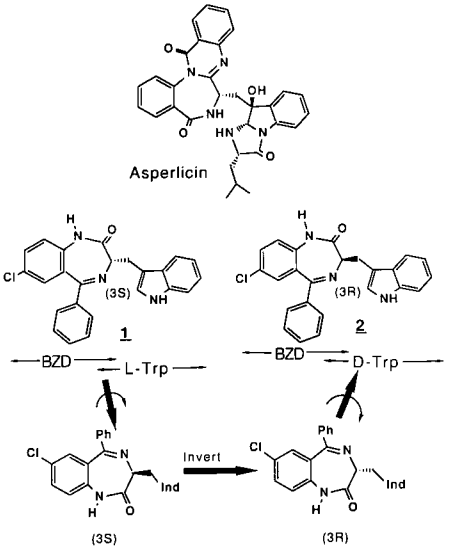

Fig. 1. Design of benzodiazepine CCK antagonists from asperlicin.

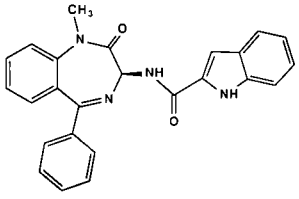

Fig. 2. CCK antagonist L-364,718.

In addition to the stereochemistry at the benzodiazepine 3-position, the nature of the linking group between benzodiazepine and indole as well as the point of attachment to indole were found to be crucial. One optimal compound designated L-364,718 incorporates a 3S-amino-5-phenyl-1,4-benzodiazepine acylated with indole-2-carboxylic acid [4] (Fig. 2). This antagonist has affinity for the peripheral CCK receptor comparable to CCK itself ($IC_{50} = 10^{-10}$M) and excellent selectivity with respect to the central CCK receptor (> 1,000-fold) and other receptors [5]. In particular, L-364,718 does not bind to the brain benzodiazepine receptor. This antagonist also inhibits the effects of CCK in vivo in a variety of animal models with long duration and oral activity. As such, L-364,718 is suitable for evaluation of the utility of a peripherally selective CCK antagonist in man.

Since L-364,718 is the first nonpeptide antagonist acting at a peptide receptor which has comparable receptor affinity to the endogenous ligand, an important question is how the interactions of antagonist and CCK with the receptor compare in molecular terms. One alternative assumes a direct structural correspondence of L-364,718 to key binding features of CCK in its active conformation, but agonist information is lacking. A second possibility is that L-364,718 could utilize, at least in part, accessory binding sites [6] near the receptor not used by CCK. There would not be complete structural correspondence between bound antagonist and agonist, and modeling comparisons attempting a fit between CCK itself and L-364,718 may not be useful. To account for this possibility, efforts have been focused on developing constrained peptide analogs of CCK which are antagonists. Such compounds may differ from CCK agonists in their bound conformation and are more likely to have receptor binding elements matching corresponding features of nonpeptide antagonists. Models of these more conformationally defined peptides should also be more readily obtained using theoretical and spectral techniques, and their comparison with L-364,718 should be more meaningful.

These studies began with the antagonist Cbz-Tyr(SO_3H)-Met-Gly-Trp-Met-Asp-NH_2 ($IC_{50} = 3$ μM) [7]. The possibility of a turn in the receptor-bound conformation was suggested when substitution of D-Trp for L-Trp gave only a 4-fold loss in pancreas receptor affinity. Furthermore, removal of the sulfate

from Tyr was found to have a negligible effect on binding, and subsequent analogs have utilized Phe in this position. Cyclization of the sequence Phe-Met-Gly-D-Trp-Met through a proline gave an analog with receptor affinity comparable to the best linear antagonist ($IC_{50} = 5.3$ μM). This result further supports the turn hypothesis. Additional analogs in which Phe and Pro were interchanged ($IC_{50} > 30$ μM) and in which Ala replaced Phe ($IC_{50} = 13$ μM) show, respectively, that backbone conformation is important in these analogs and the Phe side chain is contributing little to binding. In an attempt to gain additional receptor affinity by mimicking the C-terminal Phe of CCK, Pro was replaced by L- and D-N-δ-benzyl-Asn to give cyclo-[Phe-Met-Gly-D-Trp-Met-(L- and D-)-Asn(Bzl)]. These analogs are the most potent peptide antagonists of CCK to date ($IC_{50} = 1.2$ and 0.21 μM respectively). Importantly, they show no CCK-like agonist effects in the guinea pig ileum at concentrations as high as 10^{-5} M. The L-Asn(Bzl) analog also displays a preferred conformation in DMSO or methanol solution by NMR, and has a circular dichroism (CD) spectrum characteristic of β-turns. Determination of its solution conformation is in progress.

Current goals are to develop cyclic peptide antagonist analogs of CCK with potencies more similar to L-364,718 in order to make modeling comparisons more legitimate. Conformational models of these cyclic peptides will be constructed utilizing solution data and conformational search techniques. The ultimate objective is to establish a structural relationship between peptide and benzodiazepine with basis in experiment which may have utility in future peptide mimetic design studies.

References

1. Chang, R.S.L., Lotti, V.J., Monaghan, R.L., Birnbaum, J., Stapley, E.O., Goetz, M.A., Albers-Schonberg, G., Patchett, A.A., Liesch, J.M., Hensens, O.D. and Springer, J.P., Science, 230 (1985) 177.
2. Alho, H., Costa, E., Ferrero, P., Fujimoto, M., Cosenza-Murphy, D. and Guidotti, A., Science, 229 (1985) 179.
3. Romer, D., Buscher, H.H., Hill, R.C., Maurer, R., Petcher, T.J., Zeugner, H., Benson, W., Finner, E., Milkowski, W. and Thies, P.W., Nature, 298 (1982) 759.
4. Evans, B.E., Bock, M.G., Rittle, K.E., DiPardo, R.M., Whitter, W.L., Veber, D.F., Anderson, P.S. and Freidinger, R.M., Proc. Natl. Acad. Sci. U.S.A., 83 (1986) 4918.
5. Chang, R.S.L. and Lotti, V.J., Proc. Natl. Acad. Sci. U.S.A., 83 (1986) 4923.
6. Ariens, E.J., Beld, A.J., Rodrigues de Miranda, J.F. and Simonis, A.M., In O'Brien, R.D. (Ed.) The Receptors: A Comprehensive Treatise, Plenum, New York, 1979, p. 33.
7. Spanarkel, M., Martinez, J., Briet, C., Jensen, R.T. and Gardner, J.D., J. Biol. Chem., 258 (1983) 6746.

On the importance of the peptide bonds in the C-terminal tetrapeptide of gastrin and in the C-terminal heptapeptide of cholecystokinin

Marc Rodriguez[a], Pierre Fulcrand[a], Marie-Françoise Lignon[a], Marie-Christine Galas[a], Jean-Pierre Bali[b], Richard Magous[b], Philibert Dubreuil[a], Jeanine Laur[a] and Jean Martinez[a]

[a]*Centre de Pharmacologie-Endocrinologie, Rue de la Cardonille, 34094 Montpellier, France*
[b]*Faculté de Pharmacie, ER CNRS 228, 34000 Montpellier, France*

Introduction

Gastrin, a 17-amino acid hormone, plays a major role in the stimulation of gastric acid secretion. It was recognized early that, of the 17 amino acid residues of the molecule, only the C-terminal tetrapeptide Trp-Met-Asp-Phe-NH_2 is required for the remarkable range of physiological effects displayed by the natural hormone [1]. Cholecystokinin (CCK) has the same C-terminal pentapeptide as gastrin. CCK plays a major role in the peripheral system (stimulation of amylase secretion, gall bladder contraction) and in the central nervous system as a neuromodulator. The C-terminal heptapeptide of CCK is required for exhibiting the activities of the whole natural hormone [2]. Gastrin and CCK overlap in their activities. We have been interested in studying the role of the peptide bonds in the C-terminal tetrapeptide of gastrin and in the C-terminal heptapeptide of CCK.

Results and Discussion

We synthesized the pseudopeptides **2**, **3**, and **4**, analogs of the C-terminal tetrapeptide of gastrin (Fig. 1), in which each peptide bond, one after each other, was replaced by a CH_2NH bond [3]. Compound **2** was found to be a

BOC-Trp-Leu-Asp-Phe-NH_2 **1**
BOC-Trp$\psi(CH_2NH)$Leu-Asp-Phe-NH_2 **2**
BOC-Trp-Leu$\psi(CH_2NH)$Asp-Phe-NH_2 **3**
BOC-Trp-Leu-Asp$\psi(CH_2NH)$Phe-NH_2 **4**

Fig. 1. Tetragastrin analogs.

very potent agonist of acid secretion in the anesthetized rat. This pseudopeptide was as potent as the tetragastrin analog **1**. On the inhibition of binding of ^{125}I-[Leu^{15}]-HG-17 to its receptors on rabbit membrane mucosal cells, compound **2** showed approximately the same potency as **1** ($IC_{50} \approx 0.3$ μM for **2** and ≈ 0.5 μM for **1**). Compound **3** did not show any agonist activity, but was able to recognize the gastrin receptor with a high potency ($IC_{50} \approx 0.25$ μM). It was able to antagonize the action of gastrin on stimulation of acid secretion ($ED_{50} \approx 0.3$ mg/kg). Compound **4** has a lower affinity for the gastrin receptor. It did not show any agonist effect on acid secretion and was able to antagonize the action of gastrin ($ED_{50} \approx 15$ mg/kg). These results showed the importance of the peptide bonds of the C-terminal tetrapeptide of gastrin for the activity and prompted us to hypothesize that, for exhibiting agonist activity on acid secretion, the bond between leucine and aspartic acid has to be a peptide bond, a cleavable bond. The structural integrity of the C-terminal dipeptide appeared to be important for the binding to the gastrin receptor and crucial for the biological activity. We postulated that an enzymatic system may exist, probably located within the gastrin receptor which cleaves the C-terminal tetrapeptide of gastrin between methionine (or leucine in the analogs) and aspartic acid. The result of this cleavage is the liberation within the receptor of the dipeptide moiety Asp-Phe-NH_2 which might be the 'signal' for initiating the biological event. From these hypotheses, we investigated two directions in the design of gastrin antagonists: (1) synthesizing compounds having all the features for recognizing the gastrin receptor but which are not enzymatically cleavable between methionine (or leucine) and aspartic acid [4] and (2) synthesizing compounds having all the features for recognizing the gastrin receptor, having a peptide bond between methionine (or leucine) and aspartic acid, but modified on the C-terminal dipeptide moiety [5]. We reinforced our hypothesis on the mechanism of action of gastrin by recently showing that compound **1** was degraded in vitro by a vesicular membrane fraction from rat gastric mucosa [6], the major cleavage products being Boc-Trp-Leu and Asp-Phe-NH_2. Compound **3** was found completely stable in the incubation conditions.

We similarly studied the role of the peptide bonds of the C-terminal hep-

Z-Tyr(SO_3^-)-Met-Gly-Trp-Nle-Asp-Phe-NH_2	Z-[Nle^{31}]-CCK-7	**5**
Z-Tyr(SO_3^-)-Nleψ(CH_2NH)Gly-Trp-Nle-Asp-Phe-NH_2		**6**
Z-Tyr(SO_3^-)-Nle-Glyψ(CH_2NH)Trp-Nle-Asp-Phe-NH_2		**7**
Z-Tyr(SO_3^-)-Nle-Gly-Trpψ(CH_2NH)Nle-Asp-Phe-NH_2		**8**
Z-Tyr(SO_3^-)-Nle-Gly-Trp-Nleψ(CH_2NH)Asp-Phe-NH_2		**9**
Z-Tyr(SO_3^-)-Nle-Gly-Trp-Nle-Aspψ(CH_2NH)Phe-NH_2		**10**

Fig. 2. Analogs of the C-terminal heptapeptide of CCK.

tapeptide of CCK [7]. The replacement of each peptide bond, one at a time, by the CH_2NH bond (Fig. 2) led to compounds exhibiting the activity of the parent peptide in amylase release from guinea pig pancreatic acini, with lower potencies (Figs. 3 and 4). These pseudopeptides were able to recognize the CCK receptor on guinea pig brain membranes (Fig. 5). Interestingly, the potencies of these compounds for the pancreatic and brain guinea pig CCK receptor were different: compound **8** particularly was more potent on brain than on pancreas, whereas compound **9** had more affinity on pancreas than on brain (Figs. 4 and 5). These results confirm the heterogeneity of brain and pancreatic CCK receptors and may help in the determination of the significant parts of the CCK molecule for each type of receptor.

Conclusion

The syntheses of pseudopeptides in the gastrin and CCK family and their pharmacological evaluations led us to hypothesize about a possible mechanism of action of gastrin, to design potent gastrin antagonists, and to point out

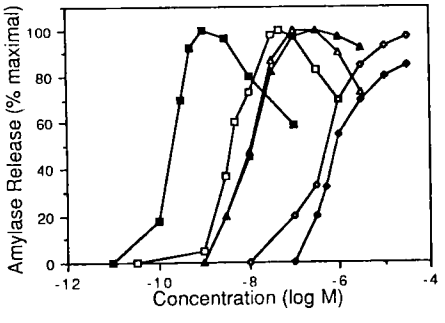

Fig. 3. The effect of Z-[Nle^{31}]-CCK-7 ***5*** *(■),* ***6*** *(□),* ***7*** *(▲),* ***8*** *(◇),* ***9*** *(△), and* ***10*** *(◆), on amylase release from guinea pig pancreatic acini. Amylase release was measured as the difference of amylase activity at the end of incubation that was released into the extracellular medium, with and without secretagogue, and expressed as the percentage of maximal stimulation obtained with CCK-8 or Z-[Nle^{31}]-CCK-7 (which represents approximately 35–40% of the total amylase contained in the acini). In each experiment, each value was determined in duplicate and the results given are the means from four separate experiments.*

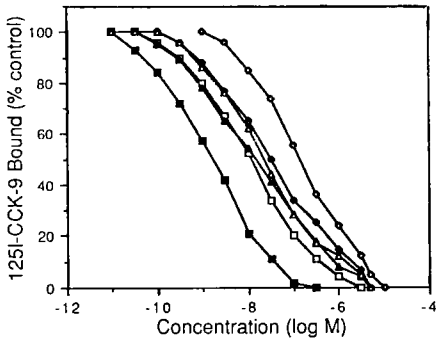

Fig. 4. Ability of compounds ***5*** *(■),* ***6*** *(□),* ***7*** *(▲),* ***8*** *(◇),* ***9*** *(△), and* ***10*** *(◆), to inhibit binding of labeled CCK-9 (^{125}I-BH-CCK-9) to guinea pig pancreatic acini. Binding of ^{125}I-BH-CCK-9 was performed as described by Jensen et al. [8]. Acini were incubated for 30 min at 37°C with various concentrations of* ***5****,* ***6****,* ***7****,* ***8****,* ***9****, or* ***10*** *plus 20 pM of labeled ^{125}I-BH-CCK-9. Values are expressed as the percentage of the value obtained with labeled CCK-9 alone. In each experiment, each value was determined in duplicate and the results given are the means from three separate experiments.*

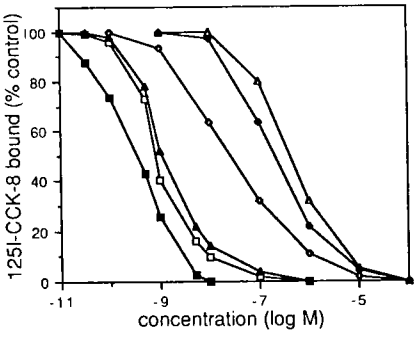

Fig. 5. Ability of compounds ***5*** *(■),* ***6*** *(□),* ***7*** *(▲),* ***8*** *(◇),* ***9*** *(△), and* ***10*** *(◆), to inhibit binding of labeled CCK-9 (^{125}I-BH-CCK-9) to guinea pig cerebral cortical membranes. Binding of labeled CCK-9 to guinea pig brain membranes was performed as described by Pelaprat et al. [9]. Brain membranes were incubated for 60 min at 25°C with various concentrations of compounds* ***5****,* ***6****,* ***7****,* ***8****,* ***9****, and* ***10*** *plus 20 pM of ^{125}I-BH-CCK-9. Values are expressed as the percentage of the value obtained with labeled CCK-9 alone. Nonspecific binding was determined in the presence of 1 μM of CCK-8. In each experiment, each value was determined in duplicate and the results given are the means from five separate experiments.*

differences between CCK analogs for the pancreatic and brain CCK receptors. These studies allowed us to evaluate the role of the peptide bonds of the C-terminal tetrapeptide of gastrin and of the C-terminal heptapeptide of CCK.

References

1. Tracy, H.J. and Gregory, R.A., Nature, 204 (1964) 935.
2. Jensen, R.T., Lemp, G.F. and Gardner, J.D., J. Biol. Chem., 257 (1982) 5554.
3. Martinez, J., Bali, J.P., Rodriguez, M., Castro, B., Magous, R., Laur, J. and Lignon, M.F., J. Med. Chem., 18 (1985) 1874.
4. Rodriguez, M., Dubreuil, P., Bali, J.P. and Martinez, J., J. Med. Chem., 30 (1987) 758.
5. Martinez, J., Rodriguez, M., Bali, J.P. and Laur, J., J. Med. Chem., 29 (1986) 2201.
6. Dubreuil, P., Lignon, M.F., Magous, R., Rodriguez, M., Bali, J.P. and Martinez, J., Drug Design and Delivery (1987) in press.
7. Rodriguez, M., Lignon, M.F., Galas, M.F., Fulcrand, P., Mendre, C., Aumelas, A., Laur, J. and Martinez, J., J. Med. Chem. (1987) in press.
8. Jensen, R.T., Lemp, G.F. and Gardner, J.D., Proc. Natl. Acad. Sci. U.S.A., 77 (1980) 2079.
9. Pelaprat, D., Zajac, J.M., Gacel, G., Durieux, C., Morgat, J.L., Sasaki, A. and Roques, B., Life Sci., 37 (1985) 2483.

Reverse turn mimics

William F. Huffman[a], James F. Callahan[a], Drake S. Eggleston[b], Kenneth A. Newlander[a], Dennis T. Takata[a], Ellen E. Codd[c], Richard F. Walker[c], Peter W. Schiller[d], Carole Lemieux[d], William S. Wire[e] and Thomas F. Burks[e]

[a]Department of Peptide Chemistry, [b]Department of Physical and Structural Chemistry and [c]Department of Reproductive and Developmental Toxicology, Smith Kline & French Laboratories, P.O. Box 1539, King of Prussia, PA 19406-0939, U.S.A., [d]Laboratory of Chemical Biology and Peptide Research, Clinical Research Institute of Montreal, Montreal, Quebec, Canada H2W 1R7 [e]Department of Pharmacology, University of Arizona, Tucson, AZ 85724, U.S.A.

Introduction

A continuing pursuit in peptide chemistry is to better understand the biologically active conformation of a given peptide as it interacts with a macromolecular receptor to produce a biological event. For peptides which interact with membrane-associated receptors, a productive approach has been to reduce the conformational flexibility of the ligand to a set of defined shapes. The retention or loss of biological activity of the resulting constrained analog can then be correlated with shape, and inferences regarding the pharmacophore can be drawn. To this end, a variety of natural and unnatural amino acids have been used to constrain the local conformation (Φ, Ψ) about a single amino acid residue or the preceding residue in a peptide sequence. Cyclization of linear peptides represents a regional conformational constraint (i.e., one which attempts to fix aspects of secondary structure such as α-helix or reverse turns). A variety of mimics have been designed to force a linear peptide sequence into various β-turn conformations. We have designed a novel mimic of the gamma turn or C-7 turn (compound **1**) and have synthesized representative examples suitable for incorporation into a model peptide, leucine enkephalin. The syntheses of mimics **2–4** (Table 1) and their incorporation into leucine enkephalin are described below.

Results and Discussion

The synthetic features incorporated in the proposed C-7 mimic **1** include (1) a *trans* olefin to replace an amide bond, (2) an ethylene bridge in place of a hydrogen bond, (3) an N,N-disubstituted amino acid, (4) a side chain R_1 replacing the native amino acid side chain in residue $i+1$, and (5) a side chain R to

Table 1 *C-7 (γ) turn mimics*

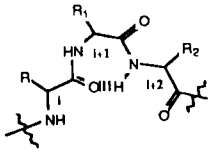

Generalized C-7 turn

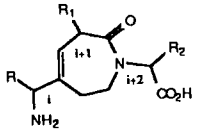

C-7 mimic

Compound	Name	R	R_1	R_2
2	γ(Gly-Gly-Phe)	H	H	CH_2Ph
3	γ(Gly-D/L-Phe-Leu)[a]	H	CH_2Ph	i-butyl
4	γ(D,L-Tyr-Gly-Gly)[b]	CH_2Ph	H	H

[a] D/L indicates a single stereoisomer (*R* or *S*) of undetermined stereochemistry.
[b] D,L indicates a mixture of stereochemistry (*R* and *S*).

represent the side chain in the i residue. General synthetic solutions to the first four of these features are exemplified by the synthesis of C-7 mimic **3** and its incorporation into leucine enkephalin as a replacement for the Gly[3]-Phe[4]-Leu[5]

Scheme 1

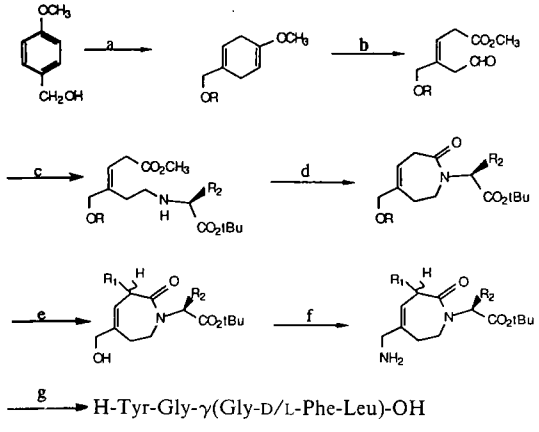

R = *t*-Bu(Ph)$_2$Si-, R_1 = benzyl, R_2 = *i*-butyl

(a) i. Li/NH_3, EtOH ii. *t*-Bu(Ph)$_2$SiCl, imidazole; 70–80% for two steps. (b) O_3, CH_2Cl_2, Me_2S, -78°, 45%. (c) Leu-O*t*Bu, $NaBH_3CN$, CH_3OH. (d) i. 1N NaOH, dioxane ii. 3N HCl, iii. DPPA, Et_3N, DMF; 37% for steps c and d. (e) i. *n*-Bu_4NF, THF, 38% ii. LDA, THF, $PhCH_2Br$, 75%. (f) i. DEAD, Ph_3P, THF, phthalimide ii. H_2NNH_2-H_2O, EtOH; 86% for steps i and ii. (g) i. Boc-Tyr-Gly-Gly-OH, DCC, HOBt, DMF, CH_2Cl_2, 72% ii. TFA, anisole iii. RPHPLC, 41% for steps ii and iii.

tripeptide (Scheme 1). A synthetic solution for the fifth feature is exemplified in the preparation of mimic **4**, the highlights of which are presented in Scheme 2.

In general, the carbon framework of the ring portion of mimic **1** can be prepared by partial reduction of an appropriate *para*-substituted anisole, selective ozonolysis of the resulting enol ether double bond, reductive amination of the intermediate aldehyde product, followed by cyclization to form the desired cycloheptene lactam. Selective alkylation strategies provide the final products containing side chains R and R_1 as depicted in Schemes 1 and 2. At this stage in the synthesis, the structure of one of the diastereoisomers about R_1 of compound **5** (where $R_2 = i$-Pr) was determined by X-ray crystallography. The stereochemistries at R_1 and R_2 were both found to be in the *S* configuration and the overall shape of the cycloheptene lactam was virtually identical to that determined theoretically with a variety of potential energy functions. Compared to an idealized γ-turn, which has torsional angles $\Psi_i = 120$, $\Phi_{i+1} = 80$, $\Psi_{i+1} = -65$, $\Phi_{i+2} = -120$ [1], the corresponding torsional angles determined by X-ray crystallography on the C-7 mimic are $\Psi_i = 128$, $\Phi_{i+1} = 56$, $\Psi_{i+1} = -67$, $\Phi_{i+2} = -123$.

The biological activity of the enkephalin analogs containing γ-turn mimics **2–4** is detailed in Table 2. Of the four peptides tested, only the molecule containing mimic **4** demonstrated any affinity for an opiate receptor. This analog retained approximately 1% of the affinity of leucine enkephalin for the delta receptor; however, in a functional assay at the delta receptor (mouse vas deferens), the

Scheme 2

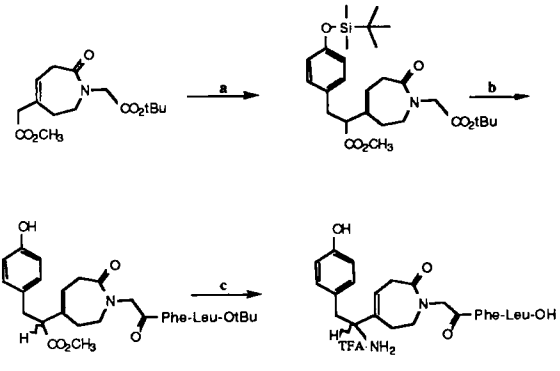

(a) i. LDA, THF ii. I-CH_2-Ph[4′-OSi(Me)$_2$-*t*-Bu] (43% for steps i and ii). (b) i. TFA, anisole, CH_2Cl_2 ii. H-Phe-Leu-O-*t*-Bu, DCC, HOBt, CH_2CH_2; 69% for b. (c) i. 1N NaOH, dioxane ii. 1N HCl iii. DPPA, Et_3N, $PhCH_2OH$, toluene; 19% for steps i.–iii. iv. HF, anisole, 50%.

Table 2 *Opiate activity of modified enkephalin analogs [2]*

	IC_{50} (nM)			
	DAGO (μ)	DPDPE (δ)	GPI (μ)	MVD (δ)
H-Tyr-Gly-γ(Gly-D/L-Phe-Leu)-OH	>100,000	20,000	>30,000	>10,000
H-Tyr-Gly-γ(Gly-D/L-Phe-Leu)-OH	40,000	9,000	>10,000	> 1,000
H-Tyr-γ(Gly-Gly-Phe)-Leu-OH	100,000	3,000	>30,000	>10,000
H-γ(D,L-Tyr-Gly-Gly)-Phe-Leu-OH	(4,000)[a]	(360)[b]	64,000	>28,500
H-Tyr-Gly-Gly-Phe-Leu-OH	25.0	3.0	246	11.4

[a] Determination made in separate assay in which IC_{50} for leucine enkephalin was found to be 9.4 nM.

[b] Determined versus the delta agonist DSLET in which the IC_{50} for leucine enkephalin was found to be 2.5 nM.

analog was virtually inactive. Apart from the important caveat that the differences between the mimic itself and an idealized γ-turn (e.g., altered angles for the α,β-vectors of the side chains or steric interactions between the ethylene bridge and the rest of the peptide or receptor) have contributed to the loss of receptor affinity, the data suggest that the biologically active conformations of leucine enkephalin at the mu and delta receptors do not contain C-7 or γ-turns about residues two, three, or four.

With the development of a mimic for the C-7 or γ-turn, it will now be possible to test hypotheses regarding the role of such reverse turns in peptides. This tool should complement the growing array of tools available to the peptide chemist to impose constraint on local and regional conformation and, thereby, to assist in the understanding of the biologically active conformations of peptides and proteins.

References

1. Rose, G.D., Gierasch, L.M. and Smith, J.A., In Anfinsen, C.B., Edsall, J.T. and Richards, F.M. (Eds.) Advances in Protein Chemistry, Volume 37, Academic Press, Orlando, 1985, p. 1.
2. For details regarding opiate binding and smooth muscle contraction assays, see the following:
   a. Paterson, S.J., Corbett, A.D., Gillan, M.G.C., Kosterlitz, H.W., McKnight, A.T. and Robson, L.E., J. Recept. Res., 4(1984) 143.
   b. Mosburg, H.I., Hurst, R., Hruby, V.J., Gee, K., Yamamura, H.I., Galligan, J.J. and Burks, T.F., Proc. Natl. Acad. Sci. U.S.A., 80(1983)5871.
   c. DiMaio, J., Nguyen, T.M.-D., Lemieux, C. and Schiller, P.W., J. Med. Chem., 25(1982) 1432.

Nonpeptide mimetics of jaspamide

Michael Kahn and Ting Su
University of Illinois at Chicago, Department of Chemistry, 829 West Taylor Street, P.O. Box 4348 (m/c 111), Chicago, IL 60680, U.S.A.

Introduction

Despite the central position which peptide and proteins occupy in the regulation of virtually all biological processes, a molecular understanding of their structure-function relationship remains in its infancy. To date, extensive and, in several cases, successful efforts have been mounted to modify peptides and proteins to examine this interplay. It should be possible, however, to utilize designed, conformationally restricted mimetics to explore this marriage of structure and function. Comprehension of this union would allow for the design of new peptides and proteins, with applications as synthetic catalysts, agricultural agents, and pharmaceutical agents.

Jaspamide (**1**) is a novel metabolite of mixed peptide/polyketide biosynthesis which was isolated from sponges of the genus *Jaspis*. Recently, Zabriskie and colleagues [1] published the X-ray structure of jaspamide. Simultaneously, Crews et al. [2] published their structure of jaspamide based upon NMR. This depsipeptide contains two rare amino acids – β-tyrosine, previously reported in the edeine peptides [3], and 2-bromoabrine, which is apparently a new amino acid. Both have an unnatural D configuration.

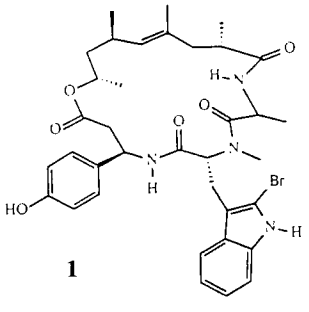

1

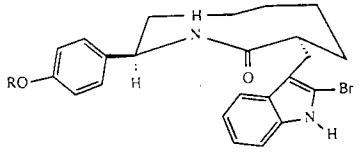

2 R = H **3** R = Me

Jaspamide exhibited potent insecticidal activity against *Heliothis virescens* (LC_{50} 4 ppm; by comparison, azadirachtin, an extremely potent insecticide, exhibited an LC_{50} of 1 ppm in this assay) [4]. Additionally, jaspamide exhibited a minimum inhibitory concentration (mic) and a minimum lethal concentration (mlc) of

25 μg/ml each against *Candida albicans*. The in vivo topical activity of a 2% solution of jaspamide against a *Candida* vaginal infection in mice was comparable to that of miconazole nitrate. It was completely inactive, however, against a variety of gram-positive and gram-negative bacteria.

Inspection of the X-ray structure of jaspamide leads one to conclude that the two key pharmacophores (i.e., the bromoindole and the phenol) are contained within a type II β-turn. Based on this analysis and our earlier investigations on the synthesis of turn mimetics [5], we have designed lactam **2** as a nonpeptide mimetic of jaspamide.

Results and Discussion

The synthesis of mimetic **3**, a protected version of **2**, is outlined in Scheme 1. Boron trifluoride-assisted opening of cyclooctadiene monoepoxide with 4-lithioanisole proceeds smoothly at −78° [6]. Subsequent Jones oxidation of the alcohol provides ketone **4**. Carbomethoxylation of the kinetic enolate of ketone **4** provides the requisite keto-ester for introduction of the indole moiety via

Scheme 1

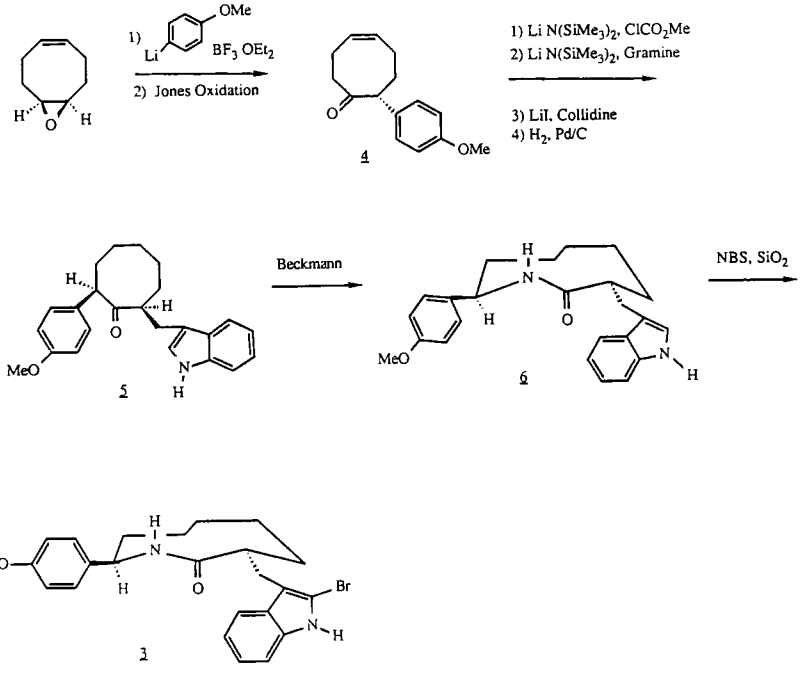

a Mannich type condensation with gramine [7]. Krapcho decarboxylation [8] provides an overall 12% yield of the *cis* ketone **5** [9] from cyclooctadiene epoxide. Utilization of the conditions recently reported by Confalone for oxime formation [10], fortuitously effects initial epimerization of the *cis* ketone and subsequent oxime formation of the *trans* derivative. Beckmann rearrangement provides lactam **6** 11, which is subsequently brominated with *N*-bromosuccinimide and silica gel [12] to afford the desired **3** in 34% yield from **5**. Gratifyingly, mimetic **3** has shown interesting preliminary activity against *H. virescens* (Houtchens, R., Dow Agricultural Chemicals Division, personal communication).

Acknowledgements

We wish to express our sincere thanks to the Camille and Henry Dreyfus Foundation, Searle Scholars Program/The Chicago Community Trust, and the University of Illinois Campus Research Board for support of this research.

References

1. Zabriskie, T.M., Klocke, J.A., Ireland, C.M., Marcus, A.H., Molinski, T.F., Faulkner, D.J., Xu, C. and Clardy, J.C., J. Am. Chem. Soc., 108 (1986) 3123.
2. Crews, P., Manes, L.V. and Boehler, M., Tetrahedron Lett., 27 (1986) 2797.
3. Wojciechowska, H., Ciaskowski, J., Chonara, H. and Borowski, E., Experientia, 28 (1972) 1423.
4. Kubo, I. and Klocke, J.A., In Hedin, P.A. (Ed.) Plant Resistance To Insects, ACS Symposium Series 208, American Chemical Society, Washington, D.C., 1983, p. 329.

5a. Kahn, M. and Chen, B., Tetrahedron Lett., 28 (1987) 1623.
b. Kahn, M., Chen, B. and Zieske, P., Heterocycles, 25 (1987) 29.
c. Kahn, M. and Devens, B., Tetrahedron Lett., 27 (1986) 4841.
d. Preliminary investigations on nonpeptide mimetics were initiated by M.K. during a postdoctoral year at Hoffmann-La Roche.

6. Eis, M.J., Wrobel, J.E. and Ganem, B., J. Am. Chem. Soc., 106 (1984) 3693.
7. Albright, J.D. and Synder, H.R., J. Am. Chem. Soc., 81 (1959) 2239.
8. Krapcho, A.P. and Lovey, A.J., Tetrahedron Lett., 14 (1973) 957.
9. The *cis* relationship between the two side-chain substituents was established via the aegis of a different NOE experiment. The thermodynamic decarboxylation conditions provide almost exclusively the *cis* ketone **5**.
10. Confalone, P.N. and Huie, E.M., J. Org. Chem., 52 (1987) 79.
11. To a solution of the oxime in methylene chloride and pyridine, one adds dimethylaminopyridine and excess methanesulfonyl chloride at 0°C. The reaction is allowed to stir for two hours to room temperature, after which saturated aqueous $NaHCO_3$ is added and allowed to stir an additional one hour.
12. Mistry, A.G., Smith, K. and Bye, M.R., Tetrahedron Lett., 27 (1986) 1051.

trans Carbon-carbon double bond isosteres of the peptide bond. General methodology and the synthesis of cholecystokinin (CCK) analogs

Y.K. Shue, G.M. Carrera, Jr., A.M. Nadzan, J.F. Kerwin, H. Kopecka and C.W. Lin

Abbott Laboratories, Neuroscience Research, Pharmaceutical Discovery Division, Abbott Park, IL 60064, U.S.A.

The replacement of amide bonds in peptides with suitable isosteric units has the potential for circumventing some of the therapeutic limitations of peptides (i.e., poor enzymatic stability, poor oral absorption, and marginal ability to cross the blood-brain barrier. Among those amide bond mimics which have been reported previously, the *trans* carbon-carbon double bond appears to be the most suitable one in terms of mimicking the rigidity, bond angle, and bond length of the amide bond [1–3]. By using natural amino acids as starting material, we have developed a general synthetic route toward *trans* carbon-carbon double bond isosteres of protected dipeptides having the general structure **1**. Four pseudodipeptides **1a**, **1b**, **1c**, and **1d** were prepared (Scheme 1) [4].

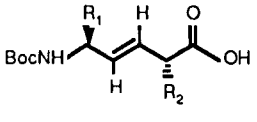

1

	R_1	R_2
a.	$CH_2CO_2C(CH_3)$	$CH_2C_6H_5$
b.	$CH_2CH(CH_3)_2$	$CH_2CO_2C(CH_3)_3$
c.	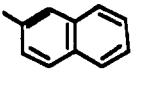	$(CH_2)_3CH_3$
d.	H	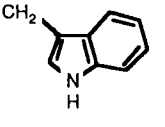

These four compounds were utilized to prepare a series of *trans*-double bond isosteres of CCK_4 and CCK_5 by employing standard peptide coupling techniques. This series along with its corresponding binding affinities for cortical CCK receptors is summarized in Table 1. The receptor binding assays were performed in the guinea pig cerebral cortex using a biologically active CCK radioligand,

Scheme 1

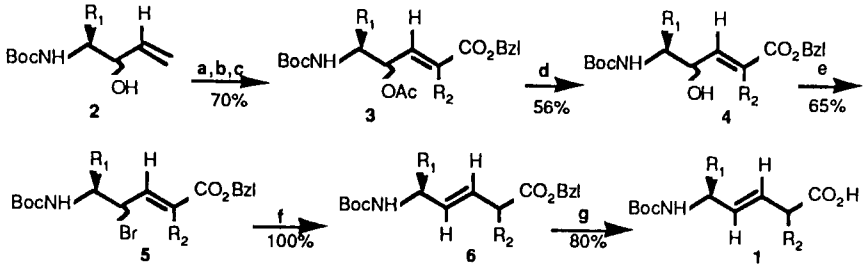

a. Ac_2O/Py., b. NMO/$NaIO_4$/OsO_4(cat.), c. $Ph_3P{=}CR_2CO_2Bzl$, d. Na_2CO_3/MeOH/45 min., e. Ph_3P/CBr_4/THF, f. Zn/HOAc, g. 1,4-Cyclohexadiene/Pd/C/MeOH.

^{125}I-Bolton-Hunter CCK_8. The replacement of the peptide linkage in CCK_4 by a *trans*-double bond at either the Trp-Leu site (entry 8), the Leu-Asp site (entries 5, 6), or the Asp-Phe site (entry 7) results in major loss of binding affinity. On the other hand, the same modification of Boc-CCK_5 at the Gly-Trp amide bond (entry 9) resulted in a 2- to 3-fold enhancement of potency.

In summary, this novel methodology provides a general route to a wide range of biologically significant modified peptide analogs which are otherwise difficult to obtain. The biological data indicate that the amide bonds in CCK_4 play a more subtle role than just providing rigidity and serving as a spacer. We are in the process of extending these studies to synthesize other amide bond surrogates having hydrogen bonding capability, such as the ketomethylene and hydroxyethylene replacements.

Table 1 *Binding affinities in guinea pig cortex*[a]

	IC50 (nM) ± *SEM (n)*
1. Boc-Trp-Met-Asp-$PheNH_2$	28 ± 4.5 (6)
2. Boc-Trp-Leu-Asp-$PheNH_2$	48 ± 7.8 (9)
3. Boc-Gly-Trp-Leu-Asp-$PheNH_2$	21 ± 7 (3)
4. Boc-β-Nal-Leu-Asp-$PheNH_2$	29.3 (2)
5. Boc-Trp-Leuψ[E-CH=CH]Asp[b]-$PheNH_2$	6,450 ± 87 (3)
6. Boc-Trp-Leuψ[E-CH=CH]Asp[b]-$PheNH_2$	10,000 ± 1,340 (3)
7. Boc-Trp-Leu-Aspψ[E-CH=CH]$PheNH_2$[c]	>10,000 (1)
8. Boc-β-Nalψ[E-CH=CH]Nle[c]-Asp-$PheNH_2$	>10,000 (1)
9. Boc-Glyψ[E-CH=CH]Trp[c]-Leu-Asp-$PheNH_2$	8.9 (1)

[a] Using ^{125}I-Bolton-Hunter CCK_8 as a radioligand.
[b] Separated pair of diastereomers at the alpha-carbon center of Asp.
[c] Mixture of diastereomers at the alpha-carbon center of Phe, Trp and Nle.

References

1. Spatola, A.F., In Weinstein, B. (Ed.) Chemistry and Biochemistry of Amino Acids, Peptides and Proteins, Marcel Dekker, New York, 1983, Vol. 7, p. 267.
2. Hann, M.M. and Sammes, P.G., J. Chem. Soc., Perkin I (1982) 307.
3. Hann, M.M. and Sammes, P.G., J. Chem. Soc. Chem. Comm. (1980) 234.
4. Shue, Y.K., Carrera, Jr., G.M. and Nadzan, A.M., Tetrahedron Lett., 28 (1987) 3225.

Conformations of cholecystokinin and their relationships to rigid molecules

Richard A. Hughes and Peter R. Andrews
School of Pharmaceutical Chemistry, Victorian College of Pharmacy Ltd., 381 Royal Parade, Parkville, Victoria, Australia 3052

Introduction

The neuropeptide cholecystokinin (CCK) and the ergopeptine alkaloids exhibit common central pharmacology, particularly via catecholaminergic systems. This led us to consider the structural and conformational similarities between the carboxy-terminal CCK tetrapeptide (CCK-4) and a representative ergopeptine, ergotamine (EA). At around the same time, a potent peripheral CCK antagonist L-364,718 (MSD) emerged [1], whose relationship with CCK-4 was similarly analyzed.

Results and Discussion

Structurally, all three compounds possess an indole system, a phenyl ring (MSD has two), and a potentially positively charged nitrogen atom. Further to this, EA has a peptidic backbone embedded within its polycyclic structure that corresponds almost atom to atom with that of CCK-4 (Fig. 1).

Conformations of CCK-4 were then sought that might match either EA or MSD. Two low energy peptide conformations were identified that might mimic EA, one from the X-ray crystal structure of CCK-4 [2] and one from an extensive Dreiding model-based, computer-assisted search procedure. An analogous search yielded a single conformation of CCK-4 related to MSD (Fig. 2).

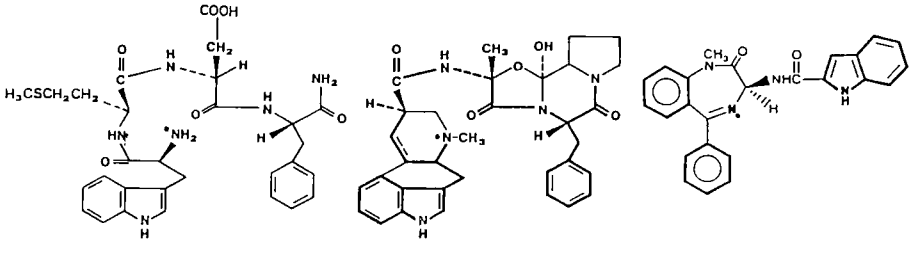

Fig. 1. CCK-4 (left), EA (middle), and MSD (right); common features are indicated in bold; potentially charged nitrogen atoms are indicated with an asterisk.

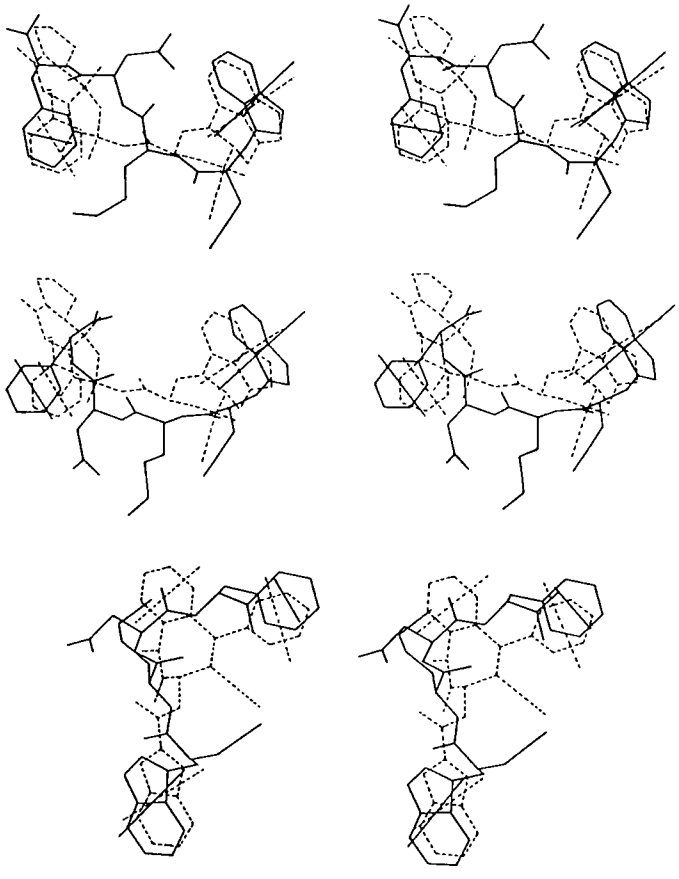

Fig. 2. Low energy CCK-4 conformations (solid lines), shown superimposed in stereo on EA (dotted lines; top and middle) and on MSD (dotted lines; bottom). Included are the receptor guidepoints attached to the common nitrogen atoms and aromatic rings of each molecule used in the modeling process.

All three conformations are similar in the position of the indole group relative to the amine; however, while the peptide chain of the two 'EA conformations' of CCK-4 is basically extended, the 'MSD conformation' has a partially folded backbone. This folding invokes a markedly different placement of the phenyl ring for CCK-4 in the 'MSD conformation' than in the 'EA conformations'. The peptide conformations described above may serve to explain the apparent difference observed between central and peripheral CCK receptors.

Acknowledgements

The work was supported in part by a Commonwealth Postgraduate Award to R.A.H.

References

1. Evans, B.E., Bock, M.G., Rittle, K.E., DiPardo, R.M., Whitter, W.L., Veber, D.F., Anderson, P.S. and Freidinger, R.M., Proc. Natl. Acad. Sci. U.S.A., 83(1986)4918.
2. Cruse, W.B.T., Egert, E., Kennard, O. and Viswamitra, M.A., Eur. Cryst. Meeting, 6(1980)274.

Acyl lysinamido phosphonates: Potent, long-acting inhibitors of angiotensin-converting enzyme

Melanie J. Loots, Michael C. Badia, David W. Cushman, Jack M. DeForrest, Donald S. Karanewsky, Maria G. Perri, Edward W. Petrillo, Jr. and James R. Powell

The Squibb Institute for Medical Research, P.O. Box 4000, Princeton, NJ 08543-4000, U.S.A.

Introduction

Recently, Almquist et al. found that replacement of the N-terminal benzoyl function in a ketomethylene acyl tripeptide analog by cyclobutanecarbonyllysine led to improved angiotensin-converting enzyme (ACE)-inhibitory potency and oral absorption [1]. By applying a similar strategy to the phosphonate acyl tripeptide analog **1c** [2], we have developed a new series of potent ACE inhibitors (**2**) with long duration of action after oral administration to rats and monkeys (Fig. 1).

Results and Discussion

Compounds **2a-d** were evaluated for inhibition of rabbit lung ACE in vitro [3] and inhibition of the angiotensin I (AI)-induced pressor response in normotensive rats (Table 1) [4]. Aminoalkyl phosphonate **1b** is much less active in vitro than the simple alkyl phosphonate **1a**; however, both **2a**, which includes

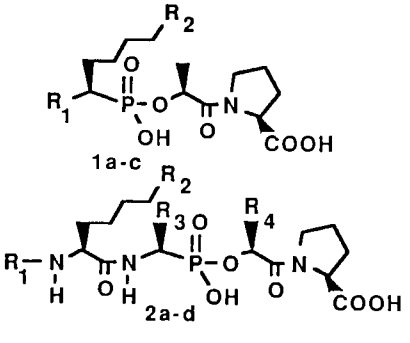

Fig. 1. Phosphonate ACE inhibitors.

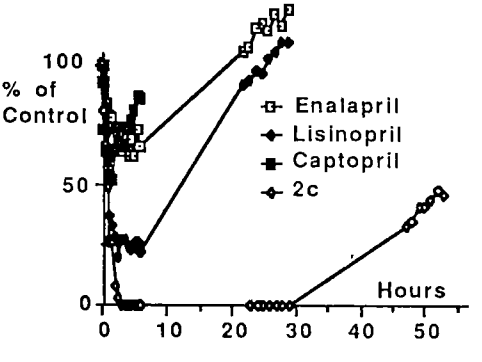

Fig. 2. %AI pressor response in monkeys at 1.5 μmol/kg, p.o.

Table 1 *Acyl lysinamido phosphonate ACE inhibitors*

No.	R_1	R_2	R_3	R_4	I_{50}[a]	ED_{50}[b]	% Inhib[c]
1a	H	Me			110	0.179	26[d]
1b	NH_2	H			1200	–	–
1c	PhCONH	H			13	0.015	20
2a	*c*-C_4H_7CO	NH_2	n-butyl	Me	6.4	0.018	88
2b	"	H	"	"	4	0.120	52
2c	*c*-C_5H_9CO	"	"	"	3.5	0.018	88
2d	H	"	"	"	22	0.060	67

[a]Rabbit lung ACE I_{50} (nM). [b]I.V. dose (μmol/kg) for 50% inhibition of AI pressor response. [c]% Inhibition of AI pressor response after 5 μmol/kg p.o. [d]50 μmol/kg dose.

structural features found in the potent pentapeptide inhibitor BPP_{5a} [5] (< Glu-Lys-Trp-Ala-Pro), and **1c** are much more potent in vitro than **1a** and **1b**. Most importantly, **2a** was more active orally than **1c**.

Removal of the amino group (**2b**) considerably reduced activity in vivo. The cyclopentylcarbonyl (**2c**) was similar to **2a** in vivo. Removal of the N-terminal acyl group (**2d**) gave diminished activity in vitro but relatively good oral activity.

Compound **2c** was compared with captopril, enalapril, and lisinopril after oral administration to monkeys (Fig. 2). Phosphonate **2c** led to complete inhibition of the AI pressor response between 5 and 30 hr after dosing; 50 hr after dosing, the AI pressor response was still inhibited by over 50%. The other compounds inhibited the response for less than 25 hr.

In summary, incorporation of structural features found in the pentapeptide BPP_{5a} into these phosphonate ACE inhibitors led not only to potent inhibition of ACE in vitro but unexpectedly to long duration of activity in rats and monkeys.

References

1. Almquist, R.G., Jennings-White, C., Chao, W.-R., Steeger, T., Wheeler, K., Rogers, J. and Mitoma, C., J. Med. Chem., 28 (1985) 1062.
2. Petrillo, E.W., Jr., Cushman, D.W., Duggan, M.E., Heikes, J.E., Karanewsky, D.S., Ondetti, M.A., O'Reilly, B., Rovnyak, G.C., Schwartz, J., Spitzmiller, E.R. and Wang, N.-Y., In Hruby, V.J. and Rich, D.H. (Eds.) Peptides: Structure and Function, Proceedings of the 8th American Peptide Symp., Pierce Chemical Company, Rockford, Illinois, 1983, p. 541.
3. Cushman, D.W. and Cheung, H.S., Biochem. Pharmacol., 20 (1971) 1637.
4. Rubin, B., Laffin, R.J., Kotter, D.G., O'Keefe, E.H., DeMaio, D.A. and Goldberg, M.E., J. Pharmacol. Exp. Therap., 204 (1978) 271.
5. Ondetti, M.A., Pluscec, J., Weaver, E.R., Williams, N., Sabo, E.F. and Kocy, O., In Meienhofer, J. (Ed.) Chemistry and Biology of Peptides, Ann Arbor Science, Ann Arbor, 1972, p. 525.

Diaminoalcohols and diaminoketones: Potent inhibitors of an enkephalin-degrading rat brain aminopeptidase

Norma G. Delaney, Eric M. Gordon, Magdi M. Asaad, David W. Cushman, Denis E. Ryono, Richard Neubeck and Sesha Natarajan

The Squibb Institute for Medical Research, P.O. Box 4000, Princeton, NJ 08543-4000, U.S.A.

Introduction

Enkephalins are rapidly inactivated in vivo by peptidases. Efforts to discover novel analgesics that potentiate endogenous enkephalins have focused primarily on inhibition of neutral endopeptidase (enkephalinase), which cleaves the Gly^3-Phe^4 bond, but aminopeptidases, which release Tyr^1, have also been strongly implicated in their physiological inactivation [1]. We therefore attempted to find novel, potent inhibitors of this enzyme class. The identity of the relevant aminopeptidase is not firmly established, but the strongest candidates are metalloenzymes [2, 3]. Potent substrate analog inhibitors of the metallopeptidase angiotensin-converting enzyme have incorporated amino alcohol [4] [-CH(OH)CH_2NH-] and aminoketone [5] (-$COCH_2$NH-) units in place of the scissile amide bond. We prepared diaminoalcohols and diaminoketones to investigate the affinity of these peptide bond surrogates for the aminopeptidase active site and to identify the minimal structural requirements for potent inhibition. N-terminal Boc-protected diaminoketones were prepared by N-alkylation of N-benzyl alkylamines or amino acid or dipeptide esters by Boc-amino acid chloromethyl ketones [5]. Standard coupling and deprotection procedures afforded diaminoketones; reduction ($NaBH_4$) prior to Boc group removal yielded diaminoalcohols. Inhibition of a soluble, puromycin-sensitive, enkephalin-degrading rat brain aminopeptidase (AP) similar to the membrane-bound enzyme called MII by Hersh [2] was assayed spectrophotometrically using L-leucine *p*-nitroanilide.

Results and Discussion

Tetrapeptide analog diaminoalcohol **1***R* is four times more potent than amastatin [6], which has a carbonyl instead of a methylene between the hydroxylated carbon and the NH of the P_1' residue. The *S*-hydroxyl epimer of **1** is about tenfold less potent. Deletion of C-terminal residues results in only a twofold loss in potency for the tripeptide analog **2***R* and a sixfold loss for

Table 1 *Inhibition by diaminoalcohols and diaminoketones*

Compound		Brain AP I_{50} (nM)	
		*R	*S
1	Leu-ψ[CH*(OH)CH_2NH]-Leu-Val-Phe-OMe	20	230
2	Leu-ψ[CH*(OH)CH_2NH]-Leu-Val-OMe	41	600
3	Leu-ψ[CH*(OH)CH_2NH]-Leu-NH_2	120	28,000
4	Leu-ψ[CH*(OH)CH_2NH]-Dcv[a]	110	5,200
Amastatin	D-Leu-ψ[CH*(OH)CONH, *S*]-Val-Val-Asp	80	
5	Leu-ψ[CH*(OH)CH_2NH, *RS*]-Phe-Leu	160	
6	Phe-ψ[CH*(OH)CH_2NH, *RS*]-Phe-Leu	580	
7	Ala-ψ[CH*(OH)CH_2NH, A[b]]-Phe-Leu	1,100	
8	Ala-ψ[$COCH_2$NH]-Phe-Leu	110	
9	Ac-Ala-ψ[$COCH_2$NH]-Phe-Leu	740,000	
10	Leu-ψ[$COCH_2$NH]-Dcv[a]	14	
11	(*S*) H_2N-CH($CH_2CH(CH_3)_2$)CO-CH_2Cl	1,600	
12	(*S*) H_2N-CH($CH_2CH(CH_3)_2$)CH_2SH	12	

[a] Dcv = des-carboxyvaline.
[b] More potent diastereomer.

the dipeptide analogs **3***R* and **4***R*. The requirement for an *R*-hydroxyl is more pronounced in the dipeptide analogs; **3***S* and **4***S* are 230- and 50-fold less active, respectively, than their epimers. Within the tripeptide framework, there is a preference for P_1 Leu (**5**) over Phe (**6**) or Ala (**7**). Diaminoketone **8** is tenfold more potent than diaminoalcohol **7**. The poor activity of the acetylated analog **9** suggests a critical requirement for a free N-terminus.

Preparation of **10**, the diaminoketone analog of **4***R*, also led to a tenfold increase in activity. This simple inhibitor has 100-fold greater activity than L-leucine chloromethyl ketone (**11**) and activity comparable to that of L-leucinethiol (**12**) [7]. The ketone carbonyl of **10** could undergo addition by an enzyme nucleophile to give a tetrahedral complex or it could bind in its hydrated form. Thus, diaminoketones and diaminoalcohols may owe their potent aminopeptidase inhibitory activity to their ability to mimic the transition state for amide bond hydrolysis.

References

1. de la Baume, S., Yi, C.C., Schwartz, J.C., Chaillet, P., Marcais-Collado, H. and Costentin, J., Neuroscience, 8 (1983) 143.
2. Hersh, L.B., J. Neurochem., 44 (1985) 1427.
3. Gros, C., Giros, B. and Schwartz, J.C., Biochemistry, 24 (1985) 2179.
4. Gordon, E.M., Godfrey, J.D., Pluscec, J., Von Langen, D. and Natarajan, S., Biochem. Biophys. Res. Commun., 126 (1985) 419.

5. Natarajan, S., Gordon, E.M., Sabo, E.F., Godfrey, J.D., Weller, H.N., Pluscec, J., Rom, M.B. and Cushman, D.W., Biochem. Biophys. Res. Commun., 124 (1984) 141.
6. Aoyagi, T., Tobe, H., Kojima, F., Hamada, M., Takeuchi, T. and Umezawa, H., J. Antibiot., 31 (1978) 636.
7. Chan, W.W.-C., Biochem. Biophys. Res. Commun., 116 (1983) 297.

Synthesis of conformationally constrained CCK-4 analogs containing a substituted gamma lactam ring

David S. Garvey, Paul D. May and Alex M. Nadzan
Abbott Laboratories, Pharmaceutical Products Division, N. Chicago, IL 60064, U.S.A.

The putative neurotransmitter/neuromodulator cholecystokinin (CCK) has been found to exist in nerve terminals throughout the central nervous system (CNS), and specific CCK binding sites have been demonstrated in numerous brain regions. The C-terminal tetrapeptide, Trp-Met-Asp-PheNH$_2$ (CCK-4), has been shown to possess high affinity for the CNS binding sites. As part of a program to design mimics of peptide neurotransmitters, we have synthesized two series of compounds in which a γ-lactam ring substituted at the 4-position with either a carboxylic acid moiety or a propyl group has been incorporated into CCK-4 at the aspartate or methionine positions, respectively (see Scheme 1).

Our starting material was the commercially available Boc-D-Asp-β-OBz (**1**), which was converted to the methyl ester **2** in 90% yield [diisopropylethylamine, methyl iodide, acetone]: mp 64°C; $[\alpha]_D$ -34.8° (c = 1.1, toluene). Compound **2** reacts with the Bredereck reagent **3** [1], following the precedence of Danishefsky et al. [2, 3] to produce the enamine **4** which is not isolated but directly hydrolyzed (2N HCl-THF) to a mixture of the hydroxymethylene isomers **5** (yield 92%, 2 steps; $<$80% ee vide infra). Reductive amination of aldehyde **5** with **6** affords the amine which cyclizes under the reaction conditions to give a mixture of lactam dipeptides **7** in 73% yield. Other products isolated were the two diastereomeric lactams (6%) derived from a small quantity of the racemate of **5** formed during the formylation reaction and the γ-lactone (9%) arising from the direct reduction of aldehyde **5**. The amino terminus of **7** was deprotected (TFA-CH_2Cl_2) and coupled to dipeptide **8** via the mixed anhydride method to give a mixture of **9a** and **9b** in 75% yield. Final deprotection (H_2, Pd/C, CH_3OH) produced the tetrapeptides **10a** and **10b** in 65% yield.

For the synthesis of the propyl substituted lactams, compound **5** was O-alkylated with allyl bromide (diisopropylethylamine, acetone) to afford **12** in 72% yield. Thermal Claisen rearrangement (Decalin, reflux, 75 min) gave **13** which was not routinely isolated but hydrogenolyzed (H_2, Pd/C, CH_3OH) to give a mixture of aldehydes **14** in 91% yield from **12**. Reductive amination with **15** under the same conditions described above produced a mixture of the lactams **16** in 65% yield. Deprotection of the amino terminus followed by active

SCHEME 1

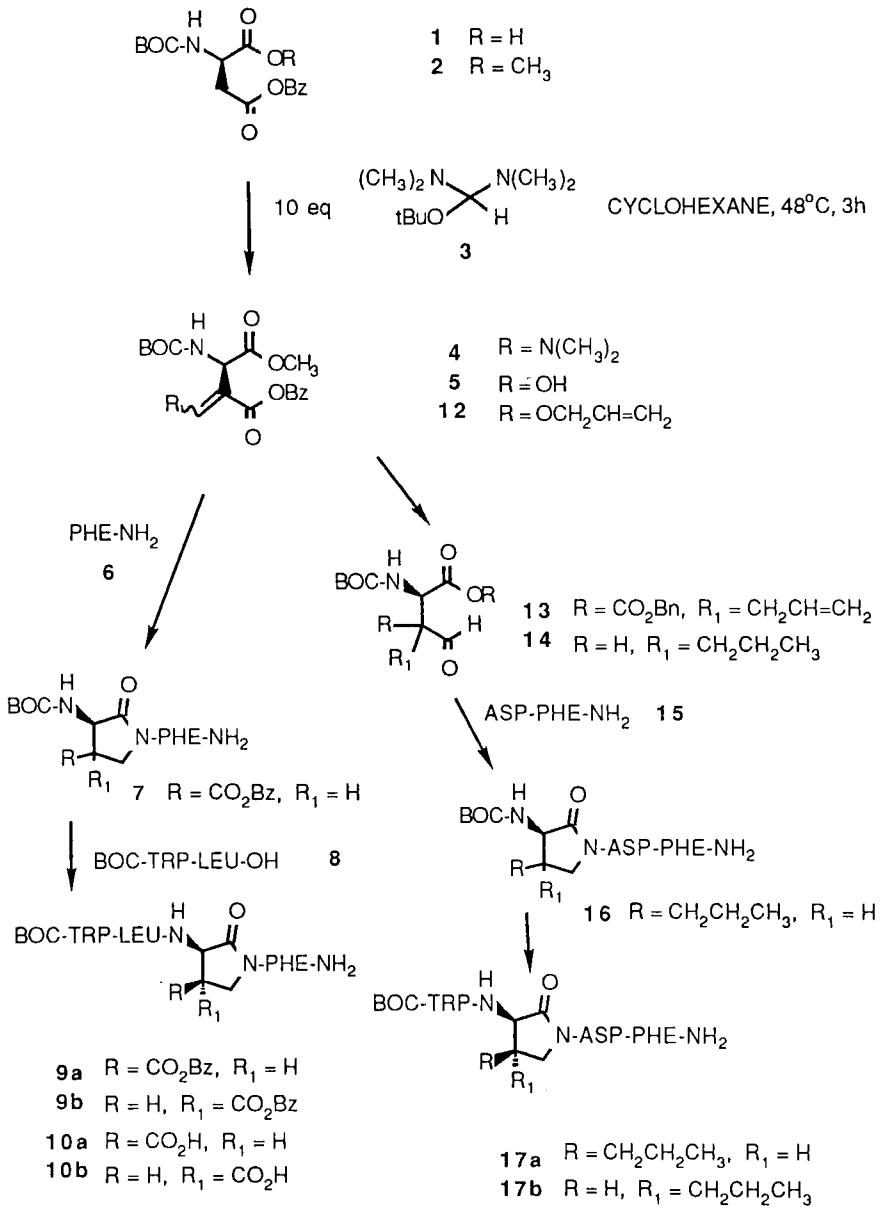
BOC-N
OR
OBz
1 R = H
2 R = CH3
10 eq
(CH3)2 N
N(CH3)2
tBuO
H
3
CYCLOHEXANE, 48°C, 3h
OCH3
4 R = N(CH3)2
5 R = OH
12 R = OCH2CH=CH2
PHE-NH2
6
13 R = CO2Bn, R1 = CH2CH=CH2
14 R = H, R1 = CH2CH2CH3
N-PHE-NH2
7 R = CO2Bz, R1 = H
BOC-TRP-LEU-OH 8
BOC-TRP-LEU-N
9a R = CO2Bz, R1 = H
9b R = H, R1 = CO2Bz
10a R = CO2H, R1 = H
10b R = H, R1 = CO2H
ASP-PHE-NH2 15
N-ASP-PHE-NH2
16 R = CH2CH2CH3, R1 = H
BOC-TRP-N
17a R = CH2CH2CH3, R1 = H
17b R = H, R1 = CH2CH2CH3

ester coupling with Boc-Trp-OSu gave the desired products **17a** and **17b** in 48% yield.

References

1. Bredereck, H., Simchen, G., Rebsdat, S., Kantlehner, W., Horn, P., Wahl, R., Hoffman, H. and Grieshaber, P., Chem. Ber., 101 (1968) 41.
2. Danishefsky, S., Berman, E., Clizbe, L.A. and Hirama, M., J. Am. Chem. Soc., 101 (1979) 4385.
3. Danishefsky, S., Morris, J. and Clizbe, L.A., Heterocycles, 15 (1981) 1205.

A dehydro-keto-methylene inhibitor of substance P degradation

A. Ewenson[a], R. Laufer[b], J. Frey[b], E. Rosenkovich[b], M. Chorev[c], Z. Selinger[b] and C. Gilon[a,*]

Departments of [a]Organic, [b]Biological and [c]Pharmaceutical Chemistry, Hebrew University of Jerusalem, Jerusalem 91904, Israel

Introduction

Substance P (SP), a putative neurotransmitter, is degraded in the mammalian central nervous system (CNS) by various enzymes, among them a specific metalloendopeptidase which has been shown to abolish SP activity [1]. In this work, we report the design, synthesis and preliminary in vitro activity of a racemic dehydro-keto-methylene pseudopeptide. This bidentate ligand apparently interacts with the active site of a rat brain SP degrading enzyme believed to inactivate the endogenous neurotransmitter.

Results and Discussion

Chemistry

We have extended our recently reported syntheses of keto-methylene pseudodipeptide analogs [2, 3] to allow the preparation of dehydro-keto-methylene pseudopeptide **6a** (see Scheme 1).

The *N*-benzoyl dehydro-keto-methylene pseudodipeptide ester, **1a**, serves as a common intermediate. In previous synthetic attempts, it proved impossible to remove the benzoyl protecting group and maintain the stereochemistry of the double bond in the dehydro-pseudodipeptide. When **1a** was hydrolyzed (HCl/HOAc) without prior reduction, *cis-trans* isomerization was observed and a low yield of product was attained. Furthermore, reintroduction of a Boc protecting group resulted in partial migration of the double bond from the side chain to the backbone. Two selective methods for the mild removal of the *N*-benzoyl group were studied. Subjecting Bz(*RS*)Phe ψ $(COCH_2)$Gly-OMe as a model compound to $SOCl_2$ at 0°C, followed by methanolysis, did not yield the expected imino ether but rather the corresponding oxazole. Attempts to avoid the formation of the oxazole by protecting the ketone as a dioxolane failed since the latter

*To whom correspondence should be addressed.

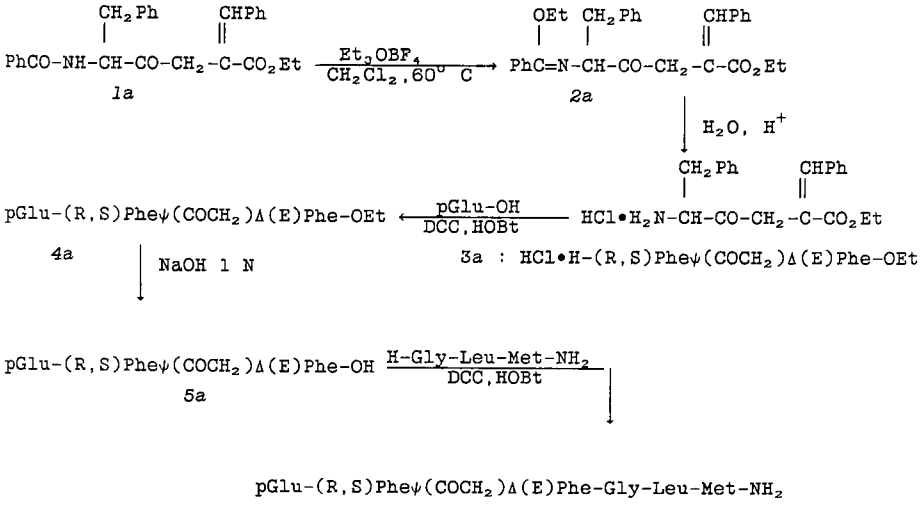

Scheme 1.

did not survive the $SOCl_2$ treatment. In the second approach (Scheme 1), Meerwein's reagent [4], Et_3OBF_4, was used. This led to a smooth conversion of the benzamide into the desired imino ether. The crude reaction mixture was subjected to mild acid hydrolysis, to yield the pure amine hydrochloride, **3a**, in 55% yield. This procedure retains the α,β-double bond in its *trans* configuration as established by ^1H NMR spectroscopy. Furthermore, no ester exchange occurs when methyl esters are treated with excess Et_3OBF_4 in a similar fashion. Preparation of the dehydro-keto-methylene pseudohexapeptide **6a** was accomplished by coupling pGlu-OH to the amine terminus of **3a**, a reaction which proceeded smoothly and in high yield. In contrast, the coupling of pseudopeptide **5a** to H-Gly-Leu-Met-NH_2 was extremely slow and plagued by side reactions, even with HOBt or DMAP catalysis. The desired product **6a** was isolated by semipreparative HPLC. Analogs **6b** and **c** (Table 1) were synthesized by classical fragment condensation, from the appropriate Boc-protected pseudodipeptides which were prepared as previously described [3].

Biological activity

The pseudohexapeptide analogs **6a, b** and **c** were assayed as inhibitors of SP degradation as followed, using a radiolabeled substrate incubated in the presence of rat brain preparations [5]. The results are summarized in Table 1. Analog **6a** was the most potent inhibitor of the group that we investigated. Compounds **6a** and **b** were devoid of spasmogenic activity using the guinea pig ileum (GPI) assay, whereas compound **6c** was a weak agonist [0.5% potency in contracting the GPI relative to (pGlu^6) SP_{6-11} = 100%].

Table 1 *Characterization and biological activities of SP keto-methylene and dehydro-keto-methylene inhibitors*

Compound	HPLC[a] (K')	AAA[b]	FABMS [M+H]	IC_{50}[c] (μM)
6a,[pGlu^6, (*RS*)Phe$^7\psi$($COCH_2$)Δ(E)Phe^8]SP_{6-11}	3.35	x = 1 Glx = 1 Gly = 1 Leu = 1 Met = 1	721	1.8
6b,[pGlu^6, (*RS*)Phe$^7\psi$($COCH_2$)(*RS*)Phe^8]SP_{6-11}	7.68	x = 1 Glx = 1 Gly = 1 Leu=1 Met = 1	723	30
6c,[pGlu^6,Gly$^9\psi$($COCH_2$)(*RS*)Leu^{10}]SP_{6-11}	6.32 7.01[d]	x = 1 Phe = 2 Glx = 1 Met = 2	723	50

[a] Merck Lichrosorb RP8, MeCN/H_2O(0.05% TFA) 62/38.
[b] x represents the free pseudodipeptide, as established independently.
[c] Established by the assay described in [5].
[d] As [a], elution conditions MeCN/H_2O(0.05% TFA) 25/75-60/40 (20 min); elemental analysis: correct C, H, N values for pseudopeptide dihydrate.

Summary

The synthetic procedure is effective for the preparation of interesting racemic peptide keto-methylene and dehydro-keto-methylene analogs. Employing this method we were able to prepare a novel dehydro-keto-methylene pseudohexapeptide **6a**, which is a potent inhibitor of SP degradation.

References

1. Lee, C.M., Sandberg, B., Hanley, M. and Iversen, L., Eur. J. Biochem., 114 (1981) 315.
2. Ewenson, A., Laufer, R., Chorev, M., Selinger, B. and Gilon, C., J. Med. Chem., 29 (1986) 295.
3. Ewenson, A., Cohen, R., Levian, D., Chorev, M., Laufer, R., Selinger, Z. and Gilon, C., In Deber, C.M., Hruby, V.J. and Kopple, K.D. (Eds.) Peptides: Structure and Function (Proceedings of the 9th American Peptide Symposium), Pierce Chemical Co., Rockford, IL, 1985, p. 639.
4. Meerwein, H., Borner, P., Fuchs, V., Sasse, J., Schrodt, H. and Spille, J., Chem. Ber., 209 (1956) 89.
5. Laufer, R., Wormser, U., Selinger, Z., Chorev, M. and Gilon, C., J. Chromatogr., 301 (1984) 415.

Synthesis and properties of some peptides related to the bicyclic β-turn dipeptide (BTD)

U. Nagai[a,*], R. Kato[a], K. Sato[b], N. Ling[b], T. Matsuzaki[c] and Y. Tomotake[c]
[a]*Mitsubishi-Kasei Institute of Life Sciences, 11-Minamiooya, Machida-shi, Tokyo 194, Japan*
[b]*The Salk Institute, P.O. Box 85800, San Diego, CA 92138, U.S.A.*
[c]*Mitsubishi Chemical Industries, Ltd., Research Centre, 1000 Kamoshida, Midori-ku, Yokohama, Kanagawa 227, Japan*

Introduction

BTD is a dipeptide building block which was designed to freeze the β-turn conformation of a peptide chain at the point of its incorporation. That is, BTD is a new type of conformational constraint. The syntheses of BTD itself [1] and some peptides containing BTD [2–4] have been reported already.

Molecular Conformation of BTD

The crystal structure of Boc-BTD-OH was elucidated by X-ray analysis. The dihedral angles corresponding to ψ_2 and θ_3 (normal β-turn nomenclature) were −161° and −69°, respectively. The β-turn of BTD was confirmed to be classified as type 2′ from the dihedral angles.

Synthesis of a BTD-Containing Analog of Mini-Somatostatin

A potent cyclic hexapeptide analog of somatostatin was reported by Veber et al. [5]. Its structure is shown in Fig. 1 together with an analog containing BTD. Based on Veber's hypothesis that the essential residues for somatostatin activity are Phe-Trp-Lys-Thr and that the Phe-Pro moiety induces the confor-

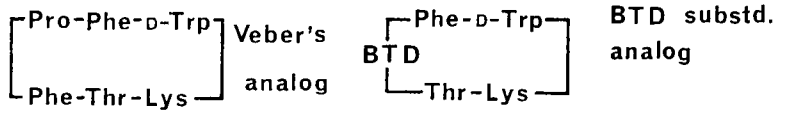

Fig. 1. Structures of the somatostatin analogs.

*To whom correspondence should be addressed.

mational constraint of the β-turn, replacement of the Phe-Pro sequence with BTD was attempted. The BTD-containing analog was synthesized by the classical solution method and showed weak activity in inhibiting growth hormone release from the pituitary. Since the analog was not thoroughly purified, it is difficult to analyze the reasons for the observed weak activity; however, it is of interest that such a designed analog showed some biological activity.

Synthesis of 8,8-Dimethyl BTD

Amino acid residues assuming β-turn conformations in the active form can be considered to play two kinds of roles; (i) inducing β-turns and (ii) having affinity with the receptor. In those cases where the second role is significant, replacement of the turn sequences with BTD having no substituent on the bicyclic nucleus cannot yield a highly active analog. It is, therefore, necessary to introduce various substituents on the BTD skeleton. As the first step for the synthesis of substituted BTD, the title compound was synthesized. The structure and physical constants are shown in Fig. 2.

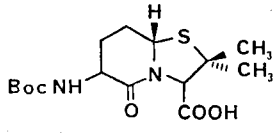

M.p ~255° (dec.)

$[\alpha]_D$ −218° (c=0.5, MeOH)

Fig. 2. Structure of 8,8-dimethyl-BTD.

References

1. Nagai, U. and Sato, K., Tetrahedron Lett., 26 (1985) 647.
2. Sato. K., Nagai, U., J. Chem. Soc. Perkin Trans. 1 (1986) 1231.
3. Nagai, U. and Sato, K., In Deber, C.M., Hruby, V.J. and Kopple, K.D. (Eds.) Peptides: Structure and Function, Proceedings of the 9th American Peptide Symposium, Pierce Chemical Co., Rockford, IL, 1985, p. 465.
4. Nagai, U., Nakamura, R., Sato, K. and Ying, S.-Y., In Miyazawa, T. (Ed.) Peptide Chemistry 1986, Protein Research Foundation, Osaka, 1987, p. 295.
5. Veber, D.F., Freidinger, R.M., Perlow, D.S., Paleveda, Jr., W.J., Holly, F.W., Strachan, R.G., Nutt, R.F., Arison, B.H., Homnick, C., Randall, W.C., Giltzer, M.S., Saperstein, R. and Hirschmann, R., Nature, 292 (1981) 55.

Tripeptide aminoalcohols: A new class of human renin inhibitors

Sesha Natarajan, Charles A. Free, Emily F. Sabo, James Lin, Ervin R. Spitzmiller, Sylvia G. Samaniego, Sandra A. Smith and Linda M. Zanoni

The Squibb Institute for Medical Research, Princeton, NJ 08540-0130, U.S.A.

Introduction

We describe in this communication the development of a novel series of low molecular weight, potent, human renin inhibitors. When we attempted to rationally design small-sized renin inhibitors, the finding that pepstatin fragment **1**, a truncated tripeptide molecule (Iva-Val-Val-Sta-OEt), binds at the active site of penicillopepsin [1] attracted our attention. Based on this observation, we reasoned that it would be appropriate to investigate whether **2**, also a tripeptide molecule (Boc-Phe-His-Sta-OEt), could effectively interact with human renin. When we synthesized and tested **2**, we observed moderate inhibition of human renin ($I_{50} = 2.7$ μM). This result encouraged us to extend the concept to develop a new series of 'tripeptide aminoalcohols' as novel inhibitors of human renin.

Results and Discussion

The concept of utilizing a β-aminoalcohol moiety as a surrogate for the scissile amide bond in the design of peptide substrate-derived 'transition state mimic' inhibitors has been successfully applied previously to angiotensin-converting enzyme and renin [2–4]. By maintaining the peptide framework of **2**, compound **3** was designed as the target 'tripeptide aminoalcohol' molecule for this investigation. When **3** was synthesized as a mixture of diastereomeric alcohols and tested, it displayed modest inhibition of human renin (Table 1). The *'R'* isomer, **4**, was approximately 30 times more potent [5] than **5**, the *'S'* isomer. In contrast to the above finding, when a diastereomer of **2**, having the hydroxyl grouping in *R* configuration, was synthesized and tested, it was found to be a weaker inhibitor of human renin ($I_{50} = 25$ μM). We next synthesized several analogs of **3** by varying the P_1 residue and the substituent on the amino grouping (Table 1). The analogs having a benzyl grouping on the amine and cyclohexylmethyl grouping at P_1 position displayed enhanced levels of inhibition (e.g., **11** vs. **3** and **12** vs. **3**). When all the above observations were combined to design an

Table 1 *Human renin inhibition by aminoalcohol analogs*

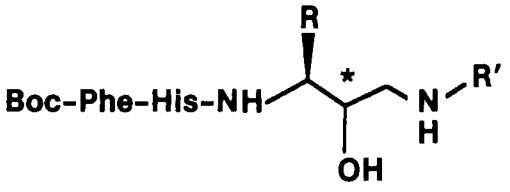

	R	R'	*	I_{50} (μM)[a]		R	R'	*	I_{50} (μM)[a]
3	*i*-bu[b]	*i*-bu	*RS*	1.6	**4**	*i*-bu	*i*-bu	*R*	0.86
5	*i*-bu	*i*-bu	*S*	27.0	**6**	*i*-bu	*n*-propyl	*RS*	1.9
7	*i*-bu	*i*-propyl	*RS*	2.5	**8**	*i*-bu	*n*-butyl	*RS*	1.5
9	*i*-bu	*i*-pentyl	*RS*	2.6	**10**	*i*-bu	chm[c]	*RS*	1.0
11	*i*-bu	benzyl	*RS*	0.34	**12**	chm	*i*-bu	*RS*	0.2
13	chm	benzyl	*R*	0.017	**14**	chm	benzyl	*S*	0.73

[a] Assays for human kidney renin were conducted at pH 7.0 using human plasma angiotensinogen (0.5 μM) as substrate.
[b] *i*-bu = *i*-butyl.
[c] chm = -CH_2-cyclohexyl.

optimal tripeptide aminoalcohol inhibitor, by choice, of a cyclohexylmethyl grouping at P_1 position, a benzyl substituent on the amine and *epi*-statine (*R*) stereochemistry for the hydroxyl grouping, the resulting molecule, **13**, displayed very potent inhibition of human renin (I_{50} = 17 nM). The corresponding '*S*' isomer, **14**, exhibited 43-fold weaker potency.

Conclusions

In summary, our findings show that 'tripeptide aminoalcohols' are potent inhibitors of human renin. A significant finding for this class of inhibitors is that the isomers with '*R*' configuration at the center bearing the hydroxyl grouping are more potent than isomers with '*S*' configuration, a finding that contrasts with what has been found in 'statine'- or 'hydroxy isostere'-containing renin inhibitors.

Acknowledgements

The authors wish to acknowledge Dr. J. Gougoutas and Ms. M. Malley for the X-ray determinations.

References

1. James, M.N.G., Sielecki, A.R. and Moult, J., In Hruby, V.J. and Rich, D.H. (Eds.) Peptides: Structure and Function, Proceedings of the 8th American Peptide Symposium, Pierce Chemical Company, Rockford, Illinois, 1983, p. 521.
2. Gordon, E.M., Godfrey, J.D., Pluscec, J., Von Langen, D. and Natarajan, S., Biochem. Biophys. Res. Commun., 126(1985)419.
3. Ryono, D.E., Free, C.A., Neubeck, R., Samaniego, S.G., Godfrey, J.D. and Petrillo, E.W., In Hruby, V.J. and Kopple, K.D. (Eds.) Peptides: Structure and Function, Proceedings of the 9th American Peptide Symposium, Pierce Chemical Company, Rockford, Illinois, 1985, p. 739.
4. Dann, J.D., Stammers, D.K., Harris, C.J., Arrowsmith, R.J., Davies, D.E., Hardy, G.W. and Morton, J.A., Biochem. Biophys. Res. Commun., 134(1986)71.
5. A slight preference for '*R*' configuration at this center was previously observed [3] with the hexapeptide aminoalcohol inhibitors.

Synthesis and antagonist activities of backbone-modified angiotensin II analogs

W. Howard Roark, Francis J. Tinney and Ernest D. Nicolaides
Department of Chemistry, Warner-Lambert/Parke-Davis Pharmaceutical Research, Ann Arbor, MI 48105, U.S.A.

Introduction

Most antagonists of angiotensin II (ANG II, Asp-Arg-Val-Tyr-Ile-His-Pro-Phe) are analogs with substitutions at positions 1 and 8 [1]. Even though potent antagonists of ANG II have been found, they are of limited therapeutic value since they have short half-lives in vivo. Recently, many investigators have sought to combat short in vivo half-lives of peptides by modifying hydrolytically susceptible amide bonds [2].

Results and Discussion

To study the effect of amide bond replacement on biological activity in the known ANG II antagonist [3, 4] [Sar^1, Leu^8] ANG II (**8**), we prepared (Scheme 1) three methyleneamino-modified analogs of this peptide and tested them for their ability to inhibit ^{125}I ANG II binding to rat adrenal homogenates [5] and for their ability to inhibit ANG II-induced contractions in isolated rat and rabbit aortae [6]. The results of these tests are in Table 1.

As evidenced in the table, a single methyleneamino modification causes almost no loss in binding. Two modifications cause only a small loss, while three modifications result in a 34-fold loss in the ability to inhibit ^{125}I ANG II binding to rat adrenal tissue homogenates. When tested for its ability to inhibit ANG II-induced contraction in aortic rings from rat and rabbit, the singly modified analog (**3**) showed only a small decrease in activity relative to the parent peptide;

Table 1 *Biological activity*

Compound	AGBI M	VAGA rat M	VAGA rabbit M
3 Mono-modified	3.7×10^{-10}	2.0×10^{-9}	3.5×10^{-9}
5 Di-modified	5.2×10^{-10}	1.4×10^{-7}	1.1×10^{-6}
7 Tri-modified	1.2×10^{-8}	2.5×10^{-8}	3.0×10^{-7}
8 Parent peptide	3.5×10^{-10}	9.0×10^{-10}	1.0×10^{-9}

Scheme 1

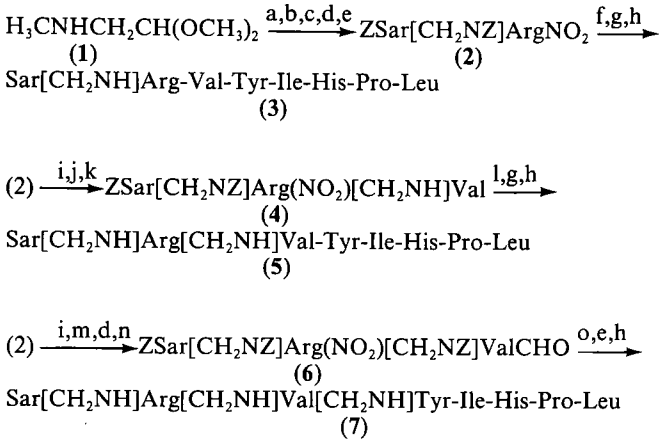

(a) ZCl, NEt_3; (b) HCl/H_2O; (c) $Arg(NO_2)OCH_3$,$NaCNBH_3$; (d) $ZCl/NaHCO_3$; (e) $NaOH/H_2O$; (f) Val-Tyr(OBz)-Ile-His-Pro-Leu-OBz; (g) HOBt, DCC; (h) H_2/Pd on C; (i) CDI, $H_3CNH(OCH_3)$, LAH; (j) Val-OtBu, $NaCNBH_3$; (k) TFA; (l) Tyr(OBz)-Ile-His-Pro-LeuOBz; (m) L-Valinol, $NaCNBH_3$; (n) $(Cl\text{-}C)_2$, DMSO, NEt_3; (o) Tyr(OBz)-Ile-His-Pro-Leu-OMe (O)

Z = carbobenzyloxy Bz = benzyl

the doubly modified derivative (**5**) showed a large (155-fold and 1100-fold in VAGA rat and VAGA rabbit, respectively) decrease in functional activity despite showing only a small decrease in binding. Finally, the tri-modified analog (**7**) showed a good correlation between binding and functional activities, with approximately a 30-fold loss in activity in all tests relative to [Sar^1, Leu^8] ANG II (**8**).

These results suggest that multiple methyleneamino amide bond replacements in [Sar^1, Leu^8] ANG II (**8**) may be made such that high binding and functional activity are maintained. Furthermore, compounds derived from modification of classical angiotensin II antagonists may lend themselves to development as valuable therapeutic agents for the treatment of hypertension.

Acknowledgements

The authors are greatly indebted to Mr. Terry C. Major and Mr. Arnold D. Essenburg for the AGBI and VAGA results.

References

1. Regoli, D., Park, W.K. and Rioux, F., Pharmacol. Rev., 69 (1974) 69.
2. Spatola, A.F., In Weinstein, B. (Ed.) Chemistry and Biochemistry of Amino Acids, Peptides and Proteins, vol. 7, Marcel Dekker, New York, 1983, P. 267.
3. Regoli, D., Rioux, F. and Park, W.K., Rev. Can. Biol., 31 (1972) 73.
4. Regoli, D., Park, W.K. and Rioux, F., Can. J. Physiol. Pharmacol., 51 (1973) 114.
5. Douglas, J.G., Michailov, M., Khoslo, M.C. and Bumpus, F.M., Endocrinology, 106 (1980) 120.
6. Hooker, C.S., Calkins, P.J. and Fleish, J.H., Blood Vessels, 14 (1977) 1.

A position seven analog of angiotensin II with potent antagonist activity

James Samanen[a], Judith C. Hempel[a], Daljit Narindray[a] and Domenico Regoli[b]

[a]*Smith Kline and French Laboratories, P.O. Box 1539, King of Prussia, PA 19406-0939, U.S.A.*

[b]*University of Sherbrooke, Sherbrooke, Quebec, Canada J1H 5N4*

Introduction

Until now, antagonist analogs of angiotensin II (AII) have only been generated through Tyr^4 or Phe^8 modifications of AII [1]. We reasoned that substitution of the lactam described by Freidinger [2] for Pro^7 in [Sar^1]-AII would give analog **1**, [Sar^1, (-L,L-lactam-Phe)^{7,8}]-AII, in which the lactam (shown in Fig. 1), with a psi angle of -111° or -144°, would prevent a C-terminal gamma turn (psi ~ 60°) inferred by ^{1}H NMR [3] and thereby prevent adoption of an agonist conformation.

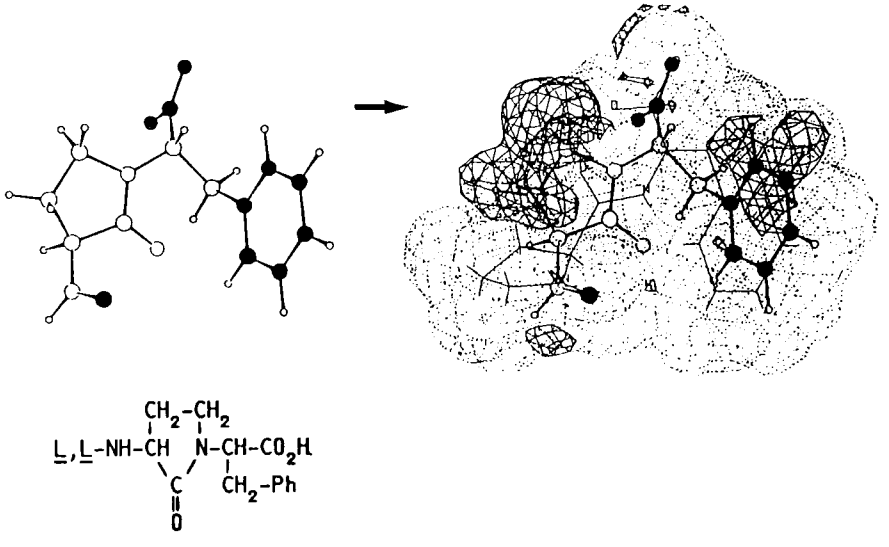

Fig. 1. -L-Lactam-L-Phe (left) and the agonist volume map [2] highlighted with divergent regions of the lactam Phe volume map. His^6-lactam^7 linkage, carboxylate and phenyl groups darkened.

Results and Discussion

Analog **1** was synthesized on Merrifield resin by standard solid phase peptide synthesis techniques from Boc-L-lactam-L-Phe [2]. In the rabbit aorta [4], analog **1** was a pure potent antagonist (pA_2 8.3), comparable to saralasin (pA_2 8.6). In vivo antagonist activity [5] was reduced (ID_{50} 100 ± 18.5 ng/rat-min), presumably due to converting-enzyme degradation [6].

Systematic search [7] (via SYBYL, Tripos Associates, St. Louis, MO) of conformations accessible to the C-terminal dipeptide of (ΔPhe^8, and Thiq^8]-AII, constrained analogs [8] that retain agonist activity, gave an agonist volume map [7], Fig. 2 [8], describing all conformers shared by these analogs. When the His^6-lactam^7 amide linkage of **1** is aligned with the His^6-Pro^7 amide linkage in the agonist model, **1** *can essentially adopt the agonist conformation* with Phe^8 side chain and carboxylate group alignments with those in the agonist conformation, Fig. 1. In this conformation, however, the lactam ethylene bridge is *not* contained within the agonist volume map (Fig. 1), suggesting the ethylene bridge could sterically interfere with receptor binding in this agonist conformation. The high affinity interaction between receptor and **1**, inferred by in vitro antagonist activity, must arise through adoption by either receptor or **1** of an *alternate conformation*, which upon binding does not end in cellular response. With the data in hand, we cannot distinguish between the two possibilities.

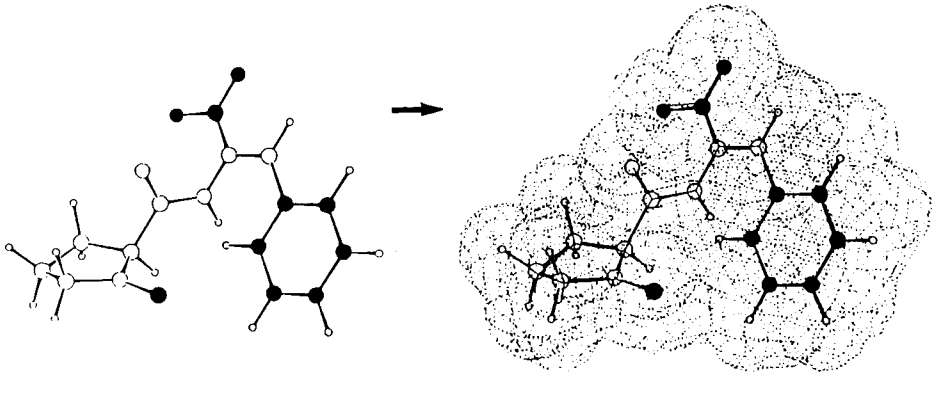

Fig. 2. -L-Pro-ΔPhe (left) and the agonist volume map [2]. His^6-Pro^7 linkage, carboxylate and phenyl groups darkened.

References

1. Bumpus, F.M. and Khosla, M.C., In Genest, J., Koiw, E. and Kuchel, O. (Eds.) Hypertension: Physiopathology and Treatment, McGraw-Hill, New York, 1977, p. 183.
2. Freidinger, R.M., Perlow, D.S. and Veber, D.F., J. Org. Chem., 47 (1982) 104.
3. Weinkam, R.J. and Jorgensen, E.C., J. Am. Chem. Soc., 93 (1971) 7038.
4. Rioux, F., Park, W.K. and Regoli, D., Can. J. Physiol. Pharmacol., 51 (1973) 665.
5. Regoli, D. and Park, W.K., Can. J. Physiol. Pharmacol., 50 (1972) 99.
6. Trachte, G.J., Ackerly, J.A. and Peach, M.J., J. Cardio. Pharm., 3 (1981) 838.
7. Sufrin, J.R., Dunn, D.A. and Marshall, G.R., Mol. Pharmacol., 19 (1981) 307.
8. Marshall, G.R., Dtsch. Apoth.-Ztg., 126 (1986) 2783.

Session III
Analytic and synthetic methods

Chair: R.B. Merrifield
The Rockefeller University
New York City, New York, U.S.A.

Asymmetric synthesis of amino acids

David A. Evans*, Ann E. Weber, Thomas C. Britton, Jonathan A. Ellman and Eric B. Sjogren

Department of Chemistry, Harvard University, Cambridge, MA 02138, U.S.A.

Introduction

Over the last several years, we have been interested in the development of new methods for the efficient asymmetric synthesis of nonproteinogenic amino acids. The synthesis of complex glycopeptides such as the potent antibiotic vancomycin [1] offers a variety of challenges in this area which are currently being pursued in this laboratory (Fig. 1). In addition to the unusual arylglycine synthons, vancomycin contains both syn and anti β-hydroxy tyrosine derivatives not readily amenable to synthesis by current reaction methodology.

Results and Discussion

Recent advances in amino acid synthesis have featured highly diastereoselective alkylation reactions of chiral glycine enolate synthons [2–4] (Scheme 1, Transform A). A complementary bond construction involves the diastereoselective electrophilic amination of chiral enolates (Scheme 1, Transform B). The advantages

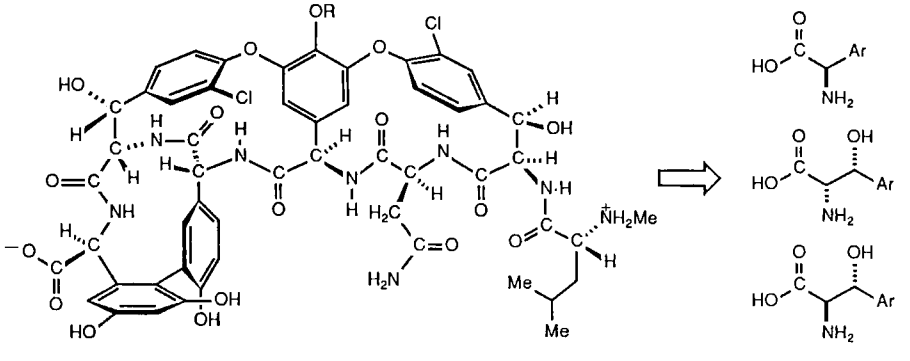

Fig. 1. Vancomycin synthons.

*To whom correspondence should be addressed.

Scheme 1

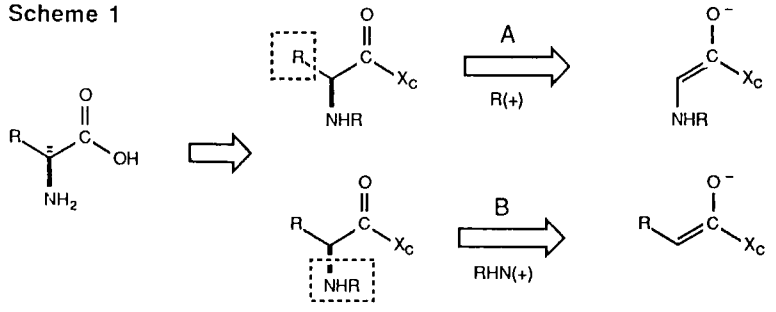

of electrophilic enolate amination are clear: The scope of the reaction is not constrained by the structure of the alkyl or aryl substituent in the amino acid target.

We have found that di-*tert*-butyl azodicarboxylate performs admirably as an electrophilic aminating agent [5]. This reagent reacts readily with lithium enolates derived from chiral *N*-acyl oxazolidinones **1** to provide the hydrazide adducts **2** in excellent yield with diastereoselectivities ranging from 97 to greater than

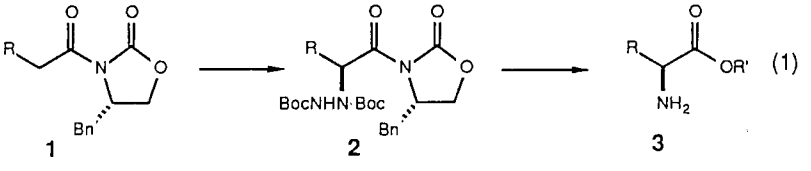

1 2 3 (1)

99% (Eqn. 1). The chiral auxiliary can be removed using either lithium hydroxide in THF/water, magnesium methoxide in methanol, or lithium benzyloxide in THF. The lithium hydroxide conditions proved to be uniquely effective for hydrolysis in base-sensitive cases such as R = aryl, providing the derived amino acid with less than 2% racemization. In this case, subsequent esterification with diazomethane followed by treatment with trifluoroacetic acid and hydrogenation with Raney nickel afforded the phenylglycine methyl ester **3** (R = Ph, R' = Me) in quantitative yield in 98% enantiomeric purity.

Several alternative enolate amination sequences which provide access to α-azido acids have also been developed (Scheme 2). Hydroxylation of the sodium enolates of *N*-acyl oxazolidinones using 3-phenyl-2-phenylsulfonyl oxaziridine provides the α-hydroxy compounds **4** with diastereoselectivities ranging from 90 (R = Ph) to greater than 99% (R = *tert*-butyl) [6]. In all cases, the minor diastereomeric product contaminants may be readily removed by column chromatography. Conversion of the hydroxy imides **4** to the corresponding azides **5** via the Mitsunobo reaction with HN_3 proceeds in excellent yield without racemization. Alternatively, *N*-acyl oxazolidinones as their derived boron enolates

Scheme 2

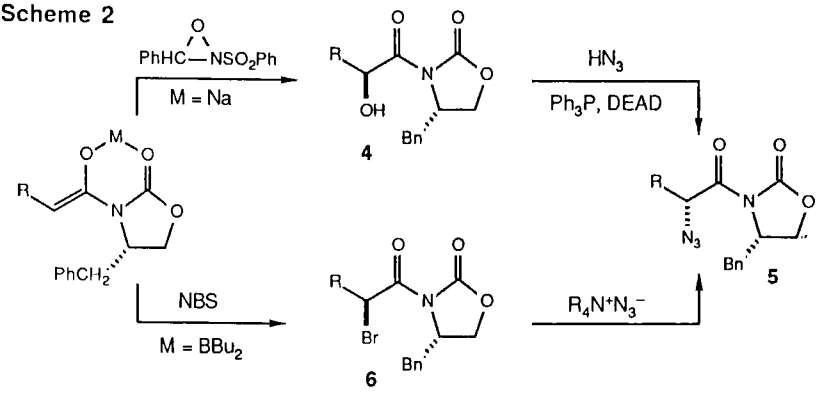

have been found to react with *N*-bromosuccinimide to give the α-bromo derivatives **6**, which also provide α-azidocarboximides when treated with tetramethylguanidinium azide [7]. The diastereoselectivity in these brominations is typically 95% for most cases. The α-azidocarboximides **5** are readily converted to the enantiomerically pure amino acids by lithium hydroxide hydrolysis and azide reduction using stannous chloride in methanol or hydrogen and palladium on carbon. Racemization-prone phenylglycine derivatives are readily obtained from **5** (R = Ar) in 98% ee following this protocol.

The preceding two-step approaches to α-azidocarboximides require S_N2 displacements by nucleophilic azide, which were found to be sluggish in hindered cases. Accordingly, a direct electrophilic azide transfer reaction has been developed which eliminates this problem [8]. Treatment of the potassium enolate derived from imide **1** with 2, 4, 6-triisopropylbenzenesulfonyl azide followed by an acetic acid quench provides the desired azide **7** in high yield with excellent stereoselectivity (Eqn. 2). Conversion to the amino acids proceeds as before.

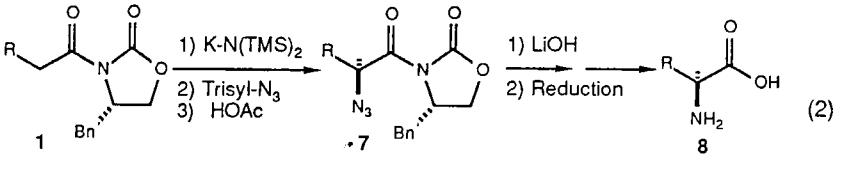

(2)

In the sterically hindered case (R = *tert*-butyl), oxazolidinone hydrolysis occurs in poor yield, with attack at the oxazolidinone carbonyl to give a predominantly ring-opened product. In contrast, hydrolysis with lithium hydrogen peroxide in THF affords the desired azido acid in 98% yield.

Syn and anti β-hydroxy amino acids are readily available via asymmetric aldol reactions of the appropriate chiral glycine enolate synthon. The syn selective

aldol reaction of a chiral protected α-aminoacetate provides syn β-hydroxy amino acids (Eqn. 3) while the syn selective aldol reaction of a chiral haloacetate followed

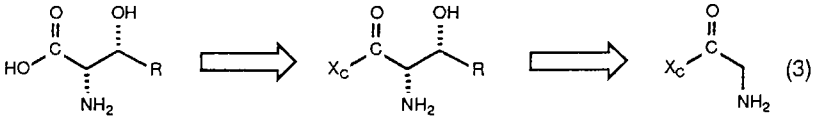

(3)

by displacement with nucleophilic nitrogen affords anti β-hydroxy amino acids (Eqn. 4).

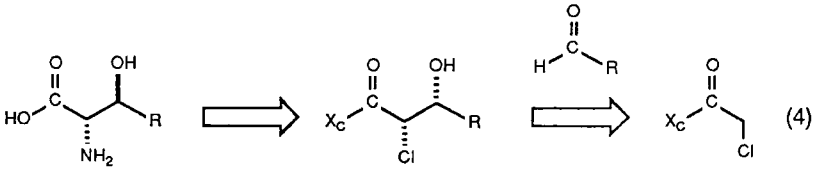

(4)

The stannous triflate-derived enolate of isothiocyanoacetyl oxazolidinone **9** undergoes a highly diastereoselective aldol reaction to afford the syn adducts as internally derived heterocycles **10** in 71–92% yields (Eqn. 5) [9]. In conjunction

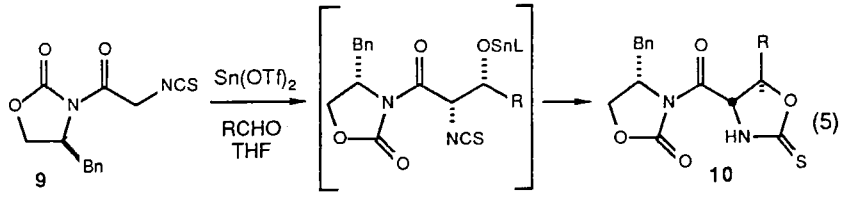

(5)

with the total synthesis of the antifungal agent echinocandin D [10], adduct **10** (R = p-BnOPhCH$_2$) was converted to N-Boc amino acid **13** in three steps (Eqn. 6) [11]. The oxazolidinone was removed by treatment with magnesium

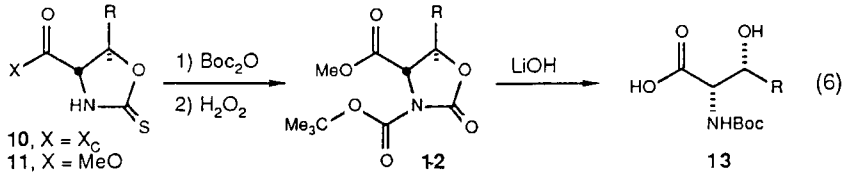

(6)

methoxide in methanol to provide methyl ester **11** in 95% yield. Following acylation with di-*tert*-butyldicarbonate and desulfurization, the resultant N-Boc oxazolidinone **12** was hydroxyzed to the desired amino acid derivative in 83% yield using aqueous lithium hydroxide.

α-Chloroacetyl oxazolidinone **14** has proven to be a useful anti β-hydroxy amino acid synthon [12]. The dibutylboron triflate-mediated aldol reaction of **14** proceeds with 95–97% diastereoselection and in moderate yield, which can be increased by using excess enolate. Adduct **18** may be readily converted to *allo*-threonine (Eqn. 8). Displacement with sodium azide (DMF, 45°C) afforded azide **19** in 70% yield, along with 10–15% of the C-2 epimer. Hydrolysis with lithium hydroxide followed by catalytic hydrogenation provided an 82% yield of *allo*-threonine (**20**). The α-bromoacetyl carboximide **16** (Eqn. 7) performs comparably in the aldol reaction; however, the azide displacement reaction of α-bromo aldol adduct **17**, which proceeds smoothly at room temperature, affords the azide with no detectable epimerization. Therefore, the α-bromo adduct **21** was chosen for use in the synthesis of the unusual hydroxyproline derivative **23** found in echinocandin D (Eqn. 9) [11]. The intriguing aspect of this synthesis

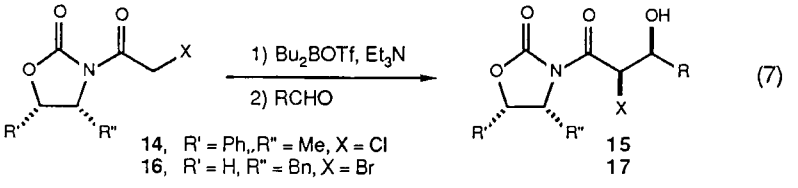

(7)

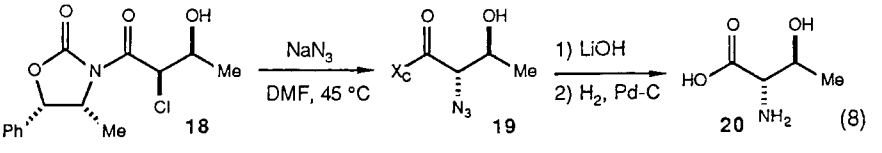

(8)

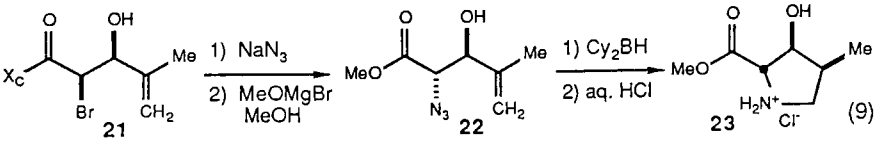

(9)

was associated with the conversion of **22** to **23**, a formal cycloalkylation of an olefinic azide promoted by dicyclohexylborane. Treatment of **22** with dicyclohexylborane gave an intermediate azido trialkylborane, which reacted in situ in an intramolecular fashion to afford a 72% yield of the desired proline derivative **23**. We are currently developing the scope of this reaction which should be generally useful for the synthesis of cyclic amino acids.

The asymmetric enolate amination reactions together with the glycine enolate aldol reaction methodology described herein are powerful tools for the synthesis of a wide variety of unusual amino acids. This methodology is currently being applied to the total synthesis of members of the vancomycin family of glycopeptides.

Acknowledgements

This research has been supported by the National Institutes of Health, the National Science Foundation, Merck, and The Eli Lilly Company. The NIH BRS Shared Instrumentation Program 1 S10 RR01748-01A1 is also acknowledged for providing NMR facilities.

References

1. Williams, D.H., Acc. Chem. Res., 17 (1984) 364.
2. Schollkopf, U., Top. Curr. Chem., 109 (1983) 66.
3. Seebach, D., Miller, D.D., Muller, S. and Weber, T., Helv. Chim. Acta, 68 (1985) 949 (and references therein).
4. Ikegami, S., Hayama, T., Katsuki, T. and Yamaguchi, M., Tetrahedron Lett., 27 (1986) 3403 (and references therein).
5. Evans, D.A., Britton, T.C., Dorow, R.L. and Delaria, J.F., J. Am. Chem. Soc., 108 (1986) 6395.
6. Evans, D.A., Morrissey, M.M. and Dorow, R.L., J. Am. Chem. Soc., 107 (1985) 4346.
7. Evans, D.A., Ellman, J.A. and Dorow, R.L., Tetrahedron Lett., 28 (1987) 1123.
8. Evans, D.A. and Britton, T.C., J. Am. Chem. Soc., 109 (1987) in press.
9. Evans, D.A. and Weber, A.E., J. Am. Chem. Soc., 108 (1986) 6757.
10. Traber, R. von, Keller-Juslen, C., Loosli, H.-R., Kuhn, M. and Wartburg, A. von, Helv. Chim. Acta, 62 (1976) 1252.
11. Evans, D.A. and Weber, A.E., J. Am. Chem. Soc., in press.
12. Evans, D.A., Sjogren, E.B., Weber, A.E. and Conn, R.E., Tetrahedron Lett., 28 (1987) 39.

Asymmetric syntheses of β-OH and β-OH, γ-alkyl α-amino acids: Analogs of the unusual cyclosporin amino acid MeBmt

Roger D. Tung*, Chong-Qing Sun, Don Deyo and Daniel H. Rich
School of Pharmacy, University of Wisconsin-Madison, 425 N. Charter St., Madison, WI 53706, U.S.A.

Stemming from our involvement in the cyclosporin system [1, 2], we have sought the development of new routes to allow ready access to the unusual amino acid MeBmt (Fig. 1, **15**), as well as to a variety of analogs to allow structure-activity assessments at that residue [3–6]. As recently reported, we have used the catalytic Sharpless epoxidation technique [7] to advantage with the parent amino acid [6]. Herein, we describe the use of asymmetric epoxidations in the synthesis of MeBmt derivatives.

Recent work in our lab has suggested that our original MeBmt synthesis [6] is amenable to considerable modification (Fig. 2). Variation of substrate, nucleophile, and protecting group allows access to a variety of analogs. We

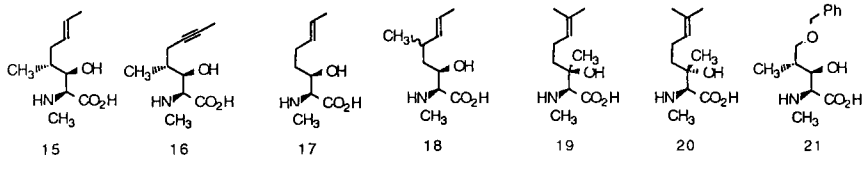

*Fig. 1. MeBmt (**15**) and analogs synthesized by asymmetric epoxidation.*

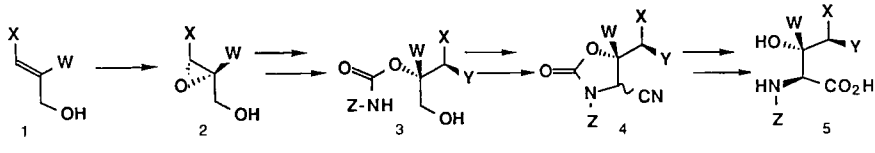

Fig. 2. Generalized synthesis of MeBmt analogs (see Ref. 6 for details).

* Present address: Department of Medicinal Chemistry, Merck Sharp and Dohme Research Laboratories, West Point, PA 19486, U.S.A.

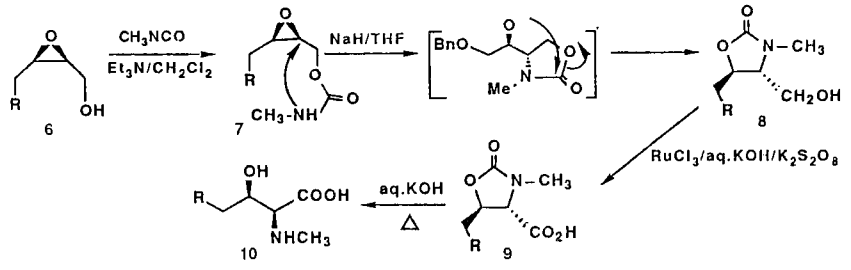

Fig. 3. Short, stereocontrolled synthesis of N*-methyl* threo *β-OH-α-amino acids.*

have recently completed the synthesis of an 'yne' derivative, wherein the olefin of the MeBmt side chain is replaced with an acetylene (Fig. 1, **16**); work is currently underway on substitutions at positions W and Y.

A shorter, enantiospecific route to a variety of *threo*, β-hydroxy-α-amino acids was suggested by Roush and Adam's report that carbamate-protected *cis* β, γ-epoxy alcohols (**4**) undergo regiospecific intramolecular opening at the β-position, followed by rearrangement to hydroxymethyl oxazolidinones (Fig. 3, **8**) [8]. Oxidation of the hydroxymethyl to carboxylate **9**, followed by hydrolytic ring cleavage, would then yield the desired amino acids **10**. This oxidation was achieved, after a number of attempts, by using a recently reported ruthenium (VI) species [9]. This reagent is compatible with olefins, and allowed reasonable yields of **5** (approximately 60–70%) with the balance being mainly starting material. Sharpless epoxidation allowed control of stereochemistry at both stereogenic centers. Starting from commercially available or readily synthesized precursors, we have synthesized several new analogs in this manner (Fig. 1, **17–20**).

Entry to the γ-methyl series via this route was made possible by Nagaoka and Kishi's [10] observation of substrate control in the mCPBA epoxidation of **12** (Fig. 4) (available in >80% yield over four steps from commercial precursor **11** [11]). Carrying this epoxide through the above route yielded an interesting oxygen isostere (Fig. 1, **21**). We are currently pursuing the corresponding methyl and ethyl ethers to give analogs closer to the parent amino acid.

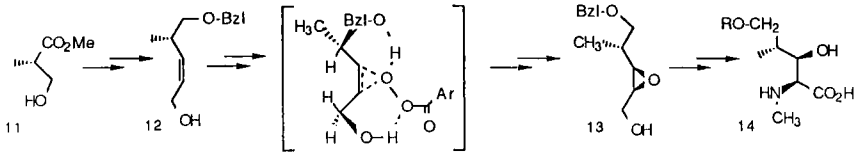

Fig. 4. ϵ-Oxygen analogs of MeBmt via Nagaoka and Kishi's substrate-controlled epoxidation.

In conclusion, we have found that asymmetric epoxidations allow convenient and versatile access to the stereocontrolled synthesis of a variety of β-OH and γ-alkyl β-OH-α-amino acids. Full experimental details and biological data for the corresponding cyclosporins will be forthcoming in due course.

Acknowledgements

Financial support from NIH (grant # AR32007) and Merck Sharp and Dohme is greatly appreciated.

References

1. Rich, D.H., Dhaon, M.K., Dunlap, B. and Miller, S.P.F., J. Med. Chem., 29 (1986) 978.
2. Tung, R.D., Dhaon, M.K. and Rich, D.H., J. Org. Chem., 51 (1986) 3350.
3. Wenger, R.M., Helv. Chim. Acta, 66 (1983) 2308.
4. Evans, D.A. and Weber, A.E., J. Am. Chem. Soc., 108 (1986) 6757.
5. Seebach, D., Juaristi, E., Miller, D.D., Schickli, C. and Weber, T., Helv. Chim. Acta, 70 (1987) 237.
6. Tung, R.D. and Rich, D.H., Tetrahedron Lett., 28 (1987) 1139.
7. Hanson, R.M. and Sharpless, K.B., J. Org. Chem., 51 (1986) 1922 (and references therein).
8. Roush, W.R. and Adam, M.A., J. Org. Chem., 50 (1985) 3752.
9. Green, G., Griffith, W.P., Hollinshead, D.M., Ley, S.V. and Schroder, M., J. Chem. Soc. Perkin Trans. I (1984) 681.
10. Nagaoka, H. and Kishi, Y., Tetrahedron, 37 (1981) 3873 (and references therein).
11. Roush, W.R., Palkowitz, A.D. and Palmer, M.A.J., J. Org. Chem., 52 (1987) 316 (and references therein).

Activation and racemization in peptide bond formation

N. Leo Benoiton and Francis M.F. Chen
Department of Biochemistry, University of Ottawa, Ottawa, Ont., Canada KIH 8M5

Introduction

Recent years have seen the introduction of several commercial peptide synthesizers which incorporate a variety of methodologies based on the use of activated forms of *N*-alkoxycarbonyl (ROCO)-amino acids obtained using an *N,N'*-dialkylcarbodiimide (C-diimide). Several intermediates have been implicated in the formation of the peptide bond, the course of the reactions depending on the stoichiometry and the order of addition of reagents and the natures of the side chain and the alkoxycarbonyl group of the activated residue. The more novel of these, the 2-alkoxy-5(4*H*)-oxazolone (AlkOx) [1], has also been identified as the first product in the decomposition of mixed anhydrides (MxAn) [2]. A clearer understanding of the reactions has issued from the finding that symmetrical anhydrides (SyAn) [3, 4], AlkOx's [1], and MxAn's [2] are stable enough to be purified by edulcoration ('to cleanse from soluble salts by washing with water'). The availability of these activated ROCO-amino acids prompted us to examine their use as derivatizing reagents [5]. Emerging from this is the finding that racemization of activated ROCO-amino acids, which can occur during their base-catalyzed esterification [6] and aminolysis [7], can also occur during aminolysis in the absence of excess base. Recognition that the extent of racemization can be correlated with the ease of cyclization of MxAn's to the AlkOx has led to the identification of iPrOCOCl as superior chloroformate for MxAn reactions. This communication contains a short review of C-diimide-mediated reactions and a description of these results. Earlier references can be found in a previous review [8].

Results and Discussion

C-diimide reacts with an ROCO-amino acid to give the *O*-acylisourea (O-AIU) which undergoes aminolysis to give the peptide. Direct detection of the O-AIU has yet to be achieved. The O-AIU has a tendency to rearrange to the inactive *N*-acylurea (N-AU), a reaction promoted by base and polar solvents. The O-AIU can also cyclize to the AlkOx, both of which react immediately with any available ROCO-amino acid to give the SyAn. All three are readily

aminolyzed by a nitrogen nucleophile, the order of reactivity being O-AIU > AlkOx > SyAn. More cyclization is associated with the use of $EtN=C=NPrNMe_2$ than the other C-diimides. The course of events depends on the availability and reactivity of the attacking nucleophile. The reaction goes in the direction of the SyAn in the absence of the nucleophile, a situation which emerges if there is an excess of reagents, when a two-phase system exists such as in solid phase synthesis, or when the nucleophile is an oxygen atom producing an ester. Cyclization and rearrangement are more pronounced for the activated β-methylamino acids which are less readily aminolyzed. AlkOx stability, as well as the point of attack by water, varies with the nature of *R*. For *R* = Bzl, hydrolysis occurs at the ring oxycarbonyl bond, producing the acid which immediately reacts with a second molecule of the AlkOx, generating SyAn [1]. For *R* = *t*Bu and Fm, hydrolysis occurs at the exocyclic bond liberating the alcohol and the *N*-carboxyanhydride. The AlkOx with *R* = Fm is the most stable to water, but the most sensitive to hydrolysis by aqueous HCO_3^-. The AlkOx itself also decomposes gradually by a self-catalyzed β-elimination, producing dibenzofulvene [4].

Additives such as 1-hydroxybenzotriazole and *N*-hydroxysuccinimide interfere by trapping the O-AIU as the ROCO-amino acid-activated ester, thus preventing the other reactions of rearrangement, cyclization, and SyAn formation. HOBt and HONSu also react immediately with an AlkOx, giving the same products. The product formed from the reaction of HOBt and an oxazolone or a SyAn is actually a mixture of two forms of the HOBt derivative [9, 10]. Based on the reaction of HOBt with 2-Me-4-iPr-5(4*H*)-oxazolone and inspection by NMR spectroscopy, we conclude there occurs initially an aminolysis by the triazole nitrogen, followed by a gradual rearrangement to the ester. Since these additives suppress but do not eliminate racemization in C-diimide couplings of peptide acids, in practice the trapping of the activated forms must not be complete.

When attack by a weak nucleophile, which implies the SyAn pathways predominate, is facilitated by the addition of a basic catalyst such as 4-dimethylaminopyridine (DMAP), the base converts the SyAn into the AlkOx [11], which can undergo some racemization before it is aminolyzed [1]. This explains why the DMAP-catalyzed esterification of a SyAn produces racemization [6]. The reaction of a *tert*-amine with a SyAn to give the AlkOx and the ROCO-amino acid anion is reversible [12]. The use of DMAP possibly could cause a second side reaction (rearrangement of the SyAn to ROCO-Xxx-(ROCO)Xxx-OH [12, 13]), which could lead to a double acylation. These issues are pertinent when esterification is used for attachment of the first residue to a support. It would be desirable to eliminate them by finding a more activated form of the ROCO-amino acid which would react with the hydroxymethyl group of the anchor without the need for a catalyst. Possibilities which come to mind are

the FmOCO-amino acid chlorides [14] and the AlkOx's [1, 4] if a satisfactory method could be found for their preparation.

An AlkOx is in principle the ideal activated form of an ROCO-amino acid because nothing is liberated by its aminolysis besides the product. In attempts to exploit their use for practical purposes, we reacted 2-EtO-oxazolones with amino acid anions. To our surprise, slight racemization was observed, part of which was attributable to the chiral lability of the compounds on storage. Subsequent experiments revealed that SyAn's of EtOCO-amino acids (Val, Phe) also underwent partial racemization (4–10%) during reaction at 23°C in aqueous DMF with amino acid anions formed by the addition of one equivalent of $NaHCO_3$. Racemization was reduced to 0.1–1.2% for reactions with the valyl derivative when the anion was formed using Na_2CO_3. This reaction of converting enantiomers to the EtOCO-L-Val-D/LXxx-OH epimers followed by their analysis by HPLC was developed as a method for determining enantiomers [15]. It is particularly suitable for determining enantiomers of arginine and histidine in a hydrolysate since all other products of the derivatization can be extracted out by an organic solvent.

The behavior of SyAn's containing cleavable protecting groups was then examined. Reactions of $(Z\text{-Val})_2O$ and $(Z\text{-Phe})_2O$ [3] with valine neutralized with one equivalent of $NaHCO_3$ in aqueous DMF at -5°C led to 11.6% and 8.6% racemization, respectively. These results were reduced to 2.0% and 0.2%, respectively, when Na_2CO_3 was the base. Similar reactions starting with Z-Val-O-COOEt and Z-Phe-O-COOEt [2] led to 31.0% and 8.4% racemization followed by 15.8% and 0.2% racemization, respectively. Thus the apparently anomalous situation that the stronger base produces less racemization had been obtained. We explain the results on the basis that aminolysis was impeded in the case of the weaker base because of incomplete deprotonation of the $-NH_3^+$. We concluded that with Na_2CO_3 as base, no racemization occurred for ROCO-Phe-anhydrides but some still occurred for ROCO-Val-anhydrides.

We had previously concluded that the first step in the decomposition of an MxAn is cyclization to the AlkOx, ultimately resulting in an apparent disproportionation of the MxAn [2]. The ease of cyclization depends on the nature of the alkyl group of the carbonate moiety of the anhydride, in the order, methyl (2-iPr-5-Me-cyclohexyl) Mn < Et/iBu << methylsulfonylethyl (Ms) [2], and the extent of racemization observed in the couplings of Z-Gly-amino acids by the MxAn method depended on the R'OCOCl, in the same order, Mn < iBu << Ms [15]. The unattractive features of MnOCOCl as a reagent prompted us to examine the suitability of iPrOCOCl (Aldrich) for MxAn reactions, since we suspected that the unique properties of the MnOCO moiety resided in the nature of the alkyl group, from a secondary alcohol. iPrOCOCl was found to be an efficient reagent for couplings by the MxAn method, and Z-Xxx-O-COOiPr and Boc-Xxx-O-COOiPr were readily obtainable by the standard procedure [2] which

includes edulcoration. The amount of urethane generated by aminolysis at the carbonate moiety of the anhydride was the same as that [15] generated by the isobutyl group. Racemization attending the aminolysis of Z-Val-O-COOR' in aqueous DMF at +5°C by D-valine neutralized with Na_2CO_3 was as follows: Et, 18.8%; iBu, 6.8%; Mn, 3.0%; iPr, 0.6%. Racemization attending the couplings of Z-Gly-Xxx-OH (Xaa = Phe, Xbb = Leu) with H-Val-OEt at +5°C using R'OCOCl and *N*-methylmorpholine and an activation time of 10 min were as follows: Xaa (DMF) Et, 28.8%; iBu, 37.6%; iPr, 6.6%; Xaa (DMF-CH_2Cl_2, 1 : 1) Et, 15.0%; iBu, 24.2%; iPr, 8.6%; Xbb (DMF) Et, 10.8%; iBu, 28.2%; iPr, 8.0%; Xbb (DMF-CH_2Cl_2, 1 : 1) Et, 36.2%; iBu, 24.8%; iPr, 3.4%. Other data indicated the same trends. The results are in accord with the observed greater resistance to cyclization of ROCO-Xxx-O-COOiPr anhydrides.

Conclusions

Activated ROCO-amino acids are susceptible to racemization when aminolyzed even in the absence of excess base. The use of iPrOCOCl in the MxAn method of coupling leads to substantially less racemization than the use of EtOCOCl or iBuOCOCl.

Acknowledgements

This work was financially supported by the Medical Research Council of Canada. The data on racemization were obtained by Mrs. Y. Lee.

References

1. Benoiton, N.L. and Chen, F.M.F., Can. J. Chem., 59 (1981) 384.
2. Chen, F.M.F. and Benoiton, N.L., Can. J. Chem., 65 (1987) 619.
3. Chen, F.M.F., Kuroda, K. and Benoiton, N.L., Synthesis, (1978) 928.
4. Paquet, A., Chen, F.M.F. and Benoiton, N.L., Can. J. Chem., 62 (1984) 1335.
5. Benoiton, N.L. and Metuzals, J., In Metuzals, J. (Ed.) Electron Microscopy and Alzheimer's Disease, San Francisco Press, San Francisco, 1986, p. 25.
6. Atherton, E., Benoiton, N.L., Brown, E., Sheppard, R.C. and Williams, B.J., J. Chem. Soc. Chem. Commun., (1981) 336.
7. Wang, S.S., Tam, J.P., Wang, B.S.H. and Merrifield, R.B., Intl. J. Pept. Protein Res., 18 (1981) 459.
8. Benoiton, N.L., In Gross, E. and Meienhofer, J. (Eds.) The Peptides - Analysis, Synthesis, Biology, Vol. 5, Academic Press, New York, 1983, p. 217.
9. König, W. and Geiger, R., Chem. Ber., 103 (1970) 788.
10. Horiki, K., Tetrahedron Lett., (1977) 1897.
11. Benoiton, N.L. and Chen, F.M.F., J. Chem. Soc. Chem. Commun., (1981) 1225.
12. Benoiton, N.L. and Chen, F.M.F., In Theodoropoulus, D. (Ed.) Peptides 1986, Walter de Gruyter, Berlin, 1987, p. 127.

13. Ahmed, F.R., Chen, F.M.F. and Benoiton, N.L., Can. J. Chem., 64 (1986) 1396.
14. Carpino, L.A., Cohen, B.J., Stephens, K.E., Jr., Sadat-Aalaee, S.Y., Tien, J.-H. and Langridge, D.C., J. Org. Chem., 51 (1986) 3732.
15. Chen, F.M.F., Lee, Y., Steinauer, R. and Benoiton, N.L., Can. J. Chem., 65 (1987) 613.

Development of methodology for arginine and *N*-alpha protection in peptide synthesis

Robert Ramage, Jeremy Green and Michael R. Florence
Department of Chemistry, University of Edinburgh, West Mains Road, Edinburgh EH9 3JJ, U.K.

Consideration of the Mtr group, **1**, for arginine protection identified a problem, in that deprotection requires strong acid for times greater than one hour and, moreover, in multi-Arg sequences the deprotection can be even slower. From previous studies [1–3] it is clear that the substituents on the benzene ring of N_G-Arg-sulphonamides control the acid stability of such derivatives. In order to maximize the inductive effects of substituents while maintaining the stereo-electronic effect of the oxygen lone-pair with respect to donation through the benzene ring to the SO_2 function, we synthesized the 2,2,5,7,8-pentamethyl-chroman-6-sulphonyl chloride, **2**, which was reacted with Z-Arg to give the stable derivative Z-Arg(Pmc)-OH, **3**. This derivative was incorporated into the sequences Z-Arg(Pmc)-Gly-Gly-OMe and Z-Leu-Arg(Pmc)-Leu-Arg(Pmc)-Gly-Gly-OMe and it was found that the new Arg protecting group was cleaved by 50% TFA in methylene chloride within 60 min.

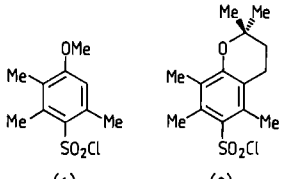

(1)

(2)

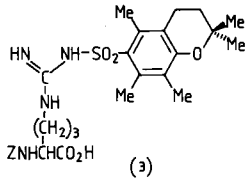

(3)

The orthogonal approach to SPPS that we adopted required a base-labile Nα protecting group analogous to the Fmoc group [4–6]. This led us to investigate the derivatives of 2,2-[bis(4-nitrophenyl)]-ethanol (BnpeOH), **4**, which was synthesized from 2,2-diphenylethyl acetate. The useful derivatives **5** and **6** can be obtained from **4** in the usual manner and reaction of a range of α-amino acids with **6**, by the method of Lapatsanis et al. [7], afforded the Bnpeoc derivatives, **7**. The Bnpeoc group is stable to acid, tertiary amines and very slowly cleaved by secondary and primary amines under forcing conditions. Indeed, some Bnpeoc amino acids may be purified as cyclohexylamine or dicyclo-

hexylamine salts. The protecting group is most effectively, and swiftly, cleaved by 1,8-diazobicyclo[5,4,0]undec-7-ene (DBU) in near stoichiometric proportions in DMF. The olefin produced, **8**, may be monitored for completion of the deprotection.

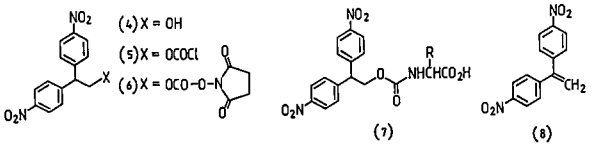

Acknowledgements

We thank Wendstone Chemicals Plc and SERC for support.

References

1. Nishimura, O. and Fujino, M., Chem. Pharm. Bull., 24 (1976) 1568.
2. Fujino, M., Wakimasu, M. and Kitada, C., Chem. Pharm. Bull., 29 (1981) 2825.
3. Yajima, H., Takeyama, M., Kanaki, J. and Mitani, K., J. Chem. Soc., Chem. Commun. (1978) 482.
4. Carpino, L.A. and Han, G.Y., J. Org. Chem., 37 (1972) 3404.
5. Atherton, E., Gait, M.J., Sheppard, R.C. and Williams, B.J., Bioorganic Chem., 8 (1979) 351.
6. Chang, C.D. and Meienhofer, J., Int. J. Pept. Prot. Res., 11 (1978) 246.
7. Lapatsanis, L., Milias, G., Froussios, K. and Kolovos, M., Synthesis (1983) 671.

Solid phase synthesis of C-terminal peptide amides under mild conditions

Fernando Albericio[a,b], Nancy Kneib-Cordonier[a], Lajos Gera[a], Robert P. Hammer [a], Derek Hudson[c] and George Barany[a,*]

[a]*Department of Chemistry, University of Minnesota, 207 Pleasant Street S.E., Minneapolis, MN 55455, U.S.A.*

[b]*Department of Organic Chemistry, University of Barcelona, Spain*

[c]*Biosearch, Inc., 2980 Kerner Blvd., San Rafael, CA 94901, U.S.A.*

An ongoing interest of these laboratories is the development of methodology for solid phase peptide synthesis which avoids the use of strong acid (e.g., anhydrous hydrogen fluoride, trifluoromethanesulfonic acid) or strong base (e.g., hydroxide, ammonia) for final cleavage from the support. Consequently, we seek anchoring linkages that can be cleaved under milder conditions by application of moderate acid (e.g., trifluoroacetic acid), light, or anhydrous fluoride ions; these anchors must be applied in conjunction with compatibly removable *Nα*-amino protecting groups.

We now report efficient preparations of the two handles **1** and **2**, which are each coupled in a single step onto amino-functionalized supports to provide a general starting point for peptide chain assembly. The group protecting the handle amino function is removed, the C-terminal residue is coupled as its *Nα*-protected free *acid*, and, ultimately, cleavage of the anchoring linkage gives the corresponding *amide*.

Handle **1**, m.p. 178–180°C, was prepared with an overall 59% yield in 5 facile steps from 4-formyl-3,5-dimethoxyphenol [1], and similar chemistry provided an isomeric handle, m.p. 116–118°C, in 25% yield from commercially available 2-formyl-3,5-dimethoxyphenol. These results embody a number of improvements over our published procedure [2], which converts 3,5-dimethoxyphenol in 15%

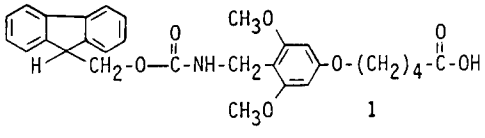

1

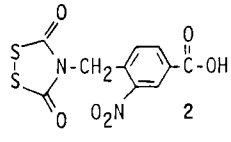

2

*To whom correspondence should be addressed.

yield for 7 steps to a crystalline *mixture* of positional isomers, m.p. 112°C. The pure handle **1** gives rise to a tris(alkoxy)benzylamide linkage, which is cleanly cleaved in 60–90% yields (depending in part on C-terminal residue) by treatment with CF_3COOH-CH_2Cl_2-CH_3SCH_3 (14:5:1) for 2 h at 25°C. By way of calibration, these conditions are more vigorous than those required to cleave peptide acids from *p*-alkoxybenzyl ester linkages, but still provide excellent acidolytic removal of peptide amides at a point when the Mtr group is only partially removed from arginine residues.

Handle **2**, m.p. 243–245°C, was obtained with an overall nonoptimized 19% yield for 3 steps from commercially available *p*-aminomethylbenzoic acid. The third, and key, step involved regioselective aromatic nitration of the appropriate Dts precursor, and illustrates a *unique* property of the Dts group in surviving severely acidic reaction conditions. Handle **2** provides a photolabile *ortho*-nitrobenzylamide linkage [3, 4], which in our hands is best cleaved by 350 nm light applied for 10 h at 25°C while the resin is suspended in a CF_3CH_2OH-CH_2Cl_2 (3:7) milieu. For simple systems, cleavage yields were in the 40–60% range, with the major desired C-terminal amide being accompanied by a small amount of the corresponding acid. Yields fell dramatically for longer peptides, but were raised back to the 50–80% range by adding 5% (v/v) of concentrated aqueous NH_4OH to the cleavage cocktail.

A number of experiments were carried out to evaluate the usefulness of handles **1** and **2** for solid phase peptide synthesis. It was demonstrated that both pure handles could be *quantitatively* attached by standard coupling protocols onto any amino-functionalized support, including aminomethyl, aminoalkyl, benzhydrylamino, and amino acyl, to give a starting point of well-defined structure for the synthesis. Compatible supports were shown to include polystyrene, polyamide, kieselguhr-encapsulated polyamide, silica, and polyethylene glycol-polystyrene graft, and syntheses could be carried out in both batchwise and continuous-flow modes. Attachment of the C-terminal amino acid residue proved to be quantitative, as assessed by the 'internal reference' amino acid technique [5]. Stepwise chain elongation could be carried out in standard ways using for temporary *N*α-amino protection the base-labile 9-fluorenylmethyloxycarbonyl (Fmoc); thiolysable dithiasuccinoyl (Dts); and, in the case of handle **2**, also acidolysable *tert*-butyloxycarbonyl (Boc) groups. Suitable targets included simple tetrapeptide amides, tetragastrin, methionine-enkephalinamide, substance P, ACP 65-74 amide, and human gastrin-I. These products were obtained in acceptable purities commensurate with the known scope and limitations of the overall synthesis protocols.

Several syntheses based on both handles were also conducted in the oxytocin family. The desired linear sequences were readily assembled with a variety of sulfhydryl protecting groups as Acm, Trt, and *S*-S*t*Bu. A beginning has been made to carry out deprotections and disulfide bridge forming reactions while

these sequences remain anchored to the support, based on the observation that the sulfur-sulfur bond survives the mild conditions used to cleave anchoring linkages derived from either **1** or **2**.

Acknowledgements

We appreciate financial support from the National Institutes of Health (GM 28934 and AM 01099), the Graduate School of the University of Minnesota, and the U.S.-Spain Committee for Scientific and Technical Cooperation.

References

1. Gruber, W., Chem. Ber., 76 (1943) 135.
2. Albericio, F. and Barany, G., Int. J. Pept. Prot. Res., 30 (1987) 206.
3. Rich, D.H. and Gurwara, S.K., Tetrahedron Lett., (1975) 301.
4. Pillai, V.R., Mutter, M. and Bayer, E., Tetrahedron Lett., (1979) 3409.
5. Matsueda, G.R. and Haber, E., Anal. Biochem., 104 (1980) 215.

Total synthesis of porcine and human cholecystokinin-33 (CCK-33) by the classical solution procedure

Yoshihiro Kurano, Terutoshi Kimura and Shumpei Sakakibara
Peptide Institute Inc., Protein Research Foundation, Minoh-shi, Osaka 562, Japan

Introduction

In 1968, porcine cholecystokinin-pancreozymin (CCK-33) was determined to be a peptide with 33 amino acid residues having an O-sulfated Tyr at position 27 [1]. Recently, the human sequence was deduced from the genomic structure and found to differ from the porcine sequence in 4 residues at position 7, 9, 10 and 15 [2]. The C-terminal octa- (CCK-8) and dodecapeptide (CCK-12) have been synthesized, but not the entire CCK-33 because of its unique structure – with porcine CCK-33 containing 3 Met, 1 Trp, and 5 Ser and human CCK-33 containing 3 Met, 1 Trp and 4 Ser. We recently reported in a short communication [3] the first synthesis of porcine CCK-33 and found the synthetic peptide to be identical to the natural isolated peptide. In the present study, we report the synthesis of human CCK-33 for which we applied the same strategy developed for the synthesis of porcine CCK-33.

Porcine: Lys-Ala-Pro-Ser-Gly-Arg-Val-Ser-Met-Ile-Lys-Asn-Leu-Gln-
Human: ---------- Met ---Ile-Val ----------

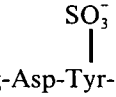

Porcine: Ser-Leu-Asp-Pro-Ser-His-Arg-Ile-Ser-Asp-Arg-Asp-Tyr-Met-
Human: Asn ----------

Porcine: Gly-Trp-Met-Asp-Phe-NH_2
Human: ----------

Results and Discussion

Two strategies are available for the synthesis of a peptide containing Tyr(SO_3^-): (1) start the synthesis with Tyr(SO_3^-) or (2) incorporate the sulfate ester group into Tyr after construction of the whole molecule. For the synthesis of CCK-

33, we applied the latter method because the sulfate group is extremely unstable under the acidic conditions used in peptide synthesis. The synthesis was carried out by the classical solution procedure applying our maximum protection strategy [4].

The protected human CCK-33 was constructed, as shown in Fig. 1, using the same segment prepared for the synthesis of porcine CCK-33, except for segments 6–8, 9–13, and 14–16. The functional group of each amino acid was protected with the following groups: cHx for Asp, Tos for Arg and His, ClZ for Lys, BrZ for Tyr, For for Trp and phenoxyacetyl (PhA) for Ser. The serine-containing segment 6–8 was prepared by reaction of tripeptide without protection of the OH group of the Ser residue with phenoxyacetic anhydride in pyridine at 0°C for 30 min. When Ser(PhA) is used as a starting material, the PhA group will migrate to the α-amino group when it is deprotected, and the peptide elongation reaction will be terminated. Protected amino acids and segments with Gly or Pro at the C-terminus were coupled by the WSCI/HOBT method. For the coupling of the protected peptides with L-amino acid residues at the C-terminus, however, we used the WSCI/HOObt method, which is known to

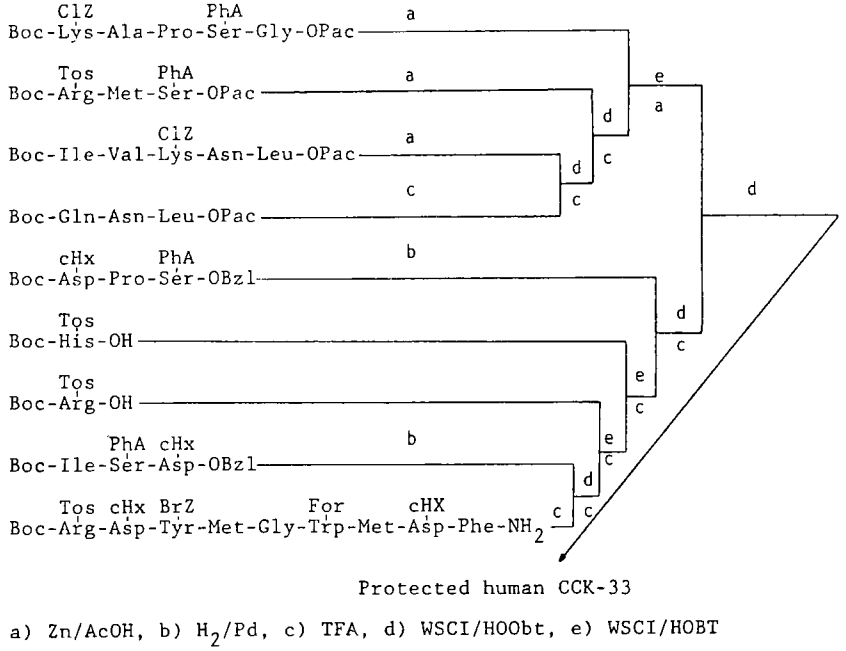

Fig. 1. Synthesis of protected human CCK-33.

minimize racemization during coupling reactions [5–6]. The fully protected peptide thus obtained was partially deprotected by the HF procedure in the presence of anisole, leaving PhA and For groups at Ser and Trp. After treatment with ammonium iodide in TFA to reduce the Met sulfoxide formed during the synthesis, each crude product was purified by Sephadex LH-20. The partially protected peptide thus purified was subjected to the sulfation reaction with 40 equivalents of pyridinium acetylsulfate [7] in TFA in an ice bath for 2 h. After precipitation by adding water, the product was treated with 40 equivalents of 0.1 NaOH in dimethylsulfoxide in an ice bath for 10 min to remove the remaining PhA and For groups. The crude CCK-33 thus obtained was purified by CM-cellulose, Butyl-Toyopearl, CM-Toyopearl, and Sephadex LH-20 to obtain the final product: $(\alpha)_D$ –76.3° (c 0.23, 1 M AcOH). The homogeneity of the synthetic

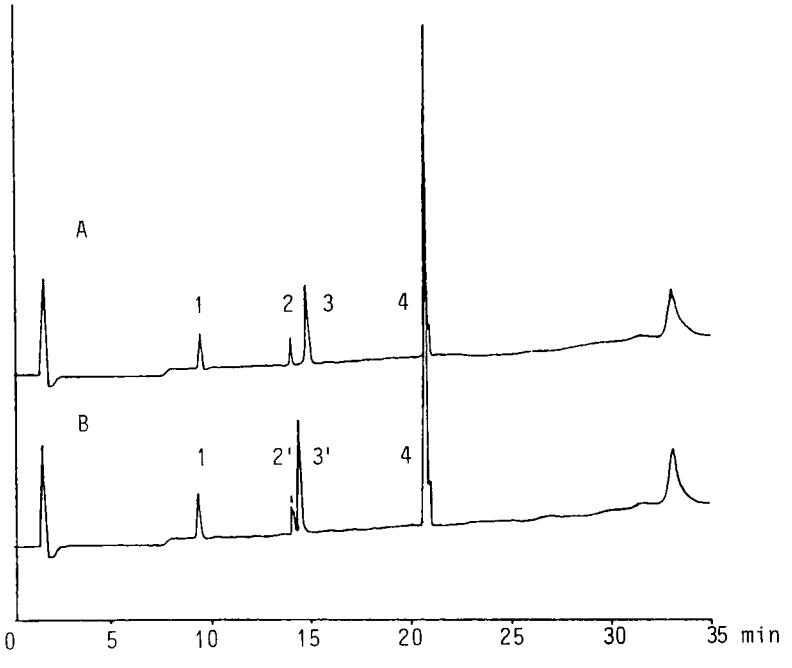

Fig. 2. Tryptic peptide mappings of synthetic porcine and human CCK-33 on HPLC.
A: Porcine CCK-33; B: Human CCK-33.
1. KAPSGR, 2: VSMIK, 2': MSIVK, 3: NLQSLDPSHR, 3': NLQNLDPSHR, 4: ISDRDYMGWMDF.
Column: Nucleosil 5C18 (4×150 mm); gradient: 1–60% MeCN in 0.1% TFA; flow rate: 1 ml/min; detection: 220 nm.

peptide was confirmed by RP- and IEX-HPLC, amino acid analysis after acid hydrolysis and aminopeptidase M (APM) digestion, and tryptic peptide mappings on HPLC. With porcine CCK-33, the material synthesized could be compared with natural, isolated porcine CCK-33, but this was not possible in the present synthesis because natural human CCK-33 is not available. Therefore, we compared the synthetic human CCK-33 with synthetic porcine CCK-33 in order to confirm its structure. The elution profile of tryptic peptide mappings of synthetic human CCK-33 on HPLC was compared with that of porcine CCK-33. As shown in Fig. 2, all peaks could be clearly assigned, and differences were observed in the chromatogram at peaks corresponding to segments 7–11 and 12–21. The biological activity of human CCK-33 was measured by comparing its effect on contraction of guinea pig gall bladder with those of synthetic porcine CCK-33 and CCK-8. The results indicated that synthetic human and porcine CCK-33 have almost the same biological activity and their relative potencies are one-fourth to one-fifth that of CCK-8.

References

1. Mutt, V. and Jorpes, J.E., Eur. J. Biochem., 6 (1968) 156.
2. Takahashi, Y., Kato, K., Hayashizaki, Y., Wakabayashi, T., Ohtsuka, E., Matsuki, S., Ikehara, M. and Matsubara, K., Proc. Natl. Acad. Sci. U.S.A., 82 (1985) 1931.
3. Kurano, Y., Kimura, T. and Sakakibara, S., J. Chem. Soc. Chem. Commun., (1987) 323.
4. Kimura, T., Takai, M., Masui, Y., Morikawa, T. and Sakakibara, S., Biopolymers, 20 (1981) 1823.
5. König, W. and Geiger, R., Chem. Ber., 103 (1976) 2024.
6. König, W. and Geiger, R., Chem. Ber., 103 (1976) 2034.
7. Penke, B., Hajnal, F., Lonovics, J., Holzinger, G., Kadar, T., Telegdy, G. and Rivier, J., J. Med. Chem., 27 (1984) 845.

Simultaneous multiple peptide synthesis: The rapid preparation of large numbers of discrete peptides for biological, immunological, and methodological studies

Richard A. Houghten*, Julio H. Cuervo, John M. Ostresh, Mairead K. Bray and Nicole D. Frizzell

Scripps Clinic and Research Foundation, Department of Molecular Biology, 10666 North Torrey Pines Road, La Jolla, CA 92037, U.S.A.

Introduction

The limiting factor in research involving large numbers (i.e., hundreds) of synthetic peptides in most instances has been the availability of the peptides. The availability of peptides, in turn, is controlled by the time and cost required for their synthesis. Currently, most laboratories do not have the necessary personnel, materials, automated equipment, and/or funds necessary to obtain large numbers of peptides.

Described here is a recently developed method of preparing peptides, termed simultaneous multiple peptide synthesis (SMPS, [1–3]) with which one person can readily synthesize 120 different 15-residue peptides in a greatly reduced amount of time (2–4 weeks) and in amounts (10–1000 mg) useful for virtually all studies. This method was designed for both the concurrent synthesis of many peptides having completely different sequences, and the concurrent synthesis of multiple analogs of the same peptide. SMPS can be used in any laboratory to produce peptides of equal or higher purity than possible with conventional manual or automated procedures.

Materials and Methods

Simultaneous multiple peptide synthesis

Detailed protocols for carrying out SMPS have been published [1–3]. In brief, 100–200 mesh resin is placed in tared polypropylene mesh packets (74 μm-mesh), having approximate dimensions of 20×20 mm. The top of the unsealed packet is numbered with a graphite-based black marking pen, the packet is closed, and the number fused into the polypropylene with a heat sealer, making an

*To whom correspondence should be addressed.

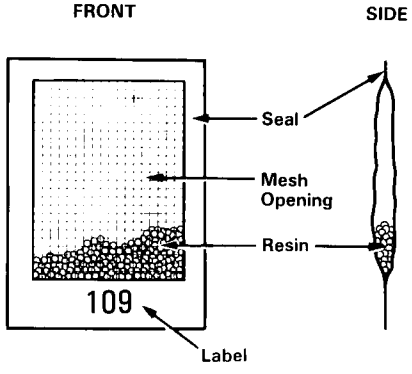

Fig. 1. Illustration of a synthesis packet.

easily readable, indelibly labeled resin packet (Fig. 1). We have found that any amount of resin from less than 25 mg to multigram amounts can be readily accommodated in these packets by simply adjusting the packet dimensions. The general SMPS procedures apply, after adjustment for different amounts of swelling, or resin particle size, to any solid phase resin used for peptide synthesis.

An example of a step-by-step SMPS protocol, utilizing N-α-Boc chemistry, appears in Fig. 2. Typically, 120 packets containing the amino acid resin(s)

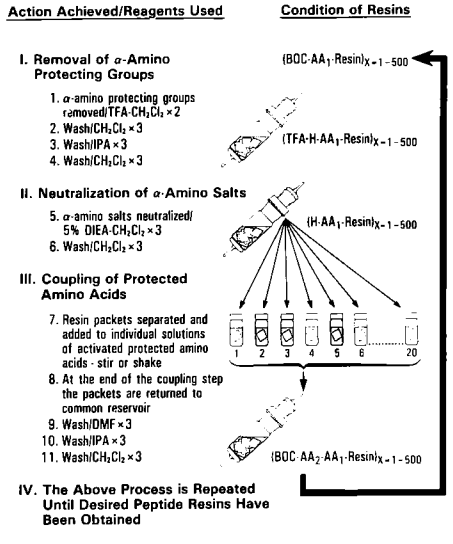

Fig. 2. Illustration of the principle of simultaneous multiple peptide synthesis (SMPS).

of choice (100 mg resin/packet) are placed in a 1000-ml, wide-mouth Nalgene polypropylene bottle. The solvents used are added to the bottle in amounts equaling 4 ml per 100 mg resin packet. All steps are carried out with vigorous agitation of the resin packets in order to ensure complete solvent transfer. Once a given wash step has been completed, the solvent is discarded into a waste reservoir, and succeeding deprotection, washing, or neutralization steps (as per the specific protocol being used) are handled in the same manner.

Following the neutralization step, the packets are removed from the common reaction bottle, separated, and organized according to the next amino acid to be added (Fig. 2 - step II. 6). When synthesizing large numbers of peptides concurrently, a computer-generated double checklist printout ensures that each packet is placed into the correct activated amino acid bottle at every coupling step [4]. For the coupling steps, an amount of amino acid is used to give a final volume of 4.0 ml/packet at a final concentration of 0.10 M. We have found that preformed symmetrical anhydrides or stoichiometric in situ activation by either dicyclohexylcarbodiimide (DCC) or diisopropylcarbodiimide (DPCDI) as activating agents works equally well. The individual coupling steps are carried out for 60 min each during vigorous shaking at room temperature. Cross contamination has not been found to occur ($>0.05\%$) when the resin packets are added to the common reaction vessel at the end of the coupling step (Fig. 2 - step III. 8). At the end of each coupling step, the completeness of the coupling can be monitored by any nondestructive method, such as that described by Gisen utilizing picric acid [5]. We have not found a decrease in peptide quality resulting from this type of monitoring. While not as sensitive as ninhydrin, this method is very rapid and can be readily carried out on the entire contents of the packet. This method also permits the observation of a variety of anomalous behavior not detected by ninhydrin. An example of this is the formation of *S-t*-butylsulfonium salts of methionine, which is evidenced by a sudden rise of picrate value after the coupling of the amino acid following methionine, the sulfonium salt being generated during the removal of the N-α-Boc group. After completion of the coupling steps, the resin packets are returned to the common reaction bottle, and the syntheses continued through additional cycles of wash, deprotection, neutralization, and coupling until completion (Fig. 2). After the final coupling step, the packets are washed thoroughly, dried, and weighed to give a preliminary indication of yield based on the resin substitution and the starting weight of resin in each packet.

The free protected peptide resins can then be cleaved using a variety of methods including hydrogen fluoride [2], but more conveniently they can be cleaved while still contained within their packets. The apparatus for the simultaneous cleavage of multiple peptide resins with liquified hydrogen fluoride (HF) illustrated in Fig. 3 is described in detail elsewhere [2, 4]. A single resin packet containing its resin is placed into each HF reaction vessel along with a Teflon-coated magnetic

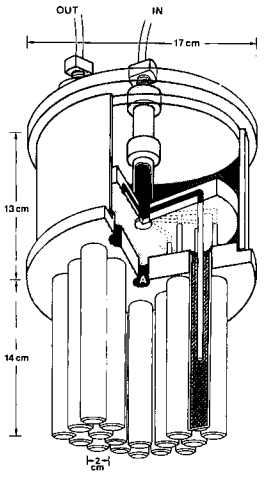

Fig. 3. Apparatus for the simultaneous cleavage of multiple protected peptide resins.

stir bar and anisole or other carbonium ion scavenger. Following HF treatment and complete removal of both the HF and scavengers, the liberated peptides are extracted from the spent resin or resin packet with 5–25% acetic acid/water and lyophilized. These are then characterized and purified to the extent necessary for the specific investigation being carried out. Cross contamination from one reaction vessel to another has not been found to occur with this multiple vessel system.

Discussion

The use of SMPS enables one to synthesize large numbers of peptides for any purpose. Our experience derived from using SMPS for over 5000 different peptides has shown that synthetic procedures which generate high quality peptides with individual free resins can be replaced with SMPS to generate these same peptides with identical or improved purity. This appears to be true for all procedures and resins normally used in standard solid phase peptide synthesis, including those encompassing *N*-α-t-Boc and *N*-α-9-fluorenylmethyloxycarbonyl (Fmoc) chemistry. A significant difference between SMPS and standard methods for single free resin solid phase synthesis [6] is the necessity for vigorous agitation of the resin-filled packets to ensure complete solvent transfer throughout their contents. This can best be achieved by vigorous shaking, but can also be accomplished by mechanical or magnetic stirring, or rocker vessel-type agitation. We have found that as much as 250 mg of resin can successfully be used to prepare a 13-residue peptide while contained in a 20×20 mm packet. For larger

amounts of resin, larger packets permit multigram quantities of resin to be used. The simultaneous multiple HF apparatus described here (Fig. 3) [2, 4] offers significant advantages over the conventional type of HF cleavage apparatus. With this new apparatus, as many as 48 individual peptide resins can be cleaved in a single day as compared to, at most, 2–4 per day with conventional systems. This apparatus also permits the simultaneous examination of as many as 24 different HF/scavenger mixtures in order to optimize cleavage conditions for a given peptide. An important safety and convenience feature over conventional HF systems is the reduced number of times that HF must be handled.

The ability to synthesize large numbers of free peptides in a reasonable time frame (weeks) and at a cost as much as 20 times less per peptide than conventional methods has a number of obvious benefits. The most fundamental, of course, is that many studies requiring large numbers of peptides would simply not be carried out without these methods. Detailed studies of the interactions of monoclonal antibodies with peptide antigens which require large numbers of discrete peptides [1, 7, 8] are greatly facilitated since the ability to work with nonsupport-bound peptides of varying length can be of critical importance. The use of support-bound short peptides for this type of study [9], while offering speed and simplicity, does not permit the necessary flexibility to vary peptide concentration, to carry out studies in solution using, for example, immunoprecipitation assays, nor does it permit the synthesis of larger sequences which were found necessary to give the precise information desired [1, 7, 8]. These methods also have immediate utility in epitope mapping and vaccine development.

For the precise tailoring of biologically active peptides in which very specific needs of specificity or length of activity are necessary, SMPS readily permits the preparation of large numbers of peptide analogs in quantities permitting full characterization and purification. An example of this approach is the synthesis of analogs of a 12-residue peptide from fibrinogen α-chain which inhibits binding of fibrinogen to platelets [10]. In this study, we were able to increase the inhibiting ability of the original sequence approximately 480-fold (120–0.2 μm) after a systematic search involving the synthesis of over 250 analogs. In another study in progress, we have prepared all of the single position omission analogs of the 53-residue epidermal growth factor.

The use of SMPS for probing solid phase synthetic methods has unparalleled utility. Since the synthesis of peptides is known to be substantially sequence dependent, the use of a single peptide to study optimization of protocols is fraught with difficulty. We have, for example, examined the base neutralization step in detail (Fig. 2 – step II. 5). This step is most often carried out using diisopropylethylamine in methylene chloride. In our study, we examined the synthesis of 8 different peptide sequences, using 7 different bases (diisopropylethylamine, triethylamine, tributylamine, *N*-methylmorpholine, piperidine, diisopropylamine, and dicyclohexylamine), 2 solvents (CH_2Cl_2 and DMF), and

2 temperatures (room temperature and 4°C). Each synthesis was carried out in duplicate for a total of 404 individual syntheses. On the average, the highest quality peptide was generated using *N*-methylmorpholine as the base component, followed by tributylamine, and then diisopropylethylamine. We also found that methylene chloride was a somewhat better solvent for the neutralization step than dimethylformamide and that substantially higher quality peptide was obtained for all bases examined if the neutralization was carried out at 4°C. Perhaps the clearest finding from this study, however, was that a substantial sequence variation exists for all of the conditions examined except temperature. Thus, for one peptide, dimethylformamide using *N*-methylmorpholine as base gave the best results, while, for another, methylene chloride using triethylamine was best. We can conclude, however, that diisopropylethylamine is clearly not the optimal base to use for neutralization of all peptides. We are currently carrying out related studies on all of the steps in the *N*-α-t-Boc and *N*-α-Fmoc protocols.

SMPS is also useful in the detailed characterization of synthetic peptides. Thus, when synthesizing a single peptide needed in high purity or a peptide needed in large amounts for commercial purposes, all of the omission or expected termination peptides can be readily synthesized along with the desired peptide. These serve not only as quality control standards, but also as a means to determine the position, or positions, of synthetic difficulty, since omission of specific individual residues can have a profound effect on peptide purity.

An early attempt by our laboratory to devise a precise set of retention coefficients from 260 substitution analogs using the approach first presented by Meek [11] failed [12, 13]. The premise of this method [11] is that the amino acid composition of a peptide as the only variable will enable accurate prediction of RPHPLC retention times. That this is not so, we believe, is the result of substantial peptide sequence variation in the induced α-helicity, amphipathicity, or overall polarity of the peptide in the RPHPLC process. Thus, peptides with sequences expected to show marked amphipathicity were retained much longer than those having identical amino acid compositions but different nonamphipathic sequences. These effects were found to cause as much as 30 min difference in retention time. Since over 300 peptides were used in this study, it would not have been carried out without the use of SMPS.

Summary

The newly developed technique of SMPS described, combined with the use of the simultaneous multiple HF cleavage apparatus, greatly facilitates the preparation of peptides. These peptides are as pure as the current chemistries permit for individual free resins. These procedures enable one person to produce large numbers (i.e., hundreds) of peptides far more rapidly (2–4 weeks) than previously possible and in amounts large enough (10–1000 mg) to enable virtually

any study involving peptides to be carried out without the need for automated peptide synthesizers.

References

1. Houghten, R.A., Proc. Natl. Acad. Sci. U.S.A., 82(1985)5131.
2. Houghten, R.A., Bray, M.K., DeGraw, S.T. and Kirby, C.J., Int. J. Pept. Prot. Res., 27(1986)675.
3. Houghten, R.A., DeGraw, S.T., Bray, M.K., Hoffmann, S.R. and Frizzell, N.D., Biotechniques, 4(1986)522.
4. Available from Multiple Peptide Systems, La Jolla, CA.
5. Gisen, B.F., Anal. Biochem., 58(1972)248.
6. Merrifield, R.B., J. Am. Chem. Soc., 85(1963)2149.
7. Houghten, R.A., Hoffmann, S.R. and Niman, H.L., In Channock, R.M. and Lerner, R.A. (Eds.) Modern Approaches to Vaccines, Cold Spring Harbor Laboratory, Cold Spring Harbor, NY, 1986, pp. 21–25.
8. Houghten, R.A., In Brown, F., Lerner, R.A. and Channock, R.M. (Eds.) Vaccines 87, Cold Spring Harbor Laboratory, Cold Spring Harbor, NY, 1987, pp. 5–10.
9. Geysen, H.M., Meloen, R.H. and Barteling, S.J., Proc. Natl. Acad. Sci. U.S.A., 81(1984)3998.
10. Ruggeri, Z.M., Houghten, R.A., Russell, S. and Zimmerman, T.S., Proc. Natl. Acad. Sci. U.S.A., 83(1986)5708.
11. Meek, J.L., Proc. Natl. Acad. Sci. U.S.A., 77(1983)1632.
12. Houghten, R.A. and DeGraw, S.T., J. Chromatogr., 386(1987)223.
13. Houghten, R.A. and Ostresh, J.M., Biochromatography, 2(1987)80.

Synthesis and characterization of peptides and proteins

Stephen B.H. Kent[a,*], Karen F. Parker[a], Dorothea L. Schiller[a], David D.-L. Woo[a], Ian Clark-Lewis[a] and Brian T. Chait[b]

[a]*Division of Biology, 147-75, California Institute of Technology, Pasadena, CA 91125, U.S.A.*

[b]*The Rockefeller University, New York, NY 10021, U.S.A.*

Introduction

The goal of total chemical synthesis of peptides and proteins is the preparation of homogeneous compounds made up of a single molecular species of known covalent structure and, for proteins, of defined tertiary structure. Classically, synthetic organic chemistry has relied on unambiguous synthetic routes and thorough structural characterization of all intermediates to establish the covalent structure of the product molecules. Peptides, once they contain more than a few amino acids, are not directly susceptible to this approach. Thus, one of the critical aspects of the total chemical synthesis of large peptides and proteins is the preparation of products with a high degree of purity and verified covalent structure. The key to the preparation of high purity synthetic products is the synthetic procedure used: a crude product containing a high proportion of the target molecule is a prerequisite to effective and reliable purification.

Here we describe the synthesis, purification, and characterization of a typical crude peptide and a small protein using the highly optimized methods developed in our laboratory.

Results and Discussion

The egg-laying hormone (ELH) of *A. californica*, a 36-residue peptide amide, was synthesized by stepwise solid phase methods using novel rapid small-scale (0.1 mmol) protocols developed in our laboratory (Kent and Parker, submitted for publication) on a completely automated peptide synthesizer expressly designed to accommodate these protocols [1]. A single solvent (DMF) was used throughout the synthetic cycle to maximize solvation of the peptide-resin. For the same reason, high-efficiency flow washes were performed and the peptide-resin was drained only before the deprotection, neutralization, and coupling steps. Reaction

*To whom correspondence should be addressed.

rates were maximized by the use of 100% TFA for removal of the N-α-Boc group and by the use of a 0.15 M (near-saturation) solution of the activated amino acid in the coupling steps. The overall cycle time for the addition of a single amino acid was approximately 20 min. An outline of a single synthetic cycle is shown in Fig. 1. Standard Boc/benzyl protected amino acids were used, compatible with final sulfonic acid (non-HF) deprotection.

Using a 4-MeBHA-resin (1.21 mmol/g), the protected 36-residue peptide chain was assembled in 14 h (overnight) with an average efficiency of 99.58% per residue, as measured by the quantitative ninhydrin assay for residual uncoupled amine on peptide-resin samples taken automatically after the addition of each residue. From 0.1 mmol starting resin, 290 mg crude protected peptide-resin was obtained. Deprotection and cleavage from the resin was performed with trifluoromethanesulfonic acid (TFMSA) [2]. The peptide was incubated with β-mercaptoethanol in 4 M guanidine·HCl 0.1 M Tris acetate adjusted to pH 8.5 for 1 h at 50°C to reduce any methionine sulfoxide. Gel filtration yielded the crude product shown in Fig. 2. The main product (62 mol% of the total products) and the two early-eluting significant byproducts (11 and 13 mol%) were isolated by reversed-phase HPLC (up to 100 mg crude product on a 1×25 cm Vydac C4 column, eluted with 0.1% TFA in acetonitrile [3]). Mass spectrometry showed that the main product had a mass of 4384.5 (calculated mass for ELH: 4384.2). The two byproducts each had a mass one unit higher, suggesting that they arose from the target product by deamidation in the 1-h incubation in pH 8.5 buffer at 50°C. The total yield of purified ELH, with full biological

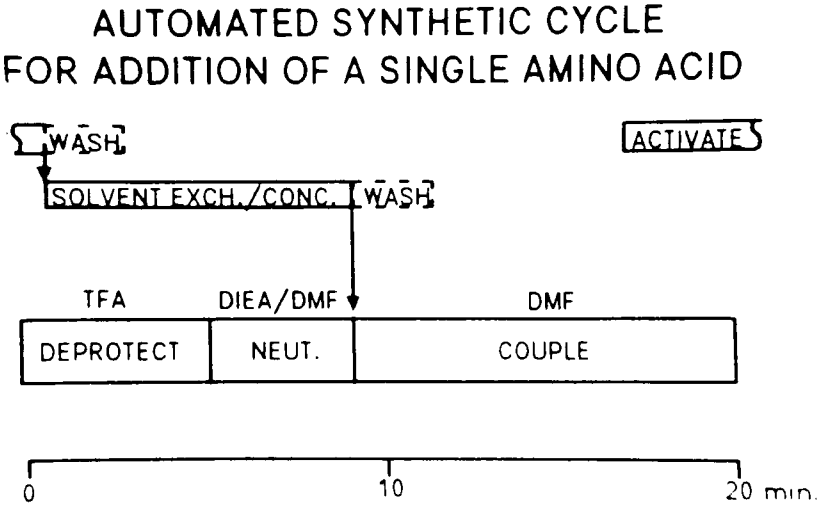

Fig. 1. Diagram of the automated protocol for rapid peptide synthesis.

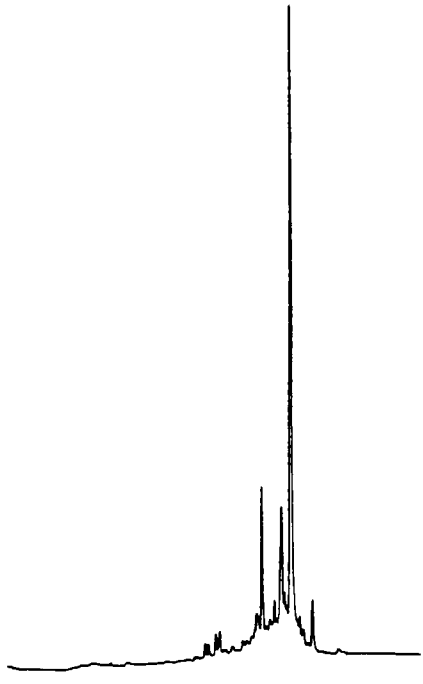

Fig. 2. Reversed-phase HPLC of the total crude synthetic products of ELH. The peptide was loaded on a Vydac C4 column and eluted with 0.1% TFA versus acetonitrile, 0–60%. Detection was at 214 nm.

activity in the egg-laying assay (performed by Felix Strumwasser, Woods Hole), was 33 mg (16 mol%, based on starting resin).

We have used these rapid small scale cycles and the chemistry described above to synthesize a number of peptides ranging from 10 to 44 amino acids in length. The peptides were purified as described [3] in yields ranging from 9 to 46%. The purified products were characterized by HPLC, the Edman degradation to establish the amino acid sequence, and mass spectrometry to determine the absence of unexpected covalent modifications.

The 50-residue mitogenic protein human transforming growth factor (TGFα) was synthesized by stepwise solid phase peptide synthesis using automated double coupling protocols as described [4]. The first coupling was performed using the preformed symmetric anhydride in DMF. In an attempt to react the residual amino groups, a second coupling was performed in a different solvent, dichloromethane, with activation of the amino acid in the presence of the peptide-resin. We have found that on the average this results in an increased coupling

yield of 0.3% per residue, which is very significant for the synthesis of long peptide chains [4]. The reaction protocols used are diagrammed in Fig. 3. The synthesis was performed on the fully automated peptide/protein synthesizer [1], using Boc/benzyl protected amino acids and final HF cleavage [5].

The protected peptide chain was assembled in 78 h without operator intervention. Quantitative Edman degradation of the peptide-resin showed an average yield of 99.65% per residue, in agreement with quantitative ninhydrin analyses of peptide-resin samples taken automatically during the synthesis. The crude product showed a major component that made up 44 mol% of the total peptide products. After folding/oxidation, a sharp early-eluting peak with the activity of TGFα was isolated by reversed-phase HPLC [3]. Correct folding of the polypeptide chain has simplified the purification by reducing conformational flexibility and burying the apolar residues, resulting in a sharper, early-eluting peak. The synthetic protein was shown to be 95% homogeneous by isoelectric focusing in an immobilized pH gradient polyacrylamide gel (Fig. 4).

Mass spectrometry of the synthetic protein gave a mass of 5546.2 compared with 5546.3 calculated for TGFα with 3 intact disulfide bonds. After reduction, the mass increased by 5.9 mass units, corresponding to the reduction of these disulfides. The location of the disulfide bonds was established by proteolysis with thermolysin followed by HPLC peptide mapping, and was found to be identical with the disulfide bonding pattern in epidermal growth factor (EGF) (Woo et al., submitted for publication).

Thus, with automated chain assembly and efficient deprotection it was possible

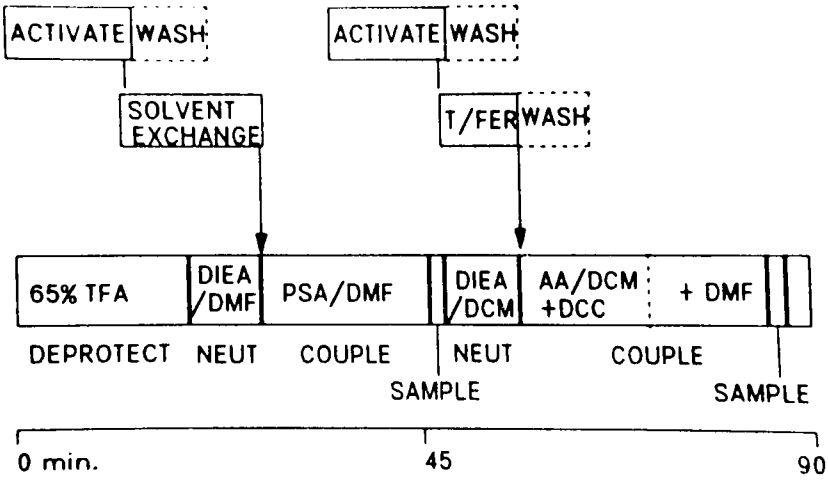

Fig. 3. Diagram of the automated double couple cycle used for the synthesis of proteins.

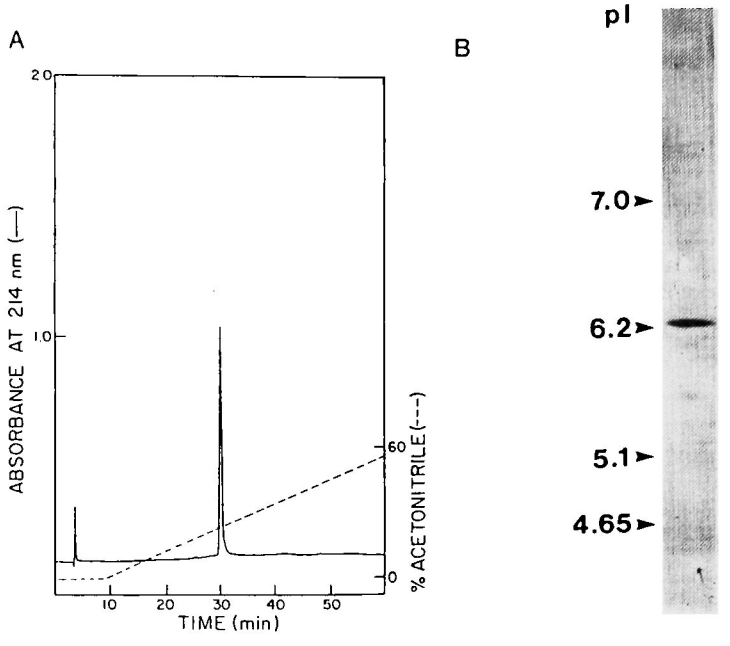

Fig. 4. Characterization of purified synthetic TGFα. (a) Reversed-phase HPLC as in Fig. 2. (b) Immobile isoelectric focusing gel, pH 4–8. The gel was electroblotted onto nitrocellulose and stained with amido black. Synthetic TGFα had an isoelectric point of 6.2.

to isolate the synthetic protein in high purity. This synthetic protein had the correct sequence of amino acids by Edman degradation, 3 intact disulfide bonds of known location, and no chemical modifications. It was then assayed and found to exhibit full biological activity (binding to the EGF receptor, mitogenic response in factor-dependent cells, anchorage-independent growth), quantitatively indistinguishable from EGF isolated from natural sources. Work is in progress to define the solution structure of this molecule using modern two-dimensional NMR techniques (in collaboration with David Live, Emory University).

Using the highly refined, solid phase synthetic chemistry and modern purification and characterization techniques described in this paper, the science of proteins is now being brought within the realm of organic chemistry.

Acknowledgements

This work was supported by funds from the NIH, NSF, the Monsanto Corporation, and Upjohn Pharmaceuticals.

References

1. Kent, S.B.H., Hood, L.E., Beilan, H., Meister, S. and Geiser, T., In Ragnarsson, U. (Ed.) Peptides 1984, Almquist and Wiksell, Stockholm, 1984, p. 185.
2. Yajima, H. and Fujii, N., In Gross, E. and Meienhofer, J. (Eds.) The Peptides – Analysis, Synthesis, Biology, Vol. 5, Academic Press, New York, 1983, p. 65.
3. Clark-Lewis, I. and Kent, S., In Kerlavage, A.R. (Ed.) Receptor Biochemistry and Methodology: The Use of HPLC in Protein Purification and Characterization, in press.
4. Kent, S. and Clark-Lewis, I., In Alitalo, K., Partanen, P. and Vaheri, A. (Eds.) Synthetic Peptides in Biology and Medicine, Elsevier Science Publishers, Amsterdam, 1985, p. 29.
5. Tam, J.P., Heath, W.F. and Merrifield, R.B., J. Am. Chem. Soc., 105(1983)6442.

Chiral synthesis of D-α,ω-diaminoalkanoic acids

Pierre L. Beaulieu* and Peter W. Schiller
Clinical Research Institute of Montreal, 110 Pine Avenue West, Montreal, Que. Canada H2W IR7

The chemical literature contains several reports on the preparation of racemic

Scheme 1

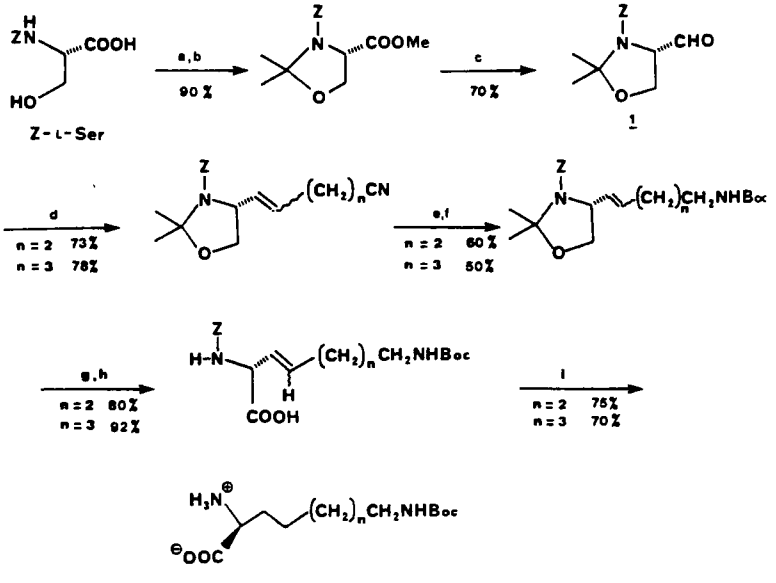

(a) CH_2N_2, Et_2O, 0°C; (b) $H_2C = C(CH_3)OCH_3$, TsOH (Cat.), CH_2Cl_2, 0°C to room temperature, 3 h; (c) DIBAL (1.2 mol equiv.), toluene, -78°C, 1 h; (d) $Ph_3P=CH(CH_2)_nCN$ (1.2 mol equiv.), THF, -78°C to room temperature, 3 h; (e) $NaBH_4$ (10 mol equiv.), $CoCl_2$ (2 mol equiv.), MeOH, 0°C to room temperature, 1 h; (f) $(Boc)_2O$ (1.2 mol equiv.), room temperature, 6 h; (g) TsOH (cat.), wet MeOH, reflux, 6 h; (h) Jones oxidation, acetone; (i) H_2 (30 psi), 20% $Pd(OH)_2/C$ (cat.), MeOH, 15 h.

*To whom correspondence should be addressed.

homolysine [1]. These procedures, however, involve multistep sequences which are not applicable to enantiospecific syntheses. At present, chiral homolysine is available only through resolution of racemic material [2]. This abstract describes our preliminary results on a general route to chiral α,ω-diaminoalkanoic acids. Masked L-serine-aldehyde **1** (Scheme 1), prepared from Z-L-serine [3], serves as the chiral starting material. It undergoes Wittig condensations with phosphonium ylides (obtained by deprotonation of the corresponding phosphonium salts with lithium diisopropylamide). The formation of geometrical isomers is of no consequence since the unsaturation is removed at a later stage. Selective reduction of the cyano group is achieved using sodium borohydride-cobalt chloride and the amine function is protected as the Boc derivative. Methanolysis under acidic conditions liberates the primary alcohol which is oxidized to the carboxylic acid with Jones' reagent. Catalytic hydrogenation over Pearlman's catalyst causes simultaneous saturation of the double bond and removal of the benzyloxycarbonyl protecting group, leading to the desired D-N^{ω}-Boc-α,ω-diaminocarboxylic acid. Catalytic tritiation could be used in the latter step to prepare labeled material. The optical purity of the products was established by 400 MHz ^{1}H and ^{19}F NMR analysis of their Mosher amides (D-N^{ω}-Boc-2,7-diaminoheptanoic acid: >95% ee, $[\alpha]_D = -10.6°$ (C = 1, 1 N HCl); D-N^{ω}-Boc-2,8-diaminooctanoic acid: >95% ee, $[\alpha]_D = -8.6°$ (C = 1, 1 N HCl). The overall process inverts the chirality of the starting material, making D-amino acids available from natural L-serine. Our method also has the advantage of delivering protected derivatives suitable for solid phase peptide synthesis without need for laborious protection-deprotection schemes. We are currently extending our approach to the synthesis of other chiral polyfunctionalized amino acids.

Acknowledgements

We thank MRCC and QHF for their financial support.

References

1. Payne, L.S. and Boger, J., Synthetic Commun., 15 (1985) 1277 (and references cited therein).
2. Bodanszky, M. and Lindeberg, G., J. Med. Chem., 14 (1971) 1197.
3. Garner, P., Tetrahedron Lett., 25 (1984) 5855.

Synthesis of anglerfish peptide YG (APY)

A. Balasubramaniam[a], D.F. Rigel[a], P.C. Andrews[b], J.E. Dixon[b], R.L. Jackson[a] and J.E. Fischer[a]

[a]*Division of G.I. Hormones, ML 558, University of Cincinnati Medical Center, Cincinnati, OH 45267, U.S.A.*

[b]*Biochemistry Department, Purdue University, West Lafayette, IN 47907, U.S.A.*

Introduction

APY is a 37-residue peptide isolated from anglerfish pancreas [1]. APY bears 64% homology to both neuropeptide Y (NPY) and peptide YY (PYY), and 43% to pancreatic polypeptide (PP); however, unlike other members of the PP family of hormones APY ends in a C-terminal glycine. These observations suggest that APY may be a new member of the PP family or may be the precursor of the amidated form. Synthesis of APY was undertaken to confirm the reported sequence and to provide sufficient quantities of peptide for biological investigations.

Results and Discussion

APY synthesis was accomplished by the stepwise solid phase method using most of the improved techniques developed in recent years [2]. The protection scheme utilized is shown below. During the synthesis the Boc group was deprotected with 50% TFA/CH_2Cl_2. Each residue was coupled twice as preformed symmetrical anhydride, first in CH_2Cl_2 and then in DMF; however, coupling of Boc-Arg(Tos), Boc-Asn, and Boc-Gln was effected both times with HOBt/DCC to avoid side reactions. Coupling was monitored by the qualitative ninhydrin test. At the end of the synthesis the DNP group was removed with 1 M benzenethiol and the N-α-Boc group was deprotected with 50% TFA/CH_2Cl_2. The free peptide was obtained by the low-high HF method [3] in 80% yield. Crude peptide purified in one step by HPLC contained 48% of the target peptide (Fig. 1).

Boc-Tyr(BrZ)-Pro-Pro-Lys(ClZ)-Pro-Glu(OBzl)-Thr(Bzl)-Pro-Gly-Ser(Bzl)-Asn-Ala-Ser(Bzl)-Pro-Glu(OBzl)-Asp(OBzl)-Trp(CHO)-Ala-Ser(Bzl)-Tyr(BrZ)-Gln-Ala-Ala-Val-Arg(Tos)-His(DNP)-Tyr(BrZ)-Val-Asn-Leu-Ile-Thr(Bzl)-Arg-(Tos)-Gln-Arg(Tos)-Tyr(BrZ)-Gly-PAM-Resin

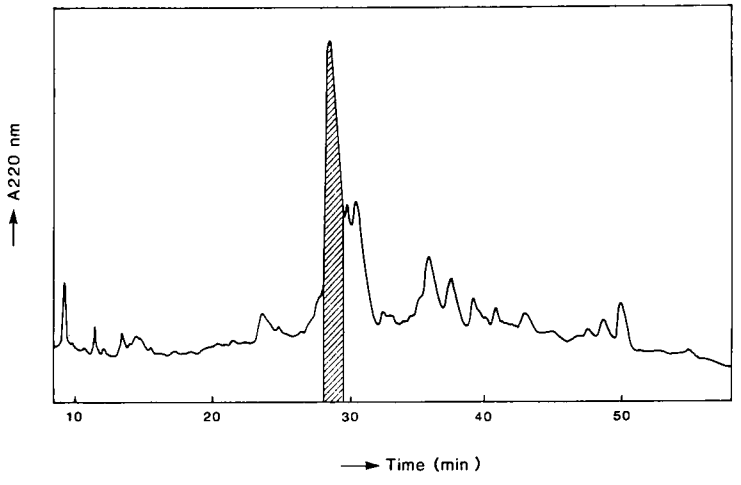

Fig. 1. Semipreparative HPLC of HF-cleaved product.

The purified product was homogeneous by analytical HPLC and had the expected amino acid composition. Integrity of the Trp residue was verified by UV analysis. The primary structure of the synthetic APY was confirmed by gas phase sequencing and mass spectrometry of the tryptic digest. Synthetic and natural APY eluted at the same time in analytical HPLC and behaved as a single compound on cochromatography. Furthermore, the trypsin-treated natural and synthetic APY gave similar HPLC profiles.

Effects of bolus injection (i.v.) of APY on blood pressure and heart rate in rats were investigated in relation to NPY, PYY and Des-37-Gly-APY. The latter peptide was isolated recently from anglerfish pancreas; the nature of the carboxyl terminal of this peptide is not yet clear (unpublished results). All the peptides except APY increased the blood pressure and decreased the heart rate (Table 1). It appears from these results that APY may not be the active form. Instead,

Table 1 *Effects of NPY, PYY, APY and Des-37-Gly-APY on the mean arterial pressure and heart rate in rats*

Peptides	Dose (nmol/kg)	ΔBlood pressure (mm Hg)	ΔHeart rate (beats/min)
NPY	3	37± 3	−50±20
PYY	3	51± 7	−33± 6
Natural APY	2	0	0
Synthetic APY	4	0	0
Des-37-Gly-APY	4	25±11	−30± 8

Des-37-Gly-APY, or more likely, Des-37-Gly-APY-NH_2 may represent the active form of APY, as for other members of the PP family of hormones. These peptides could originate from APY by the action of the proteolytic or amidating enzymes [4]. However, since only the vasoconstrictor property has been tested, the possibility of APY having other physiological functions cannot be ruled out at this stage.

References

1. Andrews, P.C., Hawke, D., Schively, J.E. and Dixon, J.E., Endocrinology, 116 (1985) 2677.
2. Merrifield, R.B., Science, 232 (1986) 341.
3. Tam, J.P., Heath, W.F. and Merrifield, R.B., Tetrahedron Lett., 23 (1982) 4435.
4. Andrews, P.C. and Dixon, J.E., J. Biol. Chem., 261 (1986) 8674.

A mild and novel approach to sulfation of serine- and threonine-containing peptides during the S_N2 deprotection step

Rolf H. Berg[a], Arne Holm[b] and James P. Tam[a]

[a]The Rockefeller University, 1230 York Avenue, New York, NY 10021, U.S.A.
[b]Department of General and Organic Chemistry, University of Copenhagen, The H.C. Ørsted Institute, Universitetsparken 5, DK-2100 Copenhagen, Denmark

Introduction

Serine-O-sulfate and threonine-O-sulfate are useful synthetic intermediates and enzyme inhibitors. Previously reported procedures for the preparation of sulfated amino acids do not discriminate between alcoholic and phenolic hydroxyl groups [1]. To avoid this limitation we have developed a mild and selective method for the sulfation of serine and threonine and for the concomitant cleavage of most benzyl-based protecting groups in peptide synthesis. This method is based on the replacement of trifluoromethanesulfonic acid (TFMSA) by sulfuric acid in the 'low-acidity' TFMSA deprotection condition [2] which contains dimethylsulfide (DMS) as the nucleophile. Under such a condition, most benzyl protecting groups are smoothly removed and serine and threonine are converted in high yields to Ser(SO_3H) and Thr(SO_3H) in a one-step reaction, but tyrosine is unaffected.

Results and Discussion

Recently, a practical mixture of TFMSA/DMS/TFA (10 : 30 : 60, v/v) operating under the S_N2 condition [2] has been found to be suitable for the removal of most benzyl-based protecting groups. Since H_2SO_4 and TFMSA are both strong acids with comparable acidity, replacement of TFMSA with H_2SO_4 in the recommended mixture should produce the same beneficial effects. Concentrated H_2SO_4 (96–98%) was treated with fuming sulfuric acid to give 100% H_2SO_4, which was used for all the following reactions. The new reagent, H_2SO_4/DMS/TFA (10 : 30 : 60, v/v), was then used for the sulfation of benzyl-protected serine and threonine at 0°C. Reaction products were analyzed by reversed-phase HPLC using fluorescence detection of a precolumn *o*-phthaldehyde derivatizing reagent in 0.1 M sodium acetate, pH 7.2 [3]. The sulfation was extremely rapid and Ser(SO_3H) and Thr(SO_3H) were found to reach yields of 85% and 70%,

respectively, within 5 min. The rapid sulfation was followed by a slow desulfation, resulting in an average yield after 4 h of 70% Ser(SO_3H) and 50% Thr(SO_3H). The rate constant of the pseudo-first-order sulfation reaction was about 0.1 min^{-1} and about 100-fold faster than the desulfation reaction. Tyr or Tyr(Bzl) was not sulfated and authentic Tyr(SO_3H) was completely hydrolyzed within a few minutes when exposed to the new reagent.

The new reagent deblocked most benzyl protecting groups including Asp(OBzl), Glu(OBzl), Ser(Bzl), Thr(Bzl), Tyr(Br-Z), Lys(Cl-Z), and His(Tos) in 4 h at 0°C completely without side reactions. Similar to other S_N2 deprotection conditions, however, such as low HF and low TFMSA conditions [1, 4], amino acid derivatives with high S_N1 character, such as Arg(Tos), steric hindrance, such as Asp(OcHex), and low basicity, such as Cys(4-MeBzl), were stable under the present deblocking condition. Also, similar to the S_N2 deprotection conditions, Met(O) was deoxygenated and converted smoothly to Met. In the presence of a thiol, such as *p*-thiocresol or ethanedithiol (2%), Trp(For) was deformylated to Trp. Cleavage of peptides from benzyl-ester resin linkage support was usually about 80% (Table 1).

The mechanism of acid-catalyzed desulfation of hydrogen sulfate esters in aqueous solution is known to proceed by cleavage of the sulfur-oxygen bond [5] and most likely via the zwitterionic species $(ROH)^+$-$(SO_3)^-$. Furthermore, the desulfation is markedly accelerated by a decrease in solvent polarity. Our findings suggest that the high concentration of DMS in the S_N2 deprotection condition greatly decreases the polarity of the acidic reagent and results in the desulfation reaction; however, the loss of SO_3 from Ser(SO_3H) and Thr(SO_3H)

Table 1 *Deprotection of protected amino acids in H_2SO_4/DMS/CF_3CO_2H (10:30:60, v/v) for 4 h at 0°C*

Protected amino acid	Yield (mol %)
Asp(OBzl)	100
Glu(OBzl)	100
Ser(Bzl)	100
Thr(Bzl)	100
Tyr(Bzl)	100
Tyr(Br-Z)	100
Lys(Cl-Z)	100
Met(O)	100
His(Tos)	100
Trp(For)	60
Glu(OcHex)	<10
Asp(OcHex)	<5
Arg(Tos)	<5
Cys(4-MeBzl)	<5

For the deformylation, 2% ethanedithiol was added.

is much less efficient than from Tyr(SO_3H), which readily explains the selectivity of the new reagent.

An important feature of our method lies in its versatility in combining two reactions in a single step. Thus, the conventional benzyl-based protecting groups and anchoring bonds of peptide-resin are smoothly cleaved, while serine and threonine simultaneously undergo sulfation. Finally, since all amino acid sulfate esters undergo complete desulfation in several organic solvents [1], the described procedure may provide a general approach to mild deprotection and cleavage of any peptide and at a low cost.

Acknowledgements

This work was supported by NIH grant CA 36544.

References

1. Penke, B., Zarándi, M., Kovács, K. and Rivier, J., In Ragnarsson, U. (Ed.) Peptides 1984, Proc. of 18th Eur. Peptide Symp., Almqvist and Wiksell International, Uppsala, 1984, p. 279.
2. Tam, J.P., Heath, W.F. and Merrifield, R.B., J. Am. Chem. Soc., 108 (1986) 5242.
3. Jones, B.N. and Gilligan, J.P., J. Chromatogr., 266 (1983) 471.
4. Tam, J.P., Heath, W.F. and Merrifield, R.B., J. Am. Chem. Soc., 105 (1983) 6442.
5. Batt, B.D., J. Chem. Soc., B (1966) 551.

Synthesis of an ε-(γ-Glu)Lys cross-linked peptide in human fibrin

Michael S. Bernatowicz[a], Catherine E. Costello[b] and Gary R. Matsueda[a,*]

[a]*The Cellular and Molecular Research Laboratory, Massachusetts General Hospital, Boston, MA 02114, U.S.A.*

[b]*Department of Chemistry, Massachusetts Institute of Technology, Cambridge, MA 02139, U.S.A.*

An efficient and practical synthesis of a two-chain 19-residue peptide (Fig. 1) containing ε-(γ-Glu)Lys has been developed. The peptide was designed as

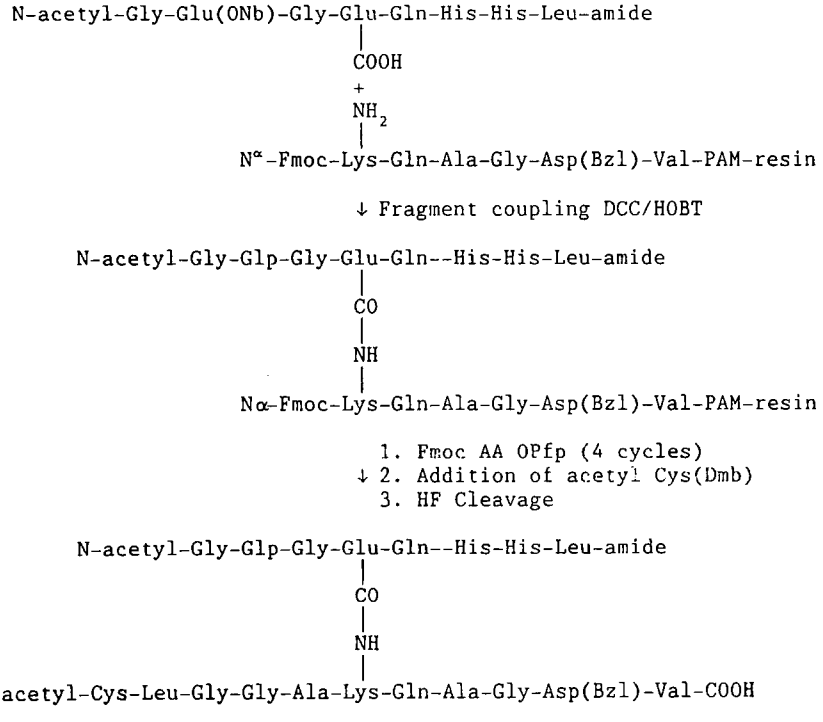

Fig. 1. Synthesis of ε-(γ-Glu)Lys cross-linked 19-residue peptide.

*Address correspondence to Gary R. Matsueda, Jackson 13, Massachusetts General Hospital, Boston, MA 02114, U.S.A.

a mimic of the proposed ϵ-(γ-Glu)Lys cross-link site formed intermolecularly between adjacent C-terminal regions of human fibrin γ-chains [1] by the enzymatic action of Factor XIIIa during the blood clotting process. A key step in the synthesis was the condensation of free-γ-glutamyl octapeptide (p-NO_2-benzyl ester of Glu-2, free N^{im}-His) to N^{α}-Fmoc-Lys-Gln-Ala-Gly-Asp(OBzl)-Val-PAM-resin using DCC/HOBT in DMF. The remaining structure was assembled by stepwise coupling of Fmoc-amino-acid-OPfp esters, except for Cys which was coupled as Boc-Cys(Dmb)-OH. Amino acid analysis and HPLC on the crude HF cleavage product indicated that the ϵ-(γ-Glu)Lys bond was formed in about 60% yield. Deprotected, homogenous peptide was isolated after a single preparative HPLC purification step in 30% overall yield. Tandem FABMS analysis of the peptide revealed that an internal pyroglutamic acid residue (Glp) was formed at Glu-2 of the octapeptide chain. We base this interpretation on the detection of a molecular ion at m/z 1970.8 and ion fragments at an m/z consistent with the presence of Glp. In a separate study, we found that cyclization is rapid and occurs under the basic conditions used for cleavage of the Fmoc group. For immunogen preparation, a reduced Cys was employed at an N-terminus to allow coupling to a carrier protein (KLH) that was bromoacetylated using *N*-succinimidyl bromoacetate [2]. The use of the two-chain 19-residue peptide as a hapten produced murine antibodies that cross-react with cross-linked fibrin.

References

1. Chen, R. and Doolittle, R.F., Biochemistry, 10(1971)4486.
2. Bernatowicz, M.S. and Matsueda, G.R., Anal. Biochem., 155(1986)95.

Use of Fmoc amino acid chlorides in peptide synthesis

Michael Beyermann[a], Dörthe Granitza[a], Michael Bienert[a], Burghard Mehlis[a], Hartmut Niedrich[a] and Louis A. Carpino[b]

[a]*AdW der DDR, Institut für Wirkstofforschung, Alfred-Kowalke-Str. 4, 1136-Berlin, G.D.R.*
[b]*Department of Chemistry, University of Massachusetts, Amherst, MA 01003, U.S.A.*

Introduction

The new technique for rapid continuous solution synthesis of peptides involving coupling by crystalline Fmoc amino acid chlorides and deblocking via 4-(aminomethyl)piperidine (4-AMP) [1] has been used for the synthesis of a varied number of tachykinin peptides. In this communication we summarize our experience with a newly developed, improved protocol [2] and discuss our efforts to suppress side reactions and monitor racemization.

Results and Discussion

Peptide synthesis

The following protocol for chain elongation has been found suitable: (A) 1.5 mmol of Fmoc-Xaa-Cl [1, 2] in 10 ml of $CHCl_3$ are added to 1 mmol of H-Yaa-OBzl (O^tBu) in 10 ml of $CHCl_3$/10 ml 5% Na_2CO_3 and stirred for 10 min. (B) The organic phase is separated and 10 ml of 4-AMP are added. (C) After 20–30 min the mixture is diluted with 80 ml of $CHCl_3$ and extracted 5× with phosphate buffer, pH 5.5. (D) The volume is reduced to 10 ml and the next cycle is started. The time required for one cycle is about one hour. Amino acid pentafluorophenyl esters may also be used when synthesis of the corresponding chlorides is impossible. Small amounts of remaining dibenzofulvene and other impurities are removed by silica gel chromatography of the protected segments. For example, the segments Z-Arg(NO_2)-Pro-Lys(Z)-Pro-O^tBu and δ-Ava-Phe-Phe-Gly-Leu-Nle-OBzl were obtained with yields of 60–70% and purities of greater than 95%.

Side reactions

During treatment of Fmoc dipeptide benzyl esters with 4-AMP, diketopiperazines (DKP) are formed (~95% cyclo [Lys(Z)-Pro] after 2 min, 10–20% cyclo(Leu-Met) within 30 min). This side reaction can be prevented by the use of C-terminal *tert*-butyl protection. The amount of cyclo(Leu-Met) or cyclo (Leu-

Nle) can be suppressed to 10% by 2-methylbenzyl protection. Cyclization can be nearly completely suppressed by reducing the time of 4-AMP treatment to 5 min in CH_2Cl_2, in which solvent the process of deblocking-adduct formation proceeds distinctly faster, as shown by model studies. Such modifications of the standard protocol should also be applicable to the Fmoc cleavage of Fmoc-Glu(OBzl)-peptides, which normally leads to 20–60% ring closure within 10 min.

Studies of racemization

Under the conditions of the protocol described, no racemization takes place (Fig. 1, Table 1). On the other hand, pretreatment of the corresponding Fmoc-Xaa-Cl with a tertiary amine led to significant racemization (Table 1), possibly via the formation of 5(4H)oxazolones [4]. Rapid addition of Fmoc Xaa-Cl to methylene chloride solutions containing one equivalent each of alanine methyl ester and triethylamine also caused no detectable racemization (Table 1).

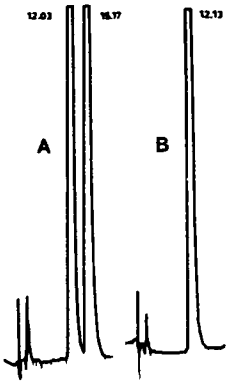

Fig. 1. HPLC racemization test, Shimadzu LC-6A, Lichrosorb RP-18, 250×4.6 mm, 10 µm, 50% acetonitrile, 50% 0.1 M NaH_2PO_4 + 0.15 M $NaClO_4$, pH 2.2, isocratic, flow 1 ml/min, detection, 220 nm, sensitivity, 0.02 AUFS.
(A) Mixture of H-L-Leu-Nle-OBzl (12.03 min) and H-D-Leu-Nle-OBzl; (B) H-L-Leu-Nle-OBzl, synthesized via Fmoc-Leu-Cl. Sensitivity 0.1–0.2%.

Table 1 *Racemization during coupling via Fmoc-Xaa-chlorides*

Xaa-Yaa-OR	Base/pretreatment (min)	Test	%D-Xaa-Yaa
Phe-Leu-OMe	aq. Na_2CO_3/–	HPLC[a]	0.1
Leu-Nle-OBzl	aq. Na_2CO_3/–	HPLC[b]	0.2
Phe-Leu-OMe	TEA /–	HPLC	0.1
Phe-Ala-OMe	TEA /1	NMR[c]	15
Val-Ala-OMe	TEA /1	NMR[c]	3
Phe-Ala-OMe	pyridine /5	NMR[c]	3

[a]Analyzed as the benzoyl derivative, see [1].
[b]See Fig. 1.
[c]60 MHz, sensitivity 3% [3].

References

1. Carpino, L.A., Cohen, B.J., Stephens, K.E., Jr., Sadat-Aalaee, S.Y., Tien, J.H. and Langridge, D.C., J. Org. Chem., 51 (1986) 3732.
2. Beyermann, M., Bienert, M., Repke, H. and Carpino, L.A., In Theodoropoulos, D. (Ed.) Peptides 1986, Walter de Gruyter, Berlin, in press.
3. Weinstein, B. and Pritchard, A.E., J. Chem. Soc. Perkin Trans. I (1972) 1015.
4. Benoiton, N.L., In Gross, E. and Meienhofer, J. (Eds.) The Peptides – Analysis, Synthesis, Biology, Vol. 5, Academic Press, New York, 1983, p. 217.

Studies of acetamidomethyl as cysteine protection: Application in synthesis of ANF analogs

Stephen F. Brady, William J. Paleveda and Ruth F. Nutt
Merck Sharp & Dohme Research Laboratories, West Point, PA 19486, U.S.A.

Introduction

Efforts to devise procedures for rapid atrial natriuretic factor (ANF) analog synthesis in these laboratories have led to a standardized protocol for efficient assembly and cyclization of linear *bis*-acetamidomethyl (Acm) peptides. Evidence for partial loss of Acm during HF cleavage of resin-bound peptides [1] prompted us to initiate studies aimed at: (1) developing procedures for assembly and acidolytic processing of Cys(Acm)-containing peptides which minimize loss of the Acm group; (2) optimizing conditions for carrying out syntheses that enable Cys(Acm) to survive multiple operations.

Results and Discussion

We focused initially on generation of byproduct *IIb* from precursor *I*, the protected resin-bound C-terminal segment of ANF [1]. This sequence was made on an automated Applied Biosystems Model 430A peptide synthesizer; manufacturer-supplied protocols were used throughout [2]. Couplings were carried out to $\geqslant 99.5\%$ completion, as assessed by quantitative ninhydrin assay. Repetitive removal of *t*-Boc was conducted in TFA with or without scavenger (see Table 1). Sulfhydryl product *IIb* was confirmed by analytical HPLC, quantitative Ellman assay, and dimerization under oxidative conditions (pH $\geqslant$ 6).

H--A-Q-S(Bzl)-G-L-G-*Cys(Acm)*-N-S(Bzl)-F-R(Ts)-Y(BrZ)- (*R*) *I*
H--A-Q-S-G-L-G-*Cys(R)*-N-S-F-R-Y--OH *IIa:* R = Acm *IIb:* R = H

As summarized in Table 1, Acm shows the highest stability when cation scavenger is used during resin-peptide assembly and when HF cleavage is conducted by the two-stage S_N2/S_N1 ('low-high') procedure (entry No. 2 versus Nos. 1 and 4). The lowest Acm loss (3%) in fact represents close to the intrinsic stability of Acm-Cys to HF (determined in a separate experiment by exposure of purified product *IIa* to high HF cleavage conditions). These findings are

Table 1 *HF cleavage of I*

Entry No.	Scavenger in assembly	HF conditions[a]	Percent *IIb*[b]
1	1% Ethanedithiol	High	7.5
2	1% Ethanedithiol	Low-High	3.0
3	None	High	13.8
4	None	Low-High	6.2
5	1% Dithioerythritol	High	11.9

[a] High = 9:1 (v/v) HF/anisole, 0°C, 60 min; Low-High = procedure described by Tam et al. [3].
[b] Normalized to Cys(Acm) *IIa* + Cys(H) *IIb* = 100.

most consistent with an *S*-benzylated Cys intermediate during the cleavage process. Employing ethanedithiol as scavenger in Boc removal during peptide assembly results in less Acm loss after HF exposure than use of dithioerythritol (entry No. 1 vs. No. 5).

We had already shown that free SH byproducts could be converted cleanly, along with Acm, to cyclic disulfide monomers if extensive processing or isolation of intermediates is avoided. We aimed to assure, in our current effort, that Acm protection could be preserved intact, through a multistep process, until final disulfide formation. Thus, we explored a general approach to bicyclic analogs, illustrated for the constrained structure *V*, based upon: (1) homodetic cyclization of *bis*-Acm linear intermediate obtained upon HF cleavage of resin-bound precursor *III*; (2) disulfide ring closure of *IV* at high dilution using iodine in aqueous acetic acid. Acm-protected *IV* was the main product after HF treatment of *III*, cyclization [1-(3-dimethylaminopropyl)-3-ethylcarbodiimide/HOBt], and nitrobenzyl group removal (zinc/50% HOAc). The strained 8-membered disulfide bridge was formed readily upon iodine-mediated Acm deprotection-cyclization.

Boc--G-R(Ts)-I-E(NO_2Bzl)-R(Ts)-I-G-A-Q-S(Bzl)-G-L-G-*C(Acm)-C(Acm)*-
F-G-(*R*) *III*
cyclo-[*C(X)*-F-G-G-R-I-E-R-I-G-A-Q-S-G-L-G-*C(X)*] *IV*: X = Acm
V: C(X) = 1/2 cystine

In summary, our experience with Acm-Cys in preparing ANF analogs has confirmed the advantages of: (1) minimal loss of Acm protection when cation scavengers are present during resin assembly and HF cleavage; (2) stability to HF allowing intermediary purification of Cys-protected peptides; (3) high yields in cyclization to monomeric disulfides.

Acknowledgements

We wish to thank Dr. H.G. Ramjit for mass spectra, Ms. J.S. Murphy for PMR determinations, and Ms. S.S. Fitzpatrick for amino acid analyses. We also thank Dr. T. Lyle for helpful discussions and Dr. D. Veber for support of this effort.

References

1. Nutt, R.F., Brady, S.F., Lyle, T.A., Ciccarone, T.M., Colton. C.D., Paleveda, W.J., Veber, D.F. and Winquist, R.J., Protides of the Biological Fluids, Vol. 34, 1986, pp. 55–58.
2. Kent, S. and Clark-Lewis, I., Synth. Pept. Biol. Med. (Proc. Labsystems Res. Symp.), 1985, pp. 29–57.
3. Tam, J.P., Heath, W.F. and Merrifield, R.B., J. Am. Chem. Soc., 105 (1983) 6442.

Analysis and enantiomeric resolution of α-alkyl-α-amino acids

Hans Brückner, Ingrid Bosch, Sibylle Kühne and Sibylle Zivny
Institute of Food Technology, University of Hohenheim, D-7000 Stuttgart 70, F.R.G.

Introduction

As pointed out several years ago [1], substitution of the C_α-hydrogen atom of protein amino acid residues by an alkyl group yields α-alkyl-α-amino acids (AAA) which give rise to significantly altered conformational torsion angles when incorporated into synthetic peptides. For this reason, and owing to the enzymatic resistance of peptide bonds formed by AAA, these sterically highly hindered [2] compounds have gained steadily increasing interest in peptide drug design. Apart from few exceptions, however, difficulties encountered in the large scale enantioselective synthesis of AAA, lack of commonly applicable methods for the preparative chemical resolution of racemates, as well as the lack of a comprehensive analytical methodology for proving the optical purity of enantiomers, discouraged the use of optically active AAA in synthetic peptide chemistry. In continuation of work described recently [2, 3], we present methods for the analytical and preparative resolution of AAA.

Results and Discussion

Fused silica capillary GC using nonchiral stationary phases enabled the baseline resolution of the diastereomeric *N*-pentafluoropropionyl (PFP) 2-alkyl esters of AAA in many cases. Among the homologous series of 2-butyl to 2-octyl esters, the pentyl esters show especially high resolution coefficients (Fig. 1). A methodologically different approach avoiding the requirement of volatile derivatives is reversed-phase (RP) HPLC and precolumn derivatization of AAA with *o*-phthaldialdehyde (OPA) and *N*-acetyl-L-cysteine (Ac-L-Cys) or *N*-*t*-butoxycarbonyl-L-Cys (Boc-L-Cys) as chiral thiol components (Fig. 2).

Furthermore, a universally applicable method for separating racemic AAA is ligand-exchange (LEC) HPLC using silica bonded L-Pro as chiral selector forming mixed copper complexes with AAA. This method also enabled the on-line assignment of the optical rotation of enantiomers using a polarimeter detector and, moreover, made feasible the preparative separation of enantiomers (Fig. 3). Although having the advantage of needing no derivatization procedure, LEC-

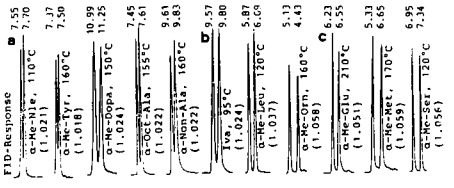

Fig. 1. GC of N-PFP DL-AAA 2-alkyl esters: (a) R(-)-2-butyl esters, (b) S(+)-2-pentyl esters, and (c) S(+)-2-hexyl esters. Column, 25 m × 0.22 mm I.D., CP-Sil 5 (Chrompack, equal to SE-30); carrier gas, hydrogen; p, 50 kPa; FID. Isothermal temperatures (°C), net retention times (min), and resolution coefficients (in brackets) are given. Me, methyl; Oct, octyl; Non, nonyl; Nle, norleucine; Iva, isovaline.

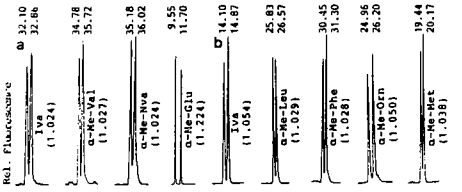

Fig. 2. RPHPLC of DL-AAA after pre-column derivatization with (a) OPA/N-Boc-L-Cys and (b) OPA/N-Ac-L-Cys. Spherisorb ODS II, µm column, 145 × 4.6 mm I.D.: eluent a, 1% tetrahydrofuran; eluent b, 50% acetonitrile in 12.5 mmol NaH_2PO_4/Na_2HPO_4 buffer, pH 7.2; gradient program, 40 min to 40% b; 25°C; flow rate, 1.5 ml/min; fluorescence detection at 344/443 nm. Sections of the chromatograms show net retention times (min) and resolution coefficients (in brackets).

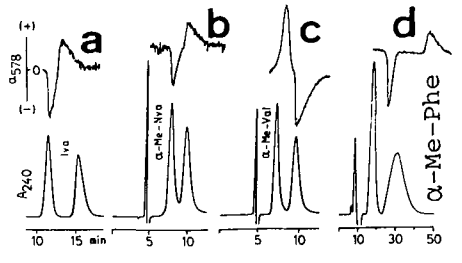

Fig. 3. Analytical (a)–(c) and 60 mg preparative (d) resolution of racemic AAA by LEC-HPLC and detection with a polarimeter detector (upper trace) and UV. Conditions (data for preparative resolution in brackets): Chiral ProCu = Daltosil, Serva, Heidelberg; column, 270(300) mm × 4.6(20) mm I.D.; 1 mmol Cu acetate in 10% acetonitrile, pH 5; flow, 1.5(10) ml/min; 40°C. The D-enantiomers elute before the L-enantiomers.

HPLC may in some cases suffer from the low solubility of hydrophobic AAA in aqueous eluents. In conclusion, the presented or recently described methods will make possible the determination and proof of the enantiomeric purity of almost any AAA.

Acknowledgements

This work was supported by the Deutsche Forschungsgemeinschaft (Br 880/3–7).

References

1. Marshall, G.R. and Bosshard, H.E., Circ. Res., Suppl. II, 30 and 31 (1972) 143.
2. Brückner, H., Bosch, I., Graser, T. and Fürst, P., J. Chromatogr., 386 (1987) 251.
3. Brückner, H., Bosch, I., Graser, T. and Fürst, P., J. Chromatogr., 395 (1987) 569.

Automated Fmoc synthesis on polystyrene resins

Hal Beilan, Dick L. Noble, Christopher P. Ashton and David P. Hadfield
Applied Biosystems Inc., Lincoln Centre Drive, Foster City, CA, U.S.A.

Introduction

The Fmoc approach to solid phase peptide synthesis is rapidly developing and is a valuable addition to the more traditional t-Boc strategy. The automation has been slow in developing compared to the rapid chemical development. The difficulty in automation is at least in part due to the particular physical properties of the 20 Fmoc amino acids.

Presented here is a method for routine, automated Fmoc synthesis using commercially available Fmoc amino acids and reagents on existing synthesis instrumentation.

Using an Applied Biosystems Model 430A Peptide Synthesizer, Fmoc amino acids are prepackaged and loaded onto the instrument prior to synthesis. The amino acids are dissolved in *N*-hydroxybenzotriazole (HOBT) in dimethylformamide (DMF) and activated in a separate vessel by the addition of diisopropylcarbodiimide (DIC) in dichloromethane (DCM). The Fmoc amino acid HOBT ester is then delivered to the reaction vessel for acylation, resulting in chain elongation. Prior to coupling, the resin is deprotected with two aliquots of 20% piperidine in DMF.

As a result of utilizing DIC/HOBT activation chemistry for all amino acids, the synthesis cycles are relatively general. Activation times are about 30 min, and all single couplings are either 30 or 60 min. Total cycle time with 30 min coupling is approximately 1.5 h. The stoichiometry of the syntheses presented here (0.5 mmol scale) is two equivalents of activated amino acid per one equivalent of free amine.

Two basic linker systems have been employed in the Applied Biosystems approach to Fmoc synthesis on polystyrene resin: PAM resins cleaved using the TFMSA/TFA method previously described (Applied Biosystems User Bulletin #3, #16); and *p*-hydroxymethylphenoxyacetic acid resin (HMP-resin) cleaved with 95% TFA (scavengers added where appropriate) or with TFMSA/TFA. Attachment of the first amino acid to the HMP-resin is accomplished automatically in the first synthesis cycle and utilizes a preformed symmetrical anhydride (PSA), dimethylaminopyridine (DMAP)-catalyzed acylation cycle.

Results and Discussion

Synthesis of ACP (65–74) (Fig. 1)

H-Val-Gln-Ala-Ala-Ile-Asp-Tyr-Ile-Asn-Gly-OH

ACP (65-74) has become a standard for solid phase peptide synthesis because of its inherent sequence-dependent coupling difficulties and has been synthesized by various procedures. It is used at installation of all Applied Biosystems peptide synthesizers to determine correct operation. A wealth of data exists on this peptide, making it an excellent choice for evaluation of the Fmoc cycles.

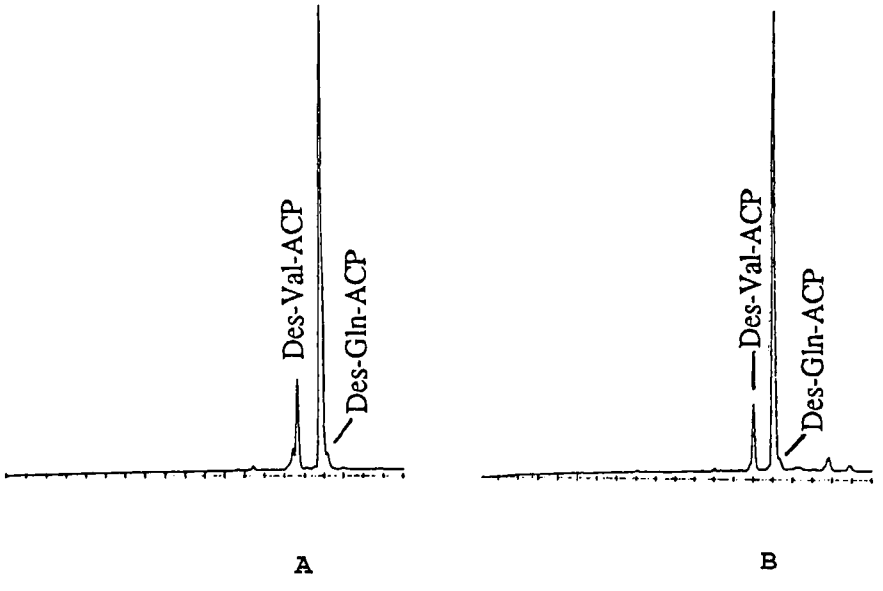

Fig. 1. (A) Fmoc chemistry on t-*Boc-Gly-PAM polystyrene resin; HOBT esters (2 equivalents; 1.0 h coupling time); TFMSA cleavage. (B) Fmoc chemistry on HMP polystyrene resin; HOBT esters (2 equivalents; 1.0 h coupling time); Gly loaded automatically by PSA/DMAP coupling; deprotected with 20% piperidine in DMF; cleaved with 95% TFA.*

Synthesis of ACTH 1–10 (Fig. 2)

H-Ser-Tyr-Ser-Met-Glu-His-Phe-Arg-Trp-Gly-OH

This peptide contains several potentially problematic amino acids, such as Met, Trp, His, and Arg. It was previously used as a model peptide at Applied Biosystems for the development of the TFMSA cleavage procedure. For the Fmoc synthesis of this peptide, the Fmoc cycles were used with the following side-chain protecting groups: *t*-Butyl for Ser, Tyr, and Glu; Mtr for Arg; and Fmoc for His.

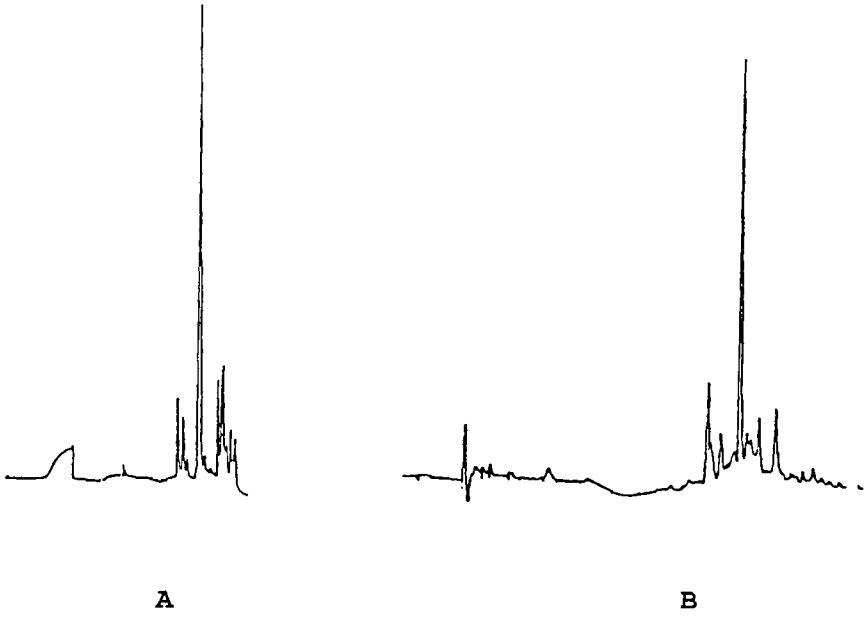

Fig. 2. (A) Fmoc chemistry on t-*Boc-Gly-PAM polystyrene resin; HOBT esters (2 equivalents; 1.0 h coupling time); TFMSA cleavage. (B) Fmoc chemistry on HMP polystyrene resin; HOBT esters (2 equivalents; 1.0 h coupling time); Gly loaded automatically by PSA/DMAP coupling; deprotected with 20% piperidine in DMF, cleaved with 95% TFA.*

Synthesis of gramicidin A (Fig. 3)

FOR-Val-Gly-Ala-(D)Leu-Ala-(D)Val-Val-(D)Val-Trp-(D)Leu-Trp-(D)Leu-Trp-(D)Leu-Trp-NH-CH_2CH_2-OH

This peptide has been synthesized several times in the past by t-Boc solid phase peptide synthesis; however, the overall yields have been reported to be generally in the 10–15% range. The peptide contains 4 Trp, 6 D-amino acids, and an N-formylated amino terminus; the C-terminal Trp forms a peptide bond with ethanolamine.

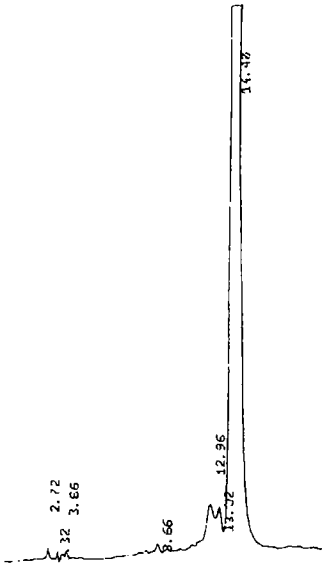

Fig. 3. The synthesis was carried out on HMP resin by standard Fmoc cycles. The N-terminal residue was coupled as the formyl-derivative. The peptide was cleaved by treatment with ethanolamine in DMF at 50°C overnight.
A total of 13.5% of the resin was removed by the resin sampler for quantitative ninhydrin monitoring.
The final protected peptide-resin recovered was 1.345 g, 93.9% theoretical.

Chemical synthesis of human epidermal growth factor (EGF) and human type α transforming growth factor (TGFα)

R. DiMarchi, E. Osborne, E. Roberts and L. Slieker
Lilly Research Laboratories, Indianapolis, IN 46285, U.S.A.

The total chemical synthesis of human EGF and human TGFα was achieved by solid phase synthetic methodology [1, 2]. Automated assembly of the protected peptides was performed by an Applied Biosystems Model 430A Peptide Synthesizer. Double coupling was routinely performed at each residue as either a preformed symmetrical anhydride or HOBt-ester. The side-chain protecting groups used throughout the synthesis were as follows: Asp(OcHex), Glu(OcHex), Arg(Tos), His(π-Bom), Cys(4-MeBzl), Lys(2,Cl-Z), Met(O), Trp(CHO), Tyr(2,Br-Z), Ser(Bzl) and Thr(Bzl).

The peptide-resins were treated with the appropriate reagents of the low-high HF cleavage method [3]. Following HF treatment, a direct and quantitative conversion to the cysteinyl-S-sulfonate derivative provided a means for chromatographic characterization and purification. High performance reversed-phase and anion-exchange analysis against an external standard revealed the EGF and TGFα sulfonates to be 5.2% and 9.5% pure, respectively. Estimation of purity by analysis of integrated peak areas without the use of an external reference was observed to over-exaggerate the purity. Cleavage in a mixture of HF/*p*-thiocresol/*m*-cresol (90 : 5 : 5) at 0° for 60 min provided a yield and purity of TGFα equal to that of the low-high method.

Properly disulfide-paired EGF and TGFα were prepared directly from the respective S-sulfonates. Conditions of conversion are analogous to those which we have previously used in the preparation of rDNA-derived IGF-I (DiMarchi and Long, manuscript submitted for publication). To a solution of crude EGF or TGFα sulfonate at 5 mg/ml in 20 mM glycine at pH 9.5 and 4°C, was added glutathione to a concentration of 6 mM. The conversion reaction was monitored continuously by reversed-phase analysis on a Zorbax C-8 column at pH 7 in 0.1 M $(NH_4)_2HPO_4/CH_3CN$. At approximately 12 h the reaction reached an equilibrium in which the EGF and TGFα were present in respective yields of approximately 35% and 60%. In the case of EGF, this level of conversion represents a dramatic improvement over that which was reportedly achieved through air oxidation of the fully reduced peptide [1].

By high-performance chromatographic analysis, it was obvious that the conversion of each peptide-S-sulfonate to disulfide had served to improve the chromatographic resolution. Presumably only derivatives closely related to the native growth factor are capable of proper disulfide pairing, and thus the remaining impurities tend to yield higher molecular weight substances. In this way, an effective means for improving chromatographic selectivity is attained. The synthetic EGF and TGFα were purified by preparative reversed-phase chromatography and determined to possess biological activity indistinguishable from naturally isolated standards.

Appreciable loss of product yield in the synthesis of EGF and TGFα was perceived possible through attenuation of minor side reaction(s) at the 6 cysteine residues. To assess this possibility a complete synthesis of EGF was completed in which all cysteine residues were substituted with alanine. Analogous handling provided the purified EGF-$(Ala)_6$ in a nearly 4-fold excess to the yield that was twice achieved in the production of EGF-$(SSO_3^-)_6$.

Our results show that in the synthesis of long peptides the S-sulfonate is a useful tool in characterization, purification, and conversion to disulfide; additionally, that proper disulfide pairing serves to facilitate purification; and finally, that there is significant opportunity for increased product yield of cysteine-containing peptides through improvements in the current methods of synthesis.

References

1. Heath, W.F. and Merrifield, R.B., Proc. Natl. Acad. Sci. U.S.A., 83(1986)6367.
2. Tam, J.P., Sheikh, M.A., Solomon, D.S. and Ossowski, L., Proc. Natl. Acad. Sci. U.S.A., 83(1986)8082.
3. Tam, J.P., Heath, W.F. and Merrifield, R.B., J. Am. Chem. Soc., 105(1983)6442.

Design, construction and application of an automated large scale solid phase peptide synthesizer: Large scale preparation of vasopressin analogs

Martin S. Edelstein, John L. Hughes, Pradip K. Bhatnagar, Jonathan E. Foster, Kenneth D. Tubman, Suresh Kalbag[a], Anasuya Patel[a], Paul Voelker[a], Daljit Narindray[b], Alan R. Culwell[c] and Michael Sherlund[c]

Department of Peptide Chemistry, Smith Kline and French Laboratories, Swedeland, PA 19479, U.S.A.

Introduction

Solid phase peptide synthesis has reached a point where its advantages over solution syntheses can be routinely applied to industrial scale processes [1, 2]. Requirements to both rapidly prepare moderate amounts of peptides on short notice and large quantities on a routine basis instigated the development of an automated large scale peptide synthesizer (ALPS) which could be used for both purposes. The ALPS has been in use for over a year and has allowed the convenient synthesis of hundreds of grams of several different peptides.

Design Criteria

Reactors

A multiple reactor design consisting of interchangeable 1 l, 10 l, or 25 l Teflon-lined, stirred, glass reactors was chosen to accommodate both large scale production and moderate scale development work. Software and plumbing must allow the four reactors to operate either synchronously or independently. Resin weights from 50 g to 7 kg can thereby be supported.

Feedback

An electronic balance provides our requirement of *direct* sensing of reactor filling and draining and (indirect) measurement of reagent and waste reservoir volumes. Custom sensors to provide for detection of stuck valves are built into each pneumatic valve.

[a,b,c] Current addresses: [a]Beckman Instruments Inc., Palo Alto, CA 94304; [b]Becton Dickinson Laboratories, Mountain View, CA 94039; [c]Applied Biosystems Inc., Foster City, CA 94409, U.S.A.

Fluid delivery

A desire to keep synthesis time comparable to laboratory scale synthesis led to the use of 6 l/min air-driven pumps.

Control system hardware

The control of 4 simultaneous syntheses requires the use of a 16-bit process scheduling computer and an 8-bit process monitoring computer.

Control system software

The software was designed to mimic a laboratory scale synthesizer. All solvent deliveries are described by volumes rather than delivery times used in many synthesizers. After synthetic commands are entered from menus, the resulting programs are checked fully for error. A complete record of all manual and automatic synthetic operations is provided in a format suitable for inclusion in a GMP record. The chemist is not required to know anything about the plumbing, electronics or computer memory requirements when writing a new program, only that he wants to deliver a specific amount of reagent to a reactor and stir for a time.

Description

Plumbing

The ALPS consists of a reagent module which contains up to 12 reservoirs. Reagents are grouped on 3 solvent manifolds such that wash solvents always occupy the positions farthest from the pumps. Three pumps with Teflon or PVDF heads generate the shear force needed to effectively scour the resin from the reactor sides via a flow-restricted shower head or clear the frit of resin debris during each solvent delivery. Waste from the reactors is pumped to any of 3 waste reservoirs.

Control

Direct control of all valves, pumps and stirrers is provided by an electropneumatic interface utilizing over 200 control points. The sensors, balances, and electropneumatic devices are directly controlled by a Motorola 6809 STD bus computer utilizing 500 I/O points. The 6809 processor receives configuration and batch-specific information from a 16-bit Motorola 68000 based processor. This processor handles all user interface functions plus scheduling functions when multiple batches are simultaneously in progress.

User interaction

The ALPS has 3 modes of operation. Every valve can be operated *manually* by use of switches on the electropneumatic interface. A *semiautomatic* mode

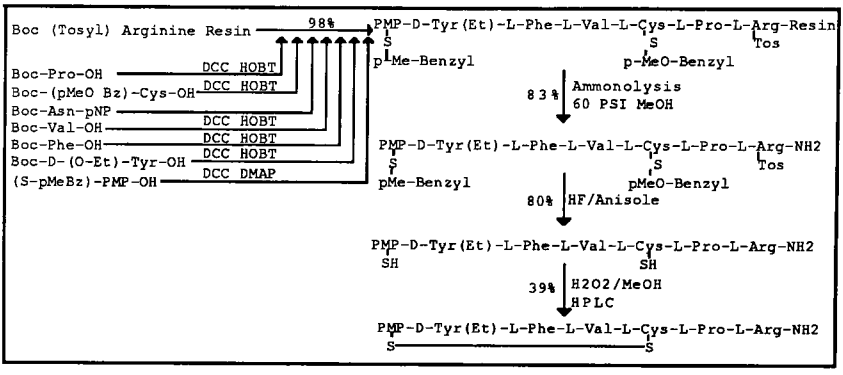

Fig. 1. Solid phase synthesis of SK&F 101926.

allows single operations to be performed. A *fully automatic* mode allows reactor-independent programs to be written. Programs are normally composed from preformed procedures. These procedures can be titled (e.g., 30-MINUTE DEBLOCK) and used by any reactor in any program. Since each residue in the amino acid sequence can be associated with its own optimized program, it is usually convenient to use the machine in automated mode, allowing the computer to load each program as needed but monitoring coupling manually.

Application to the Preparation of Vasopressin Analogs

The large scale synthesis of the vasopressin antagonist SK&F 101926 [3] is shown in Fig. 1. The synthesis was carried out using standard solid phase synthesis protocols with formation of in situ symmetrical anhydrides or HOBT esters. Cleavage of the peptide from the resin was effected by ammonolysis. HF was used to remove protecting groups. Hydrogen peroxide was used to oxidize the dithio compound to the cyclic disulfide. Monitoring the oxidation process by HPLC was essential to obtain maximal yield of cyclic peptide. Purification was

Table 1 *Summary of SK&F 101926 syntheses*

	Synthesis number			
	1	2	3	4
Resin titer (mequiv./g)	0.54	0.76	0.76	1.44
Resin (mmols)	131	190	331	288
Actual weight resin peptide (g)	383	443	750	476
Theoretical weight resin peptide (g)	370	437	766	488
% Yield (resin peptide)	103	101	98	97
Overall yield (>98% pure)	–	–	24.9	24.7

effected by reversed-phase HPLC on a 4-inch by 4-foot column packed with Vydac 201HS 15–20 (octadecylsilyl, 15–20 μm, 80 Å pore, flow rate 500 ml/min, step gradient with ammonium acetate/acetonitrile buffer) using a Separation Technology Process 2000 HPLC. Final purification was obtained by passing the material through a P-2 column and lyophilizing. Four batches of SK&F 101926 were prepared by this method on the ALPS. Batches ranged in size from 130 to 330 mmols (see Table 1). Yields of resin peptide were $100\% \pm 2\%$. Overall average yield of material after HPLC purification was 24.8%.

References

1. Colescott, R.L., Bossinger, C.D., Cook, P.I., Dailey, J.P., Enkoji, T., Flanigan, E., Geever, J.E., Groginsky, C.M., Kaiser, E., Laken, B., Mason, W.A., Olsen, D.B., Reynolds, H.C. and Skibbe, M.O., In Walter, R. and Meienhofer, J. (Eds.) Peptides – Structure and Biology, Proceedings of the Fourth American Peptide Symposium, Ann Arbor Publishing, Ann Arbor, 1975, p. 463.
2. Edelstein, M.S., Scott, P.E., Sherlund, M., Hannsen, A.L. and Hughes, J.L., Chem. Eng. Sci., 41 (1986) 617.
3. Huffman, W.F., Ali, F.E., Bryan, W.M., Callahan, J.F., Moore, M.L., Silvestri, S.S., Yim, N.C.F., Kinter, L.B., McDonald, J.E., Ashton-Shue, D., Stassen, F.L., Heckman, G.D., Schmidt, D.B. and Sulat, L., J. Med. Chem., 28 (1985) 1759.

Solid phase synthesis using high-titer resins

Martin S. Edelstein, John L. Hughes, Jonathan E. Foster and Alan R. Culwell*
Department of Peptide Chemistry, Smith Kline and French Laboratories, Swedeland, PA 19479, U.S.A.

Introduction

The development of methods suitable for the production of kilogram quantities of peptide drugs has led us to evaluate the use of high-titer chloromethyl polystyrene resin for solid phase peptide synthesis. The use of high-titer resin was anticipated to result in decreased solvent consumption and ease of workup of the resin-peptide. A series of peptides has been prepared on resin containing 4.2 mequiv. Cl/g resin and compared to peptides synthesized, under identical conditions, on 1.2 mequiv. Cl/g resin. In addition, we have recently utilized high titer resins for the large scale preparation of a vasopressin antagonist, SK&F 101926 [Pmp[1], D-Tyr(Et)[2], Val[4], des Gly[9]] AVP, on a .28-mol scale.

Results

Simultaneous synthesis of the peptides shown in Table 1 on low- and high-titer resins was carried out using standard solid phase synthesis methods on two Beckman 990 synthesizers running identical programs (except for the SK&F 101926 which was prepared on a large scale synthesizer). Amino acid-resin was prepared by a simplified cesium salt method. Double couplings were performed using in situ HOBT esters. TFA (50%) was used for deblocking and DIEA (20%) for neutralization. Acetylation was included after each coupling. No attempt was made to evaluate coupling completion by the Kaiser test. Peptides were cleaved and carefully dried to determine crude yield prior to HPLC. HPLC was performed on a Beckman HPLC system using Altex 10-μm C-18 columns and TEAP/acetonitrile as eluent.

Discussion

Sarin et al. [1] have stated that the initial interior volume of the resin may

*Current address: Applied Biosystems Inc., Foster City, CA 94409, U.S.A.

Table 1 *Peptides synthesized using high-titer resin*

	Angiotensin II		Bradykinin		SK&F 101926	
Resin titer	4.2	1.2	4.2	1.2	4.2	1.2
Resin-first amino acid titer (mequiv./g)	2.1	0.97	1.4	.84	1.4	0.76
Resin-first amino acid weight (g)	4.69	4.93	5.0	5.1	200	435
% Amino acid in resin-first amino acid	55.4	25.8	61.7	35.8	61.7	32.6
Resin-peptide weight (g)	14.5	10.2	12.5	8.3	476	750
% Peptide in resin-peptide	88	66	85	66	85	62
Yield resin-peptide	86	94	101	88	97	98
Yield cleaved peptide	89	79	97	92	98	80
% Purity HPLC	46	59	63	59	89	86
l CH_2Cl_2/ g peptide	2.26	4.57	3.9	7.0	–	6.5
Solvent savings	51%		45%		–	

not necessarily be a limiting consideration in resin-peptide swelling. To test this concept, several small peptides have been synthesized under conditions where the final resin-peptide has almost 90% peptide content. Yields and purities comparable to those found in low-loading resins were achieved with a 50% average reduction in solvent usage. In addition to decreasing synthesis cost, this method may influence the choice of a solution versus solid phase synthesis for industrial production of peptide drugs. Cleavage of the high-loading resin poses no unusual problems, and extraction of the peptide from the resin is more convenient than in comparable low-loading syntheses. In all cases observed so far, for small peptides (<10 residues), the course of synthesis for the high-titer resin-peptide paralleled that of the low-titer resin and afforded product of comparable purity and yield. Studies are underway to evaluate the use of high-titer resins for the synthesis of peptides containing 10–40 residues.

References

1. Sarin, V.K., Kent, S.B.H. and Merrifield, R.B., J. Am. Chem. Soc., 102(1980)5463.

Rapid solid phase peptide synthesis on a controlled pore glass support

Klaus Büttner[a], Helmut Zahn[a] and Wolfgang H. Fischer[b]

[a]*Deutsches Wollforschungsinstitut, Veltmanplatz 8, D-5100 Aachen, F.R.G.*

[b]*The Clayton Foundation Laboratories for Peptide Biology, The Salk Institute 10010 North Torrey Pines Road, La Jolla, CA 92037, U.S.A.*

Introduction

The most widely used supports for solid phase peptide synthesis are functionalized polymers, such as cross-linked polystyrene [1] and poly(dimethylacrylamide) [2]. The particles formed by these polymers are not very stable when swollen by the solvents used during synthesis. A more rigid support would be desirable for use in flow systems. Controlled pore glass (CPG) is such a nondeformable support.

We describe here peptide synthesis carried out on commercially available derivatized CPG employing the N_α-fluorenylmethoxycarbonyl (Fmoc) protection strategy.

Results and Discussion

Peptides corresponding to residues B 23–30 of bovine insulin and A 1–14 of mouse insulin were synthesized on a long chain alkylamine controlled pore glass (LCAA CPG, pore size 500 Å, Pierce Chemical Co.) as a support (K. Büttner, Ph.D. Thesis, in preparation). Syntheses were carried out manually in polypropylene syringes with sintered filters. Couplings and deprotections were performed in a stopped-flow mode with gentle shaking; removal of excessive reagent was achieved by a continuous flow of solvent. The synthesis strategy corresponded closely to the one developed by Atherton et al. [2] (i.e., N_α-Fmoc protected amino acids were used with *t*-butyl protection of hydroxyl and carboxyl side-chain functions). Semipermanent protection groups were employed for lysine (N_ϵ-trifluoroacetyl) and cysteine (*S*-*t*-butylsulfenyl or *S*-acetamidomethyl) side chains. Preactivation was achieved with dicyclohexylcarbodiimide (DCC) and 1-hydroxybenzotriazole (HOBt) in methylenedichloride/dimethylformamide (DMF). The primary amino groups of the glass were reacted with the linkage group 4-hydroxymethylphenoxyacetic acid. The preactivated amino acid derivative was esterified to this group in the presence of dimethylaminopyridine.

The reaction cycle consisted of (1) cleavage of the Fmoc group with 20% piperidine/DMF for 10 min, (2) removal of excess reagent by a continuous flow of DMF (<5 min), (3) coupling with preactivated amino acid derivative for 15–30 min, and (4) removal of excess reagents with a continuous flow of DMF (<5 min). The total cycle time is thus approximately 45 min. After completion of the last cycle and removal of N-terminal protection, the peptides were cleaved from the glass support with trifluoroacetic acid and purified by medium pressure liquid chromatography on a reversed-phase material.

Yields for the peptides (80–90% pure by HPLC) were approximately 70%. The amino acid composition of the peptides corresponded to the theoretical values. The octapeptide was further characterized by mass spectroscopy. The molecular ion showed the expected mass ($M_r = 1026$).

No loss of peptide chains could be detected during the synthesis indicating that the long chain alkyl amine linkage is stable under the conditions used. The support was substituted with 35 μmol primary amino groups per gram of CPG; substitution with C-terminal amino acids was 10–20 μmol/g.

Solid phase peptide synthesis on a CPG support is well suited for rapid synthesis of small amounts (~10 mg) of peptides. The mechanical properties of CPG (rigid particles, low back pressure) make this method a good candidate for use in continuous flow systems.

References

1. Merrifield, R.B., J. Am. Chem. Soc., 85 (1963) 2149.
2. Atherton, E., Gait, M.J., Sheppard, R.C. and Williams B.J., Bioorg. Chem., 8 (1979) 370.

Solid phase peptide synthesis using BOP reagent: Synthesis of growth hormone releasing factor (GRF) analogs

Alain Fournier, Ching-Tso Wang and Arthur M. Felix
Peptide Research Department, Roche Research Center, Hoffmann-La Roche Inc., Nutley, NJ 07110, U.S.A.

The BOP reagent [1] represents an attractive alternative to DCC in solid phase peptide synthesis [2]. We have evaluated the use of the BOP reagent for a series of difficult solid phase coupling reactions. To demonstrate the advantages of this approach the total synthesis of [Ala^{15}]-GRF(1–29)-NH_2 and its fragments (22–29) and (13–29) was carried out using the BOP procedure.

In the GRF(1–29) series, we observed that the couplings of Boc-Leu^{14}-OH and Boc-Val^{13}-OH, found to be particularly difficult with the conventional DCC method, proceeded to a greater extent of completion using BOP as a condensing agent. Percent completion for respective coupling of Leu^{14} and Val^{13} using DCC was 81% and 64%; using BOP was 92% and 86%. In the GRF(1–44) series the yields with BOP were compared to those obtained with the DCC/HOBt and the symmetrical anhydride (SA) procedures for the couplings of Boc-Asn^{35}-OH and Boc-Gln^{30}-OH. Again, BOP compared favorably, giving respective couplings of 67% [Asn^{35}] and 97% [Gln^{30}] while DCC/HOBt gave 55% [Asn^{35}] and SA gave 75% [Gln^{30}].

The applicability of the BOP reagent for the synthesis of a medium-size peptide using 1 coupling/cycle and only 3 equivalents of reactants was studied by synthesizing [Ala^{15}]-GRF(1–29)-NH_2. Parallel syntheses using DCC under optimal conditions (2.5 equiv./coupling; $\geqslant 2$ couplings/cycle) and DCC/HOBt (3 equiv./cycle) were also carried out. Two analytical checkpoints, (22–29) and (13–29), were chosen to evaluate the relative progress of the syntheses. The BOP reagent gave material of excellent purity at every stage of synthesis (Fig. 1b,d,f). It is comparable to the product obtained by the DCC method under optimal conditions (Fig. 1a,c,e) and much superior to what was obtained by the DCC/HOBt procedure (not shown). In fact, the synthesis using DCC/HOBt (3 equiv./coupling; 1 coupling/cycle) was stopped at the first checkpoint because the crude material was already showing large amounts of contaminants. Yields over 70% were estimated for the BOP-synthesized fragments (20–29) and (13–29) while values of about 50% were estimated for the DCC-synthesized peptides. For

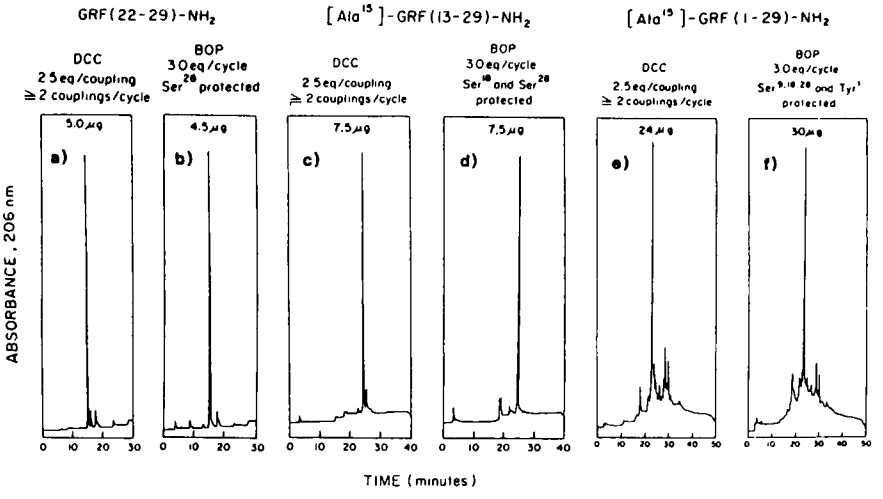

Fig. 1. Analytical HPLC of crude GRF analogs on a Merck Lichrosorb RP-8 column, 5 μm (0.46 × 25 cm). Eluent: (A) 0.1 M $NaClO_4$, pH 2.5, (B) acetonitrile. Flow rate: 1 ml/min, detection: 206 nm (0.2 AUFS). Linear gradient 20–45% (B) in 30 min for GRF (22–29)-NH_2; 30–55% (B) in 30 min for [Ala[15]]-GRF(22–29)-NH_2; 30–55% (B) in 30 min for [Ala[15]]-GRF(13–29)-NH_2; 35–60% (B) in 40 min for [Ala[15]]-GRF(1–29)-NH_2.

[Ala[15]]-GRF(1–29)-NH_2, overall yields of 14% and 12% were reached with DCC and BOP, respectively.

Martinez et al. [3] has demonstrated the feasibility of using the BOP reagent with unprotected Boc-Ser during the course of a solution phase synthesis of an IgG fragment. We applied this approach for the solid phase synthesis of the [Ala[15]]-GRF(1–29)-NH_2 fragments. The yield for the GRF(22–29)-NH_2 synthesis using unprotected Boc-Ser[28]-OH and BOP (3 equiv./coupling; 1 coupling/cycle) was comparable (49%) to that observed from a DCC synthesis (52%) using Boc-Ser[28]-(Bzl)-OH under optimal conditions (multiple couplings/cycle). Further elongation of the peptide chain (synthesis of [Ala[15]]-GRF(13–29)-NH_2) in which Ser[18] was also incorporated with its side chain unprotected, however, resulted in a substantial decrease in overall yield. Therefore, unprotected Boc(hydroxy)-amino acids can be used with the BOP condensing agent, but the number of coupling cycles after its incorporation must be minimal (< 10).

Boc-Tyr[1]-OH was also coupled successfully by the BOP procedure. Although the yield of [Ala[15]]-GRF(1–29)-NH_2 was slightly lower than with the full protection scheme (8% versus 12%), the potential of using BOP with unprotected Tyr in solid phase synthesis is also clearly established. These studies demonstrate that the BOP reagent offers several advantages over other coupling agents and is ideally suited for solid phase peptide synthesis.

References

1. Castro, B., Dormoy, J.R., Evin, G. and Selve, C., Tetrahedron Lett., 14 (1975) 1219.
2. Barany, G. and Merrifield, R.B., In Gross, E. and Meienhofer, J. (Eds.) The Peptides, Vol. 2, Academic Press, New York, 1980, pp. 1–284.
3. Martinez, J., Laur, J. and Winternitz, F., Int. J. Pept. Prot. Res., 22 (1983) 119.

Continuous flow peptide synthesis

R. Frank, H. Leban, M. Kraft and H. Gausepohl
European Molecular Biology Laboratory, 69 Heidelberg, F.R.G.

Since the introduction of the solid phase peptide synthesis technique by R.B. Merrifield in 1962 [1], continuous efforts have been made to improve and automate the method. We describe the design and operation of a new automated solid phase peptide synthesizer. Departing from Merrifield's proposals, several novel chemical procedures are applied: base-labile *N*-α-protection by the 9-fluorenyl-methoxycarbonyl (Fmoc) group [2]; *t*-butyl-based side-chain protection; *p*-benzyloxybenzyl ester anchoring of the peptide chain; and in situ activation of amino acids by benzotriazolyl-oxy-tris-(dimethylamino)-phosphonium hexa-fluorophosphate (BOP) [3]. The instrument (Fig. 1) employs a low-pressure continuous-flow reaction system, a column reactor with variable bed size, and 1% cross-linked polystyrene resin is used as solid support. Reagent flow in the synthesizer is controlled by pneumatically activated dead-volume free-membrane valves (**3**). Liquids are delivered by nitrogen pressure (**1**) or by a valveless piston pump (**7**). The main part of the synthesizer is the reaction loop, comprising the reaction column (**8**), the recirculation pump (**7**), a small volume compensation vial (**9**), a UV-flow cell (0.1 mm path length) (**4**), and valves to switch from the flow through to the recirculation mode. The reaction column contains the polystyrene resin as a loosely packed bed generating less than 0.5 bars back-pressure. UV-absorption of the reagents recirculating in the reaction loop is continuously measured at 312 nm.

Fmoc-amino acids are stored in a turntable (**6**), taken up with a pneumatically activated injection needle (**5**), and delivered to a motor-driven syringe (**2**). In this syringe, the amino acid (1-fold excess) is activated by mixing with an equimolar amount of BOP and NMM in DMF. The activated mixture is then introduced into the reaction loop and recycled. After coupling (30–45 min), the resin is washed with DMF. Deprotection is done by recycling a solution of 20% piperidine in DMF. The reaction is very rapid and under recycling conditions an absorption plateau is reached after a few minutes. This allows for quantitative determination of Fmoc-groups cleaved from the peptide. During coupling of amino acids, a similar plateau is reached. In general, after only one passage through the reactor, acylations of more than 95% are obtained. At this stage of development, the precision attainable by UV-monitoring is still below the level required for accurate determination of coupling efficiency; however, slow acylations which require

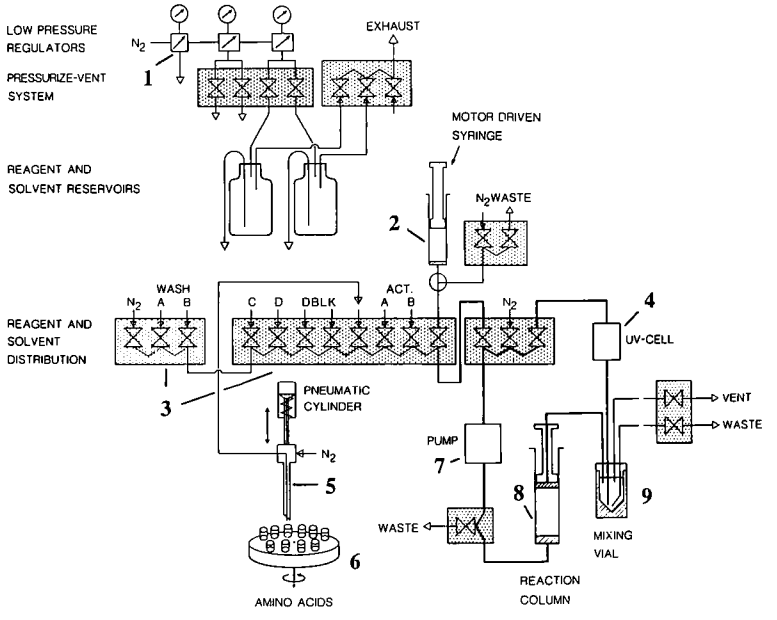

Fig. 1. Flow scheme of the instrument.

double couplings are indicated by a UV-absorption reaching the plateau as an asymptotic curve. In future developments, the slope of this curve will be used to create a signal for feedback control of the instrument. During the final cleavage and deprotection procedure, effective scavengers have to be used to prevent back addition of protecting groups [4].

Our experience has shown that the high efficiency of reagent handling under continuous flow conditions together with the mild orthogonal synthesis strategy and in situ activation of building blocks permit very rapid and reliable solid phase peptide synthesis. Furthermore, the on-line UV-monitoring of reaction progress provides a valuable set of analytical data and a reliable real time control of the instrument's correct operation.

References

1. Merrifield, R.B., Fed. Proc., 21 (1962) 412.
2. Carpino, L.A. and Han, G.Y., J. Am. Chem. Soc., 92 (1970) 5748.
3. Castro, B., Domroy, J.R., Evin, G. and Selve, C., Tetrahedron Lett., 14 (1975) 1219.
4. Frank, R. and Gausepohl, H., In Tschesche, H. (Ed.) Modern Methods in Protein Chemistry, Vol. 3, Walter de Gruyter, Berlin, New York, 1987, in press.

Two new disulfide bonding reactions for the synthesis of cystine peptides

Nobutaka Fujii, Akira Otaka, Osamu Ikemura, Toshihiro Watanabe, Hiromitsu Arai, Susumu Funakoshi and Haruaki Yajima

Faculty of Pharmaceutical Sciences, Kyoto University, Sakyo-ku Kyoto 606, Japan

Introduction

Two new disulfide bonding reactions, which can convert S-protected cysteine directly to cystine, were developed (Fig. 1). Both reactions can be handled in trifluoroacetic acid (TFA), which can dissolve any kind of peptide and protein. Usefulness of these two reactions was demonstrated in the syntheses of two cystine peptides, β-human calcitonin gene-related peptide (β-hCGRP) and oxytocin.

Results and Discussion

(1) Oxidation of S-protected cysteines with Tl(TFA)$_3$

Recently, we have found that Tl(TFA)$_3$ in TFA can cleave various S-protecting groups (*R*) of cysteine to form cystine as the sole product within 60 min at 0°C [*R* = MBzl, *t*-Bu, Ad, Acm, Trt]. Tl(TFA)$_3$ acts as a soft acid to cleave the S-protecting group and as a mild oxidant. This new procedure was successfully

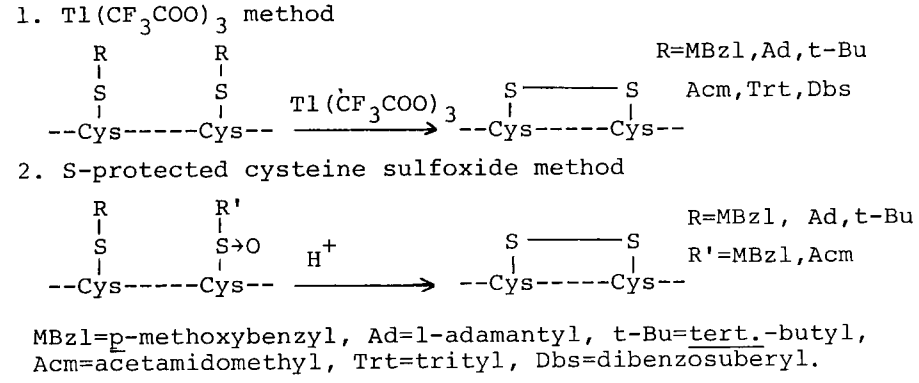

Fig. 1. Two new disulfide bonding reactions.

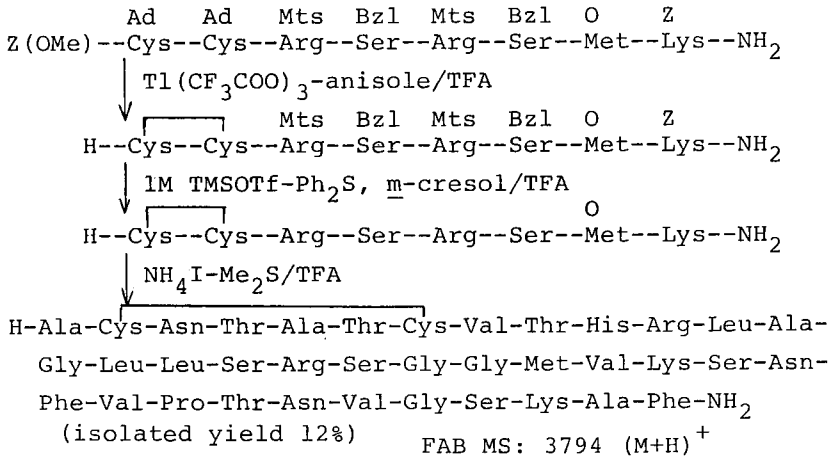

Fig. 2. Synthetic scheme for β-hCGRP.

applied to the syntheses of three model cystine peptides; oxytocin, urotensin II, and α-hCGRP [1]. Subsequently, it was applied to the problematic Met-containing peptide, β-hCGRP [2] (Fig. 2).

Protected β-hCGRP was prepared by azide condensations of 7 peptide fragments, (1–5), (6–9), (10–13), (14–16), (17–20), (21–24), and (25–37). In the final stage of the synthesis, the disulfide bond was established between two Cys(Ad) residues by treatment with $Tl(TFA)_3$. Next, the other protecting groups were cleaved with 1 M trimethylsilyl trifluoromethanesulfonate (TMSOTf)/TFA [3] in the presence of Ph_2S, and Met(O) was reduced in situ to Met by addition of NH_4I and Me_2S without affecting the disulfide bond. The overall yield (12%) after 3-step purifications, gel filtration, ion-exchange, and HPLC, was somewhat higher than that (7%) obtained in the usual air-oxidation procedure.

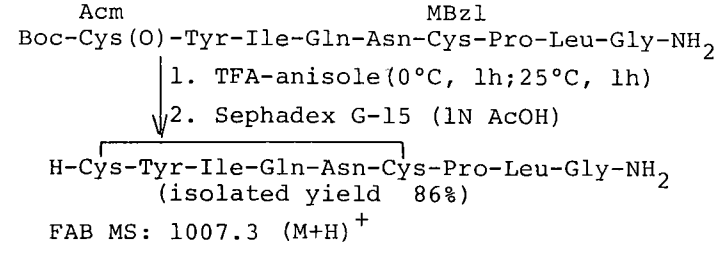

Fig. 3. Improved synthesis of oxytocin using Cys(Acm) (O).

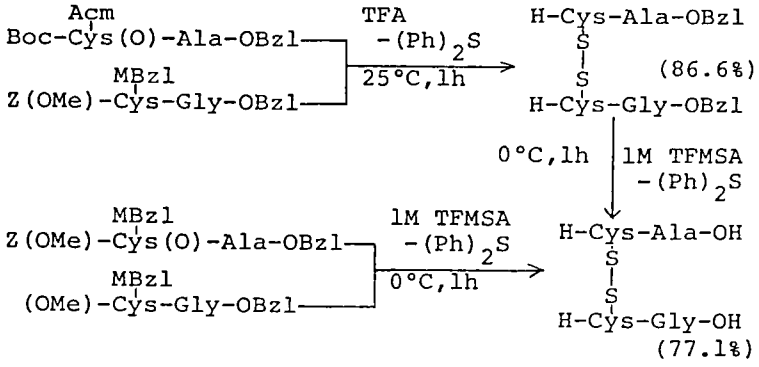

Fig. 4. Application for unsymmetrical open-chain disulfide bond formation.

*(2) Acid treatment of Cys(*R*) (O) in the presence of Cys(*R'*)*

Based on the chemical behavior of S-protected cysteine sulfoxide, Cys(*R*) (O) [4], a new disulfide bonding reaction was developed. Exposure of an equimolar mixture of Cys (*R*) (O) (*R* = Acm, MBzl) and S-protected cysteine, Cys(*R'*) (*R'* = MBzl, Ad, *t*-Bu), to 1 M trifluoromethanesulfonic acid (TFMSA) or TMSOTf in TFA was found to give cystine nearly quantitatively. Cys(Acm) (O) had enough susceptibility to react with Cys(MBzl), even in TFA, to afford cystine. This new sulfoxide-directed reaction was successfully applied to the intramolecular disulfide bond formation in the improved synthesis of oxytocin (Fig. 3), as well as the intermolecular disulfide bonding of unsymmetrical cystine peptides (Fig. 4).

The two alternative disulfide bonding reactions stated above may offer useful tactics for the syntheses of peptides containing several disulfide bonds in the same molecule.

References

1. Fujii, N., Otaka, A., Funakoshi, S., Bessho, K. and Yajima, H., J. Chem. Soc. Chem. Commun., (1987) 163.
2. Steenbergh, P.H., Höppener, J.W.M., Zandberg, J., Visser, A., Lips, C.J.M. and Jansz, H.S., FEBS Lett., 209 (1986) 97.
3. Fujii, N., Otaka, A., Ikemura, O., Akaji, K., Funakoshi, S., Hayashi, Y., Kuroda, Y. and Yajima, H., J. Chem. Soc. Chem. Commun., (1987) 274.
4. Yajima, H., Funakoshi, S., Fujii, N., Akaji, K. and Irie, H., Chem. Pharm. Bull., 27 (1979) 2151.

Kinetics of coupling reactions in solid phase peptide synthesis

Bogumil Hetnarski and R.B. Merrifield
The Rockefeller University, 1230 York Avenue, New York, NY 10021, U.S.A.

Introduction

To further characterize and evaluate solid phase peptide synthesis we have examined coupling reaction rates under pseudo-first-order and second-order conditions. The kinetics were compared as a function of activation method, solvent, concentration, temperature, polarity of side chains, chain length of the amino component, and the mass transfer rate of the carboxyl component into the solid support.

Results and Discussion

Coupling rates in CH_2Cl_2 were measured spectrophotometrically for a series of Bpoc-amino acids activated as symmetric anhydrides or mixed anhydrides with ethyl chlorocarbonate in the $10^{-5} - 10^{-4}$ M concentration range, with a 15-fold excess of Ala-OCH_2-Pam-1%-resin. The calculated k_2 values were in good agreement with corresponding data obtained under second-order conditions and ranged from 6.9 $M^{-1}s^{-1}$ for Gly to 1.3 $M^{-1}s^{-1}$ for Ile.

By analogy to the correlation of log k_2 vs. Taft σ^* constants [1], representing polarities of side chains, found in the liquid phase method [2], we demonstrated a good linear relationship of log k_2 vs. σ^* under solid phase conditions providing the coupling reaction was not dominated by steric hindrance (Fig. 1).

The effect of chain length on coupling rates was studied with $(LAGV)_n$-F-OCH_2-Pam-resin, n = 1–10. Samples were coupled with 1 equivalent of Bpoc-Ala-OC(O)OEt or $(Bpoc\text{-}Ala)_2O$ in CH_2Cl_2 and the initial rates were measured spectrophotometrically (Fig. 2). It was shown previously [3] that chain length did not affect coupling efficiency (deletion peptides) and it is demonstrated here that the length of the amino component also had no effect on the coupling rate with symmetric anhydrides. There was, however, a gradual but fluctuating decrease in rates with mixed anhydrides, which is not yet understood. In DMF as a solvent, the coupling rate constant was substitution-dependent, with lower k_2 at lower loading.

It was of interest to know whether the coupling rates during solid phase synthesis

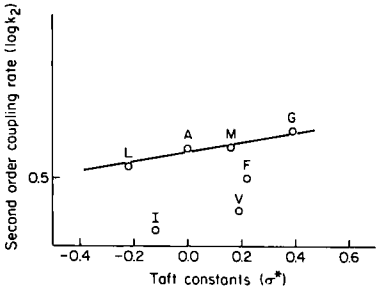

Fig. 1. Relationship of second-order rate constants (log k_2) for couplings of symmetric amino acid anhydrides with Ala-OCH_2-Pam-R vs. σ Taft constants for side chains of carboxyl components.*

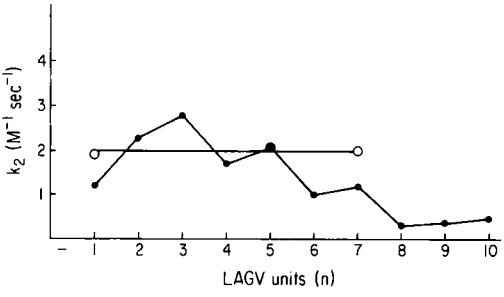

Fig. 2. Coupling of $H(LAGV)_2$-F-OCH_2-Pam-R with Bpoc-Ala-O-C(O)-OEt (•—•) and $(Bpoc\text{-}Ala)_2O$ (o—o). The data points coincide at n = 5.

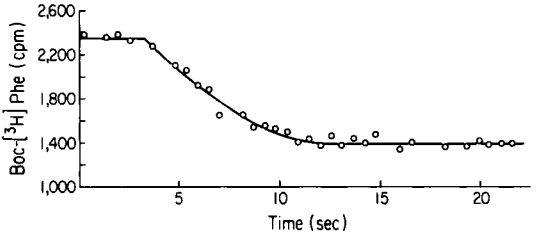

Fig. 3. Diffusion of Boc-[^{3}H]-Phe into toluene-swollen 1% cross-linked polystyrene resin.

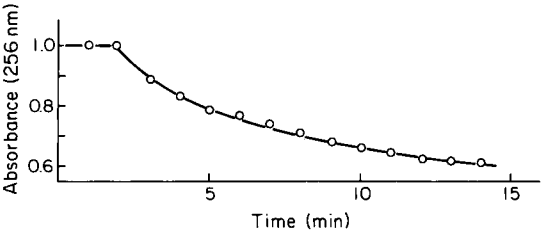

Fig. 4. Decrease in UV absorbance during coupling of aminomethyl-resin (3.0×10^{-4} M) with $(Bpoc\text{-}Ala)_2O$ (2.5×10^{-5} M) in CH_2Cl_2.

are diffusion-limited. This question was examined in four ways: (1) by measuring spectrophotometrically in a rapidly mixed system the rate of mass transfer of Bpoc-amino acids from solution into unsubstituted 1% cross-linked polystyrene beads (loss of the UV absorbance from the solution phase); (2) by determining spectrophotometrically the rate of passage of Bpoc-Ala through a 1% cross-linked polystyrene disc, $D = 7.2 \times 10^{-6}$ cm^2/s (calculated according to Crank [4]); (3) by monitoring the rate of decrease of radioactivity when solvent-swollen

beads were added rapidly to a vigorously stirred solution of Boc-[^{3}H]-Phe and the supernatant was pumped through a filter into a fraction collector (0.56 s/tube) (Fig. 3); and (4) comparing these transfer rates with coupling rates obtained from loss of UV absorbance during a reaction of aminomethyl-resin (3.0×10^{-4} M) with $(Bpoc\text{-}Ala)_2O$ (2.5×10^{-5} M) (Fig. 4).

The minimal, radiometrically determined diffusion coefficient, D, equaled 2.9×10^{-6} cm^2/s in CH_2Cl_2 and 0.84×10^{-6} cm^2/s in toluene. Under synthetic coupling conditions, with 10^{-2} M amino component (0.2 mmol/g) and 1.5×10^{-2} M symmetric anhydride, k_2 was 7.8 $M^{-1}s^{-1}$ for the reaction of $(Bpoc\text{-}Ala)_2O$ with H_2NCH_2-*R*, and to achieve the initial rate, the activated amino acid must be provided inside the bead at the rate of 2.1×10^{-5} mmol/cm^{2}s. The mass transfer was determined to be greater than 6.5×10^{-5} mmol/cm^{2}s and, therefore, we conclude that diffusion is not rate-limiting.

References

1. Taft, R.W., J. Am. Chem. Soc., 75 (1953) 4231.
2. Khurgin, Yu. and Dmitrieva, M.G., Tetrahedron, 21 (1965) 2305.
3. Sarin, V., Kent, S.B.H., Mitchell, A.R. and Merrifield, R.B., J. Am. Chem. Soc., 106 (1984) 7845.
4. Crank, J. and Park, G.S., In Crank, J. and Park, G.S. (Eds.) Diffusion in Polymers, Academic Press, New York, 1968, p. 6.

The utility of reductive alkylation in solid phase peptide synthesis

Simon J. Hocart, Ning Y. Jiang, Mary V. Nekola and David H. Coy
Peptide Research Laboratories, Department of Medicine, Tulane University School of Medicine, 1430 Tulane Avenue, New Orleans, LA 70112, U.S.A.

Introduction

Many hundreds of analogs of luteinizing hormone-releasing hormone (LH-RH) have been synthesized in the last decade in an attempt to develop potent, longer acting antagonists to the hormone. As part of our current research, we have developed facile, solid phase reductive alkylation procedures to produce a variety of new potential antagonists. Recently, we reported the effect of introducing a variety of hydrophobic alkyl and aryl groups into the side chain of Lys in positions 6(D) and 8(L) in an attempt to reduce the histamine-releasing activity of the analogs [1, 2]. In this paper, we present some initial data on the effect of the $\psi[CH_2NH]$ peptide bond isostere in the antagonists.

Results and Discussion

Solid phase reductive alkylation can be employed several ways: (i) with an aldehyde or ketone, alkyl groups can be introduced into the side chain of a dibasic amino acid or into the amino terminal to form N^{α}-alkyl amino acids in situ; (ii) alkylation with a protected amino acid aldehyde can give the $\psi[CH_2NH]$ peptide bond isostere; and (iii) alkylation of the solid phase can give the substituted amide on cleavage.

The procedures involve the reductive alkylation of a resin-bound amino group with an aldehyde or ketone in the presence of $NaCNBH_3$ in acidified DMF. The $\psi[CH_2NH]$ pseudopeptide bond was formed by reaction with a protected amino acid aldehyde, made by the reduction of the respective O,N-dimethyl-hydroxamate with $LiAlH_4$ at 0°C in an essentially racemization-free procedure (see Table 1). After alkylation, the peptides were cleaved and deprotected with anhydrous HF and purified by gel filtration and RPHPLC. Compounds were analyzed by FABMS and amino acid analysis to confirm structure and assayed in a standard rat antiovulatory assay (see Table 2) [3]. Replacement of the peptide bonds D-Phe^2~D-Phe^3, D-Phe^3~Ser^4, and Phe^7~Arg^8 produced highly soluble analogs with greatly reduced antiovulatory activities relative to the parent analog.

Table 1 *Racemization during preparation of and solid phase reductive alkylation with Boc-amino acid aldehydes*

System L-Phe-ψ[CH_2NH]Leu-NH_2 / D-Phe-ψ[CH_2NH]Leu-NH_2	R_t(RPHPLC)	6.6 min / 5.7 min	
Condition		% of isomer	
		D-L	L-L
(a) Hydroxamate formation with 0.1% DMAP, 3 equiv. $LiAlH_4$ reduction at room temperature Alkylate with $NaBH_3CN$ and			
Boc-D-Phe-CHO		94	6
Boc-L-Phe-CHO		20	80
(b) Same as (a), no DMAP			
Boc-L-Phe-CHO		11.5	89.5
(c) Same as (b), 1 equiv. $LiAlH_4$ at 0°C			
alkylate 1 h		n.d.	100
(d) Same as (c), alkylate 16 h		n.d.	100

Table 2 *Antiovulatory activities of analogs based on the structure [N-Ac-D-Nal[1], D-Phe[2,3], D-Arg[6], Phe[7],D-Ala[10]]-LHRH*

Peptide	Antiovulatory activity[a]
Parent analog	56% at 0.5 (9)
N^{α}-ethyl-D-Nal[1]	17% at 6 (6)
N^{α},N^{α}-diethyl-D-Nal[1]	0% at 12 (3)
D-Nal[1]ψ[CH_2NH]D-Phe[2]	0% at 50 (9)
D-Phe[2]ψ[CH_2NH]D-Phe[3]	0% at 12 (7)
D-Phe[3]ψ[CH_2NH]Ser[4]	0% at 12 (11)
Tyr[5]ψ[CH_2NH]D-Arg[6]	14% at 3 (7)
Phe[7]ψ[CH_2NH]Arg[8]	0% at 12 (7)

[a]Expressed as the percentage of (n) rats blocked at a dose of $\times$ μg.

Ac~D-Nal[1] and Tyr[5]~D-Arg[6] analogs, in contrast, retained considerable activity. Further work is in progress to complete the series, evaluate the histamine-releasing activity of the analogs, and perhaps correlate the results with conformational parameters.

Acknowledgements

We gratefully acknowledge the technical assistance of Ellen Shaw and Irene Brohm for conducting the antiovulatory bioassays and Etchie Yauger for liquid chromatography. This work was supported by NIH Contract NO1-HD-4-2832 to D.H.C.

References

1. Hocart, S.J., Nekola, M.V. and Coy, D.H., J. Med. Chem., 30 (1987) 739.
2. Hocart, S.J., Nekola, M.V. and Coy, D.H., J. Med. Chem., (1987) in press.
3. Vilchez-Martinez, J.A., Coy, D.H., Coy, E.J., Arimura A. and Schally, A.V., Endocrine Res. Commun., 3 (1976) 231.

A novel approach to the purification of peptides by reversed-phase HPLC: Sample displacement chromatography

Robert S. Hodges, T.W. Lorne Burke and Colin T. Mant
Department of Biochemistry and the Medical Research Council of Canada Group in Protein Structure and Function, University of Alberta, Edmonton, Alberta, Canada T6G 2H7

Introduction

Impurities resulting from peptide synthesis are usually closely related to the peptide of interest and typically require the powerful resolving capability of reversed-phase HPLC (RPHPLC) for their removal; however, the large columns required for gradient elution separation of large sample loads rapidly become prohibitively costly in terms of column packings and solvents. RPHPLC in the displacement mode, while enabling efficient separation of large amounts of sample, is difficult to optimize and often requires excessively long run times [1]. The present study describes a novel preparative method called sample displacement chromatography (SDC) for the rapid and facile separation of crude peptide mixtures on analytical columns and instrumentation. SDC can be distinguished from other types of RPHPLC in that the major separation process occurs in water.

Results and Discussion

The optimization of preparative chromatography would be greatly simplified if the only variable was sample load, i.e., if the separation process did not require the addition of organic modifier or displacer to the mobile phase. Fig. 1, Panel A, demonstrates the analytical separation profile of a crude peptide mixture. A preparative load of this mixture was applied, in 0.05% aqueous TFA, to the chromatographic system consisting of a precolumn and a larger main column connected in series. The 63 mg of peptide sample contained 45 mg of the desired peptide product (P_3) and 4.5 mg of each of four peptide impurities (I_1, I_2, I_4 and I_5). The sample was subjected to isocratic elution with 0.05% aqueous TFA for 40 min. At 15 min, the precolumn was isolated to trap the hydrophobic impurities I_4 and I_5. The overloaded peptide product competes more successfully with adsorption sites on the hydrophobic stationary phase than the more hydrophilic impurities, I_1 and I_2, which are displaced and immediately eluted

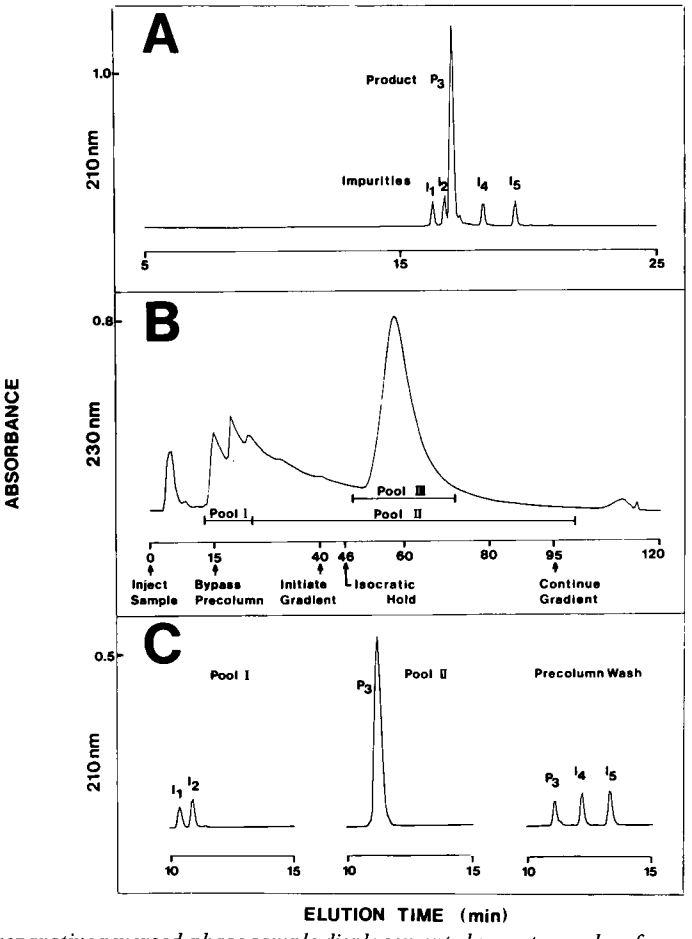

Fig. 1. Preparative reversed-phase sample displacement chromatography of a peptide product (P_3) from hydrophilic (I_1, I_2) and hydrophobic (I_4, I_5) peptide impurities. Main column: Aquapore RP 300 C_8 (220 mm × 4.6 mm I.D.). Precolumn: Aquapore RP 300 C_8 (60 mm × 4.6 mm I.D.).

Panel A: Analytical separation profile of the peptide mixture on the two-column system; conditions, linear AB gradient (2% B/min) at a flow-rate of 1 ml/min, where solvent A is 0.05% aqueous TFA and solvent B is 0.05% TFA in acetonitrile; sample load, 30μg.

Panel B: Preparative separation profile of peptide mixture; conditions, isocratic elution with 100% solvent A for 40 min at a flow-rate of 1 ml/min, followed by linear gradient elution at 1% B/min, isocratic hold (6% B) from 46 min to 95 min, and finally, continued linear gradient elution at 1% B/min. At 15 min, the precolumn was isolated from the main column. Sample load, 63 mg.

Panel C: Analytical elution profiles of Pools I and II from Panel B, and peptide components retained by the precolumn. All separations were carried out at 26°C.

from the system. Thus, the major separation process has taken place in water. Linear gradient elution (1% acetonitrile/min) was subsequently only required to elute the bulk of homogeneous peptide product from the main column. An isocratic hold (6% acetonitrile) was inserted during the gradient wash to maximize the separation of P_3 from any hydrophobic impurities which may have reached the main column; however, fraction analysis (Panel C) demonstrated that 100% of I_4 and I_5 had been retained by the precolumn. Pool II (Panel B) contained pure P_3, representing an excellent 80% recovery of homogeneous product. The potential of SDC as a preparative tool is considerable and should prove of great value to researchers in the peptide field.

References

1. Horváth, Cs., Nahum, A. and Frenz, J.H., J. Chromatogr., 218 (1981) 365.

A deprotection method using tetrachlorosilane-trifluoroacetic acid scavengers by a 'reductive acidolysis' mechanism: Application to the synthesis of a novel tachykinin peptide, scyliorhinin I

Yoshiaki Kiso, Makoto Yoshida, Tooru Kimura, Tsutomu Mimoto, Masanori Shimokura and Toshio Fujisaki

Department of Medicinal Chemistry, Kyoto Pharmaceutical University, Yamashina-ku, Kyoto 607, Japan

We have already reported that a silyl compound, methyltrichlorosilane (Cl_3SiMe), reduced Met(O) to Met in trifluoroacetic acid (TFA)-anisole within 15 min at 25°C [1] and promoted the cleavage of the Z-group and benzyl ester in TFA-soft base, dimethylselenide [2]. The usefulness of Cl_3SiMe-Me_2Se/TFA as a final deprotecting reagent was confirmed by the synthesis of the opioid peptide, amidorphin [2].

Here, we report our investigations of the reductivity and deprotecting ability of silyl compounds: tetrachlorosilane (Cl_4Si), Cl_3SiMe, and trichlorosilane ($HSiCl_3$) in the presence of various scavengers. Among these silyl compounds, Cl_4Si had the strongest reductivity in TFA-anisole at 0°C; it reduced Met(O) to Met completely within 15 min at 0°C in TFA with any species of scavengers tested, such as anisole, phenols, sulfides, selenides and thiols. Cl_4Si in TFA, however, had no reductivity in the absence of scavengers, while $HSiCl_3$ had reductivity by itself [3].

The cleavage of the Z-group and benzyl ester was examined in the presence of various soft bases in TFA to determine the optimal condition for the deprotection by silyl compound. Little difference was observed among the deprotecting ability of silyl compounds. The reaction proceeded faster when selenide was used as a soft base than when sulfide was used. In this preliminary test, no byproduct was detected. Thus, the remarkable characteristics of the deprotecting method using silyl compounds are strong reductivity and acidolytic ability.

Further, we investigated the deprotection of the methylsulfinylbenzyl (Msob) group reported by Samanen et al. [4]. The Msob group was stable in TFA-anisole, but easily removed in Cl_4Si-anisole/TFA which had strong reductivity [5]. In this deprotection reaction, the Msob group is first reduced to TFA-labile methylthiobenzyl group and then cleaved by acidolysis (i.e., the Msob group

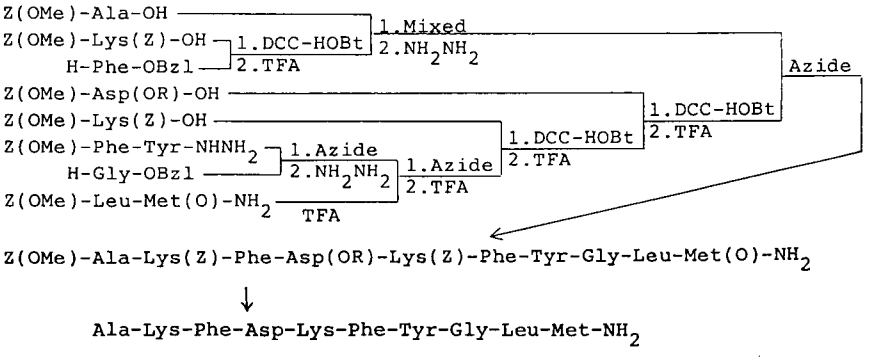

Fig. 1. Synthetic scheme for scyliorhinin I. R = *4-methylsulfinylbenzyl(Msob), Bzl or cHex.*

is deprotected by the reduction of the sulfoxide moiety and subsequent acidolysis). We propose this theory of the reductive acidolysis for this deprotection mechanism.

We applied this deprotection method to the synthesis of a novel tachykinin peptide, scyliorhinin I [6], Ala-Lys-Phe-Asp-Lys-Phe-Tyr-Gly-Leu-Met-NH_2. The synthetic scheme is illustrated in Fig. 1. The final deprotection was carried out in $SiCl_4$-Me_2Se-anisole for Asp(OMsob)-containing peptide. Protected scyliorhinin I, using Asp(OBzl) or Asp(OcHex), was deprotected by HF-Me_2Se-*m*-cresol. The purified peptides from three different routes had identical HPLC retention times. These results show that a new aspartic acid derivative, Asp(OMsob), is useful in peptide synthesis [5].

In addition, we synthesized a novel cystine-containing tachykinin peptide, scyliorhinin II, by the method shown in Fig. 2. Protected scyliorhinin II was deprotected by HF-*m*-cresol and then oxidized to form the disulfide bond by

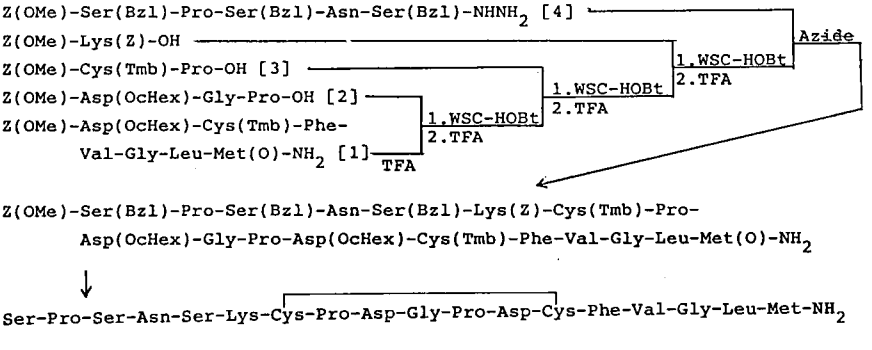

Fig. 2. Synthetic scheme for scyliorhinin II.

I_2. The obtained [Met(O)^{18}]scyliorhinin II was treated with $SiCl_4$-TFA-anisole without any effect on disulfide bond and converted to scyliorhinin II.

The contractile potencies of the synthetic peptides were examined in the isolated guinea pig ileum. Synthetic scyliorhinin I and II exhibited comparable activity to substance P.

References

1. Kiso, Y., Fujisaki, T., Shimokura, M., Okamoto, K., Kaimoto, M. and Uemura, S., Peptide Chemistry 1984 (1985) 289.
2. Kiso, Y., Fujisaki, T. and Shimokura, M., Peptide Chemistry 1985 (1986) 137.
3. Kiso, Y., Yoshida, M., Fujisaki, T., Mimoto, T., Kimura, T. and Shimokura, M., Peptide Chemistry 1986 (1987) 205.
4. Samanen, J.M. and Brandeis, E., In Deber, C.M., Hruby, V.J. and Kopple, K.D. (Eds.) Peptides: Structure and Function, Proc. 9th Am. Peptide Symp., Pierce Chemical Co., Rockford, IL, 1985, p. 225.
5. Kiso, Y., Shimokura, M., Kimura, T., Mimoto, T., Yoshida, M. and Fujisaki, T., Peptide Chemistry 1986 (1987) 211.
6. Conlon, J.M., Deacon, C.F., O'Toole, L. and Thim, L., FEBS Lett., 200 (1986) 111.

Studies related to the syntheses of pseudobactin

Teodozyj Kolasa and Marvin J. Miller
Department of Chemistry, University of Notre Dame, Notre Dame, IN 46556, U.S.A.

Introduction

Specific strains of the *Pseudomonas fluorescens-putida* group, termed plant growth-promoting rhizobacteria (PGPR), rapidly colonize various plant roots and cause statistically significant yield increases. PGPR in the soil produce extracellular siderophores which efficiently complex environmental iron and make it unavailable for growth of other potentially harmful microorganisms. The yellow-green fluorescent siderophore, designated pseudobactin, has been isolated from PGPR [1]. The structure consists of a linear hexapeptide (L-Lys-D-threo-β-OH-Asp-L-Ala-D-allo-Thr-L-Ala-D-N^{δ}-OH-cyclo-Orn) in which N^{δ} of the N^{δ}-hydroxy-ornithine is cyclized with the terminal carboxyl and the N^{ϵ}-amino group of lysine is linked by an amide bond to a fluorescent quinoline derivative (Scheme I). The iron-chelating groups consist of a hydroxamate group, an α-hydroxy acid group and an *o*-dihydroxy aromatic group. None of the three

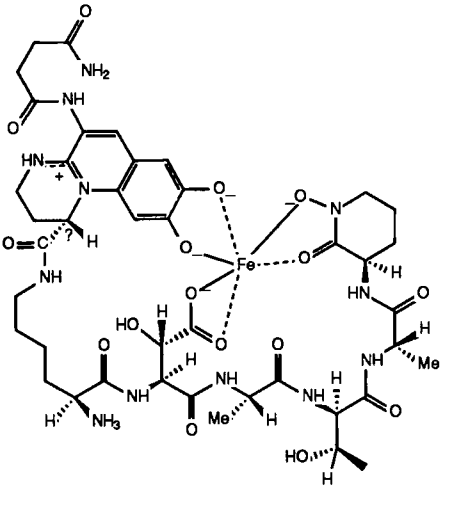

Scheme 1.

chelating groups have been observed in previously described siderophores. The alternating L- and D-amino acids in the pseudobactin sequence are also unusual and could explain why pseudobactin is not affected by trypsin, chymotrypsin, pepsin, pronase, and leucine amino aminopeptidase.

This report describes our attempts to synthesize pseudobactin.

Results and Discussion

The synthesis of the linear hexapeptide is outlined in Scheme 2. The key feature of our approach is transformation of D-glutamic acid to D-Hydroxy-norvaline by using pyroglutamic acid for differentiation of both carboxylic functions [2]. D-Hydroxy-norvaline was transformed into N^{δ}-benzyloxy-D-cycloornithine by several methods with an average of 60–70% overall yield, except one method which included the final cyclization of N^{δ}-benzyloxy-ornithine *N*-hydroxysuccinimide ester (30% yield overall). Subsequently, reaction of Boc-L-Ala-OSu with N^{δ}-benzyloxy-D-cyclo-ornithine, obtained from the N^{α}-Cbz-derivative by deprotection with HBr/AcOH, provides oily dipeptide **1** in 80% yield. The D-allo-Thr, prepared according to Morell et al. [3], was transformed to Cbz-D-allo-Thr-OSu followed by coupling with dipeptide **2**. The resulting tripeptide **2** (77% yield), after deprotection with HBr/AcOH, was converted to tetrapeptide **3** in 83% yield. The optically active di-O-acetyl-N-hydroxy-tartarimide [4] ester of N^{α}-trOC-N^{ϵ}-Cbz-L-Lys in reaction with DL-threo-β-OH-Asp(OMe)$_2$ induced a diastereoisomeric excess of N^{α}-trOC-N^{ϵ}-Cbz-L-Lys-D-threo-β-OH-Asp(OMe)$_2$ **4**, which, after chromatographic purification, gave a 60% yield of pure peptide **4**. On the other hand, optically active D-threo-β-OH-Asp was obtained according

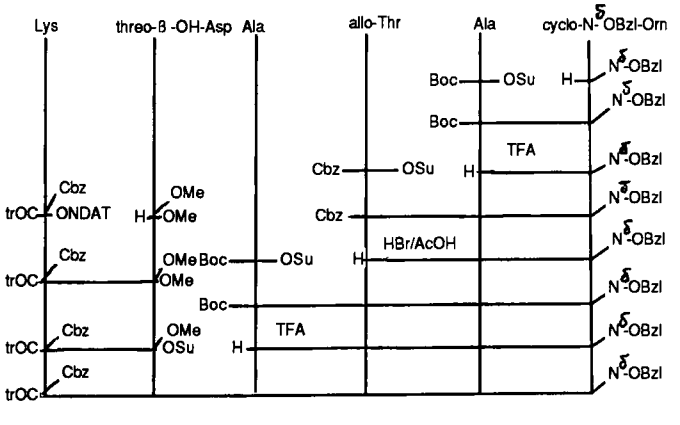

Scheme 2. A schematic diagram of the synthesis of the peptide part of pseudobactin. ONDAT stands for N*-hydroxy-diacetyltartarimide.*

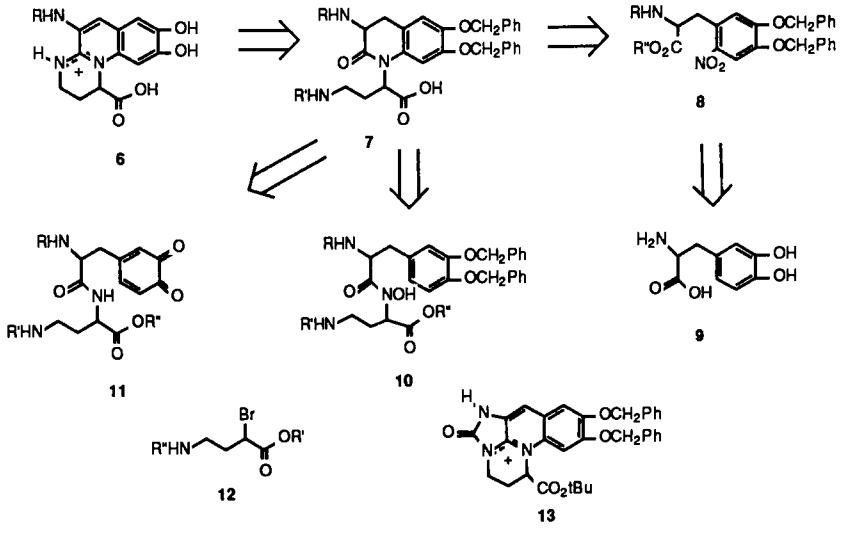

Scheme 3.

to the method of Liwschitz et al. [5]. The peptide **4** after hydrolysis and coupling with peptide **3** provided fully protected peptide **5** in 60% yield.

The approaches to the fluorescent quinoline derivative are shown in Scheme 3 as a retrosynthetic analyses. The properly protected ester of Dopa, obtained according to a known procedure [6], was nitrated with HNO_3 in acetic acid at 0–5°C to provide the *ortho*-nitro derivative in 88% yield. A one pot reduction and cyclization was accomplished in 90% yield by using Fe powder in acetic acid at 90°C for 3 h. An alkylation of the tetrahydroquinolinone derivative with an ester of α-bromo-γ-acylaminobutyric acid (refluxing THF containing NaH, 72 h) provided the desired product in 92% yield. Finally, deprotection of the γ-amino group and cyclization in xylene in the presence of air gave, in 50% yield, a chromophore which appeared to be part of another siderophore, azotobactin [7]. Formation of a fourth ring occurred even when Boc was used to protect the α-nitrogen of Dopa. More recently, the *N*-phthaloyl derivatives of Dopa and subsequent cyclization and alkylation products have been prepared. The results of subsequent cyclization attempts will be reported elsewhere.

Acknowledgements

We gratefully acknowledge the National Institutes of Health for support.

References

1. Teintze, M., Hossain, M.B., Barnes, C.L., Leong, J. and Van der Helm, D., Biochemistry, 20 (1981) 6446.
2. Gibian, H. and Klieger, E., Liebigs Ann. Chem., 640 (1961) 145.
3. Morell, J.L., Fleckenstein, P. and Gross, E., J. Org. Chem., 42 (1977) 355.
4. Teramoto, T., Deguchi, M., Kurosaki, T. and Okawara, M., Tetrahedron Lett., 22 (1981) 1109.
5. Liwschitz, Y., E.-Pfeffermann, Y. and Singermann, A., J. Chem. Soc., (C) (1967) 2104.
6. Banerjee, S.N. and Ressler, C., J. Org. Chem., 41 (1976) 3056.
7. Fukasawa, K., Goto, M., Sasaki, K., Hirata, Y. and Sato, S., Tetrahedron, 28 (1972) 5359.

Chlorotrimethylsilane-phenol as a selective deprotection reagent for the *tert*-butyloxycarbonyl group

Emil Kaiser, Sr., Teresa M. Kubiak*, James P. Tam and R.B. Merrifield**
The Rockefeller University, 1230 York Avenue, New York, NY 10021, U.S.A.

The repetitive removal of the N^{α}-*tert*-butyloxycarbonyl (Boc) group with 50% trifluoroacetic acid (TFA) in solid phase peptide synthesis is accompanied by loss of simple benzyl and benzyloxycarbonyl side-chain protecting groups and peptide chains anchored in benzyl ester linkage to the resin [1]. Such losses can be reduced by modifications of protecting groups and resin. As a different approach, Boc removal with a selective organosilicon reagent [2], chlorotrimethylsilane (CTMS) and phenol in CH_2Cl_2 solution, is described in this paper. We have found that 1 M CTMS/1 M phenol/CH_2Cl_2 deprotects Boc-amino acyl-OCH_2-copoly(styrene-divinylbenzene) resins in 1 h, and in 20 min when the phenol concentration is raised to 3 M. Alone, neither CTMS nor phenol was effective for Boc removal. The selectivity of the new reagent for *tert*-butyl vs. benzyl derivatives was about 5–10 times better than with 50% TFA/CH_2Cl_2 (Table 1).

To test the efficacy of the 1 M CTMS/3 M phenol reagent Leu-Ala-Gly-Val, Leu-enkephalin and glucagon were synthesized on a chloromethyl-resin with the usual couplings of the solid phase method [3]. The deprotection step was as follows: 1 M CTMS + 3 M phenol in CH_2Cl_2 (1×3 min and 1×17 min), CH_2Cl_2 (2×2 min), 7.2% H_2O/DMF (2×3 min), DMF (1×2 min), 10% DIEA/DMF (2×2 min), CH_2Cl_2 (3×2 min). The aqueous DMF wash was used to

Table 1 *Relative stability of benzyl protecting groups*

	% loss in 20 min[a]	
Compound	1 M CTMS-3 M phenol	50% TFA/CH_2Cl_2
Val-OCH_2-C_6H_5-*R*	0.08	0.7
Tyr(Bzl)	0.0007	0.008
Glu(OBzl)	0.0005	0.009
Ser(Bzl)	0.0012	0.013

[a]100% deprotection of N^{α}-Boc in 20 min by both reagents.

*Present address: The Upjohn Company, Kalamazoo, MI 49001, U.S.A.
**To whom correspondence should be addressed.

decompose the residual CTMS and any silylation products. Leu-Ala-Gly-Val and Leu-enkephalin were obtained in greater than 95% yield and purity. The purity and yield of glucagon showed a slight improvement over the peptide made with 50% TFA/CH_2Cl_2 deprotection. Deprotection, a shown by NMR, takes place according to Eqn. 1.

$$(CH_3)_3COCONHCHRCOOCH_2R + Me_3SiCl + C_6H_5OH \xrightarrow{CH_2Cl_2}$$

$$HCl \cdot NH_2CHRCOOCH_2R + Me_3SiOC_6H_5 + CO_2 + (CH_3)_2\text{–}C{=}CH_2 \quad (1)$$

Trimethylphenoxysilane was found by GC/MS [4] in freshly prepared 1 M TMCS-1 M phenol (Eqn. 2), and its concentration determined by NMR [5] to be 0.06 M.

$$Me_3SiCl + HOC_6H_5 \rightleftharpoons Me_3SiOC_6H_5 + HCl \quad (2)$$

Me_3SiOH, the decomposition product of CTMS formed by reaction with the water present in phenol crystals was shown by NMR [5] to be present in the 0.09–0.14 M range.

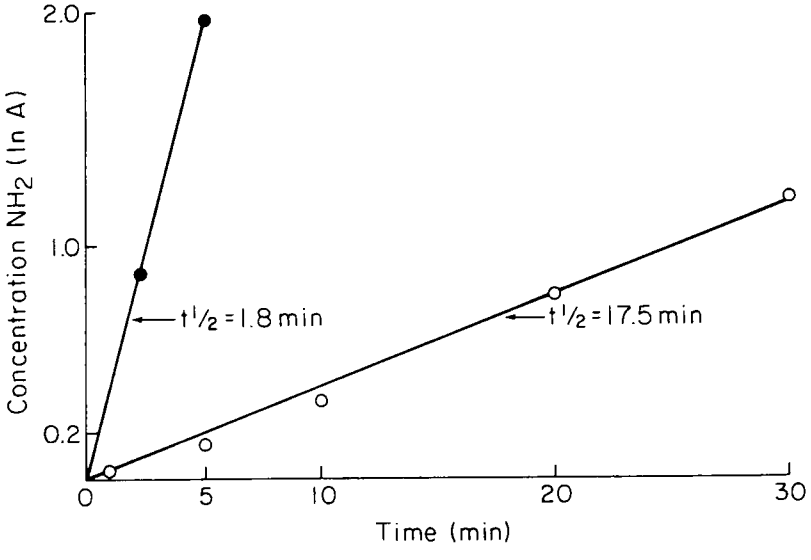

Fig. 1. Kinetic studies on Boc-Val-OCH_2-resin deprotection monitored by the quantitative ninhydrin assay [6] using HCl-free reagents: o, *1M CTMS-1 M phenol in CH_2Cl_2;* •, *1 M CTMS-3 M phenol in CH_2Cl_2.*

$$Me_3SiCl + H_2O \rightarrow Me_3SiOH + HCl \quad (3)$$

The ether and silanol concentrations remained constant for 2 h.

The question remained, whether Boc removal was due to HCl or to the action of CTMS/phenol. To examine this problem, HCl was removed by a chemical process, and acid-free reagents were obtained. In kinetic studies monitored by the quantitative ninhydrin assay [6] deprotection rates were comparable for the acid-free and HCl-containing reagents: for 1 M CTMS-1 M phenol $k = 0.037$ min^{-1}, $t_{1/2} = 17.5$ min, and for the 1 M CTMS-3 M phenol $t_{1/2} = 1.8$ min (Fig. 1). We conclude that CTMS, not HCl, is responsible for the Boc deprotection.

Acknowledgements

This work was supported by NIH Grant DK 01260.

References

1. Erickson, B.W. and Merrifield, R.B., In Neurath, H. and Hill, R.L. (Eds.) The Proteins, Vol. II, 3rd ed., Academic Press, New York, 1976, p. 255.
2. Olah, G.A. and Narang, S.C., Tetrahedron, 38 (1982) 2225 (review with references).
3. Merrifield, R.B., Vizioli, L.D. and Boman, H.G., Biochemistry, 21 (1982) 5020.
4. We wish to thank Drs. Aladar Bencsath and Frank Field for GC/MS.
5. 500 MHz 'H NMR spectrum of 1 M-CTMS-1 M-phenol in $CDCl_2$, ppm downfield from TMS phenol, 7.2 (m, 5, aromatics), 5.24 (s, OH proton), 4.84 (s, OH_2^+); CMTS, 0.410 (s, 7.97, Me); $Me_3SiOC_6H_5$, 0.250 (s, 0.54, Me); Me_3SiOH, 0.070 (s, 0.83, Me). We wish to thank Francis Picart and Dr. David Cowburn for NMR analyses and interpretation, and Dr. William Heath and James Singer for help in kinetics and purification procedures.
6. Sarin, V.K., Kent, S.B.H., Tam, J.P. and Merrifield, R.B., Anal. Biochem., 117 (1981) 147.

Synthesis of peptides containing α,α-disubstituted amino acids: Experiments related to α,α-diethylglycine

M.T. Leplawy, K. Kaczmarek and A. Redlinski
Institute of Organic Chemistry, Technical University, 90-924 Lodz, Poland

Introduction

α,α-Dialkylamino acids offer a useful addition to the arsenal of the peptide chemist, whether his major concern is stereochemistry of the peptide chain, enzymatic resistance or interesting biological effects [1-3]. Efficient incorporation of α,α-dialkylamino acids into a peptide chain requires synthetic approaches for overcoming difficulties arising from steric hindrance [4]. Reports from our own and other laboratories show the need for systematic investigation of each particular α,α-disubstituted amino acid and method of coupling [5-8]. We report here an examination of routes to peptides containing a single unit of α,α-diethylglycine (Deg) and a search for methods enabling efficient synthesis of Deg-oligohomopeptides [9].

Results

Accessibility of Deg

α,α-Diethylglycine has not been found as a constituent of natural products. It is readily accessible from 3-pentanone via the Bucherer synthesis according to published procedure [10] with an overall yield of 56–68%.

N-Protection

N-Protected Deg-derivatives are accessible in moderate yields by routine methods; however, a longer time of reaction and an excess of reagent are required. Examples: Boc-Deg, m.p. 139–141°C, yield 60% using an excess of di-*tert*-butyl-dicarbonate in portions; Z-Deg, m.p. 91–92°C, yield 55–60%; TFA-Deg, m.p. 112–114°C, after sublimation m.p. 120–121°C, yield 82% using a mixture (3:1) of trifluoroacetic acid and trifluoroacetic anhydride, room temperature, 2 days; For-Deg, m.p. 207–208°C, yield 78%; Nps-Deg-dicyclohexylammonium salt, m.p. 150–152°C, yield 50%. The removal of the Z-, Boc-, and Nps-groups proceeds without difficulty. Only a reductive approach ($NaBH_4$, aqueous EtOH, reflux) is serviceable for removal of the Tfa group.

C-Protection

Carboxyl protection (-OBu^t, -OBzl, -OMe, -OEt) requires a long reaction time and a large excess of reagent. Examples: Deg-OBu^t from Deg (20 mmol) and AcOBu^t (270 ml), 70% aqueous $HClO_4$ (20 mmol), room temperature, 5 days, oil, yield 75–80%; Boc-Deg-OBzl from Boc-Deg and Bzl-Br, triethylamine in DMF, room temperature, 3 days, m.p. 178–179°C, yield 85%; HCl·Deg-OMe using MeOH/HCl, reflux, 16 h, yield 55–65%; HCl·Deg-OEt using EtOH/HCl, reflux, 24 h, yield 60–65%. The preparative value of Deg-OMe is doubtful because the methyl group could not be removed selectively.

Peptides containing a single unit of Deg

Mixed anhydride coupling using isobutyl chloroformate is the method of choice for synthesis of Aa-Deg sequences. Example: Boc-Tyr-Deg-Gly-OMe (1 + 2 coupling) using isobutyl chloroformate and *N*-methylmorpholine, 2 days, yield 55%.

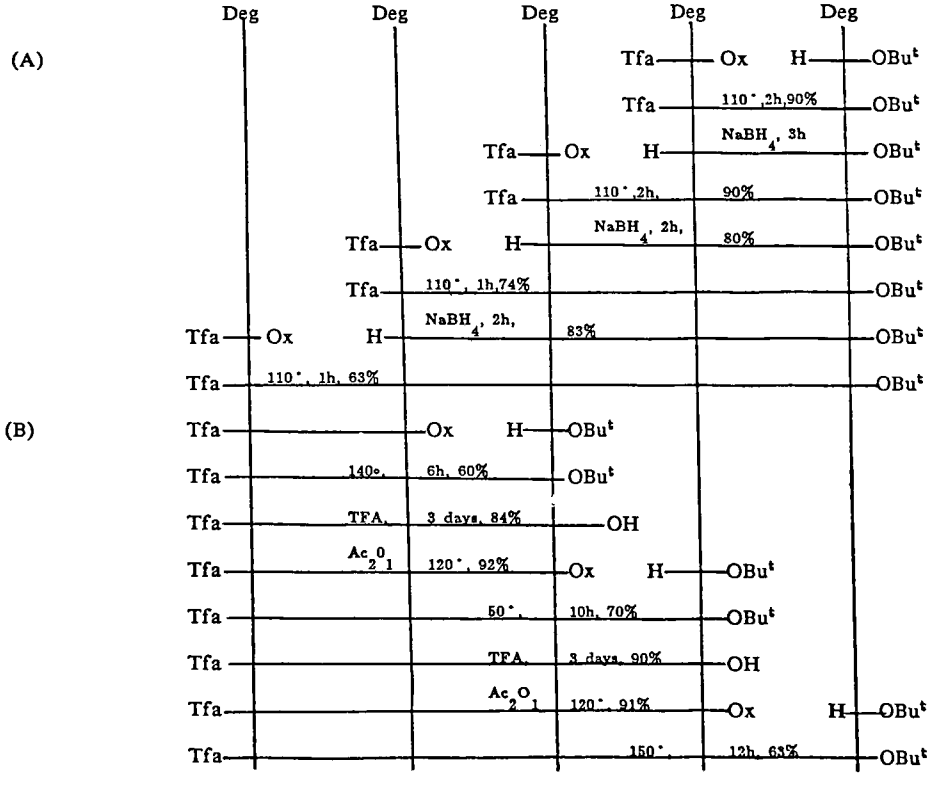

Fig. 1. Synthesis of TFA-(Deg)$_5$-OBu^t. (A) 1 + n coupling; (B) n + 1 coupling. Ox = oxazolone.

Deg-N-carboxyanhydride (prepared from Deg and phosgene, m.p. 45–47°, yield 77%) is useful in the synthesis of Deg-Aa sequences. Examples: Deg-Gly, 85%; Deg-Ala, 50%; Deg-Gly-Leu, 55%.

Examples illustrating other methods of formation of Deg-Aa sequences: Boc-Deg-Phe-Leu-OMe, using DPPA, 30 days, 1 + 2 coupling, yield 45%; Boc-Deg-Gly-OEt, using DCC, 24 h, yield 66%.

Deg-oligohomopeptides

Only the oxazolone method is serviceable for synthesis of Deg-oligohomopeptides. The efficiency of the 1 + n and n + 1 approaches proved to be comparable in the synthesis of TFA-$(Deg)_5$-OBu^t (see Fig. 1).

Acknowledgements

This work was financially supported by the Polish Academy of Sciences, grant CPBP 01.13.2.5.

References

1. Marshall, G.R., Bosshard, H.E., Kendrick, N.C.E., Turk, J., Balasubramanian, T.M., Cobb, S.M.H., Moore, M., Leduc, L. and Needleman, P., In Loffet, A. (Ed.) Peptides 1976, Editions de l'Université de Bruxelles, Brussels, 1976, p. 361 (and references therein).
2. Spatola, A.F., In Weinstein, B. (Ed.) Chemistry and Biochemistry of Amino Acids, Peptides and Proteins, Vol. 7, Marcel Dekker, New York, NY, 1983, p. 267.
3. Benedetti, E., DiBlasio, B., Pedone, C., Bavoso, A., Toniolo, C., Bonora, G.M., Leplawy, M.T. and Hardy, P., In Sasisekharan, V. (Ed.) Proc. Int. Symp. Biomol. Struct. Interactions, Suppl. J. Biosci., Vol. 8, Indian Institute of Science, Bangalore, 1985, p. 253.
4. Leplawy, M.T., Jones, D.S., Kenner, G.W. and Sheppard, R.C., Tetrahedron, 11 (1960) 39.
5. Cotton, R., Hardy, P.M. and Langran-Goldsmith, A.E., Int. J. Pept. Prot. Res., 28 (1986) 245 (and references therein).
6. Kaminski, Z., Leplawy, M.T., Olma, A. and Redlinski, A., In Brunfeldt, K. (Ed.) Peptides 1980, Scriptor, Copenhagen, 1981, p. 201.
7. Nagaraj, R. and Balaram, M., Tetrahedron, 37 (1981) 2001.
8. Schmitt, H. and Jung, G., Liebigs Ann. Chem., (1985) 321 (and references therein).
9. For conformational studies of Deg-oligohomopeptides in solid state and in solution see: Bavoso, A., Benedetti, E., DiBlasio, B., Pavone, V., Pedone, C., Toniolo, C., Bonora, G.M., Leplawy, M.T., Redlinski, A. and Kaczmarek, K., In Deber, C.M., Hruby, V.J. and Kopple, K.D. (Eds.) Peptides, Proc. 9th Am. Peptide Symp., Pierce Chemical Co., Rockford, IL, 1985, p. 193.
10. Abshire, C.J. and Planet, G., J. Med. Chem., 15 (1972) 226.

Carboxyl-terminal peptide degradation: Formation of a C-terminal derivative

Julie B. Stimmel and G. Marc Loudon*

Department of Medicinal Chemistry and Pharmacognosy, School of Pharmacy and Pharmacal Sciences, Purdue University, West Lafayette, IN 47907, U.S.A.

Introduction

In 1980 Parham and Loudon [1, 2] proposed a carboxyl-terminal peptide degradation based on the Hofmann and Curtius rearrangements (Eqn. 1; Pep = peptide attached to a glass support).

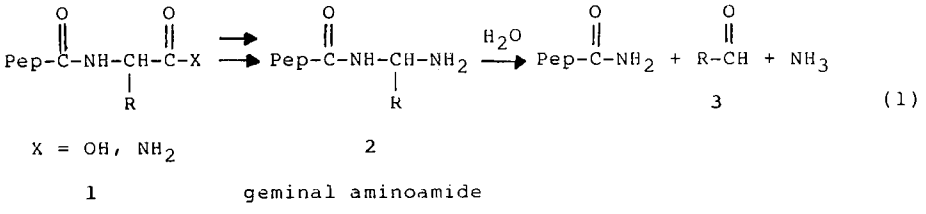

It was shown that this scheme could be applied repetitively in favorable cases with degradation yields averaging 70–80%. A disadvantage of the method, however, is that the degraded residue must be determined by difference amino acid analysis, a fact that makes the degradation unusable on all but the smallest peptides. We set out to develop the degradation further so that a well-defined derivative of the C-terminal residue is produced. Such a derivative would provide direct analysis for the identity of the C-terminal residue, in the same philosophical sense that the phenylthiohydantoin (PTH) derivatives are used to identify amino-terminal derivatives in the Edman degradation.

Results and Discussion

An obvious derivative of the C-terminal residue liberated at each cycle is the aldehyde (compound **3** in Eqn. 1); however, aldehydes were considered

*To whom correspondence should be addressed.

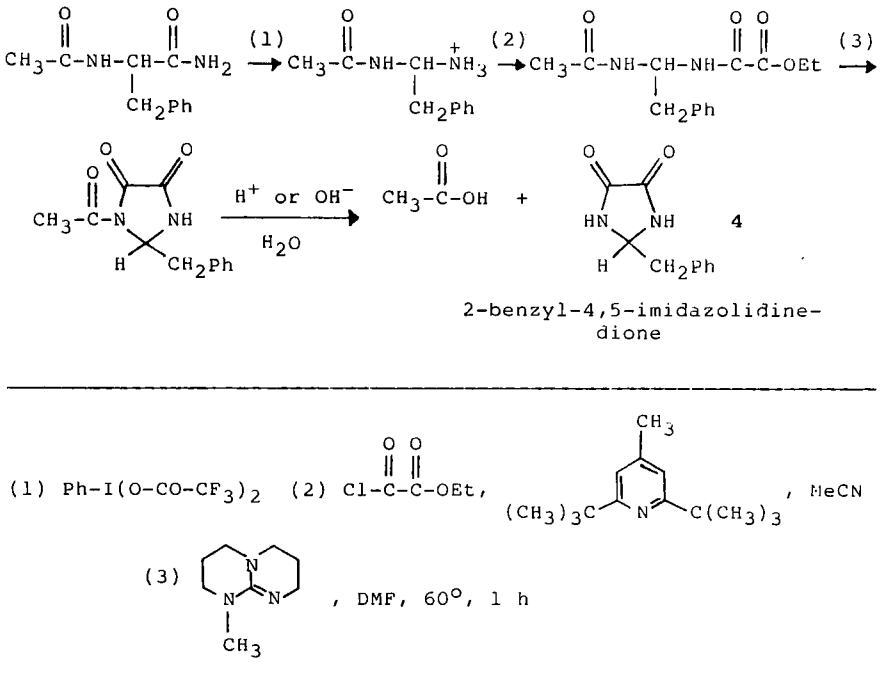

2-benzyl-4,5-imidazolidine-dione

Scheme 1. Formation of 2-substituted 4,5-imidazolidinediones (2I45D's).

unattractive because of their chemical lability, and because of the highly variable volatilities and solubilities across the range of possible amino acid residues. The key to finding a successful derivative lies in the finding [3, 4] that the geminal aminoamide derivatives (compound **2** in Eqn. 1) formed as intermediates in the degradation have a hydrolytic stability that was initially unexpected. Hence, these derivatives can in effect be used as 'trapped aldehydes' in the formation of an appropriate derivative. The derivatization procedure is summarized in Scheme 1.

It is not surprising that, once acylated on both nitrogens, geminal aminoamides have considerably increased stability to acids and bases. Hence, the scheme used to derivatize these compounds employs acylation as a first step. Following acylation with ethyl chlorooxalate, the di-acylated geminal aminoamide derivative is cyclized with the hindered base 7-methyl-1,5,7-diazobicyclo[4.4.0]dec-5-ene. The heterocyclic C-terminal derivative, a 2-substituted-4,5-imidazolidinedione (2I45D), is liberated by gentle hydrolysis.

The 2I45D derivative **4** shown in Scheme 1 (derived from phenylalanine) was, to our knowledge, the only such amino acid derivative known in the literature

prior to our work. This derivative was prepared separately by a literature route [5] and was found to be identical in all respects to the product of Scheme 1.

The chemistry in Scheme 1 was applied to the glass-immobilized peptide Gly-Phe-amide. The degradation of this peptide was monitored at various steps for consistency with the proposed chemistry. For example, amino acid analysis of the glass following formation of the geminal aminoamide showed complete loss of Phe. Following acylation, a strongly positive hydroxamate test was observed. On brief hydrolytic treatment of the glass-immobilized derivative **5**, the expected 2I45D derivative **4** was liberated from the glass in 89% isolated yield (Eqn. 2):

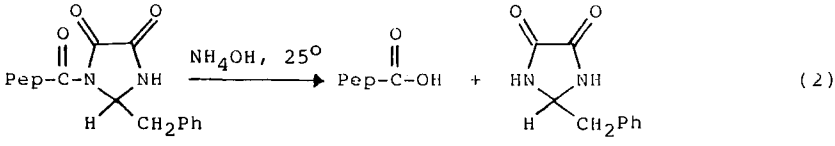

5 4 (2)

We have prepared the 2I45D derivatives from glycine and the hydrophobic amino acids, and have found them to be stable and separable by reversed-phase (C18) HPLC. Our demonstration that these derivatives can be formed and liberated in a C-terminal degradation paves the way for the development of a truly sequential process.

References

1. Parham, M.E. and Loudon, G.M., Biochem. Biophys. Res. Comm., 80(1978)7.
2. Loudon, G.M. and Parham, M.E., Biochem. Biophys. Res. Comm., 80(1978)1.
3. Loudon, G.M. and Jacob, J.M., Chem. Comm., (1980)377.
4. Loudon, G.M., Almond, M.R. and Jacob, J.M., J. Am. Chem. Soc., 103(1981)4508.
5. Wintersteiner, O., Stavely, H.E., Dutcher, J.D. and Spielman, M.A., In Clark, H., Johnson, J.R. and Robinson, R. (Eds.) The Chemistry of Penicillin, Princeton University Press, Princeton, NJ, 1949, pp. 236-239.

On-resin biotinylation of a human interleukin-1 beta analog and its convenient one-step purification

Martin R. Deibel[a], Thomas J. Lobl[a,*], Anthony W. Yem[a], Daniel E. Tracey[b] and Jeff W. Paslay[b]

[a]Biopolymer Chemistry and [b]Hypersensitivity Diseases Research, The Upjohn Company, Kalamazoo, MI 49001, U.S.A.

Introduction

There is a need to develop methods to purify low-yield chemically synthesized proteins in a rapid and efficient manner. Goodman and co-workers, while preparing small biotinylated di- and tetrapeptides as haptens [1], demonstrated that amino terminal biotinylated synthetic peptides could be synthesized and were stable to HF cleavage conditions. Goodman's approach is attractive because the synthesized peptide is fully protected except for the terminal amino group on the 'growing chain'. We decided to apply biotinylation to the purification of a 153-residue chemically synthesized interleukin-1 beta (IL-1 beta) analog where Asn^{205} was substituted with Asp (Lobl et al., manuscript in preparation). If failure sequences are terminated with a capping agent such as acetic anhydride, then only the desired full-sized peptide/protein should have a free amino terminal available for biotinylation. Analysis of the chemically synthesized IL-1 beta analog showed an on-resin yield of $\leq 9\%$ (Lobl et al., manuscript in preparation). Purification of such a low-yield protein from many similar materials is complicated. In this report, we describe our successful biotinylation on-resin of the IL-1 beta analog, its HF cleavage and one-step purification on an avidin agarose column. The method offers potential for purification when the desired product is present in low yield.

Results and Discussion

Chemical synthesis

The IL-1 beta analog was chemically synthesized on an Applied Biosystems 430A peptide synthesizer modified to double couple each residue and cap with Ac_2O/DCM. Following completion of the final coupling cycle the peptide was

*To whom correspondence should be addressed.

terminally deprotected with TFA/DCM, neutralized with DIEA/DCM, washed with DCM, DCM/MeOH (6/4) and air-dried.

Typical resin sample biotinylation procedure

Resin, DMF and NHS-Biotin (Pierce Chemical Co.) were mixed and stirred at 45°C for 10 h. The resin sample was filtered, washed with DMF, DCM and DCM/MeOH (6/4), respectively, and air-dried. The resin together with 10 mg methionine was subjected to the high-low HF cleavage [2]. Following trituration with diethyl ether the residue was extracted with buffer (6 M guanidine, 10 mM DTT, 1x Dulbecco's PBS, pH 7.0) and dialysed against PBS.

Avidin agarose chromatography

An avidin agarose column (Sigma #A-2036) was prepared and equilibrated according to the manufacturer's instructions. The extract was loaded onto the column and nonbound fraction collected. Following column washing, the bound protein was eluted with 0.1 M glycine-HCl (pH 2.0). Individual chromatography fractions were analyzed by 18% SDS–urea polyacrylamide gel electrophoresis. The completed gel was fixed in acetic acid and ethanol for 30 min, and silver-stained according to procedures recommended by BioRad.

Biotin-avidin blot detection

The gel and nitrocellulose paper were sandwiched and subjected to electro-transfer at room temperature for 18 h at 15 V. The protein-containing nitro-cellulose paper was subsequently processed as recommended by the Vectastain ABC kit specifications (Vector). The blot was visualized by incubation with 0.02% $CoCl_2$, 0.05% (w/v) 3,3'-diaminobenzidine tetrahydrochloride (Sigma), 1×PBS, and 0.2 ml of 30% hydrogen peroxide. The reaction was terminated

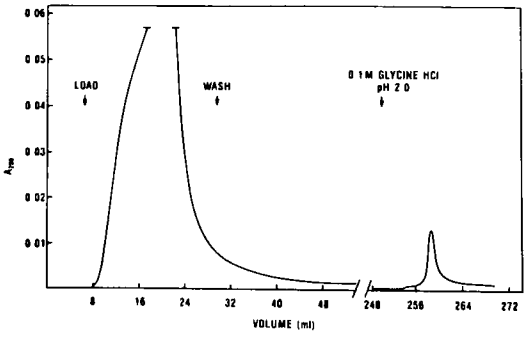

Fig. 1. Avidin agarose chromatography of the biotinylated synthetic IL-1 beta analog.

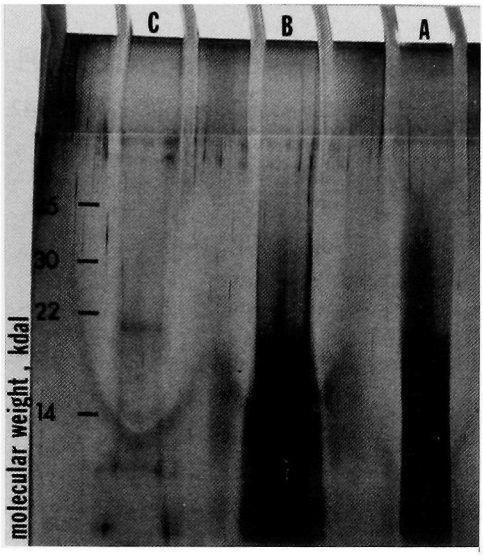

Fig. 2. SDS–urea polyacrylamide gel electrophoresis of fractions obtained from the column described in Fig. 1. Lane A: original crude solution before avidin agarose chromatography (3.8 μg total protein applied), Lane B: column load and wash pool (9.8 μg total protein applied), Lane C: 0.1 M glycine·HCl, pH 2.0 pool (0.32 μg total protein applied). The gel was stained with silver as described above.

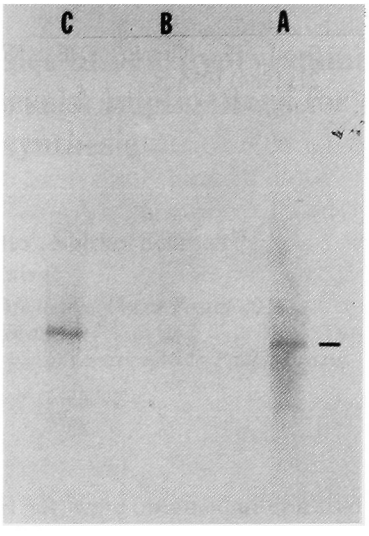

Fig. 3. Biotin-avidin detection blot of a gel run identically to that described in Fig. 2. Lanes A, B and C are described. Detection of peroxidase-conjugated protein was made as described above.

by immersion in deionized water and photographed with Polaroid type 665 film.

The elution profile on avidin agarose chromatography of the biotinylated synthetic Il-1 beta analog, shown in Fig. 1, illustrates the resolution afforded by this affinity purification method. The SDS–urea gel (Fig. 2) compares the crude HF cleavage product with the affinity purified material. Even though the desired protein is not present in high yield (based on gel profile), it is separated readily from the nonbiotinylated impurities. The biotin detection blot (Fig. 3) shows that the only detected band runs identically with the authentic recombinant IL-1 beta. We conclude from this that biotinylation offers a unique and rapid method for affinity purification of chemically synthesized proteins present in low yields on-resin. Further characterization of this method is in progress.

References

1. Scott, D., Nitecki, D.E., Kindler, H. and Goodman, J.W., Mol. Immunol., 21 (1984) 1055.
2. Tam, J.P., Heath, W.F. and Merrifield, R.B., J. Am. Chem. Soc., 105 (1983) 6442.

Synthetic and physicochemical studies of benzhydrylamine resins with different substitution levels: Implications for solid phase peptide synthesis

Clovis R. Nakaie[a], Reinaldo Marchetto[a], Shirley Schreier[b] and Antonio C.M. Paiva[a]

[a]*Department of Biophysics, Escola Paulista de Medicina, Caixa Postal 20388, 04034 São Paulo, SP, Brazil*

[b]*Department of Biochemistry, Institute of Chemistry, University of São Paulo, Brazil*

Introduction

Several batches of benzhydrylamine resins (BHAR) were obtained after a study of the kinetics of the benzoylation and reduction steps of the synthesis [1], and the effect of substitution level on their solvation properties, as well as those of model peptides bound to BHAR, were studied. Mobility and site-site interaction data were obtained by ESR spectroscopy of these compounds labeled with a nitroxyl amino acid [2].

Results and Discussion

Keeping constant the amount of benzoylation reagents (4 mmol/g of polystyrene-1%-divinylbenzene at 35°C, in nitrobenzene) and of the reduction reagents (60 mmol/g of resin at 170°C, in nitrobenzene), maximum benzoylation and reductive amination were reached around 3 h and 30 h, respectively. The high reaction rate observed in the benzoylation step should be responsible for the well-known difficulty in controlling the extent of final substitution. Maximum amino group loading was 1.4 mmol/g resin. A 2.2 mmol/g value was only obtained when benzoylation reagents were increased to 7 mmol/g resin.

The swelling properties of 5 BHAR batches (substitutions ranging from 0.05 to 2.2 mmol/g) were examined by direct microscope measurement of beads [3]. Ratios of volumes (swollen/dry) in DCM:DMF:EtOH were 5.5:2.8:1 for the unprotonated resins (independent of the substitution level) but were markedly dependent on substitution level for the protonated (trifluoroacetate) form (3.8:2:1 at 0.05 mmol/g; 1:4:7 at 2.2 mmol/g). To avoid shrinking problems with high-loaded resins in DCM, these results clearly demonstrate the need of intercalating EtOH or DMF washes with DCM before the first TEA-neutralization steps in the solid phase peptide synthesis (SPPS).

A study of the model compounds (Asn-Ala-Asn-Pro)$_n$ (n = 1–4) bound to a high-loaded (1.4 mmol/g) BHAR confirmed the dominating influence of the peptide chains on the swelling properties of the hydrophobic solid support [3], with better solvation behavior in DMF. The swollen/dry volume ratios in DCM:DMF:EtOH were 1.5:5:1 for both the unprotonated and protonated forms of Asn-Ala-Asn-Pro)$_4$-BHAR. This confirms the advantageous use of DMF for all the SPPS steps even after TFA-deprotection, when no swelling by DCM is observed. Protonated peptide-bound polymers, in contrast to the resin alone, did not swell in EtOH.

The nitroxyl amino acid Boc-2,2,6,6-tetramethylpiperidine-*N*-oxyl-4-amino-4-carboxylic acid (Boc-TOAC) (2) was coupled to BHAR and Asn-Ala-Asn-Pro-BHAR. Fig. 1A shows the effect of solvent upon ESR spectra of Boc-TOAC-BHAR (0.05 mmol/g). As expected, a greater degree of motion was observed in DCM (c) and DMF (d) whereas the lack of swelling in EtOH (b) yielded a powder spectrum (a). Relevant for SPPS, Fig. 1B clearly shows spectral line broadenings due to spin-spin exchange interactions as the extent of labeling increases (e, f, g); otherwise, the simple insertion of a tetrapeptide spacer between TOAC and the resin induces a decrease in exchange interactions (compare Fig. 1B, g and h), suggesting that the frequency of encounters is diminished in peptide-resin as compared to resin alone. In addition, the peptide-resin displays a greater degree of motion in DMF than in DCM (not shown) in accordance with the swelling results.

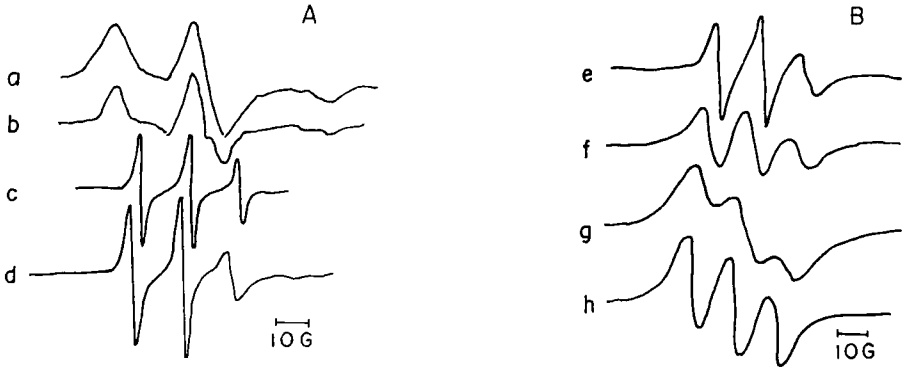

Fig. 1. ESR spectra. (A) Boc-TOAC-BHAR (0.05 mmol/g) in: (a) powder; (b) EtOH; (c) DCM; (d) DMF. (B) spectra, in DMF, of Boc-TOAC-BHAR (e, 0.14 mmol/g; f, 0.8 mmol/g; g, 1.4 mmol/g) and Boc-TOAC-Asn-Ala-Asn-Pro-BHAR, 1.4 mmol/g (h).

References

1. Piettà, P.G., Carvalho, P.F., Takahashi, K. and Marshall, G.R., J. Org. Chem., 39 (1974) 44.
2. Nakaie, C.R., Schreier, S. and Paiva, A.C.M., Biochim. Biophys. Acta, 742 (1983) 63.
3. Sarin, V.K., Kent, S.B.H. and Merrifield, R.B., J. Am. Chem. Soc., 102 (1980) 5463.

Preparation of protected peptides by the solid phase method and HF-stable, but easily removable, blocking groups

Witold Neugebauer, Ginette Champagne, Marie-Reine Lefebvre and Emanuel Escher

Department of Pharmacology, Faculty of Medicine, University of Sherbrooke, Sherbrooke, Qué. J1H 5N4, Canada

Introduction

Solid phase peptide synthesis in its many variants is by far the most common peptide synthetic procedure. The other, the solution method, is still very important to obtaining more complex peptides by means of protected fragment condensation. These fragments can be obtained either by the classical solution method or by applying variants of the solid phase method using at least a three-level protection scheme. Such three-level protection schemes are not easily accessible because they require amino acid derivatives not commercially available, special resins, etc., and thus can become very expensive. We therefore sought to find means for using relatively simple and economic procedures with the Boc-HF-Merrifield strategy to produce protected peptide sequences suitable for fragment condensation.

We propose the use of nitro-stabilized Z- and Bzl-functions which are stable against HF but readily cleaved under mild reductive conditions. With such a protection scheme protected peptides are accessible from HF-cleaved Merrifield resin. In the following, we present the application of this procedure for specifically functionalized analogs of ACTH and the preparation of peptide antigens which needed a four-dimensional orthogonal protection scheme.

Materials and Methods

The nitrobenzyloxycarbonyl function for amino protection was introduced using 4-nitrobenzyl chloroformate in the same manner as for Z-protection [1–3] and Lys was selectively acylated as the copper complex [4]. His was produced as the bis-(NO_2-Z) derivative; Arg was only N-α protected. Aspartic acid-β-nitrobenzyl ester was prepared either with the corresponding alcohol in H_2SO_4/SO_3, a variation of the Benoiton procedure [5], or by using copper-catalyzed

saponification of the diester [6, 7]. Peptide syntheses were carried out on automatic peptide synthesizers using the usual Boc-TFA scheme. Peptides were cleaved in liquid HF at 0°C for 1 h, lyophilized from 20% AcOH and filtered over LH20 in DMF, followed by preparative HPLC. After the desired derivatization, the HF-stable NO_2-Z and NO_2-Bzl groups were cleaved by hydrogenation over Pd/C under pressure for 1 h [8, 9] or by Zn in 50% HOAc for 3 h at room temperature. Cleavage of Cys(Acm) was carried out with Hg^{2+}/H_2S as reported earlier [10]. Peptide cyclizations were carried out in DMF with HOBT/DCC over a period of 6 h at room temperature or 30°C. Purifications were carried out as mentioned above.

Results and Discussion

The NO_2Z-protected amino acids (Pro and Lys) and the β-nitrobenzyl ester of Asp were subjected to HF treatment for 3 h at 0°C but in no case was partial deprotection observed. The formation of NO_2Z-amino acids was very easy and produced easily crystallized derivatives. The best way to produce the β-nitrobenzyl ester of Asp with no detectable contamination of α-ester was by catalytic saponification of the diester with LiOH in the presence of $CuSO_4$ and introduction of the Boc-group in DMSO/diisopropylethyl amine. The precursor peptides shown in Fig. 1 have been readily obtained. Peptide cyclizations also were easily achieved on the HF-cleaved and purified products. The NO_2-Z and the NO_2-Bzl group close a gap in the orthogonal protection schemes by adding a further dimension to the already existing schemes (see Table 1).

The reductive cleavage of both groups is very easily achieved by catalytic

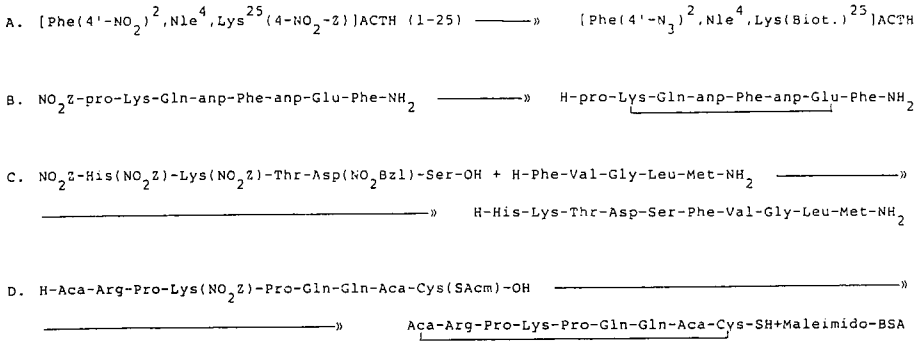

Fig. 1. Examples for synthetic applications. A = Introduction of a prostatic group into a defined position of ACTH; B = Side-chain cyclization of a substance P antagonist; C = Production of neurokinin A by fragment coupling; D = Preparation of a cyclic substance P antigen with 4-level protection; pro = D-Pro; anp = D-α-naphtylalanine; Aca = 6-aminocaproic acid.

Table 1 *Stability chart of protecting groups*

NH_2	COOH	40% TFA	HF	H_2/Pd	Hg^{2+}/H_2S
Boc	t-But	+	++	0	0
Cl_2-Z	Bzl	0	+	+	0
NO_2-Z	NO_2-Bzl	0	0	++	0
(S-Acm)		0	0	0	+

0 = stable, + = cleaved, ++ = cleaved very fast.

hydrogenation [9] and also mild reductive acidolysis with Zn in HOAc 50% but not with $NaBH_4$ or free sulfhydryls. This particular behavior is based on the two-step reaction for the cleavage (see following scheme).

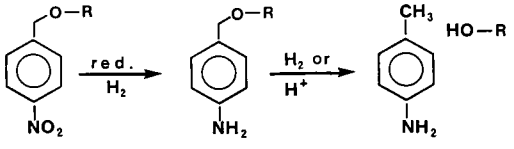

The intermediate amino benzyl function is very sensitive to acid and hydrogenation. The thus liberated toluidine is very easily separated from the peptide.

In conclusion, we have shown that these forgotten protecting groups have great potential as HF-stable protecting groups for obtaining specifically functionalized peptides or for fragment couplings of protected sequences.

Acknowledgements

This work has been supported by grants from the Medical Research Council of Canada; E.E. is a scholar of the Fonds de la Recherche en Santé du Québec. We thank Mrs. C. Théberge for secretarial help.

References

1. Carpenter, F.H. and Gish, D.T., J. Am. Chem. Soc., 74 (1952) 3818.
2. Gish, D.T. and Carpenter, F.H., J. Am. Chem. Soc., 75 (1953) 950.
3. Shields, J.E. and Carpenter, F.H., J. Am. Chem. Soc., 83 (1961) 3066.
4. Shields, J.E., McGregor, W.H. and Carpenter, F.H., J. Org. Chem., 26 (1961) 1494.
5. Benoiton, L., Can. J. Chem., 40 (1962) 570.
6. Prestidge, R.L., Harding, D.R.K., Battersby, J.E. and Hancock, W.S., J. Org. Chem., 40 (1975) 13287.
7. Prestidge, R.L., Harding, D.R.K. and Hancock, W.S., J. Org. Chem., 41 (1975) 2579.
8. Schwarz, H. and Arakawa, K., J. Am. Chem. Soc., 81 (1959) 5691.
9. Laczko, E. and Escher, E., Helv. Chim. Acta, 64 (1981) 621.
10. Escher, E., Bernier, M. and Parent, P., Helv. Chim. Acta, 66 (1983) 1355.

Application of trimethylsilyl trifluoromethanesulfonate deprotection procedure for solid phase peptide synthesis

Motoyoshi Nomizu[a], Yoshimasa Inagaki[a], Katsuhiko Asano[a], Nobutaka Fujii[b], Osamu Ikemura[b], Akira Otaka[b] and Haruaki Yajima[b]

[a]*Pharmaceutical Laboratory, Kirin Brewery Co., Ltd., Maebashi 371 Gunma, Japan*
[b]*Faculty of Pharmaceutical Science, Kyoto University, Sakyo-ku, Kyoto 606, Japan*

Introduction

Trifluoromethanesulfonic acid (TFMSA) has wide application as a deprotecting reagent both in liquid phase and solid phase peptide synthesis [1, 2]. Recently we have found that 1 M trimethylsilyl trifluoromethanesulfonate (TMSOTf)/TFA, in the presence of equimolar soft nucleophiles such as thioanisole and/or diphenylsulfide, can cleave various protecting groups currently employed in peptide synthesis more readily than 1 M TFMSA/TFA [3]. This deprotecting procedure was successfully applied to the liquid phase synthesis of several biologically active peptides. In order to evaluate the usefulness of this deprotecting procedure in solid phase peptide synthesis, three peptides – chicken calcitonin [4], α-MSH, and mammalian glucagon – were synthesized and compared with those produced by the HF deprotecting procedure.

Results and Discussion

The protected peptide was assembled on 4-methylbenzhydrylamine (MBHA) or 4-(oxymethyl)-phenylacetamidomethyl (PAM) resin using an automated peptide synthesizer (Applied Biosystems Model 430A). t-Boc amino acids with side-chain protection removable with the above reagent were employed [i.e., Asp(OChp), Glu(OBzl), Thr(Bzl), Ser(Bzl), Met(O), Tyr(BrZ), His(Tos), Lys(ClZ), Arg(Mts) and Trp(Mts)]. In the calcitonin synthesis, the SH function of 2 cysteine residues was protected with the acetamidomethyl group, which is inert to the above deprotecting reagent, as shown in Fig. 1. Deprotection and cleavage were conducted with 1 M TMSOTf/0.5 M thioanisole/0.5 M diphenylsulfide in TFA at 0°C for 2 h with fairly good yield (79%) of crude product. HPLC analysis exhibited a symmetrical main peak without any accompanying sizeable amount of side peaks (Fig. 1, A), and the elution profile compared favorably to that obtained by standard HF protocols. 1,7-Cys(Acm)-calcitonin, thus obtained, was converted directly to the natural disulfide form

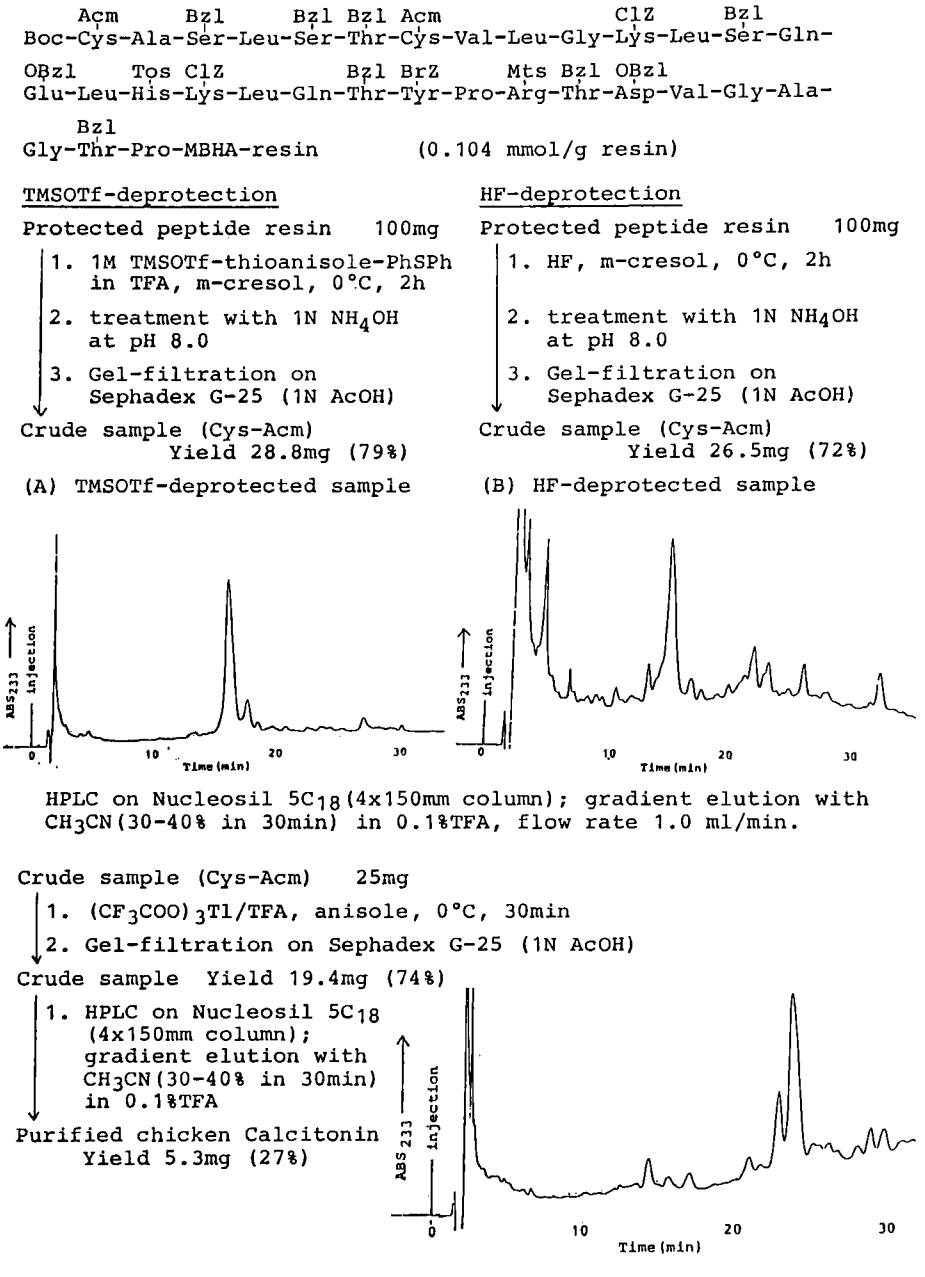

Fig. 1. Synthesis of chicken calcitonin.

by treatment with 1 equivalent of Tl $(TFA)_3$ [5]. The overall yield of purified c-calcitonin from the protected peptide resin was 16%.

Figs. 2 and 3 show HPLC patterns of crude α-MSH and glucagon synthesized in essentially the same manner. Compared to the HF procedure, no significant differences were observed, though sufficient release of α-MSH from the MBHA resin required longer treatment (5 h) at 25°C.

Based on these experimental results, we concluded that a new deprotecting procedure with TMSOTf is applicable to solid phase peptide synthesis as a practical alternative to the conventional HF procedure.

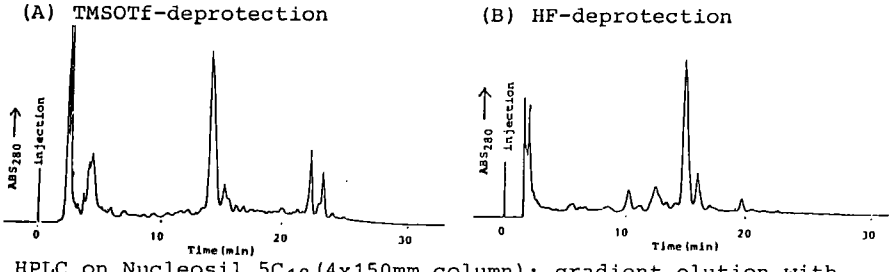

HPLC on Nucleosil $5C_{18}$ (4x150mm column); gradient elution with CH_3CN (20-40% in 30min) in 0.1%TFA, flow rate 1.0 ml/min

Fig. 2. HPLC pattern of crude α-MSH.

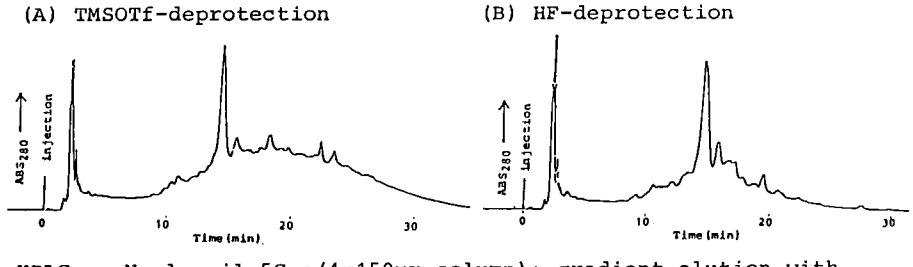

HPLC on Nucleosil $5C_{18}$ (4x150mm column); gradient elution with CH_3CN (30-50% in 30min) in 0.1%TFA, flow rate 1.0 ml/min

Fig. 3. HPLC pattern of crude glucagon.

References

1. Yajima, H. and Fujii, N., In Gross, E. and Meienhofer J., (Eds.) The Peptides, Vol. 5, Academic Press, New York, 1983, pp. 65–109.
2. Tam, J., Heath, W. and Merrifield, R.B., J. Am. Chem. Soc., 108 (1986) 5242.
3. Fujii, N., Otaka, A., Ikemura, O., Akaji, K., Funakoshi, S., Hayashi, Y., Kuroda, Y. and Yajima, H., J. Chem. Soc. Chem. Commun., (1987) 274.
4. Homma, T., Watanabe, M., Hirose, S., Kanai, A., Kangawa, K. and Matsuo, H., J. Biochem., 100 (1986) 459.
5. Fujii, N., Otaka, A., Funakoshi, S., Bessho, K. and Yajima, H., J. Chem. Soc. Chem. Commun., (1987) 163.

Improved linker resin combination for solid phase peptide synthesis

M. Mergler, R. Nyfeler, J. Gosteli and P. Grogg
BACHEM AG, Hauptstrasse 144, 4416 Bubendorf, Switzerland

Introduction

Conventional solution peptide synthesis is cumbersome and time-consuming, but has an advantage in that the fully protected intermediary fragments can be purified before coupling to other protected fragments. This is an advantage compared to solid phase peptide synthesis, where the finished product must be purified from a mixture of similar contaminants.

In this paper we want to present a resin which combines the ease of solid phase peptide synthesis with the advantage of solution synthesis. It further combines the ease of handling the polystyrene solid phase support introduced by Merrifield [1, 2] with the acid lability of a dialkoxybenzyl alcohol linker [3].

Results and Discussion

The new super acid sensitive resin (Sasrin®, see Fig. 1) is prepared by reacting chloromethyl copolystyrene/1% divinylbenzene resin with 3-methoxy-4-hydroxymethylphenol. Fluorenylmethoxycarbonyl(Fmoc)-amino acids are coupled

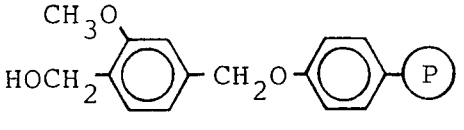

Fig. 1. Sasrin®.

to the resin using DCC and DMAP as a catalyst. The Fmoc-amino acid resins are obtained in about 80% yield. Unreacted functional groups are blocked by reaction with benzoyl chloride.

We prepared a whole range of Fmoc-amino acid resins. Side-chain protection was *t*-butyl for Asp, Ser, Thr, and Tyr; Mtr for Arg; Boc for Lys; Dod for Gln.

Loading was determined photometrically after reaction with piperidine. The

values obtained were confirmed gravimetrically by quantitative cleavage and isolation of the Fmoc-amino acids. Loading was found to be between 0.45 and 0.7 mequiv./g.

The degree of racemization was determined by gas chromatography after cleavage. The values found for D-isomer content were less than 1% and compared favorably to other resins. Peptide synthesis on Sasrin®-resin follows the general scheme of Fmoc strategy. Peptides built up on the resin can be cleaved rapidly and under very mild conditions with 0.5 - 1% TFA in CH_2Cl_2. Side-chain protection is not affected under these conditions. The resulting protected peptide fragments are obtained in high yield and purity. We have prepared protected fragments of substance P (1–3), kassinin (1–5), hANF (1–10), and hANF (4–16). The protected fragments can be used for further fragment condensation either in solution or on the resin. Fragment condensation is especially interesting in the case of multiple repetitive sequences.

Gly-Asp-Arg-Ala-Asp-Gly-Gln-Pro-Ala was found to be the structure of the immunodominant repeating peptide of the circumsporozoite protein of *Plasmodium vivax* by McCutchan et al. [4]. We prepared the dimer (i.e., the 18-amino acid peptide) by DCC/HOBt-mediated solid phase fragment coupling. The α-Boc-protected nonapeptide was first synthesized on Sasrin®-resin in a yield of 85% and with a purity of about 80% (HPLC). It was then coupled to the same sequence still attached to the resin, cleaved with 1% TFA, deprotected, and purified. The resulting octadecapeptide was of excellent purity and yield.

We have shown that synthesis, cleavage, and condensation of protected peptides on Sasrin®-resin is superior to liquid as well as to solid phase synthesis in terms of yield and purity of the final product. It is especially useful and effective for the synthesis of repetitive sequences.

References

1. Tam, J.P., DiMarchi, R.D. and Merrifield, R.B., Tetrahedron Lett., 22(1981)2851.
2. Lu, G., Mojsov, S., Tam, J.P. and Merrifield, R.B., J. Org. Chem., 46(1981)3433.
3. Sheppard, R.C. and Williams, B.J., J. Chem. Soc. Chem. Commun., (1982)587.
4. McCutchan, T.F., Lal, A.A., De la Cruz, V., Miller, L.H., Maloy, W.L., Charoenvit, Y., Beaudoin, R.L., Guerry, P. and Wistar, R., Jr., Science, 230(1985)1381.

Solid phase synthesis of acid-sensitive peptide amides

B. Penke[a], W. Gray[b], C.A. Hoeger[c] and J. Rivier[c]

[a]Institute of Medical Chemistry, Medical University of Szeged, H-6720 Szeged, Dom Ter 8, Hungary

[b]University of Utah, Department of Biology, Salt Lake City, UT 84112, U.S.A.

[c]The Clayton Foundation Laboratories for Peptide Biology, The Salk Institute, 10010 N. Torrey Pines Road, La Jolla, CA 92037, U.S.A.

Introduction

The solid phase approach to peptide synthesis [1] coupled with HPLC purification [2] is by now recognized as the methodology of choice for the synthesis of small and large quantities of polypeptides. While the N-alpha Boc protection strategy is versatile enough to be used in the synthesis of most peptides, those compounds containing acid-sensitive amino acids or sequences must be handled by other strategies. The base-labile Fmoc group is especially promising; however, while supports exist for the liberation of peptide free acids upon acid treatment, very few exist which will yield peptide amides. One of these, the 2,4-dimethoxybenzhydryl amine (2,4-DMBHA) support [3] has been successfully used in our laboratory for the synthesis of CCK-8 and GnRH [4]. We report here on the synthesis of a Gla-containing hexapeptide amide and an attempt at the synthesis of rat corticotropin releasing factor (rCRF) using this resin.

Materials and Methods

The individual peptides were synthesized employing alpha-Fmoc protection and piperidine deprotection (20% in DMF), the 2,4-DMBHA resin and the following side-chain protecting groups: Lys(Boc), Thr(tBu), Glu(γ-OtBu), Ser(tBu), Asp(β-OtBu), Arg(N^9-4-methoxy-2,3,6-trimethylbenzenesulfonyl) [Arg(Mtr)], His(Fmoc), Cys(tBu), and *gamma*-carboxy glutamic acid bis(γ-tBu)ester [Gla-$OtBu)_2$]. The Fmoc amino acids employed (with the exception of Gla) were purchased from Bachem (Torrance, CA) and were of high (>98%) purity. The peptides were liberated from the resin and deprotected as reported previously [5]. Purification was accomplished through HPLC techniques [6].

Results and Discussion

We have shown that sulfated CCK-8 and GnRH could be synthesized using

the 2,4-DMBHA resin, the Fmoc strategy and TFA cleavage/deprotection. The kinetics of cleavage and deprotection of resin-bound CCK-8 as compared to that of desulfonation of Tyr were too similar to yield CCK-8 devoid of *des*-sulfated Tyr; however, the crude material, upon HPLC purification, yielded CCK-8 in relatively good yield [4]. To further test the utility of the 2,4-DMBHA resin, we synthesized the hexapeptide Val-Tyr-Gla-Thr-His-Pro-NH_2, homologous to one of the toxic components of the venom of the cone-hunting snail *Conus magus* [7]. Cleavage of the crude peptide from the solid support by TFA/DCM/β-mercaptoethanol (49:50:1, v/v) was followed by HPLC to determine the effect, if any, of these conditions on the decomposition of Gla to Glu. After 5 h at 22°C a single major peak that does not co-elute with the corresponding Glu hexapeptide is seen. Prolonged exposure (48 h) of the peptide to these conditions, however, resulted in complete conversion of the Gla residue to Glu. The *Conus*-related hexapeptide was characterized by amino acid composition, FAB mass spectrometry and sequence analysis.

We then investigated whether the 2,4-DMBHA resin could be used for the synthesis of more complex structures such as rCRF. The assembly of this peptide was done manually and monitored by Kaiser's ninhydrin test and upon completion, a number of cleavage methods were tried [4, 5]. Workup of these cleavages was accomplished by precipitation and subsequent washing of the cleaved peptide and spent resin with diethyl ether. After extraction (CH_3CN-H_2O) and lyophilization, the crude products were analyzed by RPHPLC; no cleavage conditions used gave the desired product as the major component, irrespective of manipulations carried out on the crude peptide (gel filtration, HPLC desalting, base treatment, etc.). Explanations for such results can only be speculative at the present time; however, two possibilities come to mind: (a) instability of the peptide in the presence of large concentrations of carbocations, especially peptides containing Met (of which there are two in rCRF), and (b) the use of the somewhat acid-resistant Mtr group [8] to protect the guanidino function in Arg (of which there are four).

Conclusions

We have used the 2,4-DMBHA and Fmoc strategy to synthesize two acid-sensitive peptide amides: CCK-8 (which contains a Tyr *O*-sulfate) and a Gla-containing hexapeptide, thus opening the way for the preparation of a number of interesting native peptides containing these unusual amino acids. Our results with rCRF indicate that protecting groups and/or cleavage-deprotection conditions must be carefully evaluated; while more work in this area is indicated, it becomes also obvious that the 2,4-DMBA resin may not be acid-labile enough to the cleavage conditions currently employed to conserve the integrity of Tyr *O*-sulfate.

Acknowledgements

Research supported by NIH grant AM26741. We thank J. Dykert and C. Miller for their expert technical assistance.

References

1. Barany, G. and Merrifield, R.B., In E. Gross and J. Meienhofer (Eds.) The Peptides, Vol. 2, Academic Press, New York, NY, 1980, p. 1.
2. Burgus, R. and Rivier, J., In A. Loffet (Ed.) Peptides 1976, Editions de l'Université de Bruxelles, Brussels, 1976, pp. 85-94.
3. Pietta, P.A. and Marshall, G.R., J. Chem. Soc. Chem. Commun. (1970) 650.
4. Penke, B. and Rivier, J., J. Org. Chem., 52 (1987) 1197.
5. Wade, J. (Ed.) Workshop Manual on Fmoc-Polyamide Peptide Synthesis, Howard Florey Institute of Experimental Physiology and Medicine Press, Melbourne, Australia, 1986, p. 63.
6. Rivier, J., McClintock, R., Galyean, R. and Anderson, H., J. Chromatogr., 288 (1984) 303.
7. Olivera, B.M., Gray, W.R., Zeikus, R., McIntosh, J.M., Varga, J., Rivier, J., de Santos, V. and Cruz, L.J., Science, 230 (1985) 1138.
8. Sieber, P., Tetrahedron Lett., 28 (1987) 1637.

Structure-function relationships in the anemone *Stichodactyla helianthus* neurotoxin I: Synthesis of native sequence and Glu 8 to Gln analog

Michael W. Pennington, William R. Kem and Ben M. Dunn

Department of Biochemistry and Molecular Biology, Department of Pharmacology and Therapeutics, University of Florida, Gainesville, FL 32610, U.S.A.

Introduction

Sea anemone and scorpion polypeptide neurotoxins specifically bind to the Na^+ channel on the exterior surface of the cell membrane [1]. The receptors for the scorpion α-toxins and at least one group of the sea anemone toxins appear to be identical or have overlapping sites located at or near the voltage gate of the Na^+ channels [2]. The polypeptide neurotoxins act by slowing or blocking the inactivation of the voltage-sensitive Na^+ channels [3].

Stichodactyla helianthus neurotoxin I (ShN I) is a 48-amino acid polypeptide that contains 3 intramolecular disulfide bridges. The primary sequence of the polypeptide is shown below:

NH_2-Ala-Ala-Cys-Lys-Cys-Asp-Asp-Glu-Gly-Pro-Asp-Ile-Arg-Thr-Ala-Pro-Leu-Thr-Gly-Thr-Val-Asp-Leu-Gly-Ser-Cys-Asn-Ala-Gly-Trp-Glu-Lys-Cys-Ala-Ser-Tyr-Tyr-Thr-Ile-Ile-Ala-Asp-Cys-Cys-Arg-Lys-Lys-Lys-COOH [4].

In order to identify specific amino acid side chains involved in binding to the Na^+ channel, we have embarked on a synthetic program to provide a variety of toxin analogs for pharmacological and structural analysis. In this paper, we report on the synthesis of the native toxin and an analog incorporating the substitution of Gln for Glu 8.

Results and Discussion

Prior to the total synthesis of the native toxin sequence, a sample of reduced ShN I was subjected to the low-high HF cleavage protocol [5]. The sample was then reisolated and reoxidized in the presence of reduced and oxidized glutathione. The ShN I was then purified on a C_{18} reversed-phase (RP) column. The repurified native material was found to have nearly identical LD_{50} of 2.92

μg toxin/kg crab. Following this successful control experiment, the native sequence polypeptide was assembled using stepwise solid phase synthesis on the Applied Biosystems 430-A synthesizer. A double coupling protocol for all β-branched amino acids, as well as all amino acids containing bulky aromatic side-chain protecting groups, was incorporated into the synthesis to maximize the coupling efficiency. Quantitative ninhydrin analysis [6] of the coupling efficiency showed an overall yield of 96.1%.

Cleavage and removal of the peptide was achieved by the low-high HF method. Following HF cleavage, the peptide was desalted on Sephadex G-15. The peptide was then subjected to reoxidation in the presence of reduced and oxidized glutathione. After reoxidation, the peptide was absorbed directly onto phosphocellulose. A peptide which showed a neurotoxic response in crabs was isolated near the end of an ammonium formate gradient. This neurotoxic fraction was further purified by C_{18} RPHPLC. Amino acid analysis for this purified peptide gave the expected theoretical molar ratios of the proposed sequence.

Physical characteristics of the purified synthetic ShN I showed it to be highly homogeneous. Analytical isoelectric focusing showed a single band with identical p*I* as that of the native ShN I. No free thiol was detected by Ellman's analysis for sulfhydryl determination, however, following thiolytic reduction 6 cysteinyl residues were detected. RPHPLC analysis showed single symmetric peaks for both synthetic and native ShN I with identical retention times. Similarly, HPLC coelution of a 1 : 1 mixture of the synthetic and native ShN I showed a single symmetric peak. Circular dichroism spectropolarimetry showed the same overall conformational parameters for both of the samples. Peptide mapping experiments showed identical cleavage patterns when monitored by RPHPLC. More recently, ^{1}H NMR spectra were collected for each of the samples and shown to be identical. Dose-response data for the synthetic material matched that of the native, with an LD_{50} of 3.14 μg toxin/kg crab. Thus, we concluded that the native and synthetic structures were identical.

Next, we began probing ionic interactions by synthesizing the first substitutional analog incorporating Gln for Glu 8. Synthesis of this molecule followed the same format as that established for the native toxin except that a double coupling regimen was performed for every amino acid residue. Cleavage from the resin was different in that the standard high-HF protocol was followed. As a control, we subjected a second sample of the synthetic native sequence to the same conditions to be used on the analogs. This native sample was reoxidized, purified, and found to be identical to native toxin. Thus, the Gln 8 analog was cleaved from the resin and allowed to reoxidize in the presence of air in 50 mM NaOAc, pH 7.5 at 4°C for 10 days. The sample was purified over Sephadex G-50. A neurotoxic fraction was isolated and further purified on a C_{18} RPHPLC column. Amino acid analysis of this purified peptide agreed with the theoretical molar

ratios expected. Further characterization of this analog will give a better understanding of the ionic interactions that exist at the polypeptide receptor on the Na^+ channel.

In conclusion, we have synthesized the native sequence of the sea anemone neurotoxin ShN I. Physical and chemical data confirm that this toxin is identical to the native toxin structure. Synthesis of an analog incorporating the substitution of Gln for Glu 8 was also performed. Further characterization of this analog is currently in progress.

Acknowledgements

This work was supported by Grant GM32848, awarded by the National Institutes of Health.

References

1. Romey, G., Abita, J.P., Scheitz, H., Wunderer, G. and Lazdunski, M., Proc. Natl. Acad. Sci. U.S.A., 73 (1976) 4055.
2. Catterall, W.A. and Beress, L., J. Biol. Chem., 253 (1978) 393.
3. Catterall, W.A., Ann. Rev. Pharmacol. Toxicol., 20 (1980) 15.
4. Kem, W.R., Dunn, B.M., Parten, B.F., Pennington, M.W. and Price, D., Fed. Proc., 45 (1986) 1795.
5. Tam, J.P., Heath, W.F. and Merrifield, R.B., J. Am. Chem. Soc., 105 (1983) 6445.
6. Sarin, V.K., Kent, S.B.H., Tam, J.P. and Merrifield, R.B., Anal. Biochem., 117 (1981) 147.

Use of Fmoc amino acid oxobenzotriazine esters in continuous flow low pressure solid phase peptide synthesis

Eric Atherton, Janet C. Glass, B. Helen Matthews, Gareth P. Priestley, John D. Richards, Paul W. Sheppard and Wendy A. Wade

Cambridge Research Biochemicals Ltd., Button End, Harston, Cambridge CB2 5NX, U.K.

Introduction

Fmoc amino acid pentafluorophenyl esters (-OPfp) (Fig. 1) [1] have been shown to be highly reactive derivatives capable of rapid acylation, without undesirable side reactions, in the polar medium employed for chain assembly on polydimethylacrylamide supports [2]. The easily prepared crystalline Fmoc amino acid esters of 3-hydroxy-4-oxo-3,4-dihydro-1,2,3-benzotriazine (-ODhbt) (Fig. 2) have been proposed as alternative reagents [3]. These derivatives are reported to react with free amines in DMF at a rate comparable with symmetric anhydrides [3].

The -ODhbt esters possess 'self-indicating' properties. Free amine on the solid support results in the presence of an intense yellow coloration due to -ODhbt anion formation. The resin reverts to the original color upon completion of acylation.

A potentially serious side reaction has been reported between dicyclohexylcarbodiimide and HODhbt resulting from the reaction of the free hydroxy group on one molecule of HODhbt with another molecule of HODbht activated by dicyclohexylcarbodiimide [4]. The activated benzoate derivative produced (Fig. 3) would be liable to react with and block free amino groups. It was thought

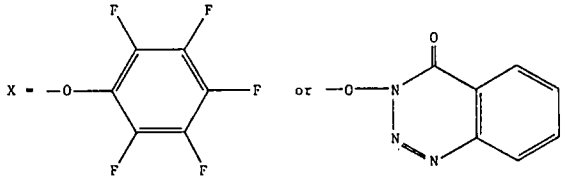

1 2

Figs. 1 and 2. Fmoc amino acid-X.

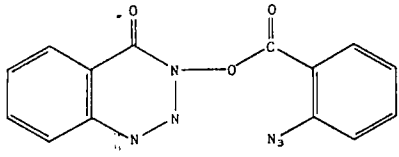

Fig. 3. Activated benzoate derivative.

possible that a similar reaction might occur between the free amino resin and the activated -ODhbt ester, resulting in chain termination. Therefore, comparative continuous flow syntheses [5] of the octapeptide dynorphin (1–8) (Fig. 4) were undertaken in order to determine the efficiency of the two classes of ester.

Results and Discussion

The preparation of active esters of arginine is not straightforward due to a side reaction leading to the formation of an unreactive lactam. We carried out extensive investigations into the synthesis and subsequent stability of active esters of Fmoc-Arg(Mtr)-OH (Mtr = 4-methoxy-2,3,5-trimethylphenyl sulphonyl). By careful control of reaction conditions, impurity levels due to the lactam were reduced to less than 10%. The -OPfp derivative was shown to be stable in its solid form and only slowly converted to the lactam in polar solvents such as DMF ($t_{1/2} = 10$ h); it did, however, rapidly convert in nonpolar solvents ($t_{1/2} = 15$ min in CH_2Cl_2). The Fmoc-Arg(Mtr)-ODhbt ester appeared to be less stable than the corresponding -OPfp derivative.

All amino acid-ODhbt esters were prepared with careful attention being paid to purity, ensuring that none of the activated benzoate (Fig. 3) was present.

The peptides were assembled by the flow methodology [5] using a polyamide-kieselguhr composite resin (0.1 mmol $\cdot$ g^{-1}) derivatized in turn with ethylene diamine, norleucine, and 4-hydroxymethylphenoxy acetic acid. The C-terminal residue was incorporated as its symmetric anhydride in the presence of a catalytic amount of 4-dimethylaminopyridine. In both assemblies acylations were complete within 25 min, with the exception of the coupling of Arg^6 to Arg^7 in the -OPfp series which took 50 min. Hydrolysis and subsequent amino acid analysis of the final peptide-resin indicated good incorporation of all residues. The peptides were cleaved from the resin by treatment with 95% TFA, 5% phenol. Side-chain protection was removed concomitantly although removal of the Mtr groups from the arginine was the rate-limiting step, taking some 22 h as determined

H-Tyr-Gly-Gly-Phe-Leu-Arg-Arg-Ile-OH

Fig. 4. Octapeptide dynorphin (1–8).

by HPLC. However, as the extinction coefficient of Mtr containing peptides is very much greater than that of the fully deprotected peptide, the reaction time allowed may be longer than necessary. Prolonged acid treatment was not deleterious to the integrity of this peptide. More recent work with dynorphin (1–13) indicates that the use of TFA with thioanisole and trimethylsilyl trifluoromethane sulphonate [6] offers a very much faster (approximately 30 min) route for the cleavage of Mtr protecting groups.

Crude chromatograms showed both peptide products to be similar and after ion-exchange chromatography identical materials were obtained in high overall yields (from -OPfp ester synthesis, 60%; from -ODhbt ester synthesis, 72%).

Conclusion

Fmoc amino acid -ODhbt esters have been demonstrated to be effective and highly reactive acylating agents in solid phase peptide synthesis. This in conjunction with their ability to suppress racemization [4] and the prospects for true automation [7] leading to real-time feedback control instrumentation demonstrates that the -ODhbt esters have considerable advantages over the related -OPfp esters.

References

1. Kisfaludy, L. and Schön, I., Synthesis, (1983) 325.
2. Atherton, E. and Sheppard, R.C., J. Chem. Soc. Chem. Commun., (1985) 165.
3. Atherton, E., Cameron, L., Meldal, M. and Sheppard, R.C., J. Chem. Soc. Chem. Commun., (1986) 1763.
4. König, W. and Geiger, R., Chem. Ber., 103 (1970) 2034.
5. Dryland, A. and Sheppard, R.C., J. Chem. Soc., Perkin Trans. 1 (1986) 125.
6. Fujii, N., Otaka, A., Ikemura, O., Akaji, K., Funakoshi, S., Hayashi, Y., Kuroda, Y. and Yajima, W., J. Chem. Soc. Chem. Commun., (1987) 274.
7. Cameron, L., Meldal, M. and Sheppard, R.C., J. Chem. Soc. Chem. Commun., (1987) 270.

Protection of histidine in peptide synthesis: A reassessment of the trityl group

Peter Sieber and Bernhard Riniker
CIBA-GEIGY Ltd., CH-4002 Basle, Switzerland

Introduction

The use of Fmoc as a base-labile N^{α}-protective group has added a new dimension to peptide synthesis. It permits side-chain protection, and linkages to the resin in solid phase syntheses, all of which are cleavable in a final mild acidolytic step. In the search for a histidine protection which would fit into this scheme, we found that the long-known, but rather neglected Trt-group assumes a new importance in combination with Fmoc.

Methods and Results

The new derivatives **1** to **3** were prepared by standard methods, starting from H-His(Trt)-OH and Trt-His(Trt)-OH [1], respectively (OTcp = 2,4,5-trichlorophenyl ester). The N^{Im}-Trt-group was shown to be located in the less hindered τ position [2]. The compounds are stable in the dry state; **1** is crystalline, **2** and **3** are amorphous solids.

1: Fmoc-His(Trt)-OH **2**: Fmoc-His(Trt)-OTcp **3**: Trt-His(Trt)-OTcp

In a first set of experiments, Fmoc-His-OH and Boc-His-OH were compared with their N^{Im}-Trt derivatives in solid phase and solution syntheses. After deprotection, the peptides were analyzed by HPLC, allowing the quantitative determination of D-His diastereoisomers. The values shown in Table 1 indicate that in most cases the derivatives of His(Trt) were less susceptible to racemization than those without Trt. The presence of N^{Im}-Trt also prevented the formation of several minor byproducts which occurred with an unprotected side chain. As observed in separate experiments, however, Trt in the τ position of His does not prevent racemization which may occur under unfavorable conditions (e.g., preactivation with DCCI + HOBt in the absence of the amino component).

Further experiments were performed to compare the reaction rates of Fmoc versus Trt in N^{α} of His(Trt) when coupled in solution with H-Val-Gly-Ala-

Table 1 *Quantitative determination by HPLC of* D-*His diastereoisomers following deprotection*

	% D-His	
	a	b
Fmoc-His (Trt)-OH	0.2	0.1
Fmoc-His-OH	1.1	0.7
Boc-His (Trt)-OH	0.3	0.5
Boc-His-OH	0.7	0.4

[a] Synthesis of H-His-Val-Val-OH on a *p*-alkoxybenzylpolystyrene resin: 3.0 His-derivative (0.3 M in DMF), 3.0 HOBt, 3.3 DCCI, 1.0 H-Val-Val-resin, 2 h, 25°C.
[b] Synthesis of H-His-Val-Gly-Ala-Pro-NH_2 in solution: 2.0 His-derivative, 2.0 HOBt, 2.2 DCCI, 1.0 H-Val-Gly-Ala-Pro-NH_2 (0.2 M in DMF), 4 h, 22°C.

Pro-NH_2. (Conditions: 1.5 Fmoc/Trt-His(Trt)-OX, 1.0 tetrapeptide, 1.5 HOBt, 1.7 DCCI for X = H; 0.04 M in DMF at 22°C). The following periods for the complete disappearance of the amino component were observed: Fmoc-His(Trt)-OH, 1 h; Trt-His(Trt)-OH, 2.5 h; Fmoc-His(Trt)-OTcp, 20 min; Trt-His(Trt)-OTcp, 4 h. The results indicate that although Trt in N^{α} decelerates the coupling rates as compared to Fmoc, Trt-His(Trt)-OTcp is a convenient and well-activated derivative for peptide syntheses. In addition, the reaction rates of the active esters **2** and **3** are increased 3–5-fold in the presence of 1 equivalent of diisopropylethylamine.

In order to evaluate the stabilities of Trt in N^{α} and N^{Im}, Trt-His(Trt)-Lys(Boc)-OMe was used as a model compound. In both positions, Trt is completely stable to nucleophiles. Table 2 shows various acidic conditions in which selective removal of N^{α}-Trt is possible (a–e), in some of these (a–c) also in the presence of *tert*-butyl-type groups.

Table 2 *Percent cleavage of* N^{α}*-Trt and* N^{Im}*-Trt in various acidic conditions*

Cleavage conditions	% cleavage of	
	N^{α}-Trt	N^{Im}-Trt
a 90% CH_3 COOH, 30 min, 20°C	100	2
b HCOOH 5% in $ClCH_2$-CH_2Cl (DCE), 8 min, 20°C	100	1
c DCE MeOH CF_3COOH (95.5:3:1.5), 5 min, 20°C	100	<1
d 0.1 N HCl in DCE MeOH dioxane (90:5:5), 10 min, 20°C	100	0
e 0.15 N HCl in 90% dioxane, 1 h, 20°C	100	<1
f 5% pyridine · HCl in MeOH, 20 min, 60°C	100	70
g 95% CF_3 COOH, 1 h, 20°C	100	100

Conclusions

The Trt group in the side chain of His is completely stable to nucleophiles, but cleavable by mild acidolysis. It reduces racemization and the formation of byproducts. This makes it ideally suited in combination with protecting groups of the *tert*-butyl type and with Fmoc in N^{α}. Fmoc-His(Trt)-OTcp and Trt-His(Trt)-OTcp, which are stable active esters, are useful for the introduction of His. The selective cleavage of N^{α}-Trt, in the presence of N^{Im}-Trt and of *tert*-butyl-type groups, is possible under various acidolytic conditions.

References

1. Barlos, K., Papaioannou, D. and Theodoropoulos, D., J. Org. Chem., 47 (1982) 1324.
2. Fletcher, A.R., Jones, J.H., Ramage, W.I. and Stachulski, A.V., J. Chem. Soc., Perkin Trans. I (1979) 2261.

A method for solid phase peptide synthesis (SPPS) of C-terminal sulfonic acid peptides: Synthesis of taurine^{16}-gramicidin A

Roger W. Roeske and Tanya P. Hrinyo-Pavlina

Department of Biochemistry, Indiana University School of Medicine, Indianapolis, IN 46223, U.S.A.

Introduction

Solid phase synthesis of peptides having C-terminal aminosulfonic acid moieties has heretofore not been successful because aminosulfonic acids (e.g., taurine) are insoluble in nonaqueous solvents. Thus, taurine cannot be used to cleave a peptide from a polystyrene resin by aminolysis. We have attached taurine to a resin by a phenyl ester link (**I**, Scheme 1) which is very stable in acids and, after peptide synthesis, is cleaved by treatment with base. The new availability of a taurine-substituted resin for SPPS of taurine^{16}-gramicidin A allowed us to circumvent the problems of the previously reported solution synthesis of this peptide [1].

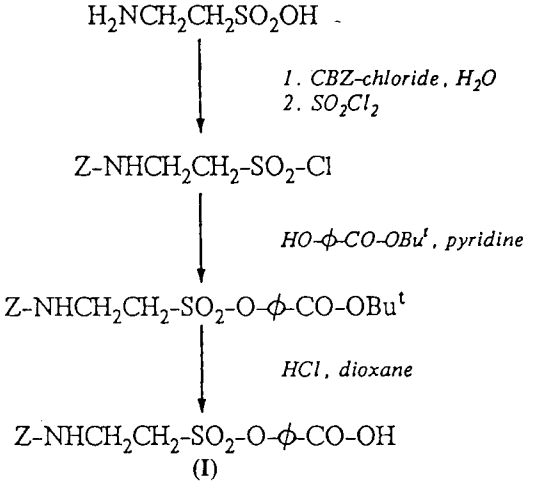

Scheme 1. Synthesis of the taurine phenyl ester derivative (I).

Experimental

Synthesis of the taurine phenyl ester derivative (**I**) is outlined in Scheme 1. The crystalline product melted at 155–156°C (uncorr.) and had an R_f (CMA, 85:15:3) of 0.58 on 0.2 mm silica gel. **I** was coupled to pMBHA resin (0.2 mequiv./g) using DCC/HOBt. The Z-group was removed by treatment with 3 N HBr/acetic acid. After neutralization with DIEA, the free amine of taurine-link-resin was coupled immediately to the first amino acid, Boc-Trp, by the symmetrical anhydride method in order to minimize intermolecular nucleophilic cleavage at nearby phenyl ester sites. Subsequent coupling reactions were carried out for 3 h with a 2.5-fold excess of Boc-amino acid, HOBt, and DCC in DMF-CH_2Cl_2 (1:1), using TFA/thioanisole deprotection. The completed taurine^{16}-gramicidin A was formylated on the resin with a 10-fold excess of *p*-nitrophenylformate in DMF. Peptide cleavage from the resin was effected with aqueous KOH in *N*-methylpyrrolidinone (NMP). A typical procedure is as follows: 300 mg peptide-resin in 3 ml NMP was treated with 25 μl of 2 N KOH and stirred at room temperature for 20 h to give >85% cleavage. After filtering the resin, the peptide was precipitated from the filtrate with ether and was purified by RPHPLC on C_{18} silica gel using MeOH/H_2O/TFA mixtures according to the published procedure [2]. The overall yield of pure product was 11%. Amino acid analysis, TLC, ^{1}H NMR, and FABMS were consistent with the expected analyses for taurine^{16}-gramicidin A.

Discussion

The taurine phenyl ester we have synthesized is linked to methylbenzhydrylamine resin via an amide bond which is stable under SPPS conditions, but readily cleaved in anhydrous HF. The phenyl ester itself is also stable under SPPS conditions, but is labile toward bases and strong nucleophiles. Hence, the cleavage of peptide from resin, concomitant with formation of the peptide sulfonate, can be achieved with simple base hydrolysis.

Gramicidin A is a pentadecapeptide containing an N-terminal formyl and a C-terminal ethanolamide (**II**).

HCO-Val-Gly-Ala-D-Leu-Ala-D-Val-Val-D-Val-Trp-D-Leu-Trp-D-Leu-Trp-D-Leu-Trp-$NHCH_2CH_2OH$

(II)

According to the widely accepted model [3], gramicidin in a lipid bilayer exists as a formyl-to-formyl dimer which adopts a β-helical conformation stabilized by hydrogen bonding to form a channel that can accommodate small ions. When the ethanolamide of gramicidin is replaced by taurine, however,

spontaneous channel formation is impossible because the sulfonic acid cannot penetrate the lipid bilayer. Preliminary studies have shown that single channel formation is observed only when taurine^{16}-gramicidin A is added to both sides of an artificial membrane ([1] and D. Busath, recent communication). We plan to continue the biophysical investigation of taurine^{16}-gramicidin derivatives; our development of the taurine-substituted resin now allows us to exploit the speed and convenience of SPPS to produce peptides for these studies.

Acknowledgements

This work was supported by the Showalter Trust of the I.U. Foundation. We thank P. Edwards for his technical assistance.

References

1. Pottorf, R., Synthesis of Peptides that Form Ion Channels in Artificial Lipid Bilayers, Ph.D. Thesis, Indiana University, 1984.
2. Gesellchen, P., Tafur, S. and Shields, J., In Gross, E. and Meienhofer, J. (Eds.) Peptides: Structure and Biological Function, Pierce Chemical Co., Rockford, IL, 1979, pp. 621-624.
3. Urry, D.W., Proc. Natl. Acad. Sci. U.S.A., 68 (1971) 672.

Preparation of new amino acids

Yolande Hervé, Derek H.R. Barton*, Josiane Thierry and Pierre Potier
Institut de Chimie des Substances Naturelles, C.N.R.S., 91190 Gif-sur-Yvette, France

Introduction

The radical decarboxylation reaction reported by Barton et al. [1] has been used with success in the field of amino acids. This reaction is particularly well adapted in modifying the side chain of optically active aspartic and glutamic acids [2–4].

The decomposition under mild conditions of the O-ester **2** of the thiohydroxamic acid **1** yields the radical R• which readily adds to electron-deficient olefins to give derivatives of synthetic value [5] (Scheme 1).

This approach has been used to transform the side chain of protected aspartic and glutamic acids.

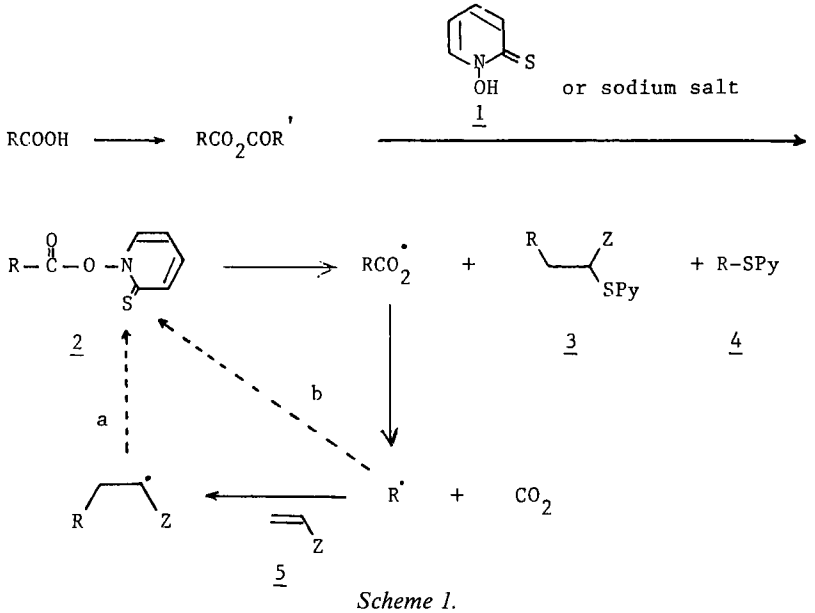

Scheme 1.

*Present address: Department of Chemistry, Texas A&M University, College Station, TX 77843, U.S.A.

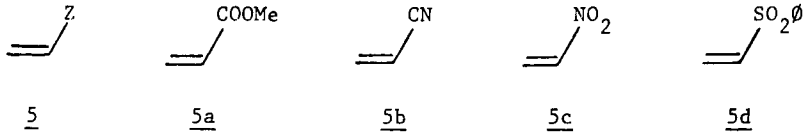

Fig. 1. Olefins chosen for addition.

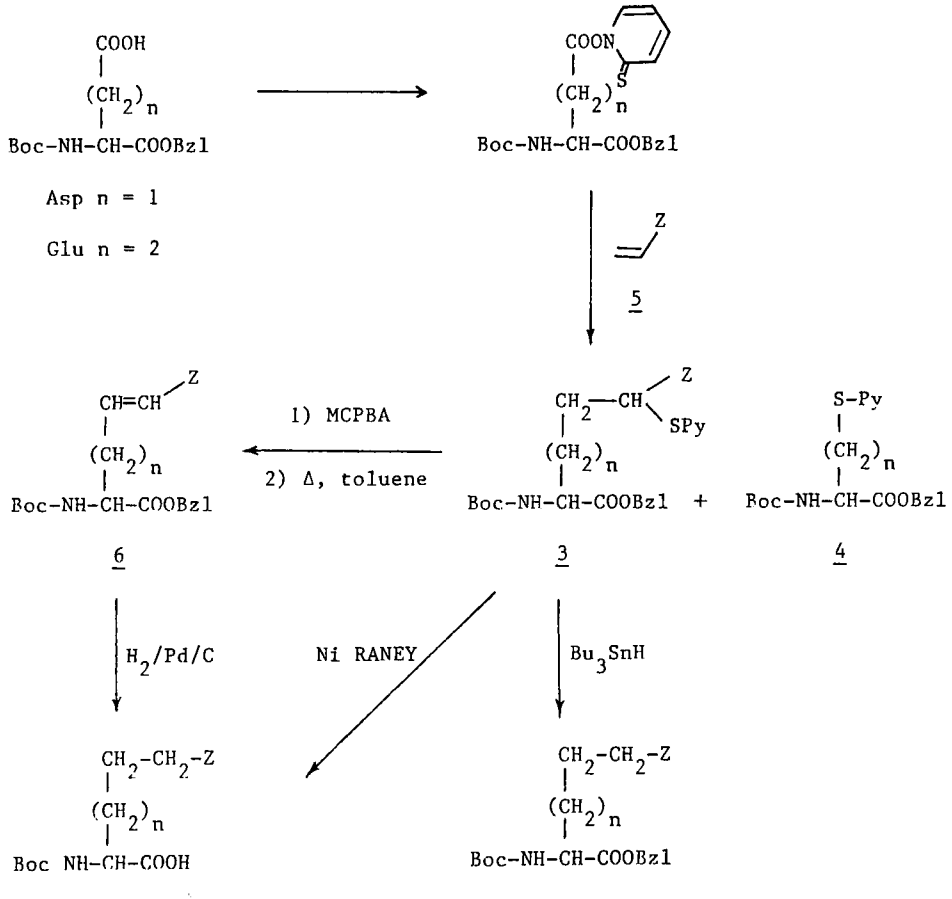

Fig. 2. Modification of Glu and Asp derivatives.

Results and Discussion

The O-ester of thiohydroxamic acid **2** has been prepared through the mixed anhydride obtained from the side-chain carboxylic acid and isobutylchloroformate. Both the sodium salt (commercial) or the triethylamine salt could be used for the ester synthesis at −15°C. The irradiation of **2** by two 100-W tungsten lamps under nitrogen in the presence of olefin **5** (5 equivalents) provides addition products with satisfactory yields (56–74%). The rearrangement product **3** is always present in small amounts (20%). The following olefins have been chosen (see Fig. 1).

The addition products are oxidized with one equivalent of *m*-chloroperbenzoic acid at room temperature. The thermolysis in refluxing toluene of the sulfoxide so obtained gives the unsaturated compound **6**, the stereochemistry being E in all cases (J = 16 Hz). The yields of this two-step transformation are good (67–91%); however, the adduct resulting from the addition on nitroethylene **5c** did not give the unsaturated compound **6c** (Fig. 2).

Thus, this method allows the easy preparation of new unsaturated amino acids, some of which could be further transformed or be used as precursors of labeled amino acids (α-aminoadipic and α-aminopimelic acids from **6a** n = 1 and n = 2).

References

1. Barton, D.H.R., Crich, D. and Motherwell, W.B., J. Chem. Soc. Chem. Commun. (1983) 939.
2. Barton, D.H.R., Hervé, Y., Potier, P. and Thierry, J., J. Chem. Soc. Chem. Commun. (1984) 1298.
3. Barton, D.H.R., Crich, D., Hervé, Y., Potier, P. and Thierry, J., Tetrahedron, 41 (1985) 4347.
4. Barton, D.H.R., Bridon, D., Hervé, Y., Potier, P., Thierry, J. and Zard, S.Z., Tetrahedron, 42 (1986) 4983.
5. Barton, D.H.R., Crich, D. and Kretzchmar, G., J. Chem. Soc., Perkin Trans. I, (1986) 39.

Protease-catalyzed synthesis of oxytocin

Pia Thorbek, Jørn Lauridsen and Fred Widmer
Carlsberg Biotechnology Ltd., Tagensvej 16, DK-2200 Copenhagen N, Denmark

Introduction

We have been working on the use of proteases for the synthesis of peptides for some time [1], and present here a summary of part of our work on oxytocin. Two reports on the enzymatic synthesis of partial oxytocin sequences have previously been published by others [2, 3].

Results and Discussion

Applying our preferred method of using alkyl esters as C-components [1] we were able to form 7 of the 8 peptide bonds enzymatically as shown below:*

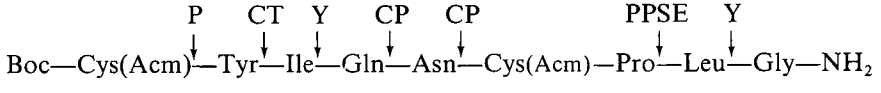

We have not found an enzyme yet which allows bond formation between cysteine and proline; this bond was thus made chemically. The synthesis is summarized in detail in Scheme 1. For further references and for background information on strategy and materials/methods of enzymatic peptide synthesis, see [1].

A point of interest is the use of Bz-Arg- as an amino blocking group of the intermediate fragment Bz-Arg-Ile-Gln-OMe. The Bz-Arg-residue increases the solubility of the peptides in polar solvent mixtures, it facilitates their work-up, and it is removable with trypsin under mild conditions to avoid deamidation side reactions. A further interesting aspect of this synthesis is the observation that the diastereomer of Cys(Acm)-Pro-Leu-OEt, resulting from racemization at cysteine (the DLL peptide), is eliminated in the subsequent enzyme coupling

---

* *Abbreviations*: CT, chymotrypsin; T, trypsin; CP, chymopapain; P, papain; Y, carboxypeptidase Y; PPSE, post-proline specific endoprotease (from *Flavobact. meningosepticum*). *Enzyme sources*: CT, T, P, CP, Sigma, St. Louis; Y, Carlbiotech, Copenhagen; PPSE, Seikagaku Kogyo, Tokyo, Japan.

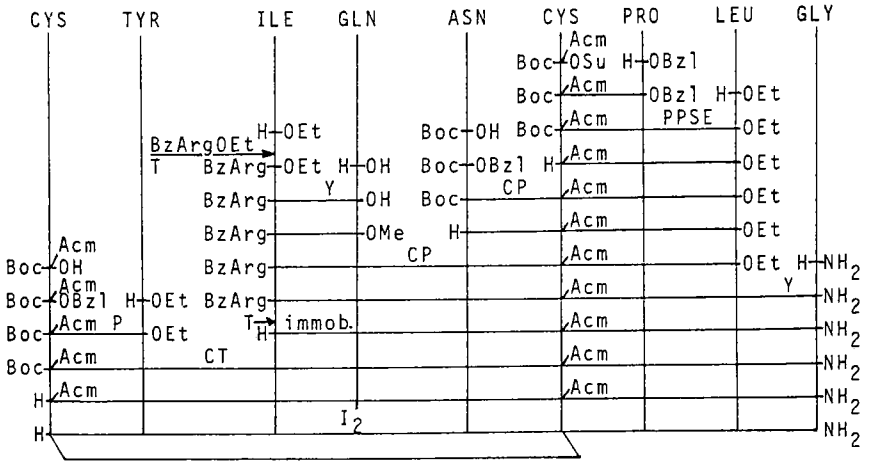

Scheme 1. Biopreparative synthesis of oxytocin.

to Boc-Asn-OBzl. Similarly if the entire tripeptide was made chemically, we found that the DDL and LDL peptides were 'purified-out' by enzymatic coupling, and thus a stereochemically purer product was obtained (Table 1).

This 'trick' can also be used to purify chemically made Ile-Gln-OMe by coupling it to Bz-Arg-OEt with trypsin (data not shown). In conclusion: even a partial enzymatic synthesis can result in stereochemically very pure peptides [4].

Early batches, which were chromatographed in systems containing HCOOH, contained a major impurity of up to 10% which increased upon standing (even at 4°C) of the lyophilizate. The impurity was identified as N^{α}-formyl-oxytocin, and could be avoided by replacing HCOOH with HOAc (cf. also [5]). A final batch purity (HPLC, 220 nm) of 95–99%, with a peptide content of 90% (rest H_2O and HOAc), could routinely be obtained [amino acid composition: Asx,0.94; Glx,0.99; Gly,1.00; Pro,1.03; Tyr,0.92; Ile,1.00; Leu,1.05; optical rotation $[\alpha]_D^{22}$ = -21.5°C (c = 0.5; H_2O); biological activity (chicken blood pressure test): 530 IU^2/mg peptide].

Table 1 *Chymopapain couplings with diastereomeric tripeptides*

Boc-Asn-OBzl	H-Cys-(Acm)-Pro-Leu-OEt	Boc-Asn-Cys-(Acm)-Pro-Leu-OEt	%
L	L L L	L L L L	60
L	D L L	L D L L	0
L	L D L	L L D L	5
L	D D L	L D D L	0

References

1. Widmer, F. and Johansen, J.T., In Alitalo, K., Partanen, P. and Vaheri, A. (Eds.) Synthetic Peptides in Biology and Medicine, Elsevier Science Publishers, Amsterdam, 1985, p. 79.
2. Tominaga, M., Pinheira, L., Muradian, J. and Seidel, W.F., In Sakakibara, S. (Ed.) Peptide Chemistry 1982, Protein Research Foundation, Osaka, 1983, p. 271.
3. Cerovsky, V. and Jost, K., Coll. Czech. Commun., 50 (1985) 2775.
4. Thorbek, P. and Widmer, F., In Deber, C.M., Hruby, V.J. and Kopple, K.D. (Eds.) Peptides: Structure and Function, Pierce Chemical Co., Rockford, IL, 1985, p. 359.
5. Viville, R., Scarso, A., Durieux, J.P. and Loffet, A., J. Chromatogr., 262 (1983) 411.

Protection of side-chain alcoholic hydroxyl groups of serine and threonine by the dimethylphosphinyl (Dmp) group

Masaaki Ueki, Mika Saito and Hidekazu Oyamada
Department of Applied Chemistry, Science University of Tokyo, 1-3 Kagurazaka, Shinjuku-ku, Tokyo 162, Japan

Introduction

Side reactions in the final deprotection step of peptide synthesis sometimes bring to naught all the efforts devoted till then. Therefore, selection of permanent protecting groups for side-chain functional groups is very important.

Benzyl-type protecting groups when cleaved under strongly acidic conditions generate highly reactive cations, which in turn modify many amino acids. Recently, we reported the usefulness of the dimethylphosphinyl (Dmp) group for the protection of the phenolic hydroxyl group of tyrosine [1]. The Dmp group could be removed without any side reaction with tetrabutylammonium fluoride as well as liquid hydrogen fluoride.

In this study we tried to extend the use of the Dmp group to the protection of alcoholic hydroxyl groups of serine and threonine.

Results and Discussion

Since dimethylphosphinyl chloride rapidly decomposes in an aqueous solution the Dmp group was introduced to Boc-Ser-OBzl and Boc-Thr-OBzl under anhydrous conditions to afford Boc-Ser(Dmp)-OBzl and Boc-Thr(Dmp)-OBzl in 85% and 81% yields, respectively. The benzyl group could then be removed by catalytic hydrogenolysis without any problem to give Boc-Ser(Dmp)-OH, mp 138–139°C, and Boc-Thr(Dmp)-OH, mp 154–155°C, in quantitative yields.

In stability there was much difference between the Dmp group attached to an alcoholic hydroxyl group (O^{al}-Dmp) and the Dmp group attached to a phenolic hydroxyl group (O^{ar}-Dmp).

The O^{al}-Dmp group could not be removed with 1 M triethylamine in methanol and 10% aqueous NH_4OH as well as tetrabutylammonium fluoride, with which the O^{ar}-Dmp was cleaved rapidly.

In stability towards mild acidic reagents, such as trifluoroacetic acid, there was no difference between two types of Dmp groups; however, some difficulty was seen in the deprotection of *O*-Dmp threonine with liquid hydrogen fluoride

(HF). When Boc-Thr(Dmp)-OH was treated with liquid HF using anisole as a scavenger under the usual reaction conditions (0°C, 1 h), 27% of the Dmp groups remained without cleavage. Since the cleavage under 'low HF' conditions (HF: dimethylsulfide: *p*-cresol; 25:65:10, v/v) gave higher recovery (91%) of Thr, other hydroxyl compounds were examined as scavengers. As expected, high recovery of Thr was obtained using *n*-butanol (97%), *s*-butanol (96%), *t*-butanol (95%), and *p*-methoxyphenol (96%). These compounds were also effective for the deprotection of resin-bound Boc-Thr(Dmp).

Applications of these results to synthesis of biologically active peptides are now in progress.

References

1. Ueki, M., Sano, Y., Sori, I., Shinozaki, K., Oyamada, H. and Ikeda, S., Tetrahedron Lett., 35 (1986) 4181.

Fmoc-polyamide continuous flow solid phase synthesis of a 74-residue fragment of human β-chorionic gonadotropin

Cui-Rong Wu[a], Vernon C. Stevens[b], Geoffrey W. Tregear[a] and John D. Wade[a]

[a]Howard Florey Institute, University of Melbourne, Parkville, Vic. 3052, Australia
[b]Department of Obstetrics and Gynecology, Ohio State University, Columbus, OH 43210, U.S.A.

Introduction

The development of a vaccine against the placental hormone human chorionic gonadotropin (hCG) should provide a safe and effective method of fertility control in the human [1]. The chemical similarities between hCG and several pituitary hormones have necessitated the use of peptide fragments as immunogens to elicit specific immune responses to hCG. The presence of a unique and extended carboxyl-terminal peptide of 30 amino acids of the β-subunit of hCG has provided the impetus for focusing in h-βCG (109–145) as a prime candidate for the development of a vaccine specific for hCG [2]; however, as the antigenicity of the peptide is low it was of interest to determine whether a synthetic polymer of h-βCG (109–145) would have improved immunogenicity. Towards this aim, we have undertaken the preparation of the linear dimer of the 37-residue peptide using the Fmoc-polyamide continuous flow method of peptide synthesis [3]. An additional purpose of this exercise was to enable an evaluation of the effectiveness of this procedure for the assembly of a long peptide.

Results and Discussion

The continuous flow solid phase synthesis of the peptide (Fig. 1) was carried out semiautomatically essentially as previously described [4]. A low-loading (0.11 mmol/g) kieselguhr-supported polydimethylacrylamide gel resin was derivatized in the usual manner. Attachment of the first residue (glutamine) onto the acid-

T-C-D-D-P-R-F-Q-D-S-S-S-S-K-A-P-P-P-S-L-P-S-P-S-R-L-
P-G-P-S-D-T-P-I-L-P-Q-T-C-D-D-P-R-F-Q-D-S-S-S-S-K-A-
P-P-P-S-L-P-S-P-S-R-L-P-G-P-S-D-T-P-I-L-P-Q

Fig. 1. Dimer sequence of h-βCG (109–145).

labile *p*-alkoxybenzyl alcohol linkage agent was successfully accomplished by a double 1-h coupling of 3 equivalents of the symmetrical anhydride of the Fmoc-amino acid, the side chain of which was protected by the 4,4′-dimethoxybenzhydryl (Mbh) group [5]. The use of this amino acid derivative prevented dehydration of the carboxamide function and other known possible side reactions. 4-Dimethylaminopyridine was used as catalyst during the esterification step. Thereafter, 3-fold molar quantities of preformed symmetrical anhydrides of protected amino acids were used throughout the remainder of the synthesis. Arginine anhydride was coupled in the presence of an equivalent amount of catalyst, *N,N′*-hydroxybenzotriazole (HOBt). Glutamine and lysine were coupled as their *p*-nitrophenyl active esters also in the presence of HOBt. The Fmoc group gave N^{α}-protection for all amino acids, and side-chain protection was afforded by the following: Arg(Mtr), Cys(Acm) and (Bu^t), Ser(Bu^t), Thr (Bu^t), Asp(OBu^t), and Lys(Boc). Each synthetic cycle consisted of (i) a 10-min deprotection with 20% piperidine/DMF, (ii) a 15-min wash with DMF, (iii) amino acid coupling for 30 min, and (iv) a 10-min wash with DMF. All couplings were monitored by the 2,4,6-trinitrobenzenesulfonic acid test and were found to be negative at the end of the allotted time. Aliquots of peptide-resin were removed during the course of the synthesis for amino acid analysis. The results together with the feedback provided by continuous spectrophotometric monitoring (310 nm) of the reaction column effluent provided additional evidence of a satisfactory assembly.

Cleavage and deprotection of the peptide-resin were effected by treatment with 95% TFA/2.5% anisole/2.5% phenol (v/v/w) for 6.5 h at room temperature. Under these conditions, little acid-mediated degradation of the peptide at the sites of Asp-Pro bonds was observed. Purification of the crude di-S-protected peptide was achieved by gel filtration on TSK-40 and preparative HPLC on a C4 column. Overall yield, based on the first amino acid on the linkage agent, was approximately 9%. The purified peptide was characterized by analytical HPLC (Fig. 2) and by high-sensitivity microsequencing of fractions resulting from tryptic digestion of the product. The data confirmed both its high purity and expected amino acid sequence.

The results of this work augur well for the Fmoc-polyamide flow synthesis of large peptides. Rates of amino acid acylation were observed to remain consistently rapid and efficient, and overall solvent consumption was low compared to other synthesis procedures. The synthetic peptide is currently being evaluated for its antifertility effect in the baboon.

Acknowledgements

This work was supported by the W.H.O. and by the National Health and Medical Research Council of Australia.

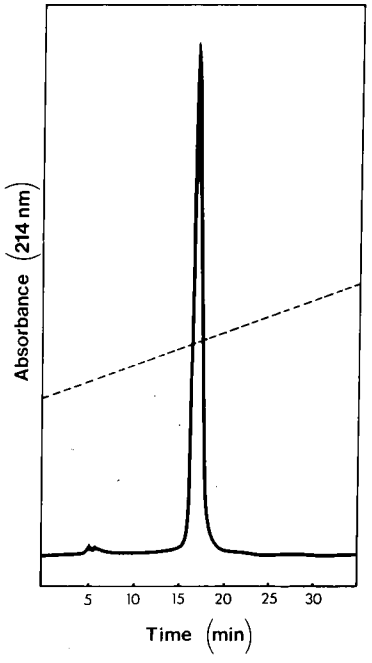

Fig. 2. HPLC of purified synthetic S-protected linear dimer of human β-CG (109–145). Conditions: Vydac C4 column (250 x 4.6 mm, 5 μm particle size), at a flow rate of 2.0 ml/min, eluting with a linear gradient of 35% B to 50% B in 35 min. Buffer A: 0.25 N triethylamine phosphate, pH 2.5. Buffer B: 40% A with 60% acetonitrile.

References

1. Stevens, V.C., Powell, J.E., Lee, A.C. and Griffin, D., Fertil. Steril., 36(1981)98.
2. Stevens, V.C., In Porter, R. and Whelan, J. (Eds.) Synthetic Peptides as Antigens (Ciba Foundation Symposium 119), John Wiley and Sons, Chichester, 1986, p. 200.
3. Atherton, E., Brown, E. and Sheppard, R.C., J. Chem. Soc. Chem. Commun., (1981)1151.
4. Wade, J.D., Fitzgerald, S.P., McDonald, M.R., McDougall, J.G. and Tregear, G.W., Biopolymers, 25(1986)S21.
5. Konig, W. and Geiger, R., Chem. Ber., 103(1970)2041.

Synthesis of human secretin

G. Wendlberger[a], W. Göhring[a], G. Hübener[a], R. Scharf[a], J. Beythien[a], Ch. Beglinger[b] and E. Wünsch[a]

[a]Max-Planck-Institut für Biochemie, Abteilung Peptidchemie, Martinsried, F.R.G.
[b]Kantonsspital, Basle, Switzerland

Sequence analysis of human secretin [1] revealed substitution of residues 15–16 of porcine secretin (i.e., Asp-Ser by Glu-Gly, the rest of the molecule being identical). This replacement should facilitate the synthesis of human secretin in view of the possible $\alpha \rightarrow \beta$-transpeptidation in this sequence portion of the porcine species [2]. Taking advantage of our previous experiences in the synthesis of porcine secretin [3], the human eicosapeptide amide was prepared following an analogous general strategy. Thereby, the fragment design was slightly modified (i) in the C-terminal region to avoid pyrrolidone-5-carbonyl-peptide formation observed to occur to significant extents during stepwise synthesis of the heptapeptide derivative 21–27 and (ii) in the N-terminal region to bypass the noxious problem of racemization encountered at the level of Phe-6 in the last fragment condensation step for porcine secretin [2]. Correspondingly the following fragments were synthesized: H-Gly-Leu-Val-NH_2, H-(25-27)-NH_2; Z-Arg(Z_2)-Leu-Leu-Gln-OH, Z-(21-24)-OH; Z-Arg(Z_2)-Leu-Gln-OH, Z-(18-20)-OH; Z-Arg(Z_2)-Glu(OBu^t)-Gly-Ala-OH, Z-(14-17)-OH; Z-Arg(Z_2)-Leu-OH, Z-(12-13)-OH; Z-Phe-Thr(Bu^t)-Ser(Bu^t)-Glu(OBu^t)-Leu-Ser(Bu^t)-OH, Z-(6-11)-OH; AdOC-His-(AdOC)-Ser(Bu^t)-Asp(OBu^t)-Gly-Thr(Bu^t)-OH, AdOC-(1-5)-OH. These fragments were assembled in sequence order via DCC/HOSu except for the cases of C-terminal glutamine fragments, where HOBt was used as a 1,2-dinucleophile. Upon acidolytic removal of the protecting groups in the presence of 1,2-ethanedithiol and anisole, the resulting crude product was purified by gel filtration on fractogel TSK-HW-40S (0.05 M ammonium acetate, pH 5.5) followed by ion exchange chromatography on CM-Sepharose fast flow (0.06 M ammonium acetate/2-propanol, 1:1, pH 6.7). Human secretin was obtained in good yields as homogenous product as judged by amino acid analysis of the acid and enzymatic hydrolysate, gas chromatographic racemization test, HPLC (Fig. 1) and HPTLC in different solvent systems. Comparative biological assays performed in vivo on 4 healthy male volunteers revealed identical hydrokinetic activity for synthetic porcine and human secretin (Fig. 2).

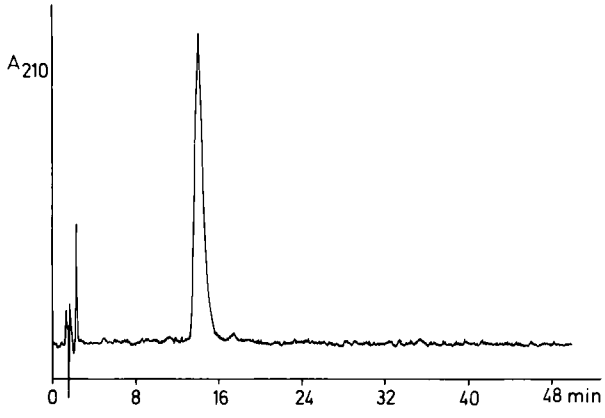

Fig. 1. HPLC (RadPakC18; eluent: 0.13 M dibutylammonium trifluoroacetate; flow rate: 2 ml/min).

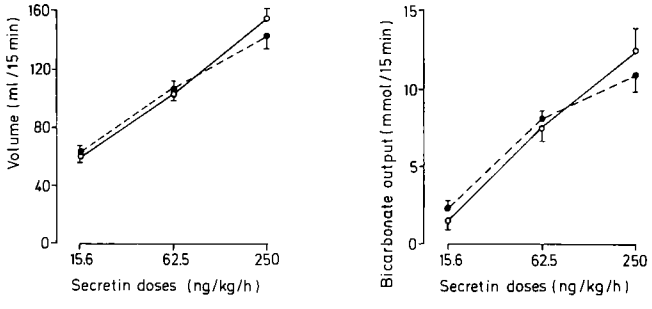

Fig. 2. Comparison of the hydrokinetic action of human (●----●) and porcine (o----o) secretin.

References

1. Carlquist, M., Jörnvall, H., Forssmann, W.-G., Thulin, L., Johansson, C. and Mutt, V., JRCS Med. Sci., 13 (1985) 217.
2. Wünsch, E., Biopolymers, 22 (1983) 493.
3. Wünsch, E., Naturwissenschaften, 59 (1972) 239.

Regiospecific synthesis of [^{13}C-2]-(2*S*, 3*S*)-*trans*-epoxysuccinyl-L-leucyl-isoamylamide

Yuichiro Yabe and Daniel H. Rich

School of Pharmacy, University of Wisconsin-Madison, 425 North Charter Street, Madison, WI 53706, U.S.A.

Introduction

(*S,S*)-*trans*-Epoxysuccinyl-Leu-Iaa (Ep-475) is an analog of E-64 [1, 2] which is a highly specific, irreversible, potent inhibitor of cysteine proteinases, e.g., papain, cathepsin B, H or L. Although these compounds are known to alkylate the sulfhydryl group in the active site cysteine [3], it has not been known whether the sulfur reacts at C-2 or C-3 in the inhibitor (Fig. 1) [4]. The title compound was synthesized in order to determine the site of alkylation by cysteine proteinases.

Results and Discussion

Reaction of the Wittig reagent, triethyl phosphonoacetate-2-^{13}C, derived from ethyl bromoacetate-2-^{13}C with 2-benzyloxyacetaldehyde [5] gave ethyl 4-benzyloxy-(E)-2-butenoate (**1**) which contained 99% ^{13}C at C-2 in 80% yield. Reduction of **1** by DIBAL-H to the alcohol (**2**, 84% yield), followed by Sharpless asymmetric epoxidation [6] gave (2*R*,3*R*)-benzyloxy-2,3-epoxy-1-butanol-2-^{13}C[**3**, >98% ee, $[\alpha]_D^{23}$ + 25.8° (c 0.36, $CHCl_3$), lit. [7] $[\alpha]_D^{25}$ + 23.0° (c 0.35, $CHCl_3$)] in 88%

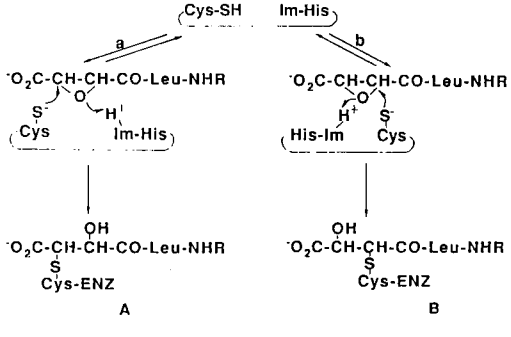

Fig. 1. Possible mechanisms for inhibition of cysteine proteinases by E-64 analogs.

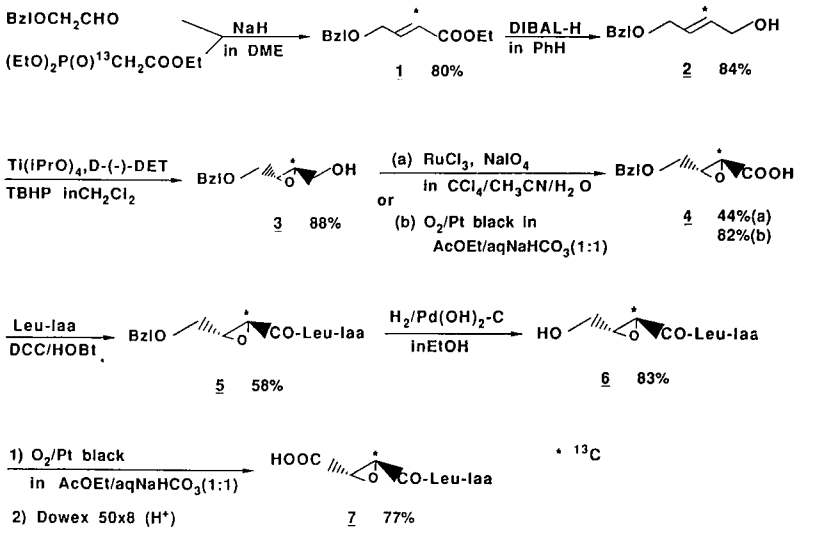

Fig. 2. Synthesis of [^{13}C-2]-Ep475 (7).

yield. The RuO_4 oxidation [8] of **3** gave the acid **4** although the yield was not good (44%). The reaction afforded four products including **4**, (2*S*,3*R*)-4-benzyloxy-2,3-epoxy-1-butylaldehyde-2-^{13}C and benzaldehyde. We then tried air oxidation of **3** over Pt black in AcOEt/aqueous $NaHCO_3$ (1:1) [9]. Although the reaction was very slow (for 5 days at room temperature), it gave only acid **4** in 82% yield. The acid **4** was coupled with Leu-Iaa by the DCC/HOBt method to give the intermediate protected epoxyalcohol peptide (**5**) in 58% yield. The benzyl group of **5** was deprotected by hydrogenation over Pearlman's catalyst to give (2*S*,3*R*)-2,3-epoxy-4-hydroxybutyryl-2-^{13}C-Leu-Iaa (**6**) in 83% yield. Air oxidation of C-4 alcohol **6** to the acid by using Pt black in AcOEt/aqueous $NaHCO_3$ (1:1) [9] completed the synthesis of [^{13}C-2]-Ep-475[7, $[\alpha]_D^{23}$ + 47.5° (c 0.2, EtOH), lit. [10] $[\alpha]_D^{20}$ + 45.5° (c 1, EtOH)] in 77% yield.

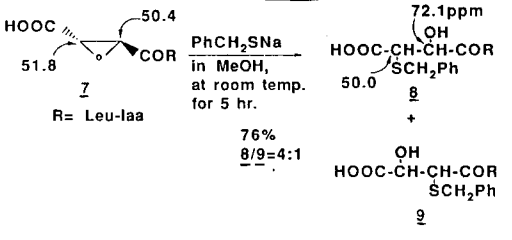

Fig. 3. Reaction of 7 with benzyl mercaptan.

To explore the chemical reactivity of the epoxysuccinyl group to mercaptans, we allowed the epoxide **7** to react with benzyl mercaptan for 5 h at pH 10. Two products (**8** and **9**) were obtained in 76% overall yield. The predominant product (**8**, 80%) is the C-3 sulfide, which is formed by attack of the mercaptan at C-3 of the epoxide, but attack at C-2(**9**, 20%) was also observed (Fig. 3). The products were assigned by the chemical shifts of the C-2 and C-3 carbons in the ^{13}C NMR spectrum. Experiments to determine the site of alkylation by papain are in progress.

Acknowledgements

We gratefully acknowledge financial support from Sankyo Co., Ltd., Japan and from Merck Sharp and Dohme.

References

1. Hanada, K., Tamai, M., Yamagishi, M., Ohmura, S., Sawada, J. and Tanaka, I., Agric. Biol. Chem., 42 (1978) 523.
2. Hanada, K., Tamai, M., Ohmura, S., Sawada, J., Seki, T. and Tanaka, I., Agric. Biol. Chem., 42 (1978) 529.
3. Hanada, K., Tamai, M., Morimoto, S., Adachi, T., Ohmura, S., Sawada, J. and Tanaka, I., Agric. Biol. Chem., 42 (1978) 537.
4. Rich, D.H., In Barrett, A.J. and Salvesen, G.S. (Eds.) Proteinase Inhibitors, Elsevier, New York, NY, 1986, p. 153.
5. Arndt, H.C. and Carrol, S.A., Synthesis, (1979) 202.
6. Katsuki, T. and Sharpless, K.B., J. Am. Chem. Soc., 102 (1980) 5974.
7. Hungerbühler, E. and Seebach, D., Helv. Chim. Acta, 64 (1981) 687.
8. Carlson, P.H.J., Katsuki, T., Martin, V.S. and Sharpless, K.B., J. Org. Chem., 46 (1981) 3936.
9. Yoshimura, J., Sakai, H., Oda, N. and Hashimoto, H., Bull. Chem. Soc. Japan, 45 (1972) 2027.
10. Barrett, A.J., Kembhavi, A.A., Brown, M.A., Kirschke, H., Knight, C.G., Tamai, M. and Hanada, K., Biochem. J., 201 (1982) 189.

Convenient synthesis of 2-methyl-3-phenylserine, a sterically hindered α,α-disubstituted amino acid

J. Zabrocki, Z. Kaminski and M.T. Leplawy
Institute of Organic Chemistry, Technical University, 90-924 Lodz, Poland

The search for more precise information about the structural features of the peptide chain essential for biological activity requires an easy access to amino acids with specifically designed side chains. We report here a new, convenient synthesis of threo- and erythro-2-methyl-3-phenylserine (**4a** and **4b**), a sterically hindered α,α-disubstituted amino acid which may be expected to gain wider interest in biological and stereochemical studies on peptide analogs. Synthetic approaches to 3-aryl-2-methylserines published before 1968 have been reviewed by Pines et al. [1], who in the same paper reported further access to this class of α,α-disubstituted amino acids via corresponding N-protected amino-β-keto esters. These β-keto esters were obtained by controlled addition (–70°C) of an aryl Grignard reagent to 4-carboalkoxy-2,4-dimethyl-5-oxo-4,5-dihydro-1,3-oxazole and then transformed into erythro- and threo-3-aryl-2-methylserines by reduction of the keto group and subsequent deprotection of the amino and carboxyl group, with an overall yield of 15%. The dominant reduction product is the erythro isomer. It should be noted that preparation of starting 4-carboalkoxy-2,4-dimethyl-5-oxo-4,5-dihydro-1,3-oxazole requires 4 additional steps, and this makes the whole synthesis rather laborious. In an alternative procedure developed for the 2-methyl-3-phenylserine [2], synthesis of the key β-keto ester intermediate methyl-2-benzamido-2-benzoylpropionate was accomplished via reaction of benzoyl chloride with oxazolone derived from *N*-benzoylalanine.

The new approach to the synthesis of 2-methyl-3-phenylserine presented in this communication (see Scheme 1) involves the base-catalyzed addition of 4-methyl-2-phenyl-5-oxo-4,5-dihydro-1,3-oxazole (**1**) to benzaldehyde followed by resolution of resulting mixture of threo- and erythro-4-methyl-2-phenyl-4-phenylhydroxymethyl-5-oxo-4,5-dihydro-1,3-oxazoles (**2**) which after 2-step hydrolysis gave threo- and erythro-2-methyl-3-phenylserines **4a** and **4b** in a ratio of approximately 3:1. We believe that this new synthesis of 2-methyl-3-phenylserine is more convenient and more efficient because formation of a cyclic system **2** containing the complete skeleton of 2-methyl-3-phenylserine can be effected in one step using easily accessible starting materials, and final products **4a** and **4b** can be obtained in better overall yield (30–38%). In contrast to the reductive

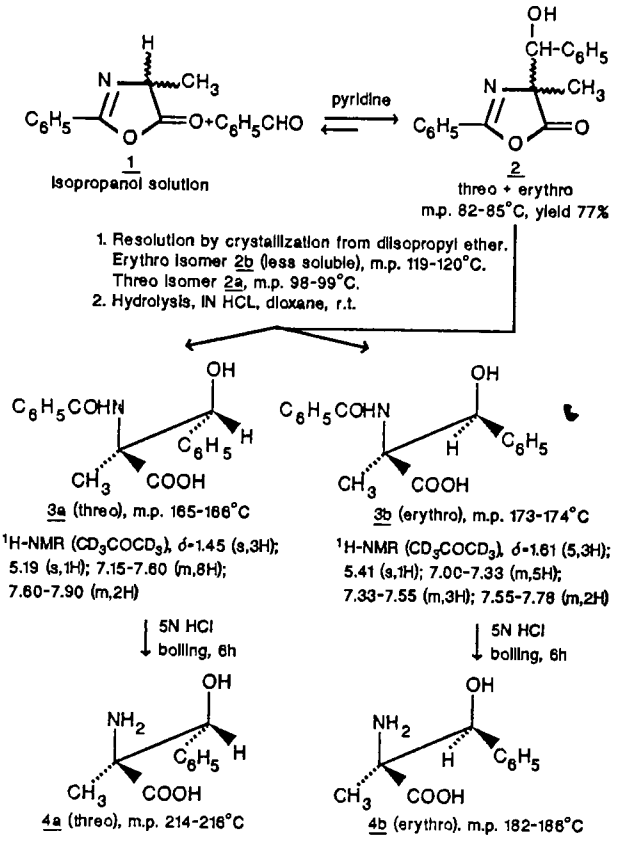

Scheme 1

procedure of Pines et al. [1, 2] giving predominantly erythro 2-methyl-3-phenylserine*, the dominant product of the present synthesis is the threo isomer. To avoid retroaddition during hydrolysis of **2**, it is necessary to carry out the first step of hydrolysis under mild acidic conditions.

Acknowledgements

This work was financially supported by the Polish Academy of Sciences, grant CPBP 01.13.2.5.

* For the sake of clarity, the erythro isomer is defined as that in which the disposition of the heteroatoms and 'aliphatic' portions (-CH_3 and -H) are similar (**4b**).

References

1. Pines, S.H., Karady, S. and Sletzinger, M., J. Org. Chem., 33 (1968) 1758.
2. Pines, S.H. and Sletzinger, M., Tetrahedron Lett., (1969) 727.

Session IV
Mechanism of action

Chair: Peter W. Schiller
Clinical Research Institute of Montreal
Montreal, Quebec, Canada

Inositol phosphates and calcium signaling

Michael J. Berridge
AFRC Unit of Insect Neurophysiology and Pharmacology, Department of Zoology, Downing Street, Cambridge CB2 3EJ, U.K.

Changes in the intracellular level of calcium play a central role in regulating a whole host of cellular responses. There are two main ways of generating calcium signals. The first method depends on having a voltage-sensitive device within the plasma membrane which responds to a change in membrane voltage with an opening of plasma membrane calcium channels or by the release of calcium from internal reservoirs particularly the sarcoplasmic reticulum of muscle. The second mechanism occurs independently of membrane potential, but is triggered by a wide range of external agonists including neurotransmitters, hormones, and growth factors. In this case, the agonist binds to specific receptors which have been referred to as calcium-mobilizing receptors because they are coupled to a transduction mechanism capable of increasing calcium entry across the plasma membrane as well as releasing calcium from internal reservoirs. Michell [1] was the first to recognize that these calcium-mobilizing receptors might mediate their effects by stimulating the hydrolysis of inositol lipids. Subsequent studies have revealed that this lipid hydrolysis generates a whole host of inositol phosphates, some of which play an integral role in calcium signaling.

Formation and Metabolism of Inositol Phosphates

The inositol phosphates used in calcium signaling are derived from a family of inositol lipids located within the plasma membrane [2–4]. The parent lipid is phosphatidylinositol, which is phosphorylated on the free hydroxyl groups of the inositol ring to form the polyphosphoinositides. The first step results in the formation of phosphatidylinositol 4-phosphate (PtdIns4P), which is further phosphorylated to form the substrate phosphatidylinositol 4,5-bisphosphate (PtdIns4,5P_2) used by the receptor mechanism to generate second messengers (Fig. 1). The key transduction event occurs when the occupied receptor stimulates the phosphoinositidase to cleave PtdIns4,5P_2 to diacylglycerol (DG) and inositol 1,4,5-trisphosphate (Insl,4,5P_3). These two products both function as second messengers in that DG activates protein kinase C [5] whereas the water-soluble Insl,4,5P_3 released to the cytosol functions to mobilize calcium [2, 6, 7]. Attention will focus on this action of Insl,4,5P_3, which is complicated because this initial

metabolite can be converted to alternative forms which may also exert a profound effect on calcium homeostasis.

There are two major pathways for metabolizing Insl,4,5P_3. The simpler of the two is a stepwise dephosphorylation to free inositol [8]. The first enzyme is a trisphosphatase which specifically removes the phosphate on the 5-position to give Insl,4P_2 (Fig. 1). This is an important step in terminating the second messenger action of Insl,4,5P_3 because Insl,4P_2 has no calcium-mobilizing activity [2, 6]. The other pathway is more complex in that it begins with a kinase reaction which specifically phosphorylates Insl,4,5P_3 on its 3-position to generate inositol 1,3,4,5-tetrakisphosphate (Insl,3,4,5P_4) [9]. The latter is then sequentially dephosphorylated to free inositol with the first step again being the removal of the phosphate on the 5-position to give Insl,3,4P_3 (Fig. 1) [10]. The next step is the dephosphorylation of Insl,3,4P_3 to Ins3,4P_2 and perhaps also to Insl,3P_2 [11]. The final dephosphorylation pathways for these intermediates remain to be worked out. The significance of this inositol tris/tetrakis pathway is that it generates additional inositol polyphosphates which could have second messenger functions, as outlined in the following section.

Inositol Phosphates and Calcium Mobilization

As discussed earlier, calcium mobilizing receptors can alter calcium homeostasis by both an influx of this ion across the plasma membrane as well as its release from internal reservoirs. There are now indications that inositol phosphates may play a role in mediating both calcium fluxes (Fig. 1). The strongest evidence

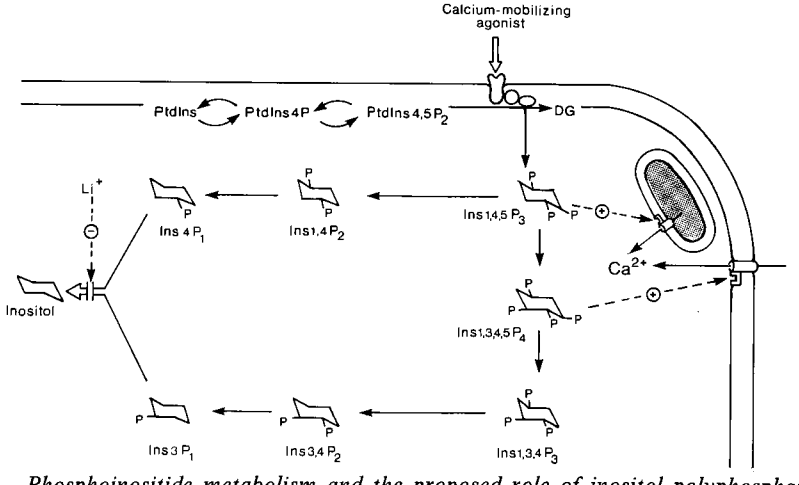

Fig. 1. Phosphoinositide metabolism and the proposed role of inositol polyphosphates in regulating the release of calcium from the endoplasmic reticulum as well as the influx of external calcium.

at present concerns the role of Insl,4,5P_3 in controlling the release of calcium from the endoplasmic reticulum. There is a constant cycling of calcium across this internal membrane system in that the passive efflux is continuously counteracted by an active pump. Insl,4,5P_3 has no effect on the pump but greatly facilitates the passive efflux component by binding to a receptor on the endoplasmic reticulum which opens a calcium channel. This Insl,4,5P_3-induced release of calcium is independent of temperature [12] which is consistent with the notion that calcium is passing through a channel. Such a flow of calcium will generate an electrical potential which would rapidly curtail further release unless it was neutralized in some way. There is evidence that this neutralization is achieved by an influx of potassium ions which are essential in order for Insl,4,5P_3 to release calcium [12]. The action of Insl,4,5P_3 seems to be insensitive to sodium but is markedly enhanced when the pH is increased from 6.7 to 7.5 [12]. When cells are stimulated, the pH often shifts to high values which would tend to enhance the calcium-mobilizing action of Insl,4,5P_3.

In order to release calcium, Insl,4,5P_3 acts through a specific receptor which presumably is connected in some way to the calcium channel. Structure–activity studies have begun to define the pharmacological characteristics of the binding site. The vicinal phosphates in the 4- and 5-positions are essential to stimulate release, whereas the phosphate on the opposite side of the molecule enhances its affinity for its receptor. The putative receptor may correspond to the specific binding sites which have been identified in various cells [13, 14]. The next step will be to isolate and purify this receptor in order to determine how it functions to regulate calcium release from the endoplasmic reticulum.

In addition to releasing calcium from intracellular stores, calcium-mobilizing receptors can also stimulate the influx of calcium across the plasma membrane, but how this is achieved is still somewhat of a mystery. The concept of a receptor-operated calcium channel (ROC) was developed from studies on smooth muscle to draw attention to the fact that neurotransmitters were capable of stimulating contractions by increasing the entry of calcium across the plasma membrane [15]. One possibility is that receptors might be linked to calcium channels, but patch-clamp studies have not provided much evidence for such a direct association. Rather, there is evidence that these plasma membrane calcium channels may be opened indirectly through the action of some internal messenger. For example, ion channels in neutrophils appear to be sensitive to an increase in intracellular calcium [16]. Another possibility is that calcium channels might be regulated by inositol phosphates because the influx of this ion across lymphocyte membranes is enhanced by Insl,4,5P_3 [17]. In the sea urchin, however, there are indications that calcium entry is induced by Insl,3,4,5P_4 [18]. There is now evidence, therefore, for a number of mechanisms, but more examples need to be studied before the role of inositol phosphates in linking calcium-mobilizing receptors to the entry of external calcium can be firmly established.

Conclusion

A characteristic feature of calcium-mobilizing receptors is that they stimulate inositol lipid hydrolysis. In particular, the highly phosphorylated lipid PtdIns4,5P_2 is cleaved to give DG and Insl,4,5P_3. The latter has a central role to play in calcium signaling by releasing this ion from the endoplasmic reticulum to give the first surge of calcium responsible for initiating a large variety of cellular responses. In order for such calcium signaling to be sustained, this ion must be brought in from the outside and inositol phosphates may also be important in regulating this influx across the plasma membrane. The Insl,4,5P_3 responsible for releasing internal calcium may also function to open similar ion channels in the plasma membrane. Another possibility is that Insl,4,5P_3 is first converted into Insl,3,4,5P_4 which is then the messenger responsible for calcium entry (Fig. 1). Since the kinase which phosphorylates Insl,4,5P_3 appears to be sensitive to calcium [19], it would seem that the entry of external calcium may depend upon an initial increase in intracellular calcium brought about by Insl,4,5P_3 prior to its conversion to Insl,3,4,5P_4. While the role of Insl,4,5P_3 in releasing intracellular calcium is firmly established, further information is required to confirm a role for the inositol phosphates in regulating calcium entry across the plasma membrane.

References

1. Michell, R.H., Biochim. Biophys. Acta, 415 (1975) 81.
2. Berridge, M.J., Biochem. J., 220 (1984) 345.
3. Downes, C.P. and Michell, R.H., In Cohen, P. and Houslay, M.D. (Eds.) Molecular Aspects of Cellular Regulation, Vol. 4 (Molecular Mechanisms of Transmembrane Signalling), Elsevier, Amsterdam, 1985, p. 3.
4. Hokin, L.E., Annu. Rev. Biochem., 54 (1985) 205.
5. Kikkawa, U. and Nishizuka, Y., Annu. Rev. Cell. Biol., 2 (1986) 149.
6. Berridge, M.J. and Irvine R.F., Nature, 312 (1984) 315.
7. Berridge, M.J., Annu. Rev. Biochem., (1987) in press.
8. Storey, D.J., Shears, S.B., Kirk, C.J. and Michell, R.H., Nature, 312 (1984) 374.
9. Irvine, R.F., Letcher, A.J., Heslop, J.P. and Berridge, M.J., Nature, 320 (1986) 631.
10. Batty, I.R., Nahorski, S.R. and Irvine, R.F., Biochem. J., 232 (1985) 211.
11. Irvine, R.F., Letcher, A.J., Lander, D.J., Heslop, J.P. and Berridge, M.J., Biochem. Biophys. Res. Commun., 143 (1987) 353.
12. Joseph, S.K. and Williamson, J.R., J. Biol. Chem., 261 (1986) 14658.
13. Spat, A., Bradford, P.G., McKinney, J.S., Rubin, R.P. and Putney, J.W., Nature, 319 (1986) 514.
14. Guillemette, G., Balla, T., Baukal, A.J., Spat, A. and Catt, K.J., J. Biol. Chem., 262 (1987) 1010.
15. Bolton, T.B., Physiol. Rev., 59 (1979) 606.

16. von Tscharner, V., Prod'hom, B., Baggiolini, M. and Reuter, H., Nature, 324 (1986) 369.
17. Kuno, M. and Gardner, P., Nature, 326 (1987) 301.
18. Irvine, R.F. and Moor, R.M., Biochem. J., 240 (1986) 917.
19. Lew, P.D., Monod, A., Krause, K.-H., Waldvogel, F.A., Biden, T.J. and Schlegel, W., J. Biol. Chem., 261 (1986) 917.

The insulin receptor: A hormone-activated transmembrane tyrosine kinase comprised of two large independently folded soluble domains

Leland Ellis

Howard Hughes Medical Institute and Department of Biochemistry, University of Texas Health Science Center, 5323 Harry Hines Boulevard, Dallas, TX 75235-9050, U.S.A.

Transmembrane Signaling by the Insulin Receptor: The Kinase Domain

The response of cells to the polypeptide hormone insulin is initiated by the binding of insulin to its cell surface receptor, an integral transmembrane glycoprotein comprised of two α-subunits (~135 kDa) and two β-subunits (~95 kDa). An immediate consequence of insulin binding is the autophosphorylation, predominantly on tyrosine residues, of the β-subunit of the receptor (reviewed in [1]). The primary sequence of the human insulin receptor (hIR) protein, deduced from the nucleotide sequence of human placental cDNAs [2, 3], predicts two large domains on either side of the cell membrane, each of which has a distinct function (insulin binding and tyrosine kinase activity, respectively; see Fig. 1). Such a topology immediately suggests two major classes of questions concerning the function of this receptor: (i) Is transmembrane signaling by the receptor a prerequisite for the physiological response of cells to insulin? If so, is autophosphorylation required? Does the IR protein-tyrosine kinase (PTK) domain convey any specificity for the response of cells to insulin? (ii) Are the extracellular and cytoplasmic domains of the IR, in the absence of the other domain, capable of independent function? That is, are these really two large independently folded soluble domains, as the deduced primary sequence suggests (Fig. 2)?

The strategy to begin to explore the role of primary structural features of the IR protein in the generation of the insulin response in cells is to introduce mutations into the hIR cDNA and, by expression of the mutant hIR proteins via the cDNA under the transcriptional control of a viral promoter (e.g., the SV-40 early promoter) in rodent CHO cells (or other mammalian cells), study the functional consequences of such alterations [4, 5]. A panel of monoclonal antibodies [6–8] directed against both extracellular and cytoplasmic epitopes of the molecule (including one antibody that blocks insulin binding and is specific for the human IR; [6]) provides the necessary reagents to study biochemically the hIR expressed in such cells.

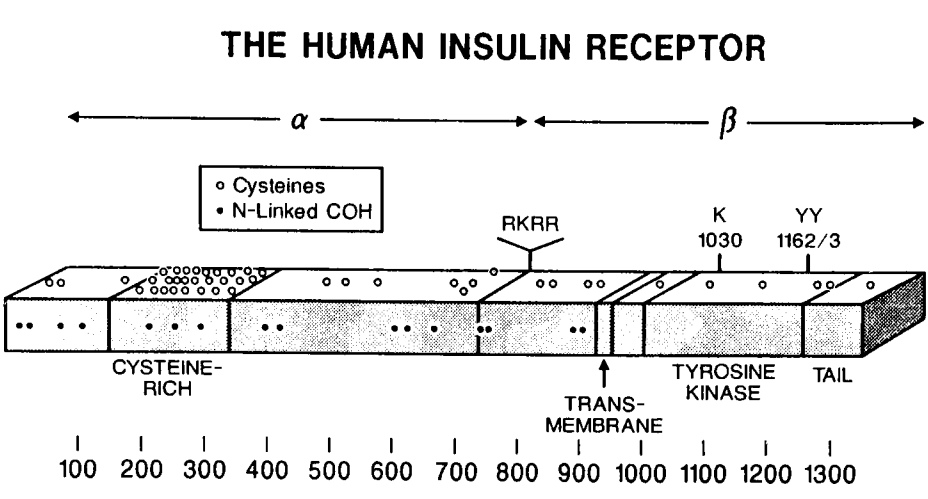

Fig. 1. Diagrammatic representation of major primary structural features of the human insulin receptor protein which are deduced from the nucleotide sequence of the human placental cDNAs [2, 3]: (i) a single chain 1382-residue (M_r 153,917) polypeptide chain precursor which is proteolytically cleaved during biosynthesis into α-subunits (735 residues; M_r 84,214) and β-subunits (620 residues; M_r 69,703); (ii) a large extracellular domain (929 residues) comprised of all of the α-subunit and approximately one-third of the β-subunit; (iii) a single predicted transmembrane domain (23 residues); and (iv) a cytoplasmic domain (403 residues; the carboxy-terminal two-thirds of the β-subunit) comprised of a protein-tyrosine kinase and a carboxy-terminal tail.

Results thus far with site-directed point mutations of tyrosine residues (1162 and 1163) and carboxy-terminal truncations in the PTK domain [5], truncations of the extracellular domain to generate insulin-independent hIR PTKs [9] and 'domain swaps' with a heterologous PTK (derived from the homologous chicken-transforming protein *v-ros*; [10]) all implicate the activity of the PTK domain in the generation of at least one aspect of the insulin response (glucose uptake). Furthermore, two cell lines that we have analyzed indicate that the PTK of the hIR is capable of autonomous activity [9]:

(i) An externally truncated hIR, which does not bind insulin, is expressed as a membrane-anchored protein in transfected CHO cells. Furthermore, this membrane-anchored hIR PTK domain mediates a constitutive insulin response in these cells (i.e., the elevated uptake of 2-deoxyglucose) in the *absence* of insulin. Thus the PTK domain of the IR, as well as the ligand binding extracellular domain, conveys specificity for the insulin response.

(ii) A functional, but soluble, hIR PTK domain has been expressed in the cytoplasm of CHO cells (Fig. 3, lane 3). When purified from such cells, this kinase is very active in vitro: it exhibits both autophosphorylation and the phosphorylation of exogenous substrates. Such cell lines do not exhibit insulin-

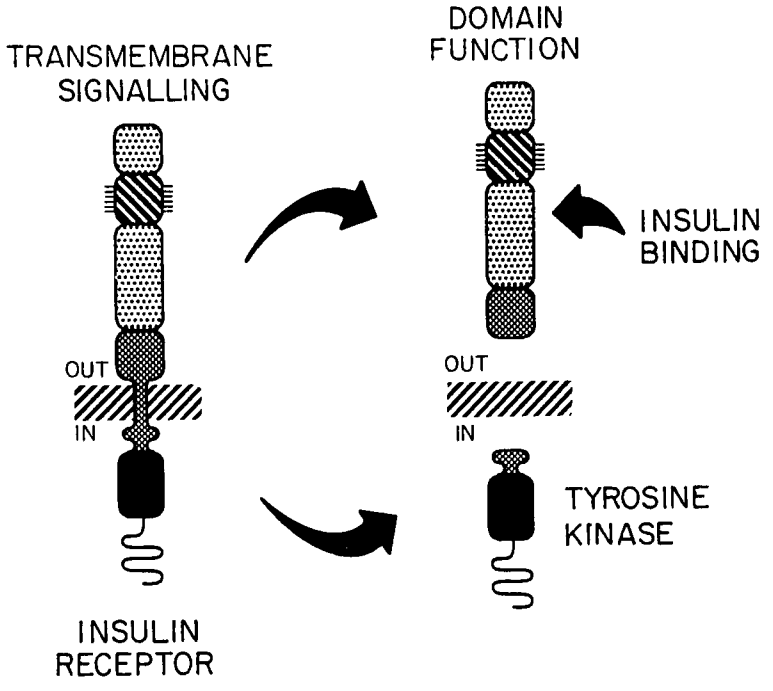

Fig. 2. Cartoon of the experimental strategy employed to explore the independence of domain function of the insulin receptor protein.

independent insulin action (see above), suggesting that the insulin-independent PTK must be membrane-anchored to mediate the response.

The Extracellular Ligand-Binding Domain

Is the extracellular domain of the IR, whose interaction with the hormone initiates the insulin response in cells, capable of autonomous function as well? The results with two chimeric receptor molecules first suggested that this may well be the case. In such chimeras the transmembrane and cytoplasmic domains of the molecule are of heterologous origin: sequences of viral/chicken (from the $P68^{gag-ros}$ transforming protein carried by the *v-ros* oncogene; [10]) and bacterial origin (from the bacterial aspartate chemotactic receptor; [11]) have thus far been utilized. Despite being tethered to the surface of cells in an entirely heterologous manner, the binding of insulin by these hybrid IRs is very near wild type. Furthermore, a range of cytoplasmic mutations of the hIR PTK domain does not compromise insulin binding by this class of mutant receptors as well [5].

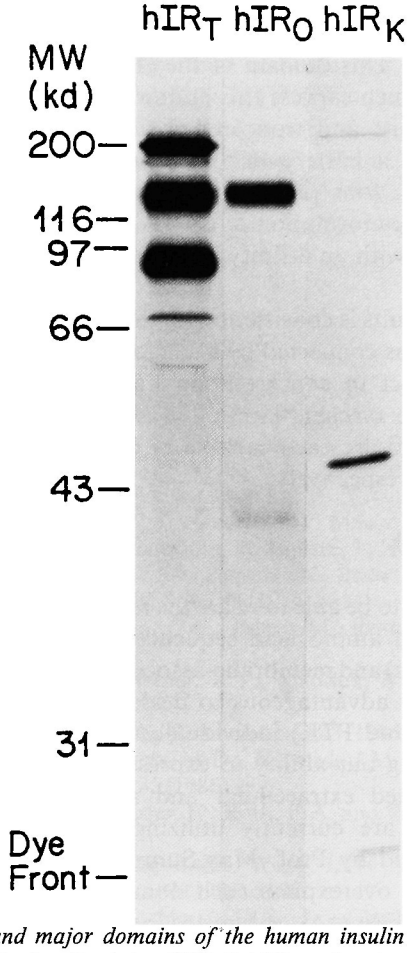

Fig. 3. Wild-type and major domains of the human insulin receptor protein expressed in CHO cell lines and visualized by SDS–PAGE and autoradiography. CHO cells were transfected with recombinant plasmids which encode the respective proteins, and cell lines which express the proteins were isolated as described [5, 6]. Cells which express the wild-type receptor (hIR$_T$, lane 1; CHO.T cells of [5], the entire extracellular ligand-binding domain (hIR$_O$, lane 2; CHO·hIRO1 cells of Ellis et al., submitted for publication) and the cytoplasmic protein-tyrosine kinase domain (hIR$_K$, lane 3; CHO·iBgl cells of [9] were metabolically labeled with [^{35}S]-methionine, and labeled proteins were immunoprecipitated by the use of anti-IR monoclonal antibodies from a nonionic detergent (TX-100) extract (lane 1), culture medium (lane 2) or an extract prepared by permeabilizing cells with the nonionic detergent saponin (lane 3), respectively.

To directly address the question of whether the extracellular domain of the IR is in fact an independently folded domain, we have now constructed an IR deletion mutant which is truncated 6 residues from the beginning of the

predicted transmembrane domain (thus comprised of 923 residues; Ellis et al., submitted for publication). This domain of the IR is in fact secreted with high efficiency from cell lines which express this mutant IR, and is processed in wild-type manner into α-subunits and truncated β-subunits (Fig. 3, lane 2). This molecule is recognized by a battery of 13 monoclonal antibodies to the IR extracellular domain [6–8], four of which block insulin binding, and two of which required the native conformation of the IR for recognition. Furthermore, this domain binds insulin, with an affinity which approximates that of the wild-type IR.

Thus the sum of these results is consistent with the idea that the IR is comprised of two large soluble domains connected by a single membrane-spanning domain, which on the one hand act in concert upon ligand-binding (transmembrane signaling: activation of the tyrosine kinase) to initiate the insulin response in cells, but on the other hand are each capable of autonomous function (ligand-binding and PTK activity, respectively).

Directions of Current Work

We would ultimately like to be able to relate the features of IR primary structure revealed from the deduced amino acid sequence to the details of IR action. Given the size (1355 residues) and membrane-associated nature of the IR molecule, it would be experimentally advantageous to deal with the two major domains of the IR (ligand-binding and PTK) individually as *soluble* molecules (Fig. 2). We are thus now exploiting our ability to express and study the two domains independently, as a secreted extracellular and a cytoplasmic PTK domain, respectively (Fig. 3). We are currently utilizing the Baculovirus insect cell expression system developed by Prof. Max Summers and colleagues at Texas A & M University [12] to overexpress each domain in sufficient quantity for detailed functional studies (Ellis et al., submitted for publication) and for attempts to crystallize each domain for 3-dimensional analysis. These efforts are now proceeding in collaboration with X-ray crystallographers Dr. Elizabeth Goldsmith (Department of Biochemistry, UTHSC in Dallas) for the PTK domain and Prof. Tom L. Blundell (Birkbeck College, London) for the extracellular domain.

Acknowledgements

The published work on the analysis of insulin receptor mutants was done while the author was a postdoctoral fellow in the laboratory of Prof. William Rutter (UCSF), in collaboration with Eric Clauser (Paris), David Morgan and Richard Roth (Stanford). The hybrid receptors (IR.ros and IAR) were studied in collaboration with Song-muh Jong and Lu-Hai Wang (Rockefeller) and Dan E. Koshland and colleagues (Berkeley), respectively. Current work is being

conducted with my colleagues Alla Levitan, Jan Sissom and Purita Ramos at the Howard Hughes Medical Institute in Dallas, in collaboration with Melanie Cobb (Department of Pharmacology, UTHSCD) and Betsy Goldsmith (Department of Biochemistry, UTHSCD). The panels of anti-IR monoclonal antibodies were generously provided by Richard Roth (Stanford) and Ken Siddle (Cambridge, U.K.). Special thanks to Flora Katz (HHMI-Dallas) for many discussions throughout the course of this work, and to Teri Baker for preparation of the manuscript.

References

1. Kahn, C.R., Annu. Rev. Med., 36 (1985) 429.
2. Ebina, Y., Ellis, L., Jarnagin, K., Edery, M., Graf, L., Clauser, E., Ou, J.H., Masiarz, F., Kan, Y.W., Goldfine, I.D., Roth, R.A. and Rutter, W.J., Cell, 40 (1985) 747.
3. Ullrich, A., Bell, J.R., Chen, E.Y., Herrera, R., Petruzzelli, L.M., Dull, T.J., Gray, A., Coussens, L., Liao, Y.C., Tsubokawa, M., Mason, A., Seeburg, P.H., Grunfeld, C., Rosen, O.M. and Ramachandran, J., Nature, 313 (1985) 756.
4. Ebina, Y., Edery, M., Ellis, L., Standring, D.N., Beaudoin, J., Roth, R.A. and Rutter, W.J., Proc. Natl. Acad. Sci. U.S.A., 82 (1985) 8014.
5. Ellis, L., Clauser, E., Morgan, D.O., Edery, M., Roth, R.A. and Rutter, W.J., Cell, 45 (1986) 721.
6. Roth, R.A., Cassell, D.J., Wong, K.Y., Maddux, B.A. and Goldfine, I.D., Proc. Natl. Acad. Sci. U.S.A., 79 (1982) 7312.
7. Morgan, D.O. and Roth, R.A., Biochemistry, 25 (1986) 1364.
8. Soos, M.A., Siddle, K., Baron, M.D., Heward, J.M., Luzio, J.P., Bellatin, J. and Lennox, E.S., Biochem. J., 235 (1986) 199.
9. Ellis, L., Morgan, D.O., Clauser, E., Roth, R.A. and Rutter, W.J., Mol. Endocrinol., 1 (1987) 15.
10. Ellis, L., Morgan, D.O., Jong, S.-M., Wang, L.-H., Roth, R.A. and Rutter, W.J., Proc. Natl. Acad. Sci. U.S.A., 84 (1987) 5101.
11. Ellis, L., Morgan, D.O., Koshland, D.E., Jr., Clauser, E., Moe, G., Bollag, G., Roth, R.A. and Rutter, W.J., Proc. Natl. Acad. Sci. U.S.A., 83 (1986) 8137.
12. Smith, G.E., Summers, M.D. and Fraser, M.J., Mol. Cell Biol., 3 (1983) 2156.

Perturbation-free modification and analysis of functional amino acid residues of a membrane protein

M. Engelhard[a], B. Hess[a] and F. Siebert[b]

[a]Max Planck Institut für Ernährungsphysiologie, Rheinlanddamm 201, D-4600 Dortmund
[b]Albert-Ludwigs Universität, Institut für Biophysik und Strahlenbiologie, Albertstr. 23, D-7800 Freiburg, F.R.G.

Bacteriorhodopsin (bR), the only protein of the purple membrane from *Halobacterium halobium* utilizes light energy to pump protons across the membrane. On light excitation, the chromophore, a protonated retinylidene Schiff base which is bound to Lys^{216}, relaxes thermally via distinct intermediates back to the ground state. These intermediates are characterized by their absorption maximum, the isomerization of the retinal and the protonation of the Schiff-base nitrogen. The proton appears in the medium during the first part of this reaction cycle, and another proton is picked up from the other side of the membrane during the later steps (for a review see [1, 2]).

For the elucidation of the intramolecular proton transfer, infrared (IR) and solid state NMR spectroscopy in combination with isotope-labeled amino acids were used, which allowed the perturbation-free analysis of structural as well as functional properties of this membrane protein. [4-^{13}C]Asp, [^{13}C]guanido-Arg, [^{18}O]Tyr, and [^{15}N]Pro were biosynthetically incorporated into the protein. The isotope enrichment was generally between 70% and 80%, with the exception of Arg, which yielded only 35%. The IR techniques (time-resolved IR, Fourier-transform IR) gave answers about the state of protonation of the ground state and the intermediates of carboxyl and tyrosyl groups and followed the time course of protonation changes [3]. It could be shown that at least three aspartic acids are cyclically protonated and deprotonated after light excitation of the chromophore. These residues are in the interior of the protein, one of which is protonated. The latter result is confirmed by the NMR data.

The solid state NMR data of [^{13}C]guanido-Arg revealed one class of Arg (most probably only one Arg) which absorbs at approximately 270 ppm (relative to tetramethylsilane). This chemical shift can only be explained by an unusual protein environment. Model studies suggest that this Arg might be bound to a Tyr residue. This would also explain the IR data of the modified tyrosine.

The results are summarized in Table 1, which shows the location of the identified amino acids, the reaction in which they take part, and the method of their detection. The number of functional amino acids identified in these experiments

Table 1 *Identified amino acids with structural and/or functional properties*

Amino acid	Method	Location	Counter-ion	Reaction[a]
Asp 1	IR, NMR?	interior	H^+	deprot/prot
2	IR	interior	$-C{=}{=}NH^+-$	deprot/prot
3	IR	interior	Arg?	deprot/prot
Arg 1	NMR	interior	Tyr?	deprot/prot?
2	NMR	interior	?	?
3	NMR	exterior	?	?
Tyr	IR	interior	Arg?	deprot/prot?
Asp	NMR	exterior	Me^{2+}?	?

[a] deprot = deprotonation; prot = protonation

would be sufficient to transport a proton from one side of the membrane to the exterior. It is also evident that the introduction of isotope-labeled amino acids into proteins opens the possibility to study functional as well as structural properties of the native unperturbed protein, employing IR and NMR methods.

References

1. Stoeckenius, W. and Bogomolni, R.A., Annu. Rev. Biochem., 52 (1982) 587.
2. Hess, B., Kuschmitz, D. and Engelhard, M., In Martonosi, A.N. (Ed.) Membrane and Transport, Vol. 2, Plenum, New York, 1982, pp. 309–318.
3. Engelhard, M., Gerwert, K., Hess, B., Kreutz, W. and Siebert, F., Biochemistry, 24 (1985) 400.

Wasp venom toxin mastoparan, a histamine releaser from mast cells, is a direct activator of GTP-binding regulatory proteins

Tsutomu Higashijima[a,*], Sonoko Uzu[b], Terumi Nakajima[b] and Tatsuo Miyazawa[a]

[a]Department of Biophysics and Biochemistry, Faculty of Science and [b]Faculty of Pharmaceutical Sciences, The University of Tokyo, 7-3-1 Hongo, Bunkyo-ku, Tokyo 113, Japan

Introduction

Mastoparan is a wasp venom toxin, Ile-Asn-Leu-Lys-Ala-Leu-Ala-Ala-Leu-Ala-Lys-Lys-Ile-Leu-NH_2 [1], that stimulates the secretion of histamine from mast cells [1], serotonin from platelets [1], catecholamines from chromaffin cells [2] and prolactin from the anterior pituitary [3]. Histamine release by mastoparan has been found to accompany the formation of inositol-1,4,5-trisphosphate (IP_3) [4], which liberates Ca^{2+} from intracellular storage [5]. The IP_3 is produced from phosphatidylinositol-4,5-bisphosphate by a phosphodiesterase whose activity is regulated by a GTP-binding regulatory protein (G-protein) [5–7]. Here we studied the direct interaction of mastoparan with a G-protein, G_o, purified from bovine brain and found that mastoparan accelerates the activation rate of G-protein as does a hormone–receptor complex.

Results

(1) Pertussis toxin treatment of mast cells inhibited the histamine release caused by mastoparan. Pertussis toxin is known to ADP-ribosylate several G-proteins and thereby render them insensitive to regulation by receptors [6]. By contrast, histamine release caused by the Ca^{2+} ionophore A23187 was not affected by pertussis toxin. (2) The rate of GTPγS binding to G-proteins, which causes their functional activation, is very slow (~$0.3 \cdot min^{-1}$ for G_o at 20°C), reflecting slow dissociation of GDP [8–11]. Mastoparan accelerated the binding of GTPγS to purified G_o in a concentration-dependent manner at more than 1 μM. Maximum acceleration caused by mastoparan was more than 10-fold. (3) The ADP-

*Present address: Department of Pharmacology, University of Texas Health Science Center at Dallas, 5323 Harry Hines Boulevard, Dallas, TX 75235, U.S.A.

ribosylation of purified G_o suppressed this effect of mastoparan but did not alter the basal rate of GTPγS binding. (4) The ability of mastoparan analogs [12], including truncated analogs, to promote GTPγS binding to purified G_o corresponded well with their ability to promote histamine release from mast cells.

Discussion

A family of G-proteins has been found to play essential roles in signal transduction by a variety of hormones and neurotransmitters [13]. G-proteins are inactive when they have bound GDP and become active when GTP (or GTPγS) is bound. In the signal transduction system, the hormone–receptor complex causes activation of the G-protein by promoting the dissociation of bound GDP [8, 14]. This lends to the activation of enzymes such as adenylate cyclase or phosphodiesterase. Recently, a GTP-binding protein has been shown to be involved in the mobilization of Ca^{2+} from intracellular Ca^{2+} storage through the formation of $InsP_3$ [5, 7]. In mast cells and some other cells, the G-protein has been shown to be a substrate of ADP-ribosylation by pertussis toxin [6].

In the present study, we showed that a G-protein is involved in mastoparan-induced histamine release because pertussis toxin blocks histamine release. We also demonstrated that mastoparan directly promotes the activation of a purified G-protein, G_o, which is a substrate of pertussis toxin. ADP-ribosylation of purified G_o by pertussis toxin inhibited the acceleration of GTPγS binding by mastoparan. These observations suggest that mastoparan regulates G-proteins in a manner similar to that of the hormone–receptor complex.

The effect of mastoparan on the acceleration of GTPγS binding to a G-protein is observed at a similar concentration range as that on histamine release from mast cells [1, 12]. And in addition, the effects of mastoparan analogs on the GTPγS binding correspond well with the activities for histamine release [12]. These results strongly suggest that the target of mastoparan for histamine-releasing activities is a GTP-binding regulatory protein, since mastoparan can penetrate into the hydrophobic interior of the phospholipid membrane [15, 16].

Acknowledgements

We thank Dr. Toshiaki Katada (Hokkaido University) and Dr. Elliott Ross (U.T.H.S.C.D.) for their helpful discussions.

References

1. Hirai, Y., Yasuhara, T., Yoshida, H., Nakajima, T., Fujino, M. and Kitada, C., Chem. Pharm. Bull., 27 (1979) 1942.
2. Kuroda, Y., Yoshida, M., Kumakura, K., Kobayashi, K. and Nakajima, T., Proc. Japan Acad., 56 (Ser B) (1980) 660.
3. Kurihara, H., Kitajima, K., Senda, T., Fujita, H. and Nakajima, T., Cell Tissue Res., 243 (1986) 311.
4. Okano, Y., Takagi, H., Tohmatsu, T., Nakashima, S., Kuroda, Y., Saito, K. and Nozawa, Y., FEBS Lett., 188 (1985) 363.
5. Berridge, M.J. and Irvine, R.F., Nature, 312 (1984) 315.
6. Nakamura, T. and Ui, M., J. Biol. Chem., 260 (1985) 3584.
7. Gomperts, B.D., Nature, 306 (1983) 64.
8. Ferguson, K.M., Higashijima, T., Smigel, M.D. and Gilman, A.G., J. Biol. Chem., 261 (1986) 7393.
9. Higashijima, T., Ferguson, K.M., Sternweis, P.C., Ross, E.M., Smigel, M.D. and Gilman, A.G., J. Biol. Chem., 262 (1987) 752.
10. Higashijima, T., Ferguson, K.M., Smigel, M.D. and Gilman, A.G., J. Biol. Chem., 262 (1987) 757.
11. Higashijima, T., Ferguson, K.M., Sternweis, P.C., Smigel, M.D. and Gilman, A.G., J. Biol. Chem., 262 (1987) 762.
12. Uzu, S., Nakajima, T., Saito, K., Wakamatsu, K., Miyazawa, T. and Fujino, M., In Kiso, Y. (Ed.) Peptide Chemistry 1985, Protein Research Foundation, Osaka, 1986, p. 229.
13. Gilman, A.G., Annu. Rev. Biochem., 56 (1987) 615.
14. Brandt, D.R. and Ross, E.M., J. Biol. Chem., 261 (1986) 1656.
15. Higashijima, T., Wakamatsu, K., Takemitsu, M., Fujino, M., Nakajima, T. and Miyazawa, T., FEBS Lett., 152 (1983) 227.
16. Wakamatsu, K., Higashijima, T., Fujino, M., Nakajima, T. and Miyazawa, T., FEBS Lett., 162 (1983) 123.

Role of the signal sequence in protein secretion

Lila M. Gierasch, Martha S. Briggs* and C. James McKnight
Department of Chemistry, University of Delaware, Newark, DE 19716, U.S.A.

Introduction

Despite considerable effort in the last 15 years, the mechanism by which proteins are secreted from cells to extracellular locations remains unclear [1]. Steps in protein secretion are viewed as commencing with a recognition of the nascent chain as it is synthesized so that it is directed to the export pathway. In eukaryotes, this step is mediated by the signal recognition particle (SRP), a complex of six polypeptide chains and a strand of ribonucleic acid. SRP has been shown to bind to the newly synthesized chain and to the ribosome and to cause a pause or arrest in translation (depending on conditions of the assay). Next, the export-competent complex of SRP, nascent chain and ribosome is targeted to the endoplasmic reticulum (ER) membrane, presumably because of a strong binding of SRP to the SRP receptor (or 'docking protein'), an integral membrane complex of two polypeptide chains, which also relieves the translation block. Subsequent steps lead to translocation of the nascent chain across the membrane and may involve a proteinaceous pore and/or receptor; energy in the form of nucleoside triphosphates appears to be required for binding and/or translocation [2]. In prokaryotes, genetic and biochemical data strongly suggest that an SRP-like factor (the *secA* gene product?) and a membrane-resident species (the *prlA* [*secY*] gene product?) play a role in export [1]; the steps outlined are therefore likely to be similar to steps in bacterial protein export.

In both eukaryotes and bacteria, a signal sequence must be present on the nascent chain in order for a protein to be handled by the export apparatus. Many signal sequences are known; they are generally N-terminal, 15–30 residues in length, and usually are cleaved during the translocation of the mature protein. There is a puzzling lack of homology among signal sequences, considering their apparently common functions in secretion: They are recognized by SRP, they are probably involved in the binding and translocation at the membrane, and they are cleaved by signal peptidase. Still, comparisons of known signal sequences have revealed general characteristics [3]. The N-terminal region of signal sequences

*Present address: Department of Chemistry, University of Pennsylvania, Philadelphia, PA 19104, U.S.A.

often contains charged residues; in prokaryotes, these are always basic. This region is followed by a hydrophobic region that is 10–12 residues in length and rich in Leu and Ala. The hydrophobic region ends on the C-terminal side with a small stretch of sequence enriched in more polar (but not usually charged) residues that are frequent participants in reverse turns in proteins. Lastly, adjacent to the cleavage site is a region with some homology among signal sequences (apparently so that it can bind to the peptidase); the '-1, -3 rule' [4] predicts that the residue adjacent to the scissile bond and the residue two away (toward the N-terminus) will be small (often Ala).

We have investigated structure/function correlations in signal sequences by synthesis and biophysical study of genetically characterized signal sequences from wild-type and export-defective mutant strains of *Escherichia coli* [5, 6]. The family of signal peptides chosen for initial study is derived from an outer membrane protein, LamB. Table 1 summarizes the signal sequences and export capacities of several *E. coli* strains with mutations in the signal region of LamB; these strains and the biochemical characterization of their export function have been reported by Stader et al. [7].

Results and Discussion

The wild-type and mutant LamB signal peptides were synthesized by solid phase methods using protocols described elsewhere [5]. Circular dichroism (CD) spectra revealed that these peptides were largely unstructured in aqueous solution and that they adopted α-helical conformations in environments that are interfacial (sodium dodecyl sulfate [SDS] micelles) or membranelike (lipid vesicles) (see data in Table 2). For most of these peptides, in fact, the content of α-helix parallels their competence to export LamB in vivo. We conclude that functional signal sequences have a strong tendency to adopt α-helical conformations in low dielectric, interfacial environments. No discrimination in helix content,

Table 1 *Sequence and in vivo export competence of* E. coli *LamB signal sequence mutant peptides studied*[a]

	1 5 10 15 20 25	% LamB exported[b]
WT	M-M-I-T-L-R-K-L-P-L-A-V-A-V-A-A-G-V-M-S-A-Q-A-M-A	100
Δ78	M-M-I-T-L-R-K-L-P ---------- V-A-A-G-V-M-S-A-Q-A-M-A	0
Δ78r1	M-M-I-T-L-R-K-L-P ---------- V-A-A-*C*-V-M-S-A-Q-A-M-A	50
Δ78r2	M-M-I-T-L-R-K-L-*L* ---------- V-A-A-G-V-M-S-A-Q-A-M-A	90
A13D	M-M-I-T-L-R-K-L-P-L-A-V-*D*-V-A-A-G-V-M-S-A-Q-A-M-A	10
G17R	M-M-I-T-L-R-K-L-P-L-A-V-A-V-A-A-*R*-V-M-S-A-Q-A-M-A	40[c]

[a] From [7].
[b] In 4 min.
[c] At longer times, this mutant exports LamB at wild-type levels.

Table 2 *Conformations of LamB signal peptides from CD spectra*[a]

	Buffer[b]			40 mM SDS		
	%α	%β	%rc	%α	%β	%rc
WT	5	15	80	60	10	30
Δ78	5	15	80	20	15	65
Δ78r1	10	10	80	35	10	55
Δ78r2	10	10	80	60	25	15
A13D	5	20	75	40	15	45
G17R	15	5	80	50	10	40

[a] Based on reference spectra from N. Greenfield and G. Fasman [9].
[b] Buffer = 5 mM Tris, pH 7.3.

however, is observed between two signal peptides that contain point mutations which introduce a charged residue in place of a neutral one: A13D, with the charge in the middle of the hydrophobic section, and G17R, with the charge in the potential turn region. The in vivo export function of these two strains is distinct: The A13D mutant is strongly export-defective, while the G17R displays a slowed kinetics of export, but wild-type amounts of LamB are exported eventually.

The possibility that signal sequences interact with lipids or proteins within the membrane led us to characterize the relative affinities of these signal peptides for organized lipid assemblies. The experimental technique applied to this question is surface tensiometry, as diagrammed in Fig. 1 (for details, see [6]). Signal

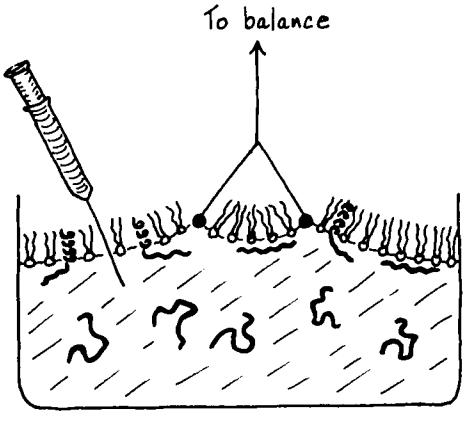

Fig. 1. Diagram of setup for following insertion of signal peptides into lipid monolayers by surface tensiometry. Surface tension is measured using a du Noüy ring. The monolayer was formed from palmitoyloleoylphosphatidylethanolamine (65 mol%) and palmitoyloleoylphosphatidylglycerol (35 mol%) to mimic the E. coli *inner membrane. For details of the protocol, see* [6].

Table 3 *Membrane insertion data for LamB signal peptides*[a]

Peptide	K_d (m/l)	$\Delta\pi_{max}$ (dynes/cm)[b]
WT	5×10^{-8}	11
Δ78	1×10^{-7}	2.5
Δ78r 2	2×10^{-7}	11
A13D	5×10^{-7}	9.5
G17R	8.5×10^{-8}	11

[a] The lipid composition is given in Fig. 1; the subphase was 5 mM Tris, pH 7.3.
[b] Initial monolayer pressure was 23.5 dynes/cm.

peptide solutions were injected from a syringe beneath a lipid monolayer, and surface pressure changes ($\Delta\pi$s) were monitored. Insertion of the peptide into the lipid monolayer is indicated by an increased surface pressure. Titrations of $\Delta\pi$ as a function of peptide concentration in the subphase show saturation-binding behavior, and thus we could extract a maximal surface pressure change and an apparent dissociation constant from the curves (see Table 3). Here we see a clear difference between the two mutants which have an additional charged residue: The G17R signal sequence, which caused a kinetic defect but still exported LamB at wild-type levels in vivo, inserts at nearly wild-type affinity. The A13D signal peptide inserts significantly less readily.

Thus, in addition to the capacity to adopt α-helical conformations, functional signal sequences display a strong tendency to interact with lipid assemblies. This may reflect a step in vivo wherein direct insertion of the signal sequence into the membrane is favored because of peptide/lipid interactions [8]. Alternatively, the affinity for lipid may be a manifestation of a property required at some other point in the export pathway. For example, using the eukaryotic paradigm, SRP must be capable of binding many signal sequences with little strict sequence homology. Perhaps this binding requires only a pattern of charge and hydrophobicity that is also conducive to favorable lipid interactions. Further dissection of the export apparatus and study of the interactions of synthetic signal sequences with the resulting components are necessary to sort out these possibilities. Nonetheless, it is likely that early in evolution secretion of proteins was a fortuitous consequence of the presence on their N-termini of primordial signal sequences that spontaneously interacted with membranes.

Acknowledgements

This research was supported by grants from the NIH and the NSF.

References

1. Recent reviews of this area include: Rapoport, T.A., CRC Crit. Rev. Biochem. 20 (1986) 73; Briggs, M.S. and Gierasch, L.M., Adv. Prot. Chem., 38 (1986) 109; Benson, S.A. and Silhavy, T.J., Annu. Rev. Biochem., 54 (1985) 101.
2. For example, see: Connolly, T. and Gilmore, R., J. Cell Biol., 103 (1986) 2253; Chen, L. and Tai, P.C., Nature, 328 (1987) 164.
3. Von Heijne, G., J. Mol. Biol., 184 (1985) 99.
4. Perlman, D. and Halvorson, H.O., J. Mol. Biol., 167 (1983) 391.
5. Briggs, M.S. and Gierasch, L.M., Biochemistry, 23 (1984) 3111.
6. Briggs, M.S., Gierasch, L.M., Zlotnick, A., Lear, J.D. and DeGrado, W.F., Science, 228 (1985) 1096.
7. Stader, J., Benson, S.A. and Silhavy, T.J., J. Biol. Chem., 261 (1986) 15075.
8. Briggs, M.S., Cornell, D.G., Dluhy, R.A. and Gierasch, L.M., Science, 233 (1986) 206.
9. Greenfield, N. and Fasman, G., Biochemistry, 8 (1969) 4108.

Membrane-catalyzed molecular mechanism of tachykinin receptor selection

Robert Schwyzer, Daniel Erne, Krzisztof Rolka, John W. Bean and David F. Sargent

Department of Molecular Biology and Biophysics, Swiss Federal Institute of Technology, CH-8093 Zürich, Switzerland

Introduction

The three mammalian tachykinins or neurokinins – substance P, neurokinin A, and neurokinin B – bind selectively to three distinct tachykinin receptor subtypes called the NK-1 (NK-P, SP-P), NK-2 (NK-A, SP-K), and NK-3 (NK-B, SP-N) sites, respectively [1]. Tachykinins from amphibians and molluscs – physalaemin, kassinin, and eledoisin – react with the same three sites, although more weakly and less selectively. The eledoisin-preferring SP-E receptor is no longer considered to be a distinct neurokinin site [1]. The complicated pharmacological patterns of neurokinins and tachykinins are attributed to a combined stimulation of receptors present on different cells in a tissue. Table 1 indicates preferred sites and their locations in pharmacologic preparations.

Results and Discussion

The type of membrane interaction and the induced membrane structures were predicted by thermodynamic calculations [2] for the peptides of Table 1 and compared with pharmacologic and binding data taken from the literature ([3] and references therein). Substance P binds reversibly to anionic lipid membranes from aqueous solutions. The C-terminal message segment folds into an α-helix which is oriented perpendicularly on the membrane surface and contacts the hydrophobic layers. The N-terminal address segment remains in aqueous surroundings. This was confirmed by circular dichroism [4], infrared attenuated total reflection spectroscopy [5], and measurement of the reduction of membrane surface charge and dipole moment by capacitance minimization. The observed intrinsic dissociation constant was identical with that predicted for neutral membranes, $K_d = 2.4 \times 10^{-4}$ M (unpublished data). Physalaemin behaved similarly, whereas eledoisin remained in the aqueous membrane compartment as a β-structure; neurokinins A and B also did not interact with the hydrophobic membrane layers (unpublished data).

NK-1 site-preferring peptides (Table 1) were predicted to have membrane structures similar to that of substance P and to bind hydrophobically with similar energies. [$C^{3,6}$, Y^{8}]SP was predicted to bind more strongly, hydrophobically, than substance P, in agreement with the observed binding data. We confirmed that the peptides containing D-amino acid residues can also form α-helices in hydrophobic environments (unpublished data). All other peptides, except antagonist C, were predicted not to bind hydrophobically to membranes. Their membrane interactions were governed by electrostatic accumulation (NK-2) or repulsion (NK-3) by the anionic biologic membranes. (Repulsion also governs the site interaction of antagonist C.) The uncharged peptides – septide, [Gly^{9}]-septide, eledoisin, and kassinin – bind to NK-2 and NK-3 sites. The preference of septide for NK-2 is attributed to a folded structure induced by proline ([3] and references therein).

Thus, neurokinin receptor subtype selection follows the same pattern as opioid receptor selection [6]. NK-1 and opioid kappa sites appear to be exposed to a hydrophobic membrane compartment and require perpendicular orientation of the peptide message domain as an α-helix. The NK-2 and opioid mu sites

Table 1 *Tachykinin amino acid sequences and preferred receptor subtypes*

NK-1 sites on postganglionic neurons (atropine-sensitive) and smooth muscle cells (atropine-insensitive):	
Substance P	Arg-Pro-Lys-Pro-Gln-Gln-Phe-Phe-Gly-Leu-Met-NH_2
Physalaemin	Pyr-Ala-Asp-Pro-Asn-Lys-Phe-Tyr-Gly-Leu-Met-NH_2
[$C^{3,6}$, Y^{8}]SP	Arg-Pro-Cys-Pro-Gln-Cys-Phe-Tyr-Gly-Leu-Met-NH_2
Antagonist A	Arg-pro-Lys-Pro-Gln-Gln-trp-Phe-trp-Leu-Met-NH_2
Antagonist B	Arg-Gln-trp-Phe-trp-Leu-Nle-NH_2
NK-2 sites on smooth muscle cells (atropine-insensitive):	
Neurokinin A	His-Lys-Thr-Asp-Ser-Phe-Val-Gly-Leu-Met-NH_2
[Gly^{9}]septide	Pyr-Phe-Phe-Gly-Leu-Met-NH_2
Septide	Pyr-Phe-Phe-Pro-Leu-Met-NH_2
[Arg^{6}, $MePhe^{8}$]- SP	Arg-Phe-MePhe-Gly-Leu-Met-NH_2
NK-3 sites on postganglionic neurons (atropine-sensitive):	
Neurokinin B	Asp-Met-His-Asp-Phe-Phe-Val-Gly-Leu-Met-NH_2
Senktide	Suc-Asp-Phe-MePhe-Gly-Leu-Met-NH_2
Antagonist C	Asp-pro-His-Asp-Phe-trp-Val-trp-Leu-Met-NH_2
[$C^{2,5}$]NKB	Asp-Cys-His-Asp-Cys-Phe-Val-Gly-Leu-Met-NH_2
NK-2 and NK-3 sites (weak, little selectivity):	
Eledoisin	Pyr-Pro-Ser-Lys-Asp-Ala-Phe-Ile-Gly-Leu-Met-NH_2
Kassinin	Asp-Val-Pro-Lys-Ser-Asp-Gln-Phe-Val-Gly-Leu-Met-NH_2

NKB = neurokinin B; SP = substance P; Suc = succinyl; lower-case pro and trp indicate D-Pro and D-Trp, respectively.

are located near the (aqueous) anionic membrane layer and prefer a folded conformation of the positively charged peptide. NK-3 and opioid delta sites may be exposed in the aqueous compartment in a positively charged local environment. These *membrane requirements* indicate membrane catalysis [7] of receptor subtype selection by tachykinins, and supplement the classical *receptor requirements* for a specific amino acid sequence and a fitting, receptor-induced conformation.

References

1. Regoli, D., Drapeau, G., Dion, S. and D'Orléans-Juste, P., Life Sci., 40 (1987) 109.
2. Schwyzer, R., Erne, D. and Rolka, K., Helv. Chim. Acta, 69 (1986) 1789.
3. Schwyzer, R., EMBO J., in press.
4. Rolka, K., Erne, D. and Schwyzer, R., Helv. Chim. Acta, 69 (1986) 1798.
5. Erne, D., Rolka, K. and Schwyzer, R., Helv. Chim. Acta, 69 (1986) 1807.
6. Schwyzer, R., Biochemistry, 25 (1986) 6335.
7. Sargent, D.F. and Schwyzer, R., Proc. Natl. Acad. Sci. U.S.A., 83 (1986) 5774.

Synthetic peptides identify a critical lysine residue in the SV-40 nuclear transport signal

Patrick Kanda, Ronald C. Kennedy and Robert E. Lanford
Department of Virology and Immunology, Southwest Foundation for Biomedical Research, San Antonio, TX 78284, U.S.A.

Introduction

Simian virus 40 (SV-40) expresses a protein, the large T-antigen, which localizes in the nucleus of infected cells and is responsible for host transformation. This protein contains a basic, contiguous stretch of seven amino acids, Pro-Lys-Lys$_{128}$-Lys-Arg-Lys-Val, which mediates its transit from the cytoplasm to the nucleus [1]. Likewise, when contained within a synthetic tridecamer peptide which has been coupled to unrelated carrier proteins, this sequence will also direct such proteins to the nucleus of mammalian cells following their microinjection into the cytoplasm [2]. In this report, we have evaluated the effects of amino acid substitutions at lysine$_{128}$ of the signal sequence with respect to the ability of these analogs to promote nuclear transport of rabbit immunoglobulin (IgG). We have also compared these transport properties with their immunologic reactivities against a monoclonal antibody.

Results and Discussion

The nuclear transport wild-type (WT) signal peptide has the following sequence: Cys-Gly-Tyr-Gly-Pro-Lys-Lys$_{128}$-Lys-Arg-Lys-Val-Gly-Gly. Substitutions at lysine$_{128}$ include L-asparagine (cT derivative), D-lysine, L-ornithine, and L-*p*-aminophenylalanine (PAF). Each was coupled to rabbit IgG and microinjected into the cytoplasm of African green monkey kidney cells. The cells were harvested, acetone-fixed, and the conjugates visualized by immunofluorescence using labeled goat anti rabbit IgG (Table 1). Of the analogs with basic side chain substitutions, only the IgG-PAF derivative did not accumulate in the nucleus. The IgG-cT conjugate also could not localize in the nucleus, in agreement with earlier studies showing that Asn$_{128}$ rendered the SV-40 large T-antigen cytoplasmic [3].

Both rabbit antisera and a mouse monoclonal antibody were raised against the WT sequence. The rabbit antisera cross-reacted against the substituted signal peptides with binding affinities similar to that of the WT signal. A mouse monoclonal anti-WT antibody was chosen which did not recognize the cT

Table 1 *Transport of modified T-signal peptides*

Peptide	Nuclear localization	Transport time
WT	+	15 min
cT	-	-
D-Lys	+	3 h
Orn	+	>6 h, <16 h
PAF	-	-

sequence (0.469 O.D. vs 0.038 O.D. at 1:2 dilution, enzyme-linked immunosorbent assay, ELISA). Its binding against the other analogs gave the following O.D.s: 0.239 (D-Lys), 0.174 (L-Orn) and 0.038 (PAF). This order of cross-reactivity correlates well with the transport properties of these surrogates relative to the WT sequence.

We conclude that recognition of the SV-40 large T nuclear transport signal incorporates a high specificity for lysine at position 128, with other basic R groups being less effective. Also, conformational elements in this region governing signal recognition may be similarly involved in the fine specificity of antibodies directed against this site.

References

1. Kalderon, D., Roberts, B., Richardson, W.D. and Smith, A.E., Cell, 39 (1984) 499.
2. Lanford, R.E., Kanda, P. and Kennedy, R.C., Cell, 46 (1986) 575.
3. Lanford, R.E. and Butel, J.S., Cell, 37 (1984) 801.

Studies on synthetic peptides of small subunit of ribulose 1,5-bisphosphate carboxylase (RuBisCO)

Judson V. Edwards[a], John M. Bland[a], Donald G. Cornell[b], Thomas E. Cleveland[a], Samuel Landry[c] and Susan G. Bartlett[c]

[a]USDA, ARS, SRRC, 1100 Robert E. Lee Blvd., New Orleans, LA 70179, U.S.A.
[b]USDA, ARS, ERRC, Philadelphia, PA, U.S.A.
[c]LSU, Biochemistry Department, Baton Rouge, LA, U.S.A.

Introduction

Over 80% of all proteins functional in the chloroplast are post-translationally transported to the organelle. Amino-terminal presequences ('transit peptides') of chloroplast proteins are believed to contain information necessary for import and compartmentalization of the protein. Transit peptides contain three major blocks (underscored below for SSU RuBisCO) of amino acid homology [1]. The shared blocks may participate in common functions performed by the transit sequence in transport events. In this regard, three approaches were taken to examine synthetic transit peptides of the small subunit of RuBisCO [1]: (i) a reconstituted chloroplast import assay, (ii) monolayer insertion analysis, and (iii) proteolytic cleavage of intermediate processing block II.

```
     5        10        15   20        25        30        35        40   45
MAPAVMAS SATTVA  PFQGLK  STAGLPVSRRSGSLGSVSN GGRI RC
     I                  II                            III
```

(1)

Methods

Peptides of (**1**) corresponding to sequences 1–44, 1–25, 15–25, 9–25, 1–9 + 15–25, and 25–44 were synthesized by solid phase methods. Uptake of labeled proteins from in vitro translation into intact chloroplasts in the presence of the above peptides (2 μM) was performed [2]. Peptide insertion into a lipid monolayer was assayed on monolayer films [3] using 2 μM peptide solutions. Peptides 15–25 and 9–25 containing homology block II were treated with both trypsin and chymotrypsin (100:1, peptide/enzyme) and the degradation products separated by RPHPLC.

Results and Discussion

Protein transport inhibition was observed at 10 μM for peptide 1–44. In the presence of a protease inhibitor, peptide 1–25 inhibited transport at approximately 50%. Peptide 1–25 inserted into the lipid monolayer resulting in increases of 5.2, 4.7, and 3.7 dynes/cm, over initial pressures of 12.2, 12.4, and 14.9, respectively. Peptide 9-25, not containing the first homology block, did not insert into the monolayer. Peptides isolated from enzyme digestion of 15–25 and 9–25 indicated proteolytic cleavage within and adjacent to block II. Chymotrypsin cleaved at residues LK (on 15–25) and FQ (on 9–25); trypsin cleaved at KS (on 15–25) at FQ and KS (on 9–25).

Both the in vitro reconstitution bioassay and the monolayer insertion study indicated the probable necessity of the first 8–9 residues associated with homology block I for chloroplast import of SSU RuBisCO. The protease degradation indicated an enzyme specificity for cleavage sites at intermediate processing block II.

Acknowledgements

The authors thank Ms. Diedre Lyons for her technical assistance.

References

1. Karlin-Newman, G.A. and Tobin, E.M., EMBO J., 5(1986)9.
2. Bartlett, S.G., Grossman, A.R. and Chua, N.-H., In Edelman, M., Hallick, R.B. and Chua, N.-H. (Eds.) Methods in Chloroplast Molecular Biology, Elsevier, Amsterdam. 1982, p. 1081.
3. Briggs, M.S., Cornell, D.G., Dluhy, R.A. and Gierasch, L.M., Science, 233(1986)206.

Biophysical studies of the fragments of the extension peptide of cytochrome *P*-450 (SCC) precursor

Haruhiko Aoyagi, Sannamu Lee, Hisakazu Mihara, Tatsuhiko Kanmera and Tetsuo Kato

Laboratory of Biochemistry, Faculty of Science, Kyushu University, Higashi-ku, Fukuoka 812, Japan

Introduction

We previously found that the N-terminal basic portion of the extension peptides of mitochondrial protein precursors was important for the import of the precursors into mitochondria by using many model peptides [1]. The extension peptide of cytochrome *P*-450 (SCC) precursor consists of 39 amino acid residues:

1	5	10	15	20	25	30	35	39
M-L-A-*R*-G-L-P-L-*R*-S-A-L-V-*K*-A-C-P-P-I-L-S-T-V-G-E-G-W-G-H-H-*R*-V-G-T-G-E-G-A-G								

We planned to synthesize several fragments of the extension peptide-containing basic amino acid residues and investigate their properties in order to obtain further information on the characteristics of the extension peptides.

Result and Discussion

Six fragments, P_{6-11}, P_{6-15}, P_{1-11}, P_{1-15}, P_{1-20} and P_{25-39}, corresponding to the residues 6-11, 6-15, 1-11, 1-15, 1-20 and 25-39, respectively, of pre-*P*-450 (SCC), were chemically synthesized by the solution method. Purity of the final products was ascertained by HPLC and amino acid analysis. P_{1-15} and P_{1-20} showed an inhibitory effect on the import of pre-*P*-450 (SCC) at 30 μM. Shorter fragments and P_{25-39} showed weak or no effects. The results indicated an essential role for the N-terminus extension peptide of approximately the first 15 residues in the import process. None of the fragments showed antibacterial activity against gram-positive (*S. aureus*, *B. subtilis*) and gram-negative bacteria (*E. coli*, *P. vulgaris*), even at 100 μg/ml.

Circular dichroism (CD) studies indicated that P_{1-15} and P_{1-20} held a random conformation in Tris-HCl buffer and a partially ordered conformation similar to α-helix or type II′ β-turn in buffer containing acidic DPPC-DPPG (3:1) liposomes as shown in Fig. 1. Other fragments had almost random conformations

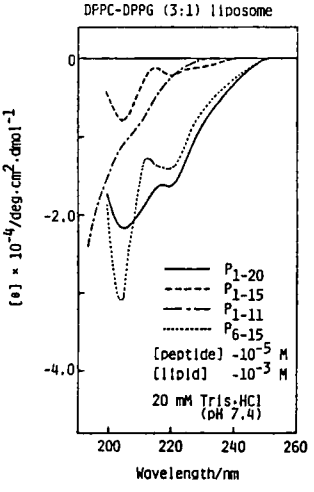

Fig. 1. CD curves of synthetic peptides.

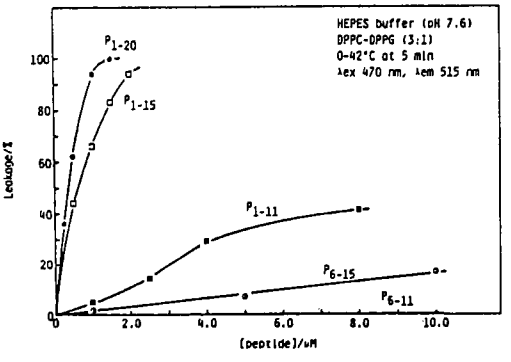

Fig. 2. Effects of synthetic peptides on dye leakage from DPPC-DPPG vesicles.

under these conditions. Hydrophobic moments $<\mu H>$ of P_{1-15} and P_{1-20} were calculated on the assumption that these fragments assume an α-helix conformation. The $<\mu H>$ values of P_{1-15} and P_{1-20} were 0.17 and 0.21, respectively, while general surface-seeking peptides and proteins have large $<\mu H>$ values greater than 0.50 [2]. These results suggest that amphiphilic helicity is not indispensable for the import of the precursor into mitochondria, although at least partially ordered conformation seems to be required.

The ability of P_{1-15} and P_{1-20} to leak carboxyfluorescein from the inside of DPPC or DPPC-DPPG (3:1) vesicles was greater than that of other fragments. P_{1-20} induced 100% leakage at 1.5 μM, and P_{1-15} showed leakage of 83% and 94% at 1.5 and 2.0 μM, respectively, in the case of acidic DPPC-DPPG vesicles, as shown in Fig. 2. The leakage ability of the fragments qualitatively parallels the degree of their inhibitory effect on the import of the precursor. Therefore, we suppose that nondrastic but mild perturbation of the mitochondrial membrane caused by the action of partially ordered structure of the peptides may be one of the requirements for the import of the precursors.

Acknowledgements

We are grateful to Prof. T. Omura and Dr. A. Ito of Kyushu University for the import-inhibitory assay.

References

1. Ito, A., Ogishima, T., Ou, W., Omura, T., Aoyagi, H., Lee, S., Mihara, H. and Izumiya, N., J. Biochem. (Tokyo), 98 (1985) 1571.
2. Eisenberg, D., Annu. Rev. Biochem., 53 (1984) 595.

Binding of dynorphin-A-(1–13) and some N-terminal fragments to neutral lipid bilayer membranes

John W. Bean, Daniel Erne, David F. Sargent and Robert Schwyzer
Department of Molecular Biology and Biophysics, Swiss Federal Institute of Technology, CH-8093 Zürich, Switzerland

Introduction

The cellular membrane plays an important role in catalyzing peptide–receptor interactions [1] as well as in determining peptide receptor subtype selectivity [2, 3]. In this investigation we have used two techniques to assess the degree of hydrophobic interaction of dynorphin (dyn) N-terminal fragments with lipid bilayer membranes. The binding of the peptides to one side of a planar 1,2-dioleoyl-*sn*-glycero-3-phosphocholine (DOPC) bilayer membrane was measured by using the capacitance minimization technique to monitor surface potential [4]. Peptide–membrane interactions were further assessed by measuring peptide-induced release of 6-carboxyfluorescein from 1,2-dipalmitoyl-*sn*-glycero-3-phosphocholine (DPPC) vesicles [5]. The measured interactions agree with the amphiphilic moment model of opiate receptor site selectivity and support previous results, indicating an N-terminal α-helical structure of dyn inserted into the membrane [2, 3, 6].

Results and Discussion

Estimated [2] and experimental K_ds for the dyn N-terminal fragments, presented in Table 1, suggest that dyn-(1–13) and dyn-(1–9) can interact significantly with a lipid membrane. Both of these peptides have strong amphiphilic moments ($\text{Å} > 340$) oriented perpendicularly to the membrane surface ($\Phi < 16°$). This particular type of interaction is predicted to be negligibly small for dyn-(1–8) and dyn-(1–7) as seen by their weaker amphiphilic moments and angles of insertion. The discrepancy between the experimental and estimated K_ds for dyn-(1–8) and dyn-(1–7) may result from a different membrane structure than for dyn-(1–9) and dyn-(1–13). A possible candidate is a folded structure, which is required by μ-receptors but not by κ-receptors [7].

It has been shown by others [8] that the depth of incorporation of peptides into the hydrophobic membrane phase directly correlates with their propensity to induce a release of 6-carboxyfluorescein from vesicles, as revealed by the

Table 1 *Measured κ-receptor selectivity, B_{max}, and K_d values of dyn N-terminal peptide fragments compared to estimated K_d, amphiphilic moment (A), and moment angle (Φ)*

Peptide	κ-Receptor selectivity[a]	B_{max}[b] (mol/Å^2)	K_d exp.[b] (mol/l)	K_d est.[c] (mol/l)	A[c] [2]	Φ[c] [2]
1–13	1	$1.0 \cdot 10^{-4}$	$3.5 \cdot 10^{-5}$ $1.1 \cdot 10^{-5}$[6]	$1.2 \cdot 10^{-5}$	400	13°
1–9	0.74	$1.0 \cdot 10^{-4}$	$9.5 \cdot 10^{-5}$	$1.2 \cdot 10^{-5}$	343	16°
1–8	0.36	$7.3 \cdot 10^{-5}$	$1.7 \cdot 10^{-4}$	$7.8 \cdot 10^{-3}$	204	18°
1–7	0.67	$3.2 \cdot 10^{-5}$	$1.8 \cdot 10^{-4}$	$1.7 \cdot 10^{1}$	265	21°

[a] κ-Receptor selectivities, as represented by reciprocal values of the potency shift caused by 100 nM naloxone in the guinea pig ileum myenteric plexus longitudinal muscle bioassay [9], normalized to dyn-(1–13).

[b] Measured on neutral planar bilayer membranes by the capacitance minimization technique.

[c] Based on an inserted α-helix, see [2].

time-dependent increase of fluorescence following addition of peptide. The relative abilities of the opioid peptides to facilitate escape of the dye from DPPC-liposomes parallel the order of calculated peptide amphiphilic moments [2] as well as κ-receptor selectivity [9] [i.e., dyn-(1–13) > dyn-(1–9) > dyn-(1–8), dyn-(1–7)] (cf. Table 1). This order does not exclude the possibility of membrane-bound conformations of the shorter fragments that are less disruptive to the bilayer membrane.

These results support our view that the classical receptor requirements for site selectivity reflect a mechanism based upon peptide–membrane interactions.

Acknowledgements

This work was supported by project grants from the Swiss Federal Institute of Technology. JWB was the recipient of a Fulbright Fellowship.

References

1. Sargent, D.F. and Schwyzer, R., Proc. Natl. Acad. Sci. U.S.A., 83 (1986) 5774.
2. Schwyzer, R., Biochemistry, 25 (1986) 6335.
3. Schwyzer, R., Biochemistry, 25 (1986) 4281.
4. Schoch, P., Sargent, D.F. and Schwyzer, R., J. Membr. Biol., 46 (1979) 71.
5. Weinstein, J.N., Yoshikami, S., Henkart, P., Blumenthal, R. and Hagins, W.A., Science, 195 (1977) 489.
6. Erne, D., Sargent, D.F. and Schwyzer, R., Biochemistry, 24 (1985) 4261.
7. Schiller, P. and DiMaio, J., Nature, 297 (1982) 74.
8. Surewicz, W.K. and Epand, R.M., Biochemistry, 23 (1984) 6072.
9. Chavkin, C. and Goldstein, A., Proc. Natl. Acad. Sci. U.S.A., 78 (1981) 6543.

Membrane-adjacent regions of receptor proteins

Charles M. Deber[a,b], Christopher J. Brandl[c], Raisa B. Deber[d], Lynn C. Hsu[a,b] and Xenia K. Young[a,b]

[a]Research Institute, The Hospital for Sick Children, Toronto, Ont., Canada M5G 1X8
[b]Department of Biochemistry, [c]Banting and Best Department of Medical Research and [d]Faculty of Medicine, Division of Community Health, University of Toronto, Toronto, Ont., Canada M5S 1A8

Since receptor function depends on rapid activation of an intracellular domain (e.g., as in receptor kinases) upon binding of an extracellular ligand, we have been examining the transmembrane (TM) segment and membrane-adjacent residues of receptors with the goal of identifying residues functional in the requisite signal transduction. We have shown (Brandl et al., submitted for publication) that residue compositions of TM regions of receptor (R) proteins ($n = 11$) could not be distinguished statistically from corresponding regions of membrane-anchored proteins (MAP) (e.g., recognition molecules, structural proteins) [i.e., those with a functional external domain attached to a single hydrophobic membrane-spanning anchor segment ($n = 16$)], and have accordingly suggested that receptor TM regions contain only the structural information necessary for inserting [1] and anchoring the receptor to the membrane bilayer.

Noting that membrane-adjacent aqueous regions in both protein categories contained relatively high concentrations of positive (Arg, Lys) residues on the cytoplasmic side of their TM region (where these residues presumably act as a stop-transfer signal during synthesis [2]), we have now extended our study to a comparison of percentages of the four charged residues among the ten membrane-adjacent external and cytoplasmic residues of receptors and MAPs. Although sample sizes (approximately 100 residues in each group) were considered too small for statistical analyses, the cytoplasmic sides in both protein categories are seen to contain substantially higher percentages of Arg and Lys residues (vs both the 10 external and the average aqueous domain residue percentages), as well as decreased percentages of negative (Asp and Glu) residues; data in Fig. 1 display these trends in all comparisons shown [except Glu (R)]. In contrast, external adjacent residues [except Arg (MAP) where external Arg = 0] show minimal variation vs corresponding total aqueous residue percentages.

Electrostatic protein/membrane attractions which can arise via Arg and Lys contacts with phosphate head groups of the lipids in the adjacent cytoplasmic region, in conjunction with the hydrophobic anchoring provided within the TM region itself, appear to mitigate against vertical displacement of local TM segments

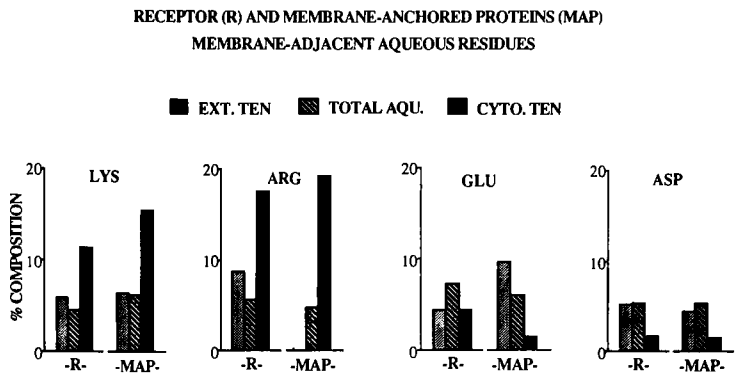

Fig. 1. Membrane-adjacent external and cytoplasmic residue percentages of the charged amino acids of R and MAPs. Residue % compositions in these regions are given and compared with overall aqueous domain percentages of the residues. Autonomous receptors used in the data base are: asialoglycoprotein-H1, asialoglycoprotein-H2, aspartate, epidermal growth factor, insulin, interleukin-2, LDL-human, serine chemoreceptor, T-cell, transferrin, and tyrosine kinase (Brandl et al., submitted for publication). See [5] for a compilation of MAP and further details relating to construction of the data base.

(i.e., for signaling purposes) from either side of the membrane. As well, helix dipole considerations [3] suggest that the high concentration of positive charge at the C-termini of the TM regions should further stabilize their existing (presumably) helical conformations. Thus, other transduction mechanisms must be considered, including receptor aggregation [4] and/or external/cytoplasmic domain–domain contact (Brandl et al., submitted for publication).

Acknowledgements

Supported by grants to C.M.D. from MRC and NSERC of Canada. C.J.B. held an MRC studentship.

References

1. Spiess, M. and Lodish, H.F., Cell, 44 (1986) 177.
2. Sabatini, D.D., Kreibich, G., Moumoto, T. and Adesnik, M., J. Cell Biol., 92 (1982) 1.
3. Shoemaker, K.R., Kim, P.S., Brems, D.N., Marqusee, S., York, E.J., Chaiken, I.M., Stewart, J.M. and Baldwin, R.L., Proc. Natl. Acad. Sci. U.S.A., 82 (1985) 2349.
4. Ullrich, A., Coussens, L., Hayflick, J.S., Dull, T., Gray, A., Tam, A.W., Lee, J., Yarden, Y., Libermann, T.A., Schlessinger, J., Downward, J., Mayes, E.L.V., Whittle, N., Waterfield, M.D. and Seeburg P.H., Nature, 309 (1984) 418.
5. Deber, C.M., Brandl, C.J., Deber, R.B., Hsu, L.C. and Young, X.K., Arch. Biochem. Biophys., 251 (1986) 68.

Ionic interactions between substrate side chains and individual subsites in the pepsin active site

Jan Pohl and Ben M. Dunn

Biochemistry and Molecular Biology, University of Florida, Box J-245, Gainesville, FL 32610, U.S.A.

Introduction

The active site of the aspartic endopeptidase family (e.g., pig pepsin) is an elongated cleft capable of binding 7 amino acids of a peptide substrate. Fruton demonstrated that elongation of a substrate from the minimum aromatic dipeptide on either side increases k_{cat}. We prepared oligopeptides long enough to fill the active site giving constant k_{cat} values; however, K_m is sensitive to the amino acid present at various positions.

Results and Discussion

We synthesized the following peptides (Applied Biosystems Model 430A synthesizer):

I	Lys-Pro-Ala-Glu-Phe-Nph-Arg-Leu
II	Lys-Pro-Asp-Glu-Phe-Nph-Arg-Leu
III	Lys-Pro-Lys-Glu-Phe-Nph-Arg-Leu
IV	Lys-Pro-Ala-Lys-Phe-Nph-Arg-Leu
V	Lys-Pro-Lys-Lys-Phe-Nph-Arg-Leu
VI	Lys-Pro-Ala-Lys-Phe-Nph-Arg-Leu-Arg-NH_2
VII	Lys-Pro-Ala-Lys-Phe-Nph-Arg-Lys-Arg-NH_2
	P5 P4 P3 P2 P1 P1′ P2′ P3′ P4′

Cleavage of purified (IEC or HPLC) peptides by pepsin between Phe and Nph (*p*-nitrophenylalanine) (37°) was studied by the absorbance change of Nph. k_{cat} values for I–VII range between 10 and 120 s^{-1} and exhibit a pH-independent plateau between pH 2.8 and 5.0, followed by a decrease with increasing pH.

The pH dependence of K_m, however, shows considerable variation. In Fig. 1, substrate I has a plateau between pH 2.5 and 6.0 in pK_m vs pH. In substrate II, Ala (P3) was replaced with Asp resulting in a decrease in binding on the plateau, but, more significantly, a decrease above pH 4.9 due to repulsion between

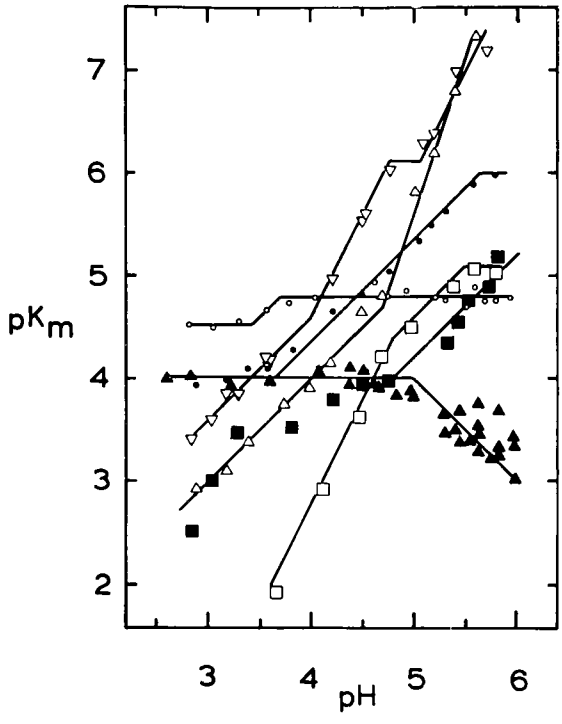

Fig. 1. Composite plot of pK_m *vs pH for substrates I (○), II (▲), III (■), IV (●), V (□), VI (▽), and VII (△).*

Glu 13 (S3 region of pepsin) and Asp in P3. For III, Lys P3, an increase in binding with pH is seen and is due to an interaction between Lys and the negative charge of Glu 13 at higher pH.

Lys in P2 (IV) improves binding (slope of the line for substrate IV is +1.0 above pH 3.4). This effect is due to a different enzyme carboxyl than Glu 13 in the S3 subsite. Lys in P2 avoids the harmful effect on binding seen with Lys in P3.

It is relevant then to consider V, with Lys in both P3 and P2. Binding at low pH is poor, with data unobtainable below pH 3.5, however, binding improves dramatically with increasing pH (pK_m vs pH for V has a slope of +2.0). Above pH 4.7, the data shift back to a slope of +1.0.

Finally, substrate VI exhibits a complex pK_m vs pH plot with regions of slope +1.0 and +2.0, suggesting that P4′ can form ionic interactions with suitable enzyme groups. For substrate VII where Lys replaces Leu at P3′, binding increases (slope +1.0) from pH 2.9 to approximately 4.6, then increases with a slope

of +3.0. This implicates the S3′ region as capable of interacting with a cationic group of the substrate. These effects result (e.g., substrate VII) in improvements in binding of 4 log units with pH (K_m values at higher pH as low as 20 nM). These effects could be exploited to design inhibitors for these enzymes to be efficient at nearly physiological pHs.

Relationship between the antiviral activity of peptides and the stabilization of membrane bilayers

Richard M. Epand[a], Roderick C. McKenzie[b], David C. Johnson[b], Thomas J. Lobl[c], H.E. Renis[d], L.L. Maggiora[c] and M.W. Wathen[d]

[a]Department of Biochemistry and [b]the Molecular Virology and Immunology Program, McMaster University, Hamilton, Ont., Canada

[c]Biopolymer Chemistry and [d]Cancer and Viral Disease Research, The Upjohn Company, Kalamazoo, MI, U.S.A.

Introduction

Viral infection of cells requires membrane fusion. Several factors, many of them interrelated, control the rate of membrane fusion. Substances which promote the hexagonal phase also promote membrane fusion, irrespective of whether the hexagonal phase or lipidic particles are actually intermediates in the fusion process. The effects of drugs on the bilayer-to-hexagonal phase transition can be used to predict how compounds modulate membrane fusion.

In addition to these nonspecific effects on the rate of membrane fusion, peptides have been designed to mimic the structure of the amino terminal sequence of viral fusion proteins [1]. Such peptides can compete with viral fusion proteins for binding to specific sites on host cell membranes, however, several of these peptides also inhibit the conversion of phospholipid bilayers to the hexagonal phase [2]. It is thus possible that peptides can inhibit viral replication by both specific and nonspecific mechanisms.

Results and Discussion

Cyclosporin is a peptide with known antiviral activity. We have shown that at low concentrations cyclosporin raises the bilayer-to-hexagonal phase transition temperature of dielaidoylphosphatidylethanolamine (DEPE) and it inhibits membrane fusion in model systems [3]. Cyclosporin also specifically inhibits virus-induced cell fusion [4].

Another group of peptides which inhibits fusion phenomenon in cells is carbobenzoxy(Z)-dipeptide-NH_2. Several of these modified dipeptides inhibit histamine release from mast cells [5], catecholamine release from adrenal chromaffin cells [5] and synaptic transmission at the neuromuscular junction [6]. All of these processes are exocytosis phenomena which require membrane

fusion. In addition, direct cell-cell fusion of myoblasts is inhibited by these peptides [7]. It has been suggested that these blocked peptides act by inhibiting a metalloendoprotease required for cell fusion. We tested the activity of several of these peptides in inhibiting the cytopathic effect of measles virus (ATCC) on Vero cells. We find that Z-Ser-Leu-NH_2, which is a potent inhibitor of myoblast fusion, also has antiviral activity at a concentration of 62 μg/ml. The peptides Z-Gly-Phe-NH_2, Z-Gly-Leu-NH_2 and Z-Gly-Gly-NH_2 which had less effect on myoblast fusion showed no antiviral activity at a concentration of 250 μg/ml. All of the Z-dipeptide-NH_2 we tested raised the bilayer-to-hexagonal phase transition temperature of DEPE. The two most potent bilayer stabilizers are Z-Gly-Phe-NH_2 followed by Z-Ser-Leu-NH_2. The Z-Ser-Leu-NH_2 may be more potent in inhibiting membrane fusion since it contains a very polar side chain which could make the membrane surface more hydrophilic. Thus the effects of these peptides on lipid properties provide an alternative mechanism to metalloprotease inhibition to explain their anti-membrane fusion activity.

Following the work of Choppin et al. [1], we synthesized a series of short peptides which resembled the amino-terminal sequence of the respiratory syncytial virus (RSV) F1 glycoprotein. The amino terminus was blocked with a Z-group, and several D-amino acid substitutions were made. The longest of these peptides was ZfLGfllG (lower case letters refer to D-amino acids). Several carboxyl-terminal deletion analogs were also studied. None of the peptides had antiviral activity against RSV; however, the full peptide had some antiviral activity against measles virus but it was also cytotoxic as was the peptide corresponding to the first 5 amino acids. The peptides which were most potent in raising the bilayer-to-hexagonal phase transition temperature of DEPE were ZfLGfl and ZfLGfll. The latter peptide had the most potent antiviral activity against measles virus. Since the amino acid sequence of these peptides more closely resembles the sequence of an RSV glycoprotein than it does the measles fusion protein, the antimeasles activity probably results from a nonspecific membrane effect. One of the differences between measles and RSV is that the measles virus fuses directly with the host plasma membrane, while RSVs are taken into the cell by endocytosis and eventually fuse with lysosomal membranes. We have noted that antiviral drugs which stabilize membrane bilayers are more effective against viruses which enter the cell by fusion with the plasma membrane. A good example of this is a comparison of two structurally related antiviral agents – amantadine and tromantadine (Cheetham and Epand, submitted for publication). Thus a variety of structurally unrelated peptides including cyclosporin, Z-L-Ser-L-Leu-NH_2 and ZfLGfll exhibit antiviral activity and they also raise the bilayer-to-hexagonal phase transition temperature. We suggest that this thermal stabilization of the bilayer phase is an indication of the ability of these peptides to inhibit membrane fusion. In the case of cyclosporin, we have directly demonstrated that it can inhibit viral-induced cell-cell-fusion. This mechanism may provide

a new approach in designing broad-spectrum antiviral chemotherapeutic agents.

Acknowledgements

This work was supported, in part, by MRC.

References

1. Choppin, P.W., Richardson, C.D. and Scheid, A., In Stuart-Harris, C.H. and Oxford, J. (Eds.) Problems of Antiviral Therapy, Academic Press, London, 1983, p. 13.
2. Epand, R.M., Biosci. Rep., 6 (1986) 647.
3. Epand, R.M., Epand, R.F. and McKenzie, R.C., J. Biol. Chem., 262 (1987) 1526.
4. McKenzie, R.C., Epand, R.M. and Johnson, D.C., Virology, 158 (1987) in press.
5. Mundy, D.I. and Strittmatter, W.J., Cell, 40 (1985) 645.
6. Baxter, D.A., Johnston, D. and Strittmatter, W.J., Proc. Natl. Acad. Sci. U.S.A., 80 (1983) 4174.
7. Couch, C.B. and Strittmatter, W.J., Cell, 32 (1983) 257.

Direct ^{13}C NMR observation of a tetrahedral species in the binding of a peptidyl ketone pseudosubstrate to penicillopepsin, a fungal aspartic proteinase

Juergen Maibaum[a], Madhup K. Dhaon[a], Paul G. Schmidt[b], Mitsuo Oka[b] and Daniel H. Rich[a]

[a]*School of Pharmacy, University of Wisconsin-Madison, 425 N. Charter St., Madison, WI 53706, U.S.A.*

[b]*Vestar Inc., 939 E. Walnut St., Pasadena, CA 91106, U.S.A.*

Introduction

Pepstatin-derived inhibitors that contain statone (4-amino-3-oxo-6-methylheptanoic acid) or ketomethylene dipeptide isosteres have been used to probe the catalytic mechanism of aspartic proteinases [1]. Previous ^{13}C NMR studies have shown that the ^{13}C labeled ketone group in statone and ketomethylene peptides is converted to a tetrahedral *gem*-diol in an enzyme-catalyzed process when these pseudosubstrates bind to pepsin [2, 3]. The X-ray crystal structure of pepsin-bound inhibitors like pepstatin has not yet been resolved, as opposed to penicillopepsin–inhibitor complexes [4]. Thus, our strategy was to develop new ketone inhibitors that would tightly bind to this fungal enzyme in order to obtain a system in which both ^{13}C NMR and X-ray crystallography could be used to analyze the tetrahedral adduct. Tight-binding inhibition of penicillopepsin ($K_i = 2.1$ nM) [5] and a refined crystal structure of the inhibitor bound to the fungal proteinase [4] have been reported recently for the lysine-statine peptide IvaValVal-LySta-OEt (**1**) (Scheme 1). We therefore considered the synthesis of the analogous lysine-statone peptide IvaValVal-LySto-OEt (**2**) [4(S),8-diamino-3-oxo-octanoic acid, LySto] as a promising approach to further elucidate the pseudosubstrate binding mode.

Results and Discussion

Attempts to prepare peptide **2** by methods that had been used in the synthesis of statone-containing inhibitors gave unsatisfactory results. Therefore, we developed a new, efficient synthetic route to **2** (Scheme 1). The γ-amino-β-ketoester **4** was prepared from diprotected L-lysine by condensation of the imidazolide with the ethyl malonate magnesium enolate. Racemization of C-4 during the synthesis of **4** was less than 3%. The tripeptide IvaValVal-OH was coupled with

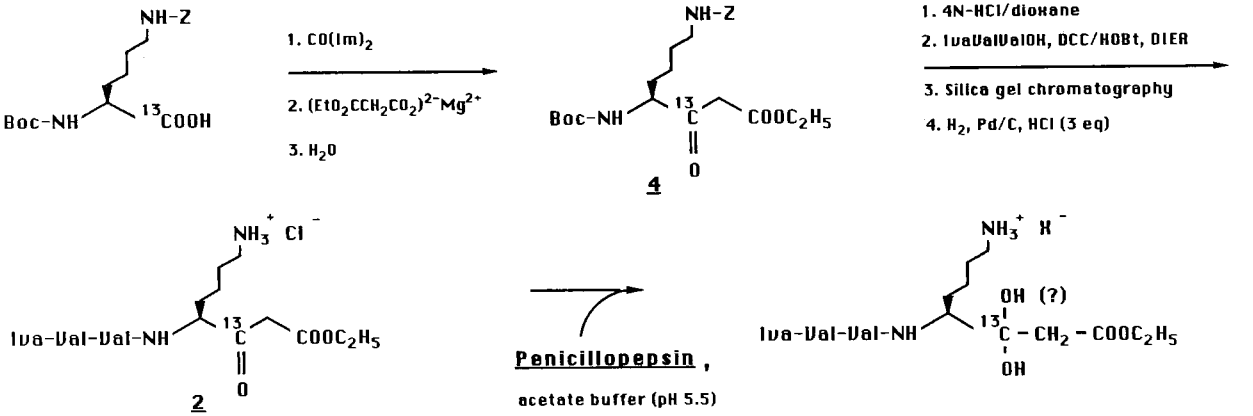

Scheme 1. Synthetic route to lysine-statone (LySto) peptide **2** *and formation of a tetrahedral adduct upon binding of the inhibitor to penicillopepsin.*

Boc-deprotected **4** as its active ester after preactivation with DCC/HOBt to give Z-protected **2** in 85–90% yield. The synthesis was repeated with IvaVal-D-Val-OH to obtain the N-protected D-Val[3] epimer **3**. Epimerization at the C-terminal valine during preactivation coupling was only 1–2%, as determined by RPHPLC. Hydrogenolysis under acidic conditions finally gave the diastereomers **2** and **3**, respectively.

The 4(S)-LySto peptide **2** is a potent slow-binding inhibitor of penicillopepsin ($K_i = 10.9$ nM, pH 5.5) and is only 5–10 times less active than the lysine-statine compound **1**. The D-Val diastereomer **3** is only a weak inhibitor of the fungal enzyme ($K_i = 1540$ nM).

The C-3 of labeled **2** (>98% ^{13}C-isotope enriched) was shown to be >95% trigonal in aqueous buffer (pH 5.5) by ^{13}C NMR spectroscopy. After addition of the inhibitor to penicillopepsin, the C-3 signal at 204.40 ppm disappeared, and a new resonance was observed near 99.2 ppm. The ^{13}C upfield shift of about 105 ppm indicates that the geometry at C-3 is converted from trigonal to tetrahedral when ketone **2** binds to the enzyme and is consistent with addition of oxygen. The tetrahedral adduct may result from enzyme-catalyzed formation of a *gem*-diol species (Scheme 1) as was found in the case of pepsin [2, 3].

Acknowledgements

We wish to thank NIH (DK20100) and the Deutsche Forschungsgemeinschaft, F.R.G. (J.M.), for financial support, and Karen Rebholz for technical assistance.

References

1. Rich, D.H., In Barrett, A.J. and Salvesen, G.S. (Eds.) Proteinase Inhibitors, Elsevier, New York, NY, 1986, p. 179.
2. Rich, D.H., Bernatowicz, M.S. and Schmidt, P.G., J. Am. Chem. Soc., 104 (1986) 3535.
3. Rich, D.H., Salituro, F.G., Holladay, M.W. and Schmidt, P.G., In Vida, J.A. and Gordon, M. (Eds.) Conformationally Directed Drug Design, ACS Symposium Series No. 251, American Chemical Society, Washington, DC, 1984, p. 211.
4. James, M.N.G., Sielecki, A.R. and Hofmann, T., In Kostka, V. (Ed.) Aspartic Proteinases and their Inhibitors, De Gruyter, Berlin, 1985, p. 163.
5. Salituro, F.G., Agarwal, N., Hofmann, T. and Rich, D.H., J. Med. Chem., 30 (1987) 286.

Activities of glucagon antagonists on normal liver: Evidence for cAMP-independent events

Roberta L. McKee[a], Dev Trivedi[b], Christian Zechel[b], David Johnson[c], Klaus Brendel[c] and Victor J. Hruby[a,b]

Departments of [a]Biochemistry, [b]Chemistry and [c]Pharmacology, University of Arizona, Tucson, AZ 85721, U.S.A.

Introduction

The peptide hormone glucagon is important in the maintenance of glucose homeostasis in animals. Although classically viewed as a hormone mediating its actions via cyclic AMP (cAMP), recent studies suggest that glucagon may in fact mediate some of its actions independent of this second messenger [1-3].

In order to obtain further insight into the basis of these observations we have examined both glucagon and one of our most potent new, totally synthetic, glucagon antagonists [*des*-amino-His[1], D-Phe[4], Tyr[5], Arg[12], Lys[17,18], Glu[21]]-glucagon ([*des*-amino-fYRKKE]glucagon) for bioactivities throughout the glycogenolytic cascade. Using a nonrecirculatory perifusion technique for thin liver slices, we can investigate hepatic hormonal mechanisms by monitoring both intracellular events and overall cellular processes simultaneously. We observe that glucagon at low concentrations and the adenylate cyclase antagonist [*des*-amino-fYRKKE]glucagon at high concentrations stimulate hepatic glycogenolysis independent of any intracellular cAMP accumulation or activation of the cAMP-dependent protein kinase. These results support the notion that glucagon can mediate physiological events independent of cAMP.

Results and Discussion

[*des*-amino-fYRKKE]Glucagon was synthesized, purified, and characterized by methods similar to those previously reported [4]. Receptor binding and adenylate cyclase activities on liver plasma membranes were measured as before [5]. The apparatus and methods for utilizing the perifusion system and for examining cAMP content, cAMP-dependent protein kinase, and glycogenolysis will be reported elsewhere (McKee, Trivedi, Hruby and Brendel, unpublished results).

[*des*-amino-fYRKKE]Glucagon displays all the properties of a classical glu-

cagon antagonist. This compound binds to the glucagon receptor with high affinity (IC_{50} = 32 nM) but is inactive in stimulating adenylate cyclase even at very high concentrations (1×10^{-5} M). Furthermore, it is a potent inhibitor of glucagon-stimulated cAMP production (pA_2 = 7.5). Despite the fact that [*des*-amino-fYRKKE]glucagon does not transduce the cAMP second messenger system, this compound can still elicit hepatic glucose production. Results in Table 1 show that although intracellular cAMP levels do not increase and cAMP-dependent protein kinase is not activated, [*des*-amino-fYRKKE]glucagon, at high doses, does stimulate glycogenolysis.

The native hormone itself also displays cAMP-independent glycogenolysis. At doses lower than those sufficient to increase cAMP accumulation or activate the corresponding kinase (0.5 nM), glucose production is observed. These results provide strong evidence that at least two glucagon-stimulated transduction mechanisms operate for hepatic glycogenolysis, one of which acts independently of cAMP. Although the mediator of the cAMP-independent glycogenolysis has yet to be identified, current studies in our laboratory and others [6, 7] suggest that calcium mobilization which is observed with low doses of glucagon may play a part in this process. Furthermore, these results demonstrate that a glucagon analog which antagonizes glucagon-stimulated cAMP production is not necessarily equivalent to a glucagon antagonist of glycogenolysis. With respect to glycogenolysis, a total glucagon antagonist must inhibit all intracellular mediators which collectively stimulate the overall cellular response.

Table 1 *Activities of perifused liver slices challenged with glucagon and [des-amino-fYRKKE]glucagon*

[Peptide] (nM)	cAMP accumulation (pmoles/mg protein)	cAMP-PK activity ratio (–cAMP/+cAMP)	Glucose production (% stimulation)
None	3.98 ± 0.65[a]	0.073 ± 0.012[a]	100 ± 1[a]
Glucagon			
1	5.21 ± 1.29	0.083 ± 0.009	122 ± 2[b]
16	8.66 ± 1.06[b]	0.189 ± 0.011[b]	156 ± 3[b]
512	15.43 ± 0.95[b]	0.516 ± 0.115[b]	219 ± 17[b]
[*des*-amino-fYRKKE]Glucagon			
512	3.42 ± 0.36	0.072 ± 0.005	99 ± 9
4,096	4.01 ± 0.28	0.061 ± 0.002	132 ± 15[b]
10,000	4.01 ± 0.88	0.093 ± 0.013	155 ± 13[b]

[a] All values are reported as the mean ± SEM.
[b] Significantly different from control, $p \leqslant 0.05$.

Acknowledgements

Supported by a grant from the U.S. Public Health Service AM 21085.

References

1. Corvera, S., Huerta-Bahena, J., Pelton, J.T., Hruby, V.J., Trivedi, D. and Garcia-Sainz, J.A., Biochim. Biophys. Acta, 804 (1984) 434.
2. Murphy, G.J., Hruby, V.J., Trivedi, D., Wakelam, M.J.O. and Houslay, M.D., Biochem. J., 243 (1987) 39.
3. Khan, B.A., Bregman, M.D., Nugent, C.A., Hruby, V.J. and Brendel, K., Biochem. Biophys. Res. Commun., 93 (1980) 729.
4. Gysin, B., Trivedi, D., Johnson, D.G. and Hruby, V.J., Biochemistry, 25 (1986) 8278.
5. McKee, R.L., Pelton, J.T., Trivedi, D., Johnson, D.G., Coy, D.H., Suerias-Diaz, J. and Hruby, V.J., Biochemistry, 25 (1986) 1650.
6. Charest, R., Blackmore, P.F., Berthon, B. and Exton, J.H., J. Biol. Chem., 258 (1983) 8769.

Crystal structure of the covalent complex formed by a peptidyl α,α-difluoro-β-keto amide with porcine pancreatic elastase at 1.78 Å resolution

Lori H. Takahashi[a], R. Radhakrishnan[b], Edgar F. Meyer, Jr.[b] and Diane Amy Trainor[c]

[a]Department of Chemistry and [b]Department of Biochemistry and Biophysics, Texas A & M University, College Station, TX 77843, U.S.A.

[c]Stuart Pharmaceuticals, Division of ICI Americas Inc., Wilmington, DE 19897, U.S.A.

Elastases (E.C.3.4.21.11) are possibly the most destructive enzymes in the body, having the ability to degrade virtually all connective tissue components. They have been directly linked to degenerative diseases [1, 2] for which no drugs are currently available.

Peptidyl fluorinated ketones have been shown to be excellent inhibitors of the elastases [3, 4]. The enhanced electrophilicity of the fluorinated ketone carbonyl was expected to facilitate an enzyme-catalyzed addition of the active site serine (Ser-195) to the ketone carbonyl forming a stable hemiketal intermediate. Additional interactions between the S′ subsites (nomenclature of Schechter and Berger, [5]) of the enzyme and the P′ fragments of the peptidyl difluoroketone inhibitors were believed to contribute to the overall tight binding. To establish unequivocally the nature of the complexation of porcine pancreatic elastase (PPE) with a peptidyl α-α-difluoro-β-keto amide, we report the crystal structure of the enzyme complexed with (S)-*N*-acetyl-L-alanyl-*N*[3,3]difluoro-1(1-methylethyl)-2,4-dioxo-4[(2-phenylethyl)aminobutyl]-L-prolinamide using 1.78 Å resolution X-ray data.

The complex was refined to $R=0.16$ using EREF [6]. Inactivation of the enzyme by the inhibitor results in the formation of a covalent bond (1.47 Å) forming a hemiketal between the inhibitor valine carbonyl carbon atom and Ser-195 $O\gamma$. A stereoview of the inhibitor in the extended binding site of PPE is shown in Fig. 1. Five hydrogen bonds (ranging from 2.58 to 2.97 Å) form between the enzyme and the inhibitor, including one between His-57 and one of the fluorine atoms. The complex forms an antiparallel β-pleated sheet hydrogen bonding arrangement with the enzyme.

The complex can be considered as a structural mimic of the tetrahedral intermediate that is formed in the pathway for substrate hydrolysis. The inhibitor can thus be regarded as a transition-state analog.

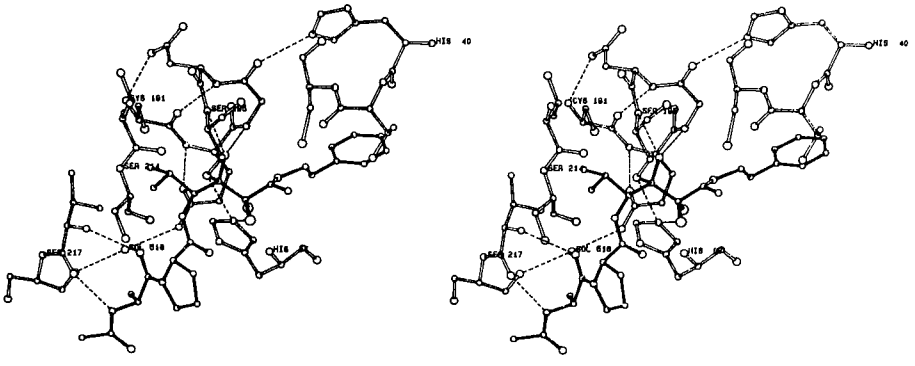

Fig. 1. A stereoview of the inhibitor (filled bonds) in the active site of porcine pancreatic elastase (unfilled bonds). Hydrogen bonds are shown by dashed lines.

References

1. Janoff, A., Annu. Rev. Med., 36 (1985) 207.
2. Stein, R.L., Trainor, D.A. and Wildonger, R.A., Annu. Rep. Med. Chem., 20 (1985) 237.
3. Imperiali, B. and Abeles, R.H., Biochemistry, 25 (1986) 3760.
4. Stein, R.L., Strimpler, A.M., Trainor, D.A., Edwards, P.D., Lewis, J.J., Mauger, R.C., Schwartz, J.A., Stein, M.M., Wildonger, R.A. and Zoppola, M.A., Biochemistry, (1987) in press.
5. Schechter, I. and Berger, A., Biochem. Biophys. Res. Commun., 27 (1967) 157.
6. Jack, A. and Levitt, M., Acta Crystallogr., 34A (1978) 931.

Session V
Protein design/engineering

Chair: Irwin Chaiken
National Institutes of Health
Bethesda, Maryland, U.S.A.

Synthetic proteins with a new three-dimensional architecture

Manfred Mutter
Institute of Organic Chemistry, University of Basel, CH-4056 Basel, Switzerland

Introduction

The considerable progress in understanding the rules which govern protein folding and topology [1, 2] has stimulated efforts to design peptide sequences with a predetermined three-dimensional conformation ('de novo design'), giving access to macromolecules with tailor-made chemical, biological, or catalytic properties [3]. In this paper, a strategy for the construction of artificial proteins with a new architecture is presented, which combines today's knowledge about secondary and tertiary structure formation of peptides and proteins with techniques of synthetic chemistry.

Results and Discussion

As depicted in Fig. 1, amphiphilic peptides with a potential for secondary structure formation are attached to a multifunctional template molecule which enhances the spatial accommodation of the peptide blocks to a well-defined tertiary structure. The formation of a hydrophobic core is considered to be

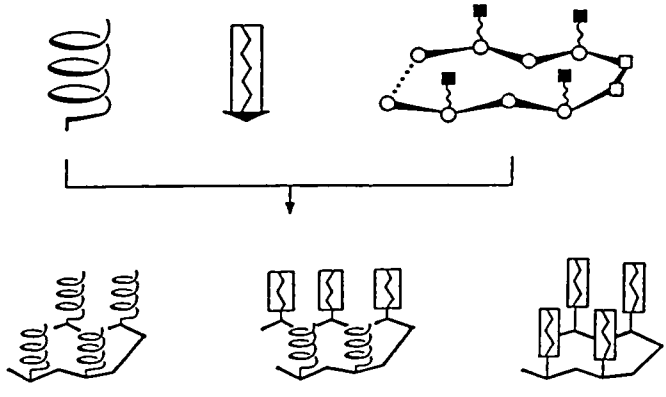

Fig. 1. Concept of template-assembled synthetic proteins (TASP).

Table 1 *Template-assembled synthetic proteins (TASP)*

TASP	Topology	Primary sequences[a]
I	$\beta\alpha\beta$	*T*: K(α_I)-P-K(β_I)-K(β_I) β_I: [T-V]$_3$ α_I: ^{1}E-A-L-Aib-A-E-L-Aib-E-L-E-A^{12}
II	4α	*T*: K(α_{II})-K-K-(α_{II})-P-G-K-(α_{II})-E-K(α_{II}) α_{II}: D-A-A-T-A-L-A-N-A-L-K-K-L^{13}
III	8α	*T*: [K(α_{III})]$_4$-P-G-[K(α_{III})]$_4$ α_{III}: A^1-L-E-A-L-L-E-A-L-A-E-A-L-E-E-A^{16}
IV	8β	*T*: [K(β_{IV})]$_4$-P-G-[K(β_{IV})]$_4$ β_{IV}:[V-K]$_4$

[a] *T* = template molecule; K(α_i) = lysine residue with helical peptide α_i attached to the side chain.

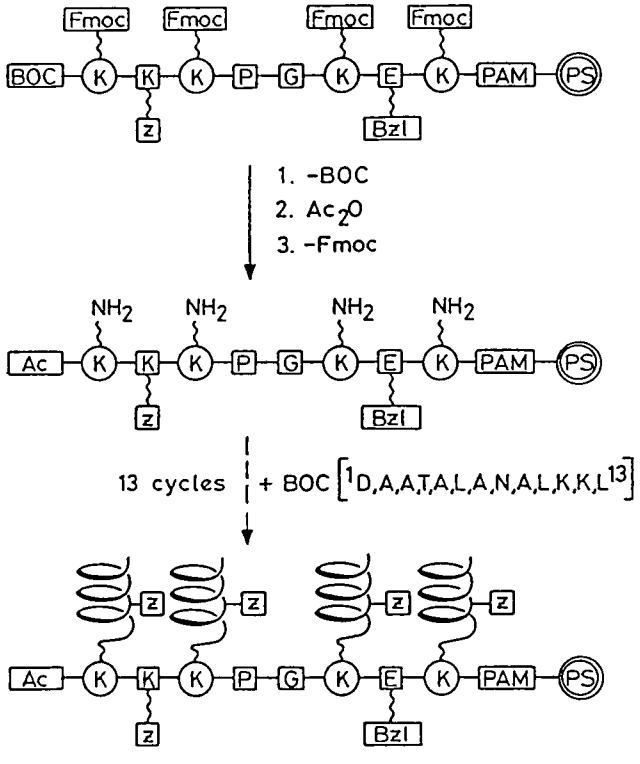

Fig. 2. Scheme for the synthesis of a 4-helix-bundle TASP (II in Table 1).

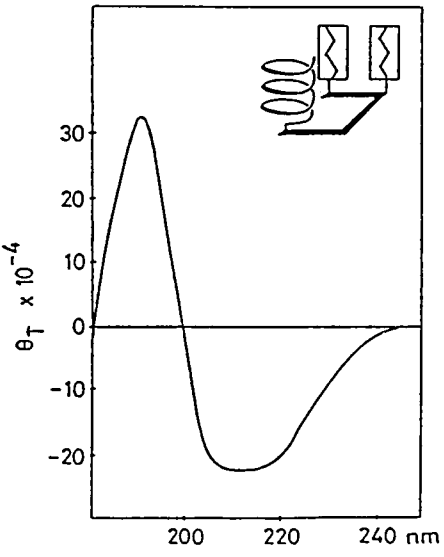

Fig. 3. CD spectra of TASP I in H_2O/TFE =8/2; 10^{-4}M.

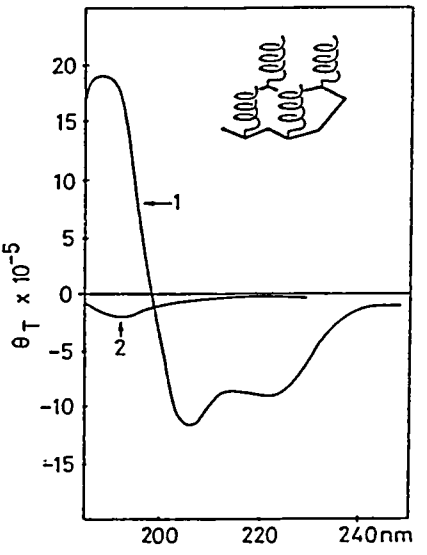

Fig. 4. CD spectra of TASP II (curve 1) and α_{II} (curve 2) in H_2O, pH 7; 10^{-4}M.

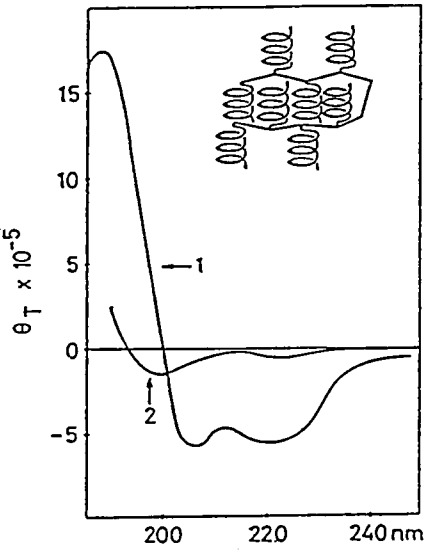

Fig. 5. CD spectra of TASP III (curve 1) and α_{III} (curve 2) in H_2O, pH 7; 10^{-4}M.

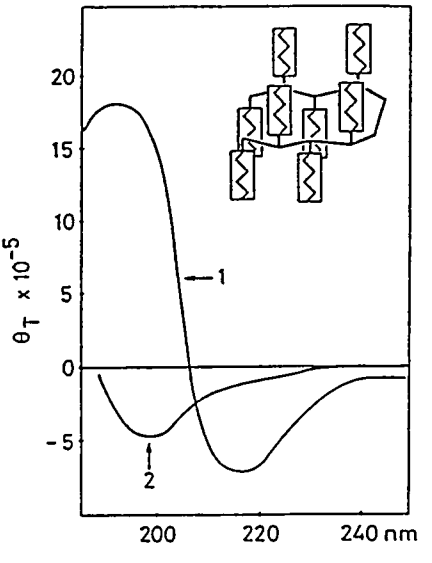

Fig. 6. CD spectra of TASP IV (curve 1) and β_{IV} (curve 2) in H_2O, pH 10; 10^{-4}M.

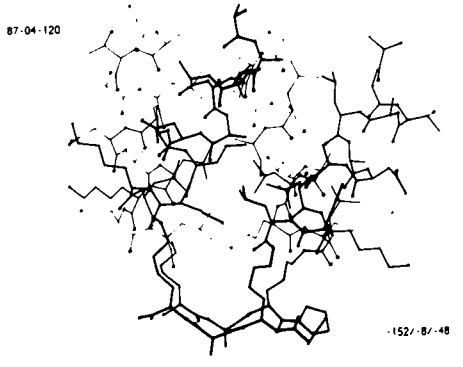

Fig. 7. Hypothetical 4-helix-bundle structure of TASP II after energy minimization by computer-assisted molecular modeling (Mutter, M. et al., in preparation).

the major driving force for the adoption of protein-like topologies. As verified by molecular modeling studies, oligopeptides with β-hairpin conformation are potent candidates for use as template molecules. The availability of a broad set of orthogonal protecting groups for the temporary protection of the attachment sites in the template (e.g., ϵ-NH_2 of K, Table 1) allows the assembly of blocks of variable sequence and mutual orientation.

According to this general concept, template-assembled synthetic proteins (TASP) of different folding topologies have been designed and synthesized by polymer-supported strategies (Mutter et al., in preparation) (Table 1). A representative protocol for the solid phase synthesis of an artificial 4-helix-bundle protein (II) is depicted in Fig. 2. Most notably, the parallel growth of the helical blocks on the template represents an extremely efficient strategy for the establishment of the structure.

Conformational studies carried out so far strongly support the formation of the hypothetical tertiary structures. As shown by the circular dichroism (CD) spectra in Figs. 3–6, the peptides adopt well-developed secondary structures (not disrupted by dilution) when assembled on the multifunctional template under a variety of experimental conditions (curve 1 in Figs. 4–6); on the other hand, the single peptides (not attached to the template) of identical sequence and chain length show unordered conformations (curve 2 in Figs. 4–6). Consequently, the

onset of stable secondary structures of these amphiphilic peptides after linkage to the template can only be rationalized by the formation of a tertiary structure (Fig. 7). Similar to the finding in natural proteins, helices and β-sheets are stabilized by long-range interactions within the hydrophobic core of the folded structures. We may conclude that the formation of a tertiary structure is not bound to the complex folding mechanism of linear polypeptide chains selected over millions of years. Rather than competing with this evolutionary process, the construction of artificial proteins with a new architecture appears to be more promising. The access to predetermined three-dimensional conformations according to the present concept will inspire chemists to create macromolecules with new properties and functions.

Acknowledgements

This work was supported by the Swiss National Science Foundation.

References

1. Jaenicke, R., Angew. Chem., Int. Ed., 23 (1984) 395.
2. Richardson, J.S., Adv. Protein Chem., 34 (1981) 167.
3. Mutter, M., Angew. Chem., Int. Ed., 24 (1985) 639.

Sequence simplification and randomization and the design of peptide recognition surfaces

Irwin Chaiken, Shoji Ando, Giorgio Fassina and Yechiel Shai
National Institute of Diabetes and Digestive and Kidney Diseases, National Institutes of Health, Bethesda, MD 20892, U.S.A.

Introduction

In the synthetic redesign of biologically active peptides and proteins, there are usually three main questions posed. First, can one determine which structural elements are important for function? Second, can the mechanistic roles of these elements be defined? And third, can one use this accumulated wisdom to formulate generalized rules for how amino acid sequence produces higher order properties? The first of these questions normally has been approached by one-site-at-a-time mutation, the bell-weather tactic of chemical modification, peptide synthesis, and, most recently, site-directed genetic engineering. Nonetheless, when trying to define molecular mechanisms and general rules for polypeptides as a group, simultaneous mutation at many sites in a sequence becomes more useful.

Two approaches we have used for multisite sequence redesign are simplification and randomization. In simplification, it is assumed that one understands enough about the importance of particular structural elements to predict how the whole sequence works together to produce function. On this basis, a model sequence is made which contains many simultaneous sequence changes but retains the most important structural elements for function. In contrast, randomization assumes ignorance, the lack of understanding of what structural elements are important, and therefore seeks to examine all possible sequence alternatives in order to identify the ones that can produce function.

Simplification and randomization can be used to understand how peptides recognize other peptides and proteins. A major continuing question in peptide and protein recognition, for example in peptide–antibody, peptide–receptor, and protein fragment complexes, is what in the sequence produces interaction and can we learn enough to regulate the affinity or specificity of the recognition process. In cases for which high resolution structures of peptide–protein complexes have been obtained, it can be deduced that recognition occurs most usually

Correspondence to: I.M. Chaiken, National Institutes of Health, Bldg. 6, Room 131, Bethesda, MD 20892, U.S.A.

with peptide components that are folded into conformationally compact structures with a well-defined part of the structure forming an exposed surface containing a relatively limited number of correctly placed contact elements. This would predict that peptides and proteins could be mimicked by greatly simplified polypeptides, in which much of the structure is replaced by a sequence which can form a conformational frame which retains groups on its surface. Of course, simplifying sequence in this way ignores flexibility, which in fact cannot be ignored in many cases. Yet, as a first order approximation, the simplification approach to sequence redesign has been successful in several systems. It also sets the stage for controlled use of randomization as a tool to learn how structural information 'fine-tunes' recognition.

The S-peptide/S-protein Interaction

In sequence design experiments with the 'prototype' system of bovine pancreatic ribonuclease S (RNase S), we have sought to 'decode' the S-peptide/S-protein recognition process by sequence simplification of S-peptide [1–4]. We prepared a series of synthetic, sequence-modeled S-peptides of which the parent sequence is shown in Fig. 1. Here, much of the sequence was replaced by Ala residues to provide a sequence-simplified poly-Ala α-helical frame. Phe-8 and Met-13 were preserved to 'recognize' the S-protein surface. The catalytically important His-12 also was retained in order to use the appearance of enzymatic activity as at least one diagnostic of functional peptide-protein interaction.

The retention of close-to-native structural properties of the semisynthetic RNase S species formed by parent, sequence-simplified S-peptide was established in solution by the enzyme activity induced upon addition to S-protein and by quantitative affinity chromatographic analysis of binding of model S-peptide to immobilized S-protein. Verification of structural mimickry upon sequence simplification was obtained by X-ray diffraction analysis of the model semisynthetic complex [3]. Model and native S-peptides were found to assume close to the same helical structure and orientation when bound to S-protein. Phe-8 and Met-13 side chains of model S-peptide make contact with the same hydrophobic area on the S-protein surface as does native S-peptide. The importance of Phe-8 and Met-13 as contact elements was verified by showing that replacement of either by Ala significantly destabilizes S-peptide/S-protein interaction (Liang, X., Dalzoppo, D., Fontana, A., Shai, Y. and Chaiken, I.M., unpublished experiments; see Fig. 1).

The results of sequence simplification offer an opportunity to evaluate the use of sequence randomization to examine what is particularly important about contact residue side chains. Met-13, a model S-peptide was synthesized (Y. Shai and I.M. Chaiken, unpublished experiments) with a large set of amino acids incorporated simultaneously into position 13 by coupling with the appropriate

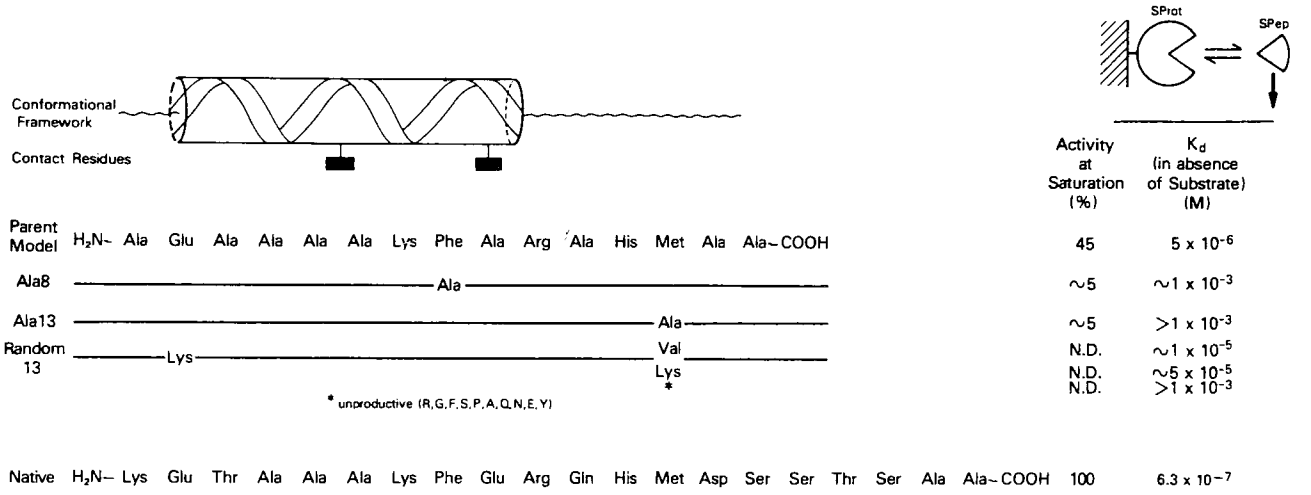

Fig. 1. Overall logic and redesign by sequence simplification and randomization of ribonuclease S-peptide recognition surface for S-protein [1–4]. Top left*: Diagram depicting critical elements of structure for S-peptide recognition. These include an α-helical conformational framework of residues 3-13 and two contact side chains at Phe-8 and Met-13.* Top right*: Diagram depicting affinity chromatographic analysis of native and mutant S-peptide interaction by elution on immobilized S-protein. Activities at saturation are the maximum enzymatic activities, relative to that of native S-peptide/S-protein complex, produced upon titrating native S-protein with sequence modeled peptide with 2',3'-cyclic cytidine monophosphate as substrate at 0.1 M Tris–HCl, pH 7.13. Values of* K_d *are for dissociation constants of native or model S-peptide binding to S-protein as determined by analytical affinity chromatography in the absence of substrate.*

mixture of N^{α}-Boc amino acids (see Fig. 1). The 'random 13' peptide mixture so produced was screened by isocratic affinity chromatography on immobilized S-protein under binding conditions to select peptides which could bind S-protein. Most of the peptide material did not bind. The small retarded peak, examined by reversed-phase HPLC, contained two peptides, the Val-13 and Lys-13 variants (Fig. 1). The former is the stronger binder and the major successful Met-13 mimic found. The Lys species is a weak S-protein binder yet strong enough to be selected in the affinity screen. The meaning of Lys mimickry is not yet fully understood but at first glance suggests the ability of the residue to use the hydrophobic $(CH_2)_4$ portion of its side chain to make a partially stabilizing hydrophobic contact with the S-protein surface.

Intramolecular Domain Recognition in Neurohypophysial Hormone Precursors

The conformation-based view of molecular recognition and the consequent use of sequence simplification and randomization for synthetic design provide a general approach to evaluate and re-engineer molecular recognition events in biological systems. We have used synthetic redesign experiments to investigate the nature and role of multimolecular assembly of neuroendocrine biosynthetic precursors of oxytocin (OT) and vasopressin (VP). These latter peptide hormones are produced in cellular pathways as parts of larger protein precursor [5–7].

We have used peptide synthesis to show that the biosynthetic precursors assemble into folded, well-ordered forms ([8, 9]; Fassina, G. and Chaiken, I.M., unpublished data). The precursor of each of these peptides (Fig. 2) contains a hormone sequence domain (H, 9 residues, 1 intradomain disulfide), a Gly-Lys-Arg tripeptide spacer/enzymatic processing region, a sequence domain for a coordinately synthesized neurophysin (NP, small protein of 10 kDa containing 7 intradomain disulfides), and a variable carboxyl terminal extension, either His in the OT precursor or an Arg-glycopeptide sequence in the VP precursor (Fig. 2). Upon completion of enzymatic processing, the folded products NP and H interact to form noncovalent complexes; and, these 1:1 complexes can self-associate. It was hypothesized that the precursors also can fold, with H and NP domains interacting intramolecularly, and that these folded precursors self-associate into at least dimers.

To test the above ideas about precursor assembly, we made hormone precursors by chemical semisynthesis. In the OT case, we synthesized the OT-GKR segment and then, after suitable side-chain protection, chemically coupled this piece to the isolated (ϵ-amino group blocked) bovine pituitary NP I (BNPI). Pro^{s}-AVP/BNPII, with sequence AVP-GKR-BNPII, also has been made. Using both circular dichroism and affinity chromatographic analysis, we found that both pro^{s}-OT/BNPI and pro^{s}-AVP/BNPII assume well-defined conformations, with compactly

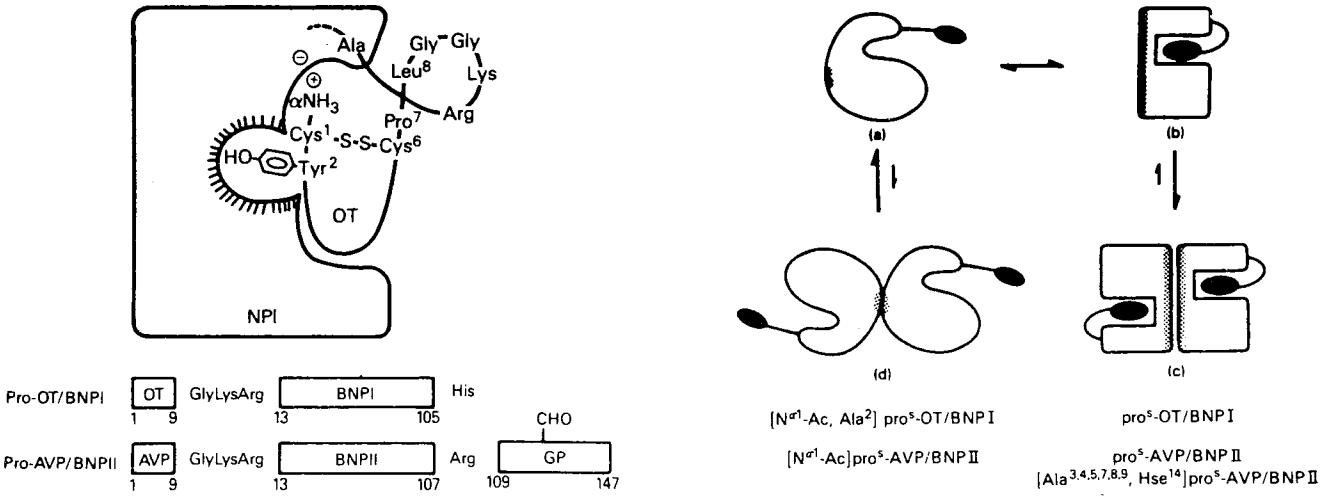

Fig. 2. Left top: *Schematic view of the intramolecular interaction between H and NP domains in OT/BNPI biosynthetic precursor, depicting the role of the α-amino and Tyr-2 side chain of the hormone in this interaction.* Left bottom: *Primary structures of pro-OT/BNPI and pro-AVP/BNPII from cDNA sequence analysis* [6]. Right: *Scheme of self-assembly of precursors and precursor mutants, emphasizing linkage, between intramolecular domain recognition and precursor self-association. Upon hormone domain binding to complementary surface of the NP domain, the conformational form of the NP domain is stabilized in which the self-association surface (dotted area) is in the high affinity state.*

folded hormone and neurophysin domains interacting with each other intramolecularly (Fig. 2).

We also have made precursor mutants by coupling synthetic OT-GKR or AVP-GKR mutants to the appropriate natural NP ([4, 9]; Fassina, G. and Chaiken, I.M., unpublished data). Folded precursor, like noncovalently liganded NP, has a high affinity potential for self-association, while incorrectly folded precursor, like unliganded NP, has a low affinity potential. By affinity chromatographic analysis, pro^5-OT/BNPI and pro^5-AVP/BNPII have affinity constants of binding to immobilized BNPII which are about one order of magnitude greater than those for BNPI and II. In cases in which the putative contact elements α-amino and Tyr-2 side chain are altered [e.g. ($N^{\alpha 1}$-acetyl) and ($N^{\alpha 1}$-acetyl, Ala^2)], folding is disrupted as judged by K^a values, on immobilized BNPII, which are similar to those for BNPI and II.

Interestingly, with pro^5-VP/BNPII, the folded structure could be mimicked with sequence-simplified mutants. In these, the disulfide loop contains Ala residues at all positions except 1/2 Cys (position 1 and 6) and contact residue Tyr-2. The linker between disulfide loop and NP also contains Ala residues at positions 7, 8, and 9. Sequence-simplified pro^5-AVP/BNPII assembles intra- and intermolecularly as does native sequence precursor (Fig. 2). Sequence modeling results for the H-NP interaction thus reflect the same view of molecular recognition as RNase S. In the hormone precursor case, the conformational frame can be viewed as the 6-residue disulfide loop and the contacts to NP are in an α-amino and Tyr-2 side chain. The sequence-simplified precursor is presently being used as a basis to examine the role of important contact residues by sequence randomization (G. Fassina, unpublished results).

Antisense Peptide Recognition

Recent data with antisense peptides do not fit easily to the orthodox view of peptide and protein recognition depicted in Figs. 1 and 2. Several studies [10–13] have suggested that synthetic peptides encoded in the base sequence of antisense DNA (Fig. 3) are able to bind to the naturally occurring sense peptides. Interestingly, sequence comparison of sense and antisense peptides has suggested a matchup in the patterns of hydropathic properties of the residues [11, 14, 15]. However, the question has remained of just what forces are responsible for antisense recognition of sense peptides. This question has become increasingly important in view of the potential to use antisense peptides as a guide to design synthetic molecules which recognize natural peptides and proteins. Such a potential has impressive implications both for the study of forces which produce peptide and protein recognition in biology and for design of affinity agents of biotechnological use in separation and analysis.

We recently began an investigation of the occurrence and nature of sense/

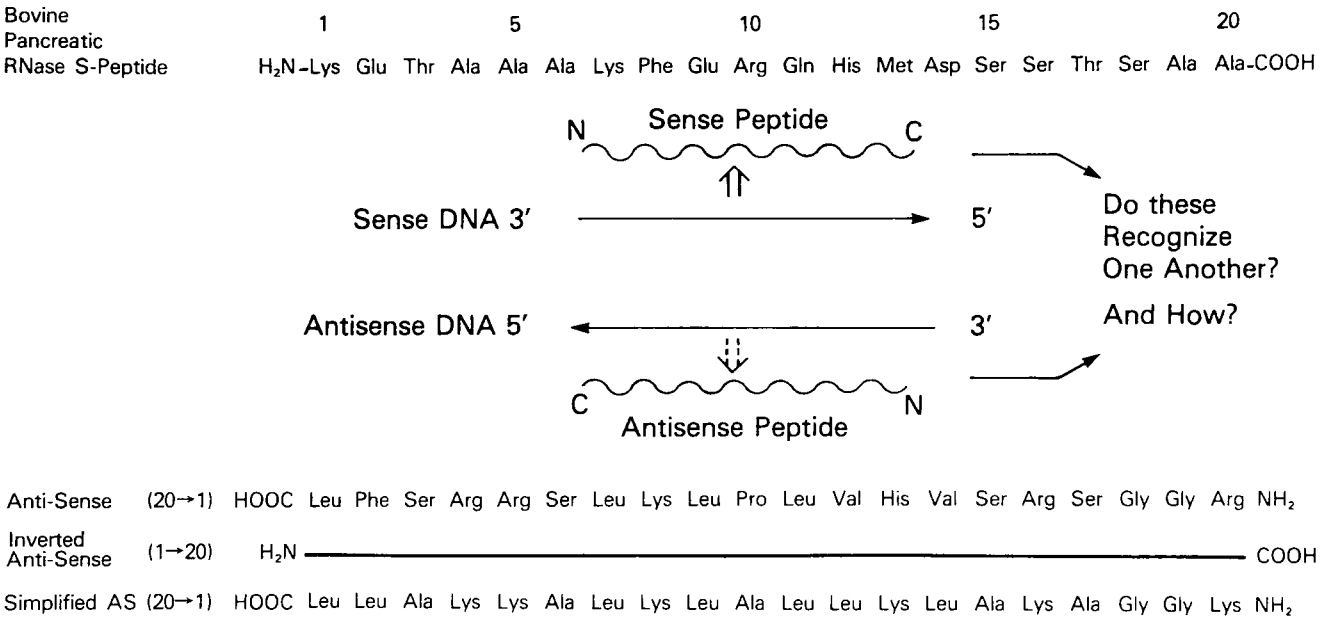

Fig. 3. Scheme depicting relationship of antisense peptide to sense peptide and the S-peptide experimental system devised to test this relationship. Antisense peptide is the sequence encoded in antisense (or complementary) DNA, while sense peptide is the native sequence encoded in the sense (coding) strand of DNA. The diagram shows the sequences of S-peptide and two synthetic antisense peptides, one [AS(20 → 1)] corresponding to antisense DNA read in a normal 3′ to 5′ direction and the other [inverted antisense or IAS (1 → 20)] with the same sequence as AS but with amino- to carboxy-terminal residue orientation reversed. The sequence for a simplified model of AS (20 → 1) also is shown.

antisense peptide recognition for the RNase S-peptide case [12, 13] using analytical affinity chromatography [16, 17] to measure interactions. With sense peptide as the immobilized molecule (M), chromatographic elution was carried out with antisense peptide (P) [either AS (antisense) or IAS (inverted antisense, same order of residues as AS but with amino-to-carboxyl orientation reversed)], either alone or in the presence of mobile sense peptide competitor (L). Such elutions allowed determination of K_d values for antisense/sense peptide interaction, both for the immobilized sense/soluble antisense interaction ($K_{M/P}$) and for soluble sense/soluble antisense interaction ($K_{L/P}$).

In one series of experiments [12], for AS (20→1), the K_d's for binding of immobilized and soluble sense peptide, respectively, were calculated to be 1.4×10^{-6}M (for $K_{M/P}$) and 3.6×10^{-5}M (for $K_{L/P}$). Strikingly, when the experiment was repeated [12] with IAS (1→20), binding to sense peptide was observed here also, and with an affinity only slightly lower than that for normally oriented antisense peptide ($K_{M/P} = 2.3 \times 10^{-6}$M, $K_{L/P} = 4.4 \times 10^{-5}$M). Since it is expected that AS and IAS peptides do not have identical three-dimensional structures or structural tendencies, a tentative conclusion is that antisense/sense peptide recognition does not require a single type of compact, folded structure. One way recognition could occur here is by a matchup of sequence in elongated peptide forms which interact with one another at many sites along the peptide chain. This view is supported by the finding that progressive shortening of antisense peptides causes stepwise decrease in sense peptide affinity and not the discontinuous decrease one might expect if only a few residues were responsible for most of the binding energy.

Given the difficulty to fit antisense/sense peptide binding into the conceptual mold of native peptide and protein interaction, a major question arises of just what is the underlying mechanism of antisense peptide recognition. We recently have begun to evaluate which elements of primary sequence are most important for antisense peptide binding (Shai, Y. and Chaiken, I.M., unpublished results). Significant sequence variation can be tolerated in antisense 20-mers with only partial loss of affinity for S-peptide. The results so far are consistent with the view that antisense/sense peptide binding occurs by interaction of the hydropathic mosaics created by the sequences. To test this view, we made [13] a simplified AS (20→1) consisting of only Lys, Ala, Leu, and Gly, in which Lys replaced His and Arg, Ala replaced Ser and Pro, and Leu replaced Phe and Val. This peptide, which substantially retains the hydropathic pattern of side chains, binds to S-peptide only slightly more weakly than the original AS (20→1). If interaction of hydropathic mosaics is a dominant theme in antisense peptide binding, it will be interesting to evaluate to what extent this mechanism also may occur with native polypeptides and proteins, both intermolecularly in the often concentrated conditions in cells and intramolecularly during protein folding.

Comments

Synthetic sequence design has proven to be a useful tool to characterize and re-engineer peptide and protein recognition events in biology. Synthetic simplification and randomization have been helpful for categorizing sequence information in native peptides and proteins and for redesigning new polypeptide sequences to mimic native, biologically active polypeptides. Synthesis, including simplification, also has been a valuable means to explore peptide recognition phenomena for the presumably 'in vitro' system of antisense peptide binding to sense peptides. The antisense results do not fit in any simple way to preconceived notions about how macromolecular recognition occurs. Nonetheless, there is reason to suspect that the forces involved in antisense/sense recognition may also occur in native peptide and protein interactions. Describing antisense/sense binding mechanisms by ongoing synthetic modeling and mutation of antisense peptides may well help to understand recognition mechanisms generally. Antisense peptides also may provide useful starting points for the design of recognition molecules for biotechnological applications. The road to designing such specific recognition molecules will likely require evaluating more fully the nature of the sequence code responsible for sense/antisense peptide recognition.

References

1. Komoriya, A. and Chaiken, I.M., J. Biol. Chem., 257 (1982) 2599.
2. Kanmera, T., Homandberg, G.A., Komoriya, A. and Chaiken, I.M., Int. J. Pept. Prot. Res., 21 (1983) 74.
3. Taylor, H.C., Komoriya, A. and Chaiken, I.M., Proc. Natl. Acad. Sci. U.S.A., 82 (1985) 6423.
4. Chaiken, I.M., Ando, S., Fassina, G., Shai, Y. and Liang, X., In Chaiken, I.M., Chiancone, E., Fontana, A. and Neri, P. (Eds.) Macromolecular Recognition: Principles and Methods, Humana Press, Clifton, NJ, 1987, in press.
5. Brownstein, M.J., Russell, J.T. and Gainer, H., Science, 207 (1980) 373.
6. Richter, D., Trends in Biochem. Sci., (1983) 278.
7. Chaiken, I.M., Fischer, E.A., Giudice, L.C. and Hough, D.T., In McKerns, K.W. and Pantic, V. (Eds.) Hormonally Active Brain Peptides, Plenum, New York, NY, 1982, p. 327.
8. Kanmera, T. and Chaiken, I.M., J. Biol. Chem., 260 (1985) 8474.
9. Ando, S., McPhie, P. and Chaiken, I.M., J. Biol. Chem., (1987) in press.
10. Bost, K.L., Smith, E.M. and Blalock, J.E., Proc. Natl. Acad. Sci. U.S.A., 82 (1985) 1372.
11. Blalock, I.E. and Bost, K.L., Biochem. J., 234 (1986) 679.
12. Shai, Y., Flashner, M. and Chaiken, I.M., Biochemistry, 26 (1987) 669.
13. Shai, Y. and Chaiken, I.M., Fed. Proc., 46 (1987) 2022.
14. Lacey, J.C. and Mullins, Jr., D.W., Origins of Life, 13 (1983) 3.
15. Blalock, J.E. and Smith, E.M., Biochem. Biophys. Res. Commun., 121 (1984) 203.

16. Swaisgood, H.E. and Chaiken, I.M., In Chaiken, I.M. (Ed.) Analytical Affinity Chromatography, CRC Press, Boca Raton, FL, 1987, p. 65
17. Fassina, G. and Chaiken, I.M., In Giddings, J.C., Gruschka, E. and Brown, P.R. (Eds.) Advances in Chromatography, Vol. 27, Marcel Dekker, New York, NY, p. 247.

A semisynthetic approach to protein engineering: Interleukin-2 redesigned

Thomas L. Ciardelli[a, b], Fred E. Cohen[c], Robert Gadski[d], Larry Butler[d], Bryan Landgraf[a] and Kendall A. Smith[a]

[a]*Dartmouth Medical School, Hanover, NH 03756, U.S.A.*
[b]*Veterans Administration Hospital, White River Jct., VT 05001, U.S.A.*
[c]*University of California, San Francisco, CA 94143, U.S.A.*
[d]*The Lilly Research Laboratories, Indianapolis, IN 46285, U.S.A.*

Interleukin-2 (IL-2, T-cell growth factor) is a lymphocytotropic hormone that mediates the T-cell proliferative immune response [1]. Structure–function studies of IL-2 have been attempted employing synthetic peptides, recombinant DNA-derived proteins and antibodies as structural probes [2]; however, despite these efforts, knowledge of the important structural relationships for this protein has remained limited.

We have employed a computer-assisted method to predict the 3-dimensional core tertiary structure of IL-2 based on its primary sequence. This method identified 4 regions of putative α-helical secondary structure along the IL-2 sequence and then assembled them to form the well-known structural motif: a 4-fold α-helical bundle [3]. The fourth and C-terminal helix was predicted to consist of 17 residues spanning the region 116-132. Closer examination of this region revealed that if this segment did assume a helical conformation, a classic amphiphilic arrangement of side chains would result. In order to test this hypothesis and obtain more precise data on the functional significance of this region, we have employed a protein engineering approach to redesign this putative C-terminal helix.

We have previously established that a biologically active protein can be reconstituted from two inactive segments: a recombinant DNA-derived fragment consisting of residues 1-99 of the IL-2 sequence and a synthetic segment corresponding to residues 105-133 via formation of the Cys-58–Cys-105 disulfide bond [4]. Therefore, we exploited the convenience of this semisynthetic approach combined with a strategy similar to that employed by Kaiser and Kezdy [5] to make 12 simultaneous amino acid substitutions directed toward enhancing helical potential in this region (Fig. 1).

The semisynthetic protein containing this altered sequence (IL-2 Var. I) exhibited approximately 4-fold greater activity than the hybrid protein having the authentic sequence (HIL-2) and provided a similar circular dichroism (CD) spectrum. A second semisynthetic protein, IL-2 Var. II, identical to the first

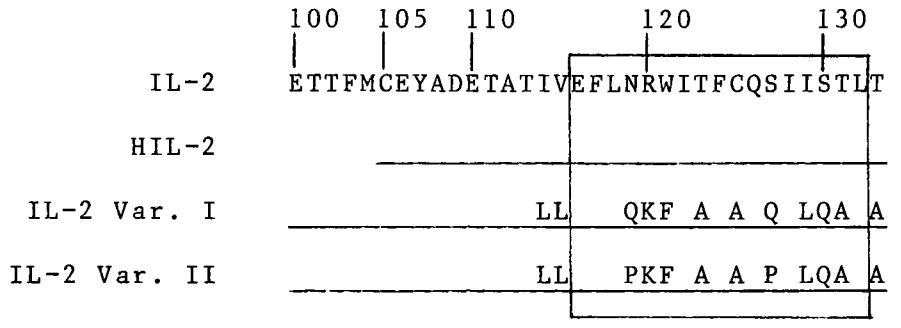

Fig. 1. The sequences of the C-terminus of IL-2 and the synthetic portion of the hybrid proteins HIL-2, IL-2 Var. I and II. Only nonhomologous residues are indicated, lines correspond to peptide length, a box surrounds the predicted helix.

except for the substitution of two helix-destabilizing Pro residues at positions 119 and 127, exhibited a CD spectrum indicating less helix and greater coil structure and was totally inactive.

Therefore, we conclude that the modeling method correctly located helical structure in this region and its integrity is critical to the stability of the bioactive conformation.

References

1. Smith, K.A., Annu. Rev. Immunol., 2 (1984) 319.
2. Ciardelli, T.L., Holley, H., Smith, K.A., Cohen, F.E., Butler, L. and Gadski, R., In Smith, K.A. (Ed.) Interleukin 2, Academic Press, New York, NY, in press.
3. Cohen, F.E., Kosen, P.A., Kuntz, I.D., Epstein, L.B., Ciardelli, T.L. and Smith, K.A., Science, 234 (1986) 349.
4. Ciardelli, T.L., Smith, K.A., Gadski, R., Butler, L., Strand, J. and Cohen, F.E., In Deber, C.M., Hruby, V.J. and Kopple, K.D. (Eds.) Peptides: Structure and Function, Proceedings of the 9th American Peptide Symposium, Pierce Chemical Co., Rockford, IL, 1985, p. 75.
5. Kaiser, E.T. and Kezdy, F.J., Science, 223 (1984) 250.

The role of cysteine residues in interleukin-3 function established by total chemical synthesis of analogs

Ian Clark-Lewis*, Leroy E. Hood and Stephen B.H. Kent
California Institute of Technology, Pasadena, CA 91125, U.S.A.

Introduction

Understanding the relationship between structure and function is critical to protein design and engineering. We have used a total chemical synthesis approach to protein structure–function studies that is based on improved chemical methods and automation of the synthetic process [1, 2]. Our work has focused on the hemopoietic growth factor, murine interleukin-3 (IL-3) [2, 3].

In an earlier study [2] we synthesized the 140-amino acid IL-3 molecule and showed that it had the expected physiochemical properties and the biological activities of the molecule isolated from natural sources. The reproducibility of the total synthesis and the high activity of the synthetic IL-3 (about 10 ng/ml gave a 50% maximal response) provided a basis for comparison of the activity of structural analogs. Synthetic forms of both the mature molecule [IL-3 (1-140)] and a further processed form [IL-3 (7-140)] that had been described previously had equivalent activity, indicating that the N-terminal 6 amino acids are not required for activity [2]. Furthermore, experiments with antibodies to a short synthetic peptide corresponding to residues 1-6 indicated that IL-3 (1-140) is the predominant form secreted by antigen-activated T cells [4].

In a further set of experiments we demonstrated that the cysteine at position 17 was essential for detectable activity. A fragment corresponding to residues 18-140, and therefore lacking this cysteine, had only barely detectable activity whereas a fragment (17-140) that included the cysteine at position 17 had high activity. The most likely explanation of this data is that cysteine-17 is involved in a critical disulfide. Based on this initial observation we have constructed a series of analogs aimed at establishing the role of disulfide bridges in determining IL-3 activity. The results are summarized below.

*Present address: The Biomedical Research Centre, The University of British Columbia, Vancouver, BC, V6T 1W5 Canada.

Results and Discussion

Clearly, when more than two cysteines are present in a protein (e.g., murine IL-3 which has four), random refolding can give rise to multiple tertiary structures, only one of which will be correct. Therefore, we synthesized full length analogs of IL-3 in which alanines were substituted for two of the four cysteines so that only two cysteines were present in each analog. This means that, on refolding, only one intramolecular disulfide bridge could form. Because the cysteine at position 17 was important for activity, we synthesized the three possible single disulfide analogs that included this cysteine. Alanines were substituted for two of the remaining cysteines. For comparison, we also synthesized a molecule with all four cysteines replaced by alanines.

Assembly of the protected 140-residue peptide chains and the deprotection steps were performed as previously described [2]. After HPLC purification, the two analogs in which Cys_{17} was paired either only to Cys_{79} or only to Cys_{140}, had readily detectable activity (490 and 470 units/mg, respectively), which was similar to that of ($Ala_{17, 79, 80, 140}$) IL-3 (790 units/mg); however, the analog in which Cys_{17} was paired to Cys_{80} had about 500-fold greater activity (3.9×10^5 units/mg) than these analogs. Interestingly this analog had about 15-fold greater activity than the partially purified synthetic molecule with the natural sequence (2.6×10^4 units/mg). This is consistent with the presence of a high proportion of aberrantly refolded molecules in the synthetic preparation containing four cysteine residues.

These results show that the formation of disulfide bonds is not absolutely required for IL-3 activity, because the analog with no cysteines had small but detectable activity, indicating that the folded form of the uncross-linked molecule gives rise to an active structure. The high activity of the [$Ala_{79, 140}$] IL-3 showed that a disulfide bridge between cysteines 17 and 80 stabilizes the tertiary structure in a functionally favorable conformation. Our results also strongly suggest that the cysteines at positions 79 and 140 are unpaired in native IL-3; however, the presence of a second disulfide between residues 79 and 140 cannot be completely ruled out and the results suggest that if this bridge does exist it would not enhance, and may decrease, IL-3 activity. This contention is supported by the fact that in the human IL-3 molecule [5], only two cysteines are present and they align with cysteines 17 and 80 in mouse IL-3 when the two sequences are computer-aligned. Future murine IL-3 analogs should be designed with only the two required cysteines to avoid the formation of aberrantly folded molecules. Finally, these results dramatically demonstrate the reproducibility and power of the total chemical synthesis approach [1, 2] to the study of structure–function relationships in proteins.

Acknowledgements

This work was supported by research grants from the National Science Foundation, the National Institutes of Health, the Monsanto Company, and Upjohn Pharmaceuticals. IC-L was supported by a C.J. Martin Travelling fellowship from the National Health and Medical Research Council, Canberra, Australia.

References

1. Kent, S. and Clark-Lewis, I., In Atitalo, K., Partanen, P. and Vaheri, A. (Eds.) Synthetic Peptides in Biology and Medicine, Elsevier, Amsterdam, 1985, pp. 29-57.
2. Clark-Lewis, I., Aebersold, R., Ziltener, H., Schrader, J.W., Hood, L.E. and Kent, S.B.H., Science, 231 (1986) 134.
3. Clark-Lewis, I. and Schrader, J.W., Lymphokines, 15 (1987) 1.
4. Ziltener, H.J., Clark-Lewis, I., Fazekas de St Groth, B., Hood, L.E., Kent, S.B.H. and Schrader, J.W., J. Immunol., 138 (1987) 1105.
5. Yang, Y.C., Ciarletta, A.B., Temple, P.A., Chung, M.P., Kovacic, S., Witek-Giannotti, J.S., Leary, A.C., Kriz, R., Donahue, R.E., Wong, G.G. and Clark, S.C., Cell, 47 (1986) 3.

Cooperativity in multiple amphipathic helical domains of apolipoprotein A-I

Jere P. Segrest, Ali Gawish, M. Iqbal, Christie G. Brouillette, Kiran B. Gupta and G.M. Anantharamaiah

Departments of Medicine, Biochemistry and Pathology and the Atherosclerosis Research Unit, University of Alabama at Birmingham Medical Center, Birmingham, AL 35294, U.S.A.

Introduction

Apolipoprotein A-I (apo A-I), the major protein component of high density lipoproteins (HDL), is a single polypeptide chain of 248 amino acid residues. Cloning and sequencing studies of apolipoprotein genes have suggested that a primordial 11-mer amino acid sequence was duplicated to produce 9 tandem-repetitive 22-mer amphipathic helical domains [1] with a Pro separating them. These domains are presumed to be involved in the lipid-associating properties of this apolipoprotein. The amphipathic α-helix is generally presumed to be the structural form of the lipid-associating domains of the exchangeable apolipoprotein classes A, C, and E from plasma lipoproteins [2]. The amphipathic helix model defines a general α-helical domain containing opposing polar and nonpolar faces with the positively charged residues occurring along the interface between the polar and nonpolar faces and negatively charged residues at the center of the polar face.

Examination of a helical wheel representation of 9 tandem domains of apo A-I indicates the presence of either a negatively or a positively charged residue at the 13th position from the N-terminus in 7 out of 9 sequences. The 13th position is close to the polar-nonpolar interface of the amphipathic helix. A 22-mer consensus amphipathic helix can be constructed which has the following sequence: Pro-Val-Leu-Asp-Glu-Phe-Arg-Glu-Lys-Leu-Asn-Glu-X-Leu-Glu-Glu-Leu-Lys-Gln-Lys-Leu-Lys (A-Icon). Based on this, 6 peptide analogs were synthesized (Table 1). The three 22-monomers differ in the presence of Glu, Arg, and Ala at the 13th position. These were synthesized to study the specificity of the ability of the amphipathic helix to associate with lipid or act as a cofactor of the enzyme lecithin:cholesterol acyl transferase (LCAT), which is involved in reverse cholesterol uptake from membranes. The three dimers are Glu and Arg dimers and a mixed dimer of Arg and Glu. These were synthesized to study the possible existence of co-operativity among the amphipathic helical domains in apo A-I for lipid association and LCAT activation properties.

The peptides were synthesized by the solid phase method of peptide synthesis as described previously [3]. Since these analogs differed in only one amino acid, they were synthesized using a two-chambered reaction vessel developed by us [4] to obtain two peptide resins simultaneously. The peptides were cleaved from the resin using the modified HF procedure and were subjected to HPLC purification and analysis.

Results and Discussion

The results of circular dichroism (CD) in buffer and in the presence of lipid are shown in Table 1.

Because the mixture of [Glu[13]] A-Icon:DMPC was turbid, the CD spectrum could not be obtained in this case. All other peptides clarified multilamellar vesicles of DMPC, and an increase in the percent helicity was observed on going from buffer to lipid. While the Glu 22-mer analog did not associate with the lipid, the dimer of this analog did clarify a turbid suspension of DMPC vesicles. Electron microscopy and nondenaturing gradient gel electrophoresis studies of the complexes showed that the sizes of the complexes formed with the monomers were a lot larger than the corresponding dimers, indicating in every case the dimers were better lipid binders than the corresponding monomers. In previous studies we have shown that the larger complexes are less stable than the smaller complexes [3]. Therefore, one can postulate that the size of the complex is inversely proportional to the lipid-associating ability of the peptides [3]. The Glu analog, although more helical in buffer than any other analog, does not interact well with DMPC. The reason for its greater helicity could be due to the formation of a salt bridge between the Glu at the 13th position and Lys at position 20 on the polar–nonpolar interface. The reason for its weak lipid-association properties is not very clear, although, we have observed such a behavior with

Table 1 Percent α-helicity of apo A-I consensus analogs[a]

Peptide	Buffer	Peptide:DMPC[b] (1:5)	TFE[b] (80%)
[Glu[13]] A-Icon[c]	32	–	57
[Ala[13]] A-Icon	22	41	65
[Arg[13]] A-Icon	24	35	63
([Arg[13]] A-Icon)$_2$	25	25	55
([Glu[13]] A-Icon)$_2$	53	58	71
[Glu[13]] A-Icon [Arg[13]] A-Icon	42	49	64

[a] As measured by ellipticity at 220 nm.
[b] DMPC = dimyristoylphosphatidyl choline; TFE = trifluoroethanol.
[c] P-V-L-D-E-F-R-E-K-L-N-E-E-L-E-E-L-K-Q-K-L-K.

model peptide analogs with the same amino acid sequence but 'reversed' in the position of charged residues [5]. We hypothesize that the difference between the Arg analog and Glu analog may be due to the more amphipathic nature of Arg which enables it to contribute to the hydrophobicity of the hydrophobic face and thus increased its lipid affinity [5].

The results of the LCAT activation experiments clearly demonstrate the existence of cooperativity in multiple amphipathic helical domains. The studies were performed using small unilamellar vesicles of egg phosphotidyl choline (PC) as substrates [3]. In all these cases, the dimers were able to activate the enzyme LCAT better than monomers. Thus, the lipid-association and LCAT-activation properties of these analogs indicate that in apo A-I there most likely exists a cooperativity among the different 22-mer tandem-repetitive amphipathic helical domains. It is interesting to note that the Arg monomer was the most active among the monomers studied. These results are in accordance with the published results of Yokoyama et al. [6], who have shown that the presence of an Arg on the nonpolar face of an amphipathic helix increases the ability of the peptide to act as a cofactor of the enzyme LCAT. It would be interesting to study the effect of His at the 13th position on the properties of the amphipathic helix, as it is present in the 22-mer tandem repeats of apo A-I.

Acknowledgements

This work was supported by NIH grant P01 HL 34341.

References

1. Luo, C-C., Li, W-H, Moore, M.N. and Chan, L., J. Mol. Biol., 187(1986)325.
2. Segrest, J.P., Jackson, R.L., Morrisett, J.D. and Gotto, Jr., A.M., FEBS Lett., 38(1973)247.
3. Anantharamaiah, G.M., Gawish, A., Iqbal, M., Khan, S.A., Brouillette, C.G. and Segrest, J.P., In Peeters, H. (Ed.) Protides of the Biological Fluids, Vol. 34, Pergamon Press, New York, NY, 1986, p. 63.
4. Anantharamaiah, G.M., Methods Enzymol., 128(1986)627.
5. Yokoyama, S., Fukushima, D., Kupferberg, J.P., Kezdy, F.J. and Kaiser, E.T., J. Biol. Chem., 25(1980)7333.
6. Epand, R.M., Gawish, A., Iqbal, M., Gupta, K.B., Chen, C.H., Segrest, J.P. and Anantharamaiah, G.M., J. Biol. Chem., 262(1987)in press.

Semisynthesis of a deletion mutant of cytochrome c by condensation of enzymatically activated fragments

Carmichael J.A. Wallace and Amanda E.I. Proudfoot
Department of Medical Biochemistry, University of Geneva, 9 avenue de Champel, CH-1211 Geneva 4, Switzerland

Introduction

We have frequently used the spontaneous resynthesis of CNBr fragments 1–65 and 66–104 of cytochrome *c* as a facile final step in the fragment condensation semisynthesis of the protein [1]. In the complex of the two fragments in aqueous buffers, residues 65 and 66 are brought into proximity, so that the subsequent aminolysis of the C-terminal homoserine lactone, normally a slow reaction, is conformationally assisted.

Enzymic resynthesis of fragments also depends for success on complex formation, but is effective in a limited number of cases. Reformation of intact cytochrome *c* from the tryptic fragments 1–38 and 39–104 has proved impossible [2]. We hoped, however, to use trypsin to activate fragment 1–38 in order to artificially induce the spontaneous resynthesis seen with the CNBr fragments.

We have found conditions in which trypsin will catalyze the addition of amino acid-active esters [3]. Using dichlorophenyl esters, high yields were subsequently obtained in fragment condensations in aqueous buffers. The dependence on conformation assistance proved much less strict than for the 1–65 and 66–104 system and the method has, therefore, general applicability.

We have used the method to synthesize analogs modified at positions 39 and 40 (Fig. 1). Typically, yields of 10–20 mg of purified protein are obtained in 1–2 weeks (Wallace et al., in preparation), making protein engineering by semisynthesis highly competitive with site-directed mutagenesis.

Since we have been interested in the role of the loop that encloses the bottom edge of the heme [4], and which includes these two residues, we wished to remove it altogether. It is only the presence or absence of the loop that distinguishes the structures of the functionally quite distinctive mitochondrial cytochrome *c* and bacterial cytochrome c_{555} [5]. In addition, this part of the protein structure fulfills the structural criteria for an Ω-loop, a recently defined element of protein secondary structure that comprises much of what was previously called random coil [6]. We hoped to test the proposition that Ω-loops may act as independent modules of folding, function, and evolution.

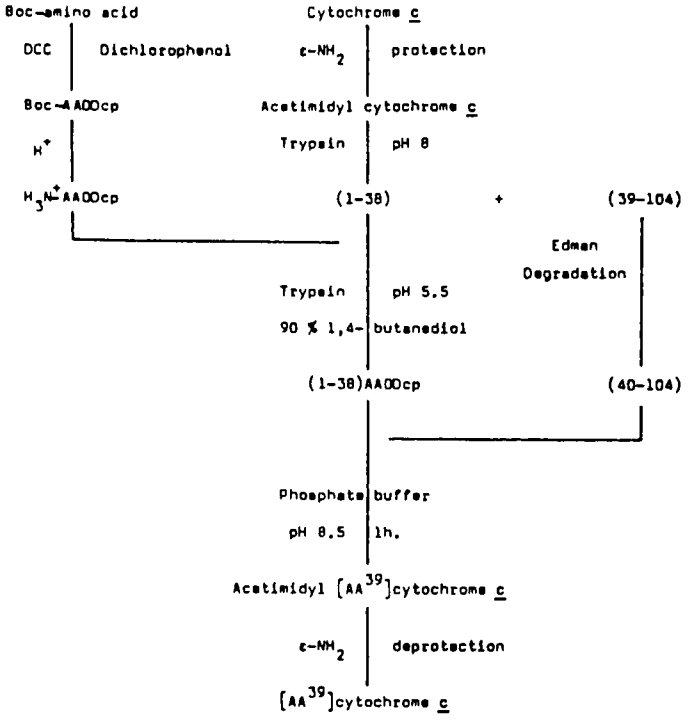

Fig. 1. A scheme for fragment condensation semisynthesis employing enzymatic activation of the N-terminal fragment.

Results and Discussion

Residues 39 and 56 are close to one another at the neck of the loop (Fig. 2), so that given a nativelike conformation for the complex and an absence of very strict conformational requirements, coupling between these two residues in the complex 1–39 and 56–104 should occur. Using the conditions optimized for coupling between 1–39 and 40–104, we have observed that indeed it does, in yields of up to 60%.

The spectrum of the purified product, *des*-(40–55) cytochrome *c*, remains identical to the mitochondrial parent, so the observed shifts in λ_{max} that characterize the bacterial cytochrome c_{555} are not a consequence of the loop deletion.

In contrast, removal of the loop reduces the midpoint oxidation-reduction potential from the 260 mV of cytochrome *c* to 130 mV. This is strikingly close to the 140 mV of the bacterial protein.

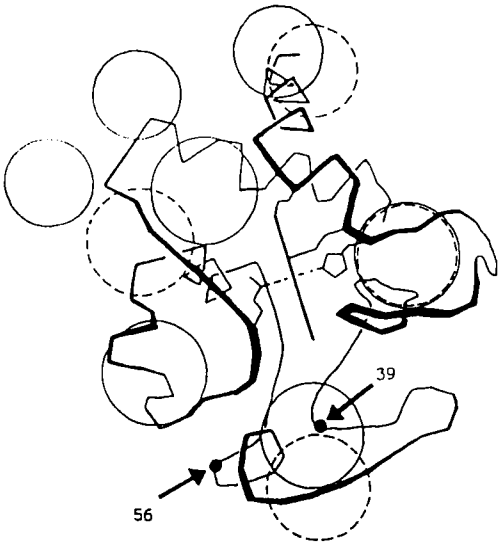

Fig. 2. The locations of residues 39 and 56, and the binding ring of amino groups (—), in cytochrome c. *The displacement of the ring in* c_{555} *(---) may explain the abnormally poor reactivity with mammalian reductase (see Fig. 3).*

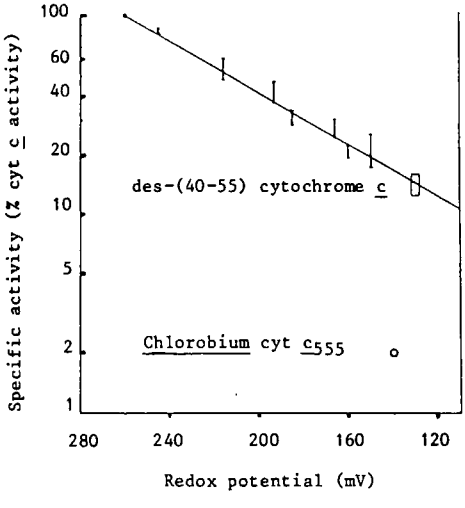

Fig. 3. The relationships between biological activity and redox potential of des-*(40–55) cytochrome* c *and* Chlorobium c_{555} *compared with those of other analogs with normal active site conformations.*

The biological activity of the analog is impaired, but by no more than would be expected given the redox potential change [4], which implies that the active site conformation is preserved (Fig. 3). The spectral data tell us that the heme crevice structure is intact. These results and the high yield obtained in the synthesis show that the loop is essential neither for folding nor the maintenance of the tertiary structure elsewhere in the molecule and support the concept of Ω-loops as independent modules of folding. Likewise, the unique and specific effect on redox potential of removal of this loop implies a role as an independent functional module.

Acknowledgements

We thank Mrs. Monique Rychner for expert technical assistance and the Swiss National Science Foundation for financial support.

References

1. Wallace, C.J.A. and Corthésy, B.E., Prot. Eng., 1 (1986) 23.
2. Proudfoot, A.E.I., Rose, K., Offord, R.E., Schmidt, M. and Wallace, C.J.A., Biochem. J., 221 (1984) 325.
3. Rose, K., Herrero, C., Proudfoot, A.E.I., Offord, R.E. and Wallace, C.J.A., Biochem. J., (1987) in press.
4. Wallace, C.J.A. and Proudfoot, A.E.I., Biochem. J., 245 (1987) 773.
5. Korszun, Z.R. and Salemme, F.R., Proc. Natl. Acad. Sci. U.S.A., 74 (1977) 5244.
6. Leszczynski, J.F. and Rose, G.D.K., Science, 234 (1986) 849.

Characterization of a two-chain structural variant of recombinant human growth hormone

Eleanor Canova-Davis, Ida P. Baldonado, Louisette J. Basa, Rosanne Chloupek, Tom Doherty, Reed J. Harris, Rodney G. Keck, Michael W. Spellman, William F. Bennett and William S. Hancock

Genentech, Incorporated, 460 Point San Bruno Boulevard, South San Francisco, CA 94080, U.S.A.

Introduction

Human growth hormone (hGH) was first expressed in *Escherichia coli* using recombinant (r)DNA techniques that resulted in production of the protein in the cytoplasm, resulting in a methionyl analog [1]. Despite the reducing environment of the cytoplasm, the extracted and purified product contains the correct disulfide bonds and tertiary structure [2]. In contrast, secretion methods allow the production in *E. coli* of hGH without the additional methionine and with the correct disulfide bond formation [3]. Whereas the secretion of correctly processed rhGH into the periplasm of *E. coli* represents a major process advantage in that the rhGH is gently extracted in an undenatured state, a certain proportion of the molecules is cleaved to a two-chain form by an enzyme that may be located in the cell membrane. A two-chain variant is present in human pituitary storage granules and is reported to have potentiated growth-promoting properties [4].

Results and Discussion

This two-chain form of rhGH was isolated by high-resolution ion exchange chromatography. An amino-terminal sequence analysis revealed the presence of two sequences in equimolar amounts and determined the new sequence to be YSKFDTNSHN-. This identified the new sequence as beginning at residue Tyr-143. Upon sodium dodecyl sulfate polyacrylamide gel electrophoresis in the presence of β-mercaptoethanol, this two-chain variant was cleaved into the two fragments previously covalently linked by the disulfide bond between cysteine residues 53 and 165.

A comparison of the two forms of rhGH by tryptic mapping shows a major difference in the peak profiles. The two chromatograms are identical except for those peaks designated by arrows (Fig. 1). The tryptic digest of the intact

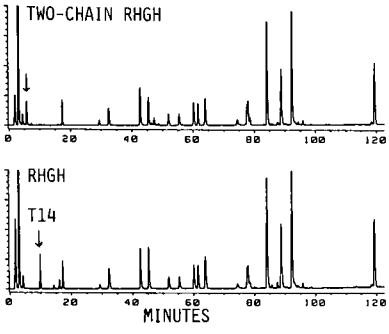

Fig. 1. Tryptic mapping of rhGH and the two-chain variant. The peptides (100 μg) were loaded onto a Nucleosil C18 column (0.46 × 15 cm, 5 μ). The gradient was from 0 to 40% acetonitrile containing 50 mM sodium phosphate, pH 2.85, run over 120 min. The profile was monitored at 220 nm.

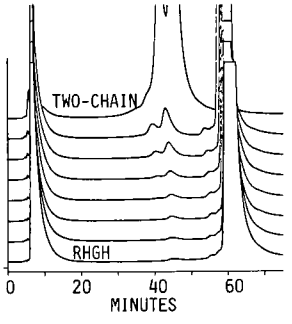

Fig. 2. The analysis of rhGH (bottom trace) plus varying amounts of two-chain rhGH (0.1, 0.5, 1, 2, 5, and 10%) by reversed-phase HPLC using a bicarbonate/acetonitrile mobile phase.

molecule contains a peptide T14 corresponding to residues 141–145 (QTYSK) eluting at 10 min. This peak is absent in the map of the two-chain form, which contains a new peak eluting at 5 min (YSK). The cleavage site can thus be unequivocally located in this peptide.

The two-chain material is resolved from the intact hormone on a reversed-phase HPLC column run in a bicarbonate mobile phase (Fig. 2). The cleaved material gives rise to peaks (one of which is deamidated) at approximately 45 min while intact rhGH elutes at approximately 60 min. It is possible to detect a 0.1% content of the two-chain variant in rhGH preparations.

The bioactivity of the two-chain form was measured by the rat weight gain assay. At equivalent doses (10 and 50 μg/day for 7 days) the two-chain form of rhGH was shown to have activity which is at least equivalent to both rhGH and Protropin®. The two-chain variant was also tested in an ELISA enzyme immunoassay in which its activity was 98.7% that of Protropin®.

In conclusion, a new two-chain variant of rhGH has been isolated and analytical techniques have shown that the variant was produced by a single proteolytic cleavage between residues Thr-142 and Tyr-143.

References

1. Goeddel, D.V., Heyneker, H.L., Hozumi, T., Arentzen, R., Itakura, K., Yansura, D.G., Ross, M.J., Miozzari, G., Crea, R. and Seeburg, P.H., Nature, 281 (1979) 544.
2. Jones, A.J.S. and O'Connor, J.V., In Gueriguian, J.L. (Ed.) Hormone Drugs,

Proceedings of the FDA-USP Workshop on Drug Reference Standards for Insulins, Somatotropins and Thyroid-Axis Hormones, U.S. Pharmacopeial Convention, Bethesda, MD, 1982, p. 335.
3. Gray, G.L., Baldridge, J.S., McKeown, K.S., Heyneker, H.L. and Chang, C.N., Gene, 39 (1985) 247.
4. Singh, R.N.P., Seavey, B.K., Rice, V.P., Lindsey, T.T. and Lewis, U.J., Endocrinology, 94 (1974) 883.

Reoxidation of basic reduced insoluble proteins: Example of neurotoxin II of the scorpion *Androctonus australis Hector*

J.M. Sabatier, H. Darbon, P. Fourquet, H. Rochat and J. van Rietschoten

U.D.C.-C.N.R.S. UA 1179, INSERM U 172, Laboratoire de Biochimie, Faculté de Médecine Secteur Nord, Bd. Pierre Dramard, F-13326 Marseille Cedex 15, France

In view of the total synthesis of the scorpion neurotoxin II of *Androctonus australis Hector* (AaH II), reoxidation of the fully reduced peptide was studied in order to set up the best conditions of renaturation. As for many proteins, reduction of the disulfide bridges yielded an insoluble peptide in neutral and alkaline conditions. AaH II is a basic 64-residue peptide cross-linked by 4 disulfide bonds. Statistical reduction of one disulfide bridge per molecule abolishes completely neurotoxic activity and binding to the receptor, the sodium channel of excitable membranes. Straight air reoxidation of fully reduced AaH II in Tris–HCl (0.1 or 0.2 M, pH 8.5 or 7.0) resulted in little soluble material (19–36% of total proteins) and very low toxicity recovery (0.2% and 2%). As the reduced toxin, however, was completely soluble in 10% acetic acid after biogel P_2 chromatography (pH 2.2), we tested reoxidation by air with a slow pH gradient in a dialysis tubing. This system is very convenient for the study of renaturation in well-defined conditions such as pH, additives, and temperature.

The pH gradient improved significantly both the recovery of peptide in solution (66%) and the overall toxicity yield (27%). A critical effect of the temperature was also observed, with the best refolding obtained between 15 and 30°C. Addition of 1 mM reduced and 1 mM oxidized glutathione greatly accelerated disulfide interchange so that the whole process was accomplished in 32 h instead of 96 h. Addition of the denaturating agent guanidinium chloride was also tested and helped increase the yield of soluble material but did not have a favorable effect on the renaturation process. A compromise had to be found in its concentration. The final conditions we tested were as follows: the reduced toxin was at a concentration of 12 μM in 10% acetic acid in the dialysis tubing and the outside buffer was composed of 0.1 M sodium phosphate, 0.1 M sodium chloride, 1 mM reduced and 1 mM oxidized glutathione, and 0.02 M guanidine hydrochloride, pH 8.0, 23°C. After 32 h, 95% of the peptide was still in solution of which 70% was completely active. HPLC, slab-gel electrophoresis, and SDS-PAGE showed that the solution was composed of: (a) 70% of a peptide identical to

the native toxin, fully active as measured by toxicity to mice and binding assays on rat brain synaptosomes; and (b) 30% of a monomeric form of peptide, fully reoxidized but with two positive charges lost (a possibility is the formation of two mixed disulfides with glutathione). These conditions seem useful for treating insoluble reduced basic proteins. See [1] for more details.

Reference

1. Sabatier, J.M., Darbon, H., Fourquet, P., Rochat, H. and van Rietschoten, J., Int. J. Pept. Prot. Res., 30(1987)125.

Trypsin-catalyzed coupling of synthetic peptides: Semisynthetic production of phospholipase A2 mutants in high yield

Jan van Binsbergen, Arend J. Slotboom and Gerard H. de Haas
Laboratory of Biochemistry, State University of Utrecht, Padualaan 8, NL-3508 TB Utrecht, The Netherlands

Pig pancreatic phospholipase A2 (PLA, EC 3.1.1.4) stereospecifically hydrolyzes the 2-acylester bond in 3-*sn*-phosphoglycerides. Monomeric substrate is bound and slowly hydrolyzed in the active site. On aggregated substrates, however, the enzyme displays considerably higher enzymatic activity [1]. The lipid binding domain (LBD) is essential for the interaction of PLA with aggregated substrates. This paper deals with substitutions of LBD residues located at the α-helical N-terminal region.

Until now, semisynthetic PLA analogs have been made by chemical coupling of synthetic peptides (mixed anhydride method), with a low yield (25–30%) [2]. As an alternative, enzymatic coupling has been performed using as a model the C-terminal porcine PLA fragment 7–124 to which hexapeptide analogs 1–6 were coupled.

The ϵ-amidinated 7–124 fragment has been obtained by tryptic digestion of ϵ-amidinated PLA, liberating the N-terminal hexapeptide Ala^1-Leu^2-Trp^3-Gln^4-Phe^5-Arg^6. The hexapeptide analogs have been made by solid phase peptide synthesis [2] and purified by HPLC. The following substitutions have been carried out: $Ala^1 \rightarrow His^1$, $Trp^3 \rightarrow Gly^3$, $Trp^3 \rightarrow Tyr^3$, and $Arg^6 \rightarrow Lys^6$. The synthetic peptides have been coupled to the 7–124 fragment (50 mg) dissolved in 3.5 ml of DMF (25% v/v) and of buffer (75% v/v) (0.2 M NaAc and 5 mM $CaCl_2$, pH 6.5), with a 5-fold molar excess of peptide over the 7–124 fragment in the presence of 15 mg of TPCK trypsin as a catalyst. The progress of the reaction can easily be monitored by HPLC and by measuring the increase in enzymatic activity. The lysine-specific protease endoproteinase Lys C (*Lysobacter enzymogenes*) has also been used for the introduction of Ac-Arg-Arg-Ala^1-Lys^6. In this mutant, the ϵ-NH_2 group of Lys^6 can be selectively acylated, followed by tryptic activation.

When the reaction was complete (usually within 12 h), the coupling was terminated by lowering the pH to 4, followed by dialysis and purification on CM cellulose.

The advantages of these trypsin-catalyzed couplings are the high yield (70–

Table 1 *Comparison of various properties of native and mutant porcine pancreatic phospholipases (PLA)*

PLA analog	Specific activity (egg yolk assay, μ equiv/min/mg)	V_{max}/micelles (L-di-C8 lecithin, μ equiv/min/mg)	kcat/K_m (monomeric dithio-C6 lecithin, s/M)
PLA (Arg^6)	250	2226	439
Lys^6	74	926	402
His^1	10	526	307
Gly^3	0	240	150
Tyr^3	24	300	234

90% after purification) and the fact that no protecting groups are required on the peptide.

As can be seen from Table 1 the activity of the mutants prepared on monomeric substrate ranges from 35% to 92%. Surprisingly, the Lys^6 mutant has a much lower activity on micellar substrates, despite its positive charge. The absence of a side chain in Gly and its role as an α-helix breaker probably explains the low activity of Gly^3-PLA. The low activity of Tyr^3-PLA on micellar substrate is most likely due to the presence of the polar hydroxyl group, which is absent in Trp. His^1-PLA retains 25% of its activity on L-di-C8 lecithin micelles at pH 6, where the His imidazole side chain is protonated. At pH 8, however, the activity of His^1-PLA decreases by 60%, while PLA activity shows a 30% increase as compared to pH 6.

References

1. Slotboom, A.J., Verheij, H.M. and de Haas, G.H., In Hawthorne, J.N. and Ansell, G.B. (Eds.) Phospholipids: New Biochemistry, Vol. 4, Elsevier, Amsterdam, 1982, p. 359.
2. Van Scharrenburg, G.J.M., Semisynthesis of Phospholipase A2, Ph.D.Thesis, Utrecht, 1984.

Protein engineering: Design and synthesis of betabellin 7

Scott B. Daniels[a], P. Anantha Reddy[a], Elisabeth Albrecht[a], Jane S. Richardson[b], David C. Richardson[b] and Bruce W. Erickson[a]

[a]*Department of Chemistry, The University of North Carolina, Chapel Hill, NC 27514, U.S.A.*
[b]*Department of Biochemistry, Duke University, Durham, NC 27706, U.S.A.*

Introduction

We are exploring the de novo design of unnatural proteins, their synthesis through peptide chemistry, and their study through biophysical techniques [1-3]. The goal is to design and construct a molecular framework that can support binding and catalytic sites. The architecture chosen is a protein with two identical peptide chains covalently joined through their carboxyl ends by a symmetric cross-linker. Each chain is designed to fold into an antiparallel beta-pleated sheet consisting of four beta strands joined by three beta turns. The pair of amphiphilic sheets is expected to adopt in water a tertiary structure having the two hydrophobic faces held together by noncovalent forces. The resulting beta-barrel bell-shaped protein is called a 'betabellin'.

The specific residues for betabellin 7 are shown in Fig. 1. The boxed cross-linker is 3,5-bis(2-aminoethyl)benzoic acid (Bab), a symmetric diamino acid first synthesized during this project [4]. Precise locations of the beta turns should be determined by Pro at the second position of each turn. Following tryptic cleavage after Lys, Edman sequencing should reveal the residues present at the first and third turns, which comprise the potential active site. The heavy iodine atoms of the Phi residues are useful for solving X-ray structures. Earlier betabellins were quite hydrophobic and difficult to dissolve because they had much lower charge density than native globular proteins. To increase its hydrophilicity, betabellin 7 contains several additional charged residues (Asp, His).

Results and Discussion

Betabellin 7 was assembled using an automated continuous-flow solid phase synthesizer developed in collaboration with Eldex Laboratories [5]. The 66-residue protein was synthesized on Bab-Bal-methylbenzhydrylaminepolystyrene by stepwise solid phase assembly of Boc-amino acids. The two amino groups of the Bab cross-linker provided two identical sites for simultaneous peptide chain assembly, which took only 32 solid phase cycles. Betabellin 7 was deprotected

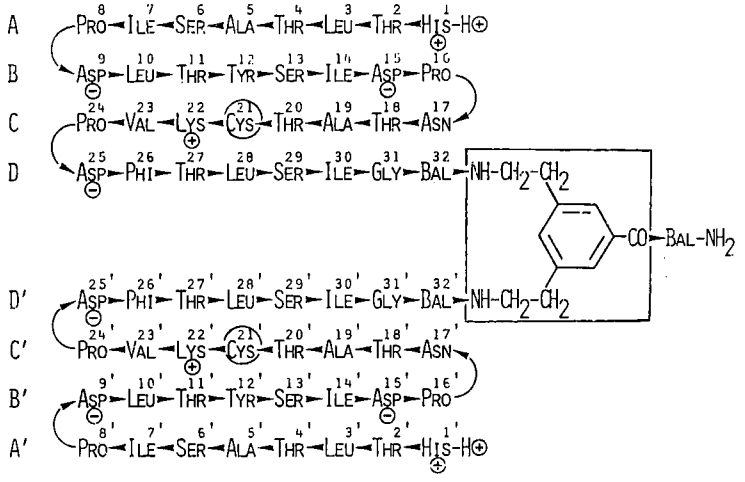

Fig. 1. Chemical structure of betabellin 7. In three dimensions, strand D' is predicted to lie over strand A (and A' to lie over D). The boxed portion is the symmetric diamino acid cross-linker Bab, Phi is 4-iodophenylalanine, and Bal is beta-alanine. The circled cysteine residues are expected to form a disulfide bridge.

and cleaved from the resin using low-high HF and gel filtered under reducing conditions on Sephadex G-50. The material eluting at the molecular weight of betabellin 7 was partitioned in a countercurrent centrifuge using butanol/acetic acid/water (4 : 1 : 5, v/v). The two major peaks had partition coefficients of 31 and 0.24. Both peaks lacked free thiol groups and gave amino acid compositions consistent with betabellin 7. Polyacrylamide gel electrophoresis showed a band near the expected molecular weight. Crystallization of the more hydrophilic material from 2-methyl-2,4-pentanediol produced small protein-like crystals.

Acknowledgements

This work was supported by contracts from the Office of Naval Research and the Army Research Office.

References

1. Daniels, S.B., Unson, C.G., Richardson, J.S., Richardson, D.C. and Erickson, B.W., Fed. Proc., 44 (1985) 694.
2. Erickson, B.W., Daniels, S.B., Reddy, P.A., Unson, C.G., Richardson, J.S. and Richardson, D.C., In Fletterick, R. and Zoller, M. (Eds.) Computer Graphics and Molecular Modeling, Cold Spring Harbor Laboratory, Cold Spring Harbor, NY, 1986, p. 53.

3. Daniels, S.B., Bobe, F.W., Reddy, P.A., Richardson, J.S., Richardson, D.C. and Erickson, B.W., Fed. Proc., 45 (1986) 1788.
4. Reddy, P.A. and Erickson, B.W., In Deber, C.M., Hruby, V.J. and Kopple, K. (Eds.) Peptides: Structure and Function, Proceedings of the 9th American Peptide Symposium, Pierce Chemical Co., Rockford, IL, 1985, p. 453.
5. Eberhard, L.M.B., Daniels, S.B. and Erickson, B.W., Fed. Proc., 45 (1986) 1788.

Phospholipid organization and motion in the presence of model amphipathic helix-forming peptides with opposite distribution of charges

Richard M. Epand[a], M. Iqbal[b], A. Gawish[b], J.P. Segrest[b], G.M. Anantharamaiah[b], W.K. Surewicz[c] and H.H. Mantsch[c]

[a]*Department of Biochemistry, McMaster University, Hamilton, Ont., Canada*
[b]*Departments of Pathology and Medicine, University of Alabama, Birmingham, AL 35294, U.S.A.*
[c]*Division of Chemistry, National Research Council, Ottawa, Ont., Canada*

Introduction

Several serum apolipoproteins, peptide hormones and peptide toxins have regularly spaced hydrophobic amino acids which would allow them to fold into an amphipathic helix; however, in addition to being able to spacially segregate hydrophobic and hydrophilic amino acid residues by folding into a helical conformation, these amphipathic helices may also have specific electrostatic interactions with phospholipids [1]. Amphipathic helical segments of serum apolipoproteins generally have positively charged amino acid residues at the polar–nonpolar interface and negatively charged residues opposite the hydrophobic face. In order to evaluate the importance of charge distribution on amphipathic helix–lipid interactions we designed and synthesized two peptides with identical amino acid composition but different distributions of charged residues [2]. One of the peptides, 18A, has the amino acid sequence Asp-Trp-Leu-Lys-Ala-Phe-Tyr-Asp-Lys-Val-Ala-Glu-Lys-Leu-Lys-Glu-Ala-Phe. Like serum apolipoproteins, this peptide would have positive charges at the hydrophobic–hydrophilic interface of an amphipathic helix. The properties of this peptide can be compared with that of reverse-18A, a peptide of opposite charge distribution and with the amino acid sequence Lys-Trp-Leu-Asp-Ala-Phe-Tyr-Lys-Asp-Val-Ala-Lys-Glu-Leu-Glu-Lys-Ala-Phe. The latter peptide has less helicity and lipid-binding affinity compared to the 18A analog. Increasing the helix-forming potential of reverse-18A increases the lipid-binding properties of the peptide compared with the unsubstituted reverse-18A [3]; however, the ability of the peptides to disrupt phospholipid bilayers is greater for the 18A analogs compared to the reverse-18A analogs. In addition to forming smaller lipoprotein particles, the modified 18A analogs were much superior to the modified reverse-18A analogs in their ability to activate the enzyme lecithin : cholesterol acyl transferase (LCAT). In this work, we compare the molecular properties of

phospholipid complexed with either [$E^{1,8}$, $L^{11,17}$]18A or with [$E^{4,9}$, $L^{11,17}$]reverse-18A (E is glutamic acid and L is leucine).

Results and Discussion

Both [$E^{1,8}$, $L^{11,18}$]18A and [$E^{4,9}$, $L^{11,17}$]reverse-18A strongly disrupt the bilayer structure of dimyristoylphosphatidylcholine (DMPC). Multilamellar suspensions of DMPC lose their turbidity within a few minutes at either 25°C or 35°C in the presence of either of these peptides, and the phase transition properties of the peptide are markedly broadened [3]. This disruption of extended bilayers of DMPC also results in a marked narrowing of the ^{1}H and ^{31}P NMR lipid resonances in the presence of either of these peptides. In addition, the ^{1}H chemical shift of the quaternary ammonium methyl groups indicates that these peptides promote the formation of smaller particles.

Although both of the peptides induce disruption of multilamellar vesicles, electron microscopy using negative staining as well as nondenaturing gradient gel electrophoresis indicate that the [$E^{1,8}$, $L^{11,18}$]18A forms smaller lipoprotein particles with DMPC than does [$E^{4,9}$, $L^{11,17}$]reverse-18A [3]. In addition, differences in the NMR properties of the lipid complexes with the two peptides can be interpreted in terms of differences in the sizes of the complexes. Both the ^{31}P and the ^{13}C line widths are narrower for the DMPC complex with [$E^{1,8}$, $L^{11,17}$]18A, and this peptide also induced a slightly greater upfield shift in the ^{1}H resonance from the quaternary ammonium group.

We investigated whether there were differences in the interaction of the charged groups of the lipid with the charged groups of the peptide. The motional properties of the phosphorous group of the lipid and of the quaternary ammonium methyl group as measured by ^{31}P-T_1 and ^{13}C-T_1, respectively, were indistinguishable for the complexes with the two peptides. In addition, FTIR measurements demonstrate that the ratio of *trans* to *gauche* rotamers of the acyl side chains is lower for these peptide–lipid complexes than it is for pure DMPC; however, the ratio of *trans* to *gauche* isomers is identical for the DMPC complexes with either of the two peptides. Thus the two peptides alter the structural properties of the lipid in the same manner and thus direct electrostatic interactions between the lipid and peptide are not likely to have a major effect on the properties of the lipid.

Another important property of lipids is the hydration of the bilayer. Increased hydration of the lipid would promote micellization. Measuring the extent of mobile water in frozen $^{2}H_2O$ solutions of the lipoprotein particles, we find that the complexes of DMPC with [$E^{1,8}$, $L^{11,17}$]18A have more unfrozen water than the complexes with [$E^{4,9}$, $L^{11,17}$]reverse-18A. The more highly hydrated and smaller lipoprotein complex formed with [$E^{1,8}$, $L^{11,17}$]18A has a larger fraction of the lipid at the edge of the discoidal lipoprotein particle. This lipid is at an interface

between lipid and protein. The molecules would not be as tightly packed at such an irregular interface as they are in a pure lipid domain. Therefore, this phospholipid would be more accessible to the enzyme LCAT. This would explain why the [$E^{1,8}$, $L^{11,17}$]18A complexes with DMPC are better LCAT substrates than the complexes formed between DMPC and [$E^{4,9}$, $L^{11,17}$]reverse-18A.

References

1. Segrest, J.P., Jackson, R.L., Morrisett, J.D. and Gotto, Jr., A.M., FEBS Lett., 38 (1973) 247.
2. Anantharamaiah, G.M., Jones, J.L., Brouillette, C.G., Schmidt, C.F., Chung, B.H., Hughes, T.A., Bhown, A.S. and Segrest, J.P., J. Biol. Chem., 260 (1985) 10248.
3. Epand, R.M., Gawish, A., Iqbal, M., Gupta, K.B., Chen, C.H., Segrest, J.P. and Anantharamaiah, G.M., J. Biol. Chem., (1987) in press.

Simulation of the crystal of *Streptomyces griseus* protease A

David H. Kitson[a], Franc Avbelj[a], John Moult[b] and Arnold T. Hagler[a]
[a]The Agouron Institute, 505 Coast Blvd. So., La Jolla, CA 92037, U.S.A.
[b]The University of Alberta, Medical Sciences Building, 113th St. & 87th, Edmonton, Alberta T6G 2H7, Canada

Introduction

The study of the structural properties of biological macromolecules, and the way in which these molecules interact with their environment and with other molecules, represents one of the most exciting fields of physical chemistry today. Conventional experimental techniques, such as X-ray crystallography, can give us an accurate picture of the macromolecule at an atomic level. They cannot, however, describe the behavior of the solvent at this level of detail due to its disordered or semiordered nature. Simulation techniques, on the other hand, provide a powerful tool for studying the solvent and will enable us to explore many questions of basic and fundamental biophysical importance. We have used Monte Carlo and molecular dynamics simulation techniques to study the energetics and dynamics of the protein and solvent in the crystal of the protein *Streptomyces griseus* Protease A (SGPA), a serine protease. The crystal structure of SGPA has been solved to high resolution (1.5 Å, R factor = 12.1%) [1].

The Experiment

The basic simulation unit consists of two proteins (with all hydrogens built on according to standard geometries), 18 sodium ions, 26 phosphate ions and 1429 water molecules. Periodic boundary conditions, with a cut-off of 15 Å, were used to simulate the crystal environment. Starting from this system (with the proteins in their crystal conformation), 10 million configurations of the solvent molecules were generated using the Metropolis Monte Carlo algorithm. Eleven picoseconds (ps) of molecular dynamics were also run (starting from a Monte Carlo configuration) with the protein kept fixed, followed by 50 ps of dynamics in which all of the system was free to move.

Analysis

Analysis of the results of the simulations can be divided into two areas: comparison of the results of the simulation with experimental data and exploration

of other fundamental questions which arise from the experimental data or the results of the simulation.

Table 1 shows the RMS deviations between the simulated and experimental structures of the protein. The RMS deviation from the experimental structure averaged both over time and over the two molecules in the asymmetric unit is 1.28 Å for all atoms and 1.11 Å for C^{α} atoms.

The motions of the counterions during the molecular dynamics show several interesting features. At the start of the 50 ps simulation one of the phosphate ions moves ≈ 3 Å in 3 ps. It then oscillates in an area of space about 1.5 Å in diameter for 10 ps. A rapid transition ('jump-diffusion', taking ≈ 1.5 ps) then takes the ion to a new position, about 1.5 Å away, around which it again oscillates for 13 ps. A final rapid transition then occurs, taking the ion to its final position where it stays until the end of the simulation. We are investigating the motion of other molecules to see how these are correlated with this type of ion motion.

We are continuing with further analyses of these simulations, including a comparison of calculated temperature factors, electron density, and structure factors with experimental values, and an examination of the effect of the protein's field on the motion of the ions. We also plan to perform simulations of SGPA including bound ligands, and of the ligands in solution, and to explore the energetics of binding of ligands to SGPA.

Table 1 *Comparison of the RMS differences between the X-ray structure of SGPA and structures averaged over various time periods of the molecular dynamics simulation*

Average structure[a]	RMS[b]			
	1[c]/X-ray	2[c]/X-ray	$\overline{1+2}$/X-ray	1/2
< 1-10>	1.18 (0.97)	0.84 (0.68)	0.86 (0.69)	1.16 (0.99)
<10-20>	1.69 (1.46)	1.26 (1.06)	1.18 (1.01)	1.83 (1.56)
<20-30>	1.76 (1.50)	1.43 (1.23)	1.27 (1.09)	1.98 (1.67)
<30-40>	1.91 (1.66)	1.46 (1.24)	1.31 (1.14)	2.17 (1.84)
<40-50>	2.11 (1.86)	1.51 (1.24)	1.44 (1.25)	2.26 (1.92)
<16-50>	1.84 (1.59)	1.43 (1.21)	1.28 (1.11)	2.06 (1.75)

[a] This column gives the time period (in picoseconds) over which the averages were calculated.

[b] The first RMS value given is for all heavy atoms. The value in parentheses is for only the C^{α} atoms.

[c] Structures 1 and 2 refer to the first and second simulated SGPA molecules, respectively.

Acknowledgements

We would like to thank the National Institutes of Health, who provided financial support for this project, and the National Science Foundation, for a grant of computer time.

References

1. Sielecki, A.R., Hendrickson, W.A., Broughton, C.G., Delbaere, L.T.J., Brayer, G.D. and James, M.N.G., J. Mol. Biol., 3134(1978)781.

Synthesis and oxidative properties of cysteine-containing fragments of bovine growth hormone

S. Russ Lehrman*, Thomas F. Holzman, Clayton J. Cole and David N. Brems
The Upjohn Company, Control Biotechnology, Kalamazoo, MI 49001, U.S.A.

Introduction

Selective disulfide bond formation occurs within cysteine-containing proteins as they renature in aqueous solution. This process has been studied for a number of proteins which include ribonuclease [1], bovine pancreatic trypsin inhibitor [2], and bovine growth hormone [3]. These studies help define pathways for disulfide bond formation, but have not determined any possible contributions of primary or secondary structure to the process.

Bovine growth hormone (bGH), a hormonal protein synthesized and released from the anterior pituitary, contains 191 residues and two disulfide bonds, spanning residues 53–164 and 181–191. To help determine structural features of bGH which allow cysteine residues 53 and 164 to form a disulfide linkage, we have synthesized two bGH fragments (see Fig. 1) which contain these cysteines, and have initiated studies of their oxidative properties and conformation.

Materials and Methods

Peptides I and II were synthesized using standard solid phase methods on an Applied Biosystems 430A (Foster City, CA). Deprotected peptides were purified on a medium pressure Vydac C4 column (20–30 μm; The Separations Group, Hesperia, CA). AAA: (I) Asx 1.0; Thr 2.7; Ser 1.5; Glx 3.0; Pro 2.2; Gly 1.0; Ala 2.2; Val 1.0; Ile 2.0; Tyr 1.0; Phe 2.3; Lys 1.0; Cys N.D.; (II) Asx 1.0; Ser 0.5; Gly 1.0; Leu 2.0; Tyr 1.0; Phe 1.0; Arg 1.0; Cys N.D.

Peptides I and II (1 mg/ml) were mixed and oxidized in 0.1 M $NaHCO_3$, pH 7.6, containing a mixture of 10 mM oxidized DTT and 1 mM reduced DTT, in the presence or absence of 5 M guanidine hydrochloride. Aliquots of the oxidation mixture were acidified and analyzed on a Bakerbond C4 column (J.T. Baker, Phillipsburg, NJ), monitored at 215 nm.

*To whom all correspondence should be addressed. The Upjohn Company, Control Biotechnology, Unit 4861-259-12, 7000 Portage Road, Kalamazoo, MI 49001, U.S.A.

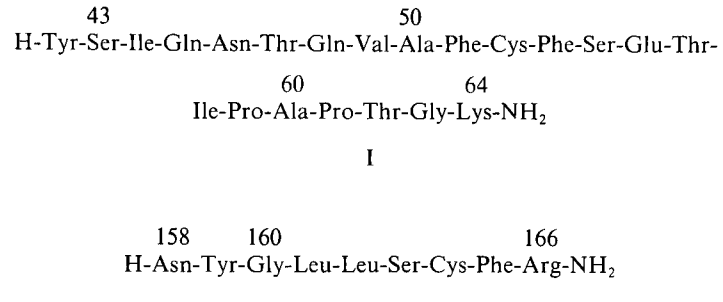

Fig. 1. Primary structure of [43–64]- and [158–166]-bGH-NH_2. Numbers above the sequence refer to residue position in the native protein.

Circular dichroism spectra of peptides I and II (1–5 nM) were obtained on a Jasco J-500C in 10 mM sodium phospate, pH 7.6, in the presence and absence of 5 M guanidine hydrochloride.

Results

Peptides I and II form a mixed disulfide only when denaturant is included in the oxidation reaction (Fig. 2, peak A). The identity of the heterodimer was confirmed by protein sequence analysis (J.J. Dougherty, data not shown). In the presence of denaturant, a minimum of 90% of peptide I forms the heterodimer, indicating selectivity in disulfide bond formation. When denaturant is omitted from the oxidizing media, peptide I forms a molecular species which elutes as a broad peak under the chromatographic conditions used. Separate experiments suggest that this species is a nondisulfide bonded aggregate. Peptide II forms a homodimer whether or not denaturant is included in the oxidizing media (Fig. 2, peak B).

The inability of peptides I and II to form the mixed disulfide in non-denaturing, aqueous solution may be due to the presence of secondary structure in one or both peptides. Circular dichroism spectra of peptides I and II were therefore obtained in the presence and absence of 5 M guanidine hydrochloride (Fig. 3). In nondenaturing solutions, the spectrum of peptide I contains a minimum of 216 nm. This absorption band suggests the presence of beta-sheet structure in this peptide. This conformation may be stabilized by intrachain hydrogen bonding (necessitating the presence of a reverse turn in the peptide backbone), or through interchain interactions, as might occur during aggregation. Further experimentation will be necessary to confirm the presence of beta-sheet structure in peptide I. The spectral measurements indicate that peptide II contains no secondary structure in aqueous solutions.

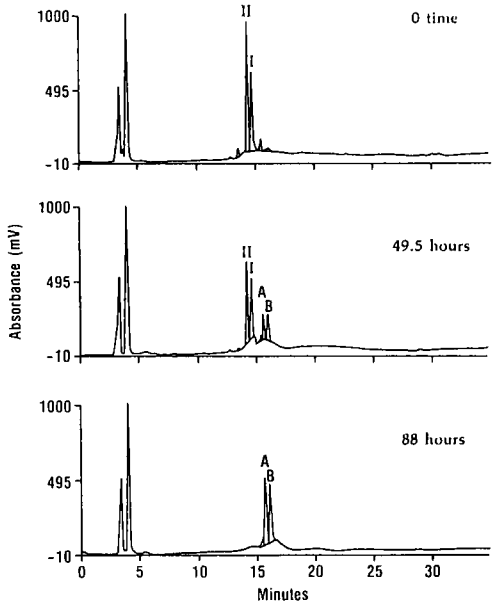

Fig. 2. HPLC analyses of the peptide I + II oxidation mixtures in aqueous solution containing 5 M guanidine hydrochloride. Aliquots (100 µl) were chromatographed from 10–70% acetonitrile (0.1% TFA), using a 40-min linear gradient. Other details are described in the text. Peaks A and B are the peptide I-II heterodimer and peptide II homodimer, respectively. Early eluting peaks are due to the addition of DTT and guanidine.

Discussion

Our data show that the peptide I-II heterodimer forms only when the two peptides are incubated in denaturing, oxidizing media. Since peptide I forms a beta-sheet-like conformation in aqueous solution, it appears that secondary structure inhibits the formation of the mixed disulfide. In addition, formation of this heterodimer occurs preferentially over the formation of the peptide I homodimer. To our knowledge, this is the first report which suggests that directional disulfide bonding occurs during the sulfhydryl oxidation of fragments derived from disulfide-containing proteins.

Cursory analysis of the primary structure for these peptides does not readily suggest reasons for this directional disulfide bond formation. The cysteine of peptide I is sandwiched between two phenylalanyl residues and is two residues removed from a glutamyl residue, while the cysteine of peptide II is situated within the sequence -Ser-Cys-Phe-Arg-Lys-. Perhaps the combined effects of the proximal aromatic residues and electrostatic interactions of nearby amino acid residues assist the preferential formation of the peptide I-II heterodimer.

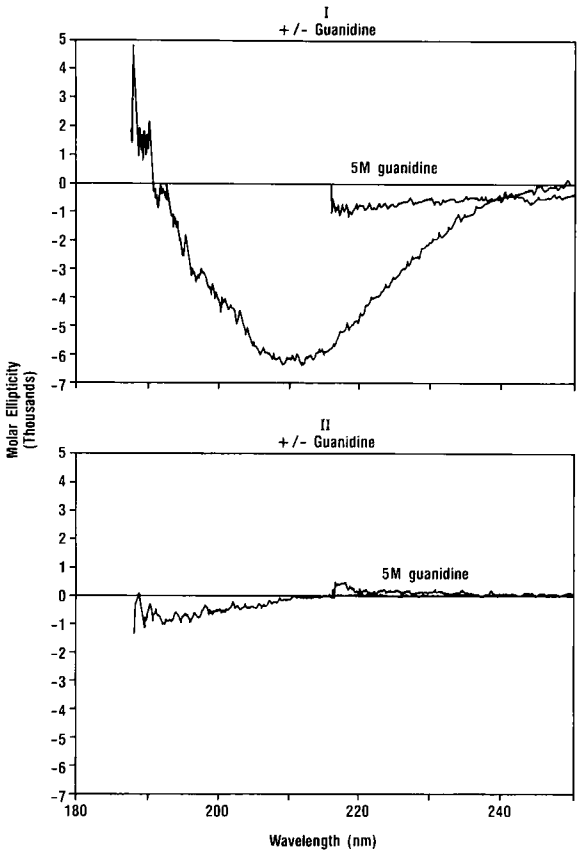

Fig. 3. Far ultraviolet circular dichroism of I and II. Peptide I (12.5 μg/ml) and II (5.0 μg/ml) were dissolved in 10 mM sodium phosphate, pH 7.6. The spectra were obtained at room temperature.

Acknowledgements

The authors thank Ms. Patricia Barr for typing the manuscript.

References

1. Anfinsen, C.B. and Haber, E., J. Biol. Chem., 236 (1961) 1361.
2. Creighton, T.E., Progr. Biophys. Mol. Biol., 33 (1978) 231.
3. Holzman, T.F., Brems, D.N. and Dougherty, J.J., Biochemistry, 25 (1986) 6907.

The role of cysteine residues in human interleukin-1β

Yoshihiro Masui, Takashi Kamogashira, Yeong-Man Hong, Yoshikazu Kikumoto, Satoru Nakai and Yoshikatsu Hirai

Laboratories of Cellular Technology, Otsuka Pharmaceutical Co., Ltd., 463-10 Kagasuno, Kawauchi-cho, Tokushima 771-01, Japan

Introduction

Interleukin-1 (IL-1) is a family of monocyte-derived polypeptide hormones which affect many different cell types involved in immunologic and inflammatory responses [1]. Recent cDNA cloning studies have shown that IL-1 activities can be mediated by at least two distinct 17.5 kDa mature proteins (IL-1α and IL-1β) [2]. In human mature protein IL-1β consisting of 153 amino acids, two Cys residues exist at the positions of 8 and 71. However, the role of these characteristic Cys residues in IL-1β on the biological function has not been clarified. In this study, the recombinant *Escherichia coli*-derived IL-1β (rIL-1β) was found to have no intramolecular disulfide bond by chemical modification. Furthermore, we investigated the influence of the Cys residues on the biological activity of IL-1β, using the site-specific mutagenesis of recombinant DNA technology.

Results and Discussion

In order to investigate whether or not an intramolecular disulfide bond exists in IL-1β, the chemical modifications of Cys in rIL-1β were carried out as follows. The reductive or direct carboxamide-methylation of rIL-β was performed in the presence of guanidine hydrochloride. In these modified proteins, about two molar carboxymethyl cysteines per protein molecule were detected by amino acid analysis following their acid hydrolyses. Direct sulfhydryl titration of rIL-1β by Ellman reagent in the presence of guanidine hydrochloride gave a value of 2.2 molar per protein molecule of rIL-1β. These results indicate that the two Cys residues in rIL-1β do not form an intramolecular disulfide bond. In addition, our comparative studies of rIL-1β and native IL-β (nIL-β) demonstrated that they were almost the same in their biological and physicochemical properties (Nakai, S., et al., unpublished data). It was therefore suggested that nIL-1β has no intramolecular disulfide bond.

Next, in order to evaluate the role of the Cys in IL-1β, modification of the

IL-1β gene was performed by site-specific mutagenesis. At first, we constructed a newly versatile plasmid (f1IL-1β1ppT) which can be used not only for isolation of the modified IL-1β gene but also for expression of the mutant proteins as shown in Fig. 1. Using this plasmid and synthetic oligonucleotide primers, some

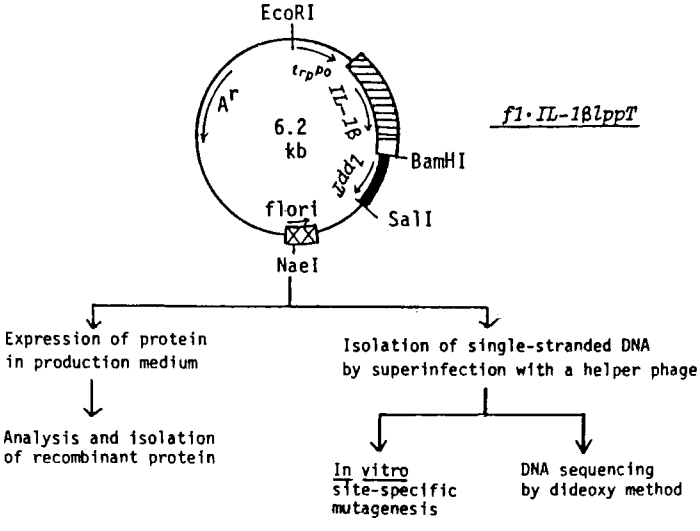

Fig. 1. The strategy for isolation and expression of IL-1β mutants using E. coli *harboring f1IL-1β1ppT plasmid. The line shows the pBR322 region including the β-lactamase gene (A^r) and the origin of replication, except for that of the promoter and operator of the tryptophan gene (trp^{po}).*
Abbreviations: 1ppT = *transcription termination region of* E. coli *lipoprotein gene; flori = the intergenic region of f1 phage gene.*

mutants, in which Cys residues at the position of 8 or 71 or both were substituted with Ala or Ser, were obtained, as shown in Table 1. The mutation of IL-1β was confirmed by sequence analysis of the DNA and amino acid composition of the purified proteins. The mutant proteins, which were produced from the mutants in *E. coli*, were purified to homogeneity by a combination of cation exchange HPLC and gel filtration HPLC. The purity of the proteins was confirmed by SDS-polyacrylamide gel electrophoresis, isoelectric focusing, analytical HPLC, amino acid composition, and amino acid sequence analysis of the amino terminal region. Only Ala was detected as an amino terminal amino acid in all purified proteins, including IL-β.

The biological and physicochemical properties of IL-1β were compared with those of the mutant proteins, as shown in Table 1. The biological activity of these proteins was determined due to the ability of growth inhibition of human

Table 1 *Biological activity and physicochemical properties of native IL-1β, rIL-1β, and its mutant proteins*

Polypeptide	Relative biological activity[a] (%)	Molecular weight[b] (kDa)	Isoelectric point [c]
native IL-1β	100	18	6.9
rIL-1β	100	18	6.9
Ala^{8} IL-1β	204	18	6.9
Ala^{71} IL-1β	187	18	6.9
Ser^{71} IL-1β	174	18	6.9
Ala^{8} · Ala^{71} IL-1β	237	18	6.9

[a] Biological activity was determined with the ability of growth inhibition for human melanoma A375 cells.
[b] Molecular weight was estimated by SDS-polyacrylamide gel electrophoresis.
[c] Isoelectric point was determined by analytical isoelectric focusing.

melanoma A375 cells. As is obvious from Table 1, the substitutions of either Cys residue with Ser as well as of either or both Cys residue(s) with Ala yield IL-1β analogs which have a little, but obviously higher biological activity than that of the natural form. We found that the deletion of Cys, especially Cys 71, however, caused the instability of proteins in *E. coli* and the decrease in their biological activities (data are not shown here). Judging from these results, the Cys residues in IL-1β were found to be substituted with Ser or Ala, but not to be eliminated for the maintenance of the functional structure of IL-1β.

Conclusion

We have demonstrated that both Cys residues in rIL-1β are not involved in the formation of disulfide bridges, nor are they essential for exerting the biological activity of IL-1β; however, in this study, the influence of the disulfide bond on the function of IL-1β was not clarified. Therefore, we plan to investigate the influence of formation of the disulfide bridge on the function of IL-1β.

References

1. Oppenheim, J.J., Kovacs, E.J., Matsushima, K. and Durum, S.K., Immunol. Today, 7(1986)45.
2. March, C.J., Mosley, B., Larsen, A., Cerretti, D.P., Braedt, G., Price, V., Gillis, S., Henney, C.S., Kronheim, S.R., Grabstein, K., Conlon, P.J., Hopp, T.P. and Cosman, D., Nature, 315(1985)641.

Synthesis of two component models of elastin

Kari U. Prasad, M. Iqbal and D.W. Urry

Laboratory of Molecular Biophysics, The University of Alabama at Birmingham, School of Medicine, University Station/P.O. Box 311, Birmingham, AL 35294, U.S.A.

Morphologically, elastic fibers can be described as a fine fibrillar coating of a large amorphous core referred to as elastin. Elastin is an insoluble, highly cross-linked and very hydrophobic protein with about 90% nonpolar amino acids and about 5% lysines. The insolubility of elastin is due to the presence of cross-links, primarily desmosine and isodesmosine (Fig. 1), which are formed from four lysine residues, two each from two different peptide chains. The cross-linking sequences KAAAK and KAAK were observed to repeat at least six times in the soluble precursor protein, tropoelastin, which is comprised of 800–850 amino acids. Determination of the amino acid sequence of porcine tropoelastin using tryptic peptides is 80% complete [1]. The largest porcine tryptic peptide is 81 residues; the dominant feature of this peptide is the repeating pentapeptide sequence $(Val\text{-}Pro\text{-}Gly\text{-}Val\text{-}Gly)_n$ with $n = 11+$ in pig. Conformational studies on oligo- and polypentapeptides of the above repeating sequence, carried out in this laboratory, resulted in the development of a new class of conformations called β-spirals in which a β-turn occurs with regularity along the helical axis. A new mechanism of elasticity, 'a librational entropy mechanism', has been put forward to explain the elastic behavior of the polypentapeptide [2–4]. This contrasts with the 'random chain-network theory' previously proposed for elastin [5]. Demonstration of the librational entropy mechanism and the nonrandom nature of elastin has been achieved by numerous physical characterizations: light and electron microscopy; circular dichroism; Raman spectro-

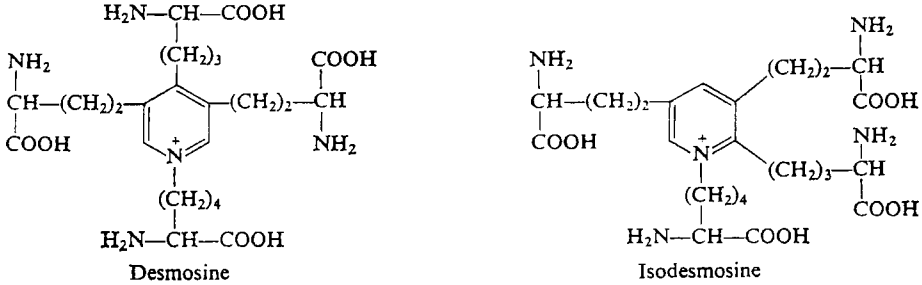

Fig. 1. Structures of desmosine and isodesmosine.

scopy; dielectric relaxation; nuclear magnetic resonance (NMR); temperature dependence of length, of force development, and of elastic modulus; and composition studies [6].

In order to develop polypeptides as models for the natural insoluble elastin, it is useful to synthesize a polypentapeptide molecule with cross-linking sequences and then polymerize them to yield very high molecular weight polymers, which on enzymatic cross-linking by lysyl oxidase could result in biomaterials with physical properties similar to elastin.

Here we report the synthesis of the two polymers $[XL\text{-}1\text{-}(VPGVG)_{15}]_n$ and $[XL\text{-}2\text{-}(VPGVG)_{15}]_n$ where XL-1 is the cross-linking sequence, AAAAKAAK-YGA, and XL-2 is the second cross-linking sequence, AAKAAAKAA.

Synthesis: The synthesis of the two monomeric peptides, AAAAKAAKYGA-

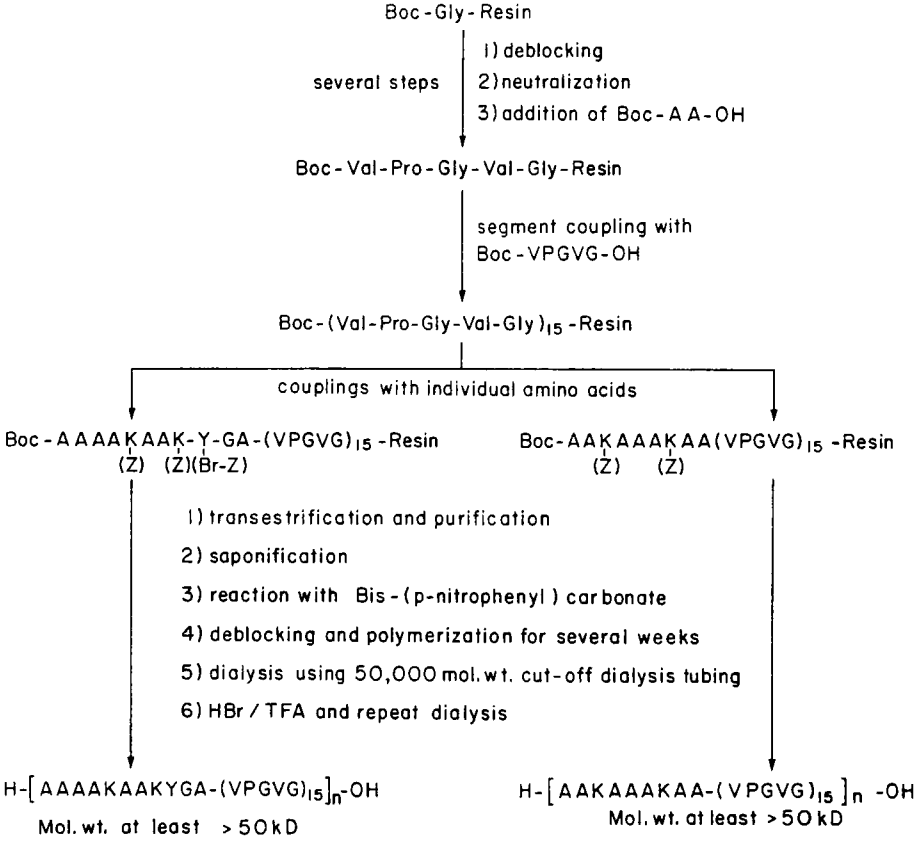

Scheme 1. Synthesis of elastin peptide models with cross-linking sequences.

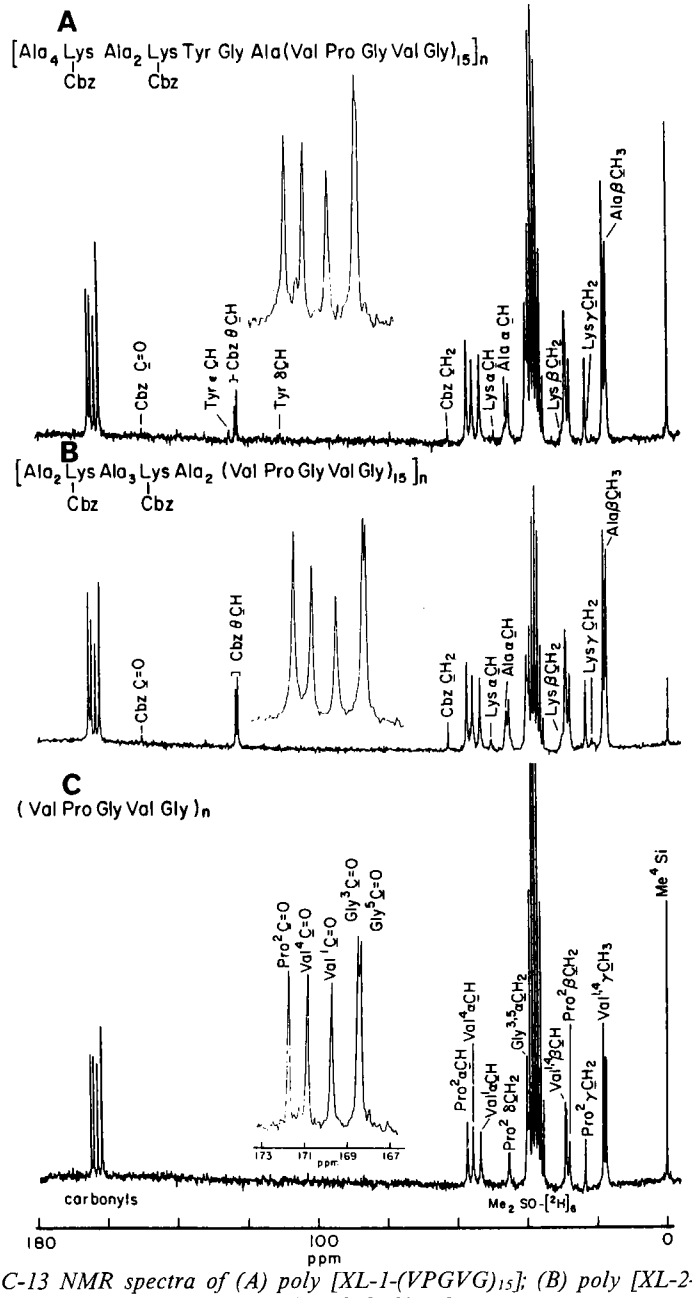

Fig. 2. C-13 NMR spectra of (A) poly [XL-1-(VPGVG)15]; (B) poly [XL-2-(VPGVG)15]; and (C) poly (VPGVG) at 25 MHz in dimethylsulfoxide.

$(VPGVG)_{15}$ and AAKAAAKAA-$(VPGVG)_{15}$, was carried out by the solid phase methodology [7] (Scheme I). The first pentamer sequence VPGVG was built on the 1% cross-linked Merrifield resin by adding a single amino acid at a time. The next 14 pentamer units were attached by the segment condensation approach using Boc-VPGVG-OH, synthesized by the classical solution methods as reported earlier [8]. The amino acids in the cross-linking sequences were once again coupled by stepwise condensation. The side-chain functional groups of Lys and Tyr were protected by Cbz and O-Br-Cbz groups, respectively. The segment condensations were carried out in DMF, TFE-CH_2Cl_2 or TFE alone in the presence of HOBt. Occasionally preformed symmetrical anhydrides of individual amino acids had to be used to ensure the completeness of the reaction. In order to check the progress of the coupling reactions, the peptides were removed from the resin as methyl esters at various stages of peptide synthesis when there were 6, 9, 12, and 15 pentamer units attached to the growing peptide chain. An approximate determination of the peptide chain length during the course of the synthesis could be obtained from a plot of ln (molecular weight) versus the midpoint of the temperature profile of turbidity ($TP\tau$) as well as from NMR end group analysis [9]. After the synthesis was completed on the resin, the Boc-protected peptides were removed as methyl esters by transesterification and purified by repeated precipitations from different solvent systems. The purity of the peptide was checked by C-13 magnetic resonance (C-13 NMR) spectra and amino acid analysis. After saponification, the peptides were converted to p-nitrophenyl esters by reacting with excess of bis (*p*-nitrophenyl) carbonate [10] for several days.

The Boc group was removed and the peptides were polymerized for 8–12 weeks in dimethylsulfoxide in the presence of *N*-methylmorpholine. After diluting with water, the polymers were dialyzed against water using a 50-kDa cutoff dialysis tubing for 15 days and the retentates were lyophilized. The purity of the polymers was again checked by C-13 NMR (Fig. 2) and amino acid analysis.

In conclusion, the feasibility of synthesizing large peptides of 86 and 84 amino acids in length and polymerizing them into polymers having molecular weights of greater than 50 kDa is demonstrated. The next step will be to remove the Z groups on lysines; submit the polymers separately, and mixed, to lysyl oxidase treatment; study the various intermediate oxidation products and also the formation of final desmosine and isodesmosine structures; and compare the mechanical properties of the insoluble matrix to those of natural elastin.

Acknowledgements

This work was supported in part by NIH Grant HL-29578 and Department of the Navy, Office of Naval Research Grant N00014-K-86-0402.

References

1. Sandberg, L.B., Leslie, J.G., Leach, C.T., Alvarez, V.L., Torres, A.R. and Smith, D.W., Path. Biol., 33(1985)266.
2. Urry, D.W., In Cunningham, L.W. and Frederiksen, D.W. (Eds.) Methods in Enzymology, Academic Press, New York, NY, 1982, p. 673.
3. Urry, D.W., Venkatachalam, C.M., Long, M.M. and Prasad, K.U., In Srinivasan R. and Sarma, R.H. (Eds.) Conformation in Biology, Adenine Press, Schenectady, NY, 1982, p. 11.
4. Urry, D.W. and Venkatachalam, C.M., Int. J. Quantum Chem., Quantum Biol. Symp. No. 10(1983)81.
5. Hoeve, C.A.J. and Flory, P.J., Biopolymers, 13(1974)677.
6. Urry, D.W., In Robert, L. and Hornebeck, W. (Eds.) Elastin and Elastases, CRC Press, Boca Raton, FL, in press.
7. Merrifield, R.B., J. Am. Chem. Soc., 85(1963)2149.
8. Prasad, K.U., Iqbal, M.A. and Urry, D.W., Int. J. Pept. Prot. Res., 25(1985)408.
9. Urry, D.W., Trapane, T.L. and Prasad, K.U., Biopolymers, 24(1985)2345.
10. Wieland, Th., Heinke, B. and Vogeler, J., Justus Liebigs Ann. Chem., 655(1961)189.

Covalent semisynthesis of α-chain of hemoglobin: Protease-catalyzed transpeptidation at the permissible discontinuity site

A. Seetharama Acharya, Youngnan J. Cho, and Girish Sahni
The Rockefeller University, 1230 York Avenue, New York, NY 10021, U.S.A.

Introduction

Protein semisynthesis is a powerful procedure for investigating the structure–function relationships of polypeptides and proteins. Unlike the genetic engineering methods for the preparation of mutants of proteins, semisynthesis offers the flexibility to introduce an unnatural amino acid or ^{13}C- or ^{15}N-amino acid at a given site. Protease-catalyzed reformation of peptide bonds in fragment complementing systems of proteins has been emerging as a very useful semisynthetic approach for the preparation of muteins [1].

The synthesis of peptide bonds by reverse proteolysis represents an equilibrium between the synthetic and hydrolytic reactions. Thus, during protein semisynthesis by this approach an equilibrium exists between the covalent form of the protein and its noncovalent fragment system. In addition, the noncovalent fragment system of a protein also represents a dynamic equilibrium between the native state in which the complementary fragments are tightly associated and the nonnative state in which the complementary fragments are dissociated [2, 3]. Therefore, it is conceivable that one could exchange a variant peptide corresponding to one of the complementary fragments of the protein with the native peptide segment of the intact protein in the presence of the appropriate protease without, in fact, having to isolate the complementary fragments (Fig. 1). The consequence of coupling the above two reversible systems is a net transpeptidation reaction at the permissible discontinuity site of the protein. This transpeptidation should succeed provided the variant peptide and the complementary fragment could interact to generate the native-like fold. The validity of this principle and the feasibility of this approach for the covalent semisynthesis of the α-chain of hemoglobin has now been investigated.

Results and Discussion

The junction around the translation products of Exon-1 and Exon-2 of α-globin [Arg-31–Met-32] represents a permissible discontinuity region of the

α-chain within its tertiary interaction. *Staphylococcus aureus* V8-protease introduces a discontinuity at the peptide bond Glu-30–Arg-31 of the chain [4]. V8-protease also catalyzes the ligation of the unprotected complementary fragments of α-globin, namely α_{1-30} and α_{31-141}, at pH 6.0 and 4°C in the presence of 30% *n*-propanol [5] with high selectivity. In order to test whether the covalent semisynthesis through the protease-catalyzed exchange route (Fig. 1) could occur, α-globin was incubated for 48 h with an equimolar amount of [^{14}C]-N$^{\alpha}$-dihydroxypropyl (DHP) α_{1-30} at pH 6.0 and 4°C (Fig. 2) in the presence of 30% *n*-propanol. The segment exchange occurs only in the presence of V8-protease. Nearly 20% of the ^{14}C-label of N$^{\alpha}$DHP-α_{1-30} is exchanged into globin. Concomitant with this exchange, α_{1-30} and small amounts of α_{1-27} are released. The exchange reaction proceeds with nearly the same overall efficiency at pH 8.0 as well.

n-Propanol is an efficient organic co-solvent for the V8-protease-catalyzed semisynthesis of α-globin; however, glycerol, the more commonly used organic co-solvent for semisynthesis, was not very efficient [5]. The protease-catalyzed semisynthesis of α-globin as well as the exchange reaction proceeded smoothly in the presence of trifluoroethanol as well as isopropanol. The propensity of *n*-propanol, trifluoroethanol, and isopropanol to induce a native-like fold in α-globin [6] appears to play a key role in the efficient semisynthesis of α-globin.

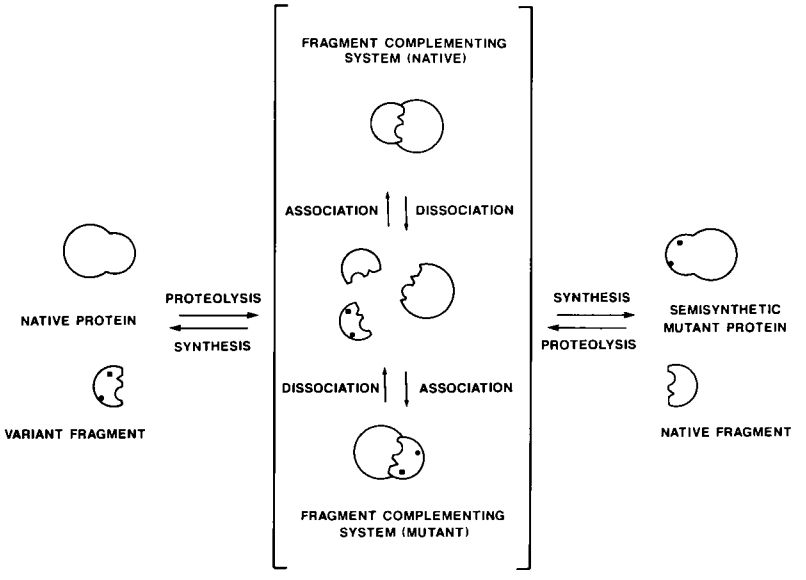

Fig. 1. Schematic representation of protease-catalyzed replacement of a segment of a protein to prepare muteins. • and ▪ represents mutations introduced through chemical synthesis.

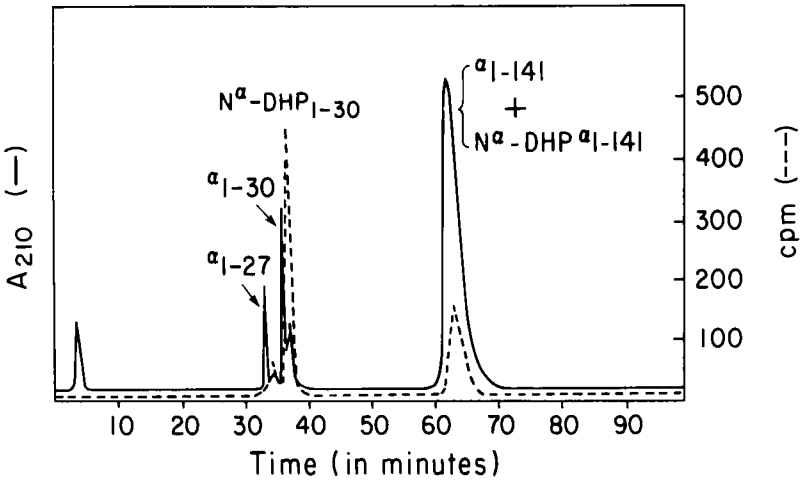

Fig. 2. RPHPLC analysis of V8-protease-catalyzed covalent semisynthesis of α-globin through segment exchange. The analysis of N^{α}-DHP-α_{1-30} incubated with α-globin for 48 h in the presence of V8-protease was carried out on a synchropak RP-300 column using 0.1% TFA and a linear gradient of CH_3CN from 5 to 70% over 100 min.

These results suggest that the V8-protease-catalyzed exchange of N^{α}DHP-α_{1-30} with the intact amino terminal 30-residue segment of α-globin could also occur in the presence of glycerol if the reaction is carried out with the α-chain (globin with bound heme). Indeed, when the reaction was carried out with the α-chain for 48 h in the presence of 50% glycerol at pH 6.0 and 4°C the segment replacement occurred with an overall efficiency comparable to that obtained using α-globin and 30% *n*-propanol.

The native-like fold of the polypeptide chain appears to be an essential element for the successful segment replacement reaction catalyzed by protease. The generality of the protease-catalyzed transpeptidation at the permissible discontinuity site of proteins appears to be a subject worthy of further investigation.

References

1. Chaiken, I.M., Crit. Rev. Biochem., 11 (1981) 255.
2. Taniuchi, H., J. Biol. Chem., 248 (1973) 5164.
3. Acharya, A.S., Manjula, B.N. and Vithayathil, P.J., Biochem. J., 173 (1978) 821.
4. Seetharam, R., Dean, A., Iyer, K.S. and Acharya, A.S., Biochemistry, 25 (1986) 5949.
5. Acharya, A.S., Khan, S.A. and Seetharam, R., In Deber, C.M., Hruby, V.J. and Kopple, K.D. (Eds.) Peptides: Structure and Function, Proceedings of the 9th

American Peptide Symposium, Pierce Chemical Co., Rockford, IL, 1985, pp. 335-338.
6. Iyer, K.S. and Acharya, A.S., Proc. Natl. Acad. Sci. U.S.A., (1987) in press.

Session VI
Nucleic acid/peptide interactions

Chair: Daniel H. Rich
University of Wisconsin
Madison, Wisconsin, U.S.A.

The structural basis for activation of *trp* repressor by L-tryptophan

R.W. Schevitz[a], R.-G. Zhang[a], C.L. Lawson[a], Z. Otwinowsky[a], A. Joachimiak[b] and P.B. Sigler[a]

[a]*Department of Biochemistry and Molecular Biology, The University of Chicago, Chicago, IL 60637, U.S.A.*

[b]*Institute of Bioorganic Chemistry, Polish Academy of Sciences, Noskowskiego 12/14, Poznan 61704, Poland*

The interactions between proteins and DNA are important elements in the regulation of gene expression. *Trp* repressor is one DNA binding protein that regulates tryptophan levels in *Escherichia coli* by controlling the transcription rate of biosynthetic genes. An important property of this repressor is that it exists in two functionally important states: (i) inactive aporepressor, which does not have the corepressor L-tryptophan bound and which cannot bind specifically to operator, and (ii) repressor, which does have L-tryptophan bound and which does bind to the operators of *trp*EDCBA, *aro*H, and *trp*R. When tryptophan levels in the cell are low, aporepressor is favored. It cannot bind to operator and interfere with polymerase access to the overlapping promoter site, and thus transcript important for tryptophan synthetase is made. Alternatively, when tryptophan levels in the cell are high, the active form of the repressor is favored; it does bind to operator and restricts access of the polymerase to the promoter site. Transcript is then not made, hence enzymes important for tryptophan synthesis are not made.

Since the three-dimensional structures of *both* aporepressor [1] and *trp* repressor [2] have been solved to high resolution, the structural features that underlie this activation can be examined. What are the structural changes produced by the binding of L-tryptophan, and how do they confer the ability to bind specifically to the operator sequence?

Trp repressor exists as a dimer; each subunit contains 107 residues that form six α-helices (labeled A through F), and they comprise more than 75% of the entire structure. Except for the loosely ordered ten N-terminal residues, the longest nonhelical segment is four residues. The helices of these two subunits are so intertwined and make such extensive intersubunit contacts that their association as a dimer is necessary for the three-dimensional integrity of *trp* repressor (Schevitz, manuscript in preparation).

Helices D and E comprise the DNA binding helix-turn-helix motif first seen

in the three-dimensional structures of corepressor [3], CAP [4] and λ-repressor [5], and predicted by Ohlendorf et al. [6] to exist in *trp* repressor on the basis of sequence homology with these proteins. Helices D and E form prominent protrusions on one side of the repressor that are separated from their symmetry-related mates in the other subunit by one turn of a B-DNA duplex. The importance of this surface, containing both helix-turn-helix motifs, for binding DNA is underscored by the observation of Kelley and Yanofsky [7] that all of the negative complementing mutants of *trp* repressor that reduced operator-specific binding were found to line this surface of the repressor exclusively.

The corepressor L-tryptophan which mediates the crucial transition between active and inactive forms does not lie in a position where it can make a direct sequence-specific interaction with the operator. Rather, it lies against the side of the E-helix near Gly-85 (Fig. 1) in the space normally occupied in homologous helix-turn-helix sequences by a large hydrophobic side chain which is often tryptophan [6]. Forming the binding site on one side of the indole ring is the adjacent residue Arg-84 which creates part of the hydrophobic surface with its aliphatic chain; Arg-84 also forms a salt bridge to the tryptophan's carboxyl end with its guanidino group. On the other side of the indole ring is Arg-54, which is held rigidly in position by an intersubunit salt bridge to Glu-47 of the opposing subunit. The α-amino group of the bound tryptophan is held in position by Ser-88 and hydrogen bonds to the carboxyl end of the opposing subunit's B-helix, mitigating the partial negative charge resulting from the helix dipole. Refinement parameters of *trp* repressor indicate that this bound tryptophan is as well localized and ordered as a typical side chain.

When the structure of aporepressor is compared in detail with the active repressor, several structural changes are seen (Fig. 1). First, in the empty L-tryptophan binding site, Arg-84 has moved to partially occupy this space with its aliphatic hydrocarbon chain, where it substitutes its guanidino group for the tryptophan's amino group in interacting with the negatively charged carboxyl end of helix B. Three water molecules also fill the binding site between Arg-54 and Arg-84. The consequence of this movement of Arg-84 is to exert a pull on helix E which causes the DNA binding domain to both undergo a conformational change and movement *en block* toward the molecular dyad. A careful analysis of the superimposed structures shows that helices A, B, and C remain unchanged with an rms difference in α-carbon positions of less than 0.5 Å, which is about the accuracy of the individual structure determinations; however, helices D and E have an rms movement of over 1.1 Å with a maximum of 4.5 Å, and these are precisely the regions believed most important in forming the sequence-specific operator interactions. Helix F with 0.6 Å rms difference between structures is little changed and seems to anchor the DNA-binding domain to the rest of the molecule.

Helices A, B, and C from *both* subunits with their intertwined arrangement

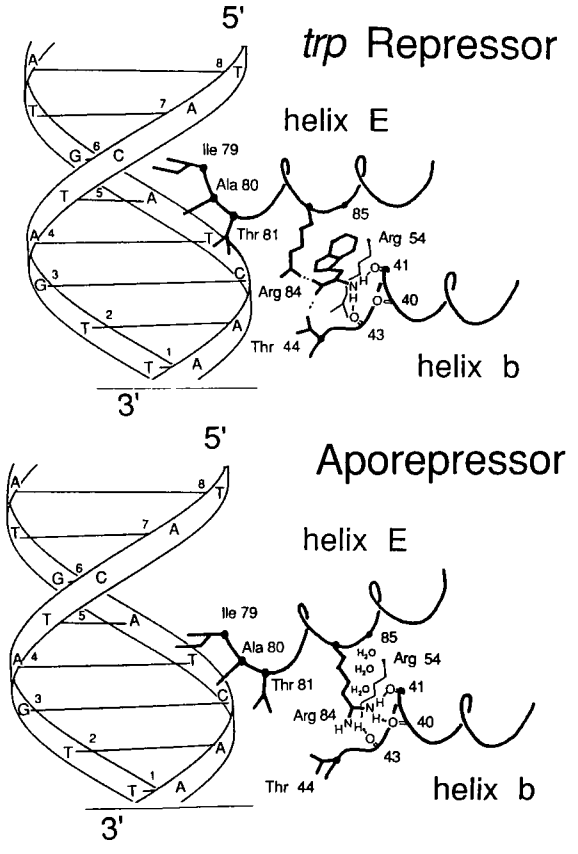

Fig. 1. The transition between aporepressor and trp *repressor.* Top*: The corepressor* L*-tryptophan positions the E-helix in* trp *repressor so that the first three residues of its N-terminal end can make deep, sequence-specific contact with the major groove of the operator.* Bottom*: In the absence of* L*-tryptophan, helix E rotates toward the molecular dyad and away from the critical bases at positions 4, 5 and 6. This also prevents the operator from approaching the aporepressor as closely as in repressor.*

thus appear to form a unified, solid structural core upon which the two more flexible, symmetrically disposed DNA binding domains pivot and bend. An analysis of the tertiary and quaternary structural interactions in *trp* repressor (Schevitz, manuscript in preparation) gives some basis for understanding this difference in local flexibility; it shows that these three helices (as well as helix F) have a much larger buried surface (and hence greater stabilizing interactions) than D and E and that the side chains in *trp* repressor that contribute to its

core are exceptionally hydrophobic. This core of the dimer is thus seen as a molecular 'scaffold' upon which the functional domains can move.

Molecular docking between *trp* repressor and operator DNA was used to find a 'best' fit between surfaces that are complementary both in shape and function groups. The most prominent interactions are between bases in the major groove of the operator at positions 4, 5, and 6 base pairs from the sequence dyad and the first three residues of helix E (Fig. 1). Specifically, Ile-79 makes a hydrophobic contact with the 5, 6 position of the pyrimidine ring of C_6 and also the 5-methyl of T_5. This is consistent with the studies of Bass et al. (manuscript submitted for publication) who have shown that only a C is acceptable at this position in the operator; our modeling of the complex indicates that a T with its 5-methyl would be sterically unacceptable, and both A and G lack a hydrophobic surface. Ala-80 and Thr-81 come close to the 5-methyl of T_4 and also appear to make a hydrophobic contact. Arg-69 and Lys-72 are able to make a variety of possible hydrogen bonds and hydrophobic contacts with base pairs 7 through 9 from the dyad; and this is presumably why these positions are not of importance for operator recognition. Thus, specific hydrophobic contacts between amino acid side chains and hydrophobic surfaces of pyrimidines in the major groove of DNA appear to be the important interactions that recognize the operator sequence.

A second crystal form of the active *trp* repressor has been solved (Lawson et al., manuscript in preparation) to 1.6 Å resolution and permits a detailed comparison between two structures which are *both* capable of binding to the operator. The surprising result is that while helices D and E of both active forms show large differences with aporepressor, they are also as different from each other! Thus, while the corepressor L-tryptophan is able to prevent the repressor from adopting the inactive aporepressor conformation, it does not fix the helix-turn-helix in a rigid and completely preformed structure that recognizes operator DNA. Rather, there is an inherent flexibility in this DNA 'reading head' that may depend upon structural adjustments in both operator *and* repressor to achieve a tight complementary fit. The prospects for directly visualizing this binding between the *trp* repressor and its operator are excellent, since good crystal forms of the complex have been obtained [8].

References

1. Zhang, R.-G., Joachimiak, A., Lawson, C.L., Schevitz, R.W., Otwinowski, Z. and Sigler, P.B., Nature, (1987) in press.
2. Schevitz, R.W., Otwinowski, Z., Joachimiak, A., Lawson, C.L. and Sigler, P.B., Nature, 317 (1985) 782.
3. Anderson, W.F., Ohlendorf, D.H., Takeda, Y. and Matthews, B.W., Nature, 290 (1981) 754.

4. McKay, D.B. and Steitz, T.A., Nature, 290 (1981) 744.
5. Pabo, C.O. and Lewis, M., Nature, 289 (1982) 443.
6. Ohlendorf, D.H., Anderson, W.F. and Matthews, B.W., J. Mol. Evol., 19 (1983) 109.
7. Kelley, R.L. and Yanofsky, C., Proc. Natl. Acad. Sci. U.S.A., 79 (1982) 3120.
8. Joachimiak, A., Marmorstein, R.Q., Schevitz, R.W., Mandecki, W., Fox, J.L. and Sigler, P.B., J. Biol. Chem. 262 (1987) 4917.

Interaction of peptide antibiotics with DNA

Terry P. Lybrand
University of Minnesota, College of Pharmacy, Health Sciences Unit F, 308 Harvard St. S.E., Minneapolis, MN 55455, U.S.A.

Introduction

The interaction of peptide antibiotics with DNA has been a topic of considerable interest for some time. One of the most extensively studied peptide antibiotics is actinomycin D (AMD, Fig. 1), a chromopeptide with chemotherapeutic activity

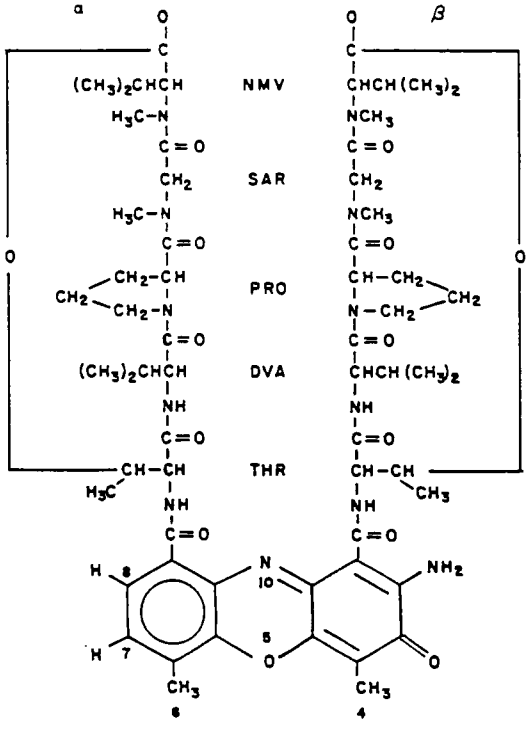

Fig. 1. Actinomycin D.

against Wilm's tumor [1] and gestational choriocarcinoma [2]. Experimental evidence indicates that the AMD chromophore intercalates on the 3′ side of guanine residues in double-helical DNA, while the cyclic pentapeptide side chains bind in the minor groove [3–7].

Computer modeling techniques, such as energy minimization, molecular dynamics simulation, and interactive computer graphics studies, have been used to investigate 'atomic resolution' details of the drug–DNA interactions and to aid in the analysis of two-dimensional nuclear magnetic resonance (NMR) studies of AMD–DNA complexes. At present, a new computational technique, the thermodynamic cycle–perturbation method, is being utilized to calculate the effect of substituent modifications in AMD on the free energy of binding to DNA. The perturbation method is also being used to suggest substituent modifications for AMD that may impart DNA sequence-selective binding properties.

Results and Discussion

Initial studies of AMD–DNA interactions utilized energy minimization techniques with gas phase models for the drug–DNA complexes [8]. Results from these energy minimization models were consistent with experimental data and suggested that some base sequence selectivity might be introduced by modified peptide side-chain interactions in the minor groove. In general, the energy-minimized structures compared quite favorably to the experimental distances from NMR studies, with only 8 of 214 compared proton-proton distances differing substantially (e.g., ≥ 1.5 Å) between computer models and experiment. Molecular dynamics simulations have now been performed on these AMD–DNA complexes, and the general agreement between computer model distances and NMR experiment improves, but several proton-proton distances are still predicted poorly by the computer models and cannot be explained easily (Creighton et al., manuscript submitted for publication). Future molecular dynamics simulations that include explicit water molecules and counterions will be performed to determine if agreement between computer models and experiment can be improved further.

Calculations to compute relative free energies of binding for AMD and AMD derivatives with substituent modifications in peptide side chains to various hexanucleotide duplex base sequences are in progress. These calculations utilize the thermodynamic cycle–perturbation method [9, 10] which allows quantitative prediction of relative free energies of binding in most cases. Until the development of this technique, it had been extremely difficult to calculate relative free energies of binding because desolvation effects and conformational changes that occur during complex formation take prohibitively long to model in computer simulations [9, 10]. The perturbation method avoids these technical problems by computing free energy changes over nonphysical thermodynamic paths. To

compute the relative free energy of binding for two ligands, A and B, to a common receptor site, R, a 'thermodynamic cycle' is constructed (see Fig. 2). Free energy changes ΔG_3 and ΔG_4 are computed in molecular dynamics simulations; these nonphysical reactions correspond to a perturbation or 'mutation' of ligand A to B while free in solution (ΔG_3) or bound in the receptor site (ΔG_4). The perturbation is effected in the simulation by use of a coupling parameter § that slowly changes the potential energy function (i.e. the Hamiltonian) from the reference system A (§ = 0) to the perturbed system B (§ = 1). At intermediate stages of the perturbation, the system is described by a 'mixed' Hamiltonian $H_§$ which changes nonlinearly from H_A to H_B as § increases from 0 to 1. The free energy change for a perturbation is computed as

$$\Delta G = {}_0\int^1 < \partial H_§/\partial § >_§ \, d§ \tag{1}$$

where $\diamond_§$ is an ensemble average from the simulation. The relative free energy of binding for the two ligands, A and B, is then calculated as

$$\Delta\Delta G = \Delta G_4 - \Delta G_3 = \Delta G_2 - \Delta G_1 \tag{2}$$

Since ΔG is a thermodynamic state function, the above equality is true.

The initial phase of these calculations addresses the effect of substituent modification in the peptide side chains on relative desolvation energies for the AMD derivatives. Frequently, relative free energies of binding for a series of related ligands to a receptor molecule are determined (or strongly influenced) by the relative desolvation energies of the ligands. Subsequent calculations will address the relative differences in intrinsic ligand–DNA interaction free energies.

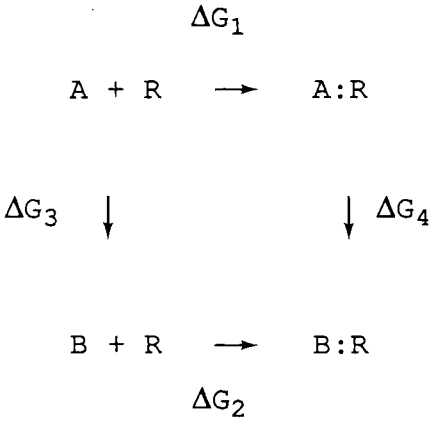

Fig. 2. A closed 'thermodynamic cycle' for relative free energy binding calculations.

Results from these calculations will then be used to suggest substituent modifications in AMD (and other peptide antibiotics) that may impart sequence-selective binding properties.

Acknowledgements

TPL is the recipient of a Damon Runyon-Walter Winchell Cancer Fund Fellowship (DRG-888). Calculations were performed in the Computer Graphics Facilities at the University of California, San Francisco (R. Langridge, Director, and T. Ferrin, Facilities Manager) supported by NIH grant RR1081 and in the Chemical Research Computing Facility at the University of Houston.

References

1. Farber, S., J. Am. Med. Assoc., 198 (1966) 826.
2. Lewis, Jr., J.L., Cancer, 30 (1972) 1517.
3. Müller, W. and Crothers, D.J., Mol. Biol., 35 (1968) 251.
4. Patel, D., Biochemistry, 13 (1974) 2388.
5. Krugh, T.R., Proc. Natl. Acad. Sci. U.S.A., 69 (1972) 1911.
6. Reinhardt, C.G. and Krugh, T.R., Biochemistry, 16 (1977) 2890.
7. Sengupta, S.K., Trites, D.H., Madhavarao, M.S. and Beltz, W.R., J. Med. Chem., 22 (1979) 797.
8. Lybrand, T.P., Brown, S.C., Creighton, S., Shafer, R.H. and Kollman, P.A., J. Mol. Biol., 191 (1986) 495.
9. Tembe, B.L. and McCammon, J.A., Comput. Chem., 8 (1984) 281.
10. Lybrand, T.P., McCammon, J.A. and Wipff, G., Proc. Natl. Acad. Sci. U.S.A., 83 (1986) 833.

Chemical synthesis of a retroviral nucleic acid binding protein

Terry D. Copeland, Louis E. Henderson, Robert Gorelick, Young Kim and Stephen Oroszlan

BRI-Basic Research Program, NCI-Frederick Cancer Research Facility, Frederick, MD 21701, U.S.A.

Introduction

The core of retroviruses contains a highly conserved, low-molecular weight, basic protein that binds to nucleic acid and is important for viral assembly. This protein of the prototype mammalian type C retrovirus, murine leukemia virus (MuLV), is designated p10 and consists of 56 residues. We have earlier determined the complete amino acid sequence [1]. The sequence of the Moloney (Mo) strain of MuLV p10 is:

A-T-V-V-S-G-Q-K-Q-D-R-Q-G-G-E-R-R-R-S-Q-L-D-R-D-Q-C-A-Y-
C-K-E-K-G-H-W-A-K-D-C-P-K-K-P-R-G-P-R-G-P-R-P-Q-T-S-L-L

MuLV p10 has been shown to bind to single-stranded nucleic acids [2, 3]. To facilitate in vitro studies on its nucleic acid binding properties, the p10 of the Mo strain of MuLV has been synthesized on a solid support.

Results and Discussion

Mo-MuLV p10 was assembled on a phenylacetamidomethyl resin, substituted with Boc-Leu, in an Applied Biosystems 430A automated synthesizer. Protected amino acids were added as the symmetric anhydrides. Arg, Asn, and Gln were double coupled. The protein was severed from the resin and protecting groups with the low-high hydrogen fluoride treatment [4] and processed as described [5]. The product was extracted into 1 N acetic acid, diluted with water and lyophilized. Purification was accomplished by reversed-phase high-performance liquid chromatography (RPHPLC) on a Waters 19 mm × 150 mm C18 column with a gradient of increasing acetonitrile content containing 0.05% TFA. The purified protein migrated on SDS–PAGE with the same apparent molecular weight as the viral protein and gave the following amino acid composition (theoretical values are in parentheses): Cys 3.1 (3), Asp 4.1 (4), Thr 2.0 (2),

Ser 2.9 (3), Glu 7.4 (8), Pro 5.6 (5), Gly 6.1 (6), Ala 2.9 (3), Val 1.3 (2), Leu 3.2 (3), Tyr 0.9 (1), His 1.3 (1), Lys 6.2 (6), and Arg 7.5 (8). Trp (1) was not determined. The Pro value is high, as Cys following acid hydrolysis results in products which can co-elute with Pro on the amino acid analyzer. Cys values were obtained as cysteic acid following oxidation with performic acid. The amino acid composition thus obtained for the synthetic p10 is in very good agreement with the expected values as obtained from the sequence of the protein. The synthetic p10 was then subjected to automated Edman degradation in an Applied Biosystems gas phase sequenator. A correct amino-terminal amino acid sequence was obtained and confirmed approximately two-thirds of the sequence. No previews or truncated peptides were observed by the sequence analysis. Therefore, we conclude that the primary structure of Mo-MuLV p10 has been synthesized.

The synthesized protein was then examined for its binding interactions with a single stranded fluorescent polyribonucleotide, polyethenoadenylic acid (ϵA), in a nonperturbing solution assay [3]. An aqueous dilute solution of poly (ϵA) was titrated with the synthetic Mo-MuLV p10. The synthetic p10 and the viral p10 both exhibited a two-phase fluorescence increase up to an end-point of 6 ± 1 nucleotides per bound p10 molecule.

Structure–function studies, employing amino acid modification, site-directed mutagenesis and chemical synthesis with selected different residues inserted into p10, are currently underway. The capability to chemically synthesize functional MuLV p10 will greatly enhance studies on the role of Mo-MuLV p10 nucleic acid binding in virus assembly and allow elucidation of other possible biological function(s).

Acknowledgements

We thank Catherine Hixson for assistance with the amino acid analyses. The research was sponsored by the National Cancer Institute, DHHS, under Contract No. NO1-CO-23909 with Bionetics Research Inc.

References

1. Henderson, L.E., Copeland, T.D., Sowder, R.C., Smythers, G.W. and Oroszlan, S., J. Biol. Chem., 256 (1981) 8400.
2. Davis, J., Scherer, M., Tsai, W.-P. and Long, C., J. Virol., 18 (1976) 709.
3. Karpel, R.L., Henderson, L.E. and Oroszlan, S., J. Biol. Chem., 262 (1987) 4961.
4. Tam, J.P., Heath, W.F. and Merrifield, R.B., Tetrahedron Lett., 23 (1982) 4435.
5. Copeland, T.D., Tsai, W.-P., Kim, Y.D. and Oroszlan, S., J. Immunol., 137 (1986) 2945.

Binding of a thynnine Z-1 fragment to DNA

F. Marchiori, G. Borin and M. Palumbo
Department of Organic Chemistry, Biopolymer Research Centre, Via Marzolo 1, I-35131 Padova, Italy

A thermodynamic and stereochemical investigation on the interaction of the synthetic fragment 13–23 (H-Arg_4-Tyr-Arg_2-Ser-Thr-Val-Ala-OMe) [Z1 (13–23)] of thynnine Z-1 to double-stranded DNA (sonicated calf thymus with average molecular weight 500,000) has been performed using the tyrosine residue as an intrinsic fluorescent probe. Taking advantage of the change in emission response of the peptide, the amount of free and DNA-bound Z1 (13–23) could be evaluated at neutral pH under different ionic strength conditions. The results are reported in Table 1 in terms of K_i, the intrinsic binding constant; ΔG, the free energy change; n, the number of nucleotide residues involved in complex formation per protamine molecule; and ω, the cooperativity parameter.

The ΔG value under physiological conditions is about −34 kJ/mol of peptide, corresponding to about 5 kJ per basic residue. These figures compare well with those reported in the literature for the interaction of DNA with clupeine YII fragments or oligolysine peptides [1, 2]. The n value is always about 7, which corresponds to the number of positively charged groups in Z1 (13–23). Thus ionic contacts should be primarily involved in the binding process. This fact is confirmed by examining the ionic strength dependence of K_i. A logarithmic plot of K_i vs ionic strength is linear with slope 6.3, corresponding to 7 charged interactions per complex unit. It can be concluded that DNA phosphates from 7 consecutive nucleotide residues participate in electrostatic binding with one fragment molecule. These figures are fully consistent with the results presented by Watanabe and Schwarz, suggesting that all 21 Arg side chains of clupeine Z are involved in DNA binding [3].

Table 1 *Thermodynamic parameters for the binding of Z1 (13–23) to double-stranded DNA at different ionic strength* (t = 25°C; pH = 7.0)

Ionic strength (M)	$K_i \times 10^{-5}$ (M^{-1})	n	ω	−ΔG kJ/mol Z1 (13–23)
0.150	11.0 ± 1	7.2 ± 0.3	0.98 ± 0.05	34.5 ± 0.4
0.175	4.3 ± 0.5	7.0 ± 0.3	1.01 ± 0.05	32.1 ± 0.4
0.200	2.1 ± 0.5	7.0 ± 0.3	0.98 ± 0.05	30.4 ± 0.4

Unlike entire protamine sequences, Z1 (13–23) does not bind cooperatively to DNA (ω is close to 1 in all cases). Thus, only peptides having a larger number of positively charged groups appear to exhibit positive cooperativity, as it is required for an effective and complete protection of the nucleic acid.

Measurements at different temperature indicate that the ΔH of complexation of Z1 (13–23) is close to 0, which is consistent with the predominant electrostatic character of the binding process.

Our findings also imply that the neutral C-terminal region of Z1 (13–23) does not interact with the polynucleotide chain and should, therefore, point outwards. Interestingly, this sequence includes serine and threonine residues, which could be available for phosphorylation even when bound to DNA. Preliminary results from our laboratory strongly suggest this hypothesis.

References

1. Arellano, A., Wehling, K. and Wagner, K.G., Int. J. Biol. Macromol., 6 (1984) 249.
2. Lohman, T.M., De Haseth, P.L. and Record, M.I., Biochemistry, 19 (1980) 3522.
3. Watanabe, F. and Schwarz, G., J. Mol. Biol., 163 (1983) 485.

Session VII
Structure-activity relations

Chair: William F. Huffman
Smith Kline and French Laboratories
Swedeland, Pennsylvania, U.S.A.

Details of the interaction of phosphorus-containing peptide inhibitors with thermolysin

Paul A. Bartlett*, David H. Drewry, John E. Hanson and Charles K. Marlowe
Department of Chemistry, University of California, Berkeley, CA 94720, U.S.A.

Introduction

With the increasing recognition of the roles that peptidases play in many biological processes has come a correspondingly heightened interest in the design of potent and selective inhibitors of these enzymes. The zinc-containing peptidases are no exception, with one of the best examples provided by the success of angiotensin-converting enzyme inhibitors as antihypertensive agents [1, 2]. The fact that inhibitor motifs can be transferred effectively within this class has provided impetus for continued investigations of the more well-characterized members, thermolysin and carboxypeptidase A. Although questions remain with regard to the mechanistic details of these enzymatic transformations, very effective inhibitors have resulted from attempts to mimic the putative tetrahedral intermediate that arises from direct addition of water to the peptide linkage. Among these, peptide analogs incorporating a phosphonic acid moiety in place of the P_1 amino acid have proven to be among the most potent, if not the most potent, inhibitors [3–8]. The 'transition state analogy' of the tetrahedral phosphorus analogs was demonstrated for a series of thermolysin inhibitors of the form Cbz-Gly^P-Leu-(AA), **1** (ZG^{P}LX) (see Scheme 1), by the correlation of inhibitor K_i values with the K_m/k_{cat} values for the corresponding substrates (Eqns. 1 and 2; Fig. 1, hollow squares; and Table 1) [8].

$$K_i = \frac{K_S}{k_{cat}} \cdot k_{noncat} \cdot K_{H_2O} \tag{1}$$

$$K_i \, \alpha \frac{K_m}{K_{cat}}, \text{ for } k_S = K_m \text{ and } k_{noncat} = \text{constant} \tag{2}$$

*To whom correspondence should be addressed.

Results and Discussion

The mode of binding of a representative phosphonamidate inhibitor, ZG^PLL (K_i = 9 nM), to crystalline thermolysin was determined by X-ray diffraction by Matthews and co-workers [9, 10]. Whereas the leucyl residues adopt quite predictable orientations in the S_2' and S_1' subsites, and the phosphonate moiety is coordinated to the zinc atom and hydrogen bonded to the carboxylate of Glu-143, the Cbz moiety is not oriented as expected for a residue in the S_2 site [11, 12]. Rather than penetrating into the binding site and hydrogen bonding with the protein backbone as postulated previously, the carbamate carbonyl oxygen projects outward, its expected position occupied by a water molecule.

Primarily because of their greater hydrolytic stability in comparison to the amidates, a related series of phosphonate esters **2** (see Scheme 1), has also been synthesized and investigated as inhibitors of thermolysin [13]. A similar correlation between inhibitor K_i values and substrate K_m/k_{cat} values was observed for these esters; however, the esters proved to be approximately 840-fold more weakly bound than the corresponding amidates (Fig. 1, hollow circles, Table 1). The constancy of this difference in binding affinity for each pair in the correlation suggested to us that inhibitors in the two series bind in a comparable manner, and that the loss in binding energy could be attributed to the loss of a hydrogen bond between inhibitor and enzyme. That this is the case was confirmed by the observation that the relevant NH of amidate ZG^PLL is hydrogen-bonded to the carbonyl oxygen of Ala-113 (distance 3 Å), and by crystallographic studies by Tronrud et al. [9], showing that the thermolysin complex of the ester analog $ZG^P(O)LL$ is virtually superimposable upon that of the complex with the amidate ZG^PLL.

The correlation of inhibitor K_i with substrate K_m/k_{cat} values for transition state analogs indicates that better inhibitors will be obtained by making the phosphonate analogs of better substrates. To explore this possibility, a series of tripeptides, **3** (see Scheme 1), was synthesized with phosphorus analogs of

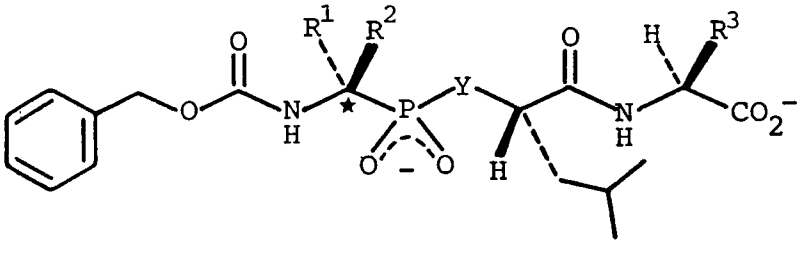

Scheme 1. **1**: $R^1 = R^2 = H$, $Y = NH$;
2: $R^1 = R^2 = H$, $Y = O$;
3: R^1 or $R^2 \neq H$, $R^3 = CH_3$, Y = NH or O.

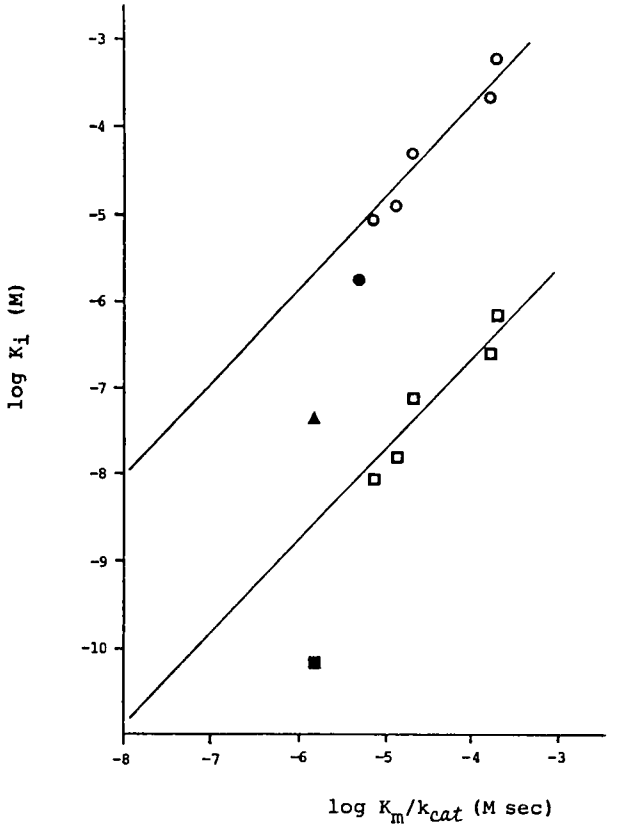

Fig. 1. Comparison of inhibitor K_i *values with* K_m/K_{cat} *values for the analogous peptide substrates;* o, *ZG*^{P}*(O)LX;* □, *ZG*^{P}*LX;* ●, *ZA*^{P}*(O)LA;* ▲, *ZF*^{P}*(O)LA;* ■, *ZF*^{P}*LA. Substrate data taken from ref.* [15]*; data on ZG*^{P} *LX analogs from ref.* [8]*; data on ZG*^{P} *(O)LX analogs from ref.* [13].

substituted amino acids at the P_1 position [14]. The P_1-substituted inhibitors for which substrate kinetic data are available [ZA^{P}LA, ZA^P(O)LA, and ZF^{P}LA] [15] proved to be *more* tightly bound than predicted by the correlation (Fig. 1, solid symbols). ZF^{P}LA, with a K_i value of 6.8×10^{-11} M, is the most potent inhibitor reported for thermolysin to date. That the P_1-substituted inhibitors do not adhere to the correlation of Fig. 1 can be attributed to a breakdown in the assumptions upon which the relationship of Eqn. 2 are based, namely that across the series of substrates, the rate-limiting step for the enzymatic reaction and the rate constants for the noncatalyzed reaction remain unchanged.

The P_1-substituted inhibitors contrast with the Gly^P analogs in the kinetic

Table 1 *Inhibition constants and second order rate constants for binding of phosphorus-containing tripeptide analogs to thermolysin*

Inhibitor	Amidates		Esters	
	K_i (nM)[a]	k_{on} ($M^{-1}s^{-1}$)[b]	K_i (nM)[a]	k_{on} ($M^{-1}s^{-1}$)[b]
$ZG^PL(D)A$	>1700	–	–	
$ZG^PL(NH_2)$	760	–	660,000	–
ZG^PLG	270	–	230,000	–
ZG^PLF	78	–	53,000	–
ZG^PLA	16.5	$>10^5$[c]	13,000	–
ZG^PLL	9.1	$>10^5$[c]	9,000	–
ZA^PLA	–		1,800	1250
ZL^PLA	–		680	480
ZF^PLA	0.068[d]	1000	45	470
$Z(D)A^PLA$	–		24,000	2.1
$Z(D)L^PLA$	–		42,000	2.8
$Z(D)F^PLA$	480	1300	30,000	400

[a] Determined by steady-state kinetics, unless otherwise indicated; dash indicates the compound was not prepared.
[b] Dash indicates slow binding not observed.
[c] Slow binding not observed; k_{on} given as lower limit only.
[d] Calculated from $K_i = k_{off}/k_{on}$.

aspects of binding as well. Whereas the Gly^P compounds bind rapidly to thermolysin ($k_{on} > 10^5$ $M^{-1}.s^{-1}$), the substituted derivatives associate with second order on-rates $\leqslant$ 1300 $M^{-1}.s^{-1}$ (Table 1). This slow-binding behavior depends solely on the presence of a substituent α to phosphorus; it is observed regardless of the size or configuration of this substituent, whether the inhibitor is a phosphonamidate or phosphonate ester, or whether it shows high or low affinity for the enzyme. Although overall slow binding is often associated with an observable two-step binding process [16], for the Phe^P analogs ZF^PLA and $ZF^P(O)LA$, a first order dependence of the association rate on [I] was observed up to [I] = 1 mM, indicating that any loose intermediates along the binding pathway for these inhibitors must have dissociation constants $\geq$ 4 mM.

In spite of the growing interest in slow-binding inhibition, it remains poorly understood at the molecular level. Specific correlations of this behavior with inhibitor or protein structure are not available, although slow binding is commonly attributed to a protein conformational change along the binding pathway [16]. For the phosphonate inhibitors, however, X-ray crystallography does not reveal any significant difference in protein conformation between the native enzyme, the complexes with the fast-binders ZG^PLL and $ZG^P(O)LL$, and the slow-binder ZF^PLA [10]. On the other hand, the latter inhibitor does adopt a different conformation in the active site than found for the Gly^P derivatives: the carbamate moiety of ZF^PLA is rotated away from the α-substituent and penetrates into the S_1 subsite as predicted previously [11]. In doing so, the carbonyl

oxygen displaces the water molecule referred to above and hydrogen bonds to the protein backbone.

In view of the lack of evidence for an overall protein conformational change and the fact that $ZF^{P}LA$ itself is not bound in an unfavorable conformation, we have considered the circumstantial evidence that displacement of water, perhaps the specific molecule referred to above, is involved in the slow-binding step. Studies on the effect of viscosity on the on-rate observed for $ZF^{P}(O)LA$ indicate that the association of this inhibitor with thermolysin is entirely diffusion-limited (unpublished results), in spite of the fact that in absolute magnitude this rate constant (1000 $M^{-1}.s^{-1}$) is several orders of magnitude below those observed for most peptide–peptidase interactions (10^{6}–10^{8} $M^{-1}.s^{-1}$) [17, 18]. This observation is consistent with a binding process that involves the diffusion-limited combination of inhibitor with a rare form of the enzyme that is in rapid equilibrium with the bulk protein. Further experiments will be required to determine whether this rare enzyme form represents a transient conformational change or the transient loss of a bound water molecule.

Acknowledgements

This work was supported by a grant from the National Institutes of Health (grant no. CA-22747). We express our appreciation to Professor Brian Matthews and his co-workers for their crystallographic studies and for fruitful discussions.

References

1. Cushman, D.W. and Ondetti, M.A., Top. Mol. Pharmacol., 1 (1981) 127.
2. Maycock, A.L., DeSousa, D.M., Payne, L.G., ten Broeke, J., Wu, M.T. and Patchett, A.A., Biochem. Biophys. Res. Commun., 102 (1981) 964.
3. Mookthiar, K.A., Marlowe, C.K., Bartlett, P.A. and van Wart, H.E., Biochemistry, 26 (1987) 1962.
4. Petrillo, Jr., E.W., Cushman, D.W., Duggan, M.E., Heikes, J.E., Karanewsky, D.S., Ondetti, M.A., O'Reilly, B., Rovnyak, G.C., Schwartz, J., Spitzmiller, E.R. and Wang, N.-Y., In Hruby, V.J. and Rich, D.H. (Eds.) Peptides: Structure and Function, Proceedings of the 8th American Peptide Symposium, Pierce Chemical Co., Rockford, IL, 1983, p. 541.
5. Galardy, R.E., Kontoyiannidou-Ostrem, V. and Kortylewicz, Z.P., Biochemistry, 22 (1983) 1990.
6. Kam, C.-M., Nishino, N. and Powers, J.C., Biochemistry, 18 (1979) 3032.
7. Weaver, L.H., Kester, W.R. and Matthews, B.W., J. Mol. Biol., 114 (1977) 119.
8. Bartlett, P.A. and Marlowe, C.K., Biochemistry, 22 (1983) 4618.
9. Tronrud, D.E., Holden, H.M. and Matthews, B.W., Science, 235 (1987) 571.
10. Holden, H.R., Tronrud, D.E., Monzingo, A.F., Weaver, L.H. and Matthews, B.W., Biochemistry (1987) in press.
11. Kester, W.R. and Matthews, B.W., Biochemistry, 16 (1977) 2506.

12. Hangauer, D.G., Monzingo, A.F. and Matthews, B.W., Biochemistry, 23 (1984) 5730.
13. Bartlett, P.A. and Marlowe, C.K., Science, 235 (1987) 569.
14. Bartlett, P.A. and Marlowe, C.K., Biochemistry (1987) in press.
15. Morihara, K. and Tsuzuki, H., Eur. J. Biochem., 15 (1970) 374.
16. Morrison, J.F. and Walsh, C.T., Adv. Enzymol., (1987) in press.
17. Hardy, L.W. and Kirsch, J.F., Biochemistry, 23 (1984) 1275.
18. Brouwer, A.C. and Kirsch, J.F., Biochemistry, 21 (1982) 1302.

Design of bradykinin antagonists

John M. Stewart and Raymond J. Vavrek
Department of Biochemistry, University of Colorado School of Medicine, Denver, CO 80262, U.S.A.

Introduction

Bradykinin (Arg-Pro-Pro-Gly-Phe-Ser-Pro-Phe-Arg; BK) and its homolog
1 2 3 4 5 6 7 8 9
kallidin (Lys-BK) are potent biologically active peptides which participate in a very broad range of physiological regulatory processes, mostly at the local, or tissue, level. They are produced in vivo by trypsin-like enzymes called kallikreins; plasma kallikrein yields BK, while tissue kallikrein yields kallidin from the same protein precursor. Evident roles for BK are in regulation of circulation and blood pressure (BK lowers blood pressure), contraction of smooth muscles of intestine and uterus, stimulation of secretion (intestinal, salivary, mucosal), initiation of inflammation (production of pain, edema, leucocyte infiltration) and regulation of neurotransmission.

It is now known that in one cell type or another, the combination of BK with its receptors can stimulate every known postreceptor mechanism. Activation of phospholipase A_2 with consequent release of arachidonic acid for production of prostaglandins and leucotrienes occurs in many tissues and may be the most common mechanism for production of BK-mediated effects, notably in inflammation and smooth muscle relaxation. Activation of guanylate cyclase is evidently involved in relaxation of some smooth muscles. In several cell types including neurones, BK activates phospholipase C with consequent conversion of phosphatidylinositol bisphosphate to inositol trisphosphate and a diglyceride; the diglyceride then stimulates kinase C, while inositol trisphosphate releases bound calcium from intracellular stores. Growth factor activity of BK in certain cells may be mediated by stimulation of tyrosine kinase activity. Smooth muscle contraction evoked by BK seems to utilize activation of a calcium-calmodulin kinase, or of adenylate cyclase as effector.

Many pathological conditions are characterized by excess BK: severe inflammation (wounds, arthritis); edema (pulmonary, traumatic, hereditary); shock (endotoxin, pancreatitis, carcinoid); pulmonary disease (edema, emphysema, anaphylaxis); rhinitis (allergic, rhinovirus, nonallergic); and pain (wounds, toxins, and venoms) [1, 2].

Given this complex array of mediators, physiological effects and pathological manifestations, it has been clear for many years that effective, specific competitive antagonists of BK receptors were critically needed, both to help unravel the complexities of BK biology and to provide new drugs for treatment of conditions characterized by BK excess. No such substances were available until 1984, when we found the first BK analogs which acted as competitive inhibitors [3].

Results and Discussion

Among the hundreds of BK-related peptides synthesized during more than two decades of investigation in this laboratory were analogs in which every amino acid in the BK sequence was replaced by its D enantiomer, singly or in various combinations; these analogs were generally inactive biologically. In our work on BK analogs with alpha-aminoisobutyric acid (Aib) replacing proline we found that [Aib^{7}]-BK was a surprisingly potent BK agonist. Since this amino acid, being neither D- nor L-, conferred these interesting properties on the analog, we investigated a large series of BK analogs having various D-amino acids at position 7. Most of these were uninteresting, but [D-Phe^{7}]-BK showed weak antagonist activity on guinea pig ileum, while being a weak agonist in rat uterus and rat blood pressure. This analog was the long-anticipated lead compound for development of true BK antagonists. Since the testing of that compound approximately three years ago, we have synthesized and tested more than 200 analogs having modifications expected to confer antagonist activity; several representative antagonists are shown in Table 1. The antagonists are highly specific for BK and related kinins, and inhibit the agonists in a competitive manner, indicating that they are acting at the BK receptor.

The first antagonist was not impressive of itself. It was a weak antagonist on guinea pig ileum (GPI), but was a weak agonist on rat uterus (RUT) and rat blood pressure (RBP) in vivo. Our first modification of this structure was to attempt to increase receptor affinity by replacing the Phe residues at positions 5 and 8 with β-(2-thienyl)-alanine (Thi); this substitution had been found earlier to produce BK superagonists by increasing the receptor affinity of the analog over that of BK [4]. This maneuver was successful; the resulting [Thi^{5,8}, D-Phe^{7}]-BK was a full order of magnitude more potent an antagonist of BK on GPI, and was also an antagonist on both RUT and RBP. Thus we see that increasing receptor affinity can enhance potency of antagonists as well as agonists. Since addition of a Lys-Lys- dipeptide to the amino end of BK made it completely resistant to hydrolytic action of angiotensin I converting enzyme (ACE), which is a major kininase in the vasculature, we added this dipeptide and other combinations of basic amino acid residues to the amino end of the early antagonists. So far, we have found addition of D-Arg- to be most useful for increasing the potency of the antagonists, although the Lys-Lys- addition may

Table 1[a] *Bradykinin (BK) antagonists*

Analog	RUT	GPI	RBP-IA
BK	100%	100%	100%
[D-Phe^7]-BK	4%	5.8	2%
[Thi^{5,8},D-Phe^7]-BK	6.5	6.3	I
D-Arg-[D-Phe^7]-BK	0.1%	6.3	I
D-Arg-[Hyp^3, D-Phe^7]-BK	6.5	5.9	I
[Phe^2, D-Phe^7]-BK	0	0	I
[Phe^3, D-Phe^7]-BK	0.1%	0	0.2%
[Phe^{2,3}, D-Phe^7]-BK	0	0	I
[Phe^2, Hyp^3, D-Phe^7]-BK	0	0	I
D-Arg-[Phe^2, D-Phe^7]-BK	0.4%	0	I
D-Arg-[Phe^3, D-Phe^7]-BK	MXD	0	I
D-Arg-[Phe^{2,3}, D-Phe^7]-BK	0	0	0.2%
D-Arg-[Phe^2, Hyp^3, D-Phe^7]-BK	6.5	0	I
[D-Phe^{2,3}]-BK	0	0	0.1%
[D-Phe^{2,7}]-BK	5.5	0	0
[D-Phe^{3,7}]-BK	5.5	0	I
[D-Phe^{2,3,7}]-BK	0	0	I
D-Arg-[Thi^{5,8}, D-Phe^7]-BK	5.5	6.1	I
D-Arg-[Hyp^3, Thi^{5,8}, D-Phe^7]-BK	6.9	6.3	I

[a] RUT/GPI = agonist activity on isolated rat uterus or guinea pig ileum relative to BK = 100%. RBP-IA = blood pressure-lowering activity in the anesthetized rat following intraaortic administration relative to BK = 100%. Antagonist potency is given as the pA_2 value and is underlined. For RBP, BK antagonism is given as I and is not quantitated.

be useful for imparting tissue selectivity to antagonists. In work with BK agonists, we had found that replacing prolines at positions 2 and/or 3 with 4-hydroxyproline (Hyp) yielded very potent agonists. Again following the presumption that substitutions which enhanced the potency of agonists might also be useful for increasing the potency of antagonists, we made similar changes in the BK antagonists and obtained new families of potent antagonists. Alterations of the antagonist structure at positions 2 and/or 3 appear to be particularly useful for yielding antagonists with tissue selectivity [5]. We report here that new antagonists with D- or L-Phe at positions 2/3 are potent and have very selective action (see Table 1). Thus, whereas [D-Phe^7]-BK is an antagonist on GPI and a very weak agonist on RUT and RBP, [D-Phe^{2,7}]-BK is an antagonist on RUT with no activity on the other two assays, [Phe^2, D-Phe^7]-BK is an antagonist on RBP with no action on GPI or RUT, and [D-Phe^{3,7}]-BK is an antagonist on RUT and RBP without any activity on GPI. Again in this series, as we had found earlier with the [Thi^{5,8}, D-Phe^7]-BK antagonists, addition of D-Arg to the N-terminus enhances antagonist potency and scope of action.

Results of investigations with BK antagonists in other systems are beginning to appear. Most of these studies have demonstrated antagonism of applied BK

by the synthetic antagonists in various biological systems, but some data are already providing evidence of involvement of BK in systems where it had been previously only postulated. For example, the antagonists have blocked BK-evoked increase in vascular permeability in rabbit skin [6, 7], release of prostaglandin E_2 from cultured human pulmonary fibroblasts [8, 9], phosphatidylinositol turnover in cultured neuroblastoma cells [10], neurotransmitter release from neurons (J.P. Huidobro-Toro, personal communication), and pain on the human blister base. It has been suggested that part of the blood pressure-lowering action of the ACE inhibitor Captopril may be due to protection of circulating BK, since ACE is a major kininase; this was recently confirmed by use of a BK antagonist [11]. The mouse writhing test (intraperitoneal injection of acetic acid) and the rat paw pressure test are standard assay systems for analgesic agents. Prostaglandins are the apparent nociceptive mediators in these systems, since both glucocorticoids (like cortisone) and cyclooxygenase inhibitors (like aspirin) produce antinociception in these tests. Although it had been suggested that BK may be the actual initial mediator, the first evidence to support this postulate came with inhibition of both responses by a BK antagonist [12].

Except for the B_1 receptor described by Regoli (which recognizes mainly [*des*-Arg^9]-BK), all actions of BK were thought to be mediated by a single class of receptors. The evidence cited above suggests that even the similar smooth muscle tissues of GPI and RUT have distinguishable BK receptor types. Recent work of Huidobro-Toro and co-workers [13] shows that neuronal BK receptors are different from smooth muscle receptors; this difference is similar to that seen in neuroblastoma cultures [10]. Additional work with new antagonist peptides and in different biological systems will be needed to establish the full story of BK receptor types. Evident usefulness of the antagonists in various in vivo systems suggests that new drugs based on these peptides may be realizable and practical.

Acknowledgements

This work was supported by NIH grant HL-26284 and a grant from the Nova Corp. We thank Virginia Callaway for amino acid analyses and Frances Shepperdson, Garima Vashistha and Irma Albinana for bioassays.

References

1. Erdos, E.G. (Ed.), Handbook of Experimental Pharmacology, Vol. 25 (Suppl.), Springer-Verlag, New York, NY, 1979.
2. Proud, D., Togias, A., Naclerio, R.M., Crush, S.A., Norman, P.S. and Lichtenstein, L.M., J. Clin. Invest., 72 (1983) 1678.
3. Vavrek, R.J. and Stewart, J.M., Peptides, 6 (1985) 161.
4. Odya, C.E., Goodfriend, T.L. and Peña, C., Biochem. Pharmacol., 29 (1980) 175.

5. Vavrek, R.J. and Stewart, J.M., In Schowen, R.L. and Barth, A. (Eds.) Molecular and Cellular Regulation of Enzyme Activity, Pergamon, Oxford, 1987, p. 73.
6. Longridge, D.J., Schachter, M., Stewart, J.M., Uchida, Y. and Vavrek, R.J., J. Physiol. (London), 372 (1986) 73.
7. Stewart, J.M., Vavrek, R.J. and Whalley, E.T., Brit. J. Pharmacol., (1985) 167.
8. Crecelius, D.M., Stewart, J.M., Vavrek, R.J., Balasubramanian, T.M. and Baenziger, N., Fed. Proc., 45 (1986) 454.
9. Crecelius, D.M., Vavrek, R.J., Stewart, J.M. and Baenziger, N.L., 10th American Peptide Symposium, St. Louis, May, 1987, Abstr. P-218.
10. Braas, K.M., Manning, D.C., Wilson, V.S., Perry, D.C., Stewart, J.M., Vavrek, R.J. and Snyder, S.H., Abstracts, Soc. Neuroscience 15th Meeting, Dallas, TX, 1985, 414.
11. Benetos, A., Gavras, H., Stewart, J.M., Vavrek, R.J., Hatinoglou, S. and Gavras, I., Hypertension, 8 (1986) 971.
12. Steranka, L.R., DeHaas, C.J., Vavrek, R.J., Stewart, J.M., Enna, S.J. and Snyder, S.H., Eur. J. Pharmacol., 136 (1987) 261.
13. Llona, I., Vavrek, R., Stewart, J. and Huidobro-Toro, J.P., J. Pharmacol. Exp. Ther., 241 (1987) 608.

Vasopressin agonists and antagonists present distinct pharmacophores at the renal V_2 receptor

Michael L. Moore and William F. Huffman

Department of Peptide Chemistry, Smith Kline & French Laboratories, 709 Swedeland Road, King of Prussia, PA 19479, U.S.A.

The design of receptor antagonists for peptide hormones presents a great challenge to the peptide chemist. There are no general rules for modifications which will turn an agonist into an antagonist. While there are some peptides for which it is possible to obtain an antagonist by the substitution of a single amino acid in the sequence, multiple substitutions, often with D-amino acids, are usually required, if antagonists can be obtained at all. Antagonists at the vasopressin renal (V_2) receptor fall into this category. The first V_2 antagonists which were active in vivo, reported by Sawyer et al. [1], contained 3 modifications: substitution of a β, β-cyclopentamethylene-β-mercaptopropionic acid at position 1, substitution of an *O*-alkyl tyrosine at position 2, and substitution of valine at position 4.

In the course of our investigations of the structure–activity relationships (SAR) of vasopressin V_2 antagonists, we have found that, while the linear sequence resembles that of vasopressin, the SAR at numerous points differs quite strikingly from that of vasopressin. These differences have led us to propose that V_2 antagonists bind to the vasopressin receptor quite differently from vasopressin and, in fact, present a distinct antagonist pharmacophore with unique SAR requirements. We have found that there are substantial species differences for SAR as well, so we have chosen to concentrate on evaluation of receptor affinity and activity in the pig, which most closely resembles the human receptor [2].

The difference between agonist and antagonist pharmacophore can be seen most prominently in the tripeptide 'tail'. For vasopressin agonists, there seem to be 3 pharmacophore elements associated with the tail. One is associated with the C-terminal glycinamide. [Mpr^1, *des*(Gly^9)]-AVP, for example, loses more than 3 orders of magnitude in binding affinity to the receptor. The second element is associated with the Arg^8 side chain. Substitution of D-Arg at position 8 causes a loss of 2–3 orders of magnitude in binding affinity to the receptor, suggestive of a 3-point type of interaction with respect to the residue 8 alpha carbon. Finally, there seems to be a hydrophobic contact with the receptor by the proline side chain. Substitution of ΔPro at position 7 substantially enhances activity [3]. In addition, the conformational constraint produced by the proline is

necessary to correctly orient the tail with respect to the rest of the molecule. Substitutions at position 7 lacking an *N*-methyl moiety have greatly reduced activity [4].

In contrast, we have shown that the C-terminal glycine can be deleted [5], the carboxamido group can be deleted [5], and the Pro^7 can be freely substituted for [6] or even deleted [7] in, antagonists, all with retention of high and approximately equipotent receptor activity. The entire tripeptide tail can be replaced by a diaminoalkane or aminoalkylguanidine attached to Cys^6 with full retention of activity. In antagonists, then, the 'tail' presents only one pharmacophore element. It does not require a conformational constraint for proper orientation. The lack of dependence of activity on chain length of the tail suggests that the site occupied by the tail is relatively close to the cyclic hexapeptide ring [8].

There are differences in SAR within the cyclic hexapeptide ring as well. In agonists, for example, Phe^3 can be substituted by an aliphatic amino acid: [Ile^3]-AVP (arginine vasotocin) is equipotent with vasopressin at the receptor. In antagonists, substitution of aliphatic amino acids for Phe^3 results in a loss of 2–3 orders of magnitude in receptor activity. Given this difference in SAR, it is unlikely that the position 3 side chain in agonists and antagonists is occupying the receptor in the same way. Since deletion of the position 3 side chain results in substantial loss of activity in both agonists and antagonists, it seems clear, however, that both are pharmacophore elements.

There are also areas in which the SAR for agonists and antagonists is similar. In agonists, Gln^4 can be substituted by aliphatic amino acids, especially valine, with retention of activity: [Mpr^1, Val^4]-AVP is equipotent in binding affinity with [Mpr^1]-AVP. Gln^4 is active in the antagonists, although its activity is slightly reduced with respect to aliphatic amino acid substitutions. We have previously shown that the α-methyl-Val^4 antagonists are quite potent while the corresponding cycloleucine (Cle) antagonists are 3 orders of magnitude less potent [9]. We interpreted this as indicating that the conformational constraint produced by an α-methyl amino acid was tolerated at position 4 but the added steric bulk of the cyclopentane ring of Cle produced an unfavorable interaction with the receptor, and that the receptor must make close contact with the antagonist molecule in the vicinity of position 4. We have found that the situation is quite similar in agonists. [Mpr^1, αMeVal^4]-AVP is a potent agonist while the corresponding Cle^4 analog loses 3 orders of magnitude in receptor affinity. Thus position 4 seems to be quite similar both with respect to SAR, conformational effects and positioning with respect to the receptor in both agonists and antagonists.

The recognition that vasopressin V_2 agonists and antagonists interact with the receptor through distinct pharmacophores has implications for peptide drug design beyond the obvious conclusion that antagonist SAR must be developed

de novo. A more detailed knowledge of the nature of both the agonist and antagonist pharmacophores is necessary in order to apply the large body of agonist SAR data to the design of antagonists. It should be possible to exploit the knowledge about the agonist pharmacophore to design antagonists with improved receptor affinity and reduced intrinsic agonist activity. Comparison of agonist and antagonist interactions with the receptor may also lead to a better understanding of the molecular nature of receptor activation and to the design of novel agonists and antagonists.

References

1. Sawyer, W.H., Pang, P.K.T., Seto, J., McEnroe, M., Lammek, B. and Manning, M., Science, 212(1981)241.
2. Stassen, F.L., Berkowitz, B.B., Huffman, W.F., Wiebelhaus, V.D. and Kinter, L.B., In Puschett, J. (Ed.) Diuretics: Chemistry, Pharmacology and Clinical Applications, Elsevier, New York, 1984, p. 64.
3. Botos, C.R., Smith, C.W., Chan, Y.-L. and Walter, R., J. Med. Chem., 22(1979)926.
4. Kolc, J., Zaoral, M. and Sorm, F., Coll. Czech. Chem. Comm., 32(1967)2667.
5. Huffman, W.F., Ali, F.E., Bryan, W.M., Callahan, J.F., Moore, M.L., Silvestri, J.S., Yim, N.C.F., Kinter, L.B., McDonald, J.E., Ashton-Shue, D., Stassen, F.L., Heckman, G.D., Schmidt, D.B. and Sulat, L., J. Med. Chem., 28(1985)1759.
6. Moore, M.L., Greene, H., Huffman, W.F., Stassen, F., Stefankiewicz, J., Sulat, L., Heckman, G., Schmidt, D., Kinter, L., McDonald, J. and Ashton-Shue, D., Int. J. Pept. Prot. Res., 28(1986)379.
7. Ali, F.E., Bryan, W., Chang, H.-L., Huffman, W.F., Moore, M.L., Heckman, G., Kinter, L., McDonald, J., Schmidt, D., Shue, D. and Stassen, F., J. Med. Chem., 29(1986)984.
8. Callahan, J.F., Ali, F.E., Bryan, W., Chang, H.-L., Greene, H., Huffman, W.F., Moore, M.L., Silvestri, J., Yim, N., Heckman, G., Kinter, L., McDonald, J., Schmidt, D., Shue, D., Stassen, F. and Sulat, L., In Deber, C.M., Hruby, V.J. and Kopple, K.D. (Eds.) Peptides: Structure and Function, Proceedings of the 9th American Peptide Symposium, Pierce Chemical Co., Rockford, IL, 1985, p. 611.
9. Moore, M.L., Huffman, W.F., Bryan, W.B., Silvestri, J., Chang, H.-L., Stassen, F., Stefankiewicz, J., Sulat, L., Schmidt, D., Kinter, L., McDonald, J. and Ashton-Shue, D., In Deber, C.M., Hruby, V.J. and Kopple, K.D. (Eds.) Peptides: Structure and Function, Proceedings of the 9th American Peptide Symposium, Pierce Chemical Co., Rockford, IL, 1985, p. 607.

Synthesis and airway smooth muscle relaxant activity of linear and cyclic vasoactive intestinal peptide analogs

David R. Bolin[a], Iou-Iou Sytwu[a], Jeanine M. Cottrell[a], Ralph J. Garippa[b], Cydney C. Brooks[b] and Margaret O'Donnell[b]

[a]Peptide Research Department and [b]Pharmacology Department, Roche Research Center, Hoffmann-La Roche Inc., Nutley, NJ 07110, U.S.A.

Introduction

Vasoactive intestinal peptide (VIP), first isolated in 1970 from porcine intestine [1], has been shown to function as both a central and peripheral neurotransmitter and is a potent bronchodilator. VIP-containing neurons innervate airway smooth muscle and exocrine glands in the lung, and VIP has been shown to be a major endogenous component of airway smooth muscle relaxation [2]. It is postulated that aberrant VIP functioning may be responsible for the bronchoconstriction, edema and mucus secretion found in bronchial asthma.

Results and Discussion

Initial in vitro and preliminary clinical [3, 4] results on VIP have indicated the potential of VIP as a therapeutic agent for bronchial asthma. A structure–activity study was initiated in order to elucidate requirements for biological activity. Peptide analogs were synthesized using standard solid phase procedures, followed by purification by HPLC and full characterization (AAA and FABMS). VIP analogs were assayed for relaxant activity on guinea pig tracheal rings. EC_{50} values, determined from full dose–response curves, were used to compare potencies with native VIP.

Synthetic fragments of VIP containing C-terminal (20-28), N-terminal (1-6, 1-13, 1-19, and 1-23) and midregions (18-23, 12-23, and 7-13) of the molecule were inactive. Elimination of His^1 or modification (3-methyl, 1-methyl, D-His, or desamino) resulted in substantial loss of potency as well as activity. Acylation of His^1 (acetyl, benzoyl, or glycyl) yielded equal or only slightly reduced potency. Replacement of Met^{17} by norleucine [5] is synthetically less problematic and increased potency slightly.

Secondary structure calculations predicted the central portion of the molecule (12-20) to be helical in nature, which is reflected in high helical content (circular dichroism, CD) in aqueous–alcohol solvents. Replacement of residues within

this region by helix-favoring residues generally enhanced potency. Replacement of Arg^{12} or Arg^{14} with Lys or Orn resulted in a 1.7 – 2.6-fold increase in potency. Replacement of Val^{19} and Tyr^{22} by Leu and Phe, respectively, reduced potency. Conservative changes in the C-terminus yielded variable results, however, it was found that replacement of both Ile^{26} and Asn^{28} by Val and Thr, respectively, doubled potency. By synthesizing combinations of the most favorable changes, a series of analogs with larger increases in potency was found (Table 1). The analog [Ac-His^1, Lys^{12}, Lys^{14}, Nle^{17}, Val^{26}, Thr^{28}]-VIP was 10-fold more potent than native VIP.

Cyclic analogs of natural peptides have been shown to enhance potency, receptor selectivity, and enzymatic stability. Site-specific cyclizations were performed on the resin-bound linear peptides using a modification of previously reported procedures [6, 7]. Standard Boc-benzyl protection was utilized except at specific amine and carboxyl sites. Lysine was protected as Boc-Lys (Fmoc). Glu and Asp residues were blocked as their side-chain Fm esters. Treatment of the blocked peptide-resin with piperidine/DMF freed the base-labile and acid sites, leaving benzyl-derived protection intact. Cyclization was performed with either DCC/HOBt or BOP followed by HF and purification. Table 2 shows the bioassay data for several cyclic VIP analogs. In general, all were over a

Table 1 *Combination replacement analogs*

	EC_{50}(nM)[a]	Potency[b]
(Nle^{17})-VIP	6.4	156%
(Ac-His^1, Nle^{17}, Val^{26}, Thr^{28})-VIP	3.5	286
(Ac-His^1, Lys^{12}, Nle^{17}, Val^{26}, Thr^{28})-VIP	2.7	370
(Ac-His^1, Lys^{12}, Nle^{17}, Thr^{25}, Val^{26}, Thr^{28})-VIP	2.1	481
(Ac-His^1, Orn^{12}, Nle^{17}, Val^{26}, Thr^{28})-VIP	1.74	575
(Ac-His^1, Lys^{12}, Lys^{14}, Nle^{17}, Val^{26}, Thr^{28})-VIP	0.98	1020

[a] EC_{50} for relaxation of guinea pig tracheal rings.
[b] Potency relative to native VIP (EC_{50} = 10 nM = 100%)

Table 2[a,b] *Cyclic analogs of VIP*

	EC_{50}(nM)[a]	Potency[b]
(His^1, Asp^3, Lys^{12}, Nle^{17}, Val^{26}, Thr^{28})-VIP	730	1.4%
(Gly-His^1, Asp^3, Lys^{12}, Nle^{17}, Val^{26}, Thr^{28})-VIP	220	5
(His^1, Asp^8, Lys^{12}, Nle^{17}, Val^{26}, Thr^{28})-VIP	–	inact.
(His^1, Lys^{12}, Glu^{16}, Nle^{17}, Val^{26}, Thr^{28})-VIP	145	7
(Gly-His^1, Lys^{12}, Glu^{16}, Nle^{17}, Val^{26}, Thr^{28})-VIP	79	13
(Ac-His^1, Asp^3, Lys^{12}, Nle^{17}, Val^{26}, Thr^{28})-VIP	170	6
(Ac-His^1, Asp^3, Lys^{12}, Lys^{14}, Nle^{17}, Val^{26}, Thr^{28})-VIP	88	11

[a, b] See footnotes to Table 1.

log less potent than VIP, yet possessed full intrinsic activity. CD results have shown that most of the cyclic analogs possessed structures similar to the linear species. This indicates that all components of receptor binding are available and that fine tuning of the ring structure may increase potency.

References

1. Said, S.I. and Mutt, V., Science, 169 (1970) 1217.
2. Said, S.I., Kitamura, S., Yoshida, T., Preskitt, J. and Holden, L.D., Ann. N.Y. Acad. Sci., 221 (1974) 103.
3. Morice, A., Unwin, R.J. and Sever, P.S., Lancet, ii (1983) 1225.
4. Barnes, P.J. and Dixon, C.M.S., Am. Rev. Resp. Dis., 130 (1984) 162.
5. Wendlberger, G., Thamm, P., Gemeiner, M., Bataille, D. and Wuensch, E., In Brunfeldt, K. (Ed.) Peptides 1980, Proceedings of the 16th European Peptide Symposium, Scriptor, Copenhagen, 1981.
6. Lebl, M. and Hruby, V.J., Tetrahedron Lett., 25 (1984) 2067.
7. Schiller, P.W., Nguyen, T. and Miller, J., Int. J. Pept. Prot. Res., 25 (1985) 171.

Structure–activity studies of atrial natriuretic factor

Ruth F. Nutt, Terry M. Ciccarone, Stephen F. Brady, C. Dylion Colton, William J. Paleveda, Terry A. Lyle, Theresa M. Williams, Daniel F. Veber, Audrey Wallace and Raymond J. Winquist

Merck Sharp & Dohme Research Laboratories, West Point, PA 19486, U.S.A.

Introduction

Atrial natriuretic factor (ANF) Arg[3]-Arg-Ser-Ser-Cys-Phe-Gly-Gly-Arg-Ile-Asp-Arg-Ile-Gly-Ala-Gln-Ser-Gly-Leu-Gly-Cys-Asn-Ser-Phe-Arg-Tyr[28] (**1**) is one of several peptides recently isolated from rat atrial tissue which exhibit potent diuretic, natriuretic, and vasorelaxant activities. Reported structure–activity studies (for review, see [1]) have demonstrated that the cyclic nature of ANF and components in the termini are major contributors to biological potency. This report deals with our attempts to define side-chain and backbone conformational features, which are crucial for eliciting high biopotency, through the use of single-point alanine substitutions.

Results and Discussion

Earlier reports have postulated Arg[27] as a primary contributor to potency in the termini of ANF [2]; however, less than a factor of 10 could be attributed to this residue. To probe for additional important determinants and to explain the greater than 100-fold loss in potency upon deletion of both termini, we synthesized singly substituted Ala analogs of **1** and several truncated derivatives and evaluated their potency as vasorelaxants (Table 1). The high potencies of analogs **2**, **3**, and **4** provide evidence for the noncritical nature of Asn, Ser, and Phe side chains in the C-terminus. These observations are consistent with our earlier conclusions drawn from the high potencies obtained upon D-residue substitution for each of these same positions [1]. Even Arg[27] was found to contribute by only a factor of 2–4 as evidenced by the potencies obtained upon Ala substitution (**5**) or deletion of the residue (**6**). A different pattern, however, emerged when the same modifications were carried out in the highly active analog **7** in which the N-terminus was deleted. In this series, removal of the Arg[27] side chain (**8**) or residue deletion (**9**) resulted in a greater than 10-fold reduction in vasorelaxant potency. These data show that high potency (20-50%) is retained upon removal of the Arg side chains in the termini of **1** as long as at least

Table 1 *Vasorelaxant potencies of ANF analogs*[a]

	ANF analog[b]	Potency[c]	
		Rabbit aorta	Rabbit renal artery
1	(3-28)	100	100
2	Ala^{24} (3-28)	84	210
3	Ala^{25} (3-28)	74	170
4	Ala^{26} (3-28)	132	340
5	Ala^{27} (3-28)	40	16
6	(3-26)NH_2	33	52
7	(7-28)	68	45
8	Ala^{27} (7-28)	4	1
9	(7-26)NH_2	6	3
10	Ala^{8} (3-28)	6	2
11	Ala^{15} (3-28)	4	3
12	Ala^{21} (3-28)	–	5
13	Ala^{11} (3-28)	53	77
14	Ala^{18} (3-28)	–	83
15	Ala^{16} (3-28)	216	279
16	Ala^{20} (3-28)	88	199
17	Ala^{22} (3-28)	94	94

[a] Analogs were synthesized either by couplings of fragments on solid support [4] or by stepwise solid phase synthesis using an Applied Biosystems 430A synthesizer. All products were purified to purity of ≥97% (HPLC).

[b] ANF (3-28) = Arg-Arg-Ser-Ser-Cys-Phe-Gly-Gly-Arg-Ile-Asp-Arg-Ile-Gly-Ala-Gln-Ser-Gly-Leu-Gly-Cys-Asn-Ser-Phe-Arg-Tyr.

[c] Determined as described in [5].

one cationic site is retained in either the C- or N-terminus. That the charged moiety can be supplied from either the C- or the N-terminus suggests a spacial proximity of the Arg residues in the two ends of ANF.

Selective side-chain deletions in the ring portion of ANF resulted in low potency (≤6% of **1**) analogs when Phe^{8}, Ile^{15}, and Leu^{21} were replaced by Ala (**10**, **11**, **12**), suggesting an important role for the hydrophobic side chains of these amino acids. Requirements for specific uncharged hydrophobic residues in position 8 are confirmed by the low potency upon replacing Phe with Tyr [3]. In contrast, high potencies (>50%) were retained upon replacement of Arg^{11} and Gln^{18} by Ala (**13**, **14**). The latter results indicate that the hydrophilic side chains in positions 11 and 18 contribute little, if any, to biological potency.

Replacement of glycine residues in positions 16, 20, and 22 by Ala resulted in highly active analogs (**15**, **16**, **17**). The increased potency of the L-Ala^{16} (**15**) over the D-Ala^{16} analog [1] (68% of parent) may indicate a preference for α-helical over β-turn structure in the bioactive conformation of ANF. For positions 20 and 22, high potencies have also been reported for the corresponding D-

Ala analogs [1]. This may be an indication for either β-turn conformation at the C-terminal portion of the ring or a high tolerance for conformational variability in this region.

References

1. Nutt, R.F. and Veber, D.F., Clin. Endocrinol. Metab., 16(1987) 19.
2. Needleman, P., Adams, S.P., Cole, B.R., Currie, M.G., Geller, D.M., Michener, M.L., Saper, C.B., Schwartz, D. and Standaert, D.G., Hypertension, 7(1985)469.
3. Misono, K.S., Grammer, R.T., Rigby, J.W. and Inagami, T., Biochem. Biophys. Res. Comm., 130(1985)994.
4. Nutt, R.F., Brady, S.F., Lyle, T.A., Ciccarone, T.M., Paleveda, W.J., Colton, C.D., Veber, D.F. and Winquist, R.J., Protides of Biol. Fluids, 34(1986)55.
5. Winquist, R.J., Faison, E.P. and Nutt, R.F., Eur. J. Pharm., 102(1984)169.

Characterization of the interaction of thrombin with the C-terminal region of the leech anticoagulant peptide hirudin

John L. Krstenansky, Simon J.T. Mao, Thomas J. Owen and Mark T. Yates
Merrell Dow Research Institute, 2110 Galbraith Rd., Cincinnati, OH 45215, U.S.A.

Hirudin is a 65-amino acid residue anticoagulant peptide secreted from the salivary glands of the medicinal leech (*Hirudo medicinalis*). It is a potent inhibitor of the cleavage of fibrinogen by thrombin through the formation of a tight complex. The kinetics of the hirudin–thrombin interaction indicate an initial rate-limiting, ionic strength-dependent interaction that is followed by a rearrangement to form a tight complex [1]. The ionic portion of the interaction has been suggested by several groups to involve the C-terminal acidic residues of hirudin with basic groups on thrombin [2, 3]. As a test of this hypothesis, unsulfated acetylhirudin$_{45-65}$ was synthesized and found to inhibit fibrinogen cleavage to fibrin and subsequent clot formation by binding to thrombin at a noncatalytic site [4]. Within the minimal sequence necessary for anticoagulant activity, hirudin$_{56-64}$ (unpublished data), Phe^{56}, Glu^{57}, Ile^{59}, Pro^{60} and Leu^{64} are particularly important since the single amino acid substitution of Ala for each of these residues results in a complete loss of anticoagulant activity (Fig. 1). Position 56 requires the presence of an L-aromatic amino acid, and position 59 requires an L-lipophilic amino acid. The presence of Pro^{60}, the activity of the D-Ala^{60} analog, and the lack of activity of the L-Ala^{60} analog suggest a conformational requirement at this site. Tyr^{63}, normally sulfated in native hirudin, was surprisingly not a critical residue although D-Tyr was not tolerated. Thus, the lipophilic residues and the single acidic Glu^{57} residue are critical for the binding of this region to thrombin and not the many acidic groups as was previously hypothesized [3].

Hirudin$_{54-65}$ is predicted as an amphipathic α-helix by Chou and Fasman [5] ($\langle P_\alpha \rangle = 1.06$, $\langle P_\beta \rangle = 0.72$, $\langle P_t \rangle = 0.84$) and Eisenberg et al. [6] analyses (hydrophobic moment maximum of 3.20 at 98°). Those residues important for activity are grouped together in such a model and occupy one face of the α-helix. The lack of activity of the Ala^{60} analog suggests that a simple α-helical conformation does not completely describe the active conformation of this peptide. Still a 'kinked' helix could not be ruled out. To test this, a means of constraining a peptide into an α-helical conformation was sought. Models indicated that an α-helix could potentially be stabilized by the introduction of a D-Cys at position i and L-Cys at position i+3 in a peptide and cyclizing to

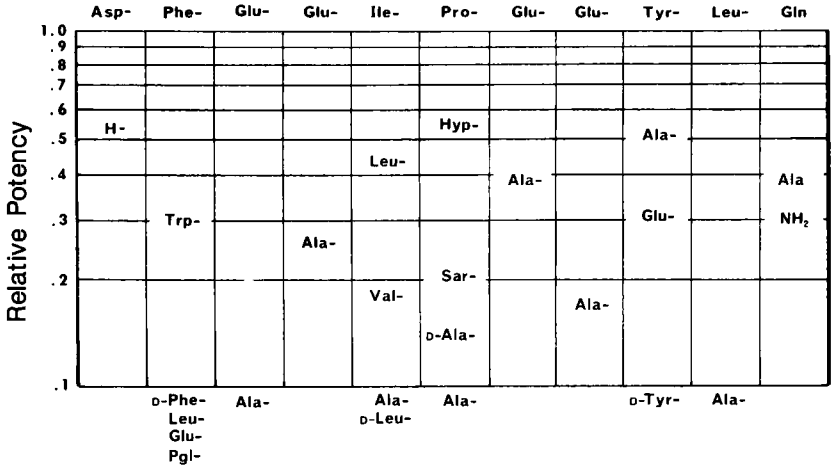

Fig. 1. Relative potency of single amino acid substitution analogs of hirudin$_{54-65}$ and hirudin$_{55-65}$ (relative potency = 1.0). The location of the amino acid on the chart indicates the relative anticoagulant potency of that analog. The natural sequence is listed at the top of each column. The substitutions listed below 0.1 relative potency had undetectable activity (relative potency <2%).

form a 14-membered ring. Thus [D-Cys^{58}, Cys^{61}]-hirudin$_{54-65}$ was synthesized and found to be active, having 14% of the potency of hirudin$_{54-65}$. Conformational analysis of the cyclic analog is currently in progress.

References

1. Stone, S.R. and Hofsteenge, J., Biochemistry, 25 (1986) 4622.
2. Tertrin, C., de la Llosa, P. and Jutisz, M. Bull. Soc. Chim. Biol., 49 (1967) 1837.
3. Magnusson, S., In Boyer, P.D. (Ed.) The Enzymes, Vol. 3, 3rd ed., Academic Press, New York, NY, 1971, pp. 282-307.
4. Krstenansky, J.L. and Mao, S.J.T., FEBS Lett., 211 (1987) 10.
5. Chou, P.Y. and Fasman, G.D., Adv. Enzymol., 47 (1978) 45.
6. Eisenberg, D., Weiss, R.M. and Terwilliger, T.C., Proc. Natl. Acad. Sci. U.S.A., 81 (1984) 140.

Characterization of parathyroid hormone antagonists

Lynn H. Caporale, Michael Chorev, Jay J. Levy, Mark E. Goldman, Patricia A. DeHaven, C. Thomas Gay, Jane E. Reagan, Michael Rosenblatt and Ruth F. Nutt

Merck Sharp & Dohme Research Laboratories, West Point, PA 19486, U.S.A.

Introduction

Parathyroid hormone (PTH) plays a key role in maintaining plasma calcium levels. Although the native hormone is an 84-residue peptide, fragments and analogs lacking the carboxy-terminal 50 amino acids as in [Tyr^{34}]PTH(1-34)NH_2 exhibit full agonist potency. In contrast, chain shortening at the amino terminus (e.g. [Tyr^{34}]PTH(7-34)NH_2) leads to antagonism. Our approaches for designing novel antagonists with improved biological profiles involve (1) stabilization against metabolic degradation, (2) elucidation of the bioactive conformation, and (3) dimerization in an attempt to increase apparent receptor affinity. Examples of PTH analogs in the three categories have been synthesized and evaluated for binding affinity in a PTH radioreceptor assay.

Results and Discussion

PTH analogs were synthesized as described previously [1] and analyzed for binding affinity in a refined radioreceptor assay (Table 1). The binding assay used [$Nle^{8,18}$,[^{125}I]Tyr^{34}]bPTH(1-34)NH_2, which was purified by HPLC (Novapak C_{18}, 32–35% CH_3CN in 0.1% TFA) and stored as aliquots in 25 mM Tris-HCl/1%BSA at −70°C. High specific binding (85%) to bovine renal cortical membranes was obtained consistently.

The analog [Tyr^{34}]bPTH(7-34)NH_2 has been shown to be an effective PTH antagonist in vivo [2]. With the goal of increasing metabolic stability by preventing potential degradation by amino peptidases, analogs **2** and **3**, containing modified amino termini, were synthesized. Binding data show that no loss in receptor affinity occurred in these analogs. The high potencies of **2** and **3** also indicate that the primary amino group of Phe^7 does not contribute to receptor binding of the antagonists.

Secondary structure prediction at Gly^{12} of PTH has postulated a β-turn [3] or an α-helix (Sander and Kabsch, manuscript in preparation). NMR spectroscopy has indicated a γ-turn at Glu^{22} [4]. Substitutions were introduced in both regions. In the antagonist series, Gly^{12} was replaced with α-amino isobutyric acid (Aib)

Table 1 *PTH receptor binding potencies of PTH analogs*

Analog	Structure	Binding [a] K_I(nM)
1	[Tyr^{34}]bPTH(7-34)NH_2	75 ± 8
2	Desamino [Tyr^{34}]bPTH(7-34)NH_2	91 ± 12
3	[$NMePhe^{7}$, Tyr^{34}]bPTH(7-34)NH_2	82 ± 14
4	[Aib^{12}, Tyr^{34}]bPTH(7-34)NH_2	51 ± 9
5	[Sar^{12}, Tyr^{34}]bPTH(7-34)NH_2	500 ± 90
6	[Tyr^{34}]hPTH(1-34)NH_2	0.7 ± 0.3
7	[D-Ala^{12}, Tyr^{34}]hPTH(1-34)NH_2	0.9 ± 0.1
8	[Ala^{12}, Tyr^{34}]hPTH(1-34)NH_2	1.0 ± 0.04
9	[Aib^{12}, Tyr^{34}]hPTH(1-34)NH_2	0.8 ± 0.1
10	[Pro^{12}, Tyr^{34}]hPTH(1-34)NH_2	590 ± 200
11	[D-Trp^{23}, Tyr^{34}]bPTH(7-34)NH_2	7.6×10^4 ± 1.5×10^4

[a] Bovine renal cortical plasma membranes were incubated with radioligand (25,000 cpm) in a Tris-containing buffer (250 μl) for 30 min at 21°C. Once equilibrium was reached, bound and free radioligand were separated by centrifugation.

(**4**), an α-helix- or 3_{10} helix-promoting modification [5], and sarcosine (Sar) (**5**), a potential helix-breaker and β-turn-promoting structure. In the agonist series, Gly^{12} was replaced by D-Ala (**7**), Ala (**8**), Aib (**9**) and Pro (**10**). The high binding affinities of the Aib, D-Ala, and Ala-containing analogs and the low affinities of the Sar and Pro analogs suggest an α-helical or 3_{10} helical conformation near position 12 of PTH. Type I or II′ β-turn conformations are contraindicated because of the low potencies of the Sar- and Pro-containing analogs and the high affinities of the Aib analogs. Although a parallel biological profile of the Gly^{12}-substituted analogs in both the antagonist and agonist series is observed, helical conformation at position 12 seems to be more critical in the agonist series.

To test for conformationally important features around position 22, the chirality of Trp^{23} was inverted in the antagonist series (**11**). A 1000-fold decrease in receptor binding was observed indicating that the conformation at position 23 plays a key role in receptor binding.

Ligand dimerization has been observed to enhance significantly the receptor binding affinity of an ACTH antagonist [6]. We have applied this concept by dimerization of the weak PTH antagonist [Tyr^{34},$Cys(Acm)^{39}$]PTH(21-39)NH_2 (**12**) to [Tyr^{34},$\overline{Cys^{39}}$]$\overline{PTH(21\text{-}39)NH_2}$)$_2$ (**13**). In an adenylate cyclase assay [7], dimer (**13**) exhibited a 25-fold increase in antagonist potency (IC_{50}, 20μM) over the monomeric derivative (**12**). This potentiation of activity upon dimerization, however, does not appear to be based upon increased receptor affinity observed in the binding assay. Further studies are in progress to explain the discrepancies in these two biological systems.

Acknowledgements

We would like to thank Dr. Dan Veber for helpful discussions.

References

1. Caporale, L., Nutt, R., Levy, J., Rosenblatt, M., Smith, J., Arison, B., Randall, W., Bennett, C., Albers-Schonberg, G., Pitzenberger, S. and Hirschmann, R., In Theodoropoulos, D. (Ed.) Peptides 1986, Proceedings 19th European Peptide Symposium, Walter DeGruyter, Berlin, 1987, in press.
2. Rosenblatt, M., N. Engl. J. Med., 315 (1986) 1004.
3. Chou, P.Y. and Fasman, C., Biophys. J., 26 (1979)367.
4. Bundi, A., Andreatta, R. and Wuthrich, K., Eur. J. Biochem., 91 (1978) 201.
5. Benedetti, E., Bavoso, A., DiBlasio, B., Pavone, V., Pedone, C., Crisma, M., Bonora, G. and Toniolo, C., J. Am. Chem. Soc., 104 (1982) 2437.
6. Fauchère, J., Rossier, M., Capponi, A. and Vallotton, M., FEBS Lett., 183 (1985) 283.
7. Caporale, L., DeHaven, P., Fisher, J., Tyler, G. and Rosenblatt, M., In Deber, C.M., Hruby, V.J. and Kopple, K.D. (Eds.) Peptides: Structure and Function, Proceedings of the 9th American Peptide Symposium, Pierce Chemical Co., Rockford, IL., 1985, p. 663.

Angiotensin II. Synthesis and biological activity of 8-(*R* and *S*)-tetrahydroisoquinoline and 7-(*R* and *S*)-(proline)thiazole analogs

Palaniappan Balasubramanian and Garland R. Marshall*
Department of Pharmacology, Washington University School of Medicine, St. Louis, MO 63110, U.S.A.

Introduction

The octapeptide angiotensin II (AII), Asp-Arg-Val-Tyr-Val-His-Pro-Phe, is a predominant hormone in blood volume homeostasis and results from a cascade of specific proteolytic events. Its biological activity has been primarily characterized by myotropic and pressor assays. During the past decade, great effort has been expended toward the understanding of the interaction of this hormone with its receptor [1–3]. The orientation of the aromatic ring at the 8 position and the free carboxylic acid group with respect to the rest of the molecule are necessary for activity [3]. Antagonism resulted when the spatial orientation of the aromatic side chain was changed from L to D [4]. Hsieh and Marshall have studied some of the modified peptides at the 8 position [5]. In continuation of our effort to understand the effect of the aromatic ring at the 8 position in relation to proline at the 7 position, we synthesized 8-(*R* and *S*-tetrahydroisoquinoline AII (**1** and **2**) and 7-(*R* and *S*)-(proline)thiazole AII (**3** and **4**) and studied their biological activity.

Synthesis

8-(*R* and *S*)-Tetrahydroisoquinoline AII (**1** and **2**) was synthesized by the solid phase procedure. Chloromethylene resin with the capacity of 0.22 meq/g was prepared according to Gisin [6]. The synthetic cycle deblocking, rinsing, and coupling steps were carried out using the double coupling procedure [7]. N-Boc protection was used throughout the synthesis with the following side-chain protecting groups: Arg(NO_2), Tyr(Cl_2BZI), and His(DNP). The peptide was cleaved using low-high HF procedure [8]. DNP was removed by stirring with C_2H_5SH and further purified by CCD(B:P:A:W, 15:10:3:12). The *R* and *S* isomers

*To whom correspondence should be addressed.

were separated by preparative RPHPLC (Vydac Column, C_{18}, 0.1% TFA in H_2O and 0.1% TFA in 60% CH_3CN + 40% H_2O).

Initially, we attempted to synthesize the Fmoc-(Pro)thiazole-OMe (**7**) as shown in Scheme 1. Compound **5** was prepared by coupling Fmoc-Pro-OH and Cys-OMe. It was then cyclized to give compound **6**. Attempts to oxidize the compound by using MnO_2, NiO_2 and DDQ have failed. We then synthesized Cbz-(*R* and *S*)-(proline)thiazole (**11** and **12**) as shown in Scheme 2. Refluxing compound **8** with *p*-TsCl and pyridine gave the nitrile, **9**, in 90% yield. This was further converted to the thioamide (**10**) by passing H_2S, NH_3 in MeOH. Reaction of the thioamide with bromopyruvate in methanol produced diastereoisomers **11** and **12**. The formation of these diastereoisomers has been discussed by Holzapfel and Pettit [9]. These were further treated with HBr/CF_3COOH and coupled with Boc-His(CH_2OCH_2Ph)-OH as shown in Scheme 3. Diastereoisomers **15** and **16** were separated by preparative TLC, and from this stage the synthesis has been carried out separately. The pentapeptide, **23**, was synthesized from Val-OMe in a stepwise procedure using PPA/DMF as a coupling reagent, and was further coupled with tripeptides **15** and **16**. The resulting octapeptide was consecutively deprotected with removal of the Boc group, and neutralized. The

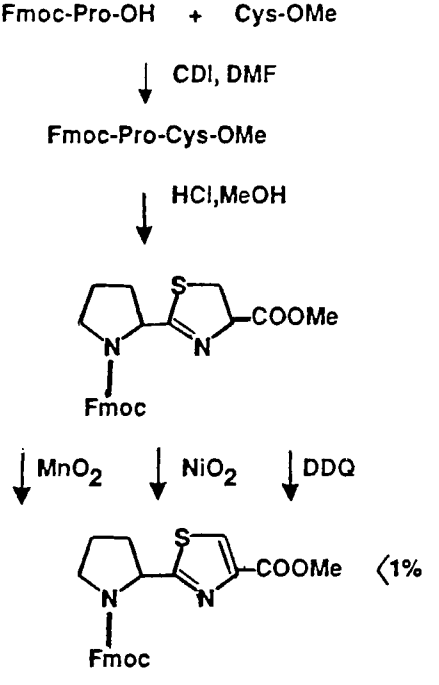

Scheme 1.

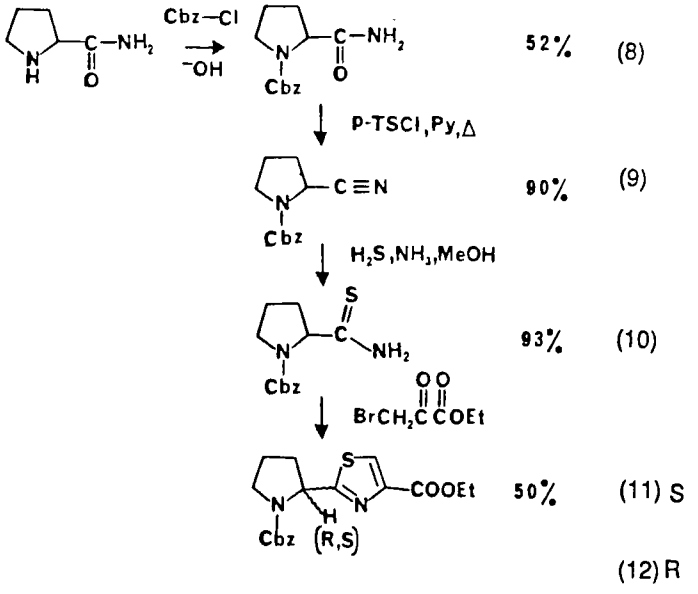

Scheme 2.

side-chain protecting groups were removed by the low-high HF procedure. The octapeptide was further purified by preparative RPHPLC and analytical RPHPLC. Biological assays were performed with Sarco female rat uterus in deJalons solution. The ED_{50} and IC_{50} have been determined, with CIBA AII used as a standard. The values are shown in Table 1.

Table 1 *Myotropic assay of analogs*

(1)	Sar-Arg-Val-Tyr-Val-His-Pro-(*S*)-Thiq	$ED_{50} = 2.8 \times 10^{-9}$ mol/ml (agonist)
(2)	Sar-Arg-Val-Tyr-Val-His-Pro-(*R*)-Thiq	$IC_{50} = 6.4 \times 10^{-10}$ mol/ml (antagonist)
(3)	Sar-Arg-Val-Tyr-Val-His-(*S*)-(Pro)Thz	No activity
(4)	Sar-Arg-Val-Tyr-Val-His-(*R*)-(Pro)Thz	No activity
Std	Asp-Arg-Val-Tyr-Val-His-Pro-Phe	$ED_{50} = 9.2 \times 10^{-13}$ mol/ml

Results and Discussion

8-(S)-Tetrahydroisoquinoline AII (**1**) shows agonist activity, and the R isomer (**2**) acts as an antagonist. The low response may be due to steric interference of the tetrahydroisoquinoline in which the phenyl ring is covalently linked to the N atom of the peptide backbone. This gives a rigid aromatic ring lacking the rotational freedom of the phenylalanine ring, which in turn cannot slide

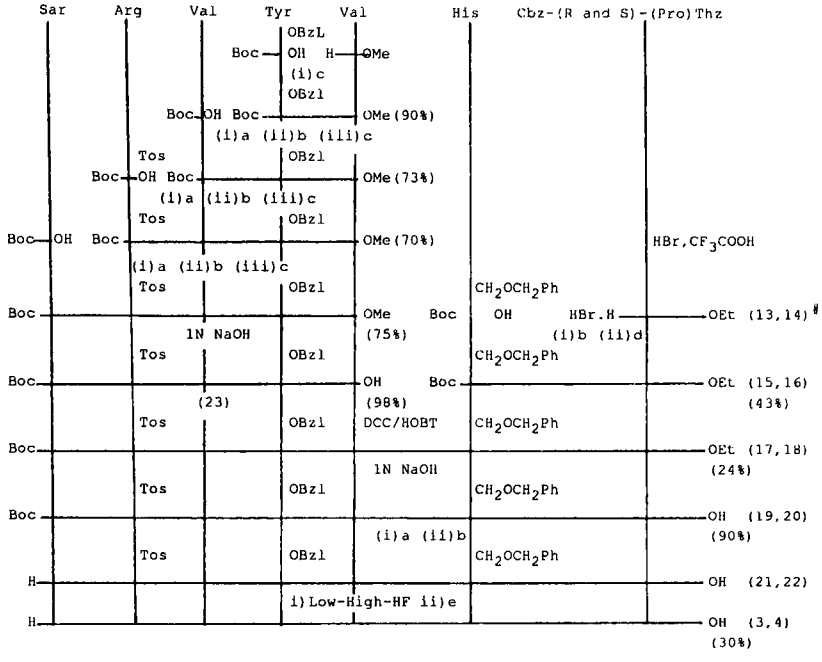

Scheme 3. a = HCl, dioxane; b = diisopropylamine in CH_2Cl_2; c = propyl phosphoricanhydride, DMF; d = diphenylphosphoryl azide, DMF; e = purified by RPHPLC followed by analytical RPHPLC (Vydac Column; Solvent A = 0.1% TFA in H_2O; Solvent B = 0.1% TFA in 60% CH_3CN and 40% H_2O).

#13, **15**, **17**, **19**, **21** and **3** correspond to 8-(*S*)-(proline)thiazole compound.

14, **16**, **18**, **20**, **22** and **4** correspond to 8-(R)-(proline)thiazole compound.

fully into the hydrophobic aromatic receptor pocket. Analogs **3** and **4** are not active. The limited orientations available to the carboxyl group constrained by the thiazole ring are either not compatible with receptor recognition, or the carbonyl of the Pro-Phe amide bond which is no longer present may play a role in binding.

Acknowledgements

The authors would like to thank the National Institutes of Health (grant number GM 24483) for support of this research.

References

1. Khosla, M.C., Smeby, R.R. and Bumpus, F.M., In Page, I.H. and Bumpus, F.M. (Eds.) Handbook of Experimental Pharmacology, Vol. 37, Springer-Verlag, Berlin, 1974, p. 126.
2. Marshall, G.R., Bosshard, H.E., Vine, W.H., Glickson, J.D. and Needleman, P., In Wesson, L.G. and Fanelli, Jr., G.M. (Eds.) Recent Advances in Renal Physiology and Pharmacology, University Park Press, Baltimore, MD, 1974, p. 215.
3. Bumpus, F.M. and Khosla, M.C., In Genest, J., Koiw, E. and Kuchel, O. (Eds.) Hypertension, McGraw-Hill, New York, NY, 1977, p. 183.
4. Gagnon, D., Park, W.K. and Regoli, D., Br. J. Pharmacol., 43 (1971) 409.
5. Hsieh, K.-H. and Marshall, G.R., J. Med. Chem., 29 (1986) 1968 (and references cited therein).
6. Gisin, B.F., Helv. Chim. Acta., 56 (1973) 1476.
7. Merrifield, R.B., Vizioli, L.D. and Boman, H.G., Biochemistry, 21 (1982) 5020.
8. Tam, J.P., Heath, W.F. and Merrifield, R.B., J. Am. Chem. Soc., 105 (1983) 6442.
9. Holzapfel, C.W. and Pettit, G.R., J. Org. Chem., 50 (1985) 2323.

NMR analysis and conformational characterization of cyclic antagonists of gonadotropin-releasing hormone

Edmund L. Baniak II[a], Lila M. Gierasch[a], Jean Rivier[b] and Arnold T. Hagler[c]

[a]*Department of Chemistry, University of Delaware, Newark, DE 19716, U.S.A.*

[b]*Clayton Foundation Laboratories for Peptide Biology, The Salk Institute, 10010 N. Torrey Pines Road, La Jolla, CA 92037, U.S.A.*

[c]*The Agouron Institute, 505 South Coast Boulevard, La Jolla, CA 92037, U.S.A.*

Introduction

The conformations of 5 cyclic analogs of gonadotropin-releasing hormone (GnRH) which have varying antagonist activities in an in-vitro assay [1] have been determined by NMR at 500 MHz. Sample preparations and spectroscopic methods used have been described in detail elsewhere [2]. The analogs studied were: Ac-*c*(Dap4-Tyr5-D-βNal6-Leu7-Arg8-Pro9-Asp10)-NH_2, I, an inactive analog; *c*(Δ^3Prol-D-pClPhe2-D-Trp3-Ser4-Tyr5-D-Trp6-NMe-Leu7-Arg8-Pro9-βAla10), II, a low potency analog; Ac-Δ^3Prol-D-pFPhe2-D-Trp3-*c*(Dap4-Tyr5-D-Trp6-Leu7-Arg8-Asp9)-Gly10-NH_2, III, having a potency similar to that of II; Ac-Δ^3Prol-D-pFPhe2-D-Trp3-*c*(Dap4-Tyr5-D-βNa16-Leu7-Arg8-Pro9-Asp10) NH_2, IV, a high potency analog; and Ac-Δ^3Prol-D-pFPhe2-D-Trp3-*c*(Asp4-Tyr5-D-βNa16-Leu7-Arg8-Pro9-Dap10)-NH_2, V, an antagonist with high in-vivo activity. By studying the conformations of constrained GnRH analogs that show bioactivity, the essential features of the bioactive conformation of the native hormone can be deduced.

Results and Discussion

All structurally significant protons of analogs I–V have been assigned. Temperature dependences of spectral parameters and magnitudes of observed NOEs show the occurrence of a β-type turn between residues 5 and 8 for all active analogs (II–V) (Table 1). This corresponds to the region of the native hormone that has been proposed to exist in a β-turn when bound at the receptor [3]. No β-turn is formed in the inactive analog (I); however, it also lacks a 3-residue segment present in the active analogs.

The $\Delta\delta/\Delta T$ data show (Table 1) that the arginine amide proton (residue 8) is sequestered only in the active analogs. All 5 analogs exist in a conformation with all *trans* peptide bonds which is in equilibrium to varying extents with

Table 1 *Observed NOEs (NH → NH) and temperature dependence of amide protons around β-turn region*

	NH → NH (residues 7 → 8)	Δδ/ΔT (ppb/degree)			
Analog	NOE magnitude	Residue 5	Residue 6	Residue 7	Residue 8
I	None	−1.9[a]	7.8	3.3	5.8
II	(NMe → NH)strong	3.5	8.2	X[b]	2.8
III	Moderate	−0.9[a]	7.1	6.4	0.0
IV	Weak	1.3	6.9	5.0	1.8
V	None	2.8	7.8	4.4	2.2

[a] Negative value suggests association of an aromatic ring side chain with the amide (at low temperatures). With increasing temperature, the aromatic ring populates more extended orientations away from the backbone.
[b] Methyl-substituted amide.

a conformation that contains one *cis* peptide bond. Magnitudes of the NOE (NH → NH) at the turn corner (Table 1) suggest that the amide protons may be further apart in the most active analogs (IV and V) than is typical for these protons at this position in a turn.

Additional experiments are in progress to determine more quantitative interproton distances, to generate 3-dimensional structures *ab initio* from these distance data and to refine calculated structures by molecular dynamics constrained by NOE distances [4].

Acknowledgements

Research supported in part by an NIH grant, GM27616 (to LMG) and an NIH contract, NO1-HD-42833 (to JER). We thank D. Hare and L. Mueller for discussions and suggestions regarding NMR techniques and data processing and G. Kupryszewski, R. Galyean and J. Varga for synthesizing the antagonists.

References

1. Rivier, J., Varga, J., Porter, J., Perrin, M., Haas, Y., Corrigan, A., Rivier, C., Vale, W., Struthers, S. and Hagler, A., In Deber, C.M., Hruby, V.J. and Kopple, K.D. (Eds.) Peptides: Structure and Function, Proceedings of the 9th American Peptide Symposium, Pierce Chemical Co., Rockford, IL, 1985, pp. 541-544.
2. Baniak, II, E.L., Rivier, J.E., Struthers, R.S., Hagler, A.T. and Gierasch, L.M., Biochemistry, 26 (1987) 2642.
3. Momany, F.A., J. Am. Chem. Soc., 98 (1976) 2990.
4. Clore, G.M., Gronenborn, A.M., Bruenger, A.T. and Karplus, M., J. Mol. Biol., 186 (1985) 435.

The *a*-mating factor of *Saccharomyces cerevisiae*: A lipopeptide?

Fred Naider[a], P. Shenbagamurthi[a], Stevan Marcus[b] and Jeffrey M. Becker[b]
[a]*Department of Chemistry, College of Staten Island, Staten Island, NY 10301, U.S.A.*
[b]*Department of Microbiology and Program in Cellular Molecular, and Developmental Biology, University of Tennessee, Knoxville, TN 37996-0845, U.S.A.*

Introduction

Peptide sex pheromones appear to be common intercellular signals in the microbial biosphere [1, 2]. The interaction of such peptides with their target cells provides an ideal model system to gain insights concerning peptide hormone–receptor interactions and peptide secretion. The yeast *Saccharomyces cerevisiae* undergoes sexual conjugation which is directed in part by diffusible peptides. The alpha-factor, one of these mating pheromones, is a tridecapeptide and has been characterized in detail [3]. The structure of the reciprocal mating pheromone, the *a*-factor, remains elusive. Although a number of reports on its structure have appeared in the literature [4, 5], no laboratory has confirmed the complete structure of the active *a*-factor nor has it been synthesized. This is despite the fact that two structural genes for the *a*-factor have been sequenced and shown to code for 36- and 38-amino acid residue peptides [6]. Based on the structural genes and the possible processing events, we have synthesized a number of peptides. In parallel studies, we have subjected culture supernatants from *MATa* cells to chemical reaction. Our results suggest that the *a*-factor is a low-molecular weight peptide which probably contains a hydrophobic modification on a cysteine residue near the carboxyl terminus of the molecule.

Methods

Putative *a*-factor peptides synthesized in our laboratory were based on the carboxyl terminus coded for by the *MFal* structural gene (Tyr-Ile-Ile-Lys-Gly-Val-Phe-Trp-Asp-Pro-Ala-Cys-Val-Ile-Ala) and reports by Duntze and co-workers of a family of dodecapeptides thought to contain *a*-factor activity [4, 5]. The dodecapeptide YIIKGVFWDPA was synthesized in solution phase using isobutylchloroformate and *N*-methyl morpholine to form mixed anhydrides and transfer hydrogenation with formic acid and palladium black to remove benzyloxycarbonyl- and benzyl ester-protecting groups. Various pentadecapeptides

were synthesized on either a PAM or benzhydrylamine resin by the solid phase technique. Coupling was accomplished using dicyclohexylcarbodiimide or DCC/1-hydroxybenzotriazole. All residues were double coupled, and coupling was monitored by ninhydrin assay. Protecting groups were removed by acidolysis, and final cleavage from the resin was by the low-high HF method. All peptides were characterized by HPLC on reversed-phase columns, thin-layer chromatography, and amino acid analysis.

Culture supernatants from *MATa* cells were filter-sterilized and lyophilized for storage at -20°C. In some cases the supernatants were partially purified by passage through a G-25 column. Activity was assayed using YEPD plates overlayed with RC757 (*MATα*) cells in noble agar. Solutions of *a*-factor were pipetted onto the overlay and the plates were incubated for 48 h at 30°C. Clear zones or halos are the indication of *a*-factor activity. In antagonism experiments, a competing peptide at various concentrations was added together with a constant amount of the culture supernatant.

Results and Discussion

As seen in Table 1 none of the dodecapeptides, pentadecapeptides, or derivatives that we synthesized caused growth arrest of the *MATα* tester strain under conditions where culture supernatant from *MATa* cells gives a clear halo. All of these peptides, however, competed with the activity present in the culture supernatant. Antagonism was greatest for the peptide YIIKGVFWDPACVIA acylated with palmitoyl chloride. Treatment of this acylated peptide with alkaline hydroxylamine resulted in a decrease in competitive activity back to that found for the underivatized pentadecapeptide. These results suggest that modification with a long-chain fatty acid significantly increases recognition of the antagonist by the *a*-factor receptor. The fact that this increased activity is eliminated by

Table 1 *Biological activity of* a*-factor-like peptides*[a]

Peptide or culture supernatant	Halo diameter (mm)	ED_{50}[b]
MATa supernatant	9.0	–
MATa supernatant + KOH/NH_2OH	0	–
YIIGVFWDPACVIA	0	1.25
YIIGVFWDPACVIA(amide)	0	1.25
YIIGVFWDPAC(palmitoyl)VIA[c]	0	0.31
YIIGVFWDPAC(palmitoyl)VIA[c] + KOH/NH_2OH	0	1.25
YIIGVFWDPA	0	5.00

[a] *S. cerevisiae* RC757 (*MATα*, *sst1-2*) was grown at 30°C on YEPD agar as a lawn and synthetic peptides or culture supernatant from a *MATa* strain were added as discrete spots. After 48 h the halo-indicating growth inhibition was measured.
[b] μg of peptide causing 50% decrease in *a*-factor activity as judged by halo assay.
[c] YIIGVFWDPACVIA treated with palmitoyl chloride.

hydroxylamine hydrolysis indicates that modification occurs on cysteine by formation of a thioester linkage.

When the *MATa* culture supernatant is treated with alkaline hydroxylamine, biological activity disappears. This result is consistent with the findings on the palmitoylated pentadecapeptide and suggests that the active *a*-factor contains a labile linkage. The *a*-factor activity passed through a G-25 column with the void volume. This would not be expected for a small peptide; however, if this peptide were to aggregate into a micelle, it would exhibit physical properties of a much larger molecule.

There are no previous reports in the literature of synthetic peptides which antagonize *a*-factor activity. Since our dodeca- and pentapeptides are sequences coded for by the *a*-factor structural genes, we believe that the biologically active pheromone is a small peptide with a sequence close to that of our synthetic analogs. The lability of the natural *a*-factor in the presence of hydroxylamine and the increased antagonism exhibited by the palmitoylated pentadecapeptide lead us to conclude that this pheromone is acylated on cysteine and thus contains a thioester linkage. Fatty acylation of proteins on cysteine linkages has recently been implicated in the export of these molecules from the cytoplasm to the cell membrane [7]. Thus fatty acylation of the *a*-factor might play a role in the secretion of this putative lipopeptide by the yeast.

Acknowledgements

This work was supported by Public Health Service grants NIH GM-22087 and NIH GM-22086.

References

1. Stephens, K., CRC Crit. Rev. Microbiol., 13 (1985) 309.
2. Gooday, G.W., Ann. Rev. Biochem., 43 (1974) 35.
3. Naider, F. and Becker, J.M., CRC Crit. Rev. Biochem., 21 (1986) 225.
4. Betz, R., Manney, T.R. and Duntze, W., Gamete Res., 4 (1981) 571.
5. Betz, R., Crabb, J.W., Meyer, H.E., Wittig, R. and Duntze, W., J. Biol. Chem., 262 (1987) 546.
6. Brake, A.J., Brenner, C., Najarian, R., Laybourne, P. and Merryweather, J., In Gething, M.J. (Ed.) Protein Transport and Secretion, Cold Spring Harbor Laboratory, Cold Spring Harbor, NY, 1985, p. 103.
7. Fujiyama, A. and Tamanoi, F., Proc. Natl. Acad. Sci. U.S.A., 83 (1986) 1266.

Receptor-selective somatostatin (SRIF) analogs

D.H. Coy[a], M.L. Heiman[a], J. Rossowski[a], W.A. Murphy[a], J.E. Taylor[b], S. Moreau[b] and J.-P. Moreau[b]

[a]Peptide Research Laboratories, Department of Medicine, Tulane University School of Medicine, New Orleans, LA 70112, U.S.A.
[b]Biomeasure, Inc., Hopkinton, MA 01748, U.S.A.

Introduction

Since there is some evidence for multiple SRIF receptors with differing recognition requirements, membrane binding assays were established for rat pituitary, brain frontal cortex, adrenal cortex, and pancreas using [^{125}I-Tyr-11]-SRIF (Amersham) as the labeled ligand. Many types of SRIF peptides and analogs were examined, ranging from the 28-residue SRIF precursor through 14- and 12-residue peptides to the SMS-201-995 octapeptide [1], H-D-Phe-Cys-Phe-D-Trp-Lys-Thr-Cys-Thr-ol, several of its longer-acting analogs [2, 3], and hexapeptides, such as cyclo (N-Me-Ala-Tyr-D-Trp-Lys-Val-Phe) [4]. A list of some of the analogs examined and their code numbers are given in Table 1.

Results and Discussion

For SRIF ring sizes greater than 8, receptor assays of this type did not reveal [5] significant differences between binding to brain and pituitary receptors. SMS-201-995 octapeptide, however, had considerably less affinity for brain receptors. This trend continued in the present work on the amidated octapeptides 1 through 3 (Table 2), all of which had significantly less affinity for cerebral cortex. A sudden and dramatic loss of binding affinity for brain receptors was observed

Table 1 *Structures of somatostatin analogs tested*[a]

1.	D-Phe-Cys-Phe-D-Trp-Lys-Thr-Cys-Thr-NH_2
2.	D-Phe-Cys-Tyr-D-Trp-Lys-Val-Cys-Thr-NH_2
3.	D-Cpa-Cys-Tyr-D-Trp-Lys-Val-Cys-Thr-NH_2
4.	D-Nal-Cys-Tyr-D-Trp-Lys-Val-Cys-Thr-NH_2
5.	D-Nal-Cys-Tyr-D-Trp-Lys-Abu-Cys-Thr-NH_2
6.	D-Phe-Cys-Tyr-D-Trp-Lys-Val-Cys-Nal-NH_2
7.	Cyclo(N-Me-Ala-Tyr-D-Trp-Lys-Abu-Phe)

[a] Cys-containing peptides were in the oxidized form. Cpa = 4-Cl-phenylalanine, Nal = β-naphthylalanine, Abu = α-aminobutyric acid.

Table 2 *In vitro analog inhibition of [^{125}I-Tyr]-SRIF-14 binding to four rat tissue types*

Peptide[a]	IC_{50} (nM)			
	Pancreas	Anterior pituitary	Adrenal cortex	Cerebral cortex
SRIF	0.37	0.91	0.27	0.53
1	0.62	0.76	0.27	4.2
2	0.38	0.16	0.35	5.8
3	0.21	1.7	0.33	5.5
4	0.39	1.2	0.26	>1000
5	0.72	1.1	0.24	>1000
6	0.01	3.9	0.02	>1000
7	–	0.23	–	0.22

[a] See Table 1.

for the D-Nal-containing analog 4. This peptide maintained its affinity for pancreas, pituitary and adrenal receptors but was devoid also of affinity for gastric mucosal receptors (J. Rossowski, manuscript in preparation), indicating similarities between these and those in the brain. The biologically active ^{125}I-labeled version of this octapeptide also failed to bind specifically to either brain or gastric mucosa, but did bind to the other tissue preparations and thus appears to be a useful specific probe for SRIF receptor types.

The octapeptide 6, containing L-Nal at its C-terminus, also completely dissociated pituitary and brain binding. In addition, however, it had extremely high affinity for pancreatic and adrenal receptors relative to its pituitary affinity and relative to the other analogs tested. It is possible that this could be due to preference for yet another subset of SRIF receptors. The hexapeptide analog 7 is representative of another major class of potent SRIF analogs. It showed equal affinity for both brain and pituitary receptors and, in preliminary experiments, for pancreatic and adrenal tissue as well.

These new octapeptide SRIFs are thus becoming useful tools for delineating the various classes of SRIF receptors and are additionally valuable therapeutically since, as well as being considerably longer acting, they should have fewer central and gastrointestinal side effects than initial members of the series or the hexapeptide series.

Acknowledgements

This research was supported in part by NIH grant DK-18370.

References

1. Bauer, W., Briner, U., Doepfner, W., Haller, R., Huguenin, R., Marbach, P., Petcher, T.J. and Pless, J., Life Sci., 31 (1982) 1133.
2. Murphy, W.A., Heiman, M.L., Lance, V.A., Mezo, I. and Coy, D.H., Biochem. Biophys. Res. Commun., 132 (1985) 922.
3. Murphy, W.A., Lance, V.A., Moreau, S., Moreau, J.-P. and Coy, D.H., Life Sci., (1987) in press.
4. Veber, D.F., Saperstein, R., Nutt, R.F., Freidinger, R.M., Brady, S.F., Curley, P., Perlow, D.S., Paleveda, W.J., Colton, C.D., Zacchei, A.G., Tocco, D.J., Hoff, D.R., Vandlen, R.L., Gerich, J.E., Hall, L., Mandarino, L., Cordes, E.H., Anderson, P.S. and Hirschmann, R., Life Sci., 34 (1984) 1371.
5. Heiman, M.L., Murphy, W.A. and Coy, D.H., Neuroendocrinology, 45 (1987) 429.

Synthesis and biological activity of novel linear and cyclic GRF analogs

Arthur M. Felix, Ching-Tso Wang, Edgar Heimer, Alain Fournier, David R. Bolin, Mushtaq Ahmad, Theodore Lambros, Thomas Mowles and Lindy Miller

Peptide and Animal Science Research Departments, Roche Research Center, Hoffmann-La Roche Inc., Nutley, NJ 07110, U.S.A.

Introduction

Structure-activity studies with hypothalamic growth hormone-releasing factor (GRF) analogs have established that the 29 amino acids at the NH_2-terminus are required for the full intrinsic activity in vitro. Conformational analysis of GRF(1–29)-NH_2 using two-dimensional NMR reveals two regions of α-helical character, between residues 6–13 and 16–29 [1]. Synthetic analogs of GRF, having increased biological potencies, were designed in which Gly^{15} was replaced by Ala in order to extend the α-helical region and maximize amphiphilic α-helical structure. Other structural modifications including multiple replacement analogs were designed to optimize the biological potency of GRF. In addition, cyclic analogs of [Ala^{15}]-GRF(1–29)-NH_2 were prepared in an attempt to enhance the short half-life (6.8 min) reported for GRF(1–44)-NH_2.

Results and Discussion

Solid phase synthesis of short segments of cyclic peptides have been reported using N^{α}-Fmoc amino acids with Boc/*tert*-butyl side-chain protection for Lys and Glu [2]. Since side-chain to side-chain cyclization by this method is often sluggish, and may lead to significant amounts of cyclic dimer, an alternate method for the solid phase cyclization was designed using BOP reagent which has been shown to be ideally suited for solid phase peptide synthesis (Fournier et al., manuscript submitted for publication). Figure 1 outlines a strategy for a synthesis which includes the use of N^{α}-Boc-amino acids with Fmoc/OFm side-chain protection for Lys/Asp. The cyclization using BOP was complete in 2 h and compared favorably to the DCC/HOBt cyclization which was only approximately 30% complete in 18 h.

Analogs of GRF(1–29)-NH_2 with increased biological activity (rat pituitary bioassay) were obtained when Gly^{15} was replaced by Ala^{15} or other helix-forming hydrophobic amino acids (Table 1). The resultant structure–activity relationships

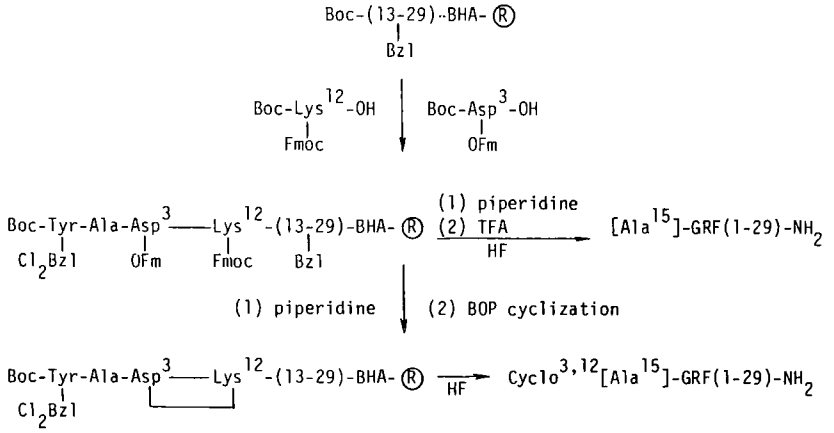

Fig. 1. Synthesis of [Ala[15]]-GRF(1–29)-NH$_2$ and Cyclo[3,12]-[Ala[15]]-GRF(1–29)-NH$_2$.

are attributed to increased α-helicity and maximization of amphiphilic structure. This was confirmed by circular dichroism studies in 75% methanol which reveal high levels of α-helicity for [Ala^{15}]-GRF(1–29)-NH$_2$. Replacement by Sar^{15}, which disrupts secondary conformation, resulted in almost complete loss of potency and a substantial decrease in α-helicity (Fig. 2). Cyclo^{3,12}-[Ala^{15}]-GRF(1–29)-NH$_2$ was inactive in the in vitro static and perifusion bioassays and had no GH-releasing activity in vivo in bovines. Linear analogs of GRF(1–29)-NH$_2$ with replacement of Tyr^1 by *des*NH$_2$-Tyr^1 or incorporation of D-Ala^2 resulted

Table 1 *Relative potencies of GRF analogs*

	Relative potency (in vitro bioassay)
GRF(1–44)-NH$_2$	1.0
GRF(1–29)-NH$_2$	0.8
[Ala^{15}]-GRF(1–29)-NH$_2$	4.0
[Aib^{15}]-GRF(1–29)-NH$_2$	3.7
[β-Ala^{15}]-GRF(1–29)-NH$_2$	5.6
[Sar^{15}]-GRF(1–29)-NH$_2$	0.04
Cyclo^{3,12}[Ala^{15}]-GRF(1–29)-NH$_2$	0.07
[*des*NH$_2$-Tyr^1]-GRF(1–29)-NH$_2$	2.5
[D-Ala^2]-GRF(1–29)-NH$_2$	1.6
[D-Ala^2,Ala^{15}]-GRF(1–29)-NH$_2$	4.97
[*des*NH$_2$-Tyr^1,Ala^{15}]-GRF(1–29)-NH$_2$	7.67

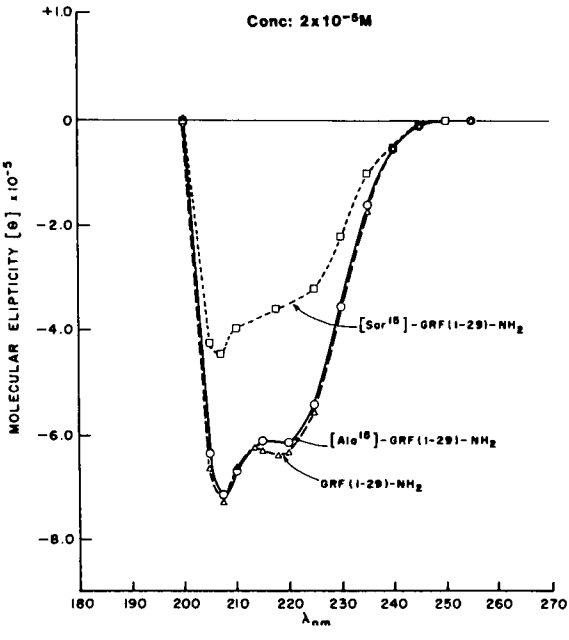

Fig. 2. Circular dichroism in 75% methanol (pH 7.4).

in increased biological activity as a result of enhanced stability of the NH_2-terminus to enzymatic degradation. The potencies of multiple replacement analogs were measured in vitro and found to have additive effects. Therefore, [*des*NH_2-Tyr[1], Ala[15]]-GRF(1–29)-NH_2 increased in potency (in vitro) to 7.67 times that of the parent compound and was found to have markedly enhanced GH-releasing activity in vivo in pigs. These multiple replacement analogs are being tested in performance enhancement trials.

References

1. Clore, G.M., Martin, S.R. and Gronenborn, A.M., J. Mol. Biol., 191 (1986) 553.
2. Schiller, P.W., Nguyen, T.M.-D. and Miller, J., Int. J. Pept. Prot. Res., 25 (1985) 171.

Weak oxytocin agonist converted to highly potent oxytocin antagonist through bicyclization

Patricia S. Hill[a], Jirina Slaninova[b] and Victor J. Hruby[a]

[a]Department of Chemistry, University of Arizona, Tucson, AZ 85721, U.S.A.
[b]Institute of Organic Chemistry and Biochemistry, Czechoslovak Academy of Sciences, 166 10 Prague 6, Czechoslovakia

Introduction

The use of conformational constraints on small peptide hormones has often led to interesting biological activity. Biophysical studies of the neurohypophyseal hormone oxytocin (H-Cys-Tyr-Ile-Gln-Asn-Cys-Pro-Leu-Gly-NH_2) and several of its agonist and antagonist analogs have led to proposed models for oxytocin–uterine receptor interaction [1–4]. The 'dynamic model' emphasizes the importance of conformational flexibility for agonist activity and relative conformational rigidity and steric effects for antagonism [3, 4]. Recently the flexibility of the potent oxytocin agonist deamino-oxytocin has been demonstrated in the crystalline state [5]. Extensive biophysical studies of a number of 1-penicillamine-containing oxytocin antagonists have indicated increased rigidity of both the peptide backbone and several amino acid side-chain groups [6]. These results and other considerations have led us to examine possibilities for further conformational constraints.

Results and Discussion

We hypothesized that suitable side-chain-to-side-chain cyclization between the amino acids in the 8- and 4-positions of deamino-oxytocin might be compatible with a strong hormone–receptor interaction. Therefore we prepared the bicyclic analog of deamino-oxytocin by lactam bond formation between the Glu^4 and Lys^8 side chains of the very weak monocyclic analog [β-Mpa^1, Glu^4, Cys^6, Lys^8]oxytocin (I). The bicyclic analog, [β-Mpa^1, Glu^4, Cys^6, Lys^8]oxytocin (II), was found to have potent antagonist activity.

Synthesis was accomplished by the solid phase method on a *p*-methylbenzhydrylamine (MBHA) resin. The peptide was cleaved from the resin and deprotected using anhydrous hydrofluoric acid. After disulfide bond formation, the monocyclic precursor peptide was purified and the bicyclic analog was formed from the monocyclic precursor using diphenylphosphorylazide (DPPA) in dilute

Table 1 *Biological activities of oxytocin and its analogs*

Compound	Rat uterotonic (IU/mg)
Oxytocin	546
[β-Mpa^1]oxytocin (deamino-oxytocin)	803
[Glu^4]oxytocin	1.5
[Lys^8]oxytocin	80
[Mpa^1, Glu^4, Cys^6, Lys^8]oxytocin (I)	0.4 ± 0.2
[Mpa^1, Glu^4, Cys^6, Lys^8]oxytocin (II)	$pA_2 = 8.2 \pm 0.2$
[Pen^1]oxytocin	$pA_2 = 6.86$

dimethylformamide. [β-Mpa^1, Glu^4, Cys^6, Lys^8]oxytocin was purified by gel filtration followed by reversed-phase high pressure liquid chromatography (RPHPLC). The purity and identity of both the monocyclic precursor and bicyclic oxytocin peptides were checked by RPHPLC, thin-layer chromatography in three solvent systems, amino acid analysis, and fast atom bombardment mass spectrometry.

The biological activities of I and II were examined using the classical in vitro rat uterus assay [7, 8] and compared with the native hormone, [β-Mpa^1]oxytocin (deamino-oxytocin), [Glu^4]oxytocin, [Lys^8]oxytocin and the antagonist analog [Pen^1]oxytocin (Table 1). The monocyclic precursor (I) had about 1/1400th the potency of oxytocin and 1/2000th that of deamino-oxytocin in the oxytocic assay. [β-Mpa^1, Glu^4, Cys^6, Lys^8]oxytocin, the bicyclic analog, however, was found to be among the most potent oxytocin antagonist analogs for the oxytocin receptor known, with a pA_2 value of 8.2. Preliminary proton nuclear magnetic resonance spectroscopy studies, including extensive temperature dependence studies, indicate increased rigidity in the bicyclic peptide which is not seen in the monocyclic precursor peptide. These results are consistent with the dynamic model of hormone action [3, 4]. Further biophysical studies comparing the conformational and dynamic properties of the bicyclic oxytocin analog with its monocyclic precursor and deamino-oxytocin are currently underway.

Acknowledgements

This work was supported by grants from the U.S. Public Health Service AM 17420 and the National Science Foundation.

References

1. Walter, R., Schwartz, F.L., Darnell, J.H. and Urry, D.W., Proc. Natl. Acad. Sci. U.S.A., 68 (1971) 1355.
2. Walter, R., Fed. Proc., 36 (1977) 1972.

3. Meraldi, J.P., Hruby, V.J. and Brewster, A.I.R., Proc. Natl. Acad. Sci. U.S.A., 74 (1977) 1373.
4. Hruby, V., In Everle, A., Geiger, R. and Wieland, T. (Eds.) Perspectives in Peptide Chemistry, S. Karger, Basel, 1981, pp. 207-220.
5. Wood, S.P., Tickle, I.J., Treharne, A.M., Pitts, J.E., Mascarenhas, Y., Li, J.Y., Husain, J., Cooper, S., Blundell, T.L., Hruby, V.J., Buku, A., Fishman, A.J. and Wyssbrod, H.R., Science, 232 (1986) 633.
6. Hruby, V.J. and Lebl, M., In Jost, K., Lebl, M. and Brtnik, F. (Eds.) Handbook of Neurohypophyseal Hormone Analogs, Vol. 1, CRC Press, Boca Raton, FL, 1987, pp. 105-155.
7. Holton, P., Brit. J. Pharmacol., 3 (1948) 328.
8. Munsick, R.A., Endocrinology, 66 (1960) 451.

Synthesis and biological activity of dicarba analogs of vasopressin antagonists

James F. Callahan[a], William F. Huffman[a], Michael L. Moore[a], Nelson C.F. Yim[a], Heidemarie G. Bryan[a], Kenneth A. Newlander[a], Victoria W. Magaard[a], Frans Stassen[b], Lewis Kinter[b], George Dytko[b], Christine Albrightson[b], Bridget Brickson[b], Nancy Caldwell[b], Grace Heckman[b] and Dulcie Schmidt[b]

[a]Department of Peptide Chemistry and [b]Departments of Pharmacology and Molecular Pharmacology, Smith Kline & French Laboratories, King of Prussia, PA 19406-0939, U.S.A.

Introduction

The disulfide bridge in vasopressin agonists can be replaced with a dicarba bridge with retention of agonist potency at the V_2-receptor [1, 2]. Considering the previously documented differences in the agonist and antagonist pharmacophores [3], it was not possible to predict the outcome of a similar replacement in a vasopressin antagonist. We therefore replaced the disulfide bridge between the Pmp^1 and Cys^6 in a represented vasopressin antagonist with a dicarba bridge and determined the effect on V_2-antagonist potency.

Results and Discussion

In order to replace the disulfide bridge in a Pmp-containing antagonist, we needed first to develop a synthesis of the unusual amino acid, 6,6-pentamethylene-2-aminosuberic acid (Pas), which incorporates the dicarba bridge. The synthesis of the appropriately protected Boc-D,L-Pas(OBn) **1** is detailed in Scheme 1. The dicarba antagonists **2** and **3** were synthesized using the solid phase method with the inclusion of the amino acid **1** as the third residue. After the final amino acid was coupled, the peptide was removed from the resin and the side chains deprotected by treatment with HF/anisole. Cyclization between the side chain of Pas and N-terminus with DPPA and TEA in DMF gave the peptide antagonists **2** and **3** which were separated by preparative reversed-phase HPLC (5μ ultrasphere ODS). The chirality of the Pas residue in **2** and **3** was determined by chiral gas-chromatographic analysis of the N-PFP, isopropyl ester derivative of the peptide hydrolysate using a Chirasil-Val III (Alltech) column. A sample of derivatized optically pure D-Pas was obtained from the action of L-amino oxidase on D,L-Pas amino acid and was used as an internal standard (D isomer eluting before L).

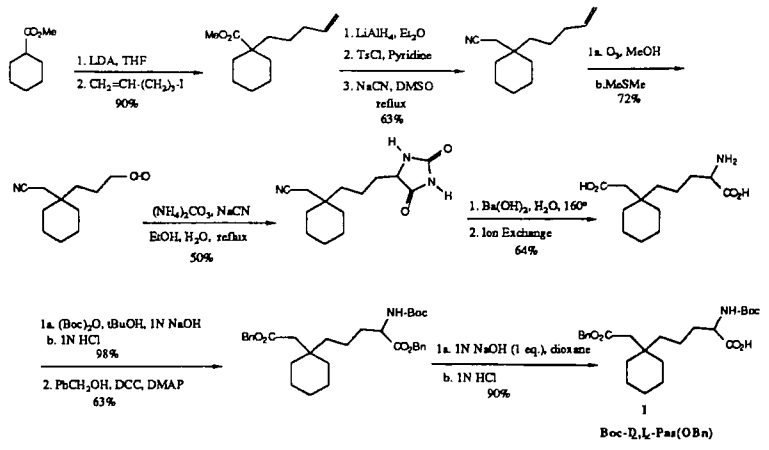

Scheme 1. Synthesis of Boc-D,L-Pas(OBn)

Both analogs **2** and **3** were shown to be antagonists of vasopressin at the V_2-receptor. The potency of the L-Pas analog **2** is similar to that observed for the analogous disulfide-containing antagonist (Table 1). In addition, the dicarba analog **2** also showed decreased partial agonist activity relative to **4** in an indomethacin pretreated dog model (C. Albrightson et al., manuscript submitted for publication).

We have shown that the disulfide can be replaced by a dicarba bridge without loss of potency at the V_2-receptor. The decrease of partial agonist activity in

Table 1 *Biological activity of dicarba vasopressin antagonists*

X-D-Tyr(Et)-Phe-Val-Asn-Y-Pro-Arg-NH_2

Compound	X	Y	Swine		Human	Rat
			K_{bind}[a] (nM)	K_i[b] (nM)	K_i[c] (nM)	ED_{300}[d] (μ/kg)
2	L-Pas		7.0(2)	3.5(3)	2.4(5)	16.2(4)
3	D-Pas		72	NT	10	30.8
4	Pmp	L-Cys	12 (9)	3.9(8)	3.6(17)	15.5(10)

[a] Binding affinity to pig renal medullary membrane preparation measured by competition with tritiated LVP.
[b] Inhibition of LVP-sensitive adenylate cyclase in pig renal medullary preparation.
[c] Inhibition of LVP-sensitive adenylate cyclase in human renal medullary preparation.
[d] Dose required to lower urine osmolality to 300 mOsm/kg H_2O in hydropenic rat.

the dicarba analog **2** indicates that there is a difference in the pharmacophore presentation of the dicarba- and disulfide-containing analogs.

References

1. Hase, S., Sakakibara, S., Wahrenburg, M., Kirchberger, M., Schwartz, I.L. and Walter, R., J. Am. Chem. Soc., 94 (1972) 3590.
2. Hechter, O., Terada, S., Spitsberg, V., Nakahara, T., Nakagawa, S. and Flouret, G., J. Biol. Chem., 253 (1978) 3230.
3. Moore, M.L., Greene, H., Huffman, W.F., Stassen, F., Stefankiewicz, J., Sulat, L., Heckman, G., Schmidt, D., Kinter, L., McDonald, J. and Ashton-Shue, D., Int. J. Pept. Prot. Res., 28 (1986) 379.

Renin inhibitors based on novel dipeptide analogs: Increased efficacy through systematic inclusion of polar functionality

Dale J. Kempf*, Ed de Lara, Jacob J. Plattner, Herman H. Stein, Jerome Cohen and Hollis D. Kleinert

Cardiovascular Research Division, Abbott Laboratories, Abbott Park, IL 60064, U.S.A.

Introduction

The poor oral bioavailability of many renin inhibitors may be due in part to low solubility in aqueous solutions. Since the primary recognition sites for renin are lipophilic in nature, the development of inhibitors incorporating polar functionality which retain high inhibitory potency poses a significant challenge. The use of polar groups at the C-terminus of a series of statine-based inhibitors to improve aqueous solubility has recently been reported [1]. We present here a systematic study of the effect of charged functionality at the N-terminus of a novel series of renin inhibitors [2].

Results and Discussion

At the outset, we felt that if the charged groups could be separated from the lipophilic recognition sites by a sufficient distance, inhibitory potency would not be dramatically affected. In order to establish an optimum separation, monoprotected ω-amino acids and ω-diacids of systematically varied length were incorporated at the N-terminus of a neutral renin inhibitor [2]. Removal of the protecting groups gave positively charged inhibitors **1–6** and negatively charged inhibitors **7–10**.

As illustrated in Table 1, the potency of charged inhibitors is dramatically dependent on the length of the alkyl chain. Thus, while the glycine derivative **1** is only moderately potent, extending the chain length to compounds **5** and **6** results in activity which matches that of prototype inhibitor **11**. Similarly, negatively charged **10** matches neutral **12**. These results suggest that no binding occurs between the enzyme and the charged moiety of either **6** or **10**. Rather, there appears to be an undefined lipophilic pocket at the P_4 site which is surpassed when the alkyl tether is greater than 4 carbons.

* To whom correspondence should be addressed.

Table 1 *Inhibition of renin by N-terminally charged compounds*

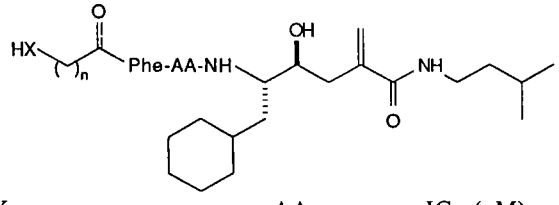

Cmpd. No.	X	n	AA	IC_{50} (nM)	% MAP[a]
1	NH	1	His	40	
2	NH	2	His	25	
3	NH	3	His	8.5	
4	NH	4	His	5.5	
5	NH	5	His	2.5	33 ± 10%
6	NH	6	His	2.2	
7	OOC	1	Leu	120	
8	OOC	2	Leu	20	
9	OOC	3	Leu	6	
10	OOC	4	Leu	3	
11		Boc-Phe-His-NHR		2.1	76 ± 8%
12		Boc-Phe-Leu-NHR		3	

[a] Mean arterial pressure expressed as % of control (78 ± 2 mm Hg) at point of maximum fall after 0.3 mg/kg bolus injection (n = 2). Reflex tachycardia was observed in those animals who had a rapid and marked fall in blood pressure.

The effect of i.v. administration of compounds **5** and **11** to salt-depleted cynomolgus monkeys is also shown in Table 1. While **11** gave moderate, short-lasting hypotensive effects, administration of **5** led to a greater than 60% fall in pressure which did not return to control levels within 60 min.

The results shown here demonstrate that renin inhibitors with increased polarity can be obtained without sacrificing inhibitory potency by incorporating charged functionality at the N-terminus. The resulting charged inhibitors show enhanced efficacy after i.v. administration. Attempts to utilize these concepts for the development of orally active renin inhibitors are in progress.

References

1. Bock, M.G., DiPardo, R.M., Evans, B.E., Freidinger, R.M., Whitter, W.L., Payne, L.S., Boger, J., Ulm, E.H., Blaine, E.H. and Veber, D.F., In Deber, C.M., Hruby, V.J. and Kopple, K.D. (Eds.) Peptides: Structure and Function, Proceedings of the 9th American Peptide Symposium, Pierce Chemical Co., Rockford, IL, 1986, p. 751.
2. Kempf, D.J., de Lara, E., Plattner, J.J., Stein, H., Cohen, J., Perun, T.J., In Abstracts of the 191st Meeting of the American Chemical Society, New York, NY, April, 1986, MEDI 10.

Tyrosine alone exhibits opiate-like activity when linked to an amphipathic hydrocarbon chain

M. Abu Khaled[a,b,*], G.M. Anantharamaiah[c], John M. Beaton[b,d] and Charles L. Watkins[e]

[a]Nutrition Sciences, [b]Neuropsychiatry Research Program, [c]Medicine and Atherosclerosis Research Unit, [d]Psychiatry and [e]Chemistry, University of Alabama at Birmingham, University Station, Birmingham, AL 35294, U.S.A.

Since the discovery of the smallest endogenous opioid peptides [Leu^5] and [Met^5] enkephalins in the brain [1], an extensive effort has been made to establish their structure–activity relationships[2]. From these studies, it appears that tyrosine at position 1 is essential; a slight alteration, even in its aromatic side chain, drastically reduces the biological activity of enkephalins [3]. Since the recent findings of the three main opioid receptor subtypes in the brain [4], namely, μ, δ, and κ, there have been tremendous efforts to design and synthesize peptides in order to understand the structural requirements for these receptor sites. For example, Deek et al. [5] synthesized 2 enkephalin analogs with restricted Tyr^1 side chains. They are: [2-amino-5-hydroxy-2-indanyl)carbonyl]- and [2-amino-6-hydroxy-2-indanyl)carbonyl]Gly-Gly-Phe-Leu-OMe. The former, with a severely restricted Tyr ^{1} side chain, was found to be virtually inactive whereas the latter, with a less restricted Tyr^1 side chain, showed 7–8 times more specificity for the μ-receptor as compared to [Leu^5] enkephalin. These results are compatible with the prediction of Horn and Rodgers [6] that the N-terminus of enkephalins may be serving the same role as found in several narcotics. Based on the above findings, we therefore hypothesize that tyrosine alone may exhibit opioid activity if appropriately transported to the receptor site(s). In order to prove our hypothesis we synthesized the following small molecules: (i) Tyr-D-Lys; (ii) Tyr-$NH(CH_2)_6$-NH_2; (iii) Tyr-$NH(CH_2)_{12}$-NH_2; and (iv) Tyr-$NH(CH_2)_{16}$-CH_3. These compounds were purified and characterized by TLC and NMR. The aliphatic hydrocarbon chain was chosen in order to have efficient lipid penetrability for crossing the blood–brain barrier and to avoid any complication arising from backbone conformational heterogeneity. Compound iv in this series is not soluble in water and, therefore, has not been tested.

Initially, the flinch-jump method employing a group of 6 rats was used for behavioral testing. All the compounds were dissolved in water and injected

*To whom correspondence should be addressed.

subcutaneously immediately prior to testing. Morphine was used for comparison. Five trials of an ascending, followed by a descending, series of 0.75-s foot shocks, delivered at 15-s intervals, were carried out. The initial shock was 0.05 mA and was altered in 0.05 mA increments, a maximum of 2.5 mA. The flinch and jump thresholds were noted. The trials were repeated at 10-min intervals. The results from the flinch-jump method indicated that all synthesized compounds have analgesic properties, but compound iii (i.e., Tyr-NH$(CH_2)_{12}$-NH_2, which is hereafter designated as T_{12}) showed better and longer lasting analgesia at a dose of 4 mg/kg. The analgesia induced by T_{12} was completely reversible by naloxone.

Further tests were carried out using only T_{12} in groups of 10 mice. In the writhing tests using phenyl-*p*-quinone in 5% aqueous ethanol, T_{12} also showed naloxone-reversible, analgesic properties. Subsequent tail-flick tests also showed the naloxone-reversible analgesic properties of T_{12}. A preliminary study to assess the receptor binding properties of T_{12} was performed by using rat brain cell membrane preparations. [^{3}H]Naloxone was used to assess the effective binding of T_{12} at the μ-receptor site as compared to morphine. The results were that T_{12} is 60% as potent as morphine. Binding of T_{12} to the δ and κ receptor sub types has not yet been completed; however, the overall results from flinch-jump, writhing, tail-flick, and rat brain cell membrane preparations support our hypothesis that tyrosine alone has opiate-like activity when appropriately transported to receptor site(s).

In an effort to compare the side-chain conformations (χ_1^1) of tyrosine in T_{12} and in [Leu^5] enkephalin, we performed 300 MHz ^{1}H NMR experiments at room temperature. The β-CH_2 protons of tyrosine of T_{12} in water (D_2O) appeared as an ABX pattern giving $^3J_{AX}=6.1$ Hz and $^3J_{BX}=9.0$ Hz, while in methanol (CD_3OD) they were A_2X giving a coupling value of 7.0 Hz. [Leu^5] enkephalin, on the other hand, showed the opposite behavior for the Tyr β-CH_2 protons. That is, in D_2O they were A_2X with $^3J_{AX}=7.0$ Hz while in CD_3OD they appeared as ABX, giving $^3J_{AX}=6.6$ Hz and $^3J_{BX}=7.9$ Hz. Following Feeney's method for determining side-chain conformations [7], both in terms of rotamer population and angle χ_1^1, it appears that the tyrosine side chain of T_{12} in aqueous medium is somewhat restricted, whereas in nonaqueous medium it rotates freely. The opposite is true for [Leu^5] enkephalin. Until each of the two β-CH_2 protons is assigned, no definite value for χ_1^1 can be determined. Once the receptor binding work is completed, and the χ_1^1 value of tyrosine has been determined by the selective deuteration of the Tyr β-CH_2 protons, it may then be possible to correlate side-chain conformation with receptor site selectivity.

References

1. Hughes, J., Smith, T.W., Kosterlitz, H.W., Fothergill, L.A., Morgan, B.A. and Morris, H.R., Nature, 258 (1975) 557.
2. Udenfriend, S. and Meienhofer, J., The Peptides: Analysis, Synthesis and Biology, Vol. 6, Academic Press, New York, NY, 1984.
3. Morley, J.S., Ann. Rev. Pharmacol. Toxicol., 20 (1980) 91.
4. Goodman, R.R. and Pasternak, G.W., In Kuhar, M. and Pasternak, G.W. (Eds.) Analgesics: Neurochemical, Behavioral and Clinical Perspective, Raven Press, New York, NY, 1904, p. 69.
5. Deek, T., Crooks, P.A. and Waigh, R.O., J. Med. Chem., 26 (1983) 762.
6. Horn, A.S. and Rodgers, J.R., Nature, 260 (1976) 795.
7. Feeney, J., J. Magn. Reson., 21 (1976) 473.

Functional residues in atriopeptin(103–125)-amide

Yasuo Konishi, Ronald B. Frazier, Gillian M. Olins, Delores J. Blehm, Foe S. Tjoeng, Mark E. Zupec and Deborah E. Whipple
Monsanto Co., 700 Chesterfield Village Parkway, St. Louis, MO 63198, U.S.A.

Abstract

A simple strategy to identify the functional residues in peptides was developed, which states that if a side chain in a peptide is functional, then removal of the side chain (the substitution for a residue with glycine) will drastically affect the function of the peptide.

This strategy was examined for atriopeptin(103–125)-amide using a rabbit aorta relaxation assay. The results showed 3 residues essential for function, i.e., Cys105-Cys121, Phe106, and Ile113, and 5 moderately functional residues, i.e., Arg109, Ile110, Arg112, Ser117, and Leu119. The results also indicated that the active conformation of the peptide was an α-helix at Arg109-Ile113 and an extended structure at Gln116-Gly120.

Strategy of Glycine Substitution

The net effect of a side chain on a peptide's function can be estimated by removing the side chain, viz., the substitution for a residue with glycine. On the other hand, if a backbone conformation available to glycine, but not to other side-chain types, is required for function, the residue must be glycine and be functional. The test for functionality of glycine is to add the smallest restrictive side chain, viz., alanine and assay for functionality.

Results and Discussion

The results of glycine substitution (Fig. 1) clearly identified 3 residues essential for function. The removal of each side chain of these residues reduced the activity of the peptide 500-, 500-, or 800-fold for Cys105-Cys121, Phe106, or Ile113, respectively. Figure 1 also shows 5 moderately functional residues. The removal of each side chain of these residues reduced the activity of the peptide 10-, 20-, 60-, 10-, or 40-fold for Arg109, Ile110, Arg112, Ser117, or Leu119, respectively. These 8 functional residues consitute two functional sites — [Phe106-Cys105-Cys121-Gly120-Leu119-Gly118-Ser117-Gln116] and [Arg109-Ile110-

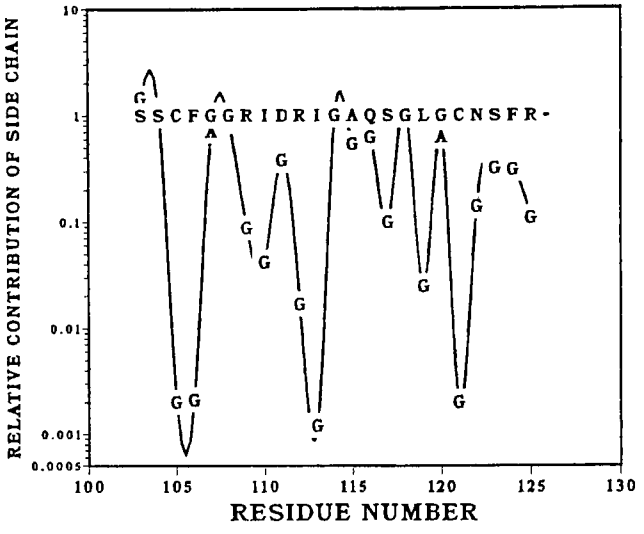

Fig. 1. The relative potency of the atriopeptin(103–125)-amide analogs with glycine substitution in the rabbit aorta assay. On the X-axis is the residue number, which was substituted by glycine, or alanine if the residue is already glycine, one residue at a time. On the Y-axis is the relative potency of the analogs against atriopeptin(103-125)-amide. For example, the substitution of Ile113 with Gly decreased the relative activity of the peptide to 0.0012 (800-fold decrease).

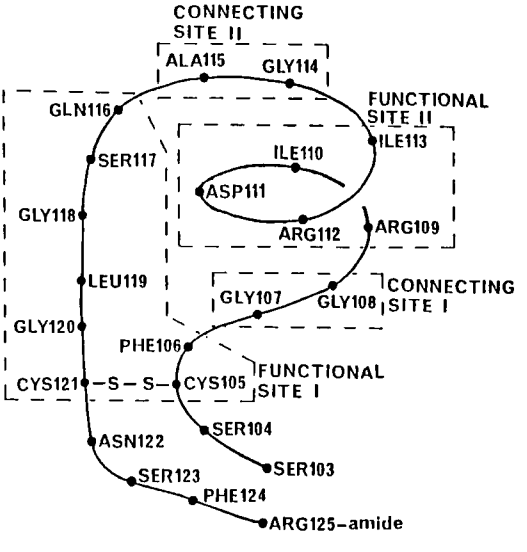

Fig. 2. A schematic sketch of the active conformation of atriopeptin (103-125)-amide.

Asp111-Arg112-Ile113] — where the residues with underline are functional. Interestingly, these two sites are connected by flexible small amino acids, Gly107-Gly108 and Gly114-Ala115.

The active conformation of the functional site, Arg109-Ile113, is suggested to be an α-helix, in which the functional residues cluster on one side of the helix and the nonfunctional residue, Asp111, localizes on the other side of the helix. The receptor may bind around Ile113 and interact with the functional residues through the hydrophobic interactions. The receptor may also position a negative charge between Arg109 and Arg112 to neutralize charge repulsion and stabilize the helix. Similarly, the active conformation of the region, Ser117-Gly120, may be an extended structure. The side chains of the functional residues, Leu119 and Ser117, can form a hydrophobic core with Phe106. The proposed active conformation of the peptide is schematically shown in Fig. 2.

Acknowledgements

We acknowledge M.G. Jennings for amino acid analysis and P. Toren and H. Fujiwara for mass spectroscopy. We also acknowledge S.T. Nugent for providing his data and G.I. Glover, J.J. Likos and C.A. McWherter for their useful discussions.

Tachykinin receptors

S. Lavielle[a], G. Chassaing[a], J. Besseyre[a], S. Julien[a], D. Loeuillet[a], A. Marquet[a], J.C. Beaujouan[b], L. Bergström[b], Y. Torrens[b] and J. Glowinski[b]

[a]CNRS UA 493, Paris VI, Tour 44-45 (3ème), 4, Place Jussieu, 75005 Paris, France
[b]INSERM U 114, Collège de France, 11, Place M. Berthelot, 75005 Paris, France

Three tachykinins and three subtypes of tachykinin receptors have been identified in mammals:

Peptides	*Receptors*	*Sequences*
Substance P (SP)	NK1	Arg-Pro-Lys-Pro-Gln-Gln-Phe-Phe-Gly-Leu-Met-NH_2
Neurokinin A (NKA)	NK2	His-Lys-Thr-Asp-Ser-Phe-Val-Gly-Leu-Met-NH_2
Neurokinin B (NKB)	NK3	Asp-Met-His-Asp-Phe-Phe-Val-Gly-Leu-Met-NH_2

In order to increase the selectivity of a highly potent cyclic analog of SP, [$Cys^{3,6}$, Tyr^8] SP [1], designed on the basis of NMR data [2], deletion in the N-terminal sequence and conformational constraints in the C-terminal region were performed. The deletion of Arg-Pro decreased the potency for the NK1 binding site on both SP(3–11) and [$Cys^{3,6}$, Tyr^8] SP(3–11), but [$Cys^{3,6}$, Tyr^8] SP(3–11) is 40 times more potent than SP(3–11) on the NK3 site. The con-

Table 1 *Binding and biological potencies of tachykinins and SP analogs*

Peptides	NK1 [3] IC_{50} (nM)	NK2 IC_{50} (nM)	NK3 [4] IC_{50} (nM)	GPI ED_{50} (nM)
SP	0.64	206	130	2.0
NKA	140	7.4	100	5.3
NKB	2,200	33	5.1	2.2
[$Cys^{3,6}$,Tyr^8] SP	0.42	955	3.0	2.2
SP(3–11)	7	160	470	2.1
[$Cys^{3,6}$,Tyr^8] SP(3–11)	8	$> 10^4$	16	3.5
[Sar^9] SP	3.1	2,900	110	2.4
[Me Leu^{10}] SP	7.4	$> 10^4$	370	2.0
[Me Met^{11}] SP	5.5	4,900	1,700	3.5
[Pro^9] SP	2.9	$> 10^4$	$> 10^4$	2.5
[Pro^{10}] SP	14	$> 10^4$	$> 10^4$	2.9
[Pro^{11}] SP	420	$> 10^4$	6,000	25
[$Cys^{3,6}$,Tyr^8,Pro^9] SP	3.1	$> 10^4$	970	2.1
[$Cys^{3,6}$,Tyr^8,Pro^{10}] SP	5.1	9,200	1,600	2.3

formational constraints (*N*-methyl amino acids, proline residues) introduced in positions 9, 10 and 11 increased the selectivity for the NK1 site. [$Cys^{3,6}$, Tyr^{8}, Pro^{9}] SP and [$Cys^{3,6}$, Tyr^{8}, Pro^{10}] SP are potent cyclic analogs as selective as SP, i.e. 200–300 times more active on the NK1 than the NK3 sites.

Collectively, these results suggest that the recognizing mechanisms of linear and cyclic analogs of SP must be similar for the NK1 binding sites and different for the NK3 binding sites.

References

1. Lavielle, S., Chassaing, G., Besseyre, J., Marquet, A., Bergström, L., Beaujouan, J.-C, Torrens, Y. and Glowinski, J., Eur. J. Pharmacol., 128 (1986) 283.
2. Chassaing, G., Convert, O. and Lavielle, S., Eur. J. Biochem., 154 (1986) 77.
3. Viger, A., Beaujouan, J.-C., Torrens, Y. and Glowinski, J., Neurochemistry, 40 (1983) 1030.
4. Beaujouan, J.-C., Torrens, Y., Viger, A. and Glowinski, J., Mol. Pharmacol., 26 (1984) 248.

Growth hormone-releasing factor analogs with potent antagonist activity

Nicholas Ling, Kazuki Sato, Mari Hotta, Teh-Chang Chiang, Hsiau-Yu Hu and Ming-Hui Dong

Laboratories for Neuroendocrinology, The Salk Institute, 10010 N. Torrey Pines Road, La Jolla, Ca 92037, U.S.A.

Introduction

Specific antagonists of human growth hormone-releasing factor (hGRF) are essential for the study of its mechanism of action and may also be important in clinical application for disorders of growth hormone secretion or diabetic retinopathy. Recently, we reported that [Asn^3, Leu^6, Val^7]hGRF(1–27)NH_2 showed antagonistic activity in the rat anterior pituitary cell culture assay [1]. However, this analog also retained partial agonistic activity. Substitution at the 2nd position of hGRF with D-alanine has been shown to increase the potency of the GRF molecule [2]. In addition, Robbrecht et al. reported that [Ac-Tyr^1,D-Arg^2]hGRF(1–29)NH_2 was able to antagonize the GRF activation of the adenylate cyclase on the plasma membrane [3]. Because of these findings, the 2nd residue of hGRF seems to be a good candidate for further investigation. For this purpose, we have synthesized a series of hGRF(1–29)NH_2 analogs which contained D-Ala, D-Ser, D-Leu, D-Phe, D-His, D-Glu, D-Lys, and D-Arg at the 2nd position and also several analogs modified at other positions.

Results and Discussion

The GRF analogs were synthesized by solid phase methodology as described previously [4] and characterized by amino acid analysis and RPHPLC. The capacity of these analogs to release growth hormone (GH) was tested in an in vitro assay using rat anterior pituitary cells [5].

In the series of analogs with single D-amino acid substitution at the 2nd position, only [D-Arg^2]hGRF(1–29)NH_2 showed significant antagonistic activity (Table 1). [L-Arg^2]hGRF(1–29)NH_2 did not show such activity, implicating the importance of the D-configuration for the arginine residue. Similar replacement of the 4th-position alanine to give [D-Arg^4]hGRF(1–29)NH_2 resulted in weak agonistic activity only.

Table 1 *Biological activity of GRF analogs in vitro*

	Relative potencies	Antagonistic activity[a]
hGRF(1–29)NH_2	1	–
[D-Ala^2]hGRF(1–29)NH_2	1.31 (0.809–2.060)[b]	–
[D-Ser^2]hGRF(1–29)NH_2	0.16 (0.106–0.237)[b]	–
[D-Leu^2]hGRF(1–29)NH_2	0.009 (0.004–0.017)[b]	–
[D-Phe^2]hGRF(1–29)NH_2	0.20×10^{-3}	–
[D-His^2]hGRF(1–29)NH_2	0.97×10^{-4}	–
[D-Glu^2]hGRF(1–29)NH_2	0.32×10^{-4}	–
[D-Lys^2]hGRF(1–29)NH_2	0.32×10^{-5}	–
[D-Arg^2]hGRF(1–29)NH_2	–	++
[L-Arg^2]hGRF(1–29)NH_2	0.77×10^{-4}	–
[D-Arg^2]hGRF(1–29)NH_2	0.54×10^{-4}	–
[Ac-Tyr^1,D-Arg^2]hGRF(1–29)NH_2	–	++
[Arg^1,D-Arg^2]hGRF(1–29)NH_2	–	+
[D-Arg^{2,29},Tyr^{30}]hGRF(1–30)NH_2	–	++
[D-Arg^{2,29},Arg^{30}]hGRF(1–30)NH_2	–	++
[D-Arg^2]rGRF(1–29)NH_2	–	++
[D-Arg^2,Ala^{15}]rGRF(1–29)NH_2	–	++

[a] – no antagonistic activity, + moderate antagonistic activity, ++ significant antagonistic activity.
[b] 95% confidence limit.

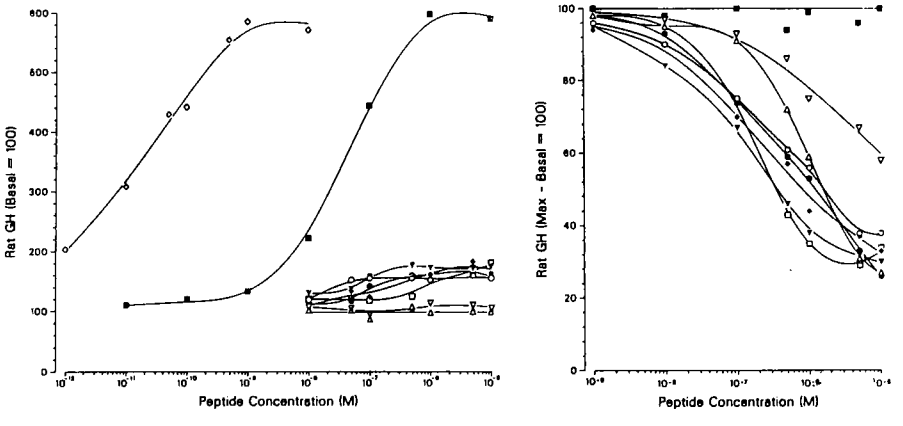

Fig. 1. Relative agonistic activity of GRF analogs compared to hGRF(1–29)NH_2 in vitro (left) and inhibition by GRF analogs on GH secretion stimulated by 10^{-9} M hGRF(1–44)NH_2 in vitro (right).
◇, hGRF(1–29)NH_2; ○, [D-Arg^2]hGRF(1–29)NH_2; △, [Ac-Tyr^1,D-Arg^2]hGRF(1–29)NH_2; ▽, [Arg^1, D-Arg^2]hGRF(1–29)NH_2; ◆, [D-Arg^{2,29},Tyr^{30}]hGRF(1–30)NH_2; ▼, [D-Arg^{2,29},Arg^{30}]hGRF(1–30)NH_2; ●, [D-Arg^2]rGRF(1–29)NH_2; □, [D-Arg^2,Ala^{15}]rGRF(1–29)NH_2; ■, [D-Arg^4]hGRF(1–29)NH_2.

In order to improve the antagonistic activity of [D-Arg^2]hGRF(1–29)NH_2, we synthesized several analogs with additional substitutions (Fig. 1). N-terminal acetylation resulted in an analog with decreased affinity to the GRF receptor, but suppression of the GH secretion was improved at higher doses. Increase of basicity at the N-terminal region gave a weaker antagonist [Arg^1,D-Arg^2]hGRF(1–29)NH_2. Two analogs, [D-Arg^{2,29},Tyr^{30}]- and [D-Arg^{2,29},Arg^{30}]-hGRF(1–30)NH_2, showed improved affinity and maximal suppression.

Since rat GRF (rGRF) was more potent than hGRF in our in vitro bioassay, we also synthesized [D-Arg^2]rGRF(1–29)NH_2; however, its antagonistic potency was not better than [D-Arg^2]rGRF(1–29)NH_2. [D-Arg^2,Ala^{15}]rGRF(1–29)NH_2 was synthesized based on the result that [Ala^{15}]hGRF(1–27)NH_2 was more potent than hGRF(1–27)NH_2 [1]. It showed considerable improvement of antagonistic activity over the [D-Arg^2]hGRF(1–29)NH_2.

The ideal antagonist should retain high affinity to the receptor but with no intrinsic activity. In the series of antagonistic analogs (Fig. 1), most of the compounds other than [Ac-Tyr^1,D-Arg^2]- and [Arg^1,D-Arg^2]hGRF(1–29)NH_2 still showed weak agonistic activity (10–20% of hGRF). It seems that modification at the N-terminal residue is required to suppress this agonistic activity, whereas modification at the 15th position is required to increase the affinity of the peptide for the receptor.

Acknowledgements

We thank M. Regno, R. Schroeder, D. Angeles, V. Bonora, and C. Wong for excellent technical assistance. The research was supported by National Institutes of Health grants (HD-09690 and AM-18811) and the Robert J. and Helen C. Kleberg Foundation.

References

1. Ling, N., Baird, A., Wehrenberg, W.B., Munegumi, T. and Ueno, N., In Joyeaux, A., Leygue, G., Morre, M., Roncucci, R. and Schmelck, P.H. (Eds.) Quo Vadis, Sanofi Recherche, Montpellier, 1986, p. 309.
2. Lance, V.A., Murphy, W.A., Sueiras-Diaz, J. and Coy, D.H., Biochem. Biophys. Res. Commun., 119 (1984) 265.
3. Robbrecht, P., Coy, D.H., Waelbroeck, M., Heiman, M.L., Neef, P., Camus, J.-C., and Chrisophe, J., Endocrinology, 117 (1985) 1759.
4. Ling, N., Esch, F., Böhlen, P., Brazeau, P., Wehrenberg, W.B. and Guillemin, R., Proc. Natl. Acad. Sci. U.S.A., 81 (1984) 4302.
5. Brazeau, P., Ling, N., Böhlen, P., Esch, F., Ying, S.-Y. and Guillemin, R., Proc. Natl. Acad. Sci. U.S.A., 79 (1982) 7909.

Transition-state analog inhibitors of human renin

Jay R. Luly, Anthony K.L. Fung, Jacob J. Plattner, Patrick A. Marcotte, Nwe BaMaung, Jeffrey L. Soderquist and Herman H. Stein
Abbott Laboratories, Cardiovascular Research Division, Abbott Park, IL 60064, U.S.A.

Introduction

Recently, we reported the synthesis of renin inhibitor **4d** which incorporated a novel amino diol as its transition-state analog binding element [1]. Although **4d** had subnanomolar binding potency and high selectivity toward renin, we found the Phe-His amide bond to be quite unstable in a chymotrypsin incubation assay. This report details recent efforts directed at the chemical stabilization of this class of inhibitors and the effects of these chemical changes on binding potency.

Results and Discussion

The amino diol fragment was prepared as shown in Fig. 1. The most efficacious diol, **3**, was isolated by flash chromatography in 20% yield from **1** [1]. Deprotection with HCl/dioxane provided the amine salt which was coupled with the appropriate dipeptide (mixed anhydride) to give inhibitors **5**. Alternatively, coupling with Boc-His (DCC/HOBT), deprotection, and coupling with the appropriate protected amino acid [2] gave inhibitors **4** and **6**. Inhibitors **5d** and **4e** were prepared in an analogous fashion using the corresponding *N*-methyl diol (derived from lithium aluminium hydride reduction of **3**) or *N*-Tos, N_{im}Bn-MeHis, respectively. The inhibitors were then evaluated in a purified renin binding assay (pH 7.0) and in a chymotrypsin incubation assay under previously described conditions [3].

Parent compounds **4a** and **4d** were found to be rapidly cleaved at the Phe-His bond. C- or N-methylation of Phe (**4b**, **4c**) resulted in stabilization of the bond, but at the expense of binding potency, whereas N-methylation of His (**4e**) or replacing Phe with 4-(OCH_3)Phe (**4f**) provided stability with minimal effect on potency. In the corresponding Phe-Leu series (**5**), the 4-(OCH_3)Phe analog (**5e**) was equipotent to the parent, and the (*N*-methyl)Leu, D-Leu, or amino diol inhibitors (**5b**, **5c**, or **5d**) were less potent. Stability of the Leu-containing analogs could not be determined due to limited solubility. Analogs **6a–e** which contain constraints from either N or C_α to the phenyl ring of **4d**

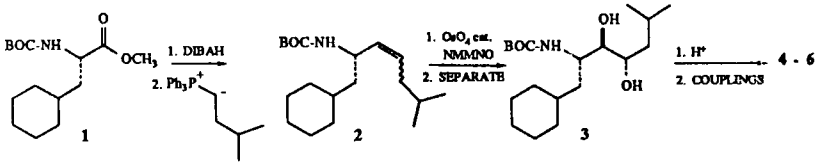

	A	R_1	R_2	R_3	R_4	X	IC_{50}, nM	Chymotrypsin Stability*
4a	Ac	H	H	H	H	H	0.75	t 1/2=1.2 min
4b	Ac	H	CH3	H	H	H	15	STABLE
4c	Ac	CH3	H	H	H	H	10	STABLE
4d	Etoc	H	H	H	H	H	0.5	t 1/2=2.8 min
4e	Etoc	H	H	CH3	H	H	2	STABLE
4f	Etoc	H	H	H	H	OCH3	1.5	STABLE
5a	Etoc	H	H	H	H	H	0.3	-----
5b	Etoc	H	H	CH3	H	H	8	-----
5c	Etoc	H	H	CH3	H	H	5800**	-----
5d	Etoc	H	H	H	CH3	H	15	-----
5e	Etoc	H	H	H	H	OCH3	0.2	-----
6a							100	***
6b							10	STABLE
6c							6	STABLE
6d							15	STABLE
6e							300	STABLE

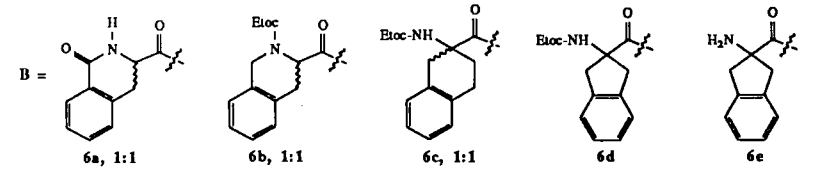

Fig. 1. Inhibitor synthesis and biological data.
** 'Stable' means less than 20% degradation over a 6-h incubation.*
*** D-Leu isomer.*
****40% degradation over a 6-h incubation.*

were found to be less potent, but quite stable. In summary, a number of modifications have been introduced into members of a novel class of renin inhibitors which render them stable to chymotrypsin. Of these changes, N-methylation of His or introduction of a 4-(OCH_3) substituent on Phe effectively preserve potency.

References

1. Luly, J.R., Soderquist, J.L., Yi, N., Perun, T.J., Kleinert, H.D., Stein, H. and Plattner, J.J., In Abstracts 192nd Meeting of the American Chemical Society, Denver, CO, April 5–10, 1987; MEDI 81.
2. (a) The N-terminal amino acids of **6c** and **6d** were prepared by a modification of a literature procedure: Pinder, R.M., Butcher, B.H., Buxton, D.A. and Howells, O.J., J. Med. Chem., 14(1971)892. (b) That of **4b** [Bollinger, F.W., J. Med. Chem., 14(1971)373] was coupled via its 5(4*H*)-oxazolone. (c) For a synthesis of **6a**, see Hein, G.E. and Niemann, C., J. Am. Chem. Soc., 84(1962)4487.
3. Luly, J.R., Plattner, J.J., Stein, H., Yi, N., Soderquist, J., Marcotte, P.A., Kleinert, H.D. and Perun, T.J., Biochem. Biophys. Res. Comm., 143(1987)44.

Peptidyl amino steroids as potential new antiarrhythmic agents

Michael Mokotoff[a], Ming Zhao[a], Qing-Jiang Liao[c], Lan K. Wong[a], William Barrington[b] and James Elson[b]

[a]Department of Pharmaceutical Sciences, School of Pharmacy and [b]Department of Medicine, School of Medicine, University of Pittsburgh, Pittsburgh, PA 15261, U.S.A.
[c]Pharmaceutical University of China, Nanjing, PR China

Introduction

Ventricular fibrillation, a major complication of acute myocardial infarction, is responsible for many of the sudden deaths occurring in the early prehospital phase [1]. In spite of the several antiarrhythmic drugs available to the clinician, there is still a need for an effective and safe long-term drug. A few years ago, Organon Labs discovered that some aminosteroids had antidysrhythmic properties. In particular one compound, Amefalone (Am), was developed to the stage of clinical testing and was shown to be an active antiarrhythmic agent when administered by the i.v. route. Pharmacological work, however, predicted a much lower level of activity following oral administration, and that, along with other reasons, led Organon to discontinue work on Am. Because of our continuing interest in peptides as potential therapeutic agents, we began a study aimed at preparing peptidyl derivatives of Am as potential prodrugs.

Results and Discussion

It was our intention to modify the 3-amino function of Am by coupling it to amino acids and peptides, thereby protecting the primary amine and thus altering the normal metabolic pathway that presumably leads to its inactivation. Initially, we chose amino acids which we would expect to be readily hydrolyzed by peptidases (Gly, Ala) or more resistant (Pro, D-Ala).

For several years we have been preparing peptides by the use of novel polymeric reagents such as PHBT [2, 3]. For the Gly series of compounds (Scheme 1), Boc-Gly was first esterified to PHBT using DIC and the resulting Boc-Gly-PHBT allowed to react with Am, affording Boc-Gly-Am in an 86% yield. The corresponding dipeptide derivatives were prepared by removal of the Boc group (TFA) from Boc-Gly-Am followed by reaction with either Boc-Ala-PHBT or its corresponding enantiomer, Boc-D-Ala-PHBT. The resulting dipeptides Boc-

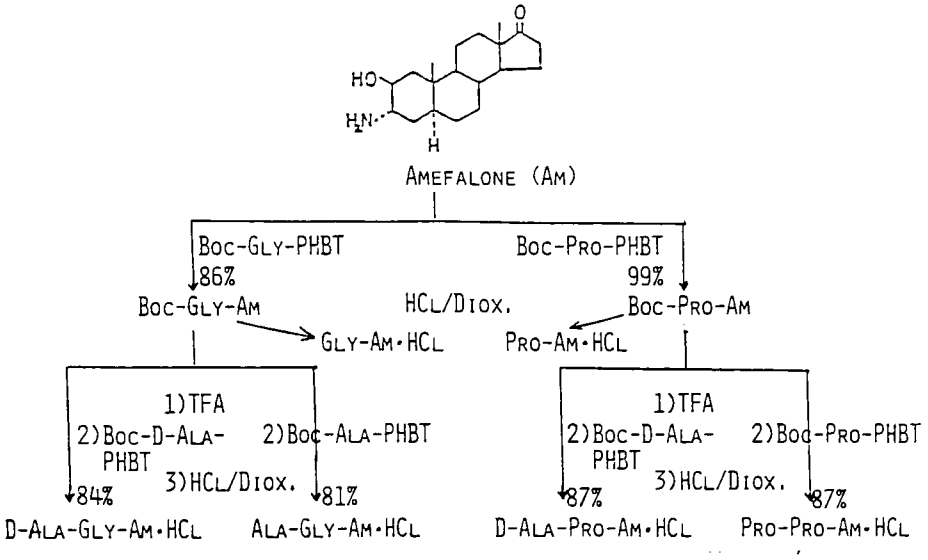

Scheme 1. Flow scheme for synthesis of peptidyl amefalone compounds.

Ala-Gly-Am and Boc-D-Ala-Gly-Am were than converted to their HCl salts in overall yields, for the three steps, of 81 and 83%, respectively. Similarly, Am was reacted with Boc-Pro-PHBT and gave Boc-Pro-Amefalone in nearly quantitative yield. Removal of the Boc group, condensation with Boc-Pro-PHBT and Boc-D-Ala-PHBT, followed by deblocking with HCl/dioxane afforded Pro-Pro-Am HCl and D-Ala-Pro-Am HCl in 87% yields (for the three steps).

Well-established antiarrhythmic drugs such as quinidine have been shown to increase action potential duration (APD) and effective refractory period (ERP) in a manner that increases the ERP/APD ratio. The clinical effect of this change decreases the period of time within the cardiac cycle when arrhythmias can be established and, furthermore, decreases the ease with which a preexisting arrhythmia can be maintained. In the past, these measurements have been made with single microelectrodes on an isolated muscle strip. In our laboratory, we have been using voltage-sensitive dyes to stain intact, beating, perfused guinea pig hearts and to simultaneously measure optical action potentials (APs) from 124 sites on the epicardium [4]. Using this technique, we have tested Am·HCl, Gly-Am·HCl, and all four dipeptide-Am hydrochlorides for their antiarrhythmic effects. Both Am·HCl and Gly-Am·HCl show desired results of increased ERP and ERP/APD ratios at concentrations as low as 0.00003 μmol/l up to the maximum concentration tested of 0.03 μmol/l. The dipeptide derivatives required a much higher concentration of drug; the minimum effective concentration being 0.01 μmol/l. Ala-Gly-Am, D-Ala-Gly-Am, and D-Ala-Pro-Am hydrochlorides

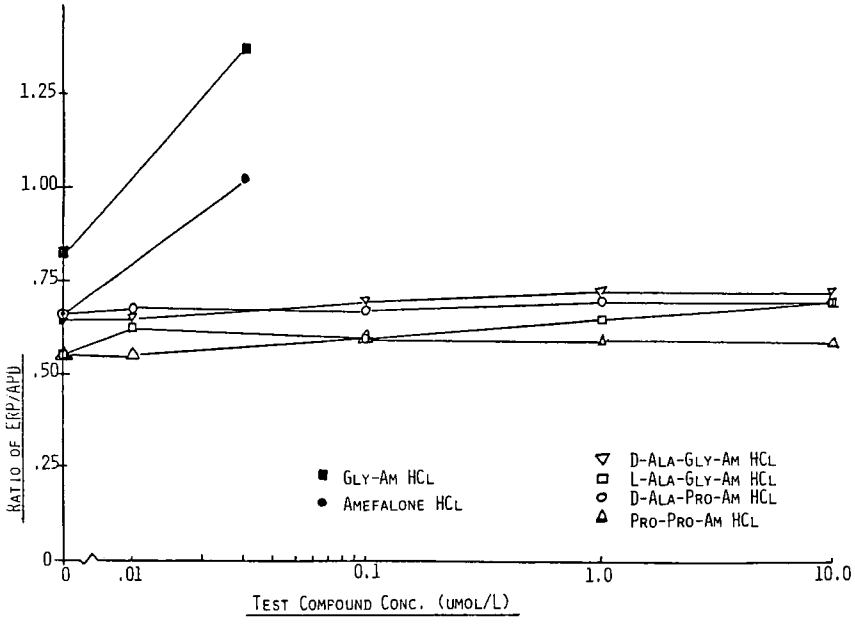

Fig. 1. Comparison of the ratio ERP/APD for all compounds tested.

showed desirable effects with some increase in APD, ERP and the ERP/APD ratio; however, these increases were all less than noted with either Am·HCl or Gly-Am·HCL (see Fig. 1).

Conclusions

All the compounds tested, with the exception of Pro-Pro-Am·HCl, changed the action potential in a manner analogous to quinidine, a well-established antiarrhythmic drug. The dipeptidyl-Am compounds require a higher concentration for the effects to be seen and appear (in these preliminary tests) to produce a smaller magnitude of change than either Am or Gly-Am hydrochlorides. Presently, all these compounds are being tested in an in vivo assay, but the results are not yet available. Since these compounds were designed as prodrugs, it is expected that the dipeptide-Am compounds will, in vivo, be hydrolyzed at different rates to free Am, and will prove to have useful antiarrhythmic properties.

References

1. Marshall, R.J. and Winslow, E., Gen. Pharmacol., 12 (1981) 315.
2. Mokotoff, M. and Patchornik, A., Int. J. Pept. Prot. Res., 21 (1983) 145.
3. Sheh, L., Mokotoff, M. and Abraham, D.J., Int. J. Pept. Prot. Res., 29 (1987) 509.
4. Salama, G., Lombardi, R. and Elson, J., Am. J. Physiol., 252 (1987) H384.

Contribution of residues B26-B30 to the receptor binding affinities of insulin analogs modified at position A1, A21 or B24

Satoe H. Nakagawa and Howard S. Tager

Department of Biochemistry and Molecular Biology, The University of Chicago, 920 East 58th Street, Chicago, IL 60637, U.S.A.

Previous studies [1] have demonstrated that (a) the truncated insulin analog *des*pentapeptide(B26-30)-[Phe^{B25}-α-carboxamide]insulin (DPI-NH_2) possesses full receptor binding affinity and (b) truncated analogs of insulin-containing substitutions of nonaromatic amino acid residues for Phe^{B25} exhibit substantially higher receptor binding affinities than the corresponding full length analogs containing identical amino acid replacements. For example, [Ser^{B25}]- and [Leu^{B25}]insulin have receptor binding affinities approximately 1% of that of natural hormone, whereas the corresponding truncated analogs have the potencies of 45% and 13%, respectively [1]. Thus, while the C-terminal pentapeptide of the insulin B-chain is not necessary for normal ligand–receptor interactions, it appears to contribute negatively to that interaction. To investigate further the importance of the C-terminal domain of the insulin B-chain in inducing conformations favorable or unfavorable for ligand binding to receptor, we synthesized and determined the receptor binding potencies of insulin analogs in which residues B26-B30 were deleted; residue Phe^{B25} was replaced by its α-carboxamide derivative; and residue A1, A21 or B24 was modified. These residues and the C-terminus of the B-chain are located in close proximity on the surface of insulin monomers as determined by studies of the crystal structure of insulin [2]. These residues are also known to be critical for the receptor binding and biological activities of the hormone from a wide variety of studies on insulin structure–activity relationships.

Truncated analogs with modifications at Gly^{A1} were obtained by (a) acylation with the acetyl group or with the *t*-butyloxycarbonyl group, (b) substitution with D-Ala or with L-Ala, (c) deletion of the amino group from Gly^{A1}, or (d) deletion of Gly^{A1}. All analogs with modifications at Gly^{A1} were derived from DPI-NH_2 by the appropriate chemical methods, involving direct acylation of Gly^{A1} or removal of Gly^{A1} by Edman degradation followed in some cases by acetylation or amino acylation. The analog with deletion of Asn^{A21} was prepared by treatment of DPI-NH_2 with carboxypeptidase A. The analogs containing

replacement of Phe^{B24} by D-Phe were prepared by semisynthesis using trypsin-assisted condensation between *des*octapeptide insulin and Gly-D-Phe-Phe-NH_2 or Gly-D-Phe-Phe-Tyr-Thr-Pro-Lys-Thr [3]. Methods for the semisynthesis of corresponding analogs containing Ser^{B25} have been described [1].

Receptor binding affinities of these analogs were assessed by competition of [(^{125}I)iodo-Tyr^{A14}]insulin binding to isolated canine hepatocytes. The potencies of the analogs relative to porcine insulin (determined by comparing the concentrations of analogs required to cause half-maximal response in binding inhibition) are as follows: porcine insulin, 100; DPI-NH_2, 100; [acetyl-Gly^{A1}]DPI-NH_2, 23; [Boc-Gly^{A1}]DPI-NH_2, 12; [D-Ala^{A1}]DPI-NH_2, 100; [L-Ala^{A1}]DPI-NH_2, 26; deamino-Gly^{A1}-DPI-NH_2, 10; *des*-Gly^{A1}-DPI-NH_2, 1.1; *des*-Asn^{A21}-DPI-NH_2, 1.6; [Ser^{B25}]insulin, 1.1; [Ser^{B25}]DPI-NH_2, 45; [D-Phe^{B24}]insulin, 170; and [D-Phe^{B24}]DPI-NH_2, 12. While the receptor binding affinities of A-chain modified analogs are comparable with the commonly obtained values for the corresponding insulin analogs with full sequences, we found that the affinity of the truncated [D-Phe^{B24}] analog is significantly decreased in comparison with the enhanced affinity (180%) of full length [D-Phe^{B24}]insulin reported by Kobayashi et al. [3]. Thus, the side chain of D-Phe in [D-Phe^{B24}]insulin apparently takes a conformation which is more favorable than that of [L-Phe^{B24}] during hormone–receptor interactions with full-length insulin, whereas the reverse is true in the corresponding truncated analog. It is the case, however, that substitutions at position B24 can induce propagated conformational change in the insulin monomer [4], and that the more favorable interactions of [D-Phe^{B24}]insulin could arise from main-chain– or side-chain–receptor contacts not actually involving the β-aromatic ring of D-Phe.

We conclude that (a) main-chain interactions involving the C-terminal domain of the B-chain and Asn^{A21} are important to maintaining effective insulin conformations even when residues B26-B30 are deleted; (b) the contribution of Gly^{A1} to insulin–receptor interactions does not depend on conformational changes involving movement of the C-terminal B-chain domain concomitant with interactions of the Phe^{B25} side chain with receptor; and (c) residues B26-B30 can play a negative role (as in B25-substituted insulins), no role (as in A1- or A21-modified insulins), or a positive role (as in [D-Phe^{B24}]insulin) in determining the affinities of insulin analogs for the hepatic insulin receptor. The variable role of residues B26-B30 probably arises from a complex interplay among each of several insulin domains during the high-affinity interactions of hormone and receptor.

References

1. Nakagawa, S.H. and Tager, H.S., J. Biol. Chem., 261 (1986) 7332.
2. Blundell, T., Dodson, G., Hodgkin, D. and Mercola, D., Adv. Protein Chem., 26 (1972) 279.
3. Kobayashi, M., Ohgaku, S., Iwasaki, M., Maegawa, H., Shigeta, Y. and Inouye, K., Biochem. Biophys. Res. Comm., 107 (1982) 329.
4. Inouye, K., Watanabe, K., Tochino, K. Kobayashi, M. and Shigeta, Y., Biopolymers, 20 (1981) 1845.

Development of selective agonists for substance P and neurokinins receptors

Guy Drapeau, Stéphane Dion, Pedro D'Orléans-Juste, Nour-Eddine Rhaleb and Domenico Regoli

Department of Pharmacology, Medical School, University of Sherbrooke, Sherbrooke, Québec, Canada J1H 5N4

Introduction

Substance P (SP), neurokinin A (NKA), and neurokinin B (NKB) are a group of related neuropeptides sharing a common C-terminal sequence: -Phe-X-Gly-Leu-Met-NH_2. Pharmacological as well as biochemical assays have revealed the existence, in mammalian tissues, of 3 receptor types for these peptides [1].

Selective pharmacological preparations containing predominantly one receptor type have been identified on the basis of the order of potency of fragments, analogs and homologs of the three neurokinins. These preparations are: the dog carotid artery (DCA), an NK-P receptor type preparation on which SP is the most potent natural agonist; the rabbit pulmonary artery (RPA), an NK-A receptor type assay sensitive to NKA; and the rat portal vein (RPV), an NK-B receptor preparation on which NKB is the most potent natural agonist.

The primary structures of the neurokinins are given below:

SP	Arg-Pro-Lys-Pro-Gln-Gln-Phe-Phe-Gly-Leu-Met-NH_2
NKA	His-Lys-Thr-Asp-Ser-Phe-Val-Gly-Leu-Met-NH_2
NKB	Asp-Met-His-Asp-Phe-Phe-Val-Gly-Leu-Met-NH_2

The naturally occurring peptides (SP, NKA and NKB), however, appear not to be selective enough for one or the other receptor type [2, 3]. For this reason, we looked for more selective agonists for each receptor. Such compounds were identified in the frame of a structure–activity study in which a large number of neurokinin derivatives and fragments were prepared, using solid phase methodology previously described [4]. All these peptides were tested in the three selective pharmacological preparations and their activities compared with the natural agonists and other selective agonists.

Table 1 *Biological activities of substance P and neurokinins related peptides*

Peptide	Preparation Receptor type	DCA NK-P RA	RPA NK-A RA	RPV NK-B RA
Substance P		100	100	100
SP-OMe		40	inact.	inact.
[Sar^9,Met(O$_2$)^{11}]SP		282	inact.	inact.
Ac[Arg^6,Sar^9,Met(O$_2$)^{11}]SP(6–11)		174	inact.	inact.
Neurokinin A		25	12,303	427
NKA(4–10)		4	24,547	933
[Nle^{10}]NKA(4–10)		0.03	5,888	< 1.0
Neurokinin B		8	2,089	7,244
Senktide		0.02	21	6,166
[β-Asp^4,MePhe^7]NKB(4–10)		0.1	10	5,495
[MePhe^7]NKB		0.1	13	30,200

RA = relative affinity expressed in percent of that of SP; DCA = dog carotid artery; RPA = rabbit pulmonary artery; RPV = rat portal vein.

Results and Discussion

In Table 1 the relative affinities of all compounds are compared with that of SP in the three pharmacological preparations. All values are expressed in percentage of the activity of SP (100%). SP methyl ester, a selective NK-P receptor agonist [5], is inactive on the NK-A and NK-B receptor type preparations but maintains only 40% of the activity of SP on the NK-P receptor. Combination of Sar in position 9 and methionine sulfone in position 11, two modifications which give selectivity for the NK-P receptor [4, 6], results in a potent and selective compound, [Sar^9,Met(O$_2$)^{11}]SP, which is inactive on both NK-A and NK-B preparations and is 2.5 times more active than SP on the NK-P receptor. A hexapeptide, N-acetyl[Sar^9,Met(O$_2$)^{11}]SP(6–11), is also a potent and highly selective agonist of the NK-P receptor.

NKA is a potent agonist of the NK-A receptor, and its fragment NKA(4–10) is even more potent on this receptor. Both compounds, however, maintain a good affinity on the other two receptors. The analog [Nle^{10}]NKA(4–10), although a weaker NK-A agonist than NKA or NKA(4–10), shows good selectivity as it is less active in the NK-P receptor system and inactive in the NK-B receptor system. Further work is needed to improve its affinity.

NKB is a potent agonist on NK-B receptors, but it also is active on the other receptors, especially the NK-A type. Senktide, succinyl[Asp^6,MePhe^8]SP(6–11) [7], is selective for the NK-B receptor, and its activity can be compared with [β-Asp^4,MePhe^7]NKB(4–10). Both compounds show an affinity near that of NKB on the NK-B receptor, while having poor affinity for the NK-P and NK-A

preparations. [MePhe^7]NKB, a full chain analog, however, is the most potent agonist of the NK-B receptor; its selectivity is combined with a high affinity, more than 4 times that of NKB for the NK-B receptor. Furthermore, this compound has the advantage over NKB of being soluble in water.

Potent and selective agonists of NK-P and NK-B receptors and a promising compound for the NK-A receptor are, therefore, available to further characterize SP and neurokinins receptors.

Acknowledgements

This work has been supported by grants from the Medical Research Council of Canada and the Quebec Heart Foundation.

References

1. Regoli, D., Drapeau, G., Dion, S. and D'Orléans-Juste, P., Life Sci., 40(1987)109.
2. Regoli, D., Drapeau, G., Dion, S. and D'Orléans-Juste, P., In Henry, J.L., Couture, R., Cuello, A.C., Pelletier, G., Quirion, R. and Regoli, D. (Eds.) Substance P and Neurokinins, Montreal 1986, Springer-Verlag, New York, NY, 1987, p. 99.
3. Drapeau, G., D'Orléans-Juste, P., Dion, S., Rhaleb, N.-E., Rouissi, N.-E. and Regoli, D., Neuropeptides, 10(1987)43.
4. Drapeau, G., Rovero, P., D'Orléans-Juste, P., Dion, S., Rhaleb, N.-E. and Regoli, D., In Henry, J.L., Couture, R., Cuello, A.C., Pelletier, G., Quirion, R. and Regoli, D. (Eds.) Substance P and Neurokinins, Montreal 1986, Springer-Verlag, New York, NY, 1987, p. 132.
5. Watson, S.P., Sandberg, B.E.B., Hanley, M.R. and Iversen, L.L., Eur. J. Pharmacol. 87(1983)77.
6. Drapeau, G., D'Orléans-Juste, P., Dion, S., Rhaleb, N.-E. and Regoli, D., Eur. J. Pharmacol., 136(1987)401.
7. Wormser, V., Laufer, R., Hart, Y., Chorev, M., Gilon, C. and Selinger, Z., EMBO J., 5(1986)2805.

Novel, subnanomolar renin inhibitors containing a postscissile site azide residue

Saul H. Rosenberg, Keith W. Woods, Jacob J. Plattner, Herman H. Stein, Hollis D. Kleinert and Jerome Cohen

Cardiovascular Research Division, Abbott Laboratories, Abbott Park, IL 60064, U.S.A.

Significant progress has been made in the development of renin inhibitors [1], yet the design of an orally active inhibitor remains a challenge. One potential solution involves a reduction in the overall size of the molecule [2]. In conjunction with another study [3], we have discovered that nanomolar potency is maintained when the entire postscissile site portion of the inhibitor is replaced by an azidomethyl group which apparently mimics the lipophilic Val^{11} side chain (**5**). Herein we report a structure-activity study which has led to a small (MW < 600), subnanomolar renin inhibitor (**15**).

The synthesis of these compounds begins by condensing Boc-cyclohexylalanal with a vinyl anion equivalent as shown in Fig. 1. Further elaboration leads to fragments **4a–h** which are coupled to the appropriate N-protected dipeptides to provide inhibitors **6–16**.

The homologue of **5** (**6**) is less active than the parent (Fig. 2). Incorporation of a 2*S*-hydroxyl (**7**) increases potency 50-fold while inclusion of a 2*R*-hydroxyl

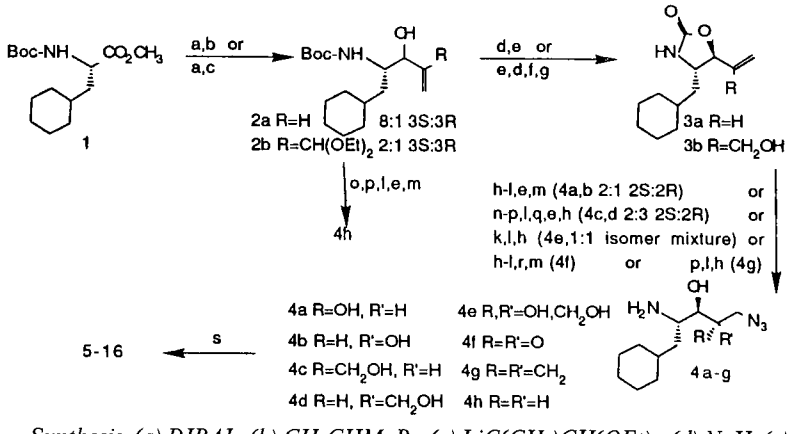

Fig. 1. Synthesis. (a) DIBAL; (b) $CH_2CHMgBr$; (c) $LiC(CH_2)CH(OEt)_2$; (d) NaH; (e) isomer separation; (f) $(HO_2C)_2$, SiO_2; (g) $NaBH_4$; (h) $Ba(OH)_2 \cdot 8H_2O$; (i) $(t\text{-}BuO_2C)_2O$; (j) Mom-Cl; (k) MCPBA; (l) NaN_3; (m) HCl; (n) TBDMSCl; (o) BH_3·THF; (p) MsCl; (q) Bu_4NF; (r) ClCOCOCl, DMSO, TEA; (s) X-AA-His-OH, HOBT, EDAC.

has little effect (**8**). This increase in potency is attributed to additional hydrogen bonding with the active site. Ketone **12** more firmly delineates the role of the 2S-hydroxyl. This compound is intermediate in activity between the parent **6** and **7**, suggesting that the second hydroxyl acts as a hydrogen bond acceptor. The loss in potency in **12** is thus due to a combination of the decreased hydrogen bonding ability of a carbonyl compared to a hydroxyl and the unfavorable geometry of an sp^2 center at this site (compare **6** and **14**). Hydroxymethyl compounds **9** and **10** are less potent than the corresponding glycols. Reintroduction of the 2-hydroxyl (**11**) increases activity but not to the original value. Replacement of the acid-labile Boc with isobutyryl gave **15** and subsequent replacement of Phe with (O-methyl)tyrosine (which stabilizes the Phe-His bond to in vitro chymotrypsin cleavage [3]) provided **16**.

Intravenous (i.v.) administration of **15** to Na-depleted monkeys resulted in a significant fall in blood pressure as illustrated in Fig. 3. Intraduodenal (i.d.) administration of **16** had similar effects, however, a comparison of i.v. and i.d. data (results not shown) suggests that the bioavailability of this inhibitor is only approximately 1%. Studies are currently underway to improve the in vivo characteristics of these and related compounds.

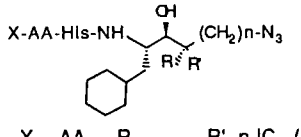

No.	X	AA	R	R'	n	IC_{50}(nM)[a]
5	Boc	Phe	H	H	0	7.5
6	Boc	Phe	H	H	1	20
7	Boc	Phe	OH	H	1	0.4
8	Boc	Phe	H	OH	1	26
9	Boc	Phe	CH_2OH	H	1	10
10	Boc	Phe	H	CH_2OH	1	370
11	Boc	Phe	CH_2OH,	OH	1	5[b]
12	Boc	Phe	O		1	5.4
14	Boc	Phe	CH_2		1	55
15	IBu[c]	Phe	OH	H	1	0.6
16	IBu	MTy[d]	OH	H	1	2

Fig. 2. In vitro activity. (a) Purified human renin, pH 6.0; (b) 1:1 isomer mixture; (c) isobutyryl; (d) (O-methyl)tyrosine.

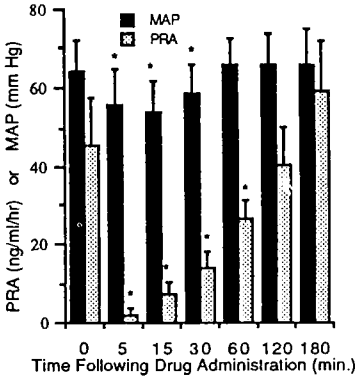

*Fig. 3. Effects of i.v. bolus injections of 15 in anesthetized, Na-depleted monkeys. * $P<0.05$ compared to time = 0; Dose: 0.1 mg/kg, i.v.; n = 4; MAP = mean arterial pressure; PRA = ng A1 generated/ml/h.*

References

1. Greenlee, W.J., Pharm. Res., in press.
2. Plattner, J.J., Greer, J., Fung, A.K.L., Stein, H., Kleinert, H.D., Sham, H.L., Smital, J.R. and Perun, T.J., Biochem. Biophys Res. Commun., 139 (1986) 982.
3. Rosenberg, S.H., Plattner, J.J., Woods, K.W., Stein, H.H., Marcotte, P.A., Cohen, J. and Perun, T.J., J. Med. Chem., 30 (1987) 1224.

Structure–activity relationships of cholecystokinin-8 analogs: Comparison of pancreatic, pyloric sphincter and brainstem CCK receptor activities with in vivo anorexigenic effects

T.K. Sawyer[a], R.T. Jensen[b], T. Moran[c], P.J.K.D. Schreur[d], D.J. Staples[a], A.E. deVaux[a] and A. Hsi[e]

[a,d]*Biopolymer and CNS Research Units, The Upjohn Company, Kalamazoo, MI 49001, U.S.A.*
[b]*Digestive Diseases Branch, National Institutes of Health, Bethesda, MD 20892, U.S.A.*
[c]*Department of Psychiatry, John Hopkins University of Medicine, Baltimore, MD 21205, U.S.A.*
[e]*Department of Chemistry, Kalamazoo College, Kalamazoo, MI 49002, U.S.A.*

Introduction

Cholecystokinin octapeptide (CCK-8, H-Asp-Tyr[SO_3H]-Met-Gly-Trp-Met-Asp-Phe-NH_2) is a neurogastric peptide hormone and neurotransmitter that possesses multiple biological activities. Specific details related to the discovery, distribution, biosynthesis, metabolism, mechanism(s) of action, and different biological effects of CCK peptides have been recently reviewed [1]. In this report, we summarize the comparative structure–activity relationships of two analogs of Ac-Asp-Tyr[SO_3H]-Nle-Gly-Trp-Nle-Asp-Phe-NH_2 (U-67827E) [2] having D-Ala or D-Trp substitutions for Gly-4 in several rat bioassay systems.

Results and Discussion

Relative to CCK-8, U-67827E was about equipotent on the pancreatic assay (Table 1); however, substitution of Gly-4 by D-Ala or D-Trp in the template of U-67827E provided congeners **1** and **2** which effected about 130- and 20-fold lower potency, respectively. In the pyloric sphincter and brainstem CCK receptor assays (Table 1), U-67827E was essentially equipotent to CCK-8; however, compounds **1** and **2** were both about 100-fold less potent than U-67827E. Based on the above results it was apparent that U-67827E was superior to derivatives **1** and **2** in the pancreas, pyloric sphincter and brainstem assays; however, the D-Trp-4 substituted compound, **2**, showed about a 10-fold greater specificity for the pancreas.

In the rat anorexigenic in vivo assay, inhibition of feeding was observed for CCK-8 in a dose–response and time-dependent manner (Table 2) in 19-

Table 1 *Comparative pancreatic, pyloric sphincter and brainstem receptor bioactivities of U-67827E analogs*[a]

Compound	EC_{50}, pancreatic amylase secretion	IC_{50}, pyloric sphincter receptor binding	IC_{50}, brainstem receptor binding
CCK-8	1.5×10^{-11} M	9.2×10^{-10} M	9.2×10^{-10} M
U-67827E	3.3×10^{-11} M	3.9×10^{-10} M	4.8×10^{-10} M
1	1.9×10^{-9} M	4.0×10^{-8} M	3.1×10^{-8} M
2	2.7×10^{-10} M	4.1×10^{-8} M	3.3×10^{-8} M

[a] Experimental methods will be published elsewhere (Sawyer et al., manuscript in preparation).

Table 2 *Comparative activities of U-67827E analogs in vivo in the rat anorexigenic assay*[a]

Compound	ED_{50} (μg/kg i.p.)	% Decrease in food consumption (10 μg/kg i.p.)		
	75 min	75 min	135 min	255 min
CCK-8	10	50	inactive	inactive
U-67827E	1	86	48	40
1	70	22	inactive	inactive
2	80	20	inactive	inactive

[a] 19-h fasted Sprague–Dawley rats (9–10/group) were injected intraperitoneally (i.p.) 15 min before powdered food was made available to them.

h food-deprived rats. U-67827E was superior (approximately 10-fold) to CCK-8, and effected significant anorexigenic activity at 4 h. Compounds **1** and **2** were similar to CCK-8 in terms of potency and duration of action. Overall, the anorexigenic activities of U-67827E and compounds **1** and **2** were relatively quite similar to the data described above for the brainstem and pyloric sphincter CCK receptor binding assays. Finally, U-67827E is the most potent CCK-8 analog which has been documented in the literature related to satiety [3], and may provide a useful molecular probe to further investigate CCK-based regulatory pathways and related neuronal and gastrointestinal functions.

References

1. Beinfeld, M.C., Neuropeptides, 3(1983)411.
2. Sawyer, T.K., Staples, D.J., Lahti, R.A., Schreur, P.J.K.D., Wilkerson, A.E., Holzgrefe, H.H. and Bunting, S., In Moody, T.W. (Ed.) Neural and Endocrine Peptides and Receptors, Plenum Publishing Corp., New York, NY, 1986, p. 541.
3. Crawley, J.N. and Beinfeld, M.C., Science, 302(1983)703.

Synthesis and activity profiles of bivalent [Leu^5]enkephalin-α-oxymorphamine hybrid opioid receptor ligands

Peter W. Schiller[a,*], Thi M.-D. Nguyen[a], Carole Lemieux[a], Dennis L. Larson[b], Guiseppe Ronsisvalle[b], Akira E. Takemori[c] and Philip S. Portoghese[b]

[a]Clinical Research Institute of Montreal, Montreal, Quebec, Canada H2W 1R7
Departments of [b]Medicinal Chemistry and [c]Pharmacology, University of Minnesota, Minneapolis, MN 55455, U.S.A.

On the basis of recent experimental evidence it has been suggested that μ- and δ-opioid receptors might coexist as distinct binding sites in an opioid receptor complex [1, 2]. Furthermore, it has been proposed that occupation of the δ-site by [Leu^5]enkephalin enhances coupling of the occupied μ-receptor to the effector system, presumably through an allosteric effect [2]. In case such a receptor complex does indeed exist, a bivalent ligand containing both a μ-selective opiate and [Leu^5]enkephalin, separated by a spacer of appropriate length, should possess activity considerably higher than the sum of the activities of each monovalent component. We, therefore, synthesized [Leu^5]enkephalin analogs containing an α-oxymorphamine (α-Oxy) moiety attached to the Glu^2 side chain either directly or via a di-glycyl spacer (Fig. 1).

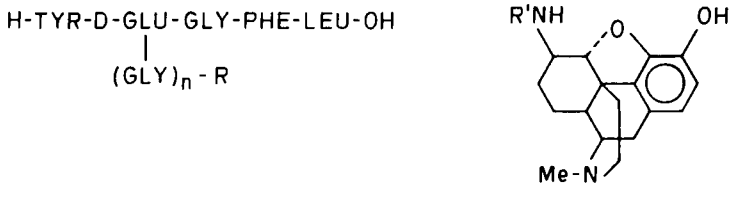

1	n = 0, R = α-Oxy	α-Oxy	R' = H
1a	n = 0, R = NH_2	1b	R' = Ac
2	n = 2, R = α-Oxy	2b	R' = Ac(GLY)$_2$
2a	n = 2, R = NH_2		

Fig. 1. Structural formulas of mono- and bivalent opioid receptor ligands.

*To whom correspondence should be addressed.

Table 1 *In vitro and in vivo opioid activities*

Compound	Binding, [^{3}H]DAGO[a]	GPI	Analgesic activity	
	K_i [nM]	IC_{50} [nM]	ED_{50} (pmol/mouse)	
1	19.1 ± 1.6	23.5 ± 0.6	0.7	(0.4 - 1.8)
1a	21.7 ± 0.5	549 ± 91	84	(64 - 114)
1b	1.81 ± 0.09	152 ± 35	5.4	(4.4 - 6.5)
2	11.1 ± 2.0	255 ± 86	5.0	(3.4 - 6.7)
2a	52.9 ± 7.7	1,050 ± 200	60	(30 - 100)
2b	5.48 ± 0.23	193 ± 20	3.1	(2.6 - 3.8)

[a] DAGO = H-Tyr-D-Ala-Gly-Phe(NMe)-Gly-Ol.

Compounds **1**, **2**, **1a** and **2a** were prepared by the solid phase method. After coupling of N$^{\alpha}$-Fmoc-D-glutamic acid -γ-*tert*-butyl ester to the resin-bound Gly-Phe-Leu segment, the D-Glu side chain was deprotected and extended by DCC couplings of α-oxymorphamine, glycine-*tert*-butyl ester or glycinamide, as necessary for the preparation of **1**, **2**, and **2a**. Subsequent Fmoc removal, followed by coupling of Boc-Tyr(OBz)-OH and HF cleavage yielded the desired products.

In the μ-receptor binding assay ([^{3}H]DAGO displacement from rat brain membranes) the bivalent ligands (**1** and **2**) showed μ-receptor affinities slightly higher than those of the monovalent enkephalin analogs (**1a** and **2a**) and significantly lower than those of the monovalent α-oxymorphamine analogs (**1b** and **2b**) (Table 1). Compared to **1** and **2**, compounds **1a** and **2a** displayed similar δ-receptor affinity, whereas binding of **1b** and **2b** to the δ-receptor was significantly weaker (data not shown). In general, the results obtained in the GPI and MVD assay were in agreement with the binding data. The exception was bivalent ligand **1** which compared to **1b** was 11 times less potent in the μ-receptor binding assay but 7 times more potent in the GPI assay. The antinociceptive potencies determined with the mouse writhing test (i.c.v. administration) were found to be in good correlation with the GPI assay data. Again, **1** showed a very significant (8-fold) potency enhancement relative to **1b**, whereas **2** and **2b** had comparable potencies. The high activity of **1** could be explained by bridging between μ- and δ-receptors, which would result in higher 'efficacy'. Alternatively, interaction of the enkephalin component in **1** with an accessory binding site in the vicinity of the μ-receptor could also be the reason for the observed efficacy enhancement.

Acknowledgements

Supported by grants from the MRCC, QHF and NIDA.

References

1. Lee, N.M. and Smith, A.P., Life Sci., 26 (1980) 1459.
2. Vaught, J.L., Rothman, R.B. and Westfall, T.C., Life Sci., 30 (1982) 1443.

Structure–function studies in a series of tachykinin antagonists containing a conformationally constrained tryptophan analog

Barry A. Morgan, Jasbir Singh*, Eugene Baizman, Harry Bentley, Doriann Keifer and Susan Ward

Sterling-Winthrop Research Institute, Rensselaer, NY 12144, U.S.A.

Introduction

We have recently reported the effects of *N*-methylation on substance P (SP) antagonist activity in a series of Pro^6, D-Trp^{7,9}SP$_{6-11}$ [1]. We now describe analogs of SP$_{6-11}$ in which a conformationally constrained tryptophan analog 2,3,4,9-tetrahydro-1H-pyrido[3,4-b]indol-3-carboxylic acid (Tpi), has been substituted for tryptophan residues. The effects of incorporation of D-Tpi at the 7 position of SP$_{6-11}$ on SP antagonist activity and antinociceptive potential was evaluated. Peptides were synthesized and tested as reported earlier [1].

Results and Discussion

We have shown that *N*-methylation of D-Trp^7 in the hexapeptide Pro^6, D-Trp^{7,9} SP$_{6-11}$ (**1**) gives rise to analog **2** (Table 1) which is a more potent antagonist

Table 1 *Pharmacology of analogs in vitro and in vivo*

Comp. No.	Structure	In vitro	In vivo		
		Guinea pig ileum pA_2 vs SP	Rotarod[b] ED_{50}	Ach writhing[b] ED_{50}	RR/Ach[c]
1	H-Pro-D-Trp-Phe-D-Trp-Leu-Met-NH_2	5.7	30	3.2	9
2	——D-Me-Trp ——	6.4	>55	0.8	>70
3	H-D-Trp ——	5.7[a]			
4	H-D-Tpi ——	6.4	>10	0.7	>14

[a] SP-like 'agonist' activity observed.
[b] Intrathecal ED_{50} μg/mouse.
[c] Ratio ED_{50}, rotarod to ED_{50}, Ach writhing.

*To whom correspondence should be addressed.

of SP than analog **1** in the guinea pig ileum assay. Elimination of proline from the N-terminus of **1** resulted in the pentapeptide **3**, which is of comparable potency to **1** as an antagonist at SP-P receptors in vitro, but which in contrast to the hexapeptide **1**, also demonstrated agonist activity in this assay. Replacement of D-Trp^7 in compound **3** by D-Tpi, a conformationally constrained analog of *N*-methyl tryptophan, however, yields pentapeptide **4** which is a more potent antagonist of SP than the hexapeptide **1**, and did not demonstrate the agonist activity shown by pentapeptide **3**.

Most SP antagonists are known to cause impairment of motor performance in the mouse, which renders the determination of antinociception unclear. Compounds **1**, **2** and **4** were assessed for effects on motor function using the rotarod (RR) test, and were also evaluated for their ability to block the nociceptive writhing response produced by intraperitoneal administration of acetylcholine (Ach) in the mouse. As shown in Table 1, analogs **1**, **2** and **4** evoked antinociception at lower doses than those which produced motor impairment, suggesting that antinociception may be independent of impairment of motor performance [2] for these compounds.

Thus incorporation of a constrained tryptophan derivative – Tpi – in the hexapeptide (**1**) resulted in a pentapeptide (**4**) which is a more potent antagonist at SP-P receptors in vitro and a more active antinociceptive agent in vivo than the hexapeptide (**1**). To our knowledge, this is the first example of a pentapeptide SP antagonist in the SP_{7-11} series. From this, we conclude that the residue at position 6 is not needed for SP-P receptor antagonist activity.

References

1. Baizman, E.R., Bentley, H., Gordon, T.D., Hansen, P.E., Kiefer, D., McKay, F.C., Perrone, M.H., Morgan, B.A., Rosi, D., Singh, J., Stevenson, J. and Ward, S.J., In Ragnarsson, U. (Ed.) Peptides, Proceedings of the 18th European Peptide Symposium, Almquist and Wiksell International, Stockholm, 1984, p. 359.
2. Rodriguez, R.E., Salt, T.E., Cahusac, P.M.B. and Hill, R.G., Neuropharmacology, 22 (1983) 173.

Potent in vivo inhibitors of rat renin

Javier Sueiras-Diaz[a], D. Michael Jones[a], D. Michael Evans[a], Michael Szelke[a], Brenda J. Leckie[b], Sheila R. Beattie[b], Elisabeth C.H. Wallace[b] and James J. Morton[b]

[a]*Ferring Research Institute, Southampton University Research Centre, Chilworth, Southampton S01 7NP, U.K.*

[b]*MRC Blood Pressure Unit, Western Infirmary, Glasgow, G11 6NT, U.K.*

Although the rat has been widely used as an experimental model in the study of hypertension, so far there have been no effective in vivo renin inhibitors available for this species. We demonstrated earlier [1] that 3-amino-deoxystatine is capable of acting as a transition state analog and produces potent in vitro inhibitors of rat renin (e.g., **2**) when inserted into the human angiotensinogen (6–13)octapeptide sequence, provided that the P_2' residue is Val rather than Ile (compare **2** with **1** in Table 1).

We have therefore investigated the insertion of Val at the P_2' position of the potent human renin inhibitor **3**. The resulting nonapeptide analog **4** exhibits an IC_{50} against rat renin [2] in the subnanomolar range. No further increase in potency is observed when the P_1' side chain is changed to that of Leu (which is the natural side chain in rat angiotensinogen) – see compound **5**.

While the 3-amino-deoxystatine compound **2** is a good inhibitor of rat renin in vitro, it completely lacks activity in vivo. In contrast, compounds **4** and **5**

Table 1 *In vitro potencies [2] of renin inhibitors **1–5***

	6 7 8 9 10 11 12 13 P_3 P_2 P_1 P_1' P_2' P_3'	IC_{50} (μM) vs Plasma renin Rat	 Human
1	Boc-His-Pro-Phe-His-Ads——Ile-His-NH_2	0.26	0.028
2	Boc-His-Pro-Phe-His-Ads——Val-Ile-His-NH_2	0.012	0.027
3	Boc-His-Pro-Phe-His-Leu$\underline{OH}$Val-Ile-His-OH	0.51	0.0007
4	Boc-His-Pro-Phe-His-Leu$\underline{OH}$Val-Val-Ile-His-NH_2	0.0008	0.008
5	Boc-His-Pro-Phe-His-Leu$\underline{OH}$Leu-Val-Ile-His-NH_2	0.0010	0.005

Ads = 3-amino-deoxystatine; $\underline{OH}$ indicates -CH(OH)-CH_2- in place of -CO-NH-.

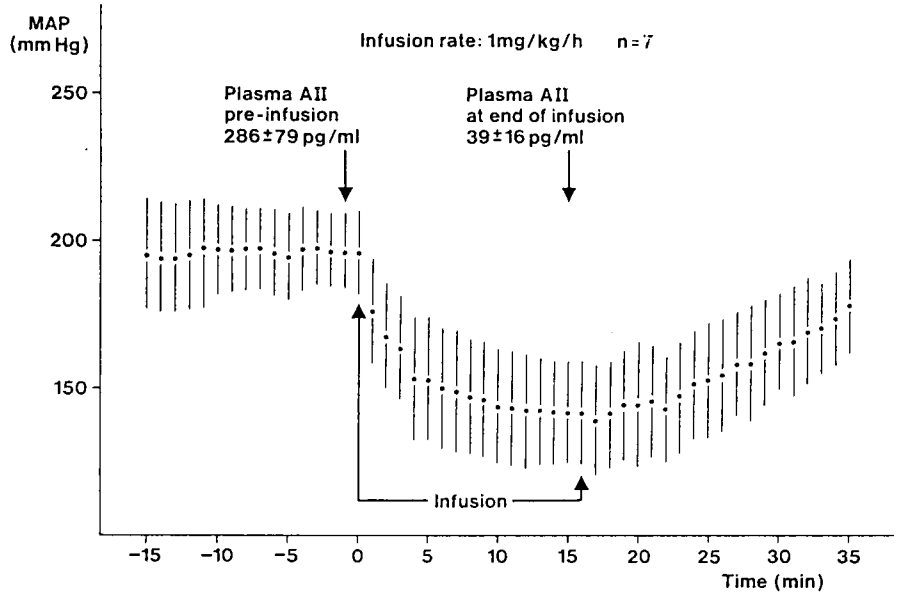

Fig. 1. In vivo activity of inhibitor **5**.

based on the hydroxy-ethylene moiety and containing Val at P_2' are highly effective inhibitors of rat renin in vivo, as shown in Fig. 1 by a marked decrease in the angiotensin-II level and mean arterial pressure during the infusion of 1 mg/kg/h of compound **5** into a group of 7 two-kidney, one-clip hypertensive rats [3].

References

1. Jones, D.M., Sueiras-Diaz, J., Szelke, M., Leckie, B.J. and Beattie, S.R., In Deber, C.M., Hruby, V.J. and Kopple, K.D. (Eds.) Peptides: Structure and Function, Pierce Chemical Co., Rockford, IL, 1985, p. 759.
2. Millar, J.A., Leckie, B.J., Morton, J.J., Jordan, J. and Tree, M., Clin. Chim. Acta, 101 (1980) 5.
3. Morton, J.J. and Wallace, E.C.H., Clin. Sci., 64 (1983) 359.

Session VIII
Immunology

Chair: John A. Smith
Harvard Medical School
Boston, Massachusetts, U.S.A.

Models and mechanisms for the immune recognition of protein antigenic sites by B-cells and T-cells

John A. Smith

Departments of Molecular Biology and Pathology, Massachusetts General Hospital and Department of Pathology, Harvard Medical School, Boston, MA 02114, U.S.A.

Introduction

A successful immune response against an invading organism (e.g., a parasite, virus, or bacterium) is dependent on cooperation between B-cells and T-cells. The immune system distinguishes between two types of antigenic sites, recognized by and interacting with antibodies (Ab) and T-lymphocyte receptors (TcRs). This article discusses what is known about the structure of these antigenic sites and their molecular interactions with IgGs, class II major histocompatibility complex (MHC) restriction elements (called Ia molecules), and TcRs.

Results and Discussion

Antibody-antigenic site recognition

The surface of a protein is mostly a continuum of overlapping antigenic sites [1, 2]. X-ray crystallography of a protein antigen(lysozyme)–monoclonal antibody complex reveals an antigenic site that contains multiple amino acids contributed by discrete linear segments and clustered together in a surface region due to folding of the protein chain [3] (Fig. 1). These residues interact with a shallow, groove-shaped, antibody combining site by a 'lock and key' mechanism without inducing structural changes in the conformation of the protein antigen [3]. Different antibodies directed against a similar region of the protein surface will likely have differing combining orientations and interactions with pertinent residues.

T-cell receptor/antigenic site recognition

In contrast to Ab recognition, T-cell recognition cannot distinguish between 'native' and 'denatured' proteins [4], because in order to invoke T-cell recognition, protein antigens must be chemically and physically modified (processed) within acidic intracellular compartments (endosomes) of antigen-presenting cells, themselves bearing Ia molecules, which function as receptors for antigenic peptides generated by poorly understood processing events. Ia molecules are present within

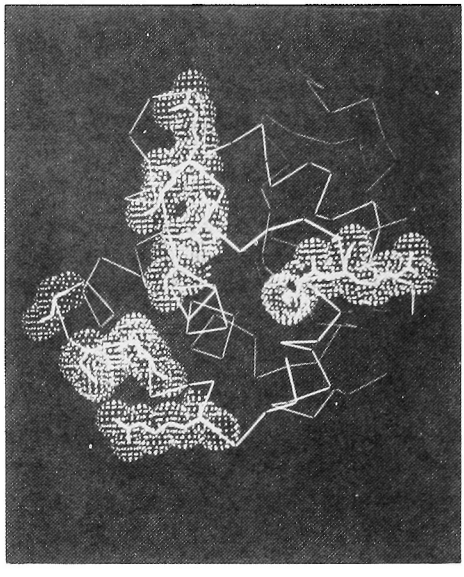

Fig. 1. The antigenic site residues determined from an antigen–antibody complex. The structure of the complex between hen egg white lysozyme and the Fab of a monoclonal anti-lysozyme antibody determined by X-ray crystallography [3]. The protein α-carbon backbone is the solid line. The van der Waals surface areas of antigenic residues (residues 13, 14, 19, 21, 22, 24, 117, 119, 121, and 125) are stippled.

the cell surface membranes of B-cells, macrophages, dendritic cells, epithelial Langerhans cells, thymic epithelial, as well as some T-cells. Although peptide binds weakly to Ia (K_D ~10^{-6}), it remains bound for a long time [5, 6]. The interactions among antigenic peptide, Ia, and TcR required for T-cell recognition of an antigenic peptide are shown in Fig. 2. Ia molecules interact with different epitopes of multisite protein antigens, although it is unclear why some peptides interact preferentially with certain Ia-presenting cells and others do not. It is now clear, however, that peptides from a large number of different protein antigens that are restricted by the same Ia will bind to and mutually compete for binding to the Ia molecule [6, 7]. Although the chemical basis for how a potentially large number of peptides, derived from a variety of foreign proteins, are able to form unique complexes with a very limited number of Ia molecules is not clear, certain peptides, restricted by a given Ia, have amino acid sequence homology with the Ia itself [8].

Synthetic peptides, containing between 7 and 17 residues, can be substituted for cellularly processed protein fragments and are the mainstay for determining the molecular details of the interactions between antigenic peptide and Ia binding site or TcR. The use of such peptides is currently shedding light on the mechanisms

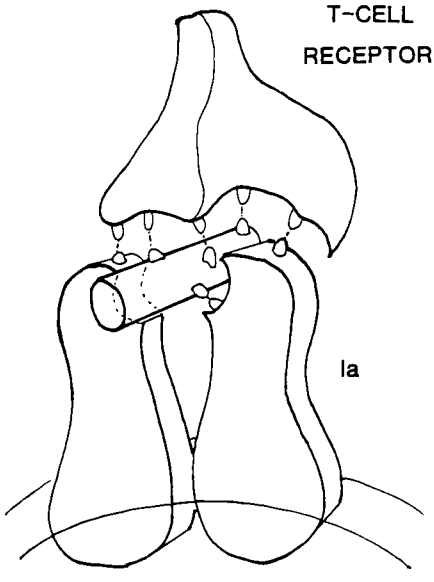

Fig. 2. Schematic representation of the Ia-peptide antigen T-cell receptor complex. The specific contact residues between peptide and Ia would be different for Ia molecules of different haplotypes (e.g., I-A^d vs I-E^k), although the overall geometry of the complex should be the same. The peptide antigen (i.e., the cylinder) binds in the polymorphic, Ia-binding site. The T-cell receptor interacts with both the peptide antigen and Ia molecule.

of antigen presentation and in the future will help clarify the mechanisms involved in antigen processing.

Although it is known that T-cells and B-cells recognize different antigenic sites [9], there are still no predictive algorithms that can determine the location of either type of antigenic sites with certainty. Clearly rational design of synthetic vaccines and immunosuppressive agents depends on a complete understanding of the nature of antigenic sites, and such knowledge will revolutionize our ability to manipulate the immune response.

Aknowledgements

This work was supported by a grant from Hoechst Aktiengesellschaft (F.R.G.). The author wishes to thank Professors M.L. Gefter and H.M. Grey, as well as Drs. J.-G. Guillet, M.-Z. Lai and T.J. Briner for numerous helpful discussions.

References

1. Benjamin, D.C., Berzofsky, J.A., East, I.J., Gurd, F.N.R., Hannum, C., Leach, S.J, Margoliash, E., Michael, J.G., Miller, A., Prager, E.M, Reichlin, M., Sercarz, E.E., Smith-Gill, S.J., Todd, P.E. and Wilson, A.C., Ann. Rev. Immunol., 2 (1984) 67.
2. Geysen, H.M., Tainer, J.A., Rodda, S.J., Mason, T.J., Alexander, H., Getzoff, E.D. and Lerner, R.A., Science, 235 (1987) 1184.
3. Amit, A.G., Mariuzza, R.A., Phillips, S.E.V. and Poljak, R.J., Nature, 313 (1985) 156.
4. Gell, P.G.H. and Benacerraf, B., Immunology, 2 (1959) 64.
5. Babbitt, B.P., Allen, P.M., Matsueda, G., Haber, E. and Unanue, E.R., Nature, 317 (1985) 359.
6. Buus, S., Sette, A., Colon, S.M., Miles, C. and Grey, H.M., Science, 235 (1987) 1353.
7. Guillet, J.-G., Lai, M.-Z., Briner, T.J., Smith, J.A. and Gefter, M.L., Nature, 324 (1986) 260.
8. Guillet, J.-G., Lai, M.-Z., Briner, T.J., Smith, J.A. and Gefter, M.L., Science, 235 (1987) 865.
9. Maizels, R.M., Clarke, J.A., Harvey, M.A., Miller, A. and Sercarz, E.E., Eur. J. Immunol., 10 (1980) 509.

A synthetic strategy for epitope mapping

H. Mario Geysen, Stuart J. Rodda and Tom J. Mason
Commonwealth Serum Laboratories, 45 Poplar Road, Parkville, Victoria 3052, Australia

Introduction

Synthetic peptides are attractive as probes for studying aspects of immunology at the molecular level, as possible diagnostic reagents, as characterized vaccine components and as hormone analogs. With the need for larger numbers of peptides for evaluation, fully automated synthesizers are widely used, and several methods have been described for the simultaneous synthesis of many peptides [1].

We describe a procedure allowing several thousand peptides to be concurrently synthesized at the rate of one residue coupled per day. With no practical restriction on the number of peptides which can be synthesized, a completely systematic approach to the location of epitopes (scan; Fig. 1) and their further resolution (replacement set; Fig. 2) becomes possible [2]. Good agreement has been shown between the results obtained from these rod-synthesized peptides and those from conventionally synthesized and purified peptides [3]. The stability of the rod-synthesized peptides on repeat testing allows their reuse for 30–60 tests.

This method has created the opportunity to address questions, which were formerly thought to be too difficult to answer, about the location of epitopes and their specificity for antibody.

Synthesis of Peptides

The method of peptide synthesis on rods has been described in detail elsewhere [2]. Briefly, specially-molded high-density polyethylene rods (diameter 4 mm) were suspended in deaerated 6% (v/v) acrylic acid in water containing 0.005 M $CuSO_4$. Gamma-irradiation at a dose of 0.8 Mrad was used to graft polymerize the monomer to the rods as polyacrylic acid. After a wash cycle, dried grafted rods were assembled into specially molded polyethylene holders designed to hold 96 rods in the format and spacing of a microtiter plate. Subsequent reactions at the tips of the rods were carried out in the wells of a specially molded polyethylene tray.

An amino group was introduced by reacting the polyacrylic acid on the rods for 2–3 days with mono-(Boc)-1,6-diaminohexane in DMF using DCC to achieve the condensation. Following a conventional Boc-deprotection cycle with TFA

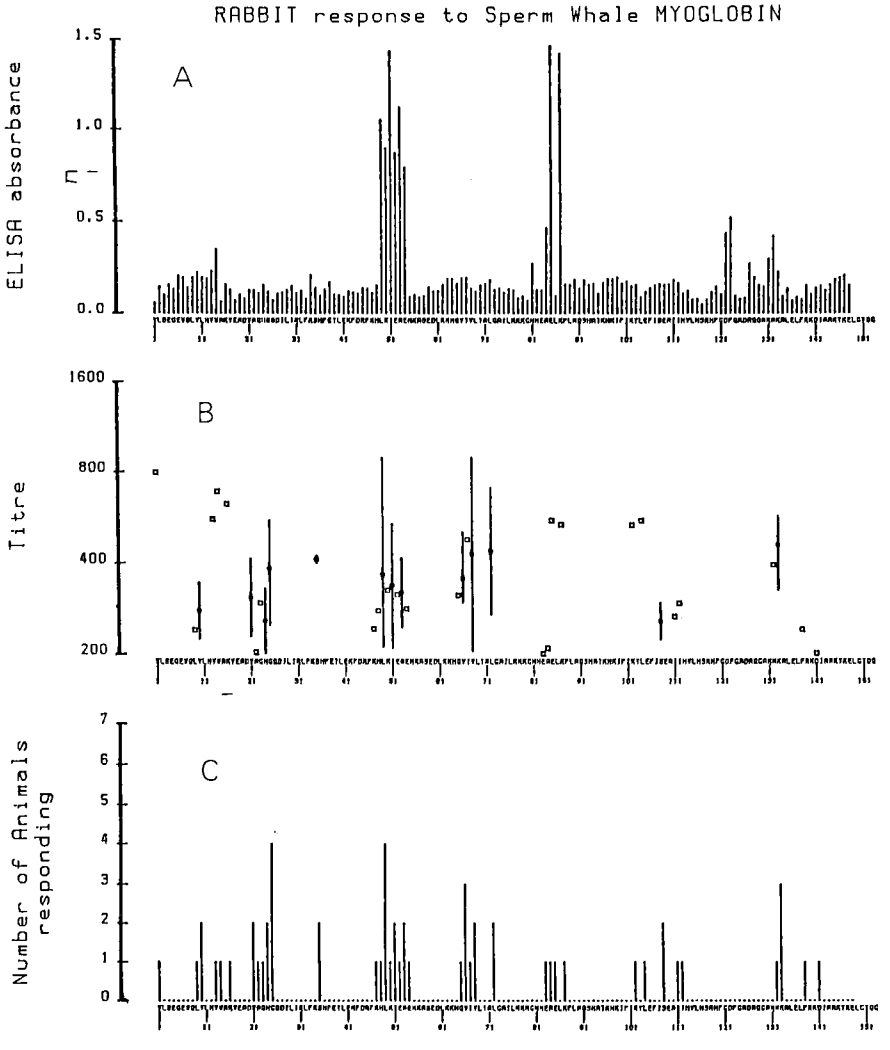

Fig. 1. Profiles of antigenic response (A–C) as a function of all possible sperm whale myoglobin (SWMb) hexapeptides. Each parameter is plotted at the sequence number corresponding to the first residue (amino-terminal) of the relevant hexapeptide. (A) Scan obtained from an individual rabbit anti-SWMb serum, used at a dilution of 1/400. The vertical axis shows the absorbance obtained at the end of the ELISA. (B) The individual titer (square) or, where more than one serum reacted, the geometric mean titer (circle) and the range of titers (vertical bar) of the antisera. Titers less than 200 (twice the slope of the test background) were ignored. (C) The frequency of the antigenic response given by the number of rabbit antisera that react with each hexapeptide.

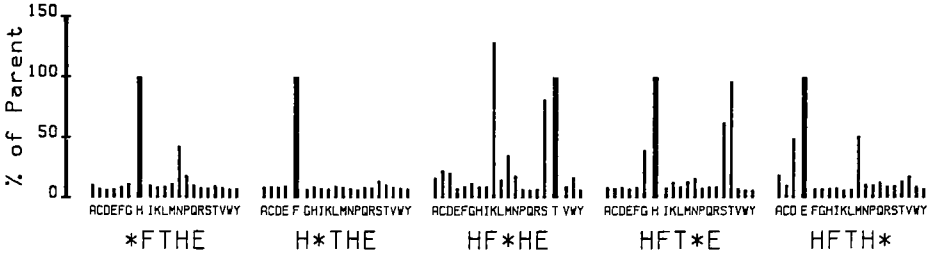

Fig. 2. Replacement set analysis, based on parent pentapeptide ^{54}HFTHE^{58} homologous with myohemerythrin. Each block of 20 ELISA values represents the results with peptides containing the single amino acid substitution identified by the single letter code beneath each bar. The position of the substitution is indicated by an asterisk in the sequence given under that block. The homologous amino acid is emphasized. ELISA values for the five copies of the parent sequence have been averaged and taken as 100% for the purposes of comparison with replacement analogs. Dilution of rabbit antiserum used was 1/1000.

Boc-β-alanine was coupled for a limited time to a target density of 50 ± 10 nmol per rod tip. Unreacted amino groups were acetylated by reaction with acetic anhydride in DMF/TEA. Successive DCC/HOBT-mediated coupling reactions were carried out overnight using side-chain protected amino acids as dictated by the sequence to be synthesized. A microcomputer program was used to calculate the requirements for the preparation of the activated amino acid solutions, and to direct the addition of the correct amino acid to each rod on each day. At the completion of the final coupling reaction, and after removal of the Boc group, the terminal amino group was acetylated. Side-chain deprotection was achieved by reaction with 50 mM boron tris(trifluoroacetate) in dry TFA [4].

Detection of Binding of Antibody by the Rod-Coupled Peptides

ELISA reactions were carried out with the appropriate serum and conjugate solutions in polystyrene microtiter trays [1]. Briefly, the tips of the rods, with the peptides still attached, were precoated using a 2% protein solution to block nonspecific adsorption of antibodies. Rods were incubated overnight in an appropriate dilution of an antiserum, washed 4 times, and incubated for 1 h in 'conjugate', comprising horseradish peroxidase-labeled goat anti-Ig, specific for the antibody species under test.

After washing to remove unbound conjugate, the level of bound conjugate was determined by the color developed by the reaction with a solution of the enzyme substrate, hydrogen peroxide in phosphate/citrate buffer, pH 4.0,

containing ABTS. Bound antibody was removed from the rods prior to retesting with another antiserum.

Rationale of Strategy

The procedure for the synthesis of peptides as described was conceived in order to provide the very large numbers of peptides required for systematic screening for sequences with biological activity. As such, the following factors were considered:

(1) By ELISA, the detection of binding of antibody only requires peptide to be present in the range of picomol [5]. This condition is satisfied by the level of peptide produced on the tips of the rods, which is typically 30–50 nmol. Furthermore, we have observed comparable test absorbances for peptide densities varying over two orders of magnitude, indicating that the test is only limited by the concentration of antibody.

(2) As in the case with the majority of serological tests, where a given antigen is determined in the presence of a large excess of extraneous protein, absolute purity of a peptide is also not a necessary requirement. The specificity of the antibody is relied upon to distinguish between the nominal sequence synthesized and the inevitable small amounts of deletion sequences, termination peptides, or other byproducts formed during the synthesis.

(3) Large numbers of 'negative control sequences' are a natural consequence of the systematic way in which peptide sets are structured. As is the usual case, peptide sets consist of closely related sequences differing by only one or two amino acids from each other. The observation of antibody binding to one peptide but failing to bind to a closely related peptide is taken as good evidence for the specificity of the test.

Stability on Repeat Testing

As a consequence of the synthesis strategy in which completed peptide remains covalently coupled to the plastic support, reuse of peptide through a number of tests only requires removal of reacting antibody between tests. When the absolute value of the absorbance is monitored over many successive tests with the same peptides, a gradual decrease is observed. Experience with many sets of peptides suggests that 30–60 useful tests can be expected before it becomes necessary to resynthesize a particular set of peptides. Peptides have been stored (dry at 4°C) for extended periods between tests, without detectable loss of activity.

Discussion

The possibility that synthetic peptides may find uses as vaccines, diagnostics

and other biologically relevant agents has focused interest on methods which provide for large numbers of peptides for evaluation. It is our experience that using the methods described, a small laboratory could readily prepare more than 1000 peptides per month. Furthermore, the format of these peptides makes them ideally suited for repeated evaluation, and utilizes the same instrumentation as is routinely used for immunological testing. Identification of a peptide(s) with the desired properties can then be followed by the preparation of larger and well-characterized qualities, using well-established solid phase synthesis procedures.

References

1. Houghten, R.A., Proc. Natl. Acad. Sci. U.S.A., 82 (1985) 5131.
2. Geysen, H.M., Rodda, S.J., Mason, T.J., Tribbick, G. and Schoofs, P.G., J. Immunol. Methods, in press.
3. Geysen, H.M., Tainer, J.A., Rodda, S.J., Mason, T.J., Alexander, H., Getzoff, E.D. and Lerner, R.A., Science, 235 (1987) 1184.
4. Pless, J. and Bauer, W., Angew. Chem., 85 (1973) 142.
5. Bittle, J.L., Houghten, R.A., Alexander, H., Shinnick, T.M., Sutcliffe, J.G., Lerner, R.A., Rowlands, D.J. and Brown, F., Nature, 298 (1982) 158.

Solid phase synthesis of biologically active antigenic peptides for T-cells

Lisa A. Casten, Pravin Kaumaya, Mark S. Anderson, John A. Smith and Susan K. Pierce

Northwestern University, 2153 Sheridan Road, Evanston, IL 60201, U.S.A.

T-cells specific for globular protein antigens do not recognize the native structure, but require that the protein be processed by an antigen-presenting cell (APC). This involves the uptake of antigen into acidic vesicles for proteolytic fragmentation, releasing a peptide which is transported to and held on the APC surface, where it is recognized by the specific T-cell in conjunction with Ia. Although the requirement for antigen processing and presentation is well established, the molecular mechanisms underlying these phenomena remain to be detailed. Of particular interest is an elucidation of the chemical features of the functional domains of the peptide fragment which allow binding to the T-cell antigen receptor and to the APC surface.

Mouse T-cells specific for pigeon cytochrome *c* (P*c*) show a high affinity cross-reaction with tobacco horn worm moth cytochrome *c* (THM*c*), and respond to equivalent concentrations of the corresponding cyanogen bromide cleavage fragments, P*c* 81–104 and THM*c* 81–103, which contain the T-cell antigenic determinant. Specific T-cell activation is dependent on lysine residues at positions 99 and 103/104 [1]. A series of peptides of increasing length representing the carboxy-terminal region of the 103 amino acid THM*c* was synthesized by solid phase synthesis, according to the Fmoc-*t*-butyl strategy, on a *p*-alkoxy-benzyl alcohol linked to a 1% cross-linked polymer of divinyl-benzene/polystyrene, Cleaved peptides were judged 98% pure by amino acid hydrolysis and HPLC analysis. Peptides shorter than 10 amino acids were biologically inactive at 10 mM, while peptides of 10–14 amino acids were able to stimulate the specific T-cell, although 10-fold higher concentrations (1 μM) were required for half-maximal responses as compared to THM*c* 81–103 (0.1 μM). The addition of a cysteine residue to the N-terminus of the synthetic THM*c* 92–103 conferred complete stimulatory activity to the peptide, which is possibly a function of the ability of the peptide to bind covalently to the APC surface, facilitating presentation to the T-cell. To further investigate the nature of the peptide domain which allows binding to the APC surface, non-stimulatory peptide analogs were assessed for their ability to compete for the cell surface binding site with the peptide antigen produced by the APC. Nonstimulatory cytochrome *c* peptides

of several species, including that of mouse, M*c* 81–104, which differ by no more than 6 amino acids, compete with the processed antigen on the APC surface and block activation of the T-cell [2]. P*c* peptides of the carboxy-terminal 7 and 8 amino acid residues, which contain the T-cell antigenic determinant but do not activate, also do not inhibit [2]. Further studies indicated that peptides which share no obvious homology with cytochrome *c*, such as peptides of the bacterial staphylococcal nuclease(Nase), block specific T-cell responses to cytochrome *c* as well as to an unrelated antigen ovalbumin (Table 1). The 9 amino terminal residues of M*c* 81–104, M*c* 81–99, are sufficient for blocking the response of the P*c*-specific T-cells, indicating that this region contains an APC binding domain; however, 3 stimulatory carboxy-terminal peptides of THM*c*, residues 90–103, 91–103, and 92–103, are capable of blocking the response of ovalbumin-specific T-cells to their processed antigen, demonstrating that this segment is also sufficient to allow the peptide to bind to the APC surface. Thus, all cytochrome *c* peptides which show blocking activity share residues 92–96. A more clear understanding of the shared features of the peptides which are able to compete with one another awaits, in part, the characterization of structures involved in holding the peptide on the cell surface and facilitating its interaction with Ia and the T-cell receptor.

Table 1 *The ability of peptides to block antigen-specific T-cell activation*

Peptides	Sequence	μM Peptide at 50% inhibition[a]	
		TP*c*9.1	AODH3.4
THM 81–103	VFAGLKKANERADLIAYLKQATK	S	60
THM 96–103	--------	-	ND
THM 97–103	-------	-	ND
THM 90–103	----------	S	225
THM 91–103	----------	S	21
THM 92–103	----------	S	145
THM Cys 92–103	C----------	S	90
P*c* 81–104	I--- I--KA----------AK	S	20
M*c* 81–104	I--- I--KG----------K-- NE	30	30
M*c* 81–99	I--- I--KG----------	300	160
Nase 61–80	FTKKMVENAKKIEVEFDKGQ	41	32
Nase 91–110	YIRADFKMVNEALVRQGLAK	52	32
Nase 101–120	EALVRQGLAKVAYVYKPNNT	43	ND

[a] The blocking ability of the peptides was determined by co-culturing P*c*-specific T-cells(TP*c*9.1) or ovalbumin-specific T-cells (AODH3.4) at 5×10^4 cells/0.2 ml with P*c*- or ovalbumin-pulsed B-cells at 2×10^5 cells/0.2 ml in the presence of competitor peptide. Culture supernatants were assayed for their interleukin-2 content, as described [2].
Abbreviations: ND, not determined; S, stimulatory; -, neither stimulation nor inhibition.

References

1. Hansburg, D., Fairwell, T., Schwartz, R.H. and Apella, E., J. Immunol., 131 (1983) 319.
2. Lakey, E.K., Margoliash, E., Fluoret, G. and Pierce, S.K., J. Immunol., 16 (1983) 721.

Recognition of peptide antigens by T-lymphocytes

Bhagirath Singh, M. Boyer, Z. Novak, E. Fraga and A. Fotedar
Department of Immunology, University of Alberta, Edmonton, Alberta, Canada

Introduction

In contrast to B-cells, T-cells do not recognize native antigens alone. Recognition of foreign antigens by T-lymphocytes usually occurs in two steps. The first step is the degradation (processing) of the antigen by the antigen-presenting cells (APC) and subsequent association of the processed antigen with the cell-surface major histocompatibility complex (MHC) molecules. The second step involves the recognition of the antigen–MHC complex by the T-cell receptor [1]. The predominant T-cell response to soluble antigens is usually Class II MHC (Ia)-restricted. Formation of the antigen–Ia complex and subsequent recognition of this complex by T-cells must depend upon the presence of specific determinants on the antigen. Furthermore, because of the antigen-processing event, local secondary structures in the fragments generated may be more important in the T-cell recognition process than the tertiary structure of the native molecule. To address these issues, we are using a synthetic polypeptide antigen of defined sequence and conformation, Poly 18, Poly Glu-Tyr-Lys-(Glu-Tyr-Ala)$_5$ and its smaller fragments [2, 3]. We have shown that immune responses to this α-helical antigen are under genetic control. Mice of H-2^d haplotype (Balb/c, B10.D2) are high responders and mice of H-2^k (CBA, C3H) and H-2^b (C3H.SW, B10) are nonresponders [2, 3]. We also found that not only the monomeric 18-residue peptide EYK(EYA)$_5$ is immunogenic, but the nonapeptide EYK(EYA)$_2$ containing the N-terminal residues is sufficient to prime H-2^d mice for Poly 18-specific antibody and T-cell responses [3]. To further analyze the system and to determine the Poly 18-specific T-cell repertoire in Balb/c mice, we have generated T-cell clones and T-cell hybridomas [4]. A number of these interleukin-2 (IL-2)-secreting hybridomas have been characterized with respect to their antigen fine specificity to determine the minimum peptide sequences required and to define the role of individual amino acid residues in the recognition of the antigen in association with the I-A^d antigens of Balb/c mice.

Results and Discussion

Based on the fine specificity analysis, Poly 18-specific T-cell hybridomas could

be divided into two groups (Table 1). Hybridomas in group A recognized Poly 18 and EYK(EYA)$_4$ peptide, whereas they were unresponsive to (EYA)$_5$. These results suggested that the lysine residue at position 3 in the EYK(EYA)$_5$ sequence of Poly 18 was critical for activation of these T-cells. It was also confirmed by the fact that antigens with ϵ-DNP lysine at residue 3 failed to activate these hybridomas. It appeared that the N-terminal glutamic and tyrosine residues at positions 1 and 2 also played an important role because their deletion in K(EYA)$_3$EYK leads to a drastic reduction in IL-2 release from the T-cells; however, alanine residues, i.e., AAK(EYA)$_3$EYK, only marginally affected the response, suggesting a structural role for these residues. The C-terminal alanine residue appeared not to be critical because it could be replaced by lysine residues without loss of biological activity. Similarly, glutamic and tyrosine residues at positions 13 and 14, respectively, were not essential for the response as they could be substituted by alanines; however, complete removal of the three C-terminal residues to generate the truncated peptide EYK(EYA)$_3$ lead to a drastic reduction of T-cell-activating capacity. We thus conclude that the minimum peptide sequence required for the activation is the 15 amino acid sequence EYK(EYA)$_4$.

Hybridomas in group B gave excellent responses with Poly 18 and (EYA)$_5$ peptide and also responded to EYK(EYA)$_4$ and (EYA)$_4$EYK antigens (Table 1). This suggested that neither position 3 nor 15 were critical for activation.

Table 1 *Fine specificity of Poly 18-specific T-cell hybridomas*

Group A hybridoma:	Poly 18-68-8	Group B hybridoma:	Poly 18-12-1
Peptides[a]	IL-2 Units[b]	Peptides[a]	IL-2 Units[b]
1 15		1 15	
EYKEYAEYAEYAEYK	665	EYAEYAEYAEYAEYA	1000
——————————A	1050	——————————K	300
AA—————————	420	—K—————————	540
—A—————————	< 10	—K——————————K	< 10
—K(DNP)—————	< 10	—K(DNP)————K	300
—————————	< 10	—AA————K	< 10
——AA—————	< 10	——AA————K	30
———AA————	< 10	———AA———K	< 10
————AA———	< 10	——————AAK	225
——————AA—	460	—————————	550
————K————	< 10	—————————	< 10

[a] Peptides were synthesized by solid phase peptide synthesis on a Beckman 990C machine by standard procedure [6]. Peptides were purified by HPLC on a C18 reversed-phase column with CH_3CN-H_2O gradient.

[b] T-cell hybridomas (5×10^4) were cultured with 10^6 irradiated antigen-presenting cells in the presence of various antigens and after 24 h supernatants were assayed for the presence of IL-2 on HT-2 cells as previously described [4].

Surprisingly EYK(EYA)$_3$EYK failed to elicit a response, indicating that the sequence of (EYA)$_4$ was important for the response. The ability of A-(EYA)$_4$ peptides to induce IL-2 release from group B hybridoma indicated that the minimum sequence for the activation is this 13-residue peptide and that the N-terminal Glu and Tyr residues at positions 1 and 2 in (EYA)$_5$ peptide probably have a structural role and not a critical role in the T-cell activation process. We find that lysine residues may have a role in the presentation of the peptide by Ia antigen. All the peptides containing a lysine residue were poorly presented by glutaraldehyde-fixed presenting cells to the group B T-cells as compared to those containing an alanine residue [5]. Glutamic and lysine residues in the C-terminal part of the (EYA)$_5$ peptide at positions 13 and 14, respectively, were not required for the antigen recognition because they could be replaced by alanine residues with only partial loss of biological activity.

It is interesting to find that any changes in the inner core of the EYK(EYA)$_4$ and (EYA)$_5$ antigens, i.e., within residues 4–12, have significant effects in the activation process of both group A and group B hybridomas. Simultaneous replacement of Glu and Tyr residues with alanine at positions 4 and 5, 7 and 8, or 10 and 11 rendered the resulting peptides incapable of activating the respective hybridomas. We therefore conclude that, in contrast to Glu and Tyr residues at positions 13 and 14, the glutamic and/or tyrosine residues at 4 and 5, 7 and 8, and 10 and 11 positions are directly involved in T-cell recognition. These may be contact residues for the T-cell receptor and/or they may interact with the Ia molecules during the process of antigen presentation. We also suggest an important role for the alanine residue at position 9. Its replacement by a lysine residue abolished the antigenicity of the peptide.

In summary, analysis of the fine specificity of group A and B hybridomas has revealed that the T-cell epitopes of Poly 18 antigen can be functionally divided into at least 2 domains of the monomeric EYK(EYA)$_5$ sequence. Group A recognizes the epitopes in the N-terminal part of the molecule, namely in EYK(EYA)$_4$ and group B determinants are in the C-terminal (EYA)$_5$ part of the molecule. Amino acids in the center of the monomeric sequence, i.e., (EYA)$_3$ from residues 4–12, must contribute to interactions with T-cell receptor and/or Ia molecules for both hybridomas. It is likely that these residues also contribute in maintaining the necessary secondary structure in the minimum peptides. Due to extensive sequence homology, the agretope site (Ia contact residues) in EYK(EYA)$_4$ and (EYA)$_5$ peptides may also be similar. The shared primary sequence in the 4–12 region of most of the peptides tested should provide identical motifs for interaction with the same Ia molecule. Single amino acid replacement studies and Ia binding studies with these two peptides will lead to a clear understanding of the role of various amino acid residues in the recognition of Poly 18 antigen by the Balb/c T-cells.

Acknowledgements

This work was supported by the Medical Research Council of Canada and the Alberta Heritage Foundation for Medical Research.

References

1. Schwartz, R.H., Ann. Rev. Immunol., 3 (1985) 239.
2. Barton, M.A., Singh, B. and Fraga, E., J. Am. Chem. Soc., 99 (1977) 8491.
3. Singh, B., Lee, K.C., Fraga, E., Wilkinson, A., Wong, M. and Barton, M., J. Immunol., 124 (1980) 1336.
4. Fotedar, A., Boyer, M., Smart, W., Widtman, J., Fraga, E. and Singh, B., J. Immunol., 135 (1985) 3028.
5. Boyer, M., Fotedar, A., Smart, W. and Singh, B., J. Cell. Biochem., Suppl. 11D (1987) T502.
6. Kilgannon, P.D., Fraga, E. and Singh, B., Mol. Immunol., 23 (1986) 311.

Structure–function relationship in protection against foot and mouth disease (FMD) by a synthetic peptide

R. DiMarchi[a], G. Brooke[a], C. Gale[a] and T. Doel[b]
[a]*Lilly Research Laboratories, Indianapolis, IN 46285, U.S.A.*
[b]*Animal Viral Research Institute, Pirbright, U.K.*

The use of a synthetic peptide vaccine for FMD has attracted much attention since it offers the advantage of a highly pure, defined, and safe alternative to the conventional vaccine [1–4]. In a previous study, we demonstrated the protection of cattle against FMD by a synthetic 40-residue peptide [4]. This represented the first example of protection in a target animal after a single immunization with a synthetic peptide under conditions typical of those used to test the potency of conventional vaccines. Of additional significance was the ability to achieve protection with a peptide free of any specific carrier protein.

Numerous issues must be addressed prior to consideration of commercial application of this peptide. The specificity, onset and duration of immunity are three items of particular concern. To a large degree, success in these three areas will be dependent upon selection of an appropriate adjuvant. From a synthetic perspective we have directed our attention at attempting to delineate the structural basis for the action of this peptide. We have prepared by solid phase synthetic methodology a number of peptides which represent various regions of the viral coat protein, VP_1 of the O_1 Kaufbeuren (O_1K) viral strain. Each peptide was purified to near-homogeneity by preparative reversed-phase chromatography.

The degree of immune protection induced by each peptide was examined in guinea pigs. Each animal was immunized with 125, 25, 5, or 1 nmol or the stated peptide in 0.2 ml of an equal volume emulsion of Freund's complete adjuvant and phosphate buffer, pH 7.6. Blood samples were removed at 27 days following vaccination and pools of the individual sera were made. All animals were challenged on day 28 with 3,000 guinea pig units of virulent O_1BFS virus.

The following peptides were synthesized and evaluated; 200–213(P14), 134–158-Leu-Pro(P27), Cys-Cys-200–213-Pro-Pro-Ser-141–158-Pro-Cys-Gly(P40), 134–158-Leu-Pro-Pro-Thr-Glu-Ala-200–213(P45), 161–213(P53), 134–213(P80). Sequences unique to VP_1 of the O_1K serotype are shown numerically with additional amino acids being shown as their three-letter code. The results of the guinea pig challenge with live virus are shown in Table 1. The most effective peptides were P40 and P45. Each of these peptides induced comparable levels of protection at doses of 125 and 25 nmol. Only one other peptide, P27, gave

Table 1 *Protection of guinea pigs vaccinated with different synthetic peptides*

	Dose level of vaccine (nmol)			
Peptide	125	25	5	1
P14	0/4	0/4	0/4	0/4
P27	3/4	0/4	0/4	0/4
P40	4/4	3/4	0/3	0/4
P45	4/4	3/4	0/3	0/4
P53	0/4	0/4	0/3	0/4
P80	1/4	0/4	0/4	0/4
Controls	0/5			

Number of guinea pigs protected/number challenged.

significant levels of protection. Neither peptide P14 nor P53, which lack the 141–158 sequence, displayed any indication of protection. Surprisingly the largest peptide, P80, which is comprised of the 141–158 and 200–213 sequences in natural linear order spaced by the viral sequence 159–199, induced an extremely poor protective response.

The serum from guinea pigs vaccinated with 125 nmol of each peptide was assayed for antibody against the immunizing peptide and each of the other peptides (Table 2). Immunization with peptide P14 failed to stimulate generation of homologous or heterologous antibody production. Peptide P27 stimulated antibody against itself which cross-reacted similarly with P40, to a lesser extent with P45, hardly at all with P80, and not at all with P14 and P53. Peptide P40 stimulated a high level of homologous antibody, which in descending order reacted to a lesser extent with P45, P27, P80 and P53. The antibody induced by P45 could be distinguished from that of P40 primarily on the basis of stronger recognition with peptides P14, P53, and P80. Peptide P53 induced antibody which displayed strong recognition of all peptides but P27. Peptide P80 provided an almost identical antibody profile to that of P53.

Our results demonstrate clearly the importance of the 141–158 epitope of VP_1 for induction of a protective response. The sequence representing residues 200–213 when presented alone or as part of 161–213 was incapable of providing protection. In contrast to P40 antisera, that of P45 displayed comparable P27 recognition, but with strong P14 binding; however, the level of protection induced by each peptide was identical. These results strongly suggest that antibody directed solely against 200–213 is of little protective value.

In combination with the major epitope (141–158), the sequence 200–213 once again provided a significant increase in the peptide potency [4]. Reversal of the linear order in the two sites from that which provided effective cattle protection served primarily to broaden the heterotypic serological cross-reactivity. Peptides P40 and P45 displayed levels of heterotypic serological recognition of the P27

Table 2 *ELISA evaluation of antipeptide sera*

Peptide on plate	P14	P27	P40	P45	P53	P80
P14	*neg*	neg	neg	2.9	2.9	2.8
P27	neg	*3.3*	2.8	2.7	neg	neg
P40	neg	3.5	*4.3*	4.0	3.2	3.3
P45	neg	2.7	3.5	*4.2*	3.9	3.9
P53	neg	neg	2.7	3.8	*3.4*	3.4
P80	neg	1.8	2.7	3.8	3.4	*3.2*

Antibody titers were determined as the $\log_{10}$ of the antiserum dilution giving 1 O.D. unit at 492 nm. Titers of 1.7 (equivalent to 50-fold dilution of antiserum) or less were considered as negative.

peptide which approach the homotypic level achieved with P27. The level of homotypic recognition in the P40 and P45 peptides is at least an order of magnitude greater than the heterotypic cross-reactivity with P27. The results support the contention that in these two peptides the 200–213 sequence induces a more nativelike structure to the 141–158 sequence and/or provides antibody which recognizes a combined epitope of the two regions. As a result of the comparable protective potency observed in peptides P40 and P45, a possible antiparallel orientation for these two separate sites on the surface of the virus can be postulated.

Of final interest is the observation that the peptide P80 provided inferior protection in comparison to peptides P40, P45 and P27. An apparent reason for this weak response was the minimal level of heterotypic cross-reaction of P80 antisera with peptide P27. Clearly this carboxy-terminal region of the VP_1 once removed from the virus is incapable of maintaining any resemblance to its natural conformation. This situation is most analogous to that reported for the isolated VP_1 protein [3]. Apparently, residues 159–213 induce an unfavorable conformation in 134–158 and/or sterically shield it from proper immunological presentation.

References

1. Kleid, D.G., Yansura, D., Small, B., Dowbenko, D., Moore, D.M., Grugman, M.J., KcKercher, P.D., Morgan, D.O., Robertson, B.H. and Bachrach, H.L., Science, 214(1981)1125.
2. Pfaff, E., Massgay, M., Bohm, H.O., Schulz, G.E. and Scaller, H., EMBO J., 1(1982)869.
3. Bittle, J.L., Houghton, R.A., Alexander, H., Shinnick, T.M., Sutcliffe, J.G. and Lerner, R.A., Nature, 298(1982)30.
4. DiMarchi, R., Brooke, G., Gale, C., Cracknell, V., Doel, T. and Mowat, N., Science, 232(1986)639.

Tubulin domains examined by antibodies from synthetic peptides

David Andreu[a], Sonsoles de la Viña[b] and José M. Andreu[b]

[a]Department of Organic Chemistry, University of Barcelona, E-08028 Barcelona, Spain
[b]CIB/CSIC, Velázquez 144, E-28006 Madrid, Spain

Introduction

Tubulin, the main constituent of microtubules and a cellular receptor for antimitotic drugs, exists as two subunits of known sequence, α and β [1, 2]. It does not crystallize well and data about its tertiary structure are limited. We are using peptide-derived antibodies to map tubulin regions involved in biologically relevant interactions such as ligand binding, proteolysis or microtubule formation. We describe our first findings in this direction.

Results and Discussion

Secondary structure analysis of tubulin gave 18 possibly exposed regions for each subunit. From those, five sequences were chosen for synthesis and antibody production. From α-tubulin, RRNLDIERPTYTN (214-226), KDYEEVGVDSVEGE (430-443) and EGEFSEAREDMAALEKDYEEVGVDSVEGE (415-443). From β-tubulin, RYPGQLNADLRKLAVN (241-256) and ESNMNDLVSEYQQYQDATAD (412-431). Peptides α(415-430), α(430-443) and β(412-431) were selected to cover the hydrophilic C-termini of both chains while minimizing their sequence homologies. All peptides were synthesized by solid phase methods, cleaved by anhydrous HF and purified to homogeneity by HPLC.

Appropriate conjugation to KLH and BSA rendered all peptides immunogenic in rabbits, raising antibodies which were cross-reactive with plate-adsorbed tubulin in ELISA. This reaction was completely inhibited by the corresponding free peptides, indicating specific recognition of the selected regions of α- and β-tubulin. In the relatively homologous C-termini, cross-reactivity among anti-α and anti-β antisera was not observed. Soluble native tubulin was also a full inhibitor in competitive ELISA; however, it would be simplistic to conclude from this that all five peptides cover exposed regions of tubulin since, even under the stabilizing conditions of the assay (3.5 M glycerol), partial denaturation of tubulin cannot completely be ruled out.

The synthetic peptides were also competitors in ELISA and indirect immu-

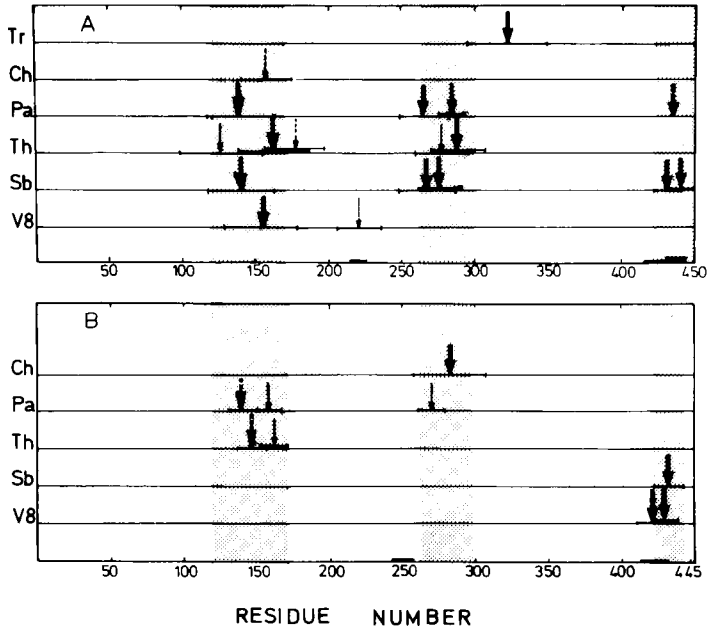

Fig. 1. Proteolytic map of tubulin. Limited proteolysis was done with trypsin (Tr), chymotrypsin (Ch), papain (Pa), thermolysin (Th), subtilisin (Sb) and S. aureus *V8 protease (V8). Apparent molecular weights of digestion fragments were determined from standard curves of protein markers; values from several assays were averaged ($\bar{x}$ + S.D.). Proteolysis fragments were aligned on the known tubulin sequences on the basis of their reaction with antipeptide antibodies. Sizes and approximate cleaving points are estimates based on apparent molecular weights. Arrows indicate cleavage points.*

nofluorescence of PTK2 cellular microtubules with antitubulin monoclonal antibodies DM1A and DM1B [3]. From the fact that α(415-443) and β(412-431) but not α(430-443), were effective inhibitors in both assays, it was concluded that determinants recognized by DM1A map in positions α(415-430) and those recognized by DM1B in positions β(412-431), not excluding other possibly recognized residues. Two conflicting reports on the localization of these epitopes have recently appeared [4, 5]. Our results provide independent confirmation, based on chemical synthesis, of the assignment made by Breitling and Little [4] using peptides obtained by extensive chemical and enzymatic cleavage of tubulin. The C-terminal regions of tubulin thus appear to be major immunogenic parts of the molecule.

Finally, our region-oriented antibodies have been useful as specific markers in proteolytic studies of tubulin. The noncovalent structure of tubulin in solution

is of limited stability and the protein unfolds, aggregates and loses activity quite readily [6]. We have chosen mild digestion conditions favoring limited proteolysis over the possibly more extensive cleavage of partially unfolded forms. Fig. 1 shows a proteolytic map of α- and β-tubulin with six common proteases. The main cleavage points for all six enzymes are located approximately in the same areas, thus allowing to define three domains for every subunit, each roughly corresponding to one third of the sequence.

In conclusion, we have shown that synthetic peptides spanning several regions of α- and β-tubulin can be successfully employed to raise noncross-reacting, monospecific antibodies which recognize determinants mapped by preexisting monoclonal antibodies and are useful in the proteolytic mapping of tubulin.

References

1. De Brabender, M. and De Mey, J. (Eds.), 3rd International Symposium on Microtubules and Microtubule Inhibitors, Elsevier, Amsterdam, 1985.
2. Postingl, H., Krauhs, E., Little, M. and Kempf, T., Proc. Natl. Acad. Sci. U.S.A., 78 (1986) 2757.
3. Blose, S.H., Meltzer, D.I. and Feramisco, J.R., J. Cell Biol., 98 (1984) 847.
4. Breitling, F. and Little, M., J. Mol. Biol., 189 (1986) 367.
5. Serrano, L., Wandosell, F. and Avila, J., Anal. Biochem., 159 (1986) 253.
6. Andreu, J.M. and Timasheff, S.N., Biochemistry, 21 (1982) 6465.

Neutralizing rabbit antibodies to synthetic human interleukin-2 (IL-2) peptides

W. Danho, R. Makofske, J. Swistok, J. Michalewsky, T. Gabriel, J. Jenson, W.-H. Tsien and M. Gately

Peptide Research and Immunopharmacology Departments, Roche Research Center, Hoffmann-La Roche Inc., Nutley, N.J. 07110, U.S.A.

Introduction

Interleukin-2 (IL-2) is one of a number of lymphokines which play a critical role in the regulation of immune responses. IL-2 provides a signal for the proliferation of activated T cells through its binding to specific cell-surface receptors.

Human IL-2 is a polypeptide with a molecular weight of 15,420 (133 amino acids). The primary sequence has been determined from the DNA sequence by Taniguchi et al. [1]. The principal goal of our program is to localize the receptor-binding site within the human IL-2 sequence and then to use this structural information to develop a specific antagonist to human IL-2. Our strategy has been to utilize the amino acid sequence data to design synthetic IL-2 peptides which are likely to contain antibody and/or cell-surface receptor binding sites, and then to use the peptides and rabbit antibodies to the synthetic peptides to map the h-IL-2 active site. The amino acid sequence of h-IL-2, therefore, was analyzed for regions with high probability for beta turns and maximum hydrophilic residues. The regions of beta turns and maximum numbers of hydrophilic amino acids were predicted by computer programs based on Chou–Fasman and Hoppe–Woods analyses. Fig. 1 shows the nine contiguous IL-2 peptides and the eight additional overlap peptides that were chosen for synthesis.

Results and Discussion

The peptides were synthesized by solid phase methodology, purified by gel filtration and preparative HPLC, and characterized by analytical HPLC and amino acid analysis. The peptides were conjugated to KLH by the MBS method and used to immunize rabbits. All antipeptide antisera were tested by ELISA and Western blot. All 17 peptide-KLH conjugates gave antisera which reacted with the free peptides. The antipeptide reactivity was specific in that the antisera reacted only with the peptide used and with intact r-IL-2 in ELISA and Western

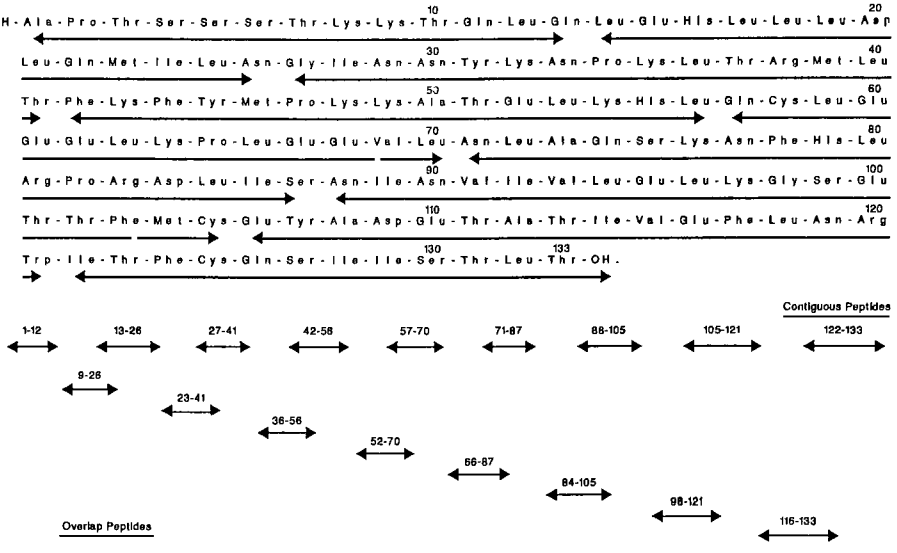

Fig. 1. The primary structure of human IL-2.

blots (only antisera raised against peptide 1-12 do not react with the intact r-IL-2). All of the anti-h-IL-2 peptide antisera were tested for their ability to inhibit binding of [^{125}I]IL-2 to PHA-stimulated peripheral blood lymphocytes [2]. Only antisera to one peptide (27-41) and its corresponding overlap peptide (23-41) significantly inhibit [^{125}I]IL-2 binding. This binding is specific since preincubation of even the highest concentration of antisera with 100 μg/ml of free peptide at 37°C for 30 min completely overrode the inhibition.

The IgG fraction of anti-(27-41) antiserum was purified on protein A-Sepharose, concentrated and tested for its ability to inhibit IL-2 activity [3]. It was demonstrated that anti-(27-41) neutralizes the bioactivity of r-IL-2 (0.1 ng/ml) at IgG concentration of 4.4 mg/ml and 1.1 mg/ml. It was also demonstrated that this neutralization is not the result of some nonspecific toxicity in two ways. First, it can be overridden with high concentrations of r-IL-2 (1.6 ng/ml; second, it can be overridden with 250 μg/ml of free peptide.

Conclusion

Only antisera to peptides 27-41 and 23-41 significantly inhibit IL-2 binding and bioactivity. Examination of the antiprotein ELISA titers indicates that this is not simply the result of high anti-IL-2 titer. The most likely explanation for its unique neutralizing ability is that the epitope with which it reacts is within

or near the binding site of h-IL-2. The location of this peptide within the predicted secondary structure of h-IL-2 supports this idea. Residues 27-41 correspond to the first predicted interhelical turn of h-IL-2 and thus are likely to be on the surface of the h-IL-2 molecule. In addition this sequence overlaps the most evolutionary conserved region of h-IL-2 (residues 36-62).

References

1. Taniguchi, T., Matsuri, H., Fujita, T., Takaoka, C., Kashima, N., Yoshimoto, R. and Hamuro, J., Nature, 302 (1983) 305.
2. Ju, G., Collin, L., Kaffka, K., Tsien, W.-H., Chizzonite, R., Crowl, R., Bhatt, R. and Killian, P., J. Biol. Chem., 262 (1987) 5793.
3. Gately, M., Wilson, D. and Wong, H., J. Immunol., 136 (1986) 1274.

Use of synthetic peptides for specific assays of proproteins: Assay of proapolipoprotein A-I

C. Martin[a], A. Barkia[b], J.C. Gesquière[a], P. Puchois[b], C. Cachera[b], J.C. Fruchart[b] and A. Tartar[a]

[a]Laboratoire de Chimie des Biomolécules and [b]SERLIA and U. INSERM 279, Institut Pasteur, 1 rue du Professeur Calmette, F-59019 Lille, France

Apolipoprotein A-I (Apo A-I) is a 243 amino acid long protein which is secreted as a proprotein (pro Apo A-I) that differs only by a 6 amino acid peptide extension at its N-terminus [1]. Assay of pro Apo A-I is of great interest as an early tracer of Apo A-I secretion; however, it is almost impossible to raise specific antibodies starting from pro Apo A-I that do not cross-react with Apo A-I because of the high homology (97%) between the two proteins. The difficulty is enhanced by the percent of circulating pro Apo A-I to Apo A-I, which is only 3–10% (Fig. 1).

In order to elicit antibodies against the protein, it would have been possible to use the hexapeptide specific for the proprotein. Nevertheless, the choice of the peptide to use for immunization was guided by 3 factors:

- sufficient length to elicit antibodies capable of reacting with the whole protein;
- specificity for the proprotein with no affinity for the mature protein;
- sufficient distance from the carrier to give good exposure during immunization.

It was possible to give a good presentation of the peptide linked to the carrier through a spacer, but in order to keep the highest similarity with the protein, we extended the 6 amino acid pro-sequence with the first 3 amino acids of the mature protein and used the nonapeptide, Arg-His-Phe-Trp-Gln-Gln-Asp-Glu-Pro. We considered that the tripeptide Asp-Glu-Pro, common to Apo A-I, would not interfere and that the nonapeptide could elicit antibodies that would not cross-react with the mature Apo A-I.

Apo AI : Asp-Glu-Pro-Pro-Gln-Ser-Pro-Trp... (243A.A.)
Pro Apo AI: Arg-His-Phe-Trp-Gln-Gln-Asp-Glu-Pro-Pro-Gln-Ser-Pro-Trp... (249 A.A.)

Fig. 1. N-terminals of apolipoprotein A-I and proprotein.

Materials and Methods

Pro A-I (1–9) was synthesized according to the Merrifield strategy [2], using tosyl groups (Arg and His) and benzyl groups (Asp and Glu) for side-chain protection. After HF treatment, using 10% *p*-cresol and 10% methylsulfide [3], the crude peptide was purified by gel filtration on a Biogel P2 and then by reversed-phase HPLC on a Whatman ODS2 column.

Purified peptide was conjugated with tetanus toxoid, using carbodiimide activation of the α-carboxyl groups of Pro-9 or of the side chains of Asp-7 and Glu-8, so that the N-terminus of the peptide was thus exposed in a similar manner as in the native protein.

Results and Discussion

After immunization of rabbits, antibodies were purified by affinity chromatography on columns prepared with the nonapeptide conjugated to 4B Sepharose by its C-terminus. The specificity of antibodies was demonstrated by immu-

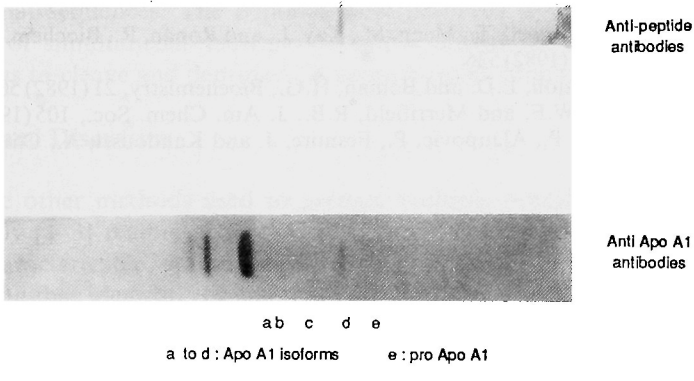

Fig. 2. Immunoblotting after isoelectric focusing of Apo HDL3.

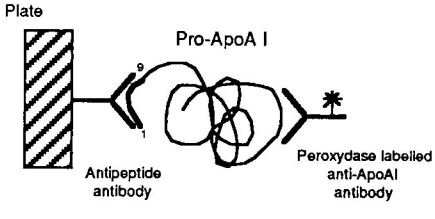

Fig. 3. Noncompetitive immunoassay.

Table 1 *Concentration of pro-Apo A-I and Apo A-I in the plasma*

	Pro-Apo A-I (mg/ml)	Apo A-I (mg/ml)	Pro-Apo A-I/Apo A-I (%)
Normolipidemic subjects, male (A)	0.084 ± 0.013	1.18 ± 0.15	6.9 ± 1.0
Normolipidemic subjects, female (B)	0.089 ± 0.015	1.18 ± 0.18	7.4 ± 0.8
(A + B)	0.087 ± 0.015	1.18 ± 0.16	7.1 ± 0.9
Tangier patient	0.0012	0.0042	29.0

noblotting after isoelectrofocusing (Fig. 2), showing no cross-reactivity with the mature protein. A noncompetitive sandwich enzyme immunoassay [4], using antipeptide antibodies coated on microtiter plates has been developed to determine pro-Apo A-I: after incubation with delipidated plasma (untreated plasma did not react), bound pro-Apo A-I was revealed by polyclonal antibodies directed against mature Apo A-I (Fig. 3). Results are shown in Table 1.

References

1. Brewer, Jr., H.B., Fairwell, T., Meng, M., Kay, L. and Ronan, R., Biochem. Biophys. Res. Commun., 113 (1982) 536.
2. Merrifield, R.B., Vizioli, L.D. and Boman, H.G., Biochemistry, 21 (1982) 5020.
3. Tam, J.P., Heath, W.F. and Merrifield, R.B., J. Am. Chem. Soc., 105 (1983) 6442.
4. Koren, E., Puchois, P., Alaupovic, P., Fesmire, J. and Kandoussi, A., Clin. Chem., 33 (1987) 38.

The determination of the precise amino acids involved, and their relative importance, in peptide antigen/monoclonal antibody interactions

Richard A. Houghten*, Jon R. Appel and John M. Sitarik
Scripps Clinic and Research Foundation, Department of Molecular Biology, 10666 N. Torrey Pines Rd., La Jolla, CA 92037, U.S.A.

Introduction

Antibody–antigen binding studies, using ELISA and immunoprecipitation assays, were conducted on over 1000 discrete analogs of haptenic peptides used to generate monoclonal antibodies. The analogs prepared consisted of 550 single and 26 multiple point replacement analogs, as well as 450 single position omission, 30 insertion, 20 truncation, and 26 D-amino acid substitution analogs of the 26 original sequences. The peptides were prepared by the recently developed method of simultaneous multiple peptide synthesis (SMPS) [1, 2] and a new apparatus to cleave and deprotect 24 peptide-resins simultaneously [3].

Results and Discussion

Unlike other methods used to prepare multiple peptides [4], those used for this study [1–3] readily generated 50–75 mg of relatively pure (average 85%), fully characterizable, nonsupport-bound peptide. In earlier work [1, 5–7], it was found that identical results were not always obtained when peptide antigen–antibody studies were carried out using ELISA and immunoprecipitation assays. To clearly establish relative differences in the residues making up the core determinant, relative IC_{50}s had to be carried out using an immunoprecipitation assay [5]. In this manner, differences in relative importance for the amino acids in the 6-residue core determinant were found to vary 10,000-fold. Thus when comparing monoclonal antibodies generated from two different clones while using a fixed concentration of each of a series of omission peptides on the ELISA plate, 4 amino acids appeared to make up the determinant in one case but 6 in the other. When lower concentrations of antigen were used, both of the antibodies saw the same 6-residue determinant [6]. These antibodies were seeing the same determinant, but with differing affinities. This resulted in the apparent absence of several amino acids in the determinant.

*To whom correspondence should be addressed.

A second difficulty was encountered when a series of analogs was prepared at a given position in a subject peptide's determinant region by substituting each of the 19 other natural amino acids for the original amino acid. This was done first for a larger 13-amino acid sequence of the original immunizing peptide (HAI residues 98–110) and then for a shorter 6-residue 'core' sequence (HAI residues 101–106) composed only of the determinant in its *N*-acetylated and C-terminal amidated form. Since this study did not readily lend itself to ELISA procedures due to the size of the short peptide series, an immunoprecipitation assay (IP) was used. The concentration of analog needed to displace the original ^{125}I radiolabeled antigen (HAI 98–110) to 50% inhibition (IC_{50}) was determined for each analog within each series. If the 6 residues consisting of the core sequence of a determinant were sufficient for giving a complete picture of the interaction of the original immunizing peptide with the antibody, then the profiles found should have been identical. This was not the case, as variations were seen throughout the profile [6]. This points to another potential difficulty in using short support-bound peptides for detailed studies of peptide antigen–antibody interactions.

In other studies, the effect of single position substitution of natural and unnatural amino acids as well as omission, insertion, truncation, multiple substitutions [6], and conformationally restrained analogs, as well as more detailed studies of the effects of residues outside the core determinant [7] on peptide antigen–antibody interaction, have been examined. In all of these studies alteration of the core determinant resulted in a decrease, or at best no change, in the antibodies' ability to see the peptide. Multiple replacements in the core determinant resulted in a decrease approximated by multiplying the individual differences with one another. In our hands, the only increase in the antibodies' ability to recognize a peptide containing the core determinant was when the length of the peptide was substantially increased in either the C- or N-terminal direction [7]. In the determination of the key interactive residues for 100 monoclonal antibodies raised against 25 different peptides, no amino acid was found to be precluded from being part of the core determinant (Fig. 1). The residues found to occur most often, relative to their overall occurrence in the immunizing peptides, were aspartic acid and tyrosine, with those occurring least often being histidine and asparagine. A wide range in sequence variation was found in the makeup of these 6-residue determinants, with examples including: -DVPDYA-, -KGKHRK-, -SAAASE-, -IWKKFE-, and -EQEGYP-.

Conclusion

The use of short, permanently support-bound peptides [4] can lead to potentially erroneous conclusions when studying peptide antigen–antibody interactions. At a fixed concentration of peptide, or if only 6 amino acid lengths of the parent

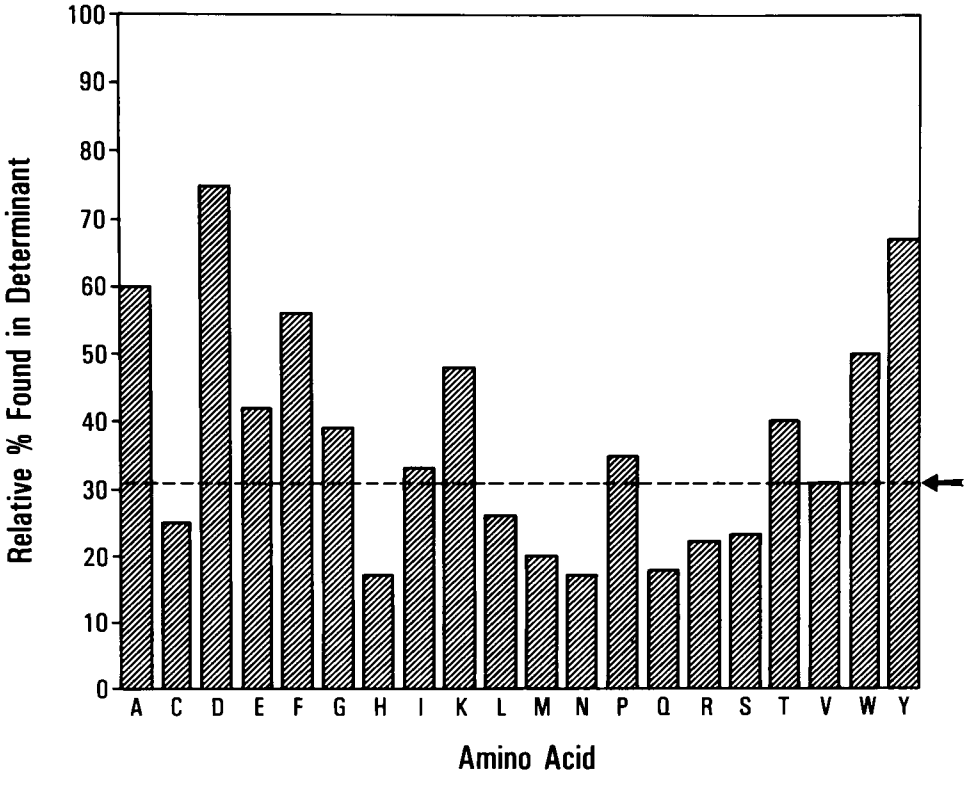

Fig. 1. The occurrence of given amino acids found in the determinant region relative to their overall occurrence in the original immunizing peptides.

sequence are examined, much of the fine specificity of interactions, as well as the exact size and specific residues constituting a determinant, can be lost [1, 5–7]. While the results presented are preliminary, several general trends in antibody–antigen interactions have begun to emerge. We have found that the majority of core determinants are comprised of 6 residues in length, with a range of 2 to 8 residues. Substitutions have resulted in decreased, or at best, equal antibody–peptide antigen binding when compared to the starting peptide. The charge effects at each end of peptides consisting of only the core determinant were found to cause significantly decreased binding (5–50-fold) and the residues outside the core determinant were found to have a substantial impact (2–20 times variation) on the binding interaction of the peptide antigen with the antibody [5, 7]. We have also found that the only instance of increasing binding ability was with peptides of increased length [7]. Related studies using more than 100 different monoclonal antibodies are in progress.

References

1. Houghten, R.A., Proc. Natl. Acad., Sci. U.S.A., 82 (1985) 5131.
2. Houghten, R.A., DeGraw, S.T., Bray, M.K., Hoffmann, S.R. and Frizzell, N.D., Biotechniques, 4 (1986) 522.
3. Houghten, R.A., Bray, M.K., DeGraw, S.T. and Kirby, C.J., Int. J. Pept. Prot. Res., 27 (1986) 675.
4. Geysen, H.M., Meloen, R.H. and Barteling, S.J., Proc. Natl. Acad. Sci. U.S.A., 81 (1984) 3998.
5. Houghten, R.A., Hoffmann, S.R. and Niman, H.L., In Channock, R.M. and Lerner, R.A. (Eds.) Modern Approaches to Vaccines, Cold Spring Harbor Laboratory, Cold Spring Harbor, NY, 1986, pp. 21–25.
6. Houghten, R.A., In Channock, R., Ginsburg, H., Lerner, R. and Brown, F. (Eds.) Modern Approaches to New Vaccines, Cold Spring Harbor Laboratory, Cold Spring Harbor, NY, 1987, pp. 5–10 (in press).
7. Houghten, R.A., In Marshak, D.R. (Ed.) Therapeutic Peptides and Proteins: Assessing the New Technologies, Cold Spring Harbor Laboratory, Cold Spring Harbor, NY, 1987, in press.

Synthesis of glycopeptides with tumor-associated antigen structure

Horst Kunz, Siglinde Friedrich-Bochnitschek and Stefan Birnbach
Institut für Organische Chemie der Universität Mainz, Becher-Weg 18-20, D-6500 Mainz, F.R.G.

Introduction

An increasing number of biological results indicate that membrane glycoproteins exhibit major functions in the regulation of cell growth. Consequently, it has been found that normal cells and tumor cells are quite different in the glycoprotein profiles of their cell membranes. The altered glycoproteins of the tumor membranes seem to be tumor-associated antigens. This has been described, in particular, by Springer et al. [1] for the so called Tn- and T-antigen glycoproteins which contain the typical structures **1** and **2**.

Tn-antigen **1** T-antigen **2**

In contrast to normal proteins, glycoproteins and glycopeptides are not easily available by gene technological methods.

Results and Discussion

The chemical synthesis of glycopeptides involves different problems: (i) the synthesis of the saccharide components, (ii) the stereoselective formation of the glycosidic bonds, and (iii) the selective deprotection of only one functional group on these complex polyfunctional molecules. The latter task is particularly difficult since the acetalic glycosidic bonds are sensitive to acids and, in the cases of the *O*-glycosyl serine and threonine derivatives (e.g., **1** and **2**, also sensitive to moderate bases).

We have solved these problems by the development of the allylic protecting groups [2]. Thus, using the allyl ester as the carboxy protecting function, we were able to synthesize *O*-glycosyl serine and threonine glycopeptides, which

are partial structures of human α_2-serum glycoprotein and of human glycophorin with Tn-antigen side chains.

A second method developed by us is the 2-pyridyl ethoxycarbonyl (Pyoc) protecting principle [3]. This stable protection can be removed – after modification – under almost neutral conditions. Using this method we succeeded in the synthesis of Tn- and T-antigen glycopeptides and in coupling of the tumor-associated membrane structures with bovine serum albumin [4]. The conjugates so obtained shall now be used for the induction of antibodies against the tumor membrane constituents.

References

1. Springer, G.F., Science, 224 (1984) 1198.
2. Kunz, H. and Waldmann, H., Angew. Chem. Int. Ed. Engl., 23 (1984) 71.
3. Kunz, H. and Birnbach, S., Tetrahedron Lett., 25 (1984) 3567.
4. Kunz, H., Angew. Chem. Int. Ed. Engl., 26 (1987) 294.

Formation of amphipathic secondary structure is correlated to T-cell antigenicity in a series of synthetic peptides from sperm whale myoglobin

Laura R. Sanza[a], Lila M. Gierasch[a], Jay A. Berzofsky[b], Gail K. Buckenmeyer[b], Kemp B. Cease[b] and Cecilia S. Ouyang[b]

[a]Department of Chemistry, University of Delaware, Newark, DE 19716, U.S.A.
[b]National Cancer Institute, NIH, Bethesda, MD 20892, U.S.A.

Introduction

Compared to the information known on antibody antigenicity and the humoral immune response, little is known about antigenic sites recognized by T-cells in the cell-mediated immune response. Antigens that invade the body can be engulfed by macrophages, processed in lysosomes and presented on the cell surface in association with a Class II major histocompatibility antigen in order for T-cells to recognize them. T-cells recognize sequences of consecutive residues within a protein made accessible by the processing event. A factor that has been proposed to make some sequences immunodominant over others is the ability of the peptide sequence, outside the constraints of the native protein, to take up amphipathic secondary structure that would stabilize it at the interface of the cell as well as with the major histocompatibility complex (MHC) protein [1]. The present study of antigenic and nonantigenic fragments from sperm whale myoglobin (SWMb) reveals that, indeed, there is a correlation between conformation and T-cell activating potential.

Results and Discussion

Synthetic peptides 132–146 and 102–118 from SWMb have been predicted to form amphipathic α-helices based on hydrophobic/hydrophilic amino acid distribution [1] and were found to activate T-cell clones from mice immunized against the whole protein [2, 3]. Using circular dichroism (CD), we find that these peptides indeed become helical in the helix-promoting environments trifluoroethanol (TFE) or aqueous sodium dodecyl sulfate (SDS); the latter also serves as a model interfacial environment (see example in Fig. 1).

SWMb 93–102 was predicted not to be amphipathic based on the sequence and was used as a control. SWMb 115–130 has a residue distribution that would be amphipathic in an α-helix, but the presence of a central Pro-Gly (120–121)

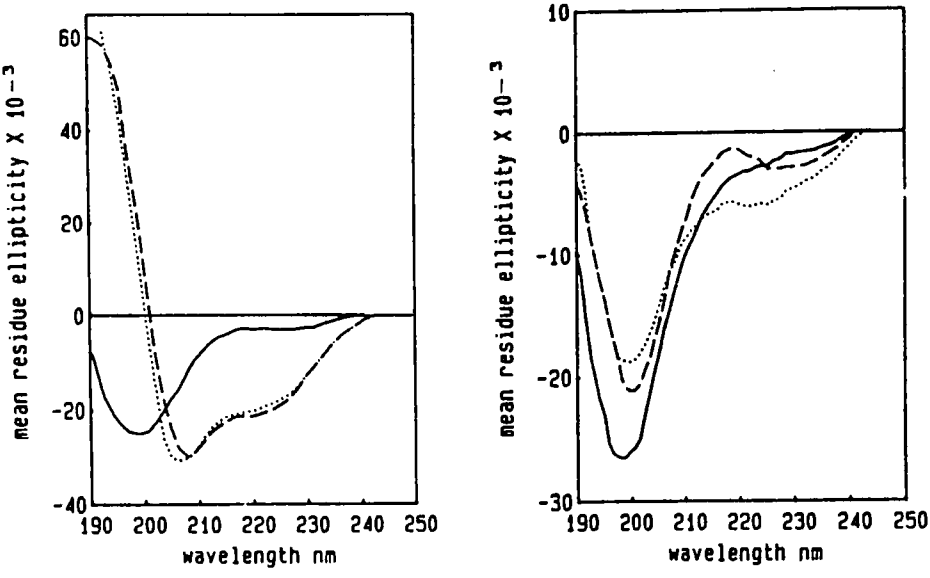

Fig. 1. CD spectra of antigenic peptide SWMb 132–146 and control peptide SWMb 93–102 in 5 m M KH_2PO_4, pH 7.4. Using Provencher's curve fitting program Contin [4], SWMb 132–146 takes up 90–100% helical structure in SDS and TFE; SWMb 93–102 is mostly random with 10–20% helical structure in SDS and TFE; both are random in buffer; ——, 5 mM KH_2PO_4 ----, 40 mM SDS, ..., 50% TFE.

sequence was expected to disfavor the helical conformation and so this was also used as a control. Neither peptide activates T-cell clones from SWMb-immunized mice or takes up significant helical structure in SDS or TFE (see example in Fig. 1). These results support the hypothesis of a correlation between T-cell antigenicity and ability to form amphipathic secondary structure.

Acknowledgements

This research was supported in part by NIH grant GM27616 to LMG.

References

1. DeLisi, C. and Berzofsky, J., Proc. Natl. Acad. Sci. U.S.A., 82 (1985) 7048.
2. Berkower, I., Buckenmeyer, G. and Berzofsky, J., J. Immunol., 136 (1986) 2498.
3. Cease, K., Berkower, I., York-Jolley, J. and Berzofsky, J., J. Exp. Med., 164 (1986) 1779.
4. Provencher, S., Computer Phys. Comm., 27 (1982) 229.

Manipulation of the immune response against a peptide from the C-terminal part of the surface protein VP_1 of foot and mouth disease virus

W.M.M. Schaaper, W.C. Puijk, D.J.A. Meijer, H. Lankhof, W.P.A. Posthumus and R.H. Meloen

Central Veterinary Institute, P.O. Box 65, 8200 AB Lelystad, The Netherlands

Introduction

In our search for a synthetic vaccine for foot and mouth disease virus (FMDV) we succeeded in locating epitopes of neutralizing monoclonal antibodies by the use of the PEPSCAN method [1]. One of them (MAb 18) was located on the surface protein VP_1 and was shown to react with a sequence eight amino acids in length, YKQKIIAP. Six amino acids were shown to be essential for and/or to contribute to binding. The octapeptide is as active as the virus itself in a competition assay with MAb 18; however, linear peptides spanning this region are hardly able to raise antibodies with antiviral activity. Because these antibodies did not show a specificity similar to that of MAb 18, we suggested that the peptides should be presented to the immune system in a different way. We speculated that by changing length or structure of the peptide the antibody specificity might be improved.

With linear 13-residue peptides it was possible to raise more potent antiviral antibodies. The specificity of these antibodies appeared to be changed when compared with the less potent antibodies of the octapeptides [2], but still differed from that of MAb 18. Here we report results with a cyclic peptide suggesting that it is possible to improve the response against the virus by manipulating the specificity of the antibodies.

Results and Discussion

The peptides Ac-YKQKIIAP-NH_2, Ac-CYKQKIIAP-NH_2 and the cyclic Ac-CYKQKIIAPC-NH_2 were used for vaccination of rabbits as indicated in Table 1. The antiserum of the nonconjugated cyclic peptide showed, in contrast to antisera of linear peptides, a modest peptide ELISA titer and an antivirus response of similar magnitude. Vaccination with this cyclic peptide is our first example where antipeptide antibodies are generated as effective against the parent peptide

Table 1 *Serological data and specificity of antisera*

Antiserum against	Link[a]	Peptide ELISA[b]	Virus ELISA	Ratio[c]	Specificity
Virus (MAb 18)	-	5.2–5.5	6.3–7.5	30	Y.QKI.AP
YKQKIIAP	GDA	5.7	2.2	0.0003	--------
CYKQKIIAP	MBS	5.3–6.3	1.8–2.9	0.0003	------AP
CYKQKIIAPC	-	2.1	1.9	1	----IIAP
└──────┘	-	2.6	3.0	2	---KIIAP

[a] Linking agent used for coupling to KLH; - indicates no coupling.
[b] YKQKIIAP.
[c] Virus ELISA/peptide ELISA. ELISA values are expressed as -Log (serum dilution) at 50% of the maximum extinction. Peptides are all acetylated at the N-terminus and in the amide form at the C-terminus.

as against the virus itself for this particular antigenic site (Table 1). When testing the specificity of the antibodies in replacement sets of peptides, we found these antisera to be specific for more amino acid residues than the linear analogs (including residues that appear to be important for the recognition by MAb 18). This brings the specificity of the cyclic peptide closer to the specificity of the MAb 18.

We speculate that the increase of the antivirus response is reflected by the improvement of the antipeptide specificity. If this speculation holds, a further step has been taken toward the rational design of peptide vaccines.

References

1. Meloen, R.H., Puijk, W.C., Meijer, D.J.A., Lankhof, H., Posthumus W.P.A. and Schaaper, W.M.M., J. Gen. Virol., 68 (1987) 305.
2. Schaaper, W.M.M., Lankhof, H., Meijer, D.J.A., Puijk, W.C. and Meloen, R.H., In Theodoropoulos, D. (Ed.) Peptides 1986, Walter de Grüyter, Berlin, in press.

Mimicking protective epitopes of foot and mouth disease virus with synthetic peptides

A.Yu. Surovoy, O.M. Vol'pina, V.M. Gelfanov and V.T. Ivanov
Shemyakin Institute of Bioorganic Chemistry, U.S.S.R. Academy of Sciences, 11781 Moscow, U.S.S.R.

Introduction

Relatively short 16 to 21-membered segments of a surface foot and mouth disease viral VP_1 protein were successfully used for preparation of respective experimental vaccines [1, 2]; however, in order to produce the desired effect the peptides had to be conjugated to a protein carrier (keyhole limpet hemocyanin, KLH). In this work, by a slight shift of the peptide segment along the VP_1 amino acid sequence, we selected and accordingly synthesized a series of peptides capable of eliciting the antiviral response in a free, nonconjugated state.

Results and Discussion

The 144–159, 145–159, 149–152, 141–152, 141–148, 136–148, and 136–152 (strain O_1K) and 131–149, 131–139, and 140–149 (strain A_{22}) segments were synthesized by the classical solution method. For all these peptides immunogenicity, antigenicity, and ability to induce virus-neutralizing response and protection in a variety of laboratory animals and cattle were investigated (Table 1). In contrast with the results obtained by Pfaff et al. [2] the 144–159 peptide conjugated to KLH as well as KLH-conjugates of peptides 141–152, 141–148, 145–159 (strain O_1K) were inactive in all in vitro and in vivo virus-inhibiting experiments. On the other hand, synthetic 136–148, 136–152 O_1K sequences as well as 131–149 and 140–149 A_{22} sequences afforded 50–100% protection both in the free state and in conjugation with KLH.

Immunogenicity of free 136–152 peptide from O_1K was studied in various mice strains. High titers of *anti*-136–152 could be obtained after immunization of BALB/c, C3H, and CBA/J mice with a nonconjugated peptide. Antibody response against 136–152 could be induced in nonresponder C57BL/6 mice by immunization with a peptide coupled to a carrier protein. This suggests that the selected regions of aphtovirus contain both the B-cell and T-cell determinants and that antibody response to this region is under the Ir-gene restriction.

In an attempt to determine more accurately the limits of the antigenic region

Table 1 *Antibody response and protection of rabbits and guinea pigs induced by different peptides from O_1K and A_{22} sequences*

Immunogen	Strain	Rabbits		Guinea pigs	
		Antipeptide titer, $\log_{10}$	Serum-neutralizing titer, $\log_2$	Serum-neutralizing titer, $\log_2$	Protection
144–159 KLH	O_1K	4.4	<1.0	<1.0	0/5
136–152 KLH	O_1K	4.4	4.1 –6.0	1.66	4/5
136–152	O_1K	4.1–5.0	2.1 –3.7	1.5	5/5
136–148 KLH	O_1K	4.1	2.1 –3.7	1.0	2/4
136–148	O_1K	4.1	2.5 –3.7	1.0	3/5
Vaccine	O_1K	–	6.5	3.5	5/5
131–149 KLH	A_{22}	4.0–4.4	4.25–5.0	4.2	3/4
131–149	A_{22}	<1.0	<1.0	4.0–4.5	4/5
131–139 KLH	A_{22}	4.0	<1.0	<1.0	0/5
131–139	A_{22}	<1.0	<1.0	<1.0	0/5
140–149 KLH	A_{22}	4.0	4.0 –4.76	–	–
140–149	A_{22}	<1.0	<1.0	3.0	3/4
Vaccine	A_{22}	–	6.5	3.8	4/5

we investigated inhibition of binding of the 136–152 peptide with *anti*-O_1K antibodies by different synthetic fragments. The minimal segment still possessing antigenic activity was 141–148, which only partially agrees with the conclusion of Geysen et al. [3] where the minimal antigenic site was formulated as 146–152.

Experiments with cattle are presently being carried out. In the first series animals were immunized with A_{22} peptides in the free form and coupled to KLH at a dose of 1 mg and boosted with the same dose after 40 days. Immunization induced high levels of virus neutralizing antibodies and protected the animals from the lethal infection. Immunization with the free, but not KLH-conjugated, 136–152 O_1K peptide induced virus-neutralizing antibodies. At the same time both preparations were unable to protect cattle from the disease.

References

1. Bittle, J.L., Houghten, R.A., Alexander, H., Shinnic, T.M., Sutcliffe, J.G., Lerner, R.A., Rowlands, D.J. and Brown, F., Nature, 298 (1982) 30.
2. Pfaff, E., Mussgay, M., Bohm, H.O., Schulz, G.E. and Schaller, H., EMBO J., 1 (1982) 869.
3. Geysen, H.M., Barteling, S.J. and Meloen, R.H., Proc. Natl. Acad. Sci. U.S.A., 82 (1985) 178.

Characterization of antibody binding sites using peptides synthesized on aminomethyl-resin

Wan-Jr Syu and Lawrence Kahan
Department of Physiological Chemistry, University of Wisconsin, Madison, WI 53706, U.S.A.

Introduction

Epitope characterization is an inevitable task for understanding antibody–antigen interactions. We describe a method to characterize epitopes based on the use of polymer-bound peptides.

Two immunoreactive segments of *E. coli* ribosomal protein S13 were synthesized (Fig. 1A). The first Boc-amino acid was manually coupled to aminomethyl-resin (Peninsula). The derivatized resin was extended by automated synthesis (Applied Biosystems). Side-chain protecting groups used were: benzyl for Thr, Ser, Asp, Glu; tosyl for Arg, His; 2-bromobenzyloxycarbonyl for Tyr; benzyloxycarbonyl for all Lys residues except Lys^{117}; and 2-chlorobenzyloxycarbonyl for Lys^{117}. Peptide-resin (10 mg) was removed after each coupling cycle and deprotected with boron tris(trifluoroacetate) (Pierce) [1]. The 2-Cl-benzyloxycarbonyl used on Lys^{117} and the 2-bromobenzyloxycarbonyl used on Tyr^{22} were not completely removed by boron tris(trifluoroacetate); however, they were used because of the known higher stability during synthesis and lack of contribution of the corresponding residues to monoclonal antibody (MAb) binding (unpublished results).

Peptide-resin samples were blocked with 10% calf serum, 10% bovine serum albumin, 1% Tween 20 in Tris/NaCl (0.1 M Tris, 0.15 M NaCl, pH 7.5), incubated with MAbs overnight at 4°C, washed with Tris/NaCl/0.05% Tween 20, incubated with alkaline phosphatase-conjugated goat antimouse IgG, washed again, and developed with *p*-nitrophenyl phosphate. Peptides were regenerated by treating with 8 M urea/0.1% sodium dodecyl sulfate/0.1% 2-mercaptoethanol.

Results and Discussion

Three MAbs to *E. coli* ribosomal protein S13, MAbs 19, 20, and 21, react with a C-terminal 34-residue fragment. Evidence from chemical modification suggested MAbs 19, 20, and 21 reacted with an epitope near the C-terminal of S13. A 23-residue peptide corresponding to the C-terminal of S13 was synthesized and the reaction of the growing peptide with these MAbs was

S13 C-terminal

P-V-R-G-Q-R-T-K-T-N-A-R-T-R-K-G-P-R-K-P-I-K-K— $NHCH_2$
95 100 105 110 115

A

S13 N-terminal

A-R-I-A-G-I-N-I-P-D-H-K-H-A-V-I-A-L-T-S-I-Y—$NH(CH_2)_3CONHCH_2$
1 5 10 15 20

← Direction of peptide synthesis

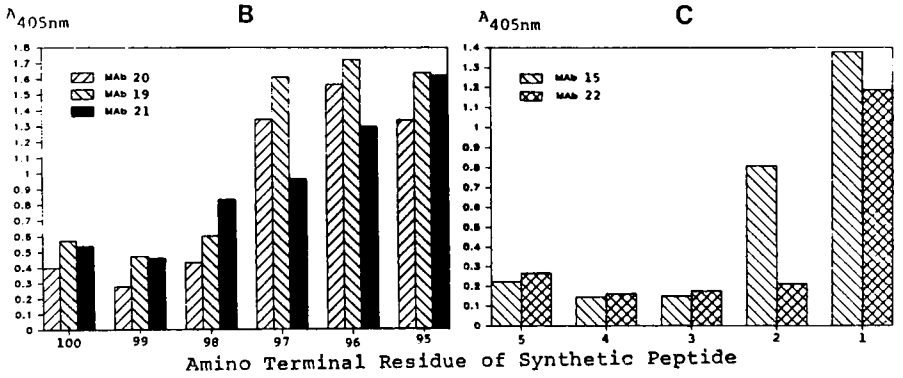

Fig. 1. (A) sequences of synthetic peptides; (B) binding of S13 C-terminal directing MAbs; (C) binding of S13 N-terminal directing MAbs. The (p)-nitrophenol product generated in the immunoassay was monitored by A_{405}. Binding to peptides of shorter length was similar to the lowest levels as shown. A single 4-aminobutyric acid residue was coupled to the resin before Tyr^{22} as a spacer.

determined. Binding of MAbs 19 and 20 increased as Arg^{97} was added (Fig. 1B), indicating the contribution of Arg^{97} to the MAb–epitope interaction. The addition of two more residues did not increase the binding of MAbs 19 and 20, suggesting the last 21 residues contain all the amino acids involved in the MAb interaction. MAb 21 bound to the C-terminal 20-residue peptide but more strongly to longer peptides. These results suggest Gly^{98}, Arg^{97}, Val^{96} and Pro^{95} affect the epitope structure.

Two MAbs directed toward the N-terminal 22 residues of S13 were similarly characterized (Fig. 1C). MAb 22 required the presence of the N-terminal residue of S13, while MAb 15 showed some binding to the peptide consisting of S13 residues 2–22.

The advantages of this approach derive from the use of sequential samples from a single synthesis and the reutilization of peptide-resin for characterization of a series of MAbs.

Acknowledgements

Supported by NIH Grant GM 22150 and NSF Grant DMB 8514305.

References

1. Geysen, H.M., Meloen, R.H. and Barteling, S.J., Proc. Natl. Acad. Sci. U.S.A., 81 (1984) 3998.

Session IX
Growth factors / oncogenes

Chair: James P. Tam
The Rockefeller University
New York City, New York, U.S.A.

Structure–activity studies of transforming growth factor

James P. Tam
The Rockefeller University, 1230 York Avenue, New York, NY 10021, U.S.A.

Introduction

Transforming growth factor type α (TGFα) and epidermal growth factor (EGF) are small proteins [1–4] of about 50 amino acids. They are characterized by their potent mitogenicity and their importance for the maintenance of growth and proliferation of mammalian cells in both normal and abnormal states. EGF is found abundantly in the submaxillary gland and is a growth factor for normal physiological functions; however, TGFα has been associated only in oncofetal states and may be an autocrine factor for rapid proliferative tissues. TGFα and EGF are secreted extracellularly as discrete soluble factors, but homologous sequences are found as domains in a diverse group of proteins that play important roles in cellular differentiation and proliferation. Proteins containing TGFα/EGF-like domains include blood coagulation factors, complements, DNA-virus gene products, and extracellular matrix [5]. The functions and biological activities of these growth factor-like domains remain unclear.

Both EGF and TGFα bind to a single class of cell surface receptor in vitro [1–3] in eliciting similar biological responses such as stimulation of tyrosine-specific protein kinase and induction of anchorage-independent growth of indicator cells in soft agar; however, they are derived from different gene products and biosynthetic processing.

To understand the relationships between the chemical structures of these growth factors and their biological properties, we used solid phase peptide synthesis to produce these growth factors, their structural variants, and shortened analogs. Our results showed that full biological activity of these growth factors required a tertiary structure maintained by the 3 disulfide pairs. Shortened analogs or extended structures without the disulfide restraint greatly reduced biological activity. Several shortened analogs, however, showed partial agonist activity and may provide useful leads to the design of therapeutic agents.

Results and Discussion

Growth factor synthesis

Recent improvements in many aspects of the solid phase methodologies have

generally facilitated the synthesis of a complex peptide such as TGFα [6]. One of the improvements is the low-high HF deprotection procedure that allows an efficient and mild condition for the removal of all protecting groups [7]. The low-high HF procedure consists of two steps in a one-pot reaction. Under the low HF condition, all of the oxygen-linked benzyl protecting groups, N^{i}-formyl of Trp and sulfoxides of protected cysteine and methionine are smoothly converted to their deprotected forms in one single operation that minimizes the formation of carbocations and hence, the alkylation side products. The continuation of the high HF reaction then removes sulfur-linked protecting groups of Cys and Arg. Thus, the low-high HF procedure combines 3 conventional steps [HF cleavage, base treatment of Trp(For), and aqueous thiol reduction of Met(O)] into a one-step reaction. Using this procedure, the syntheses of fully biologically active murine EGF and rat and human TGFα were achieved [8–10]. Furthermore, because the low-high HF procedure provided an efficient method for the deprotection of cysteinyl-containing peptides, it was used for the synthesis of human TGFα analogs for this structure–activity study.

Biological activities of synthetic TGFα

Synthetic TGFα was generally found to be as active as EGF in stimulation of anchorage-independent growth of normal rat kidney fibroblasts in culture, inhibition of histamine-stimulated gastric acid secretion, and stimulation of plasminogen activator production [9, 10]; however, the primary in vitro assays for TGFα have been the mitogenic and radioreceptor assay for the competition of [^{125}I]EGF for receptor binding in formalin-fixed A431 cells. Since a good correlation between mitogenicity and the radioreceptor assay was obtained, the latter assay was used for screening biological activities in the present study.

Structure–activity study of human TGFα

Structurally, the TGFα-EGF family is distinguished by the placement of their 6 cysteinyl residues that form the 3 disulfide loops. The first 4 cysteinyl residues form a fused ring of the first and second loop (A- and B-loop, Fig. 1) and the last 2 cysteinyl residues form the third loop (C-loop, Fig. 1). For the structure-activity studies, overlapping linear peptides containing 7 to 17 residues covering the whole molecule of TGFα (residues 1–50, TGFα-peptides: [1–9], [9–16], [16–21], [8–21], [21–32], [16–32], [34–43] and [34–50]) were synthesized and tested for their radioreceptor competing activity in A431 cells. None of these linear analogs were found to show significant radioreceptor competing activity at concentrations lower than 1 mM.

Since the linear synthetic fragments of TGFα were found to be inactive, our attention was then turned to fragments that contain disulfide linkages. These include synthetic fragments: (1) with only 1 disulfide linkage such as loop A (residues are represented in parentheses, 8–21), B (16–32) and C (34–43); (2)

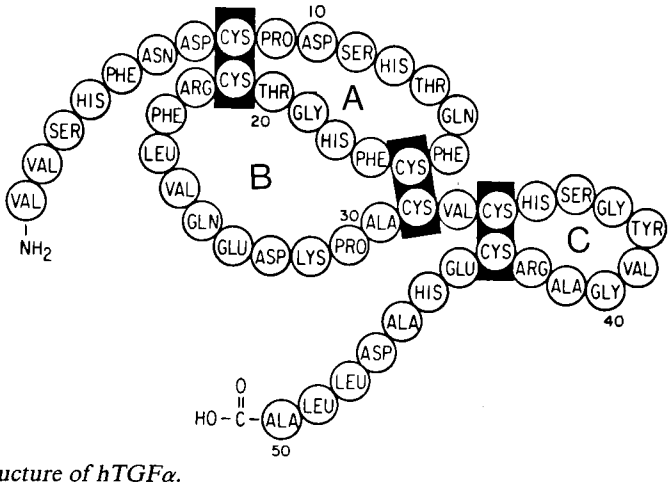

Fig. 1. Structure of hTGFα.

with 2 disulfide linkages – loop AB (8–32) and BC (16–43); and (3) with 3 disulfide linkages – loop ABC (8–50). Synthetic peptides of loops B or C showed no significant competing activity in the EGF-radioreceptor assay even in high concentrations (10^5-fold > TGFα); however, synthetic peptides containing loop A were found to be more promising and showed weak competing activity at the submicromolar level (Table 1). Peptides containing 2 disulfide linkages such as loops AB and BC showed strong activities at a range of 50–400 μM and at an effective concentration of 0.01% of TGFα. The shortened TGFα analog containing all 3 disulfide loops, TGFα-(8–50), was found to be 10–30% as active as TGFα. Taken together, these results suggest the spatial arrangements of different groups defined by the tricyclic structure of TGFα are responsible for its potency but a fragment containing loop A may have the necessary determinants for biological activities.

Previous structure–activity studies by others on EGF and rat TGFα have shown 2 regions that exhibit low but distinct activities: a portion of the B-loop in murine EGF (residue (22–31) and the C-loop of rat TGFα [11, 12]. These corresponding fragments in human TGFα were found to be inactive in both the receptor binding and the mitogen assays at a concentration of 1 mM; however, it is necessary to point out that the EGF and TGFα B-loop fragment share little common sequence homology.

Antigenic site of TGFα

The development of antibodies against TGFα would provide a possibility to obtain information concerning the tertiary structure from the internal imaging

Table 1 *Structure–activity of shortened analogs of human TGFα*

TGFα	Disulfide loop	Binding A431 IC_{50} (μM)[a]
H-(1–50)-OH	TGFα	0.01
H-(8–50)-OH	[ABC-loop]	0.03
H-(16–50)-OH	[BC-loop]	300
H-(34–50)-OH	[C-loop]	>10,000
H-(8–43)-OH	[ABC-loop]	0.1
H-(8–32)-OH	[AB-loop]	300
H-(16–43)-OH	[BC-loop]	400
H-(8–21)-NH_2	[A-loop]	4,000
H-(16–32)-NH_2	[B-loop]	>10,000
H-(34–43)-NH_2	[C-loop]	>10,000

[a] IC_{50} inhibition of binding of 3 nM [^{125}I]EGF to A431 cells.

of the antigen–antibody interactions. Of the 3 disulfide loops of TGFα and EGF (A, B and C, Fig. 1) the B-loop represents the longest of the 3, with 17 residues. Previous studies by others have shown that the antigenic site of polyclonal antibody raised against EGF is confined to a portion of the B-loop [11]. Recently, we have also raised polyclonal and monoclonal antibodies against human and rat TGFα. Using synthetic peptide fragments covering the entire molecule of TGFα to map the antigenic site, we found that the major immunodominant epitope of all TGFα-specific antibodies was confined to the B-loop. It has been demonstrated that the segmental motility of a protein correlates with the antigenicity [13]. Thus, it is not surprising that the immunodominant epitope lies within the longest loop of TGFα (B-loop) that has the greatest segmental mobility. Our data show that the B-loop is the most exposed and flexible loop of the TGFα-EGF family. Interestingly, the B-loop is also found to be the least homologous and longest of all 3 loops in other members of the TGFα-EGF family, which includes domain portions of a diverse group of proteins and provides a more suitable candidate for the development of a specific antiserum using a synthetic peptide than the previous suggested region containing the C-loop [11]. An antibody specific for the B-loop will be most desirable and will greatly minimize the possibility of cross-reaction to EGF. Indeed, our results confirmed that the polyclonal and monoclonal antibodies specific to the B-loop did not show cross-reactivity with EGF even at a high concentration.

Conclusion

Potent biological activity of human TGFα requires multiple disulfide restraint, but weak receptor binding activity is observed from the A-loop alone. The major

immunodominant epitope, however, is contained in the B-loop. Further refinements of the A-loop may lead to increased potency.

Acknowledgements

This work was supported by PHS Grant No. CA36544, awarded by the National Cancer Institute, and DHHS.

References

1. DeLarco, J.E. and Todaro, G.J., Proc. Natl. Acad. Sci. U.S.A., 75 (1978) 4001.
2. Marquardt, H., Hunkapiller, M.W., Hood, L.E., Twardzik, D.R., DeLarco, J.R. and Todaro, G.J., Proc. Natl. Acad. Sci. U.S.A., 80 (1983) 4684.
3. Derynck, R., Roberts, A.B., Winkler, M.E., Chen, E.Y. and Goeddel, D.V., Cell, 38 (1984) 297.
4. Savage, Jr., C.R., Inagami, J. and Cohen, S., J. Biol. Chem., 247 (1972) 7612.
5. Blomquist, M.C., Hunt, L.T. and Barker, W.C., Proc. Natl. Acad. Sci. U.S.A., 81 (1984) 7363.
6. Merrifield, R.B., Science, 232 (1986) 341.
7. Tam, J.P., Heath, W.F. and Merrifield, R.B., J. Am. Chem. Soc., 105 (1983) 6442.
8. Tam, J.P., Marquardt, H., Rosberger, D.F., Wong, T.W. and Todaro, G.J., Nature, 309 (1984) 376.
9. Heath, W.F. and Merrifield, R.B., Proc. Natl. Acad. Sci. U.S.A., 83 (1986) 6367.
10. Tam, J.P., Shiekh, M.A., Salomon, D.S. and Osowski, L., Proc. Natl. Acad. Sci. U.S.A., 83 (1986) 8082.
11. Komoriya, A., Hortsch, M., Meyers, C., Smith, M., Kanety, H. and Schlessing, J., Proc. Natl. Acad. Sci. U.S.A., 81 (1984) 1351.
12. Nestor, Jr., J.J., Newman, S.R., DeLustro, B.M., Todaro, G.J. and Schreiber, A.B., Biochem. Biophys. Res. Commun., 129 (1985) 226.
13. Westhof, E., Altschuh, S., Moras, D., Bloomer, A.C., Mondragon, A., Klug, A. and Van Regenmortel, M.H.V., Nature, 311 (1984) 123.

Peptide substrates and inhibitors of *N*-myristoyl transferase

Shad R. Eubanks[a], Derek S. Towery[a], Foe S. Tjoeng[a], Steven P. Adams[a], Dwight A. Towler[b], Emily Jackson-Machelski[b], Luis Glaser[b] and Jeffrey I. Gordon[b]

[a]Monsanto Company, 700 Chesterfield Village Pkwy., St. Louis, MO 63198, U.S.A.
[b]Washington University School of Medicine, 660 S. Euclid, St. Louis, MO 63110, U.S.A.

Introduction

The covalent attachment of fatty acids to specific cellular proteins in eukaryotes is a well-established phenomenon. Acyl proteins can be broadly categorized into two groups, proteins in which a fatty acid is linked to the protein through an ester or thioester linkage and proteins modified by amide-linked fatty acid. The specific amino acid residues that are fatty acylated in proteins through amide linkage have been documented for only a few proteins; however, amidation by myristic acid appears to occur exclusively on amino-terminal glycine residues. Moreover, fatty acids other than myristic acid are not found linked to amino-terminal glycine [1]. Four of the known *N*-myristoyl proteins - $p60^{src}$, cyclic AMP-dependent protein kinase catalytic subunit, calcineurin B-subunit, and murine leukemia virus gag-abl fusion protein [2] - are either protein kinases or a regulator of a phosphoprotein phosphatase (calcineurin). It has been shown recently that when avian cells are infected by Rous sarcoma virus (a transforming retrovirus), myristoylation of the viral p60 protein is required for membrane association and expression of the transforming potential of the protein, and, thus, of the virus [3]. In this report, we describe synthetic peptides that serve as effective substrates for the enzyme, *N*-myristoyl transferase (NMT), that transfers myristic acid to N-terminal glycine residues. Furthermore, we have characterized the structural requirements for substrate activity and have discovered a series of enzyme inhibitors.

Results and Discussion

A model substrate peptide (**1**) was derived in part from the N-terminal sequence of cyclic AMP-dependent protein kinase:

Gly-Asn-Ala-Ala-Ala-Ala-Arg-Arg **(1)**

An in vitro assay was developed [4] that measures the transfer of radioactive myristic acid from myristoyl CoA to the amino-terminal glycine of the synthetic peptide (**1**). The acyl peptide was identified by reversed-phase HPLC and quantitated in kinetic experiments by scintillation counting. Utilizing this assay, *N*-myristoyl transferase (NMT) was purified 80-fold from a protease-deficient strain of *S. cerevisiae* (JR 153). This preparation was suitable for experiments designed to determine the enzyme's substrate specificity; results were identical to those obtained with homogenous 11,000-fold purified enzyme.

The only conclusion about substrate activity suggested by the sequences of known myristoyl proteins was the apparent requirement for an N-terminal glycine. Systematic variation of the N-terminal residue confirmed this conclusion. As can be seen in Table 1, replacement of Gly-1 by alanine (**2**), D-alanine (**3**), β-alanine (**4**), sarcosine (*N*-methylglycine, **5**) or propionate (**6**) resulted in analogs that were inactive. This result suggested that a sterically unencumbered primary amino group is required for productive binding. Variation of the 2-position resulted in some very interesting analogs. While neutral hydrophilic residues were tolerated (**7**, **8**), D-amino acids (**9**) and negatively charged residues (**10**) did not bind the enzyme. On the other hand, when Asn-2 was substituted with hydrophobic amino acids, very impotent substrate analogs (**11**) or pure competitive inhibitors (**12–14**) were obtained. Significant alterations in the 3-(**15–17**, **23**) and the 4-position (**24**) of the peptide proved to be acceptable. Significantly, replacement of Ala-5 by Ser (**18**) resulted in a dramatic decrease in K_m, while substitution by Asp (**19**) afforded an inactive analog. Phe-5 (**20**) had little effect on the apparent K_m, but dramatically decreased the relative V_{max}. To begin to develop ideas about the conformation of the peptide in the active site, proline substitutions were examined and entries **22–26** demonstrate that only positions 3 and 4 tolerated proline.

The N-terminal octapeptide fragments corresponding to the known myristoylated proteins $p60^{src}$ (**27**), calcineurin B-subunit (**28**), and cytochrome *b*5 reductase (**29**) were synthesized and shown to be efficient substrates in vitro for NMT. Based upon the foregoing data, it is possible to suggest a consensus peptide sequence that may predict from DNA sequence information whether proteins will be myrisoylated. For example, the HTLV III gag gene encodes a surface protein known to be important for viral budding and transmission. The known DNA sequence of the HTLV III gag gene locus predicts an N-terminal octapeptide sequence Gly-Ala-Arg-Ala-Ser-Val-Ser-Gly following removal of methionine required for translation initiation. The crucial 1-, 2- and 5-positions have acceptable residues and, indeed, the peptide (**30**) is an efficient substrate for NMT. Taken together, the data predict that its gag protein will in fact be myristoylated.

Myristoylation is an important co-translational modification that is known to be essential in a model of transformation and is believed to be involved

Table 1 *Peptide substrate specificity of yeast* N-*myristoyl transferase*

	Peptide	K_m [mM]	V_{max} [%]	K_i [mM]
	1 2 3 4 5 6 7 8			
1	Gly-Asn-Ala-Ala-Ala-Ala-Arg-Arg-NH_2	0.06	100	
2	Ala-	–	–	–
3	D-Ala-	–	–	–
4	β-Ala-	–	–	– (+/–)
5	Sar-	–	–	– (+/–)
6	Prp-	–	–	– (+/–)
7	-Gln-	0.07	79	
8	-Ser-	1.7	50	
9	-D-Asn-	–	–	–
10	-Asp-	–	–	–
11	-Leu-	0.3	5	0.06
12	-Tyr-	–	–	0.16
13	-Phe-	–	–	+
14	-ChA-	–	–	+
15	-Glu-	1.8	47	
16	-Arg-	0.43	75	
17	-Phe-	0.6	121	
18	-Ser-	0.0001	3	0.00002
19	-Asp-	–	–	–
20	-Phe-	0.085	4	
21	-Ser- -Ser-	0.003	34	
22	-Pro-	–	–	–
23	-Pro-	0.5	8	
24	-Pro-	0.3	60	
25	-Pro-	–	–	–
26	Gly-Ser-Ser-Lys-Ser-Pro	–	–	–
27	Gly-Ser-Ser-Lys-Ser-Lys-Pro-Lys	0.04	43	
28	Gly-Asn-Glu-Ala-Ser-Tyr-Pro-Leu	2.3	55	
29	Gly-Ala-Gln-Leu-Ser-Thr-Leu-Gly	0.003	23	
30	Gly-Ala-Arg-Ala-Ser-Val-Ser-Gly	0.43	121	

All peptides are C-terminal amides synthesized on *p*-methylbenzhydrylamine resin by the Merrifield solid phase method. Peptides were deprotected using HF and were purified by reversed-phase HPLC. V_{max} expressed as percent of maximal rate for the parental peptide (**1**).
+ Signifies peptide was inhibitor but K_i was not measured; +/– indicates weak competitive inhibitor; Sar, sarcosine; Prp, propionyl; ChA, cyclohexylalanine.

in the activity of certain retroviruses. It is an intriguing possibility that manipulation of NMT in vivo may have therapeutic utility in such disease states. This work has begun to characterize the substrate requirements of yeast NMT, and it has produced peptides that are potent substrates and inhibitors of NMT

in vitro. These peptides may prove useful in exploring the cell biology of NMT and its potential as a therapeutic target.

References

1. Towler, D. and Glaser, L., Biochemistry, 25 (1986) 878.
2. Schultz, A. and Oroszlan, S., Virology, 133 (1984) 431.
3. Kamps, M.P., Buss, J.E., and Sefton, B.M., Cell, 45 (1986) 105.
4. Towler, D. and Glaser, L., Proc. Natl. Acad. Sci. U.S.A., 83 (1986) 2812.

Analysis of the interaction of IGF I and structural mutants of IGF I with the IGF types 1 and 2 and insulin receptors

Margaret A. Cascieri, Gary G. Chicchi, Barbara G. Green, Joy Applebaum, Nancy S. Hayes and Marvin L. Bayne

Merck Sharpe & Dohme Research Laboratories, Box 2000, Rahway, NJ 07065, U.S.A.

Insulinlike growth factor I (IGF I) is a 70-amino acid peptide with remarkable sequence homology to insulin. A model for the three-dimensional structure of IGF I has been proposed by Blundell et al. which is based on this structural homology [1, 2]. IGF I binds to the types 1 and 2 IGF receptors (IGF-R1 and IGF-R2) [3] and human serum binding proteins (hBP) [4] with high affinity. IGF I cross-reacts weakly at the insulin receptor (IR) [3]. Substitution of leucine or serine for residues 24 or 25 in the B-chain of insulin results in a dramatic loss of potency at the IR [5–7]. Site-directed mutagenesis of a synthetic gene encoding IGF I [8] has been employed to test the importance of the homologous region of IGF I in maintaining high-affinity binding to IGF-R1, IGF-R2, and hBP.

Results

The wild-type gene and the mutants were expressed in yeast using the α-1 mating factor signal sequence to direct secretion of the peptides. The peptides were purified from conditioned media by Biorex-70, Biogel P10 and C18 reversed-phase chromatography. The purity of the peptides was determined by PAGE followed by gold staining. The recombinantly derived IGF I and IGF I purified from human serum (from Dr. R.E. Humbel) are equipotent at IGF-R1 and hBP. Wild-type IGF I, which has the sequence Phe-Tyr-Phe at positions 23, 24 and 25, and [Phe23, Phe24, Tyr25] IGF I, in which the sequence is identical to the homologous region of insulin, are equipotent at IGF-R1 (Table 1). This peptide is similar to IGF I at the IGF-R2, IR, and hBP.

[Leu24] IGFI and [Ser24] IGF I are 32- and 17-fold less potent than IGF I at IGF-R1, respectively (Table 1). These peptides have 10- and 2.2-fold reduced potency at IR; however, [Leu24] IGF I, [Ser24] IGF I, and IGF I are equipotent at IGF-R2 and hBP.

IGF I, [Phe23, Phe24, Tyr25] IGF I, [Leu24] IGF I, and [Ser24] IGF I stimulate DNA synthesis in rat A10 vascular smooth muscle cells with $ED_{50} = 2.5$ nM,

Table 1 *Modification of residues 23–25 of IGF I – Effects on binding to IGF-R1, IGF-R2, IR, and hBP*

Peptide	IC_{50}[a]			
	Human placental IGF-R1 (nM)	Rat liver IGF-R2 (μM)	Human placental IR (μM)	Acid-stable hBP (nM)
IGF I	5.6 ± 0.8	0.3 ± 0.2	2.8 ± 1	0.48 ± 0.02
[Phe23,Phe24,Tyr25] IGF I	7.7 ± 0.8	0.1 ± 0.04	1.5 ± 0.3	1.2 ± 0.4
[Leu24] IGF I	180 ± 10	0.9 ± 0.6	29 ± 4	0.45 ± 0.02
[Ser24] IGF I	95 ± 6	0.6 ± 0.2	6.2 ± 0.7	0.45 ± 0.02

[a] Mean ± S.D., n = 2.

2 nM, 18 nM and 10 nM, respectively. Thus, their potencies reflect their respective affinities for the IGF-R1.

Discussion

These data show that the aromatic residue 24 of IGF I is important for maintaining affinity for the IGF-R1 and the IR. In contrast, analogs in which serine or leucine are substituted for tyrosine 24 have normal affinity for the IGF-R2 and hBP. Thus, these mutations apparently do not destabilize the tertiary structure of IGF I. Therefore, the structural determinants required for binding to the IGF-R2 and hBP are clearly different than those required for binding to the IGF-R1 and IR.

References

1. Blundell, T.L., Bedarker, S., Rinderknecht, E. and Humbel, R.E., Proc. Natl. Acad. Sci. U.S.A., 75 (1978) 180.
2. Blundell, T.L., Bedarkar, S. and Humbel, R.E., Fed. Proc., 42 (1983) 2592.
3. Rechler, M.M. and Nissley, S.P., Annu. Rev. Physiol., 47 (1985) 425.
4. Baxter, R.C., Adv. in Clin. Chem., 25 (1986) 49.
5. Tager, H., Thomas, N., Assoian, R., Rubenstein, A., Saekow, M., Olefsky, J. and Kaiser, E.T., Proc. Natl. Acad. Sci. U.S.A., 77 (1980) 3181.
6. Kobayashi, M., Haneda, M., Maegawa, H., Watanabe, N., Takada, Y., Shigeta, Y. and Inouye, K., Biochem. Biophys. Res. Comm., 119 (1984) 49.
7. Kobayashi, M., Ohgaku, S., Iwasaki, M., Maegawa, H., Shigeta, Y. and Inouye, K., Biochem. J., 206 (1982) 597.
8. Bayne, M.L., Cascieri, M.A., Kelder, B., Applebaum, J., Chicchi, G.G., Shapiro, J.A., Pasleau, F. and Kopchick, J.J., Proc. Natl. Acad. Sci. U.S.A., 84 (1987) 2638.

Conformational studies of N-terminal segments of *ras* p21 proteins

Chien-Hua Niu, Kyouhoon Han and Peter P. Roller
Laboratory of Experimental Carcinogenesis, NCI, NIH, 37/3C-28, Bethesda, MD 20892, U.S.A.

A number of human and rodent tumors contain activated *ras* genes capable of inducing a morphological and tumorigenic transformation of the NIH 3T3 cell line. The proteins encoded by the *ras* gene family are structurally and immunologically related and have molecular weights of approximately 21,000. These proteins become oncogenic when particular amino acid substitutions occur at either position 12, 13, 59, or 61. Binding of the p21 protein with GTP may initiate the cascade of events that results in tumorigenic transformation [1, 2]. To examine the conformational difference between 'nontransforming' and 'transforming' p21 proteins, two 34-amino acid residue (residue 2–35) N-terminal segments [T-E-Y-K-L-V-V-V-G-A-G(or V)-G-V-G-K-S-A-L-T-I-Q-L-I-Q-N-H-F-V-D-E-Y-D-P-T], one having glycine and the other having valine at position 12, were synthesized.

Nucleotide triphosphate binding to the two synthetic peptides was examined using the following methods: (1) *NMR spectroscopy*. Upon addition of either the Gly-peptide or Val-peptide to solutions containing GTP or ATP, the line widths of all 3 P-31 NMR signals were broadened, and all 3 phosphate resonances simultaneously shifted downfield. These results imply that a complex is formed between the peptide and nucleotides, in which the free nucleotide is in fast exchange with the bound form. (B) *Equilibrium dialysis experiments*. The binding constants obtained for the Gly-peptide and Val-peptide with GTP are 4.9×10^6 and 6.5×10^6 M^{-1}, respectively, and provide further evidence for complex formation between the nucleotides and peptides. The binding constants of the Gly-peptide and Val-peptide with GTP are 2 orders of magnitude less than those of intact p21 proteins [3]. This difference may be due to the preferential hydrogen bonding occurring between guanine and amino acid residues in the C-terminal region of p21 [4].

Peptide conformational changes upon nucleotide binding were studied by circular dichroism (CD) spectroscopy using Provencher's statistical computer program [5]. The Gly-peptide adopted a mainly β-sheet conformation (51%) in Tris buffer. When GTP was added, the conformation of this peptide shifted to a mainly random coil structure with a small increase in the amount of α-

Table 1 *Secondary structure of the Gly-peptide and Val-peptide with or without nucleotide triphosphate present*

Nucleotide	α-Helix (%)	β-Sheet (%)	Random coil (%)
A. Gly-peptide in Tris buffer			
No nucleotide	0	51 (1.2)	49 (1.2)
GTP	8 (1.4)	32 (2.5)	60 (2.6)
ATP	0	68 (4.5)	32 (4.5)
B. Val-peptide in ammonium acetate buffer			
No nucleotide	13 (0.3)	39 (0.7)	48 (0.6)
GTP	19 (0.5)	35 (0.9)	46 (0.6)
ATP	9 (1.2)	40 (3.2)	51 (1.9)

(A) 0.1 M Tris-HCl buffer (pH 7.4). Peptide concentration: 6.8×10^{-5} M. Molar ratio of nucleotide to the peptide: 20 : 1.
(B) 0.06 M ammonium acetate buffer (pH 7.4). Peptide concentration: 5.8×10^{-5} M. Molar ratio of nucleotide to the peptide: 25 : 1.
The data were obtained from the best fits between the experimental results and theoretical calculation using the CONTIN CD computer program [5]. Number in parentheses represents standard error.

helix (Table 1A). The Val-peptide in ammonium acetate buffer (Table 1B) adopted a greater amount of α-helical structure relative to that of the Gly-peptide. The results confirm that substitution of glycine with valine in the N-terminal segment of p21 proteins changes the conformation to a more α-helical structure as predicted on the basis of the algorithms of Chou and Fasman [6]. Upon addition of GTP to the Val-peptide solution, little overall conformational change was noted (Table 1B). In contrast, the conformation of the Gly-peptide in Tris buffer was substantially altered by GTP (Table 1A). These findings imply that the substitution of glycine with valine at position 12 of p21 proteins causes a restriction of local conformation which may be responsible for the alteration in transforming capability.

In conclusion, this is the first experimental demonstration that differences exist in the conformation of the N-terminal segments of nontransforming and transforming *ras* p21 proteins. Replacement of glycine with valine at position 12 of the N-terminal 34-amino acid-residue segment produces a more α-helical structure. This results in a rigidity of conformation which may contribute to the transformationally active configuration by not being able to hydrolyze GTP. GTP is hydrolyzed approximately 6 times faster by the Gly-peptide than by the Val-peptide.

References

1. Cooper, G.M. and Lane M.A., Biochim. Biophys. Acta. Rev. on Cancer, 738 (1984) 9.
2. Shih, T.Y. and Weeks, M.O., Cancer Invest., 2 (1984) 109 (and references cited therein).
3. Finkel, T., Der, C.J. and Cooper, G.M., Cell, 37 (1984) 151
4. McCormick, F., Clark, B.F.C., La Cour, T.F.M., Kjeldgaard, M., Norskov-Lauritsen, L. and Nyborg, J., Science, 230 (1985) 78.
5. Provencher, S.W. and Glockner, J., Biochemistry, 20 (1981) 33.
6. Chou, P.Y. and Fasman, G.D., Biochemistry, 13 (1974) 222.

Third loop analogs of epidermal growth factor: Bioassay studies for receptor affinity and tyrosine kinase activation

Thomas J. Lobl[a,*], Linda L. Maggiora and John W. Wilks[b]
[a]Biopolymer Chemistry and [b]Cancer and Viral Diseases Research, The Upjohn Company, Kalamazoo, MI 49001, U.S.A.

Introduction

Epidermal growth factor (EGF) stimulates the proliferation of cells through activation of a cell surface receptor containing a tyrosine protein kinase. Certain transformed cells have an amplified gene for the EGF receptor, secrete their own growth factors, and presumably sitmulate their own growth through an autocrine/paracrine mechanism [1]. Other proteins, such as transforming growth factor type α (TGFα) and vaccinia 19K protein (VVP), bind to the EGF receptor and have high homology with EGF, especially in the third disulfide loop. A number of reports in the literature suggest that fragments of EGF and TGFα have a weak affinity for the EGF receptor [2–4]. We were interested in finding an EGF/TGFα receptor antagonist, and approached the problem through a structure–activity study of EGF third loop analogs.

Results and Discussion

Chemical synthesis

The peptides used in this report were chemically synthesized by standard solid peptide synthesis methods [5] on PAM resin and HF-cleaved or on oxime resin [6] and displaced with alkyl amines. The peptides were cyclized with diiodoethane/methanol.

Bioassays

Plasma membranes were prepared from normal, term human placenta and A431 cells using previously described procedures [7, 8]. Binding assays for the EGF receptor and kinase assays were performed as described by Carpenter, Cohen and Klein et al. with modifications [7, 9, 10].

*To whom correspondence should be addressed.

Table 1 *Receptor binding and kinase activities*

Peptide	Comment	Human placenta bioassays	
		EGF-receptor[a]	Tyrosine kinase[b]
Natural third loop sequences			
CVVGYIGERC	H-EGF	89.2± 1.0	94.4±1.3
CVVGYIGERCQYRDL-NH_2	H-EGF extended	91.2± 0.8	97.8±3.2
CSHGYTGIRC	VVP	98.4± 6.1	93.3±4.9
CHSGYVGARC	TGFα	88.4± 2.6	109.3±1.8
CHSGYVGARCEHADL-NH_2	TGFα extended	87.8± 3.0	95.3±4.0
Consensus sequences			
CVIGYIGARC		101.9± 1.6	91.0±1.7
CSHGYTGERC		94.5±14	104.0±2.1
Blocked peptides			
Ac-CHSGYVGARC-OMe		101.9± 3.1	94.8±3.9
Ac-CHSGYVGARC-NHEt		100.5± 2.3	102.0±2.8
Ac-CVVGYIGERC-NHEt		95.1± 5.9	105.9±3.0
Ac-CVVGYIGERC-NH-Cyclohexyl		98.0± 3.6	91.5±2.0
Miscellaneous			
TRDL	M-EGF (44–47)	92.0± 1.1	110.3±2.1
m-EGF, 10 nM		6.8± 0.5	-

[a] Percent ^{125}I-mouse-EGF bound to the receptor. The quantity of ^{125}I-EGF (5×10^{-10} M) bound to 8 ug of placental membrane protein in the absence of any peptide was assigned a value of 100%. Peptides were tested at 10^{-4} M. Similar results were obtained for all the peptides when membranes from A431 cells were used in the binding assay. Each value is the mean +/- S.E. of 3 replicates.

[b] Percent EGF receptor and tyrosine kinase activity. The counts per min of ^{32}P incorporated into (Val^5)angiotensin II [10] by 8 ug of A431 membrane protein incubated with 100 nM mouse EGF in the absence of any other peptide was assigned a value of 100%. Peptides were tested at 1.67×10^{-4} M. Each value is the mean +/- S.E. of 3 replicates.

Results and Discussion

None of the peptides displaced [^{125}I]EGF from its receptor in the human placenta binding assay, nor did they prevent the EGF-mediated activation of the receptor tyrosine kinase (Table 1). None of the peptides activated the EGF receptor kinase when incubated with placental membranes in the absence of EGF. The peptides were tested for receptor affinity with A431 cell membranes (data not shown) and L929 cells (data not shown, R. Borchardt and I. Hidalgo),

but no significant binding was seen. Finally the peptides were tested at concentrations up to 10 μM in a vaccinia virus infection assay with L929 cells, but did not inhibit infection (data not shown, R. Borchardt and M. Hasobe). We conclude that under the assay conditions and peptide concentrations used, the peptides are inactive. Considering the literature and this data in aggregate, very high concentrations of peptide would be needed to observe third loop displacement of EGF from its receptor. High-affinity peptide binding to the EGF receptor will require portions of the ligand in addition to the third loop of EGF.

Acknowledgements

We thank R. Borchardt, I. Hidalgo and M. Hasobe of the University of Kansas for providing us with their bioassay data before publication.

References

1. Sporn, M.B. and Roberts, A.B., Nature, 313 (1985) 745.
2. Tam, J.P., Sheikh, M., Harris, P., Pileggi, N., Tsai, L. and Hampton, R., Proc. West. Pharmacol. Soc., 29 (1986) 471.
3. Komoria, A., Hortsch, M., Meyers, C., Smith, M., Kanety, H. and Schlessinger, J., Proc. Natl. Acad. Sci. U.S.A., 81 (1985) 1251.
4. Nestor, Jr., J.J., Newman, S.R., DeLustro, B., Todaro, G.J. and Schreiber, A.B., Biochem. Biophys. Res. Commun., 129 (1985) 226.
5. Merrifield, R.B., J. Am. Chem. Soc., 85 (1963) 2149.
6. DeGrado, W. and Kaiser, E.T., J. Org. Chem., 45 (1980) 1295.
7. Cohen, S., Methods Enzymol., 99 (1983) 379.
8. Hock, R.A. and Hollenberg, M.D., J. Biol. Chem., 255 (1980) 10731.
9. Carpenter, G., Methods Enzymol., 109 (1985) 101.
10. Klein, H.H., Freidenberg, G.R., Cordera, R. and Olefsky, J.M., Biochem. Biophys. Res. Commun., 127 (1985) 254.

Purification and analysis of a hepatocyte antiproliferative glycopeptide

Geneviève Auger[a], Didier Blanot[a,*], Georges A. Boffa[b], Marie-Françoise Gournay[c], Jean Van Heijenoort[a], Patrick Lambin[b], Pierrette Maes[d], Claude Nadal[c] and André Tartar[d]

[a]U.A. 1131 CNRS, Bât. 432, Université Paris-Sud, F-91405 Orsay, France
[b]CNTS, Paris, France
[c]INSERM U 22, Institut Curie, Orsay, France
[d]Institut Pasteur, Lille, France

Introduction

Nadal and co-workers have demonstrated that rat or human sera treated by trypsin liberate low-molecular weight glycopeptides which block the G_1-S transition in an in vivo system of baby rat synchronized hepatocytes [1, 2]. Recently, we have shown that the human glycopeptide is associated with α_2-macroglobulin [3, 4]. In this communication, we wish to describe the partial purification and the amino acid and sugar analyses of the glycopeptide originating from α_2-macroglobulin.

Results

Highly purified α_2-macroglobulin (5.1 g) was submitted to trypsin for 2 h at 37°C and at 1:1 molar ratio. After concentration on a PM10 Diaflo membrane in distilled water, filtration on an H1P10 hollow fiber cartridge in Tris buffer, pH 10, and concentration on a YCO5 Diaflo membrane, the crude preparation contained 1.5×10^8 inhibitory units and 57 μmol of total amino acids. It was chromatographed on μBondapak C_{18}, as previously described [2, 4], then on μBondapak NH_2 in methanol-0.1 M ammonium acetate/acetic acid buffer, pH 5.7 (55:45,v/v). The elution was achieved isocratically for 30 min at 1 ml/min, then by a decreasing gradient of methanol (from 55 to 0% for 30 min) in the same buffer. The biological activity (1.5×10^8 inhibitory units) was recovered between 30 and 36 min (fraction '32-36'), i.e. as soon as the methanol percentage decreases.

Amino acid analyses of fraction '32-36' were carried out, before and after

*To whom correspondence should be addressed.

acid hydrolysis, by the dabsyl chloride procedure [5]; 22.5 nmol and 7.1 nmol of total and free amino acids, respectively, were found. The composition in bound amino acids was (in nmol): Glx 2.6, Gly 2.3, Leu 1.4, Ala 1.3, Val 1.2, Arg 1.2, Lys 1.0, Asx 1.0, Thr 0.8, Ser 0.7, Pro 0.7, Phe 0.6, Ile 0.5, His 0.1. Furthermore, the fraction contained 6.6 nmol of sialic acid, as measured by an improved Warren assay [6].

The molecular weight of the active compound in fraction '32-36' was estimated by HPLC on Ultropac TSK G2000SW. The biological activity was eluted in fractions corresponding to M_r 3,500-4,000.

Fraction '32-36' was submitted to microsequencing with an Applied Biosystem 470A apparatus. The first cycle of the degradation yielded several peaks corresponding to the free amino acids. No peaks could be seen in the subsequent cycles. The same result was obtained after having submitted the fraction to the action of BrCN in 70% formic acid, which is consistent with the lack of methionine in the amino acid analysis.

Discussion

The present results, compared with those previously obtained [2, 4], show that α_2-macroglobulin is a much better source of factor than whole serum from rat or human; furthermore, filtration at pH 10 yields 100 times more activity than at neutral pH [7]. The factor originating from the trypsinization of 5.1 g of α_2-macroglobulin could be obtained in two chromatographic steps with a quantitative yield. A 2,530-fold purification was achieved. It should be mentioned that the behavior of this compound on μBondapak NH_2 is different from that of the active compounds released at neutral pH [2, 4]; this suggests the existence of at least two chemically different entities with the same activity in the baby rat assay.

The sialic acid and amino acid contents of fraction '32-36' are of the same order of magnitude; however, the absence of exact stoichiometry between the amino acids, and the simultaneous presence of arginine and lysine in this fraction (originating from a tryptic hydrolysis), suggest that the factor has not yet been purified to homogeneity. The absence of PTH-amino acids upon microsequencing indicates that no N-termini are present in the preparation. It is interesting to notice that the two inhibitory factors characterized up to now, the human granulopoietic chalone and the mouse epidermic chalone, possess an N-terminal pyroglutamyl residue.

The examination of the sequence of α_2-macroglobulin shows no tryptic fragment carrying at least one glycosidic chain, having a molecular weight consistent with our determination and possessing an amino acid composition similar to that of fraction '32-36'. Therefore, it seems that α_2-macroglobulin cannot be the precursor of this glycopeptide, but perhaps only its carrier.

References

1. Nadal, C., Le Rumeur, E. and Boffa, G.A., Cell Tissue Kinet., 14 (1981) 601.
2. Auger, G., Blanot, D., Van Heijenoort, J., Nadal, C. and Gournay, M.F., Eur. J. Biochem., 133 (1983) 363.
3. Boffa, G.A., Lambin, P., Rius, E. and Nadal, C., C.R. Acad. Sci. Paris, Sér. III, 300 (1985) 31.
4. Auger, G., Blanot, D., Van Heijenoort, J., Nadal, C., Gournay, M.F., Boffa, G.A. and Lambin, P., In Castro, B. and Martinez, J., (Eds.) Forum Peptides, Les Impressions Dohr, Nancy, 1986, p. 22.
5. Chang, J.Y., Knecht, R. and Braun, D.G., Methods Enzymol., 91 (1983) 41.
6. Powell, L.D. and Hart, G.W., Anal. Biochem., 157 (1986) 179.
7. Lambin, P., Nadal, C., Winchenne, J.J. and Boffa, G.A., C.R. Acad. Sci. Paris, Sér. III (1987) in press.

Structures of human TGFα fragments using two-dimensional proton magnetic resonance spectroscopy and computer simulation

Kyouhoon Han[a], Chien-Hua Niu[b], Bernard R. Brooks[c], James A. Ferretti[a] and Peter P. Roller[b]

[a]Laboratory of Chemistry, NHLBI; [b]Laboratory of Experimental Carcinogenesis, NCI; and [c]DCRT NIH, Bethesda, MD 20892, U.S.A.

Transforming growth factor alpha (TGFα) is a potent mitogenic polypeptide capable of inducing a transformed phenotype upon binding to an epidermal growth factor (EGF) receptor [1]. The amino acid sequence of human TGFα is known and shows 30% homology to EGF [1]. In addition, disposition of three disulfide bonds in EGF and TGFα is strikingly similar (Fig. 1).

A synthetic fragment of EGF including residues from 20 to 31 has been shown to exhibit biological activities similar to the whole EGF molecule [2]. A recent study on pattern recognition in the genetic code of EGF also suggested that one of the two possible receptor binding sites in EGF involves the residues from 24 to 29 [3]. We have synthesized two cyclic fragments of human TGFα: a cyclic TGF (21-32), I; and a cyclic (Ala^{21}) TGF (16-32), II.

The resonance assignments were made in water solution using the two-dimensional homonuclear Hartman–Hahn technique [4] and the interproton distances were obtained using both the two-dimensional laboratory (NOESY) and rotating (ROESY) [5] frame experiments. Structures were obtained by using these results in combination with dynamic simulation and energy minimization procedures.

Results and Discussion

Low energy structures of I and II which are consistent with the NMR data are shown in Figs. 2 and 3, respectively.

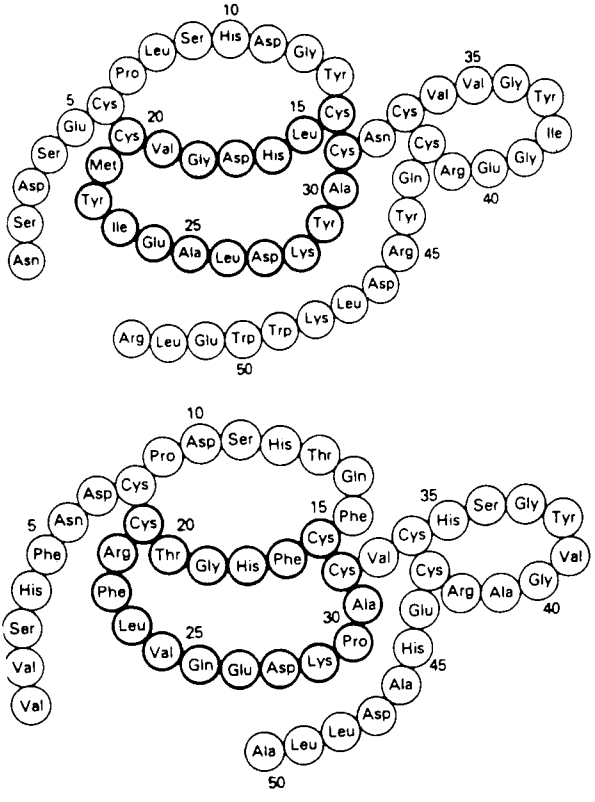

Fig. 1. Amino acid sequences of a human EGF (top) and a human TGFα (bottom). Receptor binding region in EGF and portion of TGFα under the current study are bold circled.

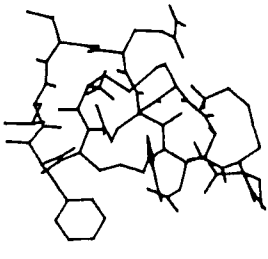

Fig. 2. Structure of cyclic TGF (21-32).

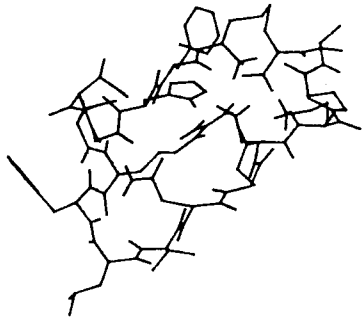

Fig. 3. Structure of cyclic (Ala^{21}) TGF (16-32).

References

1. Derynck, R., Roberts, A.B., Winkler, M.E., Chen, E.Y. and Goeddel, D.V., Cell, 38 (1984) 287.
2. Komoriya, A., Hortsch, M., Smith, M.E., Kanety, H. and Schlessinger, J., Proc. Natl. Acad. Sci. U.S.A., 81 (1984) 1351.
3. Bost, K.L., Smith, E.M. and Blalock, J.E., Biochem. Biophys. Res. Commun., 128 (1985) 1373.
4. Bax, A. and Davis, D.G., J. Magn. Res., 65 (1985) 355.
5. Bothner-By, A.A., Stephens, R.L., Lee, J., Warren, C.D. and Jeanloz, R.W., J. Am. Chem. Soc., 106 (1984) 811.

A comparative study of strategy and cleavage and methods by HF and trifluoromethanesulfonic acid: Synthesis of Shope fibroma growth factor and proteoglycan growth factor

De-Xing Wang, Yao-Zhong Lin, Gregg Caporaso, Pi-Yun Chang, Xiao-Hong Ke and James P. Tam

The Rockefeller University, 1230 York Avenue, New York, NY 10021, U.S.A.

Introduction

In an effort to improve the synthesis of complex peptides containing multiple disulfide linkages, two members of the epidermal growth factor family, the 55-residue Shope fibroma growth factor (SFGF) [1] and the 45-residue proteoglycan growth factor (PGF), were synthesized using different strategies. Both SFGF and PGF contain 6 cysteinyl residues which are strongly acid-sensitive and require mild conditions to minimize loss during cleavage. Two cleavage schemes, both based on the Boc-benzyl protecting group strategy, were designed for this purpose and incorporated in the synthesis of these growth factors as a comparative study. In the first scheme which was used for the synthesis of SFGF, we utilized Cys(MeBzl) and Arg(Tos) as protecting groups, and PAM resin [2] as the solid support with low-high HF [3] for deprotection. All protecting groups were removed in a single step giving a peptide with a free carboxylic acid. In the second scheme, which was used for the synthesis of PGF, we employed Cys(Acm) and Arg(Pme) as protecting groups, *p*-acyloxybenzhydrylamine (ABA) resin [4] as the solid support, and a gradative deprotection scheme, which used sequential cleavage steps that included low trifluoromethanesulfonic acid (TFMSA) and $Hg(OAc)_2$ to provide a peptide with an α-carboxamide terminus (Table 1).

Results and Discussion

Synthesis of SFGF and PGF was carried out by a standard protocol [5]. After the synthesis, the crude SFGF peptide-resin was cleaved in a low-HF condition containing HF/DMS/*p*-thiocresol in a ratio of 31:65:2:2 (v/v) at 0°C for 2 h, and then followed by a high-HF condition containing HF/*p*-cresol/*p*-thiocresol in a ratio of 96:2:2 (v/v) at 0°C for 1 h. Under such a condition, the oxygen-linked benzyl protecting groups were removed during the low-HF,

Table 1 *Comparison of two strategies*

Conditions	SFGF	PGF
Resin	PAM[a]	ABA[b]
Protecting group scheme	Boc-benzyl	Boc-benzyl
Arg protecting group	Tos[c]	Pme[d]
Cys protecting group	MeBzl[e]	Acm[f]
Cleavage method	Low-high HF	Low-TFMSA
C-terminus	-COOH	$-CONH_2$
Cleavage yield (%)[g]	61	87

[a] PAM-phenylacetamidomethyl, [b]ABA-*p*-acyloxybenzhydrylamine, [c]Tosyl, [d]Pme-pentamethylphenylsulfonyl, [e]4-Methylbenzyl, [f]Acetamido methyl, [g]Crude and isolated yield before refolding and oxidation.

S_N2 condition with minimal danger of alkylation side reaction. The cysteinyl protecting group was removed during the high-HF S_N1 condition. Similarly, the PGF peptide-resin was deprotected by a low-TFMSA, S_N2 condition, using TFMSA/TFA/tetrahydrothiophene (THTP)/*p*-cresol in a ratio of 10:55:30:5 (v/v) at 0°C for 2 h. HF was replaced by TFMSA in the S_N2 cleavage condition to remove the oxygen-linked benzyl protecting groups. This substitution allowed the use of a normal reaction vessel rather than a special HF apparatus. THTP was used instead of DMS to increase the acidity of the solution to accelerate the deprotection rate.

Since the ABA-resin is stable to the S_N2 cleavage conditions, the crude peptide remains attached to the resin. The release of the peptide was achieved by a combination of volatile basic solvents containing methylamine/THF/EtOH in a ratio of 10:45:45 (v/v). The crude peptide detached from resin contained an acid-labile handle (*p*-hydroxybenzhydrylamine) and together with a more acid-labile arginine protecting group (Pme), it was cleaved in a single step under solvolytic condition in TFMSA/TFA/*p*-cresol in a ratio of 2:88:10 (v/v) at 0°C for 3 h. To remove the Cys(Acm) protecting groups, the crude PGF was treated with $Hg(OAc)_2$ in 8 M urea, pH 4, for 4 h, and the mercuric salt was removed by dithiothreitol. Refolding and oxidation of both crude products were achieved in oxidized/reduced glutathione for 48 h and purified on C-18 reversed-phase HPLC. After cleavage, the yields of SFGF and PGF were 61% and 87%, respectively.

Purified SFGF or PGF gave a single peak in HPLC and the predicted amino acid ratio. Sodium dodecyl sulfate polyacrylamide gel electrophoresis analysis and enzymatic digestion of SFGF showed a single band at 6 KD and suggested proper disulfide pairings. SFGF was found to be nearly as active as TGFα in biological activity, but PGF was less than 0.1% as active in the EGF radioreceptor binding assay. Thus, our results show that the synthesis of a peptide containing

multiple disulfides could be achieved without the use of a strong acid, S_N1 treatment.

Acknowledgements

This work was supported by the National Institutes of Health (NIH), grant CA 36544.

References

1. Chang, W., Upton, C., Hu, S.L., Purchio, A.F. and McFadden, G., Mol. Cell. Biol., 7 (1987) 535.
2. Mitchell, A.R., Erickson, B.W., Ryabtsev, M.N., Hodges, R.S. and Merrifield, R.B., J. Am. Chem. Soc., 98 (1976) 7357.
3. Tam, J.P., Heath, W.F. and Merrifield, R.B., J. Am. Chem. Soc., 105 (1983) 6442.
4. Tam, J.P., J. Org. Chem., 50 (1985) 5291.
5. Tam, J.P., Int. J. Pept. Prot. Res., 29 (1987) 421.

Substrates of tyrosine-specific protein kinase: Synthetic peptides derived from lipocortins

Ronald G. Yarger, Rolf H. Berg, Susan A. Rotenberg and James P. Tam
The Rockefeller University, 1230 York Ave., New York, NY 10021, U.S.A.

Introduction

Lipocortins are proteins that inhibit phospholipase A_2 activity and also serve as substrates for tyrosine-specific protein kinase and protein kinase C [1, 2]. In addition, they may be the physiologically relevant cellular substrates of the epidermal growth factor receptor-protein kinase.

We describe here the solid phase synthesis of nine peptides (1a-c – 3a-c) based on the Tyr-21 phosphorylation site of lipocortin I (Fig. 1), and five peptides (4a-e) based on the Tyr-23 and Ser-25 phosphorylation sites of lipocortin II, to test whether they could act as substrate inhibitors and to determine their minimal structural requirements for activity.

Results and Discussion

The lipocortin I peptides were synthesized on a *p*-acyloxybenzhydrylamine resin support using the Boc group for N protection and benzyl groups for side-chain functional protection (Fig. 2). Trp(For), Tyr(BrZ), and Lys(ClZ) were also used. Each residue was coupled twice via DCC activation, first in CH_2Cl_2 and then in DMF/CH_2Cl_2 (1:2), except for Asn and Gln which were coupled using DCC/HOBt activation. Peptides were synthesized simultaneously in three

1a-c Lys-Gln-Ala-Trp-Phe-Ile-Glu-Asn-Glu-Glu-Gln-Glu-[*]-Val-Gln-Thr-Val-NH_2

2a-c Phe-Ile-Glu-Asn-Glu-Glu-Gln-Glu-[*]-Val-Gln-Thr-Val-NH_2

3a-c Asn-Glu-Glu-Gln-Glu-[*]-Val-Gln-Thr-Val-NH_2

4a-e Leu-Glu-Gly-Asp-His-Ser-Thr-Pro-Pro-Ser-Ala-[*]-Gly-[#]-Val-Lys-Ala

*Fig. 1. Lipocortins I and II synthetic peptides. * = L-Tyr, D-Tyr, or L-Phe; # = D-Ser or L-Ala.*

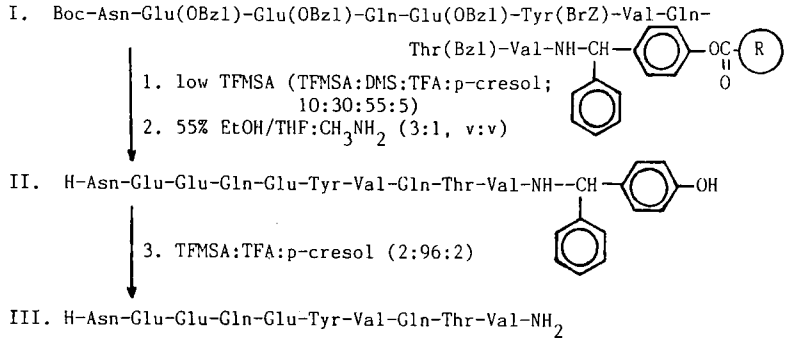

Fig. 2. Scheme for parallel synthesis of lipocortin I peptides.

reaction vessels (for L-Tyr, D-Tyr, and L-Phe analogs), one-third of the peptide-resin being removed after the Asn-16 and Phe-13 couplings. The reaction progress was followed using the qualitative ninhydrin test and amino acid analysis. The weakly electron-withdrawing *p*-acyloxybenzhydrylamine linkage provided the required acid stability for repetitive TFA treatments and subsequent S_N2 removal of benzyl groups. Liberation of peptides was accomplished in two stages. Methylaminolysis in 55% EtOH/THF released the peptide-ABA handle from the resin while 2% TFMSA treatment yielded the peptide carboxamides [3]. The peptides were then purified by HPLC on a C-18 column using a gradient of CH_3CN in 0.05% TFA.

The lipocortin II peptides were synthesized on a PAM resin support with similar protecting group chemistry and also using His(DNP). These were prepared in separate vessels in a parallel fashion, allowing for synthesis of the five analogs. After thiolytic removal of the DNP group and acidolytic cleavage of the terminal Boc group, the peptides were cleaved from the resin by low TFMSA treatment [4] in the reaction vessels at 0°C. The peptides were obtained by precipitation in cold diethyl ether and purified by reversed phase HPLC. These peptides were found to be effective competitive substrate inhibitors of $pp60^{src}$ autophosphorylation in the range of 10–100 μM.

Acknowledgements

This work was supported by NIH grant CA 36544.

References

1. Pepinsky, R.B. and Sinclair, L.K., Nature, 321 (1986) 81.
2. Gould, K.L., Woodgett, J.R., Isacke, C.M. and Hunter, T., Mol. Cell. Biol., 6 (1986) 2738.
3. Tam, J.P., J. Org. Chem., 50 (1985) 5291.
4. Tam, J.P., Heath, W.F. and Merrifield, R.B., J. Am. Chem. Soc., 108 (1986) 5242.

Session X
Neurochemistry

Chair: John M. Stewart
University of Colorado Health Sciences Center
Denver, Colorado, U.S.A.

Receptor-mediated peptide transport through the blood–brain barrier

William M. Pardridge

Department of Medicine, Division of Endocrinology and Brain Research Institute, UCLA School of Medicine, Los Angeles, CA 90024, U.S.A.

The potential for peptides as neuropharmaceuticals in humans is limited by the restricted transport of these water-soluble molecules through the brain capillary wall, [i.e., the blood–brain barrier (BBB)]. Unlike capillaries in nonbrain organs, which have pores that allow for free diffusion of peptides and other small molecules from blood into the organ interstitial space, the capillaries of vertebrate brain have no pores [1]. Consequently, water-soluble molecules in the circulation gain access to the brain interstitial space only via specific transport processes localized at the lumenal and antilumenal borders of the brain capillary endothelium, which makes up the BBB in vivo [2]. For example, numerous transport systems have been characterized for circulating nutrients, thyroid hormones, or water-soluble vitamins such as thiamine [3]. Steroid hormones traverse the BBB via free diffusion based on the high lipid solubility of these molecules; however, steroid hormone transport through the BBB is still regulated since plasma proteins selectively deliver steroid hormones to the brain via plasma protein-mediated transport [4].

Peptides may be transported through the BBB via one of two mechanisms. First, the peptides may undergo free diffusion through the porous capillaries perfusing the tiny circumventricular organs (CVOs) surrounding the ventricles (e.g., the median eminence, the organum vasculosum of the lamina terminalis (OVLT), subfornical organ, area postrema or choroid plexus [5]). The capillaries perfusing the brain proper, however, have a surface area of 100–200 cm^2/g (which, in the human brain, is equivalent to the size of a paddle tennis court), and this is estimated to be about 5,000-fold greater than the surface area of capillaries perfusing the CVOs. Therefore, water-soluble peptides are barred from entry into the vast area of brain interstitial space, unless the peptides have an affinity for specialized peptide transport systems within the BBB. The second mode of entry of circulating peptides from blood into brain is receptor-mediated transport through the brain capillary endothelial wall [6]. This process is believed to be comprised of three sequential steps: (a) receptor-mediated endocytosis at the lumenal border of the BBB; (b) diffusion of the receptor–peptide complex or free peptide through the 0.3 μm of endothelial cytoplasm; and (c) receptor-

mediated exocytosis of the peptide at the antilumenal border of the brain capillary endothelium. The BBB peptide transcytosis hypothesis was first put forward in 1985 on the basis of insulin receptor studies in isolated human brain capillaries (see [6]). These experiments showed that insulin is endocytosed by isolated human brain capillaries subsequent to membrane receptor binding. The BBB peptide transcytosis hypothesis has recently been confirmed with in vivo experiments using thaw-mount autoradiography and HPLC analysis of blood and brain radioactivity to show net transport of unmetabolized blood-borne[^{125}I]insulin through the BBB of rabbits and into brain interstitial space [7]. Subsequent studies have identified specific receptor transport systems for insulinlike growth factor (IGF)-1, IGF-2, transferrin, and cationized albumin [6]. Native albumin, which has an isoelectric point of ~4, does not undergo receptor-mediated transport through the BBB and enters the cerebrospinal fluid (CSF) slowly with a halftime of 1–2 days, however, cationization of albumin to an isoelectric point of 8.5 results in both marked uptake of the cationized plasma protein into the CSF endocytosis in isolated brain capillaries [6].

In addition to the BBB peptide receptors that are believed to be transport systems, there are undoubtedly peptide receptors in the brain capillary for numerous other functions. For example, peptides such as parathyroid hormone or vasoactive intestinal peptide have been shown to alter brain capillary adenyl cyclase [9], and cyclic nucleotides alter the BBB permeability [10]. Arginine vasopressin and angiotensin II have been shown to alter brain capillary water permeability [11, 12]. Bradykinin results in an increase in pinocytotic activity in the brain microcirculation [13]. Another major mode of interaction of peptides with the brain capillary is via capillary aminopeptidase. The N-terminal tyrosine of both [Tyr^1]-somatostatin and leucine enkephalin is rapidly cleaved by the aminopeptidase activity of isolated brain capillaries [14, 15].

In summary, recent studies have shown numerous and dynamic modes of interactions of neuropeptides with the brain capillary which makes up the BBB in vivo. Although some neuropeptides (e.g., enkephalins) do not appear to have a significant affinity for a specific receptor-mediated transcytosis system [15], other circulating peptides (e.g., insulin, IGFs, transferrin) do enter the brain interstitial space via these pathways [6].

References

1. Brightman, M.W., Exp. Eye Res., 25 (1977) 1.
2. Pardridge, W.M., Ann. Rev. Physiol., 45 (1983) 73.
3. Pardridge, W.M., Fed. Proc., 45 (1986) 2047.
4. Pardridge, W.M., Am. J. Physiol., 252 (1987) E157.
5. Weindl, A., In Ganong, W.F. and Martini, L. (Eds.) Frontiers in Neuroendocrinology, Oxford University Press, New York, NY, 1973, p. 3.

6. Pardridge, W.M., Endocr. Rev., 7 (1986) 314.
7. Duffy, K.R. and Pardridge, W.M., Brain Res., 420 (1987) 32.
8. Griffin, D.E. and Giffels, J., J. Clin. Invest., 70 (1982) 289.
9. Huang, M. and Rorstad, O.P., J. Neurochem., 43 (1984) 849.
10. Joo, F., Temesvari, P. and Dux, E., Brain Res., 278 (1983) 165.
11. Raichle, M.E. and Brubb, Jr., R.L., Brain Res., 143 (1978) 191.
12. Gruff, Jr., R.J. and Raichle, M.E., Brain Res., 210 (1981) 426.
13. Unterberg, A., Wahl, M. and Baethmann, A., J. Cereb. Blood Flow Metab., 4 (1984) 574.
14. Pardridge, W.M., Eisenberg, J. and Yamada, T., J. Neurochem., 44 (1985) 1178.
15. Pardridge, W.M. and Mietus, L.J., Endocrinology, 109 (1981) 1138.

Neuropeptide co-transmitters in physiologically identified motor neurons in *Aplysia*

Philip E. Lloyd* and David P. Lotshaw
Department of Pharmacological and Physiological Sciences, University of Chicago, 947 East 58th, Chicago, IL 60637, U.S.A.

Introduction

Neuropeptides constitute the largest variety of intercellular messengers in the nervous system. The overall complexity of vertebrate central nervous systems (CNS) has made it difficult to establish the physiological and behavioral role of neuropeptides. One method of circumventing these difficulties is to take advantage of preparations with reduced complexity, such as vertebrate peripheral nervous systems or the relatively simple CNS of invertebrates. The CNS of the gastropod mollusc *Aplysia* is well suited for such studies because it is comprised of a relatively small number of neurons, many of which are very large and can be identified in each preparation. Radioenzymatic microassays with sufficient sensitivity to measure the levels of conventional transmitters such as acetylcholine, serotonin, histamine, and dopamine in single neuronal cell bodies dissected from *Aplysia* ganglia have been developed. We are now developing procedures to measure neuropeptides in single neurons. These procedures permit a group of neurons to be physiologically characterized by recording and stimulating via an intracellular electrode. Selected neurons are marked by the injection of a vital dye. Ganglia are then incubated in organ culture with [^{35}S]methionine and individual neurons removed and extracted. These extracts are run on HPLC and the resulting samples counted. These procedures permit us to relate the levels of peptide synthesis to the physiological properties of a neuron.

Our studies have concentrated on a group of about a dozen large neurons, termed the ventral cluster, present in the buccal ganglia. These are motor neurons which control muscles involved in producing biting and swallowing movements. They are of interest because they contribute to the neural processes which underlie a robust form of behavioral plasticity in *Aplysia*, namely, an arousal of the feeding system on exposure to food [1]. One aspect of this arousal is an increase in the magnitude of each bite which appears to be due, in part, to the presence of specific neuropeptides in these neurons along with their conventional trans-

*To whom correspondence should be addressed.

mitters. The precise complement and rates of syntheses of the peptides differ for different neurons within the cluster. The dominant peptides synthesized by these neurons are the two small cardioactive peptides, SCP_A (ARPGYLAFPR-Mamide) [2], SCP_B (MNYLAFPRMamide) [3], and FMRFamide [4]. The two SCPs are cleaved from a single precursor [5] and appear to have identical physiological functions [6]. FMRFamide is cleaved from another precursor [7]. Although there is some similarity of sequence at the carboxyl terminal of the SCPs and FMRFamide, they have markedly different physiological actions.

Evidence for the presence of these peptides in the ventral cluster neurons first came from immunocytological studies [8, 9]. We have now developed procedures to determine not only what peptides are synthesized by individual physiologically characterized neurons in this cluster, but also to quantify their rates of synthesis. The results from these experiments should provide answers to the question of the physiological role of neuropeptide co-transmitters in an experimentally accessible neural preparation.

Methods

The connective tissue sheath was dissected from the buccal ganglia to expose neurons of the ventral cluster. Innervation to the feeding muscles through select nerves was left intact. Motor neurons were identified by visual criteria (location, size, pigmentation), and the nature and location of contractions produced by intracellular stimulation. Select neurons were stained by electrophoretic injection of a vital dye (Fast green). The ganglia were transferred and labeled in 1 ml sterilized (0.2 μm filtered) *Aplysia* blood containing 2.5 mM colchicine, antibiotics, and 0.2 mC/ml [^{35}S]methionine (Amersham) for 20 h at 15°C. This was followed by a 4-h chase in a medium consisting of 1/2 filtered blood: 1/2 L15 culture medium (Flow Labs; 0.5 mM cold methionine) with added physiological salts. After the chase period, neurons were identified visually and dissected in a solution of 50% propylene glycol/50% ASW at -20°C. The cell bodies were placed in a microtube containing 50 μl of 0.01 M trifluoroacetic acid (TFA) with 2 nmol of synthetic SCP_A, SCP_B, and FMRFamide (Peninsula). This solution was filtered and subjected to a low-resolution screening HPLC run (counterion: TFA) on a Brownlee RP-300 C8 column with an acetonitrile gradient and aliquots of the fractions counted. The remaining portions of selected samples with the retention time of known peptides were then run with high resolution on an acetonitrile gradient with heptafluorobutyric acid (HFBA) replacing TFA.

Results

More than 100 neurons have been identified by physiological criteria and analyzed for peptide synthesis. Because of the large number of neurons sampled,

the initial screening by HPLC was designed to be a rapid, but low-resolution, gradient. Aliquots of the samples of interest were then run on a second higher-resolution gradient with a different counterion to confirm tentative peptide identities.

Individual neurons of the buccal ganglia show dramatic differences in their levels of neuropeptide synthesis. Examples of identified neurons of similar size that are at the extremes of peptide synthesis are shown in Fig. 1. The levels of unincorporated methionine were a good indicator of the size of each neuron. Similar levels of unincorporated methionine were found in the two neurons shown in Fig. 1, making it possible to compare them directly. The SCPs are being synthesized in neuron B1 at a rate at least 100-fold higher than any Met-containing peptide in neuron B4. Motor neurons of the ventral cluster generally demonstrate rates of peptide synthesis intermediate between these two extremes. Fig. 2 shows the combined low- and high-resolution HPLC procedures used to identify an FMRFamide-synthesizing ventral cluster motor neuron. Fig. 3 shows the same

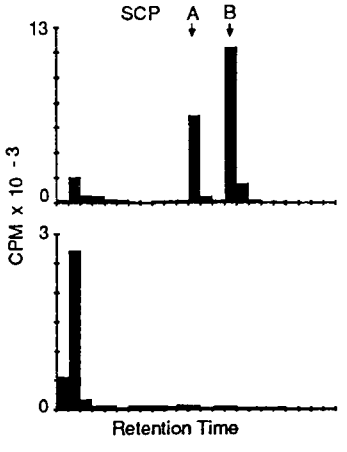

Fig. 1. Low-resolution screening HPLC procedure (counterion: TFA) demonstrates the extremes of peptide synthesis in two identified neurons from the buccal ganglia. Top histogram is from an extract of neuron B1 showing equimolar synthesis of SCP_A (1 Met residue) and SCP_B (2 Met residues). Bottom histogram is from neuron B4. Levels of unincorporated Met (fraction No. 2) are similar in the two neurons reflecting their similar size (note different scales).

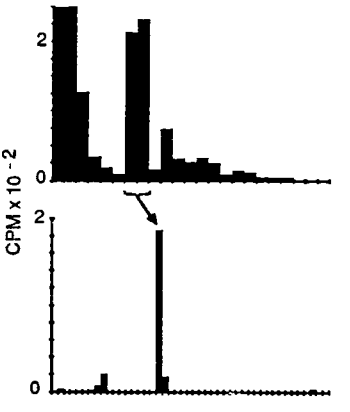

Fig. 2. Two-step procedure used to identify a ventral cluster motor neuron which synthesizes FMRFamide. Top histogram: Low-resolution screening HPLC (TFA) of neuron extract. Bottom histogram: High-resolution HPLC (HFBA) confirms the peptide was FMRFamide. Half of the two indicated samples was retained for the second HPLC step.

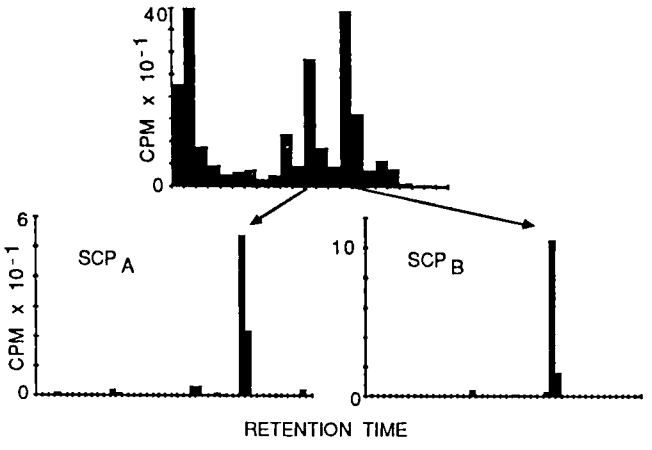

Fig. 3. Two-step procedure used to identify a ventral cluster motor neuron which synthesizes the two SCPs. Details are the same as for Fig. 2 except high-resolution HPLC was carried out separately for each of the SCP peaks.

procedure used to identify an SCP-synthesizing neuron. Both of the neurons described in Figs. 2 and 3 had previously been characterized physiologically by their actions on individually identified feeding muscles. Many of the ventral cluster neurons have been identified in ganglia from a number of individuals and the neurons consistently demonstrate similar patterns of peptide synthesis. This suggests that the synthesis and expression of neuropeptides in these neurons is selectively regulated, and thus is likely to be of physiological importance.

Discussion

In this report, we have described our protocol for measuring peptide synthesis in single motor neurons. It is important to emphasize that these procedures are carried out after the physiological properties have been determined by stimulating the neuron via an intracellular electrode and monitoring its actions on its target muscles. These procedures have several advantages over the more commonly used alternative of staining the neurons with an intracellularly injected fluorescent dye and doing immunocytology with antisera to the SCPs or FMRFamide. The major advantages of the radiolabeling procedure are: (i) it is considerably more reliable; (ii) it yields quantitative information on the rates of peptide synthesis; (iii) it is less labor-intensive if the number of neurons analyzed per ganglia is limited (i.e. < 10). One disadvantage of the procedure is that it requires that the peptide of interest contain a Met (or Cys) residue. This

appears to be due to a combination of high specific activity available for these residues and the low endogenous pools of these amino acids in the ganglia. Fortunately, all the peptides we have studied contain Met residues.

The peptides that we have shown to be present in ventral cluster neurons potently modulate feeding muscles [10, 11]. We have also demonstrated that these peptides are transported from the ganglia to presumptive release sites in the feeding muscles [12]. Our present challenge is to design physiological experiments that will elucidate the actions of the peptides released from the motor neurons themselves and to determine how this release contributes to the arousal observed when the animal feeds. The experimental tractability of the system should permit us to determine the physiological roles of peptide co-transmitters in feeding behavior in *Aplysia*.

Acknowledgements

Supported by NIH NS 23569 and Whitehall Foundation grants.

References

1. Weiss, K.R. and Kupfermann, I., In Ferrenelli, J.A. (Ed.) Aspects of Behavioral Neurobiology, Vol. 3, Soc. Neurosci. Symposia, Bethesda, MD, 1977, p. 66.
2. Morris, H.R., Panico, M., Karplus, A., Lloyd, P.E. and Riniker, B., Nature, 301 (1982) 643.
3. Lloyd, P.E., Kupfermann, I. and Weiss, K.R., Peptides, 8 (1987) 179.
4. Price, D.A. and Greenberg, M.J., Science, 197 (1977) 670.
5. Mahon, A.C., Lloyd, P.E., Weiss, K.R., Kupfermann, I. and Scheller, R.H., Proc. Natl. Acad. Sci. U.S.A., 82 (1985) 3925.
6. Lloyd, P.E., Trends Neurosci., 9 (1986) 428.
7. Schaefer, M., Picciotto, M., Kreiner, T., Taussig, R. and Scheller, R.H., Cell, (1985) 457.
8. Lloyd, P.E., Mahon, A.C., Kupfermann, I., Cohen, J.L., Scheller, R.H. and Weiss, K.R., J. Neurosci., 5 (1985) 1851.
9. Lloyd, P.E., Frankfurt, M., Stevens, P., Kupfermann, I. and Weiss, K.R., J. Neurosci., 7 (1987) 1123.
10. Lloyd, P.E., Kupfermann, I. and Weiss, K.R., Proc. Natl. Acad. Sci. U.S.A., 81 (1984) 2934.
11. Weiss, K.R., Lloyd, P.E., Cropper, E.C., Frankfurt, M. and Kupfermann, I., Soc. Neurosci. Abstr., 12 (1986) 947.
12. Lloyd, P.E., Soc. Neurosci. Abstr., (1987) in press.

Distinct endogenous ligands for PCP and sigma opioid receptors

Debora A. DiMaggio[a,b,*], Patricia C. Contreras[b] and Thomas L. O'Donohue[a,b]
[a]*Department of Pharmacology, St. Louis University, St. Louis, MO, U.S.A.*
[b]*CNS Diseases Research, G.D. Searle and Company, St. Louis, MO, U.S.A.*

Phencyclidine [PCP, 1-(1-phenylcyclohexyl) piperidine, angel dust, whack, lovely] is now a commonly abused drug in many of the major cities throughout the United States. In humans, PCP abuse produces euphoria and excitation, and very often leads to violent and aggressive behavior, amnesia, and psychotic disturbances. The mechanisms through which these various behaviors are induced by PCP administration are not yet clear; however, it is believed that many of these effects of PCP are mediated through specific interactions with PCP receptors. Several investigators have described high affinity binding sites for PCP in the central nervous system (CNS) which appear to have many properties of receptors, and have characterized the binding [1, 2], as well as the distribution [3, 4], of these specific binding sites. It appears that PCP receptors play a role in mediating stereotyped behavior and ataxia [5] in rodents.

Sigma opioids such as cyclazocine and *N*-allylnormetazocine (SKF 10,047) also induce PCP-like psychoses. Based on this similarity of effect between sigma opioids, PCP, and PCP analogs in various species, it was believed that PCP and sigma opioids exert their psychotomimetic effects through the same mechanism, perhaps through the same population of receptors. Furthermore, it was shown that sigma opioids inhibit the binding of [^{3}H]PCP to rat brain homogenates [3, 6]. Subsequent studies, however, indicate that distinct classes of binding sites exist for PCP and sigma opioids due to differences in distribution and potencies [7–9].

Since much evidence points to separate receptor populations for sigma opioids and PCP, it is likely that two separate endogenous ligands specific for these distinct receptors are present in the CNS. Two such putative endogenous ligands have already been described [10, 11]. Previous reports detail the purification of these ligands [11, 12]. These ligands have been named alpha- and beta-endopsychosin, representing PCP- and SKF-active material, respectively.

* Present address: G.D. Searle and Co., 700 Chesterfield Village Parkway, Mail Zone AA5C, St. Louis, MO 63198, U.S.A.

Results and Discussion

In fractions from earlier chromatographic runs, it was evident from the binding studies that PCP- and SKF-active material had distinct elution profiles. Whereas most PCP activity eluted between 18 and 86 min, the SKF activity eluted in two broad regions (20–42 min and 90–120 min). The first SKF-active region overlapped with PCP activity. This overlap is not surprising, since the endogenous ligand for the PCP receptor may also interact with the sigma receptor considering the functional and pharmacological similarities between the receptors. [^{3}H]SKF 10,047 also appears to bind to both PCP and sigma opioid receptors. Since the second SKF-active region did not overlap with the PCP-active region, these active fractions were subjected to further reversed-phase chromatography until apparent homogeneity, the main criterion being baseline resolution of the absorbance peak. Pronase digestion of the peak material completely abolished SKF activity, indicating that the SKF-active material is at least partially peptide.

PCP-active material from early chromatographic runs was shown to be selective for PCP receptors, with a distinct distribution in the CNS [10]. This PCP-active material, which was protease-sensitive, was purified to homogeneity using reversed-phase methodology [12].

Amino acid analysis of this SKF-active material was similar to, yet distinct from, the amino acid composition of the PCP-active material [12]. A partial sequence determination of the SKF-active material yielded sequence information on a 12-amino acid fragment. This fragment was synthesized and shown to be active in the sigma opioid receptor assay. Antibodies have been generated against the synthetic fragment, as well as synthetic peptide fragments containing amino acid substitutions in the terminal regions. The antibodies are presently being assessed for binding and staining characteristics. Both the SKF-active fragment and the endogenous PCP-active material appear to be PCP-like. PCP-active material mimicked the effects of PCP in both behavioral and electrophysiological tests [10]. PCP-active fractions inhibited spontaneous firing of cerebellar neurons and induced contralateral turning after intranigral injections in rats.

Chemical and biological characterization of PCP- and SKF-active material from porcine brain inidcates that these endogenous putative ligands for the PCP and sigma opioid receptors are distinct. It is likely that both ligands interact with both receptors with different affinities, as the data indicate that the peptides are structurally related. Complete chemical characterization and synthesis of both endogenous peptides, and the discovery of selective receptor ligands will allow for detailed studies on the physiological and pathophysiological significance of these endogenous ligands.

References

1. Vincent, J.P., Kartalovski, B., Geneste, P. Kamenka, J.M. and Lazdunski, M., Proc. Natl. Acad. Sci. U.S.A., 76 (1979) 4678.
2. Zukin, S.R. and Zukin, R.S., Proc. Natl. Acad. Sci. U.S.A., 76 (1979) 5372.
3. Quirion, R., Hammer, Jr., R.P., Herkenham, M. and Pert, C.B., Proc. Natl. Acad. Sci. U.S.A., 78 (1981) 5881.
4. Contreras, P.C., Quirion, R. and O'Donohue, T.L., Neurosci. Lett., 67 (1986) 101.
5. Contreras, P.C., Rice, K.C., Jacobson, A.E. and O'Donohue, T.L., Eur. J. Pharmacol., 121 (1986) 9.
6. Zukin, R.S. and Zukin, S.R., Mol. Pharmacol., 20 (1981) 246.
7. Su, T.P., J. Pharmacol. Exp. Ther., 223 (1982) 284.
8. Tam, S.W., Proc. Natl. Acad. Sci. U.S.A., 80 (1983) 6703.
9. Contreras, P.C., Quirion, R. and O'Donohue, T.L., Proc. Soc. Neurosci., 11 (1985) 583.
10. Quirion, R., DiMaggio, D.A., French, E.D., Contreras, P.C., Shiloach, J., Pert, C.B., Everist, H., Pert, A. and O'Donohue, T.L., Peptides, 5 (1984) 967.
11. Contreras, P.C., DiMaggio, D.A. and O'Donohue, T.L., Synapse, 1 (1987) 57.
12. DiMaggio, D.A., Contreras, P.C. and O'Donohue, T.L., In Clouet, D.H. (Ed.) NIDA Research Monograph 64, National Institute on Drug Abuse Office of Science, Rockville, MD, 1986, p. 24.

Comparison of amyloid from Alzheimer's disease with synthetic peptide

Lawrence K. Duffy[a], Daniel A. Kirschner[b], Catharine L. Joachim[a], Alison Sinclair[b], Hideyo Inouye[b] and Dennis J. Selkoe[a]

[a]Center for Neurologic Diseases, Brigham and Women's Hospital and [b]Department of Neuroscience, Children's Hospital and Department of Neurology and Neuropathology, Harvard Medical School, Boston, MA 02115, U.S.A.

Alzheimer's disease (AD) is characterized by differential progressive deposition of three neuropathological lesions: (a) neurofibrillary tangles in neuronal cell bodies; (b) senile plaques having a central amyloid core; and (c) cerebral amyloid angiopathy. Glenner and Wong have isolated a low molecular weight protein, called the β-peptide, from congophilic meningeal vessels in AD and have reported the amino acid sequence of the first 28 residues [1]. Recently, a gene coding for the β-amyloid precursor protein has been mapped to chromosome 21 and the complete sequence of the precursor protein has been proposed [2]. Our own protein sequence studies of the AD meningeal amyloid indicate that precursor protein residues 597 to 636 are deposited into fibrils as chymotrypticlike cleavage peptides of various lengths [3]. Earlier, we found that the amyloid cores had a blocked or buried amino terminal [4] and now have shown that extended collagenase treatment can release β-peptide fragments.

Previous X-ray diffraction patterns from purified amyloid cores showed β-pleated sheet type of protein conformation with spacings at about 4.8 and 11 Å [5]. Also, HPLC-isolated meningeal amyloid β-protein has now been shown to have a similar X-ray diffraction pattern to that of amyloid cores, i.e., a β-pleated sheet. Castano et al. [6] have observed by electron microscopy the in vitro formation of amyloidlike fibrils from synthetic β-peptide. We have now observed X-ray patterns from partially dried, oriented pellets of β-peptide. The patterns show characteristic cross β-spacings: a strong meriodional arc at 4.76 Å and a diffuse equatorial arc at 10.6 Å. These spacings and the other ones that we observed at wide angles are similar to those reported for β-keratin. The series of small angle intensity maxima along the equator indicate the fibril is tubular with a diameter of 71 Å and that the wall is composed of two or three cross β-pleated sheets.

When the synthetic β-peptide length was increased to 45 amino acids to encompass some of the proposed membrane spanning region, it became very insoluble and 88% formic acid had to be used initially to solubilize it. X-ray

patterns from this peptide (β-45) in the presence of 25% trifluoroacetic acid showed β-pleated sheet spacings at about 11 Å and 4.7 Å spacings; similar but weaker patterns have been recorded for cerebral vascular amyloid (Fig. 1).

Chemical modification of amyloid and the β-28 (28-Ala) synthetic peptide indicated that the lysine at position 16 may be important in both antibody recognition and fibril formation [7]. An analog peptide, β-28 (16-Ala) was synthesized and produced polymorphic structures whose assemblies were five or six β-sheets instead of two or three. Using an inhibition-ELISA assay, we found a differential inhibition loss of 20% of binding of antibody to β-28-coated plates with β-28 (16-Ala) (Fig. 2). This suggests that Lys-16 is exposed in the

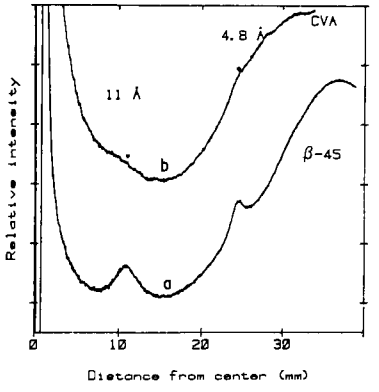

Fig. 1. Densitometer scans of X-ray patterns from (a) 25% TFA hydrated gel of β-45, and (b) vapor-hydrated lyophilate of cerebral vascular amyloid (CVA) protein isolated by HPLC. The positions of the interchain spacing (4.76 Å) and the intersheet spacing (~11 Å).

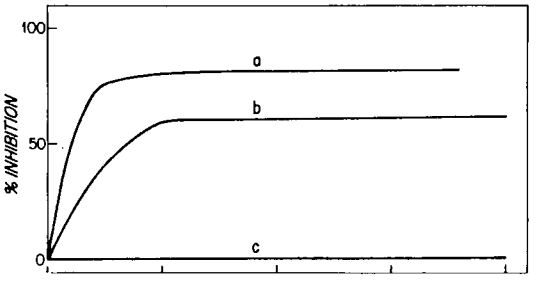

Fig. 2. Decreased ability of a peptide with alanine at position 16 [28 (16-Ala); line b] to inhibit the antipeptide antibody. A synthetic peptide (β-peptide residues 17–28) did not inhibit the antibody binding at all (line c). Line a is the control inhibition curve using β-28.

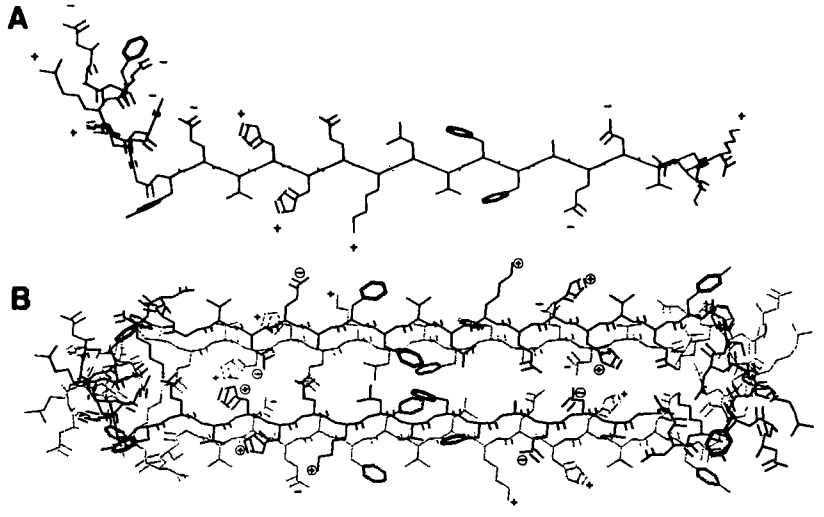

Fig. 3. (a) Schematic model of β-28 viewed in the H-bond direction to show the amino acid side chains and the polarity of charge. The conformations of the amino-terminal sequence proximal to and the short sequence distal to the β-strand are not known. (b) Model of the tetrameric subunit that may constitute the wall of the β-28 fibril. The view, which is in the direction of the axis of the fibril, is tilted slightly in order to reveal more clearly the four antiparallel β-strands and the side chains.

amyloid fibrils and that alanine at that position promotes intersheet stacking. These studies show that the AD amyloid behavior can be examined using synthetic peptides and a preliminary model of an amyloid peptide fibril can be developed (Fig. 3). Further studies using peptide analogs can be used to test this model.

Acknowledgements

This work was supported in part by grants from AFAR and ADRDA.

References

1. Glenner, G.G. and Wong, C.W., Biochem. Biophys. Res. Commun., 120 (1984) 885.
2. Kang, J., Lamarre, H.-G., Unterbeck, A., Salbaum, J.M., Masters, C.L., Grzeschik, K.-H., Multhaup, G., Beyreuther, K. and Muller-Hill, B., Nature, 325 (1987) 733.
3. Joachim, C.L., Duffy, L.K. and Selkoe, D.J., J. Neuropathol. Exp. Neurol., 46 (1987) 396 (abstract).
4. Selkoe, D.J., Abraham, C.R., Podlisny, M.B. and Duffy, L.K., J. Neurochem., 46 (1986) 1820.

5. Kirschner, D.A., Abraham, C. and Selkoe, D.J., Proc. Natl. Acad. Sci. U.S.A., 83 (1986) 503.
6. Castano, E.M., Ghiso, J., Prelli, F., Gorevic, P.D., Migheli, A. and Frangione, B., Biochem. Biophys. Res. Commun., 141 (1986) 782.
7. Duffy, L.K., Kates, J., Podlisny, M.B., Walsh, R., Galibert, L. and Selkoe, D.J., Protides Biol. Fluids, 34 (1986) 193.

Cyclic CCK-8 analogs highly selective for central receptors

B. Charpentier[a], I. Marseigne[a], A. Dor[a], D. Begué[a], C. Durieux[a], D. Pélaprat[a], M. Reibaud[b], J.L. Zundel[b], J.C. Blanchard[b] and B.P. Roques[a]

[a]Département de Chimie Organique, U266 INSERM, UA498 CNRS, Faculté de Pharmacie, 4 avenue de l'Observatoire, F-75006 Paris, France

[b]Rhône-Poulenc Santé, F-94403 Vitry-sur-Seine, France

Introduction

The sulfated peptide cholecystokinin $(CCK)^{26-33}$ (CCK-8) is present in high concentrations in mammalian brains where it seems to play a neurotransmitter role [1]. Central and peripheral CCK-8 binding sites probably corrrespond to two different biochemical entities [2]. Nevertheless, the respective role of both receptors in CCK-8-induced pharmacological responses (such as reduction of food intake or inhibition of locomotor activity) still remains controversial. It was, therefore, of major interest to design selective ligands for central CCK receptors. Recently, highly selective antagonists of peripheral CCK binding sites have been synthesized [3], but, until now, no specific ligands for the central receptors have been reported. In solution, CCK-8 exists preferentially under folded conformations characterized by an N-terminal β-turn and a C-terminal folding [4]. Therefore, cyclic analogs mimicking the N-terminal folding of the native peptide have been synthesized, and are the first described highly selective ligands for the central CCK receptors [5].

Results and Discussion

Owing to its high potency and stability, Boc $[Nle^{28,31}]CCK^{27-33}$ was chosen in preference to native CCK-8 as the parent compound. Boc-D-Asp-Tyr(SO_3H)-Nle-D-Lys-Trp-Nle-Asp-Phe-NH_2 (**1**) and Boc-γ-D-Glu-Tyr(SO_3H)-Nle-D-Lys-Trp-Nle-Asp-Phe-NH_2 (**2**) are characterized by an internal amide bond between the side-chain amino group of a D-Lys^{29} residue and either the β-carboxyl group of a D-Asp^{26} residue (compound **1**) or the α-carboxyl group of a D-Glu^{26} residue (compound **2**). These peptides were synthesized in liquid phase using a fragment condensation method [6]. The final cyclic peptides were obtained by condensation of the cyclic fragment Boc-D-X-Tyr-Nle-D-Lys-Trp-OH with the C-terminal

*To whom correspondence should be addressed.

tripeptide H-Nle-Asp(OBzl)-Phe-NH_2. Finally, the Tyr residue was sulfated by means of SO_3-pyridine. Competition experiments using [^{3}H]Boc [$Nle^{28,31}$] CCK^{27-33} as radioligand showed that compounds **1** and **2** have a high affinity for brain CCK binding sites (**1**: $K_I = 5.1$ nM; **2**: $K_I = 0.49$ nM). In contrast these peptides have a low affinity for guinea pig pancreas binding sites (**1**: $K_I = 910$ nM; **2**: $K_I = 970$ nM). The selectivity of the two cyclic peptides, as compared with CCK-8, for central receptors was clearly confirmed by their weak potencies in stimulating amylase secretion ($EC_{50} > 1000$ nM) and contracting guinea pig ileum ($EC_{50} > 1000$ nM). These results show that compounds **1** and **2** are the first described highly selective ligands of brain CCK-8 receptors, with the selectivity ratios K_I (pancreas)/K_I (brain) = 179 for **1** and 1979 for **2**. Finally, the introduction of conformational constraints on native peptides appears to be a powerful means of designing receptor-specific ligands.

References

1. Vanderhaeghen, J.J., Signeau, J.C. and Gepts, W., Nature, 221 (1975) 557.
2. Sakamoto, C., Williams, J.A. and Goldfine, I.D., Biochem. Biophys. Res. Commun., 124 (1984) 497.
3. Evans, B.E., Block, M.G., Rittle, K.E., Dipardo, R.M., Whitter, W.L., Veber, D.F., Anderson, P.S. and Freidinger, R.M., Proc. Natl. Acad. Sci. U.S.A., 83 (1986) 4918.
4. Fournié-Zaluski, M.C., Belleney, J., Lux, B., Durieux, C., Gérard, D. Gacel, G., Maigret, B. and Roques, B.P., Biochemistry, 25 (1986) 3778.
5. Charpentier, B. and Roques, B.P., French Patent No. 87-02770.
6. Charpentier, B., Durieux, C., Menant, I. and Roques, B.P., J. Med. Chem. 30 (1987) 962.

Structural requirements for the satiety effect of CCK-8

James D. Rosamond[a], Jeanne M. Comstock[a], Nancie J. Thomas[a], Anne M. Clark[a], James C. Blosser[a], Roy D. Simmons[a], Daniel L. Gawlak[a], Mary E. Loss[a], Susan J. Augello-Vaisey[a], Arno F. Spatola[b] and Deanne E. Benovitz[b]

[a]*Pharmaceutical Division, Pennwalt Corporation, P.O. Box 1710, Rochester, NY 14623, U.S.A.*

[b]*Department of Chemistry, University of Louisville, Louisville, KY 40292, U.S.A.*

Introduction

Cholecystokinin (CCK-8) (H-Asp-TyrSE-Met-Gly-Trp-Met-Asp-Phe-NH_2, SE = sulfate ester) has been shown to produce satiety in a dose-related manner in a variety of species including man (see Stacher [1] for a review). Limited structure–activity relationship (SAR) studies have indicated that the satiety effect of CCK-8 depends on the presence of the sulfate ester group [2] and the presence of the sulfated tyrosine moiety in the seventh position from the C-terminus [3]. Based on this information, a detailed SAR study of CCK-8 was undertaken. To guide the design of potent, long-acting anorectic agents, synthesized peptides were evaluated for potency to contract guinea pig gallbladder [4] and for stability to peptidase activity from homogenates of dog kidney cortex.

Results and Discussion

Peptides were synthesized by appropriate solid phase techniques [5] and purified to homogeneity by ion-exchange and/or reversed-phase chromatography. Since the major CCK-8 metabolizing organ found in the dog was the kidney [6], CCK-8 degradation in dog kidney cortex homogenate was studied. The cleavage sites identified were the Asp^1-$TyrSE^2$, Gly^4-Trp^5, and Asp^7-Phe^8 bonds. A study of D-amino acid replacements showed (see Table 1, analogs 2-6) that replacement of Asp^1 with D-Asp or $TyrSE^2$ with D-TyrSE was well tolerated (i.e., kidney stability was improved while gallbladder and anorectic potencies were either improved or only slightly reduced). Thus, chirality was not required at positions 1 and 2 for potent anorectic activity. Replacement of Gly^4 with D-Ala, Ala, Sar, Pro, or Aib (analogs 7-11) resulted, with the exception of D-Ala (analog 7), in major losses in gallbladder and anorectic potencies with little improvement in kidney stability. Thus, replacement of Gly^4 with D-Ala may be useful in multi substitution analogs. Replacement of Trp^5 with MeTrp or Phe^8 with MePhe (analogs 12-13) produced interesting results especially in the case of MePhe.

Table 1 *Analog stability versus gallbladder and anorectic activity*

No.	CCK-8 analogs	Rel. kidney homog. ($t_{1/2}$)	Rel. GP gall-bladder (EC_{50})	MAD (μg/kg) half-hour feeding period	MAD (μg/kg) three-hour feeding period
1	CCK (reference compound)	1.0[a]	1.0[b]	3[c]	30[c]
2	[D-Asp[1]]CCK-8	3.1	0.4	0.3	30
3	[D-Tyr[2]]CCK-8	5.8	1.8	3	30
4	[D-Trp[5]]CCK-8	1.8	270	300	> 300
5	[D-Asp[7]]CCK-8	1.1	59.5	30	300
6	[D-Phe[8]]CCK-8	0.8	40.4	30	300
7	[D-Ala[4]]CCK-8	5.8	5.2	30	300
8	[Ala[4]]CCK-8	1.2	1680	> 300	> 300
9	[Sar[4]]CCK-8	1.6	NT[d]	300	300
10	[Pro[4]]CCK-8	2.0	75	> 300	> 300
11	[Aib[4]]CCK-8	4.2	179	> 300	> 300
12	[MeTrp[5]]CCK-8	2.4	NT	30	30
13	[MePhe[8]]CCK-8	0.2	0.7	0.3	3
14	For-CCK-7	2.3	0.5	⩽ 0.3	3
15	Suc-CCK-7	3.6	1.5	⩽ 0.3	0.3
16	iBuOCO-CCK-7	6.4	1.9	⩽ 0.3	0.3
17	HppSE-CCK-6[e]	3.5	0.5	⩽ 0.3	3
18	HppSE-[D-Ala[2],MePhe[6]]CCK-6	> 99	2.3	3	30
19	For-[MePhe[7]]CCK-7	6.3	0.12	⩽ 0.3	0.3
20	Suc-[MePhe[7]]CCK-7	2.7	0.14	⩽ 0.3	0.3
21	iBuOCO-[MePhe[7]]CCK-7	6.9	0.13	⩽ 0.3	⩽ 0.3
22	HppSE-[MePhe[6]]CCK-6	19.0	0.003	⩽ 0.3	3

[a] Relative kidney homogenate half-life values are multiples of the value obtained for CCK-8 (4.3 ± 1 min).

[b] Relative in vitro guinea pig gallbladder EC_{50} values are multiples of the value obtained for CCK-8 (2.7 nM) [4].

[c] MAD (minimum anorectic dose, i.p.) is the lowest dose which significantly inhibits feeding in the 21-h fasted rat [7].

[d] NT is not tested.

[e] Hpp is the 3-(4-hydroxyphenyl)propionyl moiety; SE is sulfate ester.

Even though the latter analog's anorectic potency was 10 times greater than CCK-8 its kidney stability was 5 times less. The Asp[7]-MePhe[8] bond, however, was stable in kidney homogenate, while the molecule as a whole was rapidly degraded. Thus, replacement of Phe[8] with MePhe may be useful in multi-substitution analogs.

When compared with CCK-8, analogs 14-17 which contain acyl group replacements (i.e. For, Suc, iBuOCO, or HppSE) for part or all of the Asp[1]-TyrSE[2] moiety were found to be 2-3 times more stable and to have perhaps 100 times higher anorectic potencies than CCK-8. Combining these leads, HppSE-

[D-Ala^2, MePhe^6]CCK-6 (analog 18) was synthesized. This analog was found to be at least 100 times more stable than CCK-8 and only two times less potent on the gallbladder; however, its anorectic potency was unchanged. Replacement of D-Ala with native Gly produced more potent analogs as demonstrated with analogs 19-22. For example, HppSE-[MePhe^6]CCK-6 (analog 22) was 19 times more metabolically stable than CCK-8 and some 300 times more potent than CCK-8 on the gallbladder. Its anorectic potency was 10–100 times higher.

In summary, rationales for the design of anorectic analogs of CCK-8 resulted in agents with improved anorectic and gallbladder potency and greater metabolic stability. A strong correlation (Spearman's, $r = -0.81$, $P < 0.001$) was established between gallbladder potency (EC_{50}) and anorectic potency (percent inhibition for the half-hour feeding period at 30 μg/kg).

References

1. Stacher, G., Psychoneuroendocrinology, 11 (1986) 39.
2. Gibbs, J., Young, R.C. and Smith, G.P., Nature, 245 (1973) 323.
3. Lorenz, D.N., Kreielsheimer, G. and Smith, G.P., Physiol. Behav., 23 (1979) 1065.
4. Rubin, B., Engel, S.L., Drungis, A.M., Dzelzkalns, M., Grigas, E.O., Waugh, M.H. and Yiacas, E., J. Pharm. Sci., 58 (1969) 955.
5. Rosamond, J.D., Comstock, J., Blosser, J.C. and Augello-Vaisey, S.J., In Deber, C.M., Hruby, V.J. and Kopple, K.D. (Eds.) Peptides: Structure and Function, Pierce Chemical Co., Rockford, IL, 1985, p. 241.
6. Lonovics, J., Hajnal, F., Mara, P., Szabó, I. and Varró, V., Acta Hepato-Gastroenterol., 26 (1979) 222.
7. Cox, Jr., R.H. and Maickel, R.P., J. Pharmacol. Exp. Ther., 181 (1972) 1.

A study of the substrate specificity of carboxypeptidase H

Nigel J. Darby[a], Lloyd D. Fricker[b], Kamela Maruthainar[a] and Derek G. Smyth[a]
[a]*National Institute for Medical Research, The Ridgeway, Mill Hill, London NW7 1AA, U.K.*
[b]*Albert Einstein Medical College, Yeshiva University, The Bronx, NY 10461, U.S.A.*

Introduction

Several natural paptides have been found to occur in forms that lack a C-terminal amino acid. Thus, in the pars intermedia of the pituitary, β-edorphin also occurs in two shortened forms, β-endorphin 1-27 and 1-26, one of which lacks a terminal histidine residue [1]. Using a synthetic peptide based on a sequence present in the C-terminal region of porcine β-endorphin, D-Tyr-Ala-His-Lys-Lys, we have examined the possibility that β-endorphin 1-26 might arise from β-endorphin 1-27 by the action of carboxypeptidase H (CpAse H), although this enzyme is known to have a specificity for lysine and arginine [2].

Results and Discussion

Digestion of D-Tyr-Ala-His-Lys-Lys with CpAse H under conditions that allowed complete removal of the two lysine residues led to the release of < 0.5% of the histidine (Fig. 1). The removal of both Lys and His was blocked

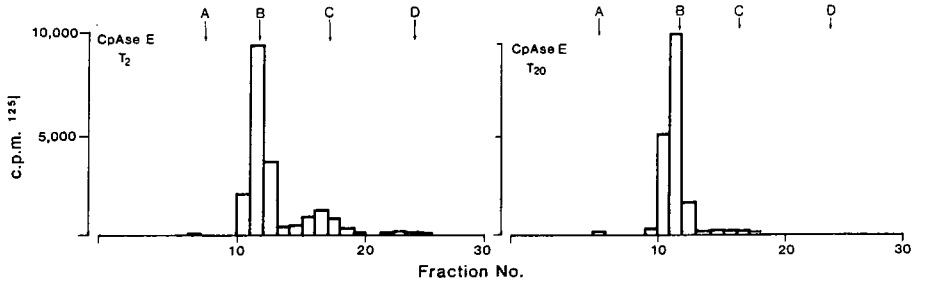

Fig. 1. Digestion of ^{125}I-D-Tyr-Ala-His-Lys-Lys (4 × 10^4 cpm; 10 nmol labeled using 1 mCi Na^{125}I) with CpAse H (0.5 μg) was carried out for 2 h or 20 h in 0.25 ml of 50 mM NaOAc 6 mM CoCl, at pH 5.7, 37°C. Products were analyzed by cation-exchange chromatography. A, B, C and D indicate the elution positions of iodinated D-Tyr-Ala, D-Tyr-Ala-His, D-Tyr-Ala-His-Lys and D-Tyr-Ala-His-Lys-Lys, respectively.

by preincubation of the enzyme for 20 min with 10 μM guanidino-ethylmercapto-succinic acid (GEMSA). In similar experiments with secretory granules from porcine pituitary, incubation of the pentapeptide at pH 5.7 led to rapid removal of lysine followed by an extremely slow release of histidine; the release of both Lys and His was again prevented by preincubation with 10 μM GEMSA.

The results demonstrate that CpAse H is capable of removing C-terminal histidine but at a very slow rate, despite the basic nature of this amino acid at pH 5.7. On the basis of this observation it is possible that the formation of β-endorphin 1-26 in vivo could be explained by prolonged exposure of β-endorphin 1-27 to CpAse H; however, a different carboxypeptidase might be involved and the action of an endopeptidase cannot be excluded.

References

1. Zakarian, S. and Smyth, D.G., Biochem, J., 202 (1982) 561.
2. Fricker, L.D. and Snyder, S.H., Proc. Natl. Acad. Sci. U.S.A., 79 (1982) 3886.

Relationship between the conformational properties of a new series of hexapeptides derived from DSLET and DTLET and their opioid delta selectivity

Marie-Claude Fournié-Zaluski[a], Joel Belleney[a], Gilles Gacel[a], Bernard Maigret[b] and Bernard P. Roques[a]

[a]U266 INSERM, UA498 CNRS, 4 avenue de l'Observatoire, F-75006 Paris, France
[b]UA422 CNRS, F-67000 Strasbourg, France

The introduction of the bulky *t*-butyl group in position 2 and/or 6 in the sequence of DSLET **1** [1] (Tyr-D-Ser-Gly-Phe-Leu-Thr, K_{i_δ} = 4.80 nM, K_{i_μ} = 31 nM) induced a large increase in opioid δ-selectivity, without loss of affinity (Delay-Goyet et al., submitted for publication) [DSTBULET **2** (Tyr-D-Ser(OtBu)-Gly-Phe-Leu-Thr, K_{i_δ} = 4.9 nM, K_{i_μ} = 404 nM) and BuBu **3** (Tyr-D-Ser(OtBu)-Gly-Phe-Leu-Thr(OtBu), K_{i_δ} = 4.2 nM, K_{i_μ} = 460 nM)]. Conversely, in DTLET **4** [2] (Tyr-D-Thr-Gly-Phe-Leu-Thr), the introduction of a *t*-butyl group on Thr^2 produced a large decrease in the affinity and selectivity for δ-receptors (DTBU-LET: Tyr-D-Thr(OtBu)-Gly-Phe-Leu-Thr, K_{i_δ} = 980 nM, K_{i_μ} = 4,500 nM) (Delay-Goyet et al., submitted for publication). Correlation between the biological properties of these peptides and their conformational characteristics was studied by ^{1}H NMR spectroscopy and theoretical calculations.

Results and Discussion

(1) ^{1}H NMR study

The ^{1}H NMR spectra of compounds **1**, **2**, and **3** showed large similarities in their preferential conformations in solution, characterized by (i) a folding of the C-terminal part of the peptides with, most probably, a γ-turn around Leu^5 stabilized by a hydrogen bond between the CO of Phe^4 and the NH of Thr^6 and (ii) a folding of the backbone on the N-terminal with a γ-turn centered around Ser^2. The Gly^3 residue might occur as a hinge between these two-folded parts of the backbone, with coupling constants and nuclear Overhauser effects corresponding to ϕ and ψ angles of around +120°. The lateral chains of the aromatic residues are preferentially in the t^- orientation. For the inactive compound **5**, the main conformational change corresponds to a reorientation of the N-terminal part of the backbone by rotation around the Thr^2 residue without changes in the folding tendency of the C-terminal part of the peptide.

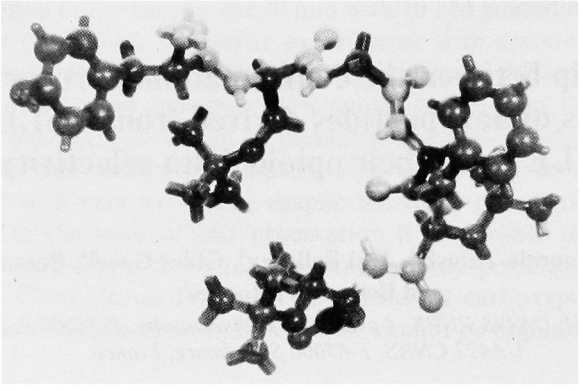

Fig. 1. Molecular model of the preferential conformation in solution of Tyr-D-Ser(OtBu)-Gly-Phe-Leu-Thr(BuBu3).

(2) Conformational calculations

Different behaviors have been found for the active molecules **1**, **2**, **3**, and **4** and the inactive molecule **5**. These differences mainly occur in the distances between (i) the Tyr^1-Phe^4 aromatic rings, (ii) the NH_3^+ $-CO_2^-$ groups, and (iii) the oxygen atoms of the Ser and Thr residues, respectively. Energy refinement of all these molecules shows that, for the active compounds, the residue in position 2 is mainly found in the C_7 conformation and the residue in position 3 near the right-handed α-helix. Phe^4 is mainly in the β-sheet region of the Ramachandran map, and Leu^5 is able to move easily from a C_7^{ax} position to a β-turn of type II position. The overall shape of all the active molecules is in close correspondence with the most stable structure found for the cyclic peptide DPLPE [3].

References

1. Delay-Goyet, P., Zajac, J.M., Rigaudy, P., Foucaud, B. and Roques, B.P., FEBS Lett., 183 (1985) 439.
2. Zajac, J.M., Gacel, G., Petit, F., Dodey, P., Rossignol, P. and Roques, B.P., Biochem. Biophys. Res. Commun., 111 (1983) 390.
3. Belleney, J., Roques, B.P. and Fournié-Zaluski, M.C., Int. J. Pept. Prot. Res., 30 (1987) 356.

Interaction of the dogfish cyclic tachykinin scyliorhinin II with tachykinin NK-1 and NK-2 binding sites

John L. Krstenansky and Stephen H. Buck
Merrell Dow Research Institute, 2110 E. Galbraith Road, Cincinnati, OH 45215, U.S.A.

Tachykinins are a large family of peptides that share the C-terminal sequence of Phe-Xxx-Gly-Leu-Met-NH_2. They interact with the multiple tachykinin receptors with varying potencies and specificities [1]. Substance P (H-Arg-Pro-Lys-Pro-Gln-Gln-Phe-Phe-Gly-Leu-Met-NH_2) and neurokinin A (H-His-Lys-Thr-Asp-Ser-Phe-Val-Gly-Leu-Met-NH_2) are examples of two mammalian tachykinins. Substance P exhibits a preference for rat submandibular salivary gland receptors (NK-1 receptors) over hamster urinary bladder receptors (NK-2 receptors) with binding affinities of 0.3 nM and 130 nM, respectively (NK-1 selectivity: NK-2/NK-1 = 433). Neurokinin A prefers NK-2 receptors having a binding affinity of 0.8 nM versus 50 nM for NK-1 receptors (NK-2 selectivity: NK-1/NK-2 = 63). Currently available structure–activity relationships for the tachykinins suggest that Phe^8 of substance P is quite important for NK-1 affinity and Asp^4 of neurokinin A is an important feature for NK-2 specificity.

Recently, Conlon et al. [2] reported the isolation of two new tachykinins from dogfish gut. One of these, scyliorhinin II, contains a pair of Cys residues and is presumably cyclic. The sequence of scyliorhinin II (H-Ser-Pro-Ser-Asn-Ser-Lys-Cys-Pro-Asp-Gly-Pro-Asp-Cys-Phe-Val-Gly-Leu-Met-NH_2) is quite similar to neurokinin A, having what are considered to be the important features for NK-2 receptor specificity. Further, the cyclic structure might also be expected to lend some receptor selectivity due to the conformational restraint that cyclization imposes.

The solid phase syntheses of scyliorhinin II and the C-terminal fragment analog scyliorhinin II_{7-18} were performed with *p*-methylbenzhydrylamine resin using Boc amino acids that were double coupled as their symmetrical anhydrides, with the exception of Asn which was coupled by the DCC/HOBT methodology. Deprotection and cleavage using HF containing 5% anisole at 0°C for 40 min was followed by oxidative cyclization with potassium ferricyanide and then purification by gel filtration and preparative reversed-phase HPLC. Homogeneity of the final product was confirmed by analytical HPLC and TLC. Identity of the materials was established by amino acid analysis and fast-atom bombardment mass spectrometry. Receptor binding of [^{125}I]-Bolton-Hunter-substance P (Amersham) to NK-1 sites in rat submandibular gland membranes and of [^{125}I]-His^1-

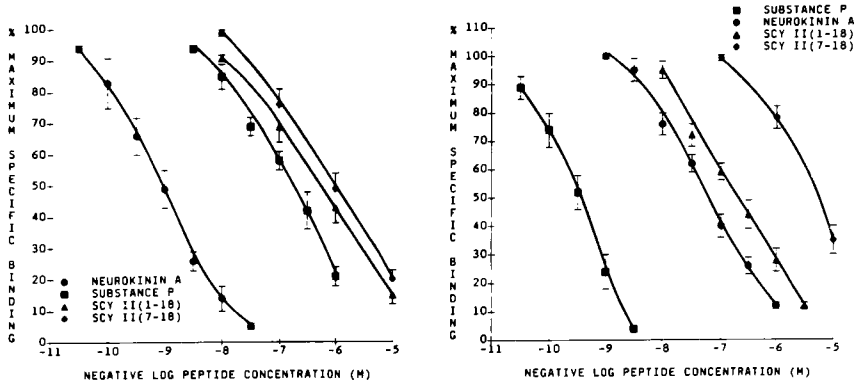

Fig. 1. Receptor binding of tachykinin peptides at NK-2 (left panel) and NK-1 (right panel) tachykinin receptors.

neurokinin A (Amersham) to NK-2 sites in hamster urinary bladder membranes was carried out as previously described [3].

Surprisingly, scyliorhinin II exhibited little receptor selectivity. The K_i of this peptide on NK-1 receptors was 200 nM and on NK-2 receptors it was 500 nM. In fact there was a slight preference for NK-1 receptors (NK-2/NK-1 = 2.5). Scyliorhinin II_{7-18} had slightly less affinity for the NK-2 receptors than the parent compound (K_i = 900 nM), but a much lower NK-1 affinity (IC_{50} = 5000 nM) giving it more of the initially expected NK-2 selectivity (NK-1/NK-2 = 5.6). Thus, this fragment is not specific enough to be useful as a selective NK-2 agonist. The potencies of both of these peptides are rather low relative to substance P or neurokinin A. The conformational restriction of the cyclization is not favorable for optimum NK-2 interaction and probably accounts for the low potency at this receptor. Considering that scyliorhinin II does not contain the functional groups considered favorable for NK-1 receptor interaction, it binds to these receptors surprisingly well, indicating that the conformation of the cyclic tachykinin is tolerated at the NK-1 receptor.

References

1. Regoli, D., Drapeau, G., Dion, S. and D'Orleans-Juste, P., Life Sci., 40 (1987) 109.
2. Conlon, J.M., Deucon, C.F., O'Toole, L. and Thim, L., FEBS Lett., 200 (1986) 111.
3. Burcher, E. and Buck, S.H., Eur. J. Pharmacol., 128 (1986) 165.

Theoretical conformational analysis of μ-selective cyclic opioid peptide analogs

Brian C. Wilkes* and Peter W. Schiller

Clinical Research Institute of Montreal, 110 Pine Avenue West, Montreal, Quebec, Canada H2W 1R7

We recently developed a systematic procedure for determining the allowed low energy conformations of the highly μ-receptor-selective cyclic opioid peptide analog H-Tyr-D-Orn-Phe-Asp-NH_2 (**1**), using the software package SYBYL (Tripos Associates, St. Louis, MO) [1]. A comprehensive grid search of the 13-membered ring structure devoid of the exocyclic Tyr-1 residue and the Phe-3 side chain resulted in only four low energy conformations. These four structures served as templates for studies including the Tyr-1 residue and the Phe-3 side chain. Despite the apparent rotational freedom around the exocyclic rotatable bonds, only a limited number of low energy side-chain configurations were found. The lowest energy conformation is characterized by a tilted stacking arrangement of the two aromatic rings (Fig. 1, **1**). No hydrogen bonds were found in low energy conformations of this compound.

This conformational analysis was extended to six 13-membered ring cyclic analogs related to **1** which display considerable diversity in their μ-receptor affinity and selectivity [2]. Two potent μ-selective analogs. H-Tyr-D-Orn-Phe-D-Asp-NH_2 and H-Tyr-D-Asp-Phe-Orn-NH_2 (Fig. 1, **2**) show a stacking arrangement of the two aromatic rings in their lowest energy conformations similar to that observed in the lowest energy conformer of **1**.

Compounds studied which show reduced μ-receptor affinity as compared to **1** were unable to adapt the tilted stacking interaction observed for the potent μ-agonists described above. Thus, the lowest energy conformation of H-Tyr-D-Orn-Phg-Asp-NH_2 (Phg = phenylglycine) is characterized by an almost fully stacked, parallel arrangement of the two aromatic rings (Fig. 1, **3**). The lack of stacking observed with the weakly active analog H-Tyr-D-Orn-Phe(NMe)-Asp-NH_2 (Fig. 1, **4**) is caused by steric interference of the bulky *N*-methyl group. Analysis of the weak μ-agonist H-Tyr-L-Orn-Phe-Asp-NH_2 revealed that chiral inversion at the 2-position also precludes a low energy stacking configuration. It is concluded that a specific tilted stacking interaction of the aromatic rings

*To whom correspondence should be addressed.

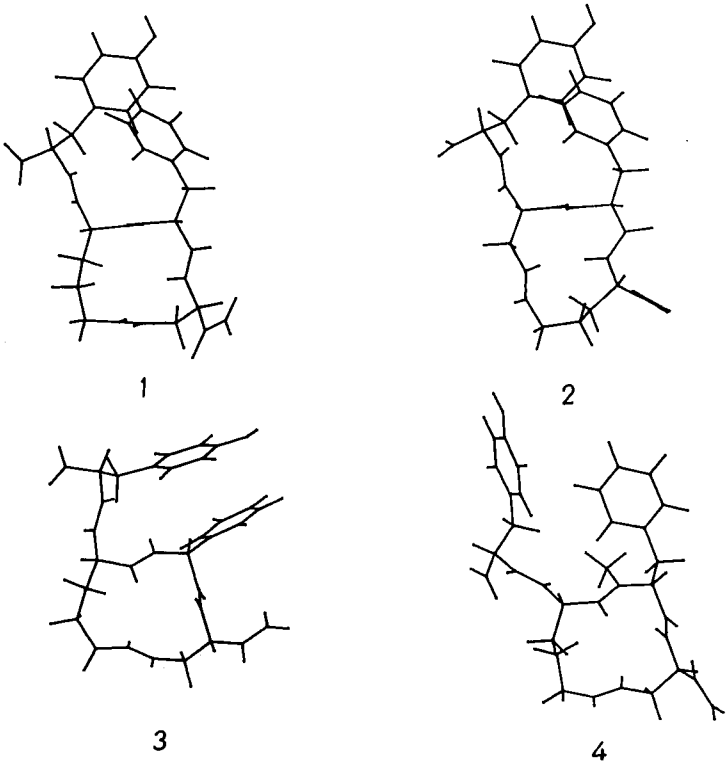

Fig. 1. Lowest energy conformers of cyclic opioid peptide analogs. **1***: H-Tyr-D-Orn-Phe-Asp-NH_2.* **2***: H-Tyr-D-Asp-Phe-Orn-NH_2.* **3***: H-Tyr-D-Orn-Phg-Asp-NH_2.* **4***: H-Tyr-D-Orn-Phe(NMe)-Asp-NH_2.*

may represent an important structural requirement for binding at the μ-receptor, at least in this series of compounds.

Acknowledgements

Supported by grants from the MRCC, QHF, and NIDA.

References

1. Wilkes, B.C. and Schiller, P.W., Biopolymers, (1987) in press.
2. Schiller, P.W., Nguyen, T.M.-D., Maziak, L.A., Wilkes, B.C. and Lemieux, C., J. Med. Chem., in press.

Session XI
New biological areas

Chair: Victor J. Hruby
University of Arizona
Tucson, Arizona, U.S.A.

Peptide sequences specified by complementary RNAs represent binding sites for proteins or peptides which interact

Kenneth L. Bost and J. Edwin Blalock

Department of Physiology and Biophysics, University of Alabama at Birmingham, Birmingham, AL 35294, U.S.A.

Introduction

Previously, we observed that hydrophobic amino acids encoded by the 'sense' strand of DNA were complemented by codons for hydrophilic amino acids on the 'antisense' strand and vice versa [1, 2]. Because of this pattern in the genetic code, peptides encoded by complementary strands of nucleic acids (i.e., complementary peptides) tend to be of an opposite hydropathic nature at each residue along their primary amino acid sequence. Since peptide hormones have been predicted to have well-defined amphiphilic conformations in the presence of their receptors [3, 4], we speculated that a pair of complementary peptides might form or impose such amphiphilic structures and bind one another.

Results and Discussion

To test this hypothesis, we synthesized peptides specified by RNA sequences complementary to the mRNA sequences for corticotropin (ACTH), γ-endorphin and luteinizing hormone releasing hormone (LHRH). A peptide encoded by the RNA complementary to the mRNA for ACTH (designated HTCA) was capable of binding ACTH with specificity and high affinity (K_d 0.3 nM) [2]. When considering ligand–receptor interactions, HTCA behaved like an ACTH receptor binding site [5]. We reasoned further that antibody against this complementary peptide (HTCA) might recognize an ACTH receptor binding site. This assumption was confirmed upon demonstrating that anti-HTCA antibodies could compete for the same binding site as ACTH on Y-1 adrenal cells. Furthermore, the antibody behaved as an agonist of ACTH, inducing Y-1 adrenal cells to steroidogenesis [5]. Taken together, these initial studies demonstrate the potential for generating, in a predetermined fashion, peptides that not only bind ligands but are also antigenically related to receptor binding sites. To demonstrate the generality of this method, peptides encoded by RNAs complementary to the mRNAs for γ-endorphin [5] and LHRH [6] were

synthesized. These complementary peptides also represented receptor-like binding sites since antibodies directed against each peptide recognized the respective hormone receptor binding site and blocked binding of the appropriate ligand [6, 7]. These examples advance the hypothesis that contact points between receptors and their ligands can be defined by regions of complementarity between the respective sequences.

Conceptually, at least two predictions can be made based on this hypothesis. If a comparison between known ligand and receptor sequences is made (1) regions of complementarity would be found, and (2) these regions would represent ligand–receptor binding sites. In fact, the presence of such complementarity was demonstrated by searching the nucleotide sequences for three ligand–receptor pairs [8]. For all three cases (epidermal growth factor, interleukin-2, transferrin, and their respective receptors) significant regions of complementarity were found in areas which would be logical for binding sites. If these sequences truly represent contact points, it should be possible to generate peptides which would block ligand binding and inhibit or enhance biological responses.

To test this prediction, peptides corresponding to the previously defined regions of complementarity between IL-2 and its receptor [8] were synthesized. A complementary sequence identified in IL-2, Leu-Glu-His-Leu-Leu-Leu (unpublished observations), and an analog, Leu-Glu-Arg-Ile-Leu-Leu [9], blocked an IL-2-mediated biological response by competing with IL-2 for receptor binding sites. When coupled to a carrier protein, these peptides effectively blocked [^{125}I]-IL-2 binding. An analog of the corresponding complementary sequence identified in the IL-2 receptor, Glu-Leu-Met-Asp-Asp-Asp, also inhibited IL-2 biological activity and binding, presumably by complexing directly with IL-2. Binding of the two complementary sequences to one another was further demonstrated by the ability of the receptor sequence to block the inhibitory effect of the IL-2 sequence. Thus, we were able to successfully predict a contact point for this receptor–ligand combination, and more importantly to use this information to block IL-2 activity. As a control, a second set of complementary sequences occurring in IL-2 and its receptor [8] were synthesized. Since the peptide, Tyr-Arg-Met-Gln-Leu, is found only in the signal sequence of IL-2 and not in the mature (processed) IL-2 molecule, we did not expect and did not find any inhibitory activity using this peptide [9]. Thus, to summarize the initial investigations, it has been shown that peptides specified by complementary strands of nucleic acids have the ability to bind one another. Furthermore, regions of complementarity between ligands and their receptors can be defined, and these sequences, in at least one instance, represent contact points. Using this approach, it was possible not only to identify binding site sequences, but also to synthesize peptides which possessed biological activity. In an effort to define a biological system where the use of complementary structures would be an ongoing process

which might rely on complementary sequences, we have begun to investigate 'immunoglobulin networks' within the immune system.

To this end, we have demonstrated that immunization with complementary peptides results in the production of antibodies which have an idiotype–anti-idiotype relationship [10]. Specifically, a portion of the antibodies produced against ACTH bound to anti-HTCA antibodies at or near the respective antigen binding sites. Similar results were obtained using antibodies against β-endorphin and antibodies against its complementary peptide. These results suggest that complementary sequences located within the hypervariable regions of such antibody pairs may represent the idiotypic and antiidiotypic determinants.

Acknowledgements

Support for this work came, in part, from Triton Biosciences, Inc. and the Comprehensive Cancer Center at the University of Alabama at Birmingham.

References

1. Blalock, J.E. and Smith, E.M., Biochem. Biophys. Res. Commun., 121 (1984) 203.
2. Blalock, J.E. and Bost, K.L., Biochem, J., 234 (1986) 679.
3. Kaiser, E.T. and Kezdy, F.J., Science, 223 (1984) 249.
4. Snell, C.R., Biochim. Biophys. Acta, 787 (1984) 53.
5. Bost, K.L., Smith, E.M. and Blalock, J.E., Proc. Natl. Acad. Sci. U.S.A., 82 (1985) 1372.
6. Mulchahey, J.J., Neill, J.D., Dion, L.D., Bost, K.L. and Blalock, J.E., Proc. Natl. Acad. Sci. U.S.A., 83 (1986) 9714.
7. Carr, D.J.J., Bost, K.L. and Blalock, J.E., J. Neuroimmunol., 12 (1986) 329.
8. Bost, K.L., Smith, E.M. and Blalock, J.E., Biochem. Biophys. Res. Commun., 128 (1985) 1373.
9. Weigent, D.A., Hoeprich, P.D., Bost, K.L., Brunck, T.K., Reiher, W.E. and Blalock, J.E., Biochem. Biophys. Res. Commun., 139 (1986) 367.
10. Smith, L.R., Bost, K.L. and Blalock, J.E., J. Immunol., 138 (1987) 7.

Didemnin and its biological properties

Kenneth L. Rinehart
Roger Adams Laboratory, University of Illinois, 1209 W. California St., Urbana, IL 61801, U.S.A.

Discovery and Chemistry

During the 1978 Alpha Helix Caribbean Expedition we noted that samples of a compound tunicate, subsequently identified as *Tridemnum solidum*, regularly possessed potent antiviral activity against herpes simplex virus, type 1 (HSV-1) [1]. This was later confirmed and expanded during in vitro studies at The

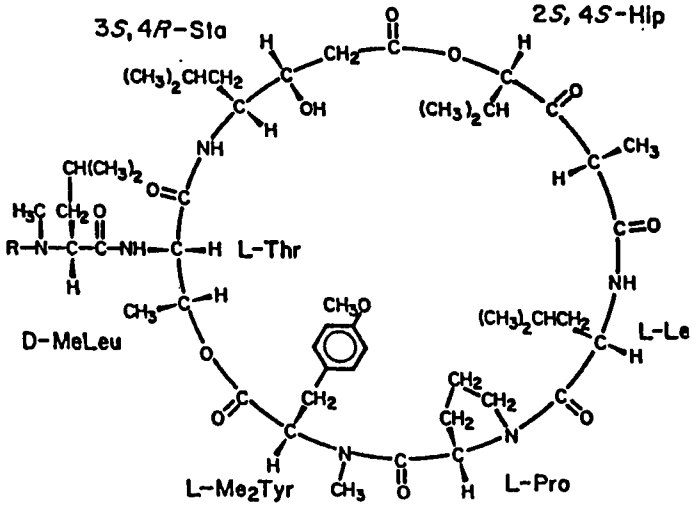

Upjohn Company against a number of DNA (HSV-1, HSV-2, vaccinia) and RNA (influenza A, parainfluenza 3, equine rhino, and Coxsackie A21) viruses [2]. Isolation studies at the University of Illinois yielded five major didemnin components (A–E) and several minor components (didemnins F-L) [3–6]. The structures assigned in 1984 to didemnins A–E (**1–5**) are shown, the stereochemistry of the Hip (hydroxyisovalerylpropionic acid) unit having been defined as 2*S*,4*S* at that time [4, 7]. In 1983 we succeeded in converting didemnin A, the most abundant component, to didemnin B, the most active, in good yield, and in late 1986 we completed a total synthesis of structure **1** [8]. While a number of the properties of synthetic **1** matched those of native didemnin A, minor differences in HPLC behavior in some solvents, in circular dichroism, and in ^{1}H NMR spectra required a revision of the structures assigned to the didemnins to include an isostatine unit, -NHCH[CH(CH_3)C_2H_5]CHOHCH_2CO-, instead of the (3*S*, 4*R*)-statine unit shown, -NHCH[CH_2CH(CH_3)$_2$]CHOHCH_2CO-.

Antiviral Activity

In studies by Renis and co-workers the purified didemnins differed by as much as an order of magnitude in their activity against DNA and RNA viruses, with didemnin B being the most potent, reducing virus titers of HSV-2 by nearly 1 log at 0.1 μg/ml [9–11]. The antiviral activity of didemnins has also been confirmed in other laboratories against a variety of DNA viruses, including varicella zoster virus and cytomegalovirus (ID_{50} 0.02 μg/ml for didemnin B; E. DeClercq and T. Sakuma, University of Leuven, Belgium, personal communication) and a number of strains of dengue virus (ID_{50} approximately 0.2 μg/ml for didemnin A) [12]. If anything, the didemnins are somewhat more active against RNA viruses than against DNA viruses: didemnin B shows 2- and 3-log reductions of equine rhino and parainfluenza-3 viruses at 0.05 μg/ml [6, 10]. A number of lethal RNA viruses (Venezuelan equine encephalomyelitis, yellow fever, sandfly fever, Rift Valley fever, and a Pichinde virus) are inhibited as well [13]. For example, didemnin B has ID_{50} 0.04 μg/ml against Rift Valley fever virus whereas the ID_{50} for ribavirin is approximately 50 μg/ml [14]. Fish viruses have also recently been shown to be inhibited by didemnin B [15].

The didemnins were early shown to be effective in vivo against vaginal herpes simplex, type 2, infections in mice [9], but treatment of cutaneous herpes infections with didemnin B was much less successful [16]. An appropriate dose regimen of didemnin B saved most mice infected with Rift Valley fever, but higher doses led to mortality [13]. Unfortunately, didemnin B is ineffective against a number of viruses, including rabies virus (F. Bussereau, Institut Pasteur, Paris, personal communication), Semliki Forest virus [16], and, most disappointingly, the AIDS virus HTLV-3 (M. Matsukura, National Cancer Institute, personal communication).

Antitumor Activity

The initial shipboard screening of *T. solidum* extracts for antiviral activity indicated a high level of cytotoxicity [1]. In subsequent testing at the Upjohn Co. by Li et al. didemnins were shown to have exceedingly potent activity against cultured L1210 cells (ID_{50} 0.001–0.0022 μg/ml for didemnin B) [2, 9, 11]. The antitumor activity for the didemnins was independently noted at the National Cancer Institute on material supplied by Weinheimer [17]. In vitro activity of didemnin B has also been demonstrated against a number of human tumor stem cell lines in two laboratories [18, 19]. Unfortunately, the cytotoxicity is manifested by the didemnins against normal cells to approximately the same degree as against tumor cells [20]. Nevertheless, in vivo assays demonstrated that didemnin B is effective against both P388 leukemia and B16 melanoma in mice as well as against a sarcoma [21, 22]. Moreover, tests against Yoshida ascites tumors in mice indicated comparable responses to didemnin and *cis*-diaminedichloroplatinum (II) but at a much lower concentration of didemnin B [23]. The in vivo results against leukemia, melanoma, and the sarcoma were felt to warrant clinical trials, and these are currently under way [21]. In preclinical studies in mice, rats, and dogs, a number of reversible toxic effects of didemnin B were noted [21], and in Phase I clinical trials no unexpected toxic effects have been observed [24]. In one study, the dose-limiting response was determined to be nausea and vomiting with some elevation of transaminase activity [25, 26]; in the other study, involving more frequent doses, some reversible liver toxicity was observed [27, 28]. Phase II clinical trials are just getting under way.

Immunoregulation

Noting some structural similarity between cyclosporin A and didemnin B, Montgomery et al. at the University of Arizona tested didemnin B as a potential immunoregulator [29–32]. They found that didemnin B inhibits T-cell mitogenesis at approximately a 1000-fold lower concentration than cyclosporin A; but, in contrast to cyclosporin A, didemnin B also inhibits B-cell mitogenesis. In the mixed lymphocyte reaction both compounds were inhibitory, didemnin B again at a 1000-fold lower concentration. More recently, scientists at Merck have demonstrated that didemnin B inhibits concanavalin A-stimulated interleukin II secretion (J. Boger et al., personal communication). The initial in vitro studies by the Arizona group were soon followed by in vivo graft versus host reaction studies in which didemnin B inhibited splenomegaly in a dose-related fashion [31]. In addition, Stevens has shown some extension of duration of rat heart grafts (L.E. Stevens, LDS Hospital, Salt Lake City, UT, personal communication), and Montgomery et al. have seen enhanced retention of mouse skin grafts [32].

The immunoregulatory properties of didemnin B are somewhat complicated in that blood chemistry remains relatively normal, with blood leukocytes and hemagglutinating antibodies being slightly elevated rather than depressed; a similar situation exists for bone marrow cells. Overall, the immunoregulatory picture remains unclear.

Other Activities

Quite recently, Gschwendt et al. have demonstrated that didemnin B inhibits tetradecanoylphorbol acetate-induced mouse ear edema, that alkaline phosphatase is inhibited in mouse dorsal skin, and that the same 100-kDa protein seems to be phosphorylated by both cyclosporin A and didemnin B [33, 34].

Modes of Action

The didemnins have been observed to exert a number of inhibitory effects on macromolecular synthesis. Inhibition of protein synthesis most nearly matches the overall cytotoxicity, while DNA synthesis is inhibited somewhat less and RNA synthesis much less than protein synthesis [30, 35]. These activities are presumed to account for the cytotoxicity, and the antiviral activity may simply result from killing the viral-infected cells. The immunoregulatory activity, however, appears to be somewhat different and may well involve inhibition of prolactin binding to T-cells [32, 36]. It is especially significant that didemnin B and cyclosporin A appear to undergo competitive binding to prolactin.

Structure–Activity Relationships

From the differences in activity between didemnins B and A [2, 9–11] it is clear that the didemnins are ideally suited for structure–activity studies. Most of the *N*-acylated didemnin analogs prepared have activity quite similar to that of didemnin B (K.L. Rinehart, L.H. Li and H.E. Renis, unpublished results), while acylation on both the isostatine hydroxyl and *N*-methylleucine appears to lead to retention of the antiviral activity but diminution of the cytotoxicity. Replacement of isostatine by norstatine in nordidemnin B causes a slight reduction in activity [37]. Reduction of the keto group in the Hip unit decreases both antiviral and antitumor activity dramatically. Finally, one recently studied semisynthetic didemnin was approximately 10-fold more inhibitory of T-cell mitogenesis than didemnin B (D.W. Montgomery and C.F. Zukoski, personal communication).

Summary

The didemnins are exceedingly potent antiviral, antitumor, and immunosuppressive agents. Thus far, their toxicity to normal cells has limited their clinical promise as antiviral agents and their effectiveness as anticancer agents remains to be demonstrated in Phase II clinical trials. What is abundantly clear at present, however, is that the very low concentrations required for biological activity allow room for considerable modification and extensive structure–activity studies. There is hope that a useful drug may be derived from these structurally novel compounds.

References

1. Rinehart, Jr., K.L., Shaw, P.D., Shield, L.S., Gloer, J.B., Harbour, G.C., Koker, M.E.S., Samain, D., Schwartz, R.E., Tymiak, A.A., Weller, D.L., Carter, G.T., Munro, M.H.G., Hughes, Jr., R.G., Renis, H.E., Swynenberg, E.B., Stringfellow, D.A., Vavra, J.J., Coats, J.H., Zurenko, G.E., Kuentzel, S.L., Li, L.H., Bakus, G.J., Brusca, R.C., Craft, L.L., Young, D.N. and Connor, J.L., Pure Appl. Chem., 53(1981)795.
2. Rinehart, Jr., K.L., Gloer, J.B., Hughes, Jr., R.G., Renis, H.E., McGovren, J.P., Swynenberg, E.B., Stringfellow, D.A., Kuentzel, S.L. and Li, L.H., Science, 212(1981)933.
3. Rinehart, Jr., K.L., Gloer, J.B., Cook, Jr., J.C., Mizsak, S.A. and Scahill, T.A., J. Am. Chem. Soc., 103(1981)1857.
4. Rinehart, Jr., K.L., Anal. Chem. Symp. Ser., 24(1985)119.
5. Gutowsky, R.E., M.Sc. Thesis, University of Illinois at Urbana-Champaign, Urbana, IL, 1984.
6. Rinehart, Jr., K.L., Cook, Jr., J.C., Pandey, R.C., Gaudioso, L.A., Meng, H., Moore, M.L., Gloer, J.B., Wilson, G.R., Gutowsky, R.E., Zierath, P.D., Shield, L.S., Li, L.H., Renis, H.E., McGovren, J.P. and Canonico, P.G., Pure Appl. Chem., 54(1982)2409.
7. Nagarajan, S., Ph.D. Dissertation, University of Illinois at Urbana-Champaign, Urbana, IL, 1984.
8. Rinehart, K.L., Kishore, V., Nagarajan, S., Lake, R.J., Gloer, J.B., Bozich, F.A., Li, K.-M., Maleczka, Jr., R.E., Todsen, W.L., Munro, M.H.G., Sullins, D.W. and Sakai, R., J. Am. Chem. Soc., 109(1987)6846.
9. Rinehart, Jr., K.L., Gloer, J.B., Wilson, G.R., Hughes, Jr., R.G., Li, L.H., Renis, H.E. and McGovren, J.P., Fed. Proc., 42(1983)87.
10. Renis, H.E., Court, B.A., Eidson, E.E., Swynenberg, E.B., Gloer, J.B. and Rinehart, Jr., K.L., 21st International Conference on Antimicrobial Agents and Chemotherapy, Chicago, IL, Nov. 4–6, 1981, No. 189.
11. Li, L.H., Renis, H.E., McGovren, J.P. and Rinehart, Jr., K.L., Proc. Am. Assoc. Cancer Res., 22(1981)255.
12. Maldonado, E., Lavergne, J.A. and Kraiselburd, E., P.R. Health Sci. J., 1(1982)22.
13. Canonico, P.G., Pannier, W.L., Huggins, J.W. and Rinehart, Jr., K.L., Antimicrob. Agents Chemother., 22(1982)696.
14. Stephen, E.L., Jones, D.E., Peters, C.J., Eddy, G.A., Loizeaux, P.S. and Jahrling,

P.B., In Smith, R.A. and Kirkpatrick, W. (Eds.) Ribavirin: A Broad Spectrum Antiviral Agent, Academic Press, New York, NY, 1980, pp. 169–183.
15. Ji, R., Yoshimizu, M. and Kimura, T., Proceedings of the 12th Annual Meeting of Japan Society of Fish Pathology, March, 1987.
16. Weed, S.D. and Stringfellow, D.A., Antiviral Res., 3 (1983) 269.
17. Suffness, M. and Douros, J., J. Nat. Prod., 45 (1982) 1.
18. Jiang, T.L., Liu, R.H. and Salmon, S.E., Cancer Chemother. Pharmacol., 11 (1983) 1.
19. Rossof, A.H., Johnson, P.A., Kimmell, B.D., Graham, J.E. and Roseman, D.L., Proc. Am. Assoc. Cancer Res., 24 (1983) 315.
20. Crampton, S.L., Adams, E.G., Kuentzel, S.L., Li, L.H., Badiner, G. and Bhuyan, B.K., Cancer Res., 44 (1984) 1796.
21. Clinical Brochure on Didemnin B (NSC 325319). Prepared by the Division of Cancer Treatment, National Cancer Institute, Bethesda, MD, June, 1984.
22. Didemnin B: NSC-325319. In NCI Investigational Drugs: Pharmaceutical Data (NIH Publication No. 85-2141), March, 1985, pp. 117–178.
23. Fimiani, V., Oncology, in press.
24. Chun, H.G., Davies, B., Hogh, D., Suffness, M., Plowman, J., Flora, K., Grieshaber, C. and Leyland-Jones, B., Invest. New Drugs, 4 (1986) 8279.
25. Dorr, A., Schwartz, R., Kuhn, J., Bayne, J. and Von Hoff, D.D., Proc. Am. Soc. Clin. Oncol., 5 (1986) 39.
26. Dorr, F.A., Kuhn, J.G., Phillips, J. and Von Hoff, D.D., J. Clin. Oncol. (1987) in press.
27. Stewart, J.A., Tong, W.P., Hartshorn, J.N. and McCormack, J.J., Proc. Am. Soc. Clin. Oncol., 5 (1986) 33.
28. Tong, W.P., Webster, L.K., Hartshorn, J.N., Stewart, J.A. and McCormack, J.J., Proc. Am. Assoc. Cancer Res., 27 (1986) 1113.
29. Montgomery, D.W. and Zukoski, C.F., Fed. Proc., 42 (1983) 374.
30. Montgomery, D.W. and Zukoski, C.F., Fed. Proc., 43 (1984) 368.
31. Montgomery, D.W. and Zukoski, C.F., Transplantation, 49 (1985) 49.
32. Montgomery, D.W., Celniker, A. and Zukoski, C.F., Transplantation, 43 (1987) 133.
33. Gschwendt, M., Kittstein, W. and Marks, F., Cancer Lett., 34 (1987) 187.
34. Gschwendt, M., Kittstein, W. and Marks, F., Carcinogenesis, 8 (1987) 203.
35. Li, L.H., Timmins, L.G., Wallace, T.L., Krueger, W.C., Prairie, M.D. and Im, W.B., Cancer Lett., 23 (1984) 279.
36. Russell, D.H., Buckley, A.R., Montgomery, D.W., Larson, N.A., Gout, P.W., Beer, C.T., Putnam, C.W, Zukoski, C.F. and Kobler, R., J. Immunol., 138 (1987) 276.
37. Gloer, J.B., Ph.D. Dissertation, University of Illinois at Urbana-Champaign, Urbana, IL, 1983.

Identification of two distinct regions of an alternatively spliced site in human plasma fibronectin that promotes cell-type specific adhesion

Martin J. Humphries[a,b], Akira Komoriya[c], Steven K. Akiyama[a,b], Kenneth Olden[a,b] and Kenneth M. Yamada[b]

[a]*Howard University Cancer Center, Washington, DC 20060, U.S.A.*
[b]*NCI, National Institutes of Health, Bethesda, MD 20892, U.S.A.*
[c]*Rorer Biotech Inc., Rockville, MD 20850, U.S.A.*

Introduction

Organization and development of cells, tissues, and organs require not only growth and differentiation factors but also the presence of an extracellular matrix. One well-characterized component of the matrix is fibronectin. Fibronectin exists primarily as a heterodimer with a molecular weight of about 450 kDa. Two similar subunits are joined by two disulfide bonds (see Fig. 1). The domains are defined by limited proteolysis and each domain contains distinct binding specificity, e.g., binding to collagen, fibrin, heparin, or cells. A key cell attachment site in fibronectin for fibroblasts has been recently shown to be the tetrapeptide Arg-Gly-Asp-Ser (RGDS) [1–3]. In addition to the cell binding domain containing the RGDS amino acid sequence, we recently identified another domain that promotes adhesion of B16-F10 melanoma cells but not fibroblastic baby hamster kidney (BHK) cells [4]. This cell-type specific adhesion site is localized to the type III connecting segment (III CS), a region of fibronectin that undergoes complex alternative splicing. We report here further localization of cell-type specific adhesion sites within the III CS domain.

Results and Discussion

A total of six overlapping synthetic peptides spanning the entire III CS domain (120 amino acid residues) was synthesized by the solid phase method and purified by reversed-phase liquid chromatography on C18 SynChropak RP-P columns (250 × 10 mm) using a water/acetonitrile gradient of 10–50% containing 0.1% TFA. The six synthetic peptides were the residues 1–25, 23–47, 45–68, 66–92, 90–109, and 107–120 of the III CS domain and were designated as CS1 to CS6, respectively (see [4] for the amino acid sequences). The six CS peptides were designed with a 3-amino acid overlap so that every possible tetrapeptide was

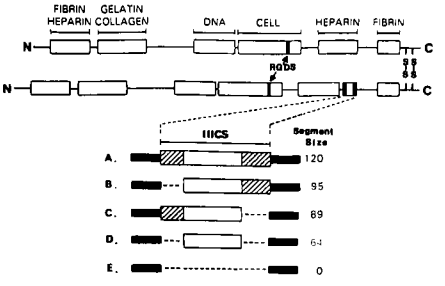

Fig. 1. Schematic representation of the domain structure of human fibronectin and the five possible derivatives arising from alternative splicing of the III CS region.

contained within at least one peptide. In additon, CS1 was designed to contain an entire alternatively spliced segment consisting of residues 1–25 of the III CS.

In order to evaluate the ability of the CS peptides to mediate cell adhesion of melanoma cells, each peptide was synthesized with an N-terminal cysteine residue to allow coupling of the peptides to an IgG using the cross-linking reagent *N*-succinimidyl-3-(2-pyridyldithio)propionate. As shown in Fig. 2, only two of the conjugates, CS1-IgG and CS5-IgG, exhibited cell-spreading activity for the cells. The abscissa shows the initial solution-phase coating concentration of peptide-IgG conjugates. The amount of conjugate or fibronectin actually bound to the substrate was determined by utilizing radiolabeled peptides in the conjugate preparations and determining the radioactivity of excised duplicate wells coated by conjugates. Analysis of the amino acid sequence of CS5 revealed a tetrapeptide Arg-Glu-Asp-Val (REDV), which resembles the now classic cell adhesion sequence RGDS. CS5-IgG, however, was 320-fold less active than fibronectin itself on a molar basis, whereas CS1-IgG was found to be only 2.4-fold less active. These results suggest that the CS1 region may be the major site for fibronectin interaction with the B16-F10 melanoma cell surface. The adhesion-promoting activities of CS1-IgG and CS5-IgG were additive, as were the adhesion-

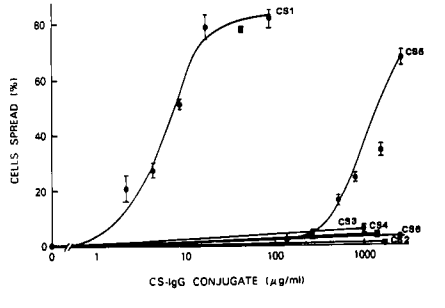

Fig. 2. Concentration dependence of the spreading of B16-F10 melanoma cells on substrate-adsorbed CS-IgG conjugates.

inhibitory activities of the free peptides (data not shown). These findings suggest that both regions of the III CS can function separately or together in mediating the interactions of melanoma cells with fibronectin.

References

1. Ruoslahti, E. and Pierschbacher, M.D., Cell, 44 (1986) 517.
2. Akiyama, S.K. and Yamada, K.M., Adv. Enzymol., 59 (1987) 1.
3. Hynes, R., Annu. Rev. Cell Biol., 1 (1985) 670.
4. Humphries, M.J., Akiyama, S.K., Komoriya, A., Olden, K. and Yamada, K.M., J. Cell Biol., 103 (1986) 2637.

Melanin-concentrating hormone: Structure-activity studies of a new hormone

Mac E. Hadley[a], Ana M.L. Castrucci[c] and Victor J. Hruby[b]

Departments of [a]Anatomy and [b]Chemistry, University of Arizona, Tucson, AZ 85721, U.S.A. and [c]Departmento de Fisiologia Geral, University of São Paulo, SP, CP11176, Brazil

Introduction

Melanin-concentrating hormone (MCH) is a heptadecapeptide, Asp-Thr-Met-Arg-Cys-Met-Val-Gly-Arg-Val-Tyr-Arg-Pro-Cys-Trp-Glu-Val, which is synthesized by hypothalamic neurons and stored within the neurohypophysis of some vertebrates [1, 2]. This melanotropic peptide stimulates melanosome (melanin granule) aggregation within teleost melanocytes. We synthesized MCH [3] and fragment analogs of the hormone and determined the structural requirements for the melanotropic activity of the neuropeptide [4].

Results and Discussion

In an in vitro fish skin (melanosome-aggregating) bioassay, the potency ranking was: MCH = MCH_{5-17} > MCH_{1-14} > MCH_{5-14}. The minimum effective dose (MED) of MCH is about 10^{-12}M. The N-terminal tetrapeptide sequence, Asp-Thr-Met-Arg, is not required for MCH-like activity since MCH_{5-17} is equipotent to the native hormone. MCH_{1-14}, which lacks the C-terminal tripeptide ring extension, exhibits about 1/10th the activity of MCH, indicating a contribution of one or more C-terminal amino acids, for full agonistic activity. MCH_{5-14}, possesses about 1/300th the activity of MCH. Surprisingly, MCH stimulates melanosome dispersion rather than aggregation in the in vitro frog and lizard skin bioassays. The N-terminal tetrapeptide sequence of MCH is required for this melanocyte-stimulating hormone (MSH)-like activity since MCH_{1-14}, but not MCH_{5-17} and MCH_{5-14}, exhibited such activity.

When the fragment analogs were used at a high concentration (10^{-5}M), it was revealed that the peptides possessing the intact NH_2-terminus (MCH_{1-17} and MCH_{1-14}) exhibited autoantagonism [5]. The MCH_{5-17} and MCH_{5-14} analogs, in contrast, only exhibited melanin concentrating activity. The contrasting activities of MCH_{1-17} and MCH_{5-17} (which were equipotent and full agonists at a low concentration) were clearly shown when they were used over the complete dose–response range, including supermaximal concentrations. The melanosome-

aggregating activity of MCH diminished as the concentration was increased above 10^{-8}M, whereas the activity of MCH_{5-17} was uncompromised at even the highest concentrations employed (10^{-5}M). Self-antagonism of MCH at high concentrations appears to relate to the NH_2-terminal tetrapeptide, which is responsible for the intrinsic MSH-like activity of the hormone. Calcium is required for the MSH-like activity but not the MCH-like action of MCH on fish melanocytes. Since MCH autoantagonism is also Ca^{2+}-dependent, it is likely that self-antagonism is due to the MSH-like activity of MCH.

It would be expected that the actions of two different peptide hormones that exhibit opposing actions should be mediated through separate cellular receptors. This view is supported by the observation that the actions of MSH were inhibited in CA^{2+}-free medium, whereas the actions of MCH under similar experimental conditions were uncompromised. The demonstration that MCH only exhibits melanosome aggregating activity on teleost melanocytes (not on tetrapod, frog, and lizard melanocytes) is further proof that the two receptors are separate. Tetrapods apparently lack MCH or MCH-like melanocyte receptors. It is possible that MCH functions as a humoral hormone only in teleostean fishes.

Although MCH and MSH do not share any apparent primary structural similarity, they may nevertheless be evolutionarily related and possess some common topological (three-dimensional) feature of structure. Alternatively, both molecules may have derived MSH-like activity, and by inference structural similarity, by convergent evolution. How a linear amino acid sequence determines the three-dimensional topology of a peptide or protein is still not understood. Given the relatively small size of MSH and MCH, these peptides may provide useful models for the determination of the relationship between primary structure and three-dimensional structure especially by examining conformationally constrained analogs with specific activities.

Both MSH and MCH are present within the brain and/or the pituitary gland of several vertebrates. Indeed, MCH has been reported to inhibit corticotropin secretion from the isolated rat pituitary gland [6]. This observation suggests that MCH may be a peptidergic neurohormone functioning as a hypophysiotropic factor. If these melanotropic peptides play a role as neuroregulatory hormones, then their actions are probably mediated through separate receptors. The present studies provide a useful beginning for an understanding of these putative peptidergic receptors.

Acknowledgements

Supported in part by PHS grant AM-17420 and NSF grant DCB-8615706.

References

1. Enami, M., Science, 121 (1955) 36.
2. Naito, N., Nakai, Y., Kawauchi, H. and Hayashi, Y., Cell Tissue Res., 242 (1985) 41.
3. Wilkes, B.C., Hruby, V.J., Sherbrooke, W.C., Castrucci, A.M.L. and Hadley, M.E., Biochem. Biophys. Res. Commun., 122 (1984) 613.
4. Hadley, M.E., Zechel, C., Wilkes, B.C., Castrucci, A.M.L., Visconti, M.A., Pozo-Alonso, M. and Hruby, V.J., Life Sci., 40 (1987) 1139.
5. Castrucci, A.M.L., Hadley, M.E., Wilkes, B.C., Zechel, C. and Hruby, V.J., Life Sci., 40 (1987) 1189.
6. Baker, B.I., Bird, D.J. and Buckingham, J.C., J. Endocrinol., 106 (1985) R5-R8.

Synthesis and biological activity of peptides inhibiting herpes simplex virus ribonucleotide reductase

Pierrette Gaudreau[a], Jacques Michaud[b], Suman Rakhit[c], Jean-Marie Ferland[c], Jean Gauthier[c], Yves Langelier[b] and Paul Brazeau[a]

[a]Neuroendocrinology Laboratory, Notre-Dame Hospital Research Center and [b]Montreal Cancer Institute, 1560 Sherbrooke St. E., Montreal, Canada H2L 4M1
[c]Bio-Mega Inc., Laval, Quebec, Canada

Introduction

Herpes simplex virus (HSV-1, HSV-2) ribonucleotide reductase is formed by the association of two nonidentical subunits. The C-terminus of the subunit 2, H-Tyr-Ala-Gly-Ala-Val-Val-Asn-Asp-Leu-OH(H2 7–15), has been shown to completely inhibit the reductase activity without affecting the host isoenzyme [1]. The inhibition is also reversible and noncompetitive with respect to the substrate [1].

In order to establish the relationship between chemical requirements and inhibitory potency, a series of peptides, including fragments and analogs of H2 7–15, were synthesized by solid phase methodology and tested in vitro on viral reductase [1].

Material and Methods

N^{α}-Boc amino acid derivatives were esterified to a chloromethylated resin by the cesium salt method. N^{α}-Boc-amino acid side chains were protected as follows: Asp, Glu, Ser, Thr(0-Bzl), Cys(S-4-MeBzl); Tyr(0-2-Br-Z); Arg(N^{g}-Tos). Coupling was achieved by preformed symmetrical anhydrides except for N^{α}-Boc-Asn, which was coupled with dicyclohexylcarbodiimide/hydroxybenzotriazole, and its completion ascertained by the Kaiser test. The N^{α}-amine was deprotected with 40% TFA/CH_2Cl_2 and neutralized with 5% DIEA/CH_2CH_2. After completion of the synthesis and removal of the last N^{α}-Boc group, deprotection of the amino acid side chains and cleavage of the peptides from the resin were performed with anhydrous liquid hydrogen fluoride at −15°C for 30 min and at 0°C for 30 additional min, in the presence of 10% anisole. The peptides were purified in one step by preparative HPLC (Partisil 10 ODS-3 (2.2×50 cm) C18, 10-μm particles or Vydac (5.7×30 cm) C18, 15-μm particles] using appropriate linear gradients of aqueous 0.01% TFA (pH 2.9) and

Table 1 *Primary structure and inhibitory potency of HSV H2 7–15 fragments and analogs*

Name	Primary Structure	IC_{50}[a] (μM)	RI[b] (%)
	1 2 3 4 5 6 7 8 9 10 11 12 13 14 15		
H2 1–15	H-Glu-Cys-Arg-Ser-Thr-Ser-Tyr-Ala-Gly-Ala-Val-Val-Asn-Asp-Leu-OH	42[d]	143
H2 2–15	H-Cys-Arg-Ser-Thr-Ser-Tyr-Ala-Gly-Ala-Val-Val-Asn-Asp-Leu-OH	37[d]	162
H2 3–15	H-Arg-Ser-Thr-Ser-Tyr-Ala-Gly-Ala-Val-Val-Asn-Asp-Leu-OH	35[d]	171
H2 4–15	H-Ser-Thr-Ser-Tyr-Ala-Gly-Ala-Val-Val-Asn-Asp-Leu-OH	29[d]	207
H2 5–15	H-Thr-Ser-Tyr-Ala-Gly-Ala-Val-Val-Asn-Asp-Leu-OH	31[d]	193
H2 6–15	H-Ser-Tyr-Ala-Gly-Ala-Val-Val-Asn-Asp-Leu-OH	29[d]	207
H2 7–15	H-Tyr-Ala-Gly-Ala-Val-Val-Asn-Asp-Leu-OH	36[c]–60[d]	100
H2 8–15	H-Ala-Gly-Ala-Val-Val-Asn-Asp-Leu-OH	283[c]	13
H2 9–15	H-Gly-Ala-Val-Val-Asn-Asp-Leu-OH	225[c]	16
H2 10–15	H-Ala-Val-Val-Asn-Asp-Leu-OH	190[c]	19
H2 11–15	H-Val-Val-Asn-Asp-Leu-OH	760[c]	5
[Tyr^8]-H2 8–15	H-Tyr-Gly-Ala-Val-Val-Asn-Asp-Leu-OH	330[d]	18
[Tyr^9]-H2 9–15	H-Tyr-Ala-Val-Val-Asn-Asp-Leu-OH	340[d]	18

Results are expressed in percentage of the activity obtained in control experiments without peptide and represent the mean of two (H2 1–15) or four (others) assays that varied less than 10% with each other.

[a] IC_{50}, concentration of peptide producing 50% of the maximal inhibition;

[b] RI, relative inhibition in percentage compared to H2 7–15; specific activity of viral enzyme preparations.

[c] 50 μg = 30 $U \cdot mg^{-1}$.

[d] 75 μg = 21.6 $U \cdot mg^{-1}$.

H2 12–15, H2 13–15, H2 7–12, H2 7–13, H2 7–14, [Tyr^{11}]-H2 11–15 and [Tyr^{12}]-H2 12–15 were inactive at 2 mM.

acetonitrile. Their homogeneity was assessed by analytical HPLC (>95%) and their amino acid composition confirmed by quantitative amino acid analysis after acidic hydrolysis and leucine aminopeptidase digestion (peptide content ≥78%). Ribonucleotide reductase activity was measured in vitro on viral reductase partially purified from HSV-1-infected confluent BHK-21/C13 cells as described elsewhere [1].

Results and Discussion

The inhibitory activity of HSV H2 7–15 and its fragments and analogs is reported in Table 1. Deletion of Tyr^7 generated an octapeptide with a markedly reduced inhibitory potency ($IC_{50} = 280$ μM) when compared to the nonapeptide ($IC_{50} = 36$ μM). In contrast, deletions of Ala^8 and Gly^9 did not substantially modify the IC_{50} obtained with H2 8–15. Deletion of Ala^{10} had a marked effect, increasing the IC_{50} to 760 μM. Subsequent removal of Val^{11} completely abolished activity, rendering the H2 12–15 and H2 13–15 devoid of inhibitory potency, at concentrations up to 2 mM. N-terminal fragments H2 7–14, H2 7–13 and H2 7–12 were also inactive at 2 mM. Hence, the minimum active core is the pentapeptide H2 11–15.

To ascertain whether the space between Tyr^7 and Ala^{10} is an important determinant of the inhibitory activity and possibly to find shorter peptides than H2 7–15 that retain high potency, C-terminal fragments H2 9–15, H2 10–15, H2 12–15 and H2 13–15 were extended at their N-terminus by a tyrosyl residue. [Tyr^8]-H2 8–15 and [Tyr^9]-H2 9–15 had a lower inhibitory potency (IC_{50}s = 330 μM and 340 μM, respectively) than H2 7–15, while [Tyr^{11}]-H2 11–15 and [Tyr^{12}]-H2 11–15 were inactive at 2 mM. These results indicate that the amino acid chain length is critical for maximum bioactivity.

Finally, to determine whether H2 7-15 corresponded to the complete active core, *N*-extended peptides corresponding to the C-terminus of the H2 subunit were studied. As shown in Table 1, the sole extension by Ser^6 increased the inhibitory potency 2-fold, while longer peptides had a similar potency (H2 4–15) to, or a lower inhibitory potency (H2 1–15) than, H2 6–15.

These data indicate that the minimum active core exhibiting maximal activity is the decapeptide H2 6–15. Altogether, these observations could help to design a new generation of viral reductase inhibitors.

Reference

1. Cohen, E.A., Gaudreau, P., Brazeau, P. and Langelier, Y., Nature, 321 (1986) 441.

The synthesis and characterization of 81- and 88-residue peptides: Conserved structures in the protein components of cartilage proteoglycan aggregates

Peter J. Neame, G.M. Anantharamaiah, James E. Christner and John R. Baker
Atherosclerosis Research Unit, University of Alabama at Birmingham, 705 DH, University Station, Birmingham, AL 35294, U.S.A.

Introduction

Aggregates of proteoglycan (PG) with hyaluronic acid (HA) are major components of cartilage and are stabilized by the link proteins (LP). We have previously reported the primary structure of the LP [1], and have recently determined the primary structure of the fragment of the PG which binds to both HA and LP (hyaluronic acid binding region: HABR) [2]. The similarity between these two glycoproteins is striking. The LP consists of 339 amino acids with three disulfide-bonded loop structures. Both LP and HABR have two loop structures containing two disulfide bonds each in the COOH-terminal half of the molecule. A third loop with a single disulfide bond is in the NH_2-terminal region; however, the protein core of the intact PG has a molecular weight of approximately 250 kDa versus 40 kDa for the LP. Our hypothesis is that the internally duplicated loops are involved in protein–protein interactions, while the single loop structure near the NH_2-terminal binds to HA. Our objective was to synthesize peptides which could be utilized to dissect the structure–function interrelationships in these molecules. We have synthesized an 88-residue peptide, which represents amino acids 42–129 of rat chondrosarcoma LP [1], and an 81-residue peptide which represents an HABR duplicate loop. The latter peptide is approximately 50% identical to either of the two COOH-terminal loops in LP (Fig. 1).

Results and Discussion

The syntheses were performed by the solid phase method on an Applied Biosystems 430A automated peptide synthesizer. The efficiency was monitored by ninhydrin and amino acid analyses, and 10 residues were analyzed by Edman degradation at the midpoint and at the end. The estimated cumulative step yield was $18 \pm 4\%$ for the 88-residue peptide and $24 \pm 5\%$ for the 81-residue peptide.

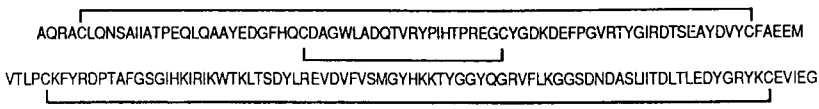

Fig. 1. The structures of (top) the 81- and (bottom) 88-residue peptides showing desired disulfide bonds.

The 'low HF'-treated resins were extracted with 4 M guanidine HCl, 50 mM Tris, pH 7.4 and the extracts dialyzed against water. The precipitate which formed during dialysis was analyzed by SDS–PAGE, UV spectrum, and tryptic and chymotryptic peptide mapping. Many of the larger fragments obtained by the two latter methods were identical to those from LP (88-residue peptide) or HABR (81-residue peptide), indicating success in the synthesis. The peptides were refolded by incubation in 2 M guanidine HCl, 50 mM Tris–HCl, pH 8.5, 3.8 mM EDTA, 10 mM reduced glutathione, 1 mM oxidized glutathione for 24 h at room temperature, in an effort to obtain native structures. The products were examined by gel filtration and by SDS–PAGE. Both peptides exhibited some polymerization and dimerization; this was particularly pronounced with the 81-residue peptide. The 81-residue peptide existed primarily as polymeric material or as a dimer, with a proportion as trimer or tetramer. The latter species were partially eliminated by reduction, though even extensive reduction did not eliminate dimeric material. Analysis of the products of refolding revealed one type of disulfide bond. It appears that the 81-residue peptide is, therefore, aggregated through noncovalent links as well as covalent cross bridges. This is apparent from Fig. 2, which shows that even after reduction, aggregated material is present.

Efforts to analyze the interactions of these peptides by adsorption to Sepharose-immobilized LP or HA were hampered by their insolubility. The peptides were adsorbed to the immobilized ligands in 0.4 M guanidine–HCl, pH 7.4 (conditions which allow formation of aggregates of the native macromolecules), and eluted with 4 M guanidine; however, there appeared to be no difference between the voided and eluted material. It is likely that these peptides are interacting largely by strong hydrophobic forces.

Our results show that large, partially purified peptides can be utilized in efforts to dissect the mechanism of aggregation in cartilage PG.

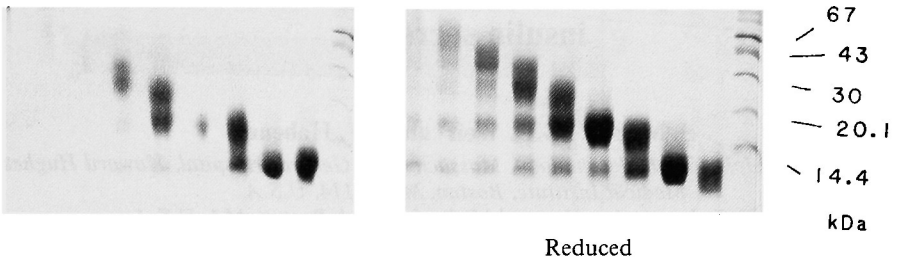

Fig. 2. SDS–PAGE analysis of the refolded 81-residue peptide. The gel on the left is an analysis of fractions from a Sephacryl S-200 column run in 4 M guanidine, pH 6.5. The gel on the right is an analysis of the same fractions after reduction in 1% SDS, 5 mM DTT at 100°C for 3 min.

Acknowledgements

Supported by grants HL 34343, AR 35322 and CA 13148.

References

1. Neame, P.J., Christner, J.E. and Baker, J.R., J. Biol. Chem., 261 (1986) 3519.
2. Neame, P.J., Christner, J.E. and Baker, J.R., J. Biol. Chem. (1987) in press.

Glucagonlike peptide I (7–37) is a potent stimulator of insulin secretion

S. Mojsov[a], G.C. Weir[b] and J.F. Habener[a]

[a]*Laboratory of Molecular Endocrinology, Massachusetts General Hospital, Howard Hughes Medical Institute, Boston, MA 02114, U.S.A.*

[b]*Joslin Laboratories, Harvard Medical School, Boston, MA, U.S.A.*

Introduction

Glucagonlike peptide I is a newly-discovered peptide, the structure of which was predicted from the nucleotide sequence of the glucagon gene [1–3]. The glucagon gene encodes a precursor, preproglucagon, that contains in addition to glucagon, the sequences of two glucagon-like peptides, termed GLP-I and GLP-II. The structures of GLP-I and GLP-II were deduced to consist of 37 and 33 amino acids, respectively, because they are flanked at their amino and carboxy termini by dibasic residues that typically are the sites cleaved in the processing of prohormones. The amino acid sequence of GLP-I is completely conserved among all mammalian species analyzed so far and is closely related to the glucagon/vasoactive intestinal/secretin peptides; however, this structural similarity starts at position 7 of the sequence of mammalian GLP-I(1–37) that is preceded by an arginine residue at position 6. Because there are many examples of prohormones that are processed at single basic residues (e.g., neurophysin and a number of growth factors), we postulated that GLP-I can exist in at least two forms: a 37-amino acid peptide termed GLP-I(1–37) and a 31-amino acid termed GLP-I(7–37). We have found that both forms of the peptides are liberated during the tissue-specific post-translational processing of proglucagon in the intestine and the pancreas [4]. The similarity in structure of GLP-I to glucagon and gastric inhibitory polypeptide, two peptides that stimulate insulin secretion, suggested to us that GLP-I might be involved in the regulation of insulin secretion. To test this hypothesis we synthesized GLP-I(1–37) and GLP-I(7–37) by the stepwise solid phase method and tested their insulinotropic effect in the rat-perfused pancreas [5].

Results and Discussion

The results of perfusions of separate pancreases each with synthetic (GLP-I(7–37) and GLP-I(1–37) are shown in Figs. 1A and B. GLP-I(7–37) at 10^{-9}

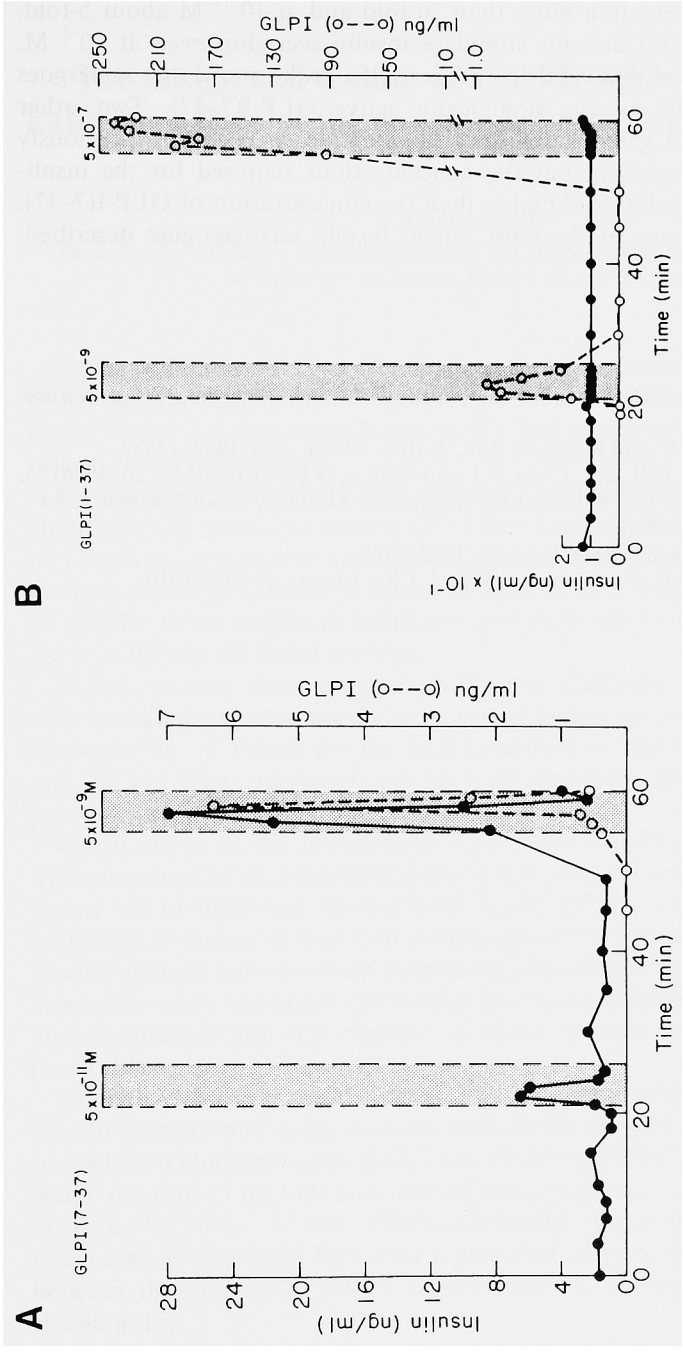

Fig. 1. Insulinotropic effects of separate perfusions with GLP-I(7–37) (Panel A) and GLP-I(1–37) (Panel B). Panel A is representative of six independent perfusions and Panel B of two separate perfusions with each of the respective peptides. Stippled areas represent the duration of perfusion with each of the peptides at the concentrations indicated. Insulin (solid lines) and the amount of GLP-I peptide perfused (dashed lines) were measured by radioimmunoassays. The concentration of GLP-I(7–37) at 10^{-11} M is below the sensitivity of the radioimmunoassay (see [6]).

M stimulated insulin secretion more than 20-fold and at 10^{-11} M about 5-fold. In contrast, GLP-I(1–37) did not stimulate insulin secretion even at 10^{-7} M. These two results suggest that GLP-I(1–37) is itself a prohormone that undergoes proteolytic cleavage to release biologically active GLP-I(7–37). Two other peptides, glucagon and gastric inhibitory polypeptide, were shown previously to stimulate insulin secretion, but the concentrations required for the insulinotropic effect were 10–100-fold higher than the concentration of GLP-I(7–37). Thus, GLP-I(7–37) is one of the most potent insulin secretagogues described.

References

1. Bell, G.I., Sanchez-Pescador, R., Laybourn, P.J. and Najarian, R.C., Nature, 304 (1983) 368.
2. Heinrich, G., Gros, P. and Habener, J.F., J. Biol. Chem., 259 (1984) 14087.
3. Seino, S., Welsh, M., Bell, G.I., Chan, S.J. and Steiner, D.F., FEBS. Lett., 20 (1986) 25.
4. Mojsov, S., Heinrich, G., Wilson, I.B., Ravazzola, M., Orci, L. and Habener, J.F., J. Biol. Chem., 261 (1986) 11880.
5. Merrifield, R.B., J. Am. Chem. Soc., 95 (1963) 2149.
6. Mojsov, S., Weir, G.C. and Habener, J.F., J. Clin. Invest., 79 (1987) 616.

The design and testing of specific inhibitors of tissue kallikrein: Role of the enzyme in blood pressure regulation

James Burton

Biomolecular Medicine, Evans Department of Clinical Research, University Hospital, 75 East Newton Street, Boston, MA 02118, U.S.A.

Tissue kallikrein (E.C. 3.4.21.35) is a serine proteinase with varied actions which include: production of lysyl-bradykinin (kallidin); activation of renin, pro-insulin and atrial natriuretic factor (ANF); and participation in various catabolic roles ([1] and refs. therein).

Several high-affinity inhibitors of tissue kallikrein such as aprotinin and the chloromethylketones are known [2]. These compounds cannot be used in vivo to unequivocally answer questions about the biologic role of tissue kallikrein because of lack of specificity. Research reported here deals with the development of specific tissue kallikrein inhibitors and their use to determine the effect of tissue kallikrein on blood pressure.

Initial research demonstrated that tissue kallikrein could be inhibited by substrate analogs based on the sequence of kininogen around the arginyl-serine cleavage site. K_i values for the best inhibitors in this series were between 50 and 200 μM. The compounds exhibit good specificity, blocking only nonspecific proteases such as trypsin [3].

Modification of the hexapeptide KKI-5 (Ac-Pro-Phe-Arg-Ser-Val-Gln-NH_2) by replacement of the acetylprolyl group at P_3 with the prochiral cyclohexylacetyl group led to inhibitors having both better affinity and specificity for tissue kallikrein. Proteases chosen four routine specificity testing included tonin, which has the greatest sequence homology to tissue kallikrein; plasma kallikrein, which cleaves the same substrate; and trypsin which was inhibited by KKI-5. Proteases and receptors commonly involved in blood pressure control were also tested (see Table 1).

In vivo KKI-7 reverses the increase in regional blood flow in the rat caused by administration of exogenous rat tissue kallikrein [4]. To determine the effect of KKI-7 on blood pressure, KKI-7 was dissolved in 50% (v/v) propylene glycol–water solution (5 mg/ml) and infused into conscious, salt-replete rats at a rate of 200 $\mu g \cdot kg^{-1} \cdot min^{-1}$. In 50% of the rats tested (8/16), mean arterial blood pressure rose between 20 and 30 Torr over a period of 10 min. The dose–response curve between the amount of KKI-7 infused and the increase in blood pressure is shown in Fig. 1.

Table 1 *Tests for the specificity of tissue kallikrein*

Protease	Species	K_I (μM) KKI-5	KKI-7
Tissue kallikrein	Human	156	4
Trypsin	Cow	30	12
Tonin	Rat	843	ND
Plasma kallikrein	Cow	1255	244
Renin	Human	ND	-
Converting enzyme	Rabbit	400	-
Angiotensin II receptor	Rat	ND	ND
Kallikrein receptor	Rat	ND	ND
Vasopressin (V1) receptor	Rat	ND	ND
β_1 and β_2 receptor	Chicken	ND	ND
α_1 and α_2 receptor	Chicken	ND	ND
ANF receptor	Rat	-	ND

ND = not detectable; - = not done.

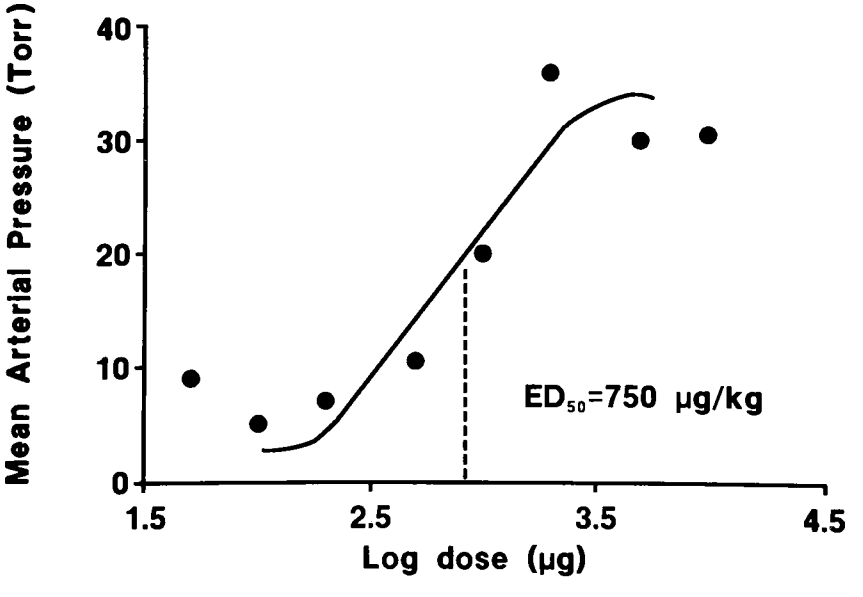

Fig. 1. Effect of KKI-7 on blood pressure in rats.

Effects of the tissue kallikrein inhibitor on blood pressure are similar to those seen when the Stewart–Vavrek kinin receptor blockers are infused, although the latter compounds must be used at much higher doses to obtain similar results [5].

The biological effects reported here are subject to many interpretations, and a convincing case for the effect of tissue kallikrein in the control of blood pressure can be made only after additional experiments. Results reported here, however, are consistent with the idea that tissue kallikrein does play an important role in blood pressure homeostasis. The hypotensive effects of the converting enzyme inhibitors in animals and humans having low plasma renin activities could be explained by the ability of converting enzyme inhibitors to potentiate circulating kinins.

References

1. Okunishi, H., Spragg, J. and Burton, J., Hypertension, 7 (1985) 172.
2. Fitz, H., Fink, E. and Truscheit, E., Fed. Proc., 38 (1979) 2753.
3. Okunishi, H., Spragg, J. and Burton, J., Hypertension, 8 (1986) 1114.
4. Okunishi, H., Spragg, J. and Burton, J., Agents Actions, (1987) in press.
5. Benetos, A., Gavras, H., Stewart, J.M., Vavrek, R.J., Hatinoglou, S. and Gavras, I., Hypertension, 8 (1986) 971.

Detection of new peptaibol antibiotics (mycotoxins) in species and strains of the fungal genus *Trichoderma*

Hans Brückner, Christine Kussin and Thomas Kripp
Institute of Food Technology, University of Hohenheim, D-7000 Stuttgart 70, F.R.G.

Introduction

A unique group of membrane-active polypeptides which are characterized by the presence of several α-aminoisobutyryl (Aib) residues has been recognized in molds of mainly the genera *Trichoderma, Emericellopsis, Stilbella,* and *Gliocladium* [1]. These peptides may be designated peptaibol antibiotics, or mycotoxins, depending on which activity is emphasized (standards are available from BACHEM AG, Hauptstr. 144, CH-4416 Bubendorf, Switzerland). In the course of a systematic screening program for these compounds we have further developed our specific methods which now enable the detection of peptaibols directly in the mycelia of molds.

Materials and Methods

Malt extract agar slants or petri dishes were seeded with a spore suspension of *Trichoderma.* After vigorous growth and sporulation occurred (usually after 7–14 days at 25°C), the mycelium was extracted three times with methanol/dichloromethane (1 : 1, v/v). The combined extracts were filtered, evaporated to dryness in heavy walled vials, and hydrolyzed with 6 N HCl at 110°C for 18 h (or propionic acid/concentrated HCl at 150°C for 1 h). After evaporation to dryness, the residue was esterified with 2.5 N HCl in 1-propanol and, after evaporation, acylated with 50 μl pentafluoropropionic anhydride in 200 μl dichloromethane (20 min at 100°C). After evaporation to dryness, the residue was dissolved in 100 μl dichloromethane and a 0.6 μl sample was injected into a capillary column. The PFP-Aib 1-propyl ester eluted either first or second (Fig. 1).

Results and Discussion

As a result of the high hydrophobicity of peptaibols, the extraction procedure allows specific, highly sensitive, and rapid chemical screening of toxins of a large number of molds grown on malt extract agar. Under the experimental

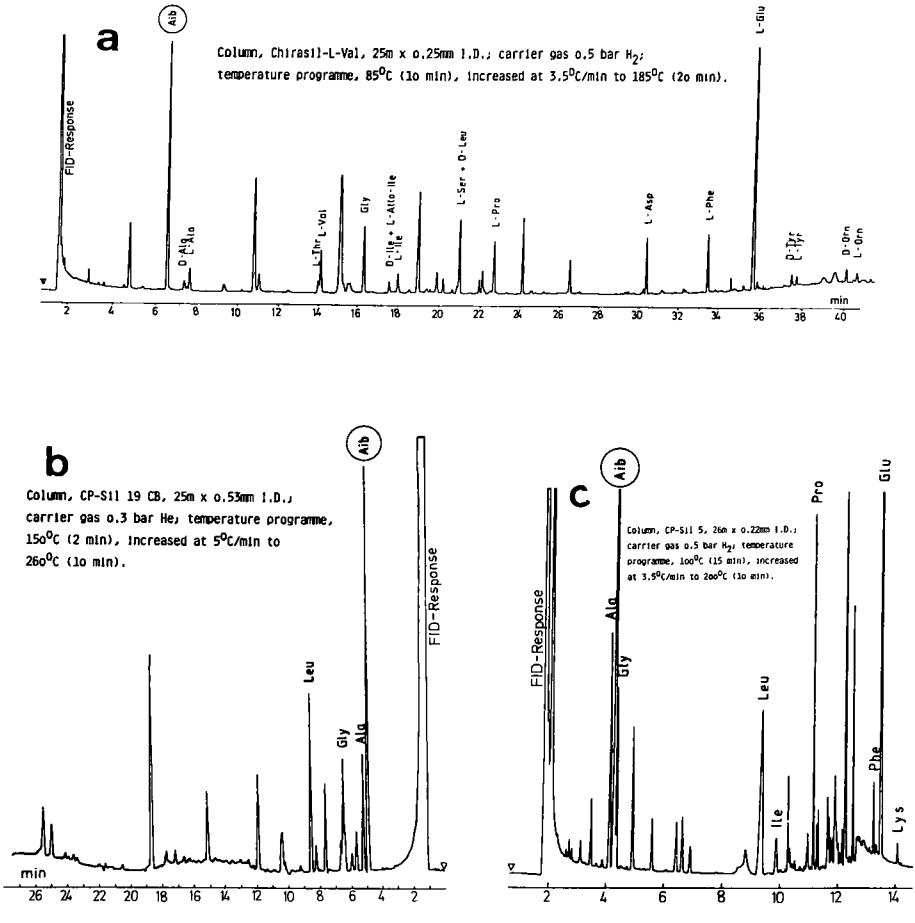

Fig. 1. Examples for the gas chromatography detection of Aib in molds using various fused-silica columns (Chrompack, Middelburg, The Netherlands): (a) Tr. hamatum *IMI 204016; (b)* Tr. aureoviride *IMI 112068; (c)* Tr. pseudokoningii *CBS 816.68.*

conditions described, peptaibols have been found in all species of *Trichoderma* and most of the strains (Table 1), and very recently in many species and strains of *Gliocladium* (e.g., *Gl. virens* WPL 258A, IFO 9169, CBS 512.66). These findings should be taken into account when discussing the mode of action in use of *Trichoderma* (or *Gliocladium*) as fungal antagonists [2]. Moreover, with regard to recommendations by various national food and drug administrative bodies concerning the employment of molds in biotechnology and food production, the above findings also have to be considered with regard to the cytotoxic,

Table 1 *New species and strains of* Trichoderma *found to produce significant amounts of Aib-containing peptides*

Trichoderma species	Culture collection number
Tr. album	BKM/GM/F-57
Tr. aureoviride	IMI 91968, IMI 112068
Tr. hamatum	NRRL 15951, NRRL 1762, IMI 204016, CBS 961.68
Tr. koningii	IMI 54963, CBS 817.68
Tr. lignorum	NRRL 8138, PWi-30 7805
Tr. longibrachiatum	CBS 816.68, CBS 936.69
Tr. piluliferum	IMI 185209
Tr. pseudokoningii	CBS 818.68
Tr. reesei	QM 6a, QM 9123, AM 9136
Tr. saturnisporum	CBS 330.70
Tr. todica	ATCC 36963, NRRL 3091
Tr. virgatum	ATCC 24961
Tr. viride	NRRL 3153, ATCC 18652, ATCC 32630, ATCC 32173

membrane-active, and antibiotic properties of peptaibols, the significance and biological activity of which have not yet been fully explored [3].

Acknowledgements

Supported by the Deutsche Forschungsgemeinschaft (BR 880/3-1).

References

1. Brückner, H. and Przybylski, M., Chromatographia, 19 (1984) 188.
2. Carlisle, D., New Scientist, 114 (1987) 35.
3. Brückner, H., Gehrlein, B. and Kiess, M., In Chmiel, H., Hammes, W.P. and Baileyi, J.E. (Eds.) Biochemical Engineering: A Challenge for Interdisciplinary Cooperation, Gustav Fischer Verlag, Stuttgart, 1987, p. 450.

Structure–activity relationships for insect hypertrehalosemic hormone: The importance of side chains and termini

Mary M. Ford, Timothy K. Hayes and Larry L. Keeley
Laboratories for Invertebrate Neuroendocrine Research, Department of Entomology, Texas A & M University, College Station, TX 77843, U.S.A.

Hypertrehalosemic hormone (HTH) is a blocked neutral peptide (Table1) as isolated from the tropical cockroach, *Blaberus discoidalis* [1]. The hormone exerts control over energy metabolism through increasing hemolymph sugar concentrations, an action similar to vertebrate glucagon. HTH is a member of a large family of hormones related to locust adipokinetic hormone and crustacean pigment concentrating hormone. These hormones control a wide range of physiological processes (e.g., protective coloration in crustaceans; lipid, carbohydrate and free amino acid metabolism, and heartbeat rate in insects). At least nine octa- to deca-peptide amides of the HTH family have been identified [2]. Each is uncharged, blocked at the N-terminus by pyroglutamic acid (pGlu), and has a Phe^4 and Trp^8. Chou–Fasman analysis predicts a high β-turn potential for each peptide at residues 5-8 [3].

We have synthesized 13 analogs of HTH and tested the analogs in vivo to measure hemolymph sugar concentrations in *B. discoidalis* [1]. These analogs were designed to replace each amino acid residue outside the putative β-turn region with an Ala residue. Amino acids favorable to β-turn formation were used to replace the naturally occurring residues in the 5-8 positions (Table 1). Since Gly does not have an asymmetric α-carbon, replacement analogs for positions 7 and 9 were D- and L-amino acid residues. This study has identified that $pGlu^1$, Phe^4 and Trp^8 are essential for the hypertrehalosemic effect of HTH in *B. discoidalis*.

Results and Discussion

$pGlu^1$, Phe^4 and Trp^8 are essential for the biological activity of HTH. Replacement of Phe^4 and Trp^8 results in a complete loss in biological activity (Table 1). When tested in preliminary antagonist studies, [*N*-Ac-Ala^1]-HTH, [Ala^4]-HTH, and [Ser^8]-HTH failed to block the action of HTH (1 pmol) even though the putative antagonist:hormone ratio was as high as 1000:1 (unpublished data). Thus, these residues of HTH are required for initial recognition and binding

Table 1 *Replacement analog series for insect HTH*

Analog[a]	HTH_{50}[b] (pmol)	Max. act. (Trehalose $\mu g/\mu l$)
1 2 3 4 5 6 7 8 9 10 pGlu-Val-Asn-Phe-Ser-Pro-Gly-Trp-Gly-Thr- NH_2	1	78
Ac-Ala-Val-Asn-Phe-Ser-Pro-Gly-Trp-Gly-Thr-NH_2	1000	NR
pGlu-Ala-Asn-Phe-Ser-Pro-Gly-Trp-Gly-Thr-NH_2	10	85
pGlu-Val-Ala-Phe-Ser-Pro-Gly-Trp-Gly-Thr-NH_2	150	NR
pGlu-Val-Asn-Ala-Ser-Pro-Gly-Trp-Gly-Thr-NH_2	NA	NA
pGlu-Val-Asn-Phe-Gly-Pro-Gly-Trp-Gly-Thr-NH_2	10	63
pGlu-Val-Asn-Phe-Ser-Gly-Gly-Trp-Gly-Thr-NH_2	150	80
pGlu-Val-Asn-Phe-Ser-Pro-Asn-Trp-Gly-Thr-NH_2	1	73
pGlu-Val-Asn-Phe-Ser-Pro-Asn-Trp-Gly-Thr-NH_2	1.5	80
pGlu-Val-Asn-Phe-Ser-Pro-Gly-Ser-Gly-Thr-NH_2	NA	NA
pGlu-Val-Asn-Phe-Ser-Pro-Gly-Trp-Ala-Thr-NH_2	30	74
pGlu-Val-Asn-Phe-Ser-Pro-Gly-Trp-Ala-Thr-NH_2	80	NR
pGlu-Val-Asn-Phe-Ser-Pro-Gly-Trp-Gly-Ala-NH_2	1	87
pGlu-Val-Asn-Phe-Ser-Pro-Gly-Trp-Gly-Thr-OH	35	59

[a] Double underline = replacement L amino acid;
Single underline = replacement D amino acid;
Ac = acetyl-.

[b] HTH_{50} = Amount of analog required to reach half the maximum activity of HTH.
NR = Maximum activity not reached within the limits of analog solubility.
NA = No activity detected.

to the hormone receptor. Phe[4] and Trp[8] are located on opposite ends of the putative β-turn which suggests that the side chains of these amino acids may form a coordinated aromatic bond. This aromatic interaction may stabilize the hormone conformation recognized by the receptor and/or directly interact with receptor aromatic groups.

The impact of residue 5-7 replacement on the potency of the respective HTH analog correlated with the bend frequency data used in Chou–Fasman calculations for β-turn predictions [3]. For example, Gly is found in the f_i position of protein β-turns slightly less often than Ser. [Gly[5]]-HTH is only slightly less potent than HTH. On the other hand, Gly is found much less often at the f_{i+1} position than Pro and [Gly[6]]-HTH is much less potent than HTH. Asn and Gly occur with approximately the same frequency in the f_{i+2} position and replacement of Gly[7] with D- or L-Asn produced no detectable change in potency. These results suggested the importance of β-turn formation in biologically active conformation of HTH.

Acknowledgements

The authors wish to thank the Texas Agricultural Experiment Station, US Public Health Service [Grant TMP(AHR) R01 NS20137-03 to TKH] and the US Department of Agriculture [Grant 86-CRCR-1-2008 to TKH] for assisting in the support of this research. Further, we would like to thank the Texas Agricultural Experiment Station's Biotechnology Support Laboratory for technical support.

References

1. Hayes, T.K., Keeley, L.L. and Knight, D.W., Biochem. Biophys. Res. Commun., 140(1986)674.
2. Goldsworthy, G.J., Mallison, K., Wheeler, C.H. and Gade, G., J. Insect Physiol., 32(1986)433.
3. Chou, P.Y. and Fasman, G.D., In Snell, E.E., Boyer, P.D., Meister, A. and Richardson, A.A. (Eds.) Annual Review of Biochemistry, Vol. 47, Annual Reviews, Palo Alto, CA, 1978, p. 251.

Structure elucidation of the major cytotoxic component of *Tridemnum cyanophorum*

Bertrand Castro[a], Patrick Jouin[a,*], Adrien Cavé[a], Michel Dufour[a], Bernard Banaigs[b] and Christian Fransisco[b]

[a]*CCIPE, Rue de la Cardonille, F-34094 Montpellier-Cedex, France*

[b]*Biologie et Chimie des Végétaux Marins, Université des Sciences, F-66025 Perpignan-Cedex, France*

The marine environment provides a number of interesting biologically active compounds. Didemnins, a class of compounds isolated from a *Tridemnum* species, have been extensively studied by Rinehart, Jr. et al., for their potent antiproliferative effects against a variety of tumor cell lines [1]. The more potent didemnin B **1a** exerts immunosuppressive effects as well [2]. We report the structure determination of an analog of didemnin B (compound **1b**) with antineoplastic activity that was extracted from a different *Tridemnum* species (see Scheme 1).

The symbiotic association between a Didemnid Ascidian (*Tridemnum Cyanophorum*) and a unicellular alga (*Cyanophyta*) has been identified and collected by Dr. F. Lafargue along the coast of Guadeloupe. The methanolchloroform extract of this biological material was purified by chromatographic techniques, providing a major fraction of compound **1b**.

In an in vitro prescreening, compound **1b** markedly inhibited growth of L 1210 cells (ID_{50} 0.2 μg/ml). This product was also active in vivo against P 388 leukemia in mice at the dosage level of 0.12 mg/kg (intraperitoneal administration on days 1, 5, 9; $T/C > 128\%$).

From analytical data, compound **1b** appeared very similar to didemnin B [1]; however, a 360 MHz ^1H NMR study clearly indicates the presence of a *sec*-butyl side chain instead of one of the isobutyl side chains present in didemnin B. From the NMR data, we concluded that 3-hydroxy-4-amino-5-methylheptanoic acid **2b** (biogenetically derived from isoleucine) was present in compound **1b** in place of the 6-methyl analog statine **2a** (derived from leucine), which is present in didemnin B. (This structure was independently elucidated by M. Guyot, D. Davoust and E. Morel, personal communication.)

We suspected that this novel γ-amino β-hydroxy acid **2b** was present in the HPLC profile of the compound **1b** hydrolysate, using precolumn derivatization technique with OPA-ME as reagent for fluorescence determination of primary amines. As expected, both Thr and Leu residues were unambiguously detected,

*To whom correspondence should be addressed.

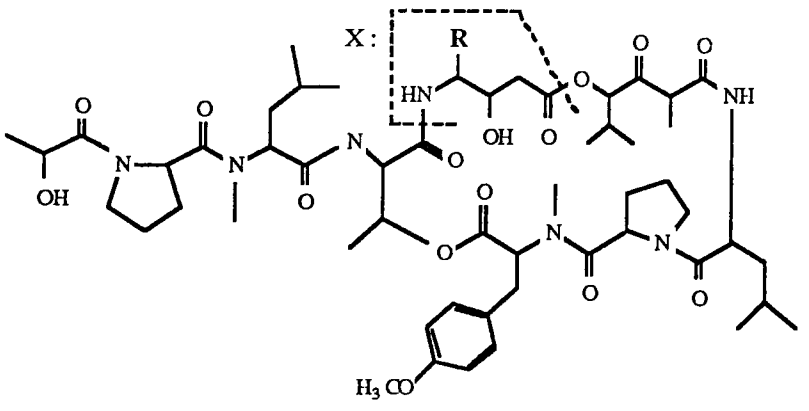

Didemnin B **1a** (X = Sta **2a**) R = CH_2-$CH(CH_3)_2$

Compound **1b** (X = Iso-Sta **2b**) R = $CH(CH_3)$-C_2H_5

Scheme 1.

but the latter peak showed a 2-fold higher integration, and we found that only the synthetic 3R4S5S isomer of **2b** could not be separated from Leu in this system; the other isomers of **2b**, as well as the *syn*- and the *anti*-statines **2a**, gave a different response. These experiments are still in progress.

The study of other naturally occurring and synthetic products of this class is in progress.

References

1. Rinehart, Jr., K.L., Glover, J.B. and Cook, Jr., J.C., J. Am. Chem. Soc., 103 (1987) 1857.
2. Montgomery, D.W. and Zukoski, C.F., Transplantation, 40 (1985) 49.

Backbone modification of synthetic poly-α-L-amino acids

Joachim Kohn[a,*] **and Robert Langer**[b]

[a]*Department of Chemistry, Rutgers, The State University of New Jersey, Piscataway, NJ 08855-0939, U.S.A.*

[b]*Department of Applied Biological Sciences, Massachusetts Institute of Technology, Cambridge, MA 02139, U.S.A.*

Introduction

Synthetic poly(amino acids) have served as model compounds for polypeptides and proteins [1]. Several attempts were made to find industrial applications for poly(amino acids) [2] and recently their use as biomaterials for implantable drug delivery devices, sutures, biomembranes, or skin replacements [3] has been suggested. Since many synthetic poly(amino acids), however, are insoluble, high-melting materials [4] that tend to absorb a significant amount of water when exposed to an aqueous environment [5], the number of useful engineering materials or biomaterials among them is extremely small as compared to the vast number of already synthesized poly(amino acids).

These problems may possibly be circumvented by suitable structural modifications of the poly(amino acid) backbone. In order to test this hypothesis, we developed several reaction schemes in which amino acids and dipeptides are polymerized via their side chains by nonamide bonds [6–8].

Results and Discussion

1-Hexadecanoyl-4-hydroxy-L-proline methyl ester (N-Pal-Hpr-Me, **1**) was poly-

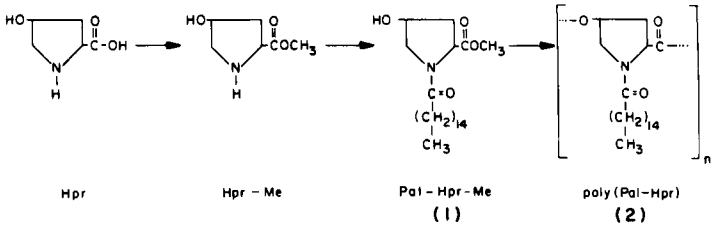

Scheme 1.

*To whom correspondence should be addressed.

merized by a transesterification reaction involving the C-terminus and the side-chain hydroxyl group (Scheme 1) [7]. The resulting polymer (**2**) can be regarded as a structural isomer of conventional O-protected poly(hydroxyproline). Presently, molecular weights (M_w) as high as 50,000 have been obtained (H. Yu, doctoral thesis). Palmitic acid was selected as the N-terminal protecting group in order to impart a high degree of hydrophobicity to the polymer. Poly(Pal-Hpr-ester) was found to be highly tissue-compatible, and its applicability as a biomaterial is presently under investigation.

The approach of 'side-chain polymerization' can be extended to dipeptides as monomers as shown by the polymerization of N-Z-tyrosyl-tyrosine alkyl esters (**3**) by a polycondensation reaction involving both tyrosine hydroxyl groups (Scheme 2) [7]. The resulting polymer is a strictly alternating copolymer, containing an equimolar ratio of amide bonds and iminocarbonate bonds. It is noteworthy that the amino acid side chains have become an integral part of the polymer backbone, while the amino acid termini assume the position of pendent chains and can be used (after deprotection) for the attachment of ligands or cross-linkers. The structure of polymer **5** has been confirmed by IR, NMR, and elemental analysis, and molecular weights (M_w) close to 20,000 have been obtained ([7] and J. Kohn, unpublished results).

In order to test the influence of the dipeptide protecting groups on the properties of the resulting polymer, we synthesized the ethyl, hexyl, and palmityl esters of N-Z-Tyr-Tyr and prepared the corresponding polymers (polyCTTE, polyCTTH, and polyCTTP) according to Scheme 2. These polymers represent a homologous series differing only in the length of the alkyl group attached to the C-terminus. In this series the melting range decreased with increasing length

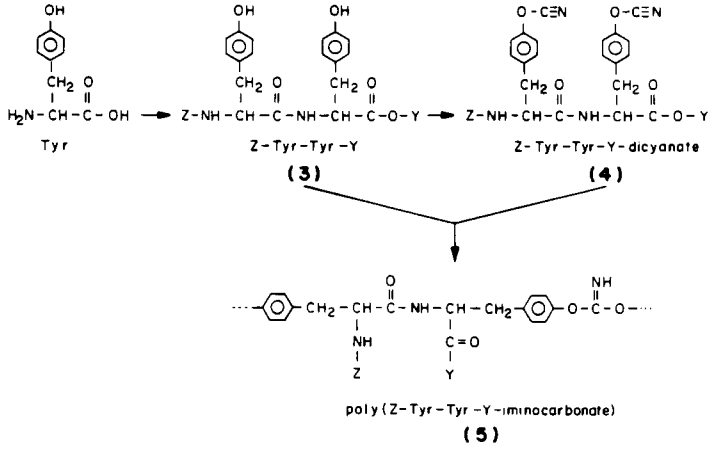

Scheme 2.

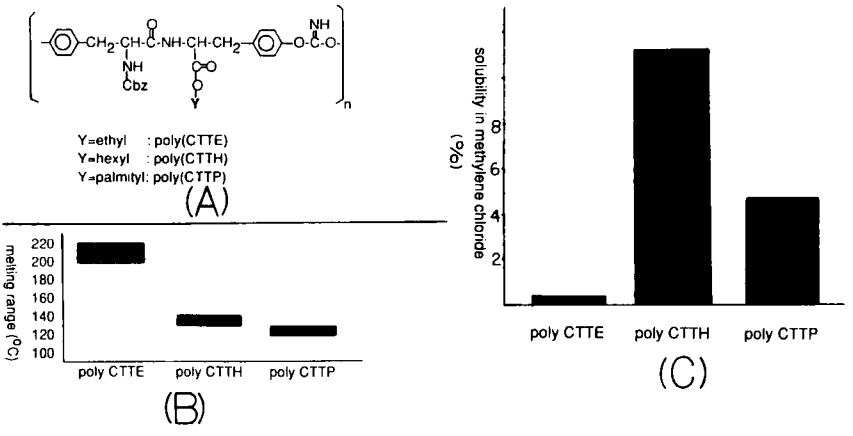

Fig. 1. Variation of some polymer properties as function of the C-terminus protecting groups: (A) molecular structures of a series of homologous polymers; (B) variation of polymer melting range; and (C) variation of polymer solubility in methylene chloride.

of the C-terminal protecting group, while solubility in organic solvents (shown for methylene chloride, Fig. 1) was greatest for the hexyl ester. Based on preliminary observations, we expect to find similar variations in mechanical properties (tensile strength) and rate of biodegradation. These results indicate that it might be possible to optimize the physical and mechanical properties of side-chain polymerized pseudopoly(amino acids) by properly selecting the N- and C-terminal protecting groups.

One important limitation for the use of synthetic poly(amino acids) as biomaterials is their relatively slow rate of biodegradation. Hence, with the exception of certain derivatives of poly(glutamic acid) [5], synthetic poly(amino acids) cannot be used for the formulation of biodegradable, implantable drug delivery devices. For example, if poly(tyrosine) is implanted subcutaneously in the back of male CD-1 mice, the implant persists for over one year, causing moderately severe inflammation at the implantation site. Since the incorporation of hydrolytically labile aminocarbonate bonds into the polymer backbone can be expected to increase the rate of biodegradation, we used polyCTTH as implant material. Contrary to the behavior of poly(tyrosine), polyCTTH disappeared from the implantation site within about one year causing only a very slight and transitory inflammatory tissue response [9].

Acknowledgements

This work was supported by NIH Grant GM 26698, by a Biomedical Research Support Grant (PHS RR 07058-21), and by a grant from the Research Council of Rutgers University.

References

1. Katzir, E., In Blout, E.R., Bovey, F.A., Goodman, M. and Lotan, N. (Eds.) Peptides. Polypeptides, and Proteins, Proceedings of the Rehovot Symposium on Poly(amino acids), Polypeptides, and Proteins, Wiley, New York, NY, 1974, pp. 1-13.
2. Block, H., Poly(γ-benzyl-L-glutamate) and other Glutamic Acid Containing Polymers, Gordon and Breach, New York, NY, 1983.
3. Anderson, J.M., Spilizewski, K.L. and Hiltner, A., In Williams, D.F. (Ed.) Biocompatibility of Tissue Analogs, Vol. 1, CRC Press, Boca Raton, FL, 1985, pp. 67-88.
4. Bamford, C.H., Elliott, A. and Hanby, W.E., Synthetic Polypeptides, Academic Press, New York, NY, 1956.
5. Sidman, K.R., Schwope, A.D., Steber, W.D., Rudolph, S.E. and Poulin,S.B., J. Membr. Sci., 7 (1980) 277.
6. Kohn, J. and Langer, R., In Proceedings of the ACS Division of Polymeric Materials Science and Engineering, Vol. 51, American Chemical Society, 1984, p. 119.
7. Kohn, J. and Langer, R., J. Am. Chem. Soc., 109 (1987) 817.
8. Kohn, J. and Langer, R., U.S. Patent 4,638,045 (1987).
9. Kohn, J., Niemi, S.M., Albert, E.C., Murphy, J.C., Langer, R. and Fox, J.G., J. Immunol. Meth., 95 (1986) 31.

Peptide derivatives specific for a *Plasmodium falciparum* protease involved in red blood cell invasion by merozoites

Roger Mayer[a], Isabelle Picard[a], François Bernard[b], Philippe Lawton[b], Philippe Grellier[b], Joseph Schrevel[b] and Michel Monsigny[a]

[a]*Centre de Biophysique Moléculaire, CNRS, F-45071 Orléans Cédex 2, France*
[b]*Laboratoire de Biologie Cellulaire, Université de Poitiers, F-86022 Poitiers, France*

Introduction

It has become clear that the spreading of antimalarial drug-resistant parasites requires new therapeutic approaches to reduce the dramatic worldwide resurgence of malaria. As the invasion of red cells by merozoites is a key event during malarial infection, the inhibition of invasion appears as an attractive biological approach. In order to understand the molecular aspect of the highly specific interaction between erythrocytes and merozoites, we have recently developed new fluorogenic hydrosoluble peptidic substrates for the assay of *Plasmodium berghei* and *chabaudi* proteases (rodent parasites) [1]. In this report, we present preliminary data on the characterization of a neutral endopeptidase from *P. falciparum* merozoites (human parasites) and on the development of specific peptidic inhibitors as potential new antimalarial drugs.

Results and Discussion

Peptides were synthesized by the classical dicyclohexylcarbodiimide method in the presence of 1-hydroxybenzotriazole. The C-terminal end of the peptide, at the proteolytic site, was substituted by a 3-amino-9-ethylcarbazol group (AEC) [2] to obtain sensitive fluorogenic substrates. The N-terminal end of the substrate was acylated by a hydrosolubilizing gluconoyl group (GlcA) which also prevents the substrate from aminopeptidase degradation. The substrates were purified at a preparative scale by reversed-phase HPLC. Their specificity was determined by monitoring the release of the fluorescent amine in the presence of parasite extracts and of plasma from parasite-free erythrocytes.

Experiments were performed with cultured *P. falciparum* FCR3 Gambia strain synchronized at the schizont stage. When the parasitemia reached 10–15%, purified merozoites were obtained from red blood cells by saponin lysis and the endopeptidase activity of the parasite extract was monitored by a fluorometric

assay using the substrate GlcA-Val-Leu-Gly-Lys-AEC [1]. The protease responsible for this activity has been isolated either by chromatofocusing of the *P. falciparum* enzyme extract on a 'Mono P' column followed by gel filtration on a 'Superose 12' column of the most active chromatofocusing fraction, or by affinity chromatography using ClcA-Val-Leu-Gly-Lys-Sar-OH immobilized on a matrix of Ultrogel ACA 34 through a hexamethylene diamine arm.

These purification procedures lead to an endopeptidase of molecular weight 68,000, with an optimal pH value close to 7.5 and an isoelectric point of 4.35.

This endopeptidase splits peptide bonds specifically after a basic amino acid and preferentially after lysine. It displays a high specificity toward substrates having a glycyl residue in the P_2 position. The protease exhibits a distinct preference for hydrophobic nonaromatic residues such as leucine at position P_3. The role of the P_4 residue seems predominant: a bulky valine side chain leads to a good substrate; the highest specificity, however, is obtained with a threonyl residue while a seryl residue strongly lowers the specificity.

From these results, specific peptidic inhibitors of this endoprotease were synthesized by replacing the fluorescent amine of the substrates by alkyl- or hydroxyalkyl amines. As an example, the tetrapeptide GlcA-Val-Leu-Gly-Lys-NHEt quantitatively inhibits the penetration of the merozoites into the erythrocytes in in vitro experiments. These preliminary results support the view that this endoprotease is implicated in the invasion process of the merozoites into erythrocytes and that this biological approach could lead to the development of a new antimalarial therapy.

References

1. Schrevel, J., Bernard, F., Maintier, C., Mayer, R. and Monsigny, M., Biochem. Biophys. Res. Commun., 124 (1984) 703.
2. Monsigny, M., Kieda, C. and Maillet, T., Embo, J., 1 (1982) 303.

Author index

Subject index

ISBN 90-72199-01-4